NASA/CP—2007-214667

Minnowbrook I
1993 Workshop on End-Stage Boundary Layer Transition

March 2007

NASA STI Program . . . in Profile

Since its founding, NASA has been dedicated to the advancement of aeronautics and space science. The NASA Scientific and Technical Information (STI) program plays a key part in helping NASA maintain this important role.

The NASA STI Program operates under the auspices of the Agency Chief Information Officer. It collects, organizes, provides for archiving, and disseminates NASA's STI. The NASA STI program provides access to the NASA Aeronautics and Space Database and its public interface, the NASA Technical Reports Server, thus providing one of the largest collections of aeronautical and space science STI in the world. Results are published in both non-NASA channels and by NASA in the NASA STI Report Series, which includes the following report types:

- TECHNICAL PUBLICATION. Reports of completed research or a major significant phase of research that present the results of NASA programs and include extensive data or theoretical analysis. Includes compilations of significant scientific and technical data and information deemed to be of continuing reference value. NASA counterpart of peer-reviewed formal professional papers but has less stringent limitations on manuscript length and extent of graphic presentations.

- TECHNICAL MEMORANDUM. Scientific and technical findings that are preliminary or of specialized interest, e.g., quick release reports, working papers, and bibliographies that contain minimal annotation. Does not contain extensive analysis.

- CONTRACTOR REPORT. Scientific and technical findings by NASA-sponsored contractors and grantees.

- CONFERENCE PUBLICATION. Collected papers from scientific and technical conferences, symposia, seminars, or other meetings sponsored or cosponsored by NASA.

- SPECIAL PUBLICATION. Scientific, technical, or historical information from NASA programs, projects, and missions, often concerned with subjects having substantial public interest.

- TECHNICAL TRANSLATION. English-language translations of foreign scientific and technical material pertinent to NASA's mission.

Specialized services also include creating custom thesauri, building customized databases, organizing and publishing research results.

For more information about the NASA STI program, see the following:

- Access the NASA STI program home page at *http://www.sti.nasa.gov*

- E-mail your question via the Internet to *help@sti.nasa.gov*

- Fax your question to the NASA STI Help Desk at 301–621–0134

- Telephone the NASA STI Help Desk at 301–621–0390

- Write to:
  NASA Center for AeroSpace Information (CASI)
  7115 Standard Drive
  Hanover, MD 21076–1320

NASA/CP—2007-214667

Minnowbrook I
1993 Workshop on End-Stage Boundary Layer Transition

John E. LaGraff
Syracuse University, Syracuse, New York

Proceedings of
Minnowbrook I—1993 Workshop on End-Stage Boundary Layer Transition
sponsored by Syracuse University
Blue Mountain Lake, New York
August 15–18, 1993

Prepared under Grant NAG3–621

National Aeronautics and
Space Administration

Glenn Research Center
Cleveland, Ohio 44135

March 2007

This report contains preliminary findings, subject to revision as analysis proceeds.

Contents were reproduced from the best available copy as provided by the authors.

Contents were reproduced from author-provided presentation materials.

This work was sponsored by the Fundamental Aeronautics Program at the NASA Glenn Research Center.

Level of Review: This material has been technically reviewed by technical management.

Available from

NASA Center for Aerospace Information
7115 Standard Drive
Hanover, MD 21076–1320

National Technical Information Service
5285 Port Royal Road
Springfield, VA 22161

Available electronically at http://gltrs.grc.nasa.gov

Acknowledgments

The workshop co-chairs would like to express their appreciation for financial support given in 1993 to the workshop by the following organizations:

NASA Lewis Research Center (now NASA Glenn), Heat Transfer Branch
NASA Langley Research Center, Experimental Flow Physics Branch
U.S. Army Vehicle Propulsion Directorate, Aviation Systems Command
U.S. Air Force:
    Office of Scientific Research (AFOSR)
    European Office of Aeronautical Research and Development (EORAD)
    Asian Office of Aeronautical Research and Development (AORAD)
Syracuse University

The contribution of the local organizing committee members from Syracuse University is acknowledged: Professors Eric F. Spina, Hiroshi Higuchi, Edward A. Bogucz, Jacques Lewalle, Fredric A. Lyman, and Thong Q. Dang.

The work of Dr. David E. Ashpis from NASA Glenn Research Center in bringing this volume to print as a NASA report is greatly appreciated.

Special thanks to Lorraine Feher, Editorial Assistant, Pat Webb, Coordinator, Jeff Abbott, Computer Operator III, and Lisa Pukach, Desktop Publishing Assistant, of LTID Publishing Services at NASA Glenn, for their dedication in producing this volume.

Contents

ORIGINAL WORKSHOP ANNOUNCEMENT

SYRACUSE UNIVERSITY/MINNOWBROOK

WORKSHOP
ON
End-Stage Boundary Layer Transition
15-18 August 1993
Blue Mountain Lake, New York, USA

It is proposed to organize a workshop which has a primary focus on experimental measurements in transitional boundary layers. It is the intent of the organizing committee to emphasize experimental results in the 3-D breakdown region of transition where hairpin vortices and turbulent bursts/spots tend to dominate the flow. Computational and analytical work supporting the interpretation of events in this regime will also be welcomed. The topic area was selected as a focus because, 1) relatively little has been reported in the region, 2) recent advances in instrumentation techniques hold the promise of direct time-resolved measurements in this region, and 3) the region is of significant engineering interest since it is here that transport processes are rapidly changing. It is the intent of the workshop to focus on potential applications including high free stream turbulence environments and airfoil design. Past and present phenomenological measurements which give insight into the physics of the end-stage region are of particular interest. It is expected that the workshop will be small, focused, and highly interactive. A small number of keynote talks will be given as a review. A representative of each major research group known to be active in the field will be invited to discuss their current and/or past work.

The major objective of the workshop will be to clarify our current understanding of the physics of end-stage transition. Proposals for future experiments will be included in the final report.

Workshop Co-Chairman:

Prof. John E. LaGraff - Syracuse University, Dept. Mech. & Aero. Eng., Syracuse, NY 13244 (tel. 1-315-443-4366; Fax 315-443-9099; JLAGRAFF@SUVM.ACS.SYR.EDU)

Prof. T.V. Jones - Oxford University, Dept. Eng. Science, Oxford OX13PJ, UK (tel. 44-865-246-561; Fax 865-722-274)

Prof. J.Paul Gostelow - University of Technology, PO Box 123, Broadway NSW 2007, Australia (tel. 61-2-330-2603; Fax 2-330-2611)

4/93

MINNOWBROOOK CONFERENCE
End Stage Transition Workshop
15-18 August 1993

Sunday - 15 August 1993

2:30 pm
Minnowbrook Center Open to Participants

3 - 5:30 pm
Visit to Adirondack Museum (optional)

6:00 pm - Dinner

7:30 pm
Organization Comments - J.E. LaGraff
Intro. to Goals and Focus of Workshop- J.P. Gostelow

8:00 pm
The Many Worlds of Transition Research
R. Narasimha (30 minutes)

9:00 pm - Social

Monday - 16 August 1993
8:00 am Session 1
Approach to Bursting

moderator: J. Lewalle
a) M.V. Morkovin - Keynote - (30 min)
b) R.E. Blackwelder
c) J.M. Kendall
d) M. Gaster
e) D. Nosenchuck

9:30 am - Discussion

BREAK

10:30 am Session 1a

moderator: E.A. Bogucz
e) T.C. Corke
f) F. Smith
g) C. Smith
h) B. Singer

11:30 am - Discussion

12:15 - LUNCH

2:00 pm Session 2 - Engineering Models and Turbomachinery Applications

moderator: T. Okiishi
a) H. Hodson- Keynote (30 min)
b) C. Fraser
c) D.A. Ashworth
d) G.J. Walker

3:15 pm - Discussion

BREAK

4:15 pm Session 2a

moderator: M. Crawford
e) T. Wang
f) T. Okiishi
g) D.Wisler
h) F. Simon
i) M. Platzer

5:30 pm - Discussion

7:00 pm - Dinner

Tuesday - 17 August 1993
8:00 am Session 3 - Turbulent Spots & Breakdown

moderator: E.F. Spina
a) I. Wygnanski - Keynote (30 nin)
b) J.P. Gostelow
c) T.V. Jones
d) I. Poll
e) T. Cebeci

9:30 am - Discussion

BREAK

10:30 am Session 3a

moderator: T.V. Jones
f) R. Kimmel
g) T. Simon
h) A. Seifert
i) E. Malkiel

11:30 am - Discussion

12:15 LUNCH

2:00 pm Session 4
Numerical & 3-D Effects

moderator: S. Robinson
a) E. Reshotko - Keynote (30 min)
b) T. Herbert
c) M.M. Rai
d) N.D. Sandham
e) M. Crawford

3:30 pm - Discussion

BREAK

4:30 pm Session 4a

working group meeting

6:30 pm - Dinner

8/9/93

8:00 am
Report of Session Chairs/moderators
Report of ad-hoc working groups?
Wrap-up discussion- Narasihma

10:00 am
Conclusion of workshop

10:30 am
Vans leave for Syracuse Airport

12 noon
Lunch for remaining participants

1:00 pm
Vacate center

Opening Remarks

J. Paul Gostelow
Workshop Co-Chair

The title of this workshop is End-Stage Boundary Layer Transition and I think we would all be happy to accept, as terms of reference, the study of the completion of the transition process. It was suggested, in the brochure, that the focus would be on experimental measurements and I hope that we are happy to accept that as a major emphasis - although a significant number of the presentations will be concerned with numerical simulation of the processes. Such a balance is entirely appropriate. I imagine you would agree that in a complex question like transition, we need all the help we can get, from whatever source.

Now, transition as a field tends to spawn as many opinions as there are participants and at this stage, I would like to inject a note of controversy, right from the start. I do so to set the scene for Roddam Narasimha's keynote presentation to follow and hopefully to spark discussion. The brochure implies that end-stage transition is synonymous with "the 3-D breakdown region of transition where hairpin vortices and turbulent bursts/spots tend to dominate the flow". Well, I have made as many measurements of spots as most people and I do not believe the above statement to be universally true. Some of us will be showing results where such parameters as free-stream turbulence level are systematically varied. Ted Okiishi, for example, will be showing fairly clearly, that on a turbine cascade at turbulence levels above 1%, spots do indeed dominate the flow. However, below 1% turbulence level in an adverse pressure gradient transition occurs without a hint of a spot.

You may think that in highlighting this distinction, I am nit-picking but I would contend that it is precisely such difficulties which have led to a division of the transition community into completely separate groups which have not communicated. The fundamental fluid dynamics community works in low turbulence wind tunnels and sees many things, but not spots - unless they choose to trigger them officially. The turbomachinery community, for example, usually works under higher free-stream, turbulence levels and therefore, usually sees spots.

Transition is still a rich and complex set of phenomena and if, as a result of this workshop, we can get a feel for the extent and role of these scenarios, we shall be doing well.

We chose this 2 1/2 day format and this magnificent, but remote, location to encourage total immersion in End-Stage Boundary Layer Transition with a minimum of distraction and maximum opportunity for interaction-which should be as informal as we can make it.

In your presentations, we do ask you to stick strictly to the 15 minute limit. All we want you to do is to highlight and summarize your contribution and to provoke discussion. Since this is a relatively informal meeting, it does provide an off-the-record opportunity to let your hair down. You should feel free to provoke discussion without it being held against you in the printed word. We want the presentations to be free-wheeling and adaptive - so feel free to change your presentation according to the way the meeting is going - don't be bound by your abstract. Of course, we do want to know what you have been doing in your research, but we also want your broader views on the topic - and as you know, there are as many views on transition as there are participants. A workshop can be a useful forum for presenting early results and future plans and for getting advice on how to analyze or interpret them. A workshop can also be a forum for conjectures and - if you must - refutations.

We have commissioned a small number of keynote addresses, the first of which, from Roddam Narasimha, we shall hear shortly.

What I would finally like to stress, is the role of the session moderators. These are really the key people of the workshop. For that reason, I shall name them now - they are Jacques Lewalle, Ed Bogucz, Ted Okiishi, Mike Crawford, Eric Spina, Terry Jones and Steve Robinson. These people have the critical role of controlling the presentation sessions, teasing out the unanswered or unresolved questions which arise from the session. Then we want them to make judgments on the questions which, by discussion or other means, are acceptable to clearer elucidation, program or resolution during the workshop. To achieve this, we expect that they will need to assemble small teams to work on those problems and to report agreement, disagreement and progress back to the full meeting on Wednesday morning. If you walk around late at night and see a lot of little huddles going on, you will know that the workshop is working.

THE MANY WORLDS OF TRANSITION RESEARCH

R. Narasimha

Indian Institute of Science and Jawaharlal Nehru Centre
for Advanced Scientific Research
Bangalore 560 012

The transition from laminar to turbulent flow in a boundary layer is a complex phenomenon that may take different routes, each involving distinct stages governed by different, often not-yet unraveled dynamical principles. There are, surprisingly, questions concerning virtually every stage in the process, beginning with receptivity to external disturbances, the linear stability of spatially developing flows, different possible nonlinear end games, the formation and propagation of turbulent spots and the emergence of fully developed turbulent flow. There seems no doubt that the flow has to be seen as a forced, nonlinear spatio-temporal system, but the system is so complex that to extract simple insights is still very difficult.

There is evidence that there is no transition in the boundary layer if there is no forcing; and further that different kinds of forcing may select different routes to turbulence - an issue that we shall shortly return to. A proper specification of the disturbance environment is therefore essential, although what is 'proper' is not clear. In controlled wind tunnel experiments, the disturbance has often been created by wavemakers of some kind - 2D vibrating ribbons (following Schubauer & Skramstad), point sources (as Gaster has done, using small surface-mounted loudspeakers), oblique waves (Corke, with surface films) etc. In such experiments the disturbance is often harmonic in time, but does not have to be; some interesting results have been obtained by Gaster using white noise forcing. The transition scenario obtained in these cases is not in general the same: while what we may call the "canonical" route charted by Klebanoff and others in a low-disturbance environment involves 2D TS waves, peak-valley splitting in the spanwise direction, appearance of spikes and the formation and growth of turbulent spots. Morkovin has emphasized how in high-disturbance environments the canonical route may be by-passed, and the flow may proceed "directly" to the transition zone consisting of spots short-circuiting the slow build-up on a viscous time scale that is so characteristic of the canonical route. I believe it is still to be established whether the TS mechanism is necessarily irrelevant on a by-pass route; waves may not actually be "visible", but the response of the flow to the disturbance environment might still be describable through TS transfer functions. A genuine by-pass would occur when the disturbance level is so high that significant mean flow distortion may be expected to occur, as for example when roughness may induce local inflexion points in the velocity profile that lead to turbulence on a short inviscid time-scale. Meanwhile the existence of a "spot-less" route, involving a gradual filling up of the spectrum rather than a catastrophic collapse into a turbulent spot, has been demonstrated by the Novosibirsk group, and investigated by Corke at Illinois,

although the disturbance environment required to 'select' spot-less transition may have to be specially contrived.

We thus broadly distinguish between three classes of routes: the canonical (slow-build-up, rapid collapse into spots), the by-pass (short road to spots/turbulence), and what we may call the "scenic" (long spot-less road involving spikes in the velocity signal that may behave like solitary waves, followed by gradual spectral filling). Many variations on these routes are possible (there are bylanes everywhere), and some of these have been described elaborately by Morokvin.

The emergence of three-dimensionality from 2D TS waves can be described by a weakly nonlinear theory that accounts for parametric resonance when the basic flow is modulated by finite amplitude 2D TS waves, by the application of Floquet techniques, as Herbert has shown. But is the emergence of stochasticity from the waves characterizing instability, in the later non-linear stage, a form of dynamical chaos? Some physical models describe the gross features of the transition process in the framework of nonlinear dynamical-system theory (e.g. Bhat, Narasimha & Wiggins; interestingly, their equations have some commonality with a set proposed by Herbert, and some crucial differences as well: see Appendix). Gaster's experimental investigations sketch the way that a continuous spectrum may arise in boundary layers excited in different ways, in particular by combinations of harmonic and stochastic forcing. One promising method of identifying a low-dimensional dynamical system underlying observations of transition has been recently proposed by Healey. My own personal view is that it would be surprising if there were no connection between dynamical chaos and boundary layer transition. One way to find out would be an experiment in which some easily-recognized milestone on the route to turbulence, such as e.g. the first appearance of turbulent spots, is determined for different levels of stochastic forcing keeping the deterministic (say harmonic) forcing always of the same amplitude (see Figure 1). If say the Reynolds number at onset is independent of the stochastic forcing as it is diminished while the harmonic forcing is unchanged, we should be able to attribute the stochasticity at onset to nonlinear mechanisms alone, rather than to the stochasticity of the forcing itself. If the end-stage in transition were to be describable in terms of a low-dimensional nonlinear system there would be a considerable conceptual simplification in understanding the process, possibly with many benefits in applications. However, it must be admitted that as of today nonlinear system theory has made no significant contribution to our ability to predict any feature of the transition process.

Once spots are generated they grow and fill the boundary layer, taking it asymptotically to a fully turbulent state. The growth of intermittency in this transition zone, and the development of various boundary layer properties, has been studied extensively on flat plates. However, even here there have been various questions. The hypothesis of concentrated breakdown (Narasimha), postulating that turbulent spots are born in a relatively narrow band around a suitably defined onset location, has worked well in a variety of flows, although there is no direct observational evidence of the region over which breakdowns do occur in actual practice. It seems clear, especially if the disturbance environment is not violent, that no breakdowns can occur over the slow build-up phase in the canonical route; equally there would not be many breakdowns once the intermittency is substantially different from zero, and there can be none when the flow is fully turbulent. So a hypothesis that most breakdowns should occur over a relatively restricted region should be reasonable. It is in fact surprising how closely measurements obey the

resulting intermittency distribution, as Gostelow and Fraser have recently found. However we are in no position yet to explain why spots are born where they actually are.

There are also unresolved questions about spot propagation, especially possible interference from other spots in the neighbourhood, and about the possibility of each spot giving birth to offspring in pockets of the neighbourhood (e.g. the wing tips) that the spot excites (as in Wygananski's observations). Are the offspring autonomous spots, or do they eventually merge with the parent to make it grow bigger? There are also issues concerning the propagation of spots in pressure gradients (studied by Wygnanski, Narasimha and Gostelow), in skew and diverging flows (Jahanmiri et al.), etc. Very few studies have been made here, and surprises may be in store. In our study of spots in a distorted duct (no pressure gradient but streamlines diverging on plate), it was found that the spot does not necessarily propagate across streamlines always, and can have a highly unsymmetrical structure (fatter on the outside of the bend as the spot traces a curved trajectory).

In turbomachinery, where the free-stream disturbance levels are not only high but may involve travelling wakes from upstream rotor stages hitting stator blades, transition is a major feature of the boundary layer flow, as Reynolds numbers tend to be in the awkward range of $5x10^5$ to $2x10^6$. In addition the flow is rendered complex by the possible presence of separation bubbles, reverse transition etc. Wake-hitting induces a transition zone that is also intermittent, but this time due to the propagation and growth of "slabs" of turbulence stretching across the span of the blade (rather than arrow-headed Schubauer-Klebanoff spots). There has however been some evidence that there are S-K spots concealed in the turbulent slabs induced by the wakes. What precisely such slabs and concealed spots do to the flow remains to be investigated.

Finally, does the emerging turbulent boundary layer remember its origins? Does it differ depending on the route taken to turbulence? If the "standard" boundary layer defined by Coles is to have any meaning, there must be an asymptotic state independent of the route by which it is reached. It must then necessarily have a well-defined virtual origin that can be obtained by extrapolation backwards, helping to determine an onset location, irrespective of how dispersed breakdown is and indeed of which of the three classes of routes to turbulence is selected by the disturbance environment. This question has not been directly addressed either.

What is striking after so many years of transition research is that there is not a single investigation which traverses the whole route from fully laminar to fully turbulent flow: we each seem to live in our own world, and look at stability or breakdown or spot propagation or solitary waves or intermittency or turbulent boundary layer or whatever, to the exclusion of the other aspects of the transition process. The time has come to make a few grand experiments that go the whole way and traverse the different major routes. This is not going to be a simple task, but transition is not a simple problem. Such experiments may even require new facilities (long test sections, wide control over disturbance environment, etc.).

The existence of multiple paths to turbulence raises an obvious question: what selects the route? Clearly the disturbance environment (in which we include not only free-stream turbulence but noise, vibration, roughness etc.) must be the major determinant. That suggests that we ought to start delineating what nonlinear scientists call the "basin of attraction" for each of the "attractors" (strange or

otherwise) that dot the transition landscape (Figure 2). Morkovin estimates that, given the numerous factors that can induce transition, the space of disturbances may have something of the order of 10 to 20 dimensions. To map things in such a high-dimensional space seems hopeless, and (even if feasible) will certainly be an expensive and tedious task; but it would be interesting even to sketch sections or projections of the basins of attraction in subspaces of fewer dimensions: e.g. it should not be difficult (Figure 3) to determine the location of transition onset as a function of the characteristics of 2D and spanwise-periodic components of the disturbance made by a wave maker (which one can conceive of as consisting of appropriate strips of thin film on a flat plate, programmed to produce both spanwise uniform and periodic disturbances). I do not think we have a clue yet on what the boundaries of the different regimes will be: aligned or staggered lambda vortices, spots or spotless transitions, etc.

Clearly, there is still a great deal of interesting work to be done before one can say that the transition problem is understood. I hope this meeting can chart the course of future investigations.

APPENDIX

LOW-DIMENSIONAL NONLINEAR SYSTEMS

Herbert 1988:

$$\frac{d\hat{A}}{dt} = a_o\hat{A} + a_1\hat{A}^2 + a_2B^2$$

$$\frac{dB}{dt} = b_oB + b_1\hat{A}\,B$$

where $\hat{A} = A - A^*$

A^* — amplitude of basic periodic flow

$\hat{A}$ ~ amplitude of 2D secondary instability

B ~ amplitude of 3D subharmonic or fundamental instability

Narasimha & Bhat (1988), Bhat, Narasimha & Wiggins (1990)

$$\frac{dU}{dt} = a_oU + a_1U^3 + a_2u|u|$$
$$\qquad\qquad\quad (*) \qquad\quad (*)$$

$$\frac{du}{dt} = b_ou + b_1\,U\,|u|$$
$$\qquad\qquad\quad (*)$$

Note differences in starred terms.

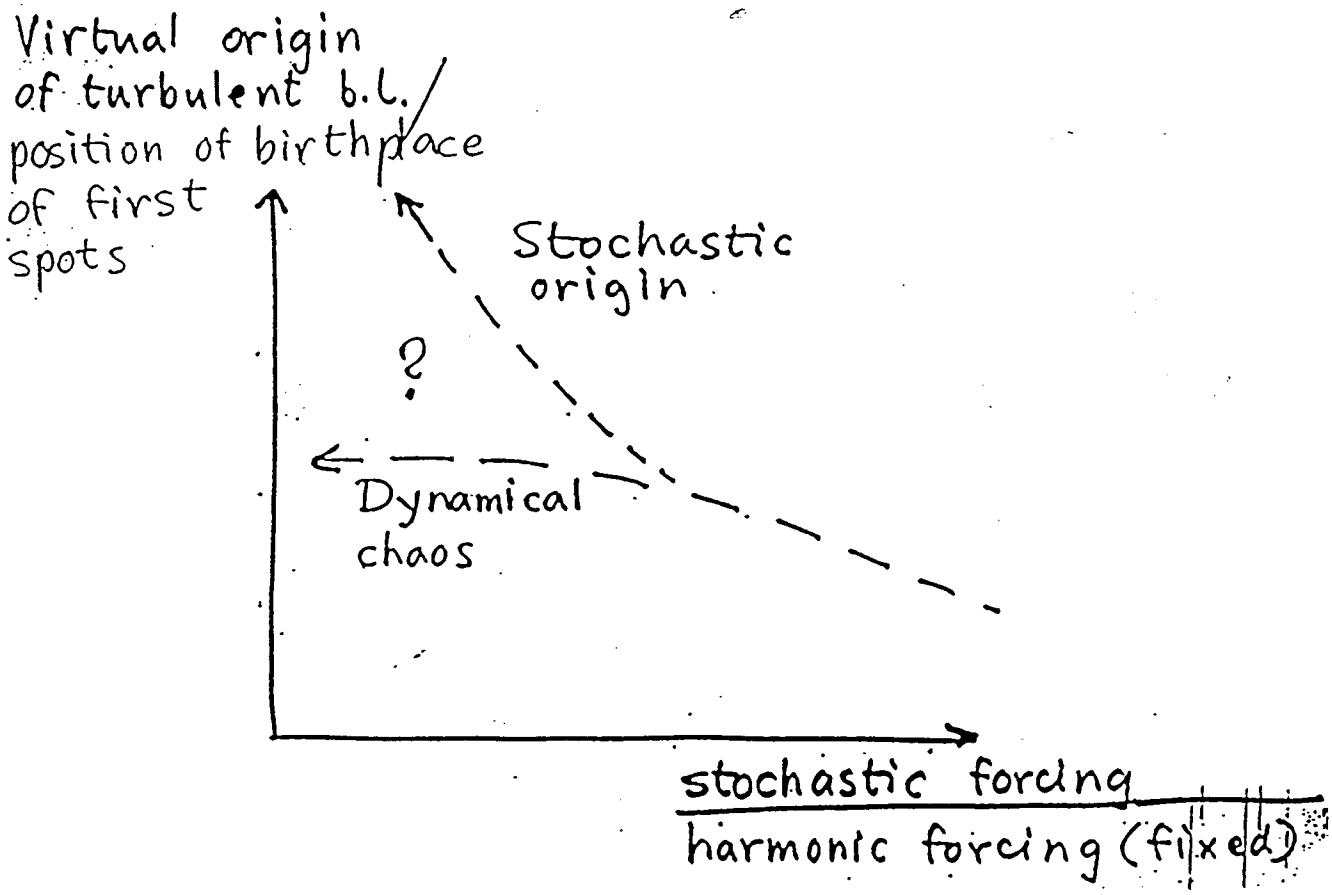
Virtual origin
of turbulent b.l./
position of birthplace
of first
spots
Stochastic
origin
?
Dynamical
chaos
stochastic forcing
harmonic forcing (fixed)

FIG 1

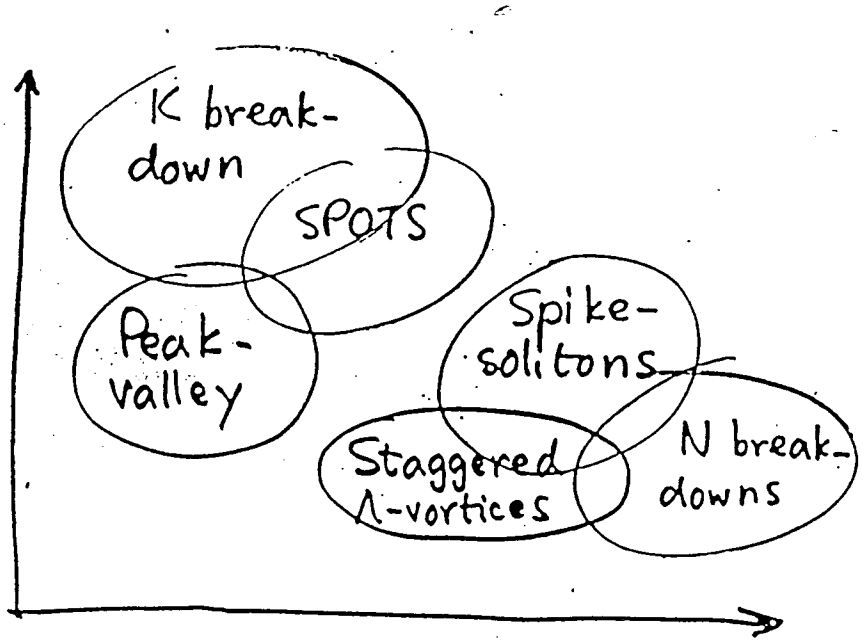

ATTRACTORS IN SOME SUITABLE DISTURBANCE SPACE
(Positions in diagram NOT significant

FIG. 2

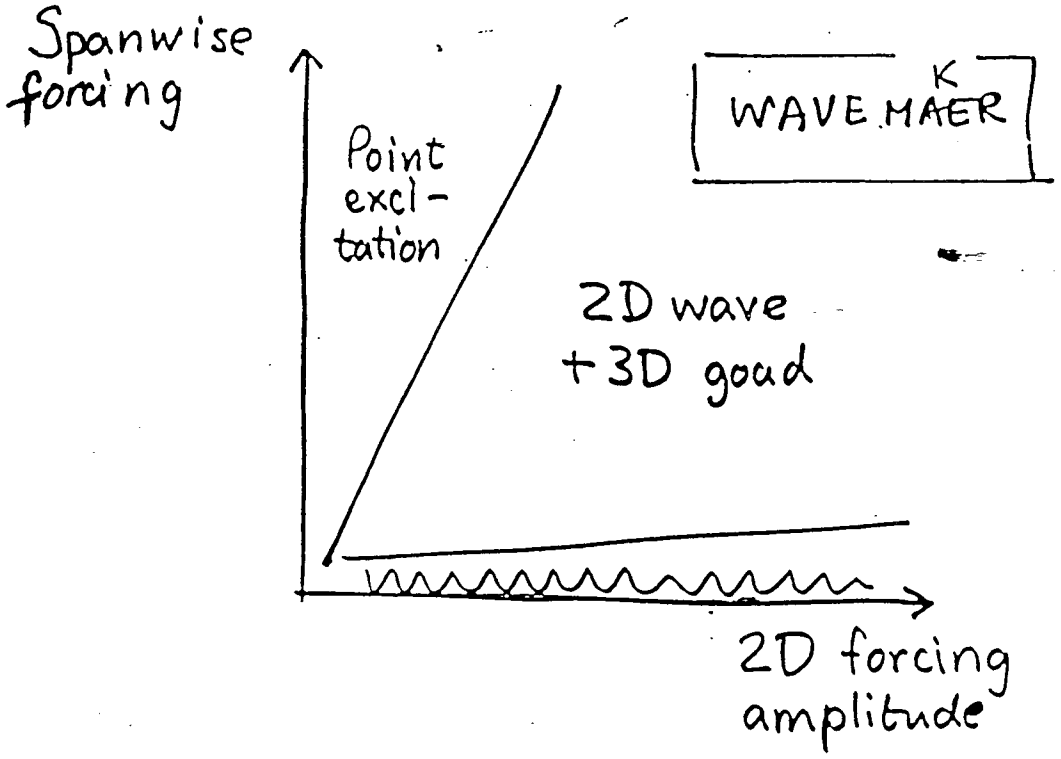
Spanwise forcing
Point excl-tation
WAVE MAKER
K
2D wave
+3D goad
2D forcing amplitude

FIG. 3

From Disturbances to Instabilities, to Breakdown to Turbulence: the Physics of Transition in Boundary Layers

Mark V. Morkovin
Professor Emeritus, Illinois Institute of Technology

In order to understand the end-stages of boundary layer transition in low as well as high disturbance environments (including bypass transition) it is desirable to establish a unified view of the sequences of physico-mathematical phenomena that lead from laminar flow to self-sustained "bursting" in wall turbulence. The dominant driving disturbances: oncoming free turbulence, unsteady pressure fields (including sound), inhomogeneous density fields, inhomogeneities in wall geometry (including distributed roughness) etc., all force disturbed motions within the boundary layer via multiple competitive receptivity mechanisms. For small disturbances, a sequence of (often linearizable) instabilities then leads to sporadic local bursting very near the wall which can sustain turbulence. The local seeds of turbulence then somehow propagate (as in case of idealized Emmons' spots) to engulf quite rapidly the surrounding disturbed but still laminar regions. The instability sequences differ with basic parameters and with the nature of internalized ("received") boundary-layer disturbances, thus providing highly non-unique roads to turbulence. There may be fewer modes of the final onset of bursting, the criteria for which are not yet clear.

For larger disturbances (even more non-unique) the instabilities will generally bypass the linearizable primary amplified modes (T.S. waves, steady and unsteady cross flow modes, Goertler modes) and amplify nonlinearly and "inviscidly", roughly starting with the secondary instability phenomena. Special attention is called to "algebraically" growing instabilities, which theoretically can grow from rather small disturbances, but must be "environmentally realizable". The final "bursting" breakdown process is likely to be similar to that for the non-bypass cases. In both small and large disturbance cases, the number of governing parameters is large, ten to twenty or more.

In prediction of transition and in modeling of its end stages, idealization and simplification is unavoidable. The purpose of this lecture is to establish a common vocabulary for the various processes and their dominant mechanisms. Then we should be able to compare various theoretic-empirical methods, both in terms of the success in correlating (limited) data and in terms of the essential physics retained in the idealizations (as a guide to its generality).

END STAGES of TRANSITION

Could be for either LOW-DISTURBANCE ROAD involving HIGHER INSTABILITIES

or BYPASSES with STRONG - (S) WEAK - (W) DISTURBANCES

DEFINITELY NON-LINEAR (non-superposable, NON-UNIQUE)

∴ information primarily from EXPERIMENTS Direct Numer. Soln → • PARTICULAR SOLUTIONS

↓

GOVERNED by In. Cond + Bound C.

INCREDIBLY RICH PATTERNS OF BEHAVIOR

CONCEPTUAL GENERALIZATIONS?

via CLASSIFICATIONS

of distinguishable MECHANISMS

of functional CLASSES of DISTURBANCES I.C. and B.C.

PRIMARY PARAMETERS

(NON-LINEARITY → • CHANGES IN THE BASE FLOW
• THRESHOLDS)

AMPLITUDE - DEPENDENT CHANGES OF FIELDS on the ROADS to TURBULENCE

FOR APPLICATIONS SIMPLIFICATIONS AND IDEALIZATIONS ARE UNAVOIDABLE

CONSISTENCY OF "PHYSICS" "GUARDIAN of Reliability and Concept generality

illustration: role of EMMONS' SPOTS in highly disturbed environments

illustration:

FINAL BREAKDOWN Initiation of self-sustained BURSTING → is LOCAL, SPORADIC, probably caused by EXTREMA of DISTURBANCES

CAN IT BE CORRELADED BY A SINGLE AVERAGE MEASURE : % Tu ?

(S1)

SYSTEMS APPROACH TO

TRANSITION

from

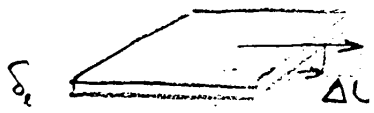

Thin, finite δ_{lam} SLABS or SHEATHS

with LAMINAR VORTICITY $\vec{\Omega}(Y)$ DISTRIBUTION

at lower $Re \sim \frac{\Delta U_\infty \delta_t}{\nu}$ QUASI-2D, QUASI STEADY

streamwise L_x
spanwise L_y $\gg \delta_{lam}$

BL's (MIXING L's, JETS, WAKES, etc

SUBJECTED TO ENVIRONMENTAL

weak $|\Delta\vec{v}| \ll \Delta U_\infty$ Free-stream AND Boundary disturbances with characteristi

NONHOMOGENEITIES in x, z, t

longer scales and times (except for ROUGHNESS)

INEVITABLY AS Re ↑ to

SCALE DISCREPANCIES

finite δ_{tu} SLABS or COLUMNS

with TURBULENT VORTICITY $\vec{\Omega}(x, Y, z, t)$ DISTRIBUTIONS

with space-time DISORDER (chaos)

(A) with "large coherent eddies" $L_z \sim \delta_{tu}$, $L_x \sim 3\delta_{tu}$

(B) with fine "wall-scaled", $l^+ \sim 100 \ll \delta_{tu}$, NONLINEAR INSTABILITY with a threshold, referred to as BURSTING for SHORT (Killed in relaminarization!)

See S.K. ROBINSON 1991 Ann. Rev. Fluid Mech.

STRONG Ex with Z asymmetry

• $Re_{t\,min}$

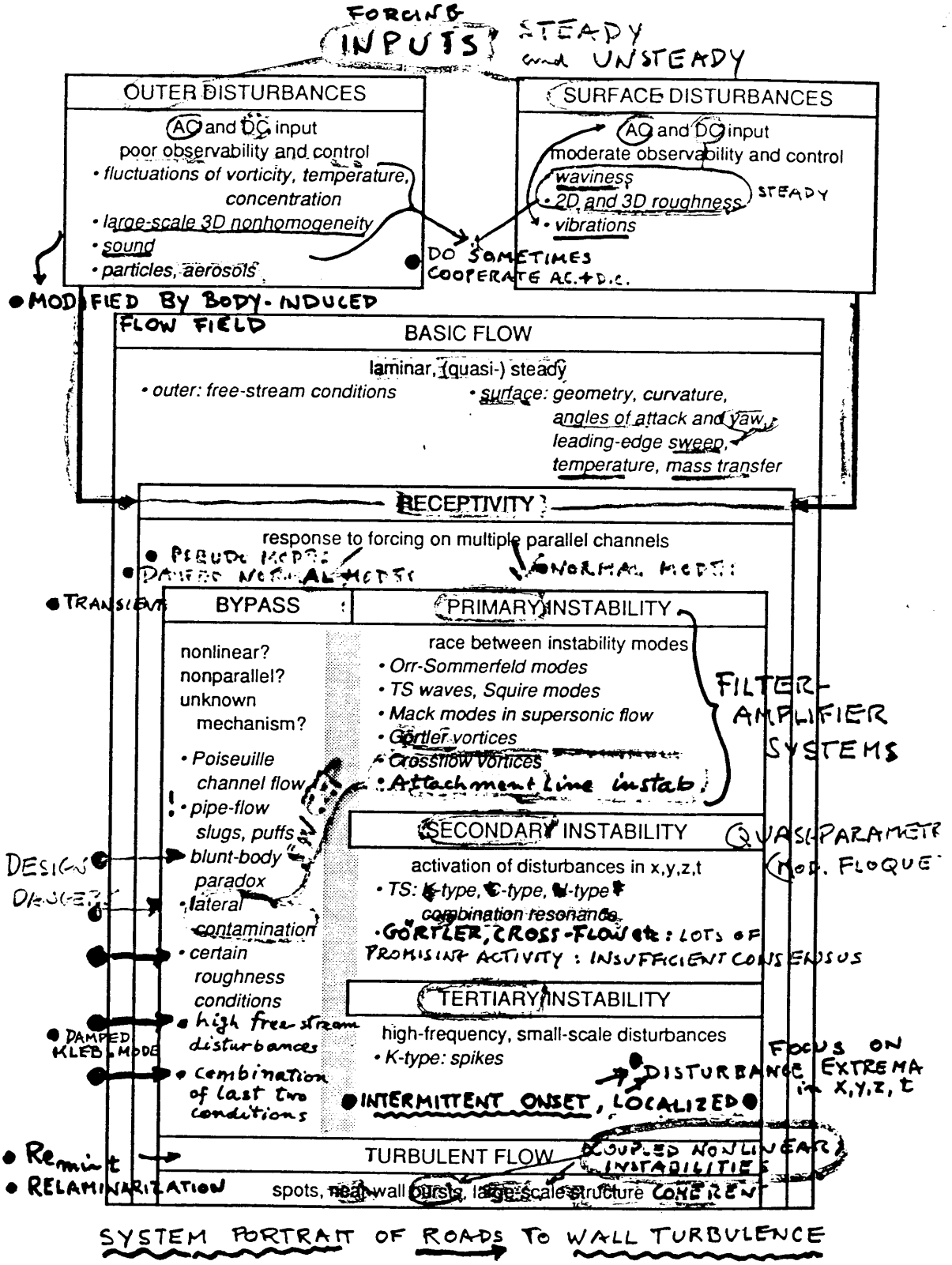
FORCING INPUTS
STEADY and UNSTEADY
OUTER DISTURBANCES
AC and DC input
poor observability and control
• fluctuations of vorticity, temperature, concentration
• large-scale 3D nonhomogeneity
• sound
• particles, aerosols
SURFACE DISTURBANCES
AC and DC input
moderate observability and control
• waviness
• 2D and 3D roughness
• vibrations
STEADY
DO SOMETIMES COOPERATE AC.+D.C.
MODIFIED BY BODY-INDUCED FLOW FIELD
BASIC FLOW
laminar, (quasi-) steady
• outer: free-stream conditions
• surface: geometry, curvature, angles of attack and yaw, leading-edge sweep, temperature, mass transfer
RECEPTIVITY
response to forcing on multiple parallel channels
PERTURB MODES
DAMPED NORMAL MODES
NORMAL MODES
TRANSIENT
BYPASS
nonlinear?
nonparallel?
unknown mechanism?
• Poiseuille channel flow
• pipe-flow slugs, puffs
• blunt-body paradox
• lateral contamination
• certain roughness conditions
• high free-stream disturbances
• combination of last two conditions
PRIMARY INSTABILITY
race between instability modes
• Orr-Sommerfeld modes
• TS waves, Squire modes
• Mack modes in supersonic flow
• Görtler vortices
• Crossflow vortices
• Attachment-line instab.
FILTER-AMPLIFIER SYSTEMS
SECONDARY INSTABILITY
activation of disturbances in x,y,z,t
• TS: K-type, C-type, H-type combination resonance
• GÖRTLER, CROSS-FLOW etc: LOTS OF PROMISING ACTIVITY : INSUFFICIENT CONSENSUS
QUASI-PARAMETR (Mod. FLOQUET)
TERTIARY INSTABILITY
high-frequency, small-scale disturbances
• K-type: spikes
INTERMITTENT ONSET, LOCALIZED
DISTURBANCE
Focus on EXTREMA in x,y,z,t
DESIGN
DAMPED KLEB. MODE
Remint
RELAMINARIZATION
TURBULENT FLOW
spots, near-wall bursts, large-scale structure
COUPLED NONLINEAR INSTABILITIES
COHERENT
SYSTEM PORTRAIT OF ROADS TO WALL TURBULENCE

J. KENDALL '92

FREESTREAM FLUCTUATION RECORDS

Ø.65 SEC DURATION EACH
u'/U_o = Ø.22 %

STATIONARY INPUT

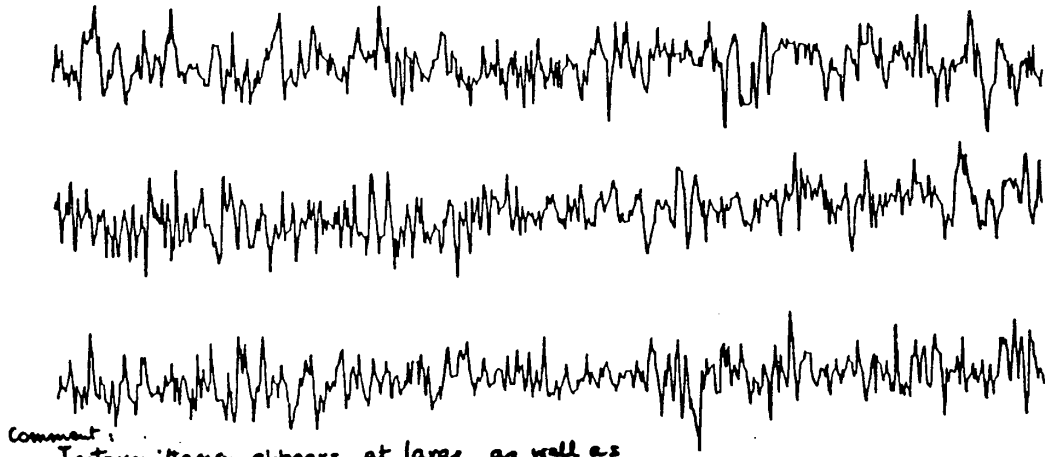

Comment:
Intermittency appears at large as well as fine scales of Tu – e.g. in dissipation. Fractal nature.

YET DISCRETE OUTPUT

P'_w AT SEQUENTIAL STATIONS

u'/U_o = Ø.18%

LINEAR WAVE PACKETS

EXTRA STRONG

higher instability

NON LINEAR!

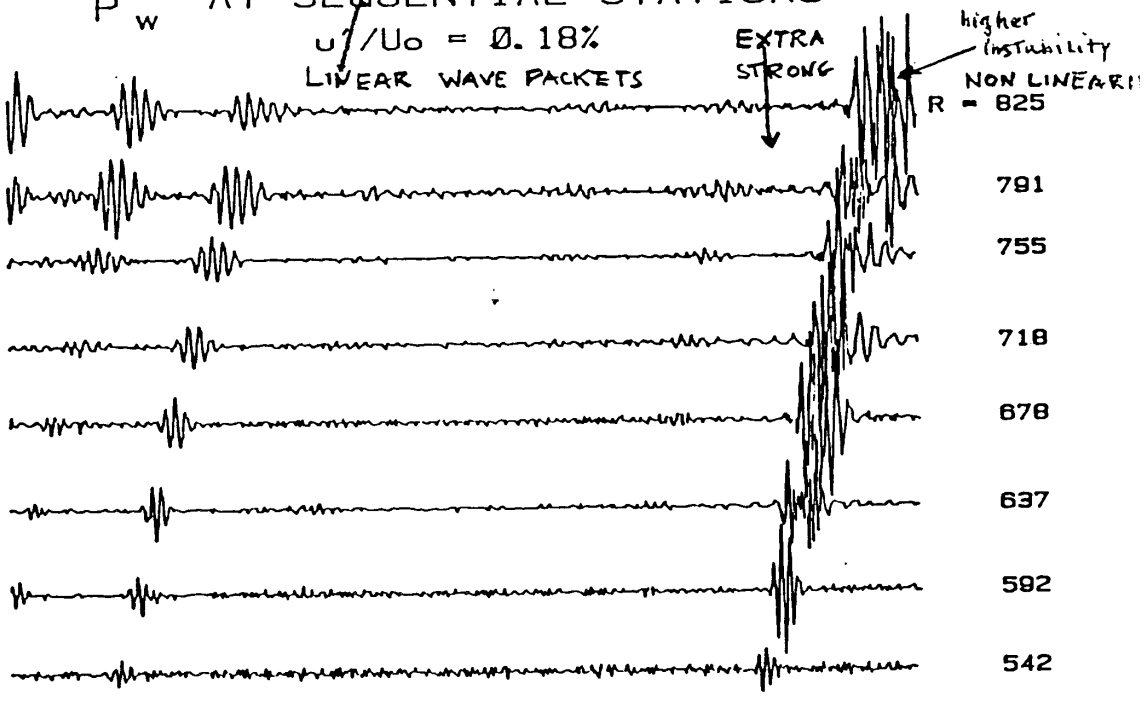

NASA/CP—2007-214667

FUNCTIONALITY OF DISTURBANCE CLASSES

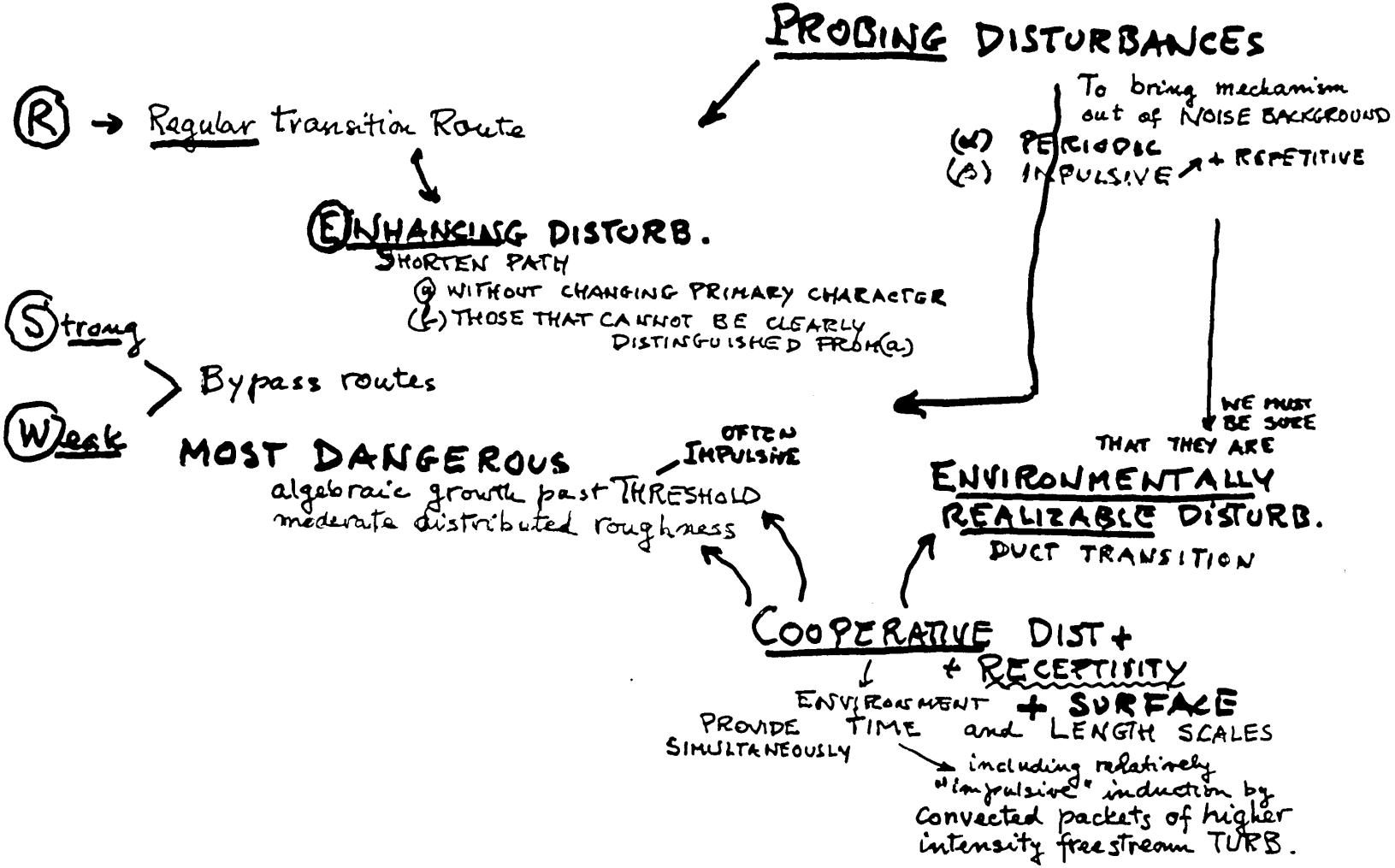

ROUGHNESS CAN FUNCTION IN ALL THESE CATEGORIES
BUT BEWARE OF —

'A New Direction in Hydrodynamic Stability : Beyond Eigenvalues" ON PSEUDOSPECTR
S. Reddy and T. Driscoll, submitted to SCIENCE 12/93 ; Cornell U. Adv. Comp Res Inst. CTC92TR115 L. and A. Trefethen

TRANSIENT DISTURBANCES

Can lead to substantial "algebraic" growth even when disturbances are

(W) (Weak) – a property of nonsymmetric PDE operators (for which eigenfunctions are not independent = non normal e.g. Schmid, Henningson, Khorrami & Malik : "A study of eigenvalue sensitivity for hydrodynamic stability operators", Theor. & Comp. Fluid Dyn (in Press 1993). In a system with damped eigenmodes, the growth may be sufficient (before ultimate decay) to modify the system nonlinearly and lead to a bypass (as observed experimentally for most duct and plane Couette flows) For (S) (stronger) disturbances this road to turbulence may be competitive with "REGULAR" paths, based on amplified eigenfunctions and higher-order instabilities.

Obviously, the (W) category represents the larger danger in design. ON THE OTHER HAND, these disturbances are [ARTIFICIAL] and question remains whether and how they can be (actually) (induced) by a given DISTURBANCE ENVIRONMENT

ONLY THE CLASS OF [ENVIRONMENTALLY REALIZABLE] DISTURBANCES is practically relevant. HOWEVER, conceptually it is important to understand the mechanisms – they can even be used as TRIPPERS.

Groups at MIT : Landahl, Breuer, Hennigson, Reddy, Schmid (Gustafson of Swedish KTH) and Lehigh Univ: Charles Smith, Haji-Haidari, J.D.A Walker, B. Taylor etc. have done both experimental and theoretical work using pseudospectra Butler, K. and Farrell, B (1992): "3-dimensional optimal perturbations in viscous flows" Phys. Fl. A, 4(8) used variational theory to find alg. growing flows undoubtedly related to "Klebanoff damped modes" $< Re_{cr}$.

L. TREFETHEN's PSEUDO MODES for NON-NORMAL OPERATORS (Book forthcoming) applied to linearized Navier-Stokes eqs forced by $e^{-i\omega t} v(x,y,z)$ imposed at every point in the shear layer. The response is gauged in terms the resolvent matrix of the system. Its norm $\to \infty$ for v. eigen solutions at ω_{ev} and can be large for complex ω near ω_{ev}. When ω_{ev} is slightly damped (Im(ω) just below zero) mode-responses with ω near ω_{ev} can be substantially amplified i.e. PSEUDO-RESONANT. ⊙ The forcing functions $v(x,y,z)e^{-i\omega t}$ would have to be induced by the environment. Which of these are environmentally realizable?

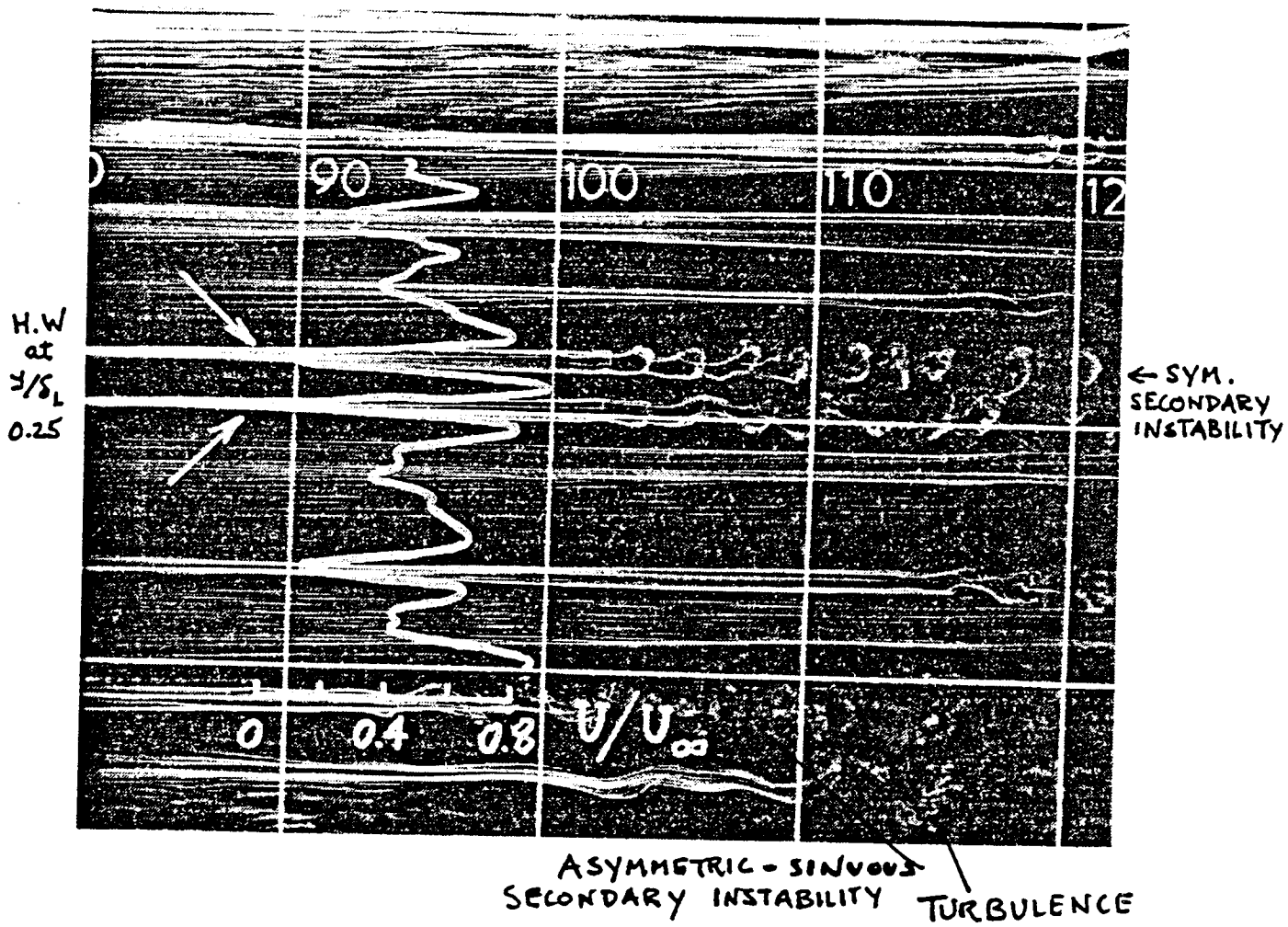

Figure 4.3: Spanwise variation of the mean streamwise velocity at y/δ_L = 0.25 superimposed on the flow visualization of figure 4.2a.

(3.21e)

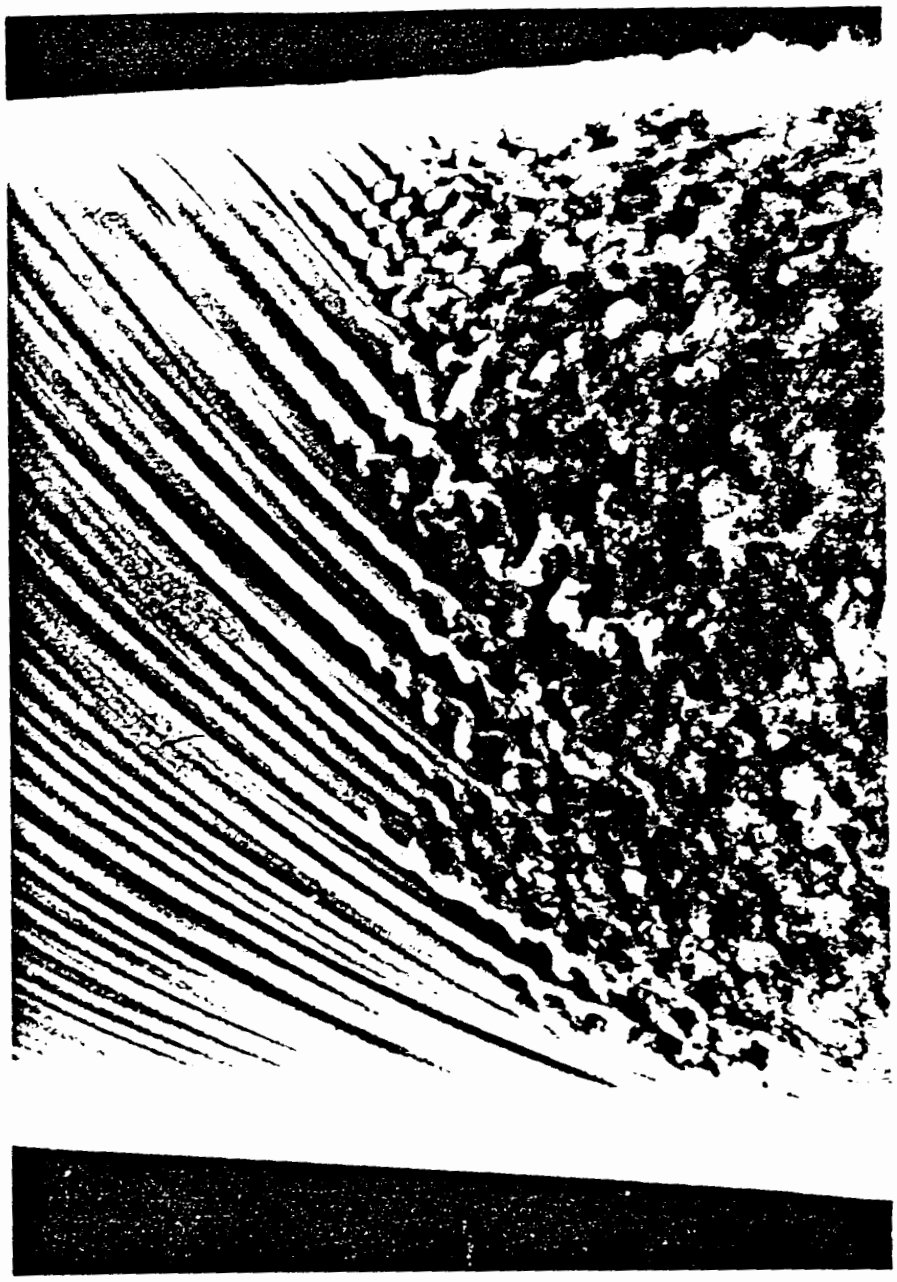

J. KEGELMAN

Figure 65: Enlargement of Striations Illustrating Striation Breakdown ($V_s/U_\infty = 0.825$, $Re_L = 0.814 \times 10^6$)

WHAT IS FREE-STREAM TU that gives "NATURAL" TRANSITION?

Grid Tu
Screen Tu
Tu in any WTunnel
Tu in Turbomachinery
Tu in atmospheric flight

Even when nearly homogeneous and nearly isotropic
(it) has unknown coherent structures and intermittencies ~ fractals.
masked by the one-dimensional time signals and spectra of hot wires

BÖTTCHER

- Born in separated shear layers; fed by $\overline{v_{tang} \cdot v_{nom}} \frac{\partial V_{tang}}{\partial n}$
- wakes from upstream decays in absence of mean flow grad $\vec{V}$
- and rejuvenates when comes on

→ near stag regions in contractions over wings and blades

- carry streamwise vorticity $\vec{\Omega}$ (Klebanoff, Kottke)
  - ↘ direct feeding of Görtler instab. and Crossflow Zero f instab.

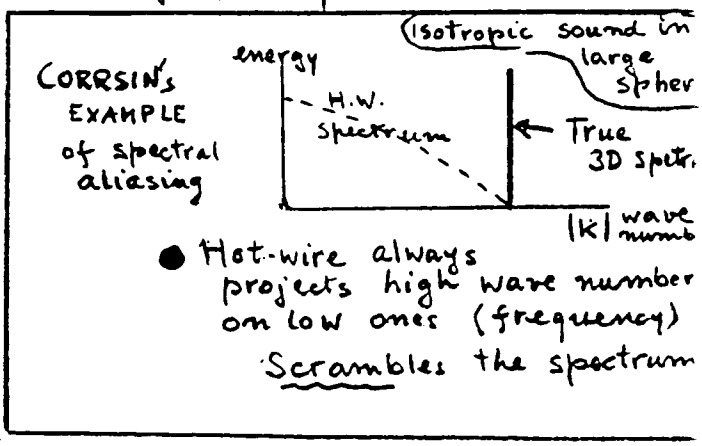

- Hot-wire always projects high wave number on low ones (frequency)
  Scrambles the spectrum

To understand:
Concentrate on the sporadic energetic extremal events
(possibly enhanced by "probing" periodic disturbances)

Then Two-point space-time correlations in free stream one in f-s, one in BL

Kendall ( ) showed that disturbances associated with the slightly damped were moving towards the wall.

KLEBANOFF MODE RESPONSE
↓ dominated by Low frequency Streamwise Vortices which generate large u' fluctuations (with theoretical low v' and w')
agreement with Butler and Farrel 1992 theory

Such disturbed motion then influences Subsequent instabilities especially secondary instabilities

Initiation of Turbulent Spots in a Laminar Boundary Layer by Rigid Falling Particulates

R.F. Blackwelder, F.K., Browand, C. Fisher and P. Tanaguichi
University of Southern California
Los Angeles, CA 90089-1191

A transitional laminar boundary layer is developed on a 1m wide 5m long flat plate in a 0.6m deep water channel with a freestream velocity of 15-50cm/s. A particulate dispenser under computer control ejects individual particles having diameters of $\frac{1}{6}\delta$ into the free stream. The particulates are introduced with an initial velocity of U_∞ in the direction of the free stream. They have differing specific gravities of 1.03-2.7 which introduces an additional non-dimensional parameter relating the time taken to traverse the boundary layer to the convective time scale. The particulates produce a wake in the upper region of the boundary layer as they sink towards the wall. Visualization data taken over the range $5 \cdot 10^4 < Re_x < 5 \cdot 10^5$ indicate that turbulent spots are produced by the disturbances due to the wake rather than by the particulates themselves. This suggests that the spot formation process in this case may be inviscid in nature and may not be strongly influenced by the presence of the wall.

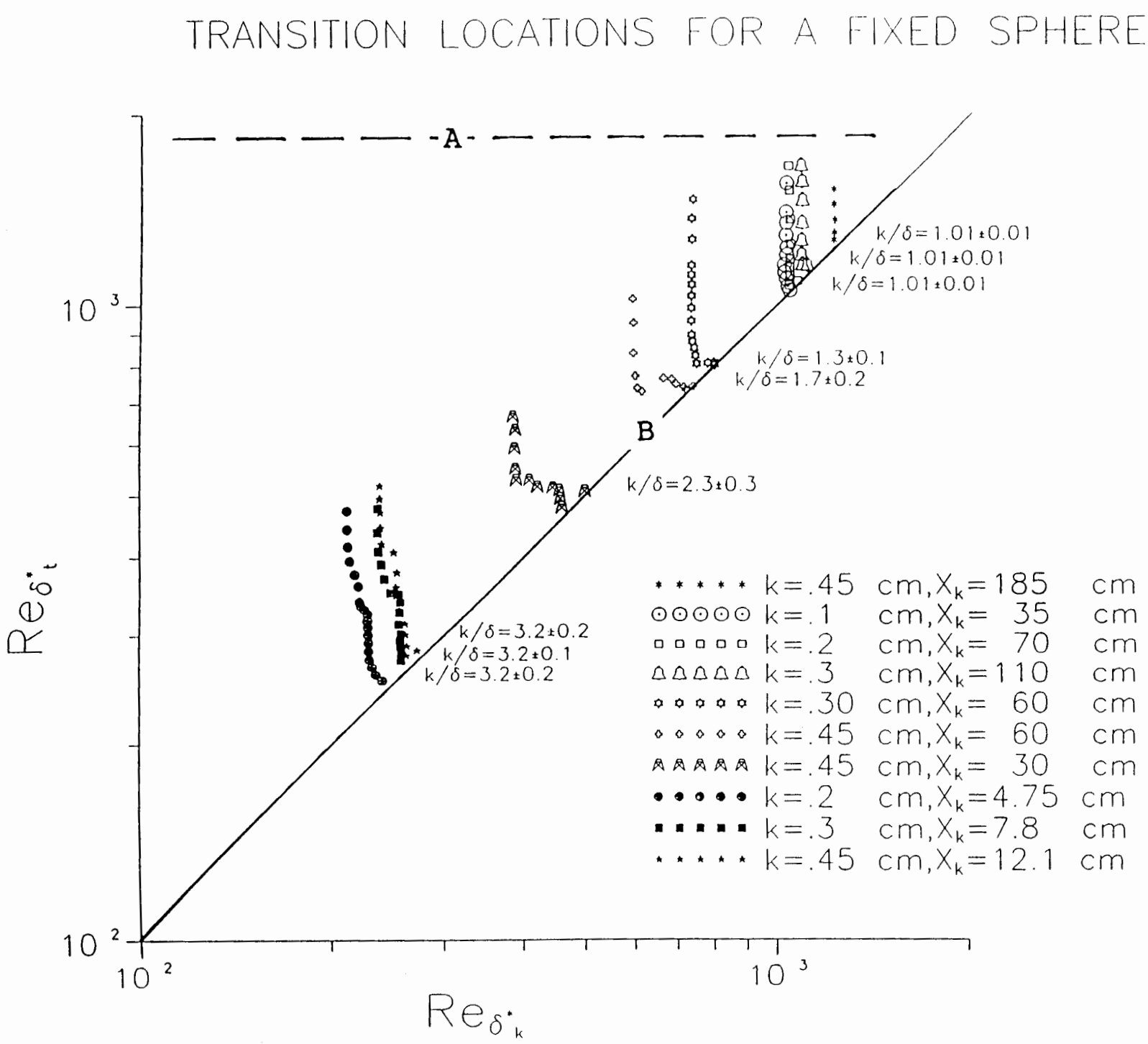
TRANSITION LOCATIONS FOR A FIXED SPHERE
-A-
B
k/δ=1.01±0.01
k/δ=1.01±0.01
k/δ=1.01±0.01
k/δ=1.3±0.1
k/δ=1.7±0.2
k/δ=2.3±0.3
k/δ=3.2±0.2
k/δ=3.2±0.1
k/δ=3.2±0.2
k=.45 cm, X_k=185 cm
k=.1 cm, X_k= 35 cm
k=.2 cm, X_k= 70 cm
k=.3 cm, X_k=110 cm
k=.30 cm, X_k= 60 cm
k=.45 cm, X_k= 60 cm
k=.45 cm, X_k= 30 cm
k=.2 cm, X_k=4.75 cm
k=.3 cm, X_k=7.8 cm
k=.45 cm, X_k=12.1 cm
10^3
10^2
10^2
10^3
Re_δ*_t
Re_δ*_k

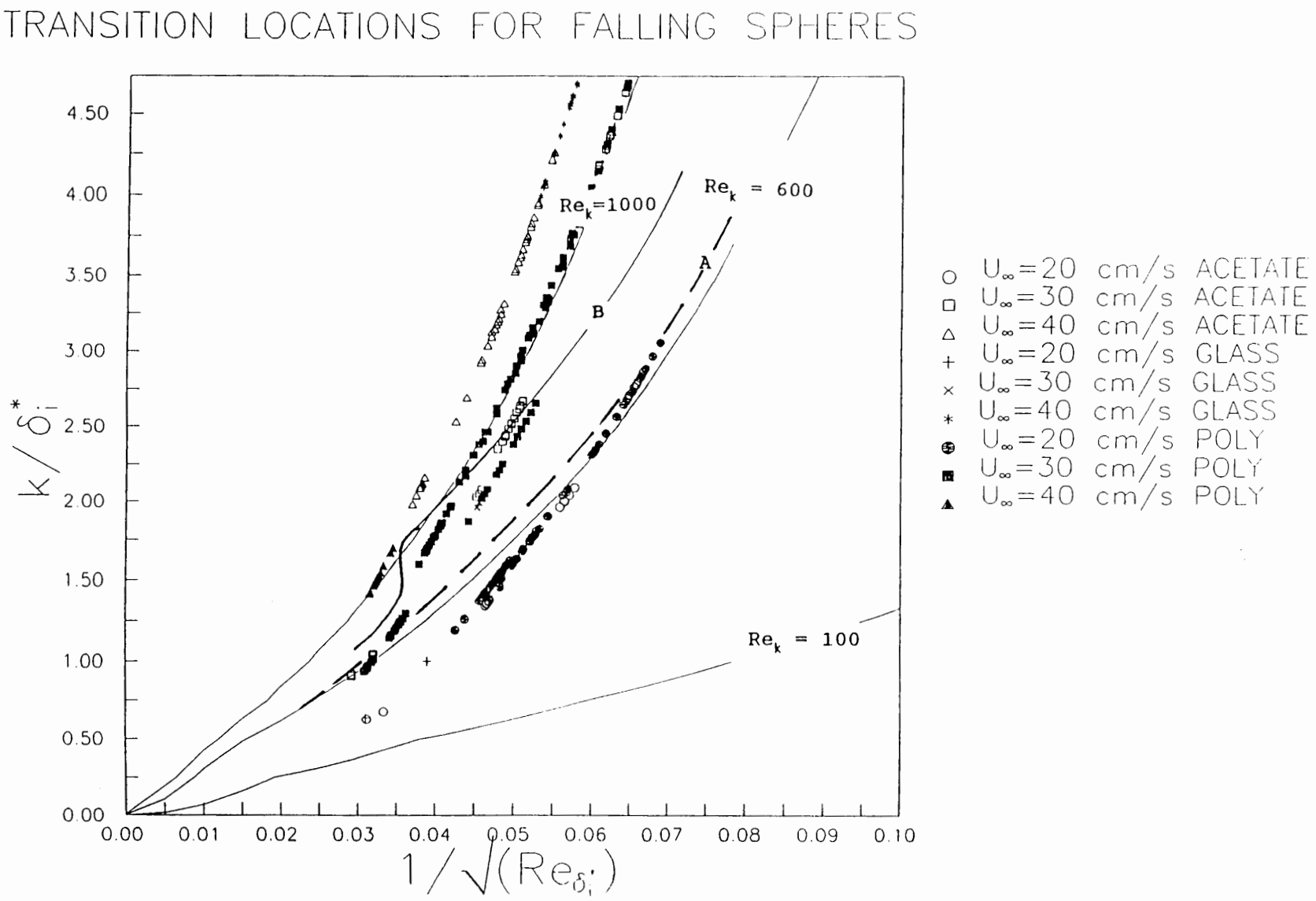
TRANSITION LOCATIONS FOR FALLING SPHERES
k/δ_i^*
$1/\sqrt{(Re_{\delta_i^*})}$
Re_k=1000
Re_k = 600
Re_k = 100
A
B
U_∞=20 cm/s ACETATE
U_∞=30 cm/s ACETATE
U_∞=40 cm/s ACETATE
U_∞=20 cm/s GLASS
U_∞=30 cm/s GLASS
U_∞=40 cm/s GLASS
U_∞=20 cm/s POLY
U_∞=30 cm/s POLY
U_∞=40 cm/s POLY

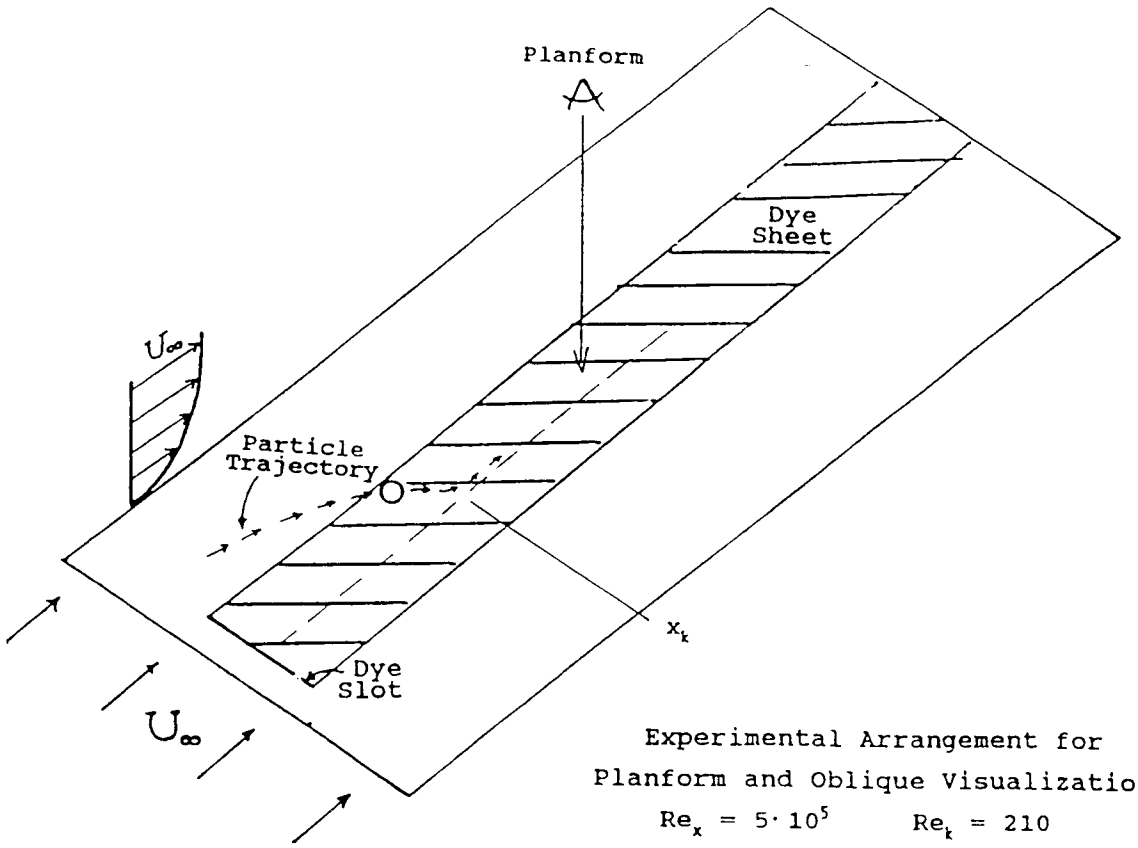

Experimental Arrangement for
Planform and Oblique Visualization
$Re_x = 5 \cdot 10^5$ $Re_k = 210$

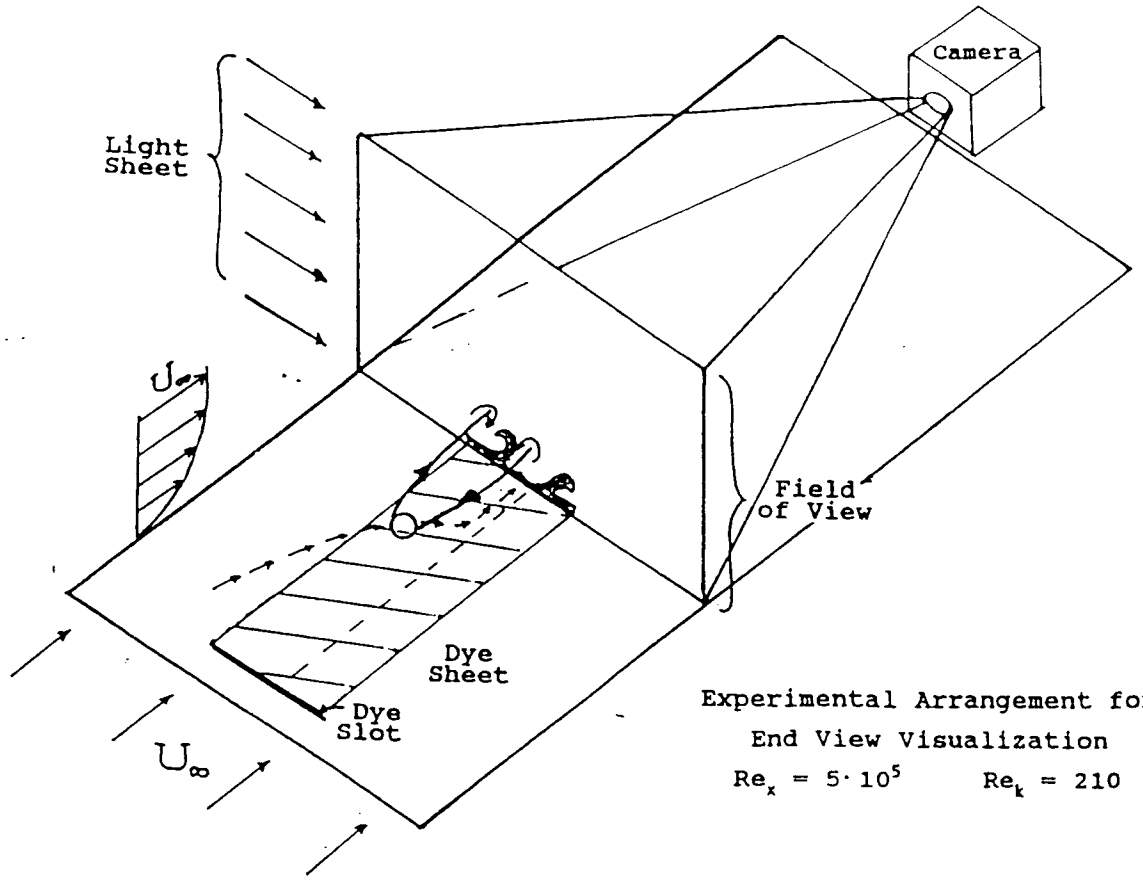

Experimental Arrangement for
End View Visualization
$Re_x = 5 \cdot 10^5$ $Re_k = 210$

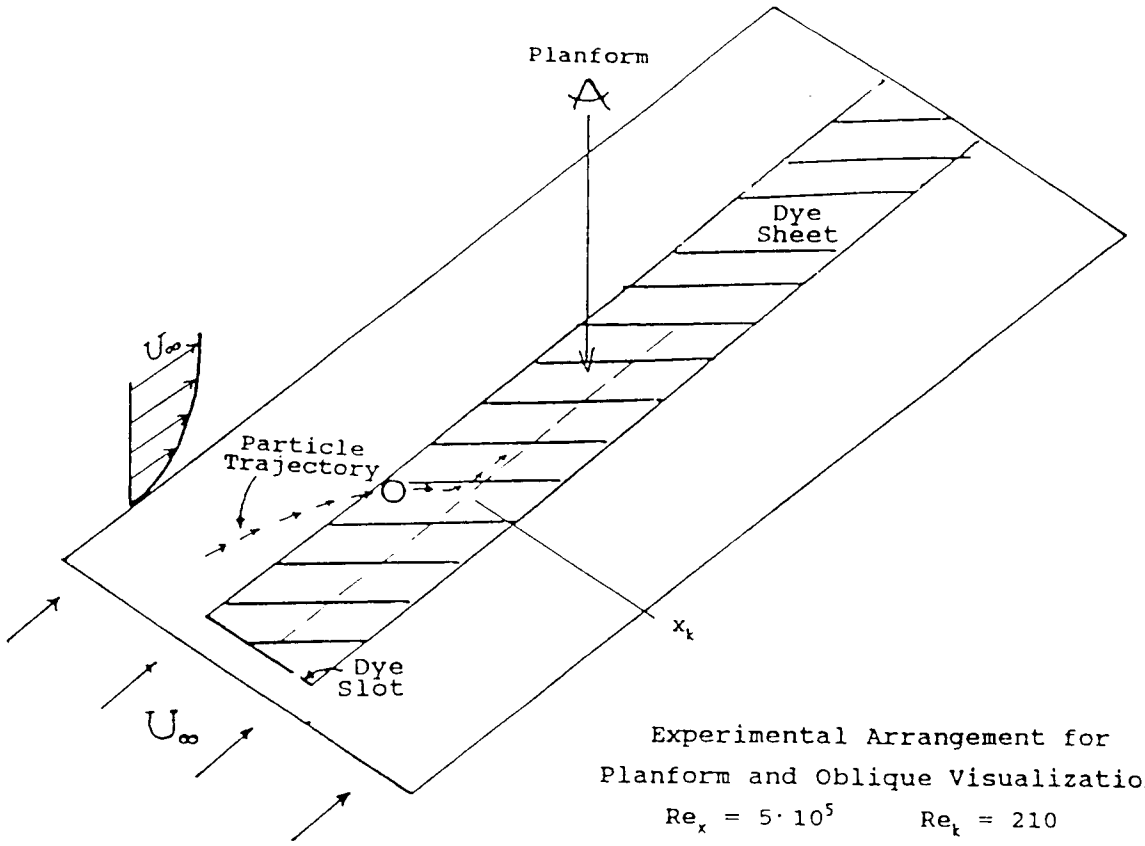

Experimental Arrangement for
Planform and Oblique Visualization
$Re_x = 5 \cdot 10^5$ $Re_k = 210$

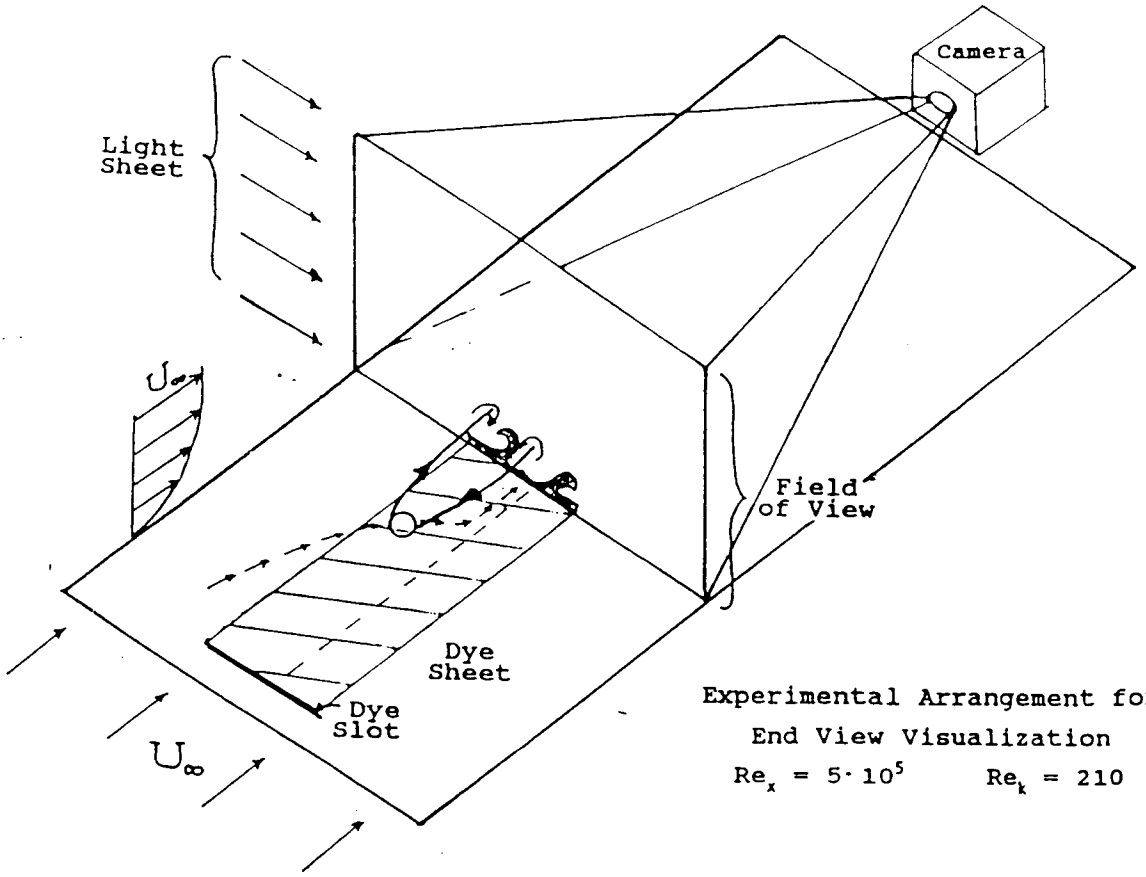

Experimental Arrangement for
End View Visualization
$Re_x = 5 \cdot 10^5$ $Re_k = 210$

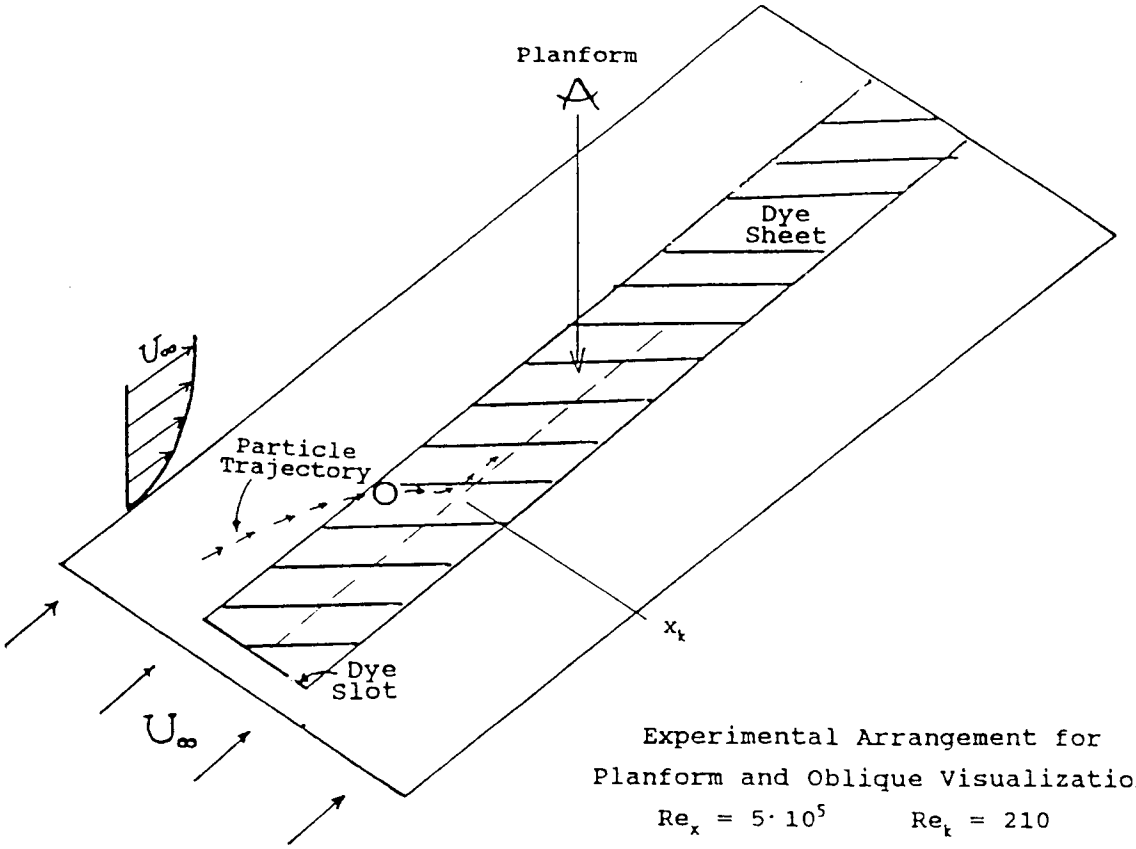

Experimental Arrangement for
Planform and Oblique Visualization
$Re_x = 5 \cdot 10^5$ $Re_k = 210$

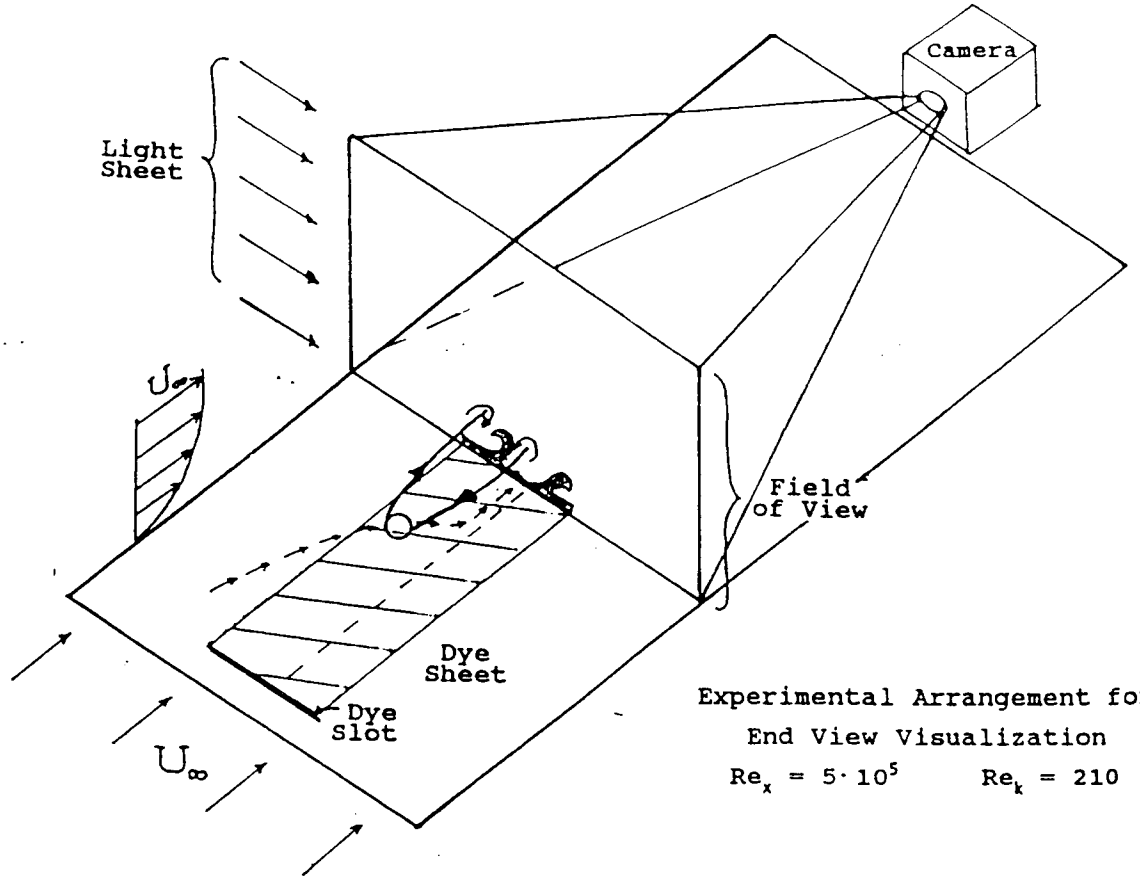

Experimental Arrangement for
End View Visualization
$Re_x = 5 \cdot 10^5$ $Re_k = 210$

CONCLUSIONS

- Transition with a fixed particle with $k \leq \delta^*$ is characterized by Re_k alone.

- Moving particulates produce additional unsteady vortical disturbances which are not correlated by Re_k.

- Transition may be induced by the particle's wake and not by the particulate directly.

- The parameter

$$\frac{\tau_H}{t_\delta} = \frac{(\gamma-1)(\gamma+\frac{1}{2})\cdot g\cdot d^4}{18^2\cdot\nu^2\cdot\delta} = (\gamma+\tfrac{1}{2})\,\frac{d}{\delta}\,Re_d$$

  appears to govern the disturbance strength and transition.

Boundary Layer Receptivity to Weak Freestream Turbulence

Notes on Figures Presented at End-Stage Transition Workshop

J. M. Kendall, Jet Propulsion Laboratory

Prepared August 15, 1993; revised September 15, 1993

Work sponsored by NASA

Fig. 1 shows the experimental configuration. The tunnel is about 8 ft long by 2 ft square. In most cases the wind speed is set to 11.6 m/s. Three different plates are used. Each is a quarter-inch thick, extends wall-to-wall, and has a semi-elliptical leading edge. The two extremes in bluntness are shown, being half a 14:1 ellipse and half a 5:1 ellipse. The plate surface pressure is uniform to better than 0.01q, except near the leading edge, or whenever a condition of lift is intentionally applied to the plate. Turbulence is created in the setting chamber by means of eight 1/16-inch hypodermic tubes stretched normal to the flow and pressurized at any controlled value up to 6 psi.. Each has twenty-one 0.006-inch holes spaced at 1-inch intervals along its mid-section of length, and directed upwind. The tubes are spaced vertically at 1.25-inch intervals. The turbulence so created is carried to the test section, where it is found to be spatially uniform over a suitably large cross-sectional area and axial length. *Fig. 2* presents spectra of the stream turbulence in the empty tunnel for jet-array pressures of 1 psi to 6 psi. The T-S range extends between 80 and 150 Hz, approximately, for the present conditions. The primary method of fluctuation measurement is by use of microphones installed on the reverse side of the plate. A description of the method and its advantages has been given in AIAA 90-1504. Mean and fluctuating flow measurements are also made by means of various hot-wire probes and rakes carried on a computer-controlled x-y-z traverse mechanism. *Fig. 3* shows the layout of a four-foot plate carrying 64 microphones, the outputs of which are digitized simultaneously. The location of a single driver used for creating controlled T-S packets is also indicated.

The boundary layer responds to the turbulence in three (seemingly) distinct ways. First, in examining the broadband u'-fluctuation profile across the layer at some station (given in terms of R, the square-root of the x-Reynolds number) where T-S waves have not yet grown to prominence, one finds that the most obvious motion is what is referred to as Klebanoff's mode (not to be confused with his peak-valley breakdown mechanism) because he first described it in 1970 or 1971. *Fig. 4* shows this motion, together with that variation which would result from a thickening/thinning motion of the layer, a similitude pointed out by him. The vertical placement of the curve is arbitrary. Some general characteristics of this mode are:

(1) Long, narrow, high amplitude.
(2) $u'/Uo \propto x^{0.5}$, approx.; downstream, the peak typically exceeds five percent rms.
(3) The distribution in η is as for thickening /thinning of the layer.
(4) The lateral scale is established by the turbulence scale and is $\cong 2\delta$.

The statement as to the narrowness of the disturbances follows from lateral correlation measurements made within the layer and in the stream and shown in *Fig. 5*.

When one band-limits the signal and examines only those frequency components expected from stability theory to be most-amplified near a particular station, then one finds a second kind of motion, one which is far weaker than the first, as in *Fig. 6*. A single peak occurs near the outer edge of the layer for the more-forward stations. Note, however, that at the two more-downwind stations the T-S eigenmode has begun to appear near the wall. Therefore, this motion does not resemble the T-S eigenmode, even though the temporal frequencies are similar. Some characteristics of this mode are:

(1) Possesses the frequency of the T-S mode.
(2) Propagation speed = *Uo;* hence λ differs from T-S.

Results on the packet rms amplitude under a variation in the stream turbulence level are given in *Fig. 12*. The results pertain to a specific frequency within the unstable portion of the TS band. The ordinate is the wall pressure fluctuation component due to TS waves at a particular frequency, shown with arbitrary scale. The abscissa is the component of the freestream turbulence at the *same frequency* as the turbulence level was raised. Each curve corresponds to a particular axial station. The minimum critical R for the parallel-flow boundary layer is near 300. Thus, it is possible to detect TS components at stations as far forward as that point, but it must be pointed out that packets, if present there, could not be distinguished by eye amid the total signal. Isolation of the TS component at the forward stations therefore relied upon the technique of measuring the spectrum with turbulence present and then subtracting the spectrum measured with no added turbulence. The figure shows that the response to turbulence was linear at the forwardmost station, but that it became increasingly nonlinear with increase of x. Further evidence of the nonlinear response to turbulence is given in *Fig. 13*. There, the average amplitude of the passing packets, detected individually through analysis of the time- series records, is presented as a function of R for four levels of turbulence. It appears that a rapid rise in amplitude commenced well downstream of the minimum critical Reynolds number, corresponding to the formation of packets.

Recent studies have made use of the 64-microphone array, together with simultaneous hot-wire measurements. *Fig . 14* summarizes some results. It can be seen in the left frame that packets forced by means of the driver indicated in Fig. 3 are much wider than those induced by turbulence. The lateral variation in peak strength is shown for five turbulence-induced packets passing the station R = 831 at various times. These have been selected from the great number recorded such as to be approximately similar in strength to the forced ones. Clearly, the ones due to turbulence are narrow. The right side shows that turbulence- induced packets are sometimes much stronger than the strongest ones which can be forced without serious waveform distortion due to incipient breakdown. Also seen there is an intercomparison of microphone and hot-wire signals.

Fig. 15 gives time traces for several microphones and for a five-wire vertical rake. Two large, and several small, packets are seen in the microphone traces. The effect of the largest is also to be seen in one of the hot-wire records. The hot wires also reaffirm in a general way the presence of T-S-range frequencies in the outer layer, as well as a predominance of low frequencies in the inner layer. Five instants of time have been selected to display the instantaneous profiles given in *Fig. 16*. Substantial distortion is apparent.

Figs. 17 and *18* show the time history of repetitively forced packets. The results are presented in the form of 60 time traces, with each "box" corresponding to a microphone shown in Fig. 3 (the layout here is inverted top-to-bottom, and no traces are included for the four centerline sensors not part of a lateral array.) Fig. 17 is for a quiescent stream, and Fig. 18 is for a weakly turbulent one. The (relative) amplitude range of display differs in the two cases, and is indicated in the figures. The results within the former figure are as expected, but the addition of turbulence has greatly altered the packet development, rendering the packet locally both stronger and locally weaker than in the quiescent case, and has also produced an additional, unsynchronized, packet which has grown to become a burst. *Fig. 19* shows a turbulence-induced packet which breaks down to become a burst.

Some results on the packets can be summarized as follows. The turbulence-induced ones:

(1) Mainly arise at stations downstream of the min. crit. Reynolds number.
(2) Possess a strength not in linear proportion to the stream turbulence
(3) Travel at the expected speed.
(4) Have slightly higher frequency content than forced ones.
(5) Possess the expected amp. dist. in the near-wall region, but not in the outer region.
(6) Are surprisingly narrow.

MICROPHONE LAYOUT
122-cm PLATE

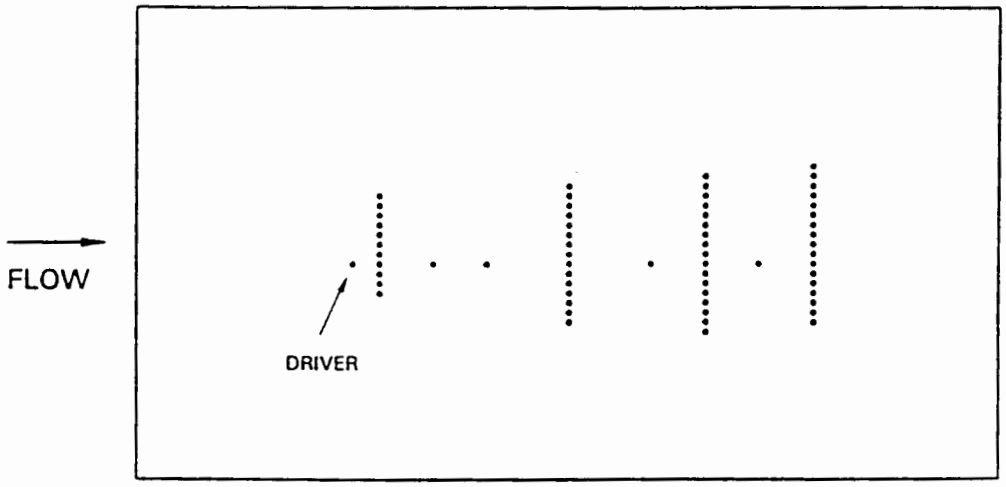

3.

K - MODE FLUCTUATIONS
DUE TO FREESTREAM TURBULENCE

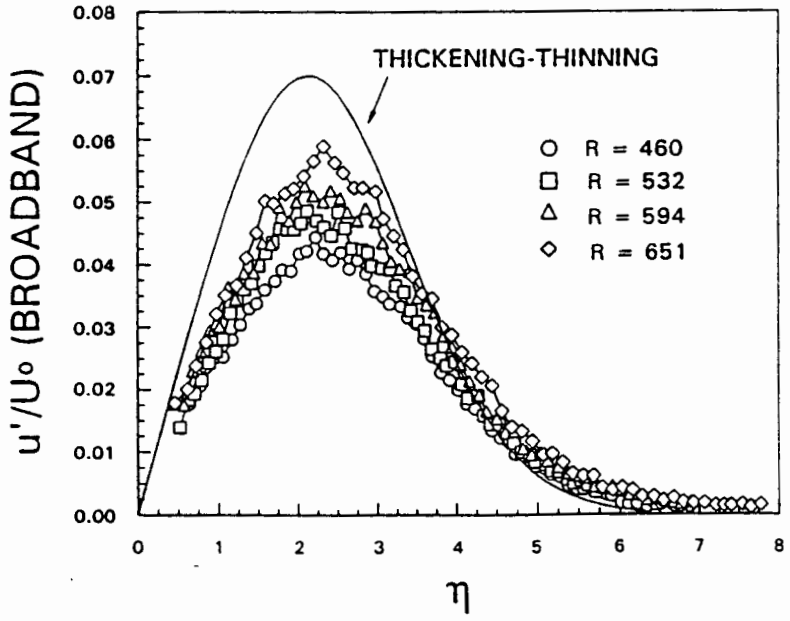

4.

THREE EXAMPLES:

FREESTREAM FLUCTUATION RECORDS

0.65 sec DURATION EACH

u'/Uo = 0.22 %

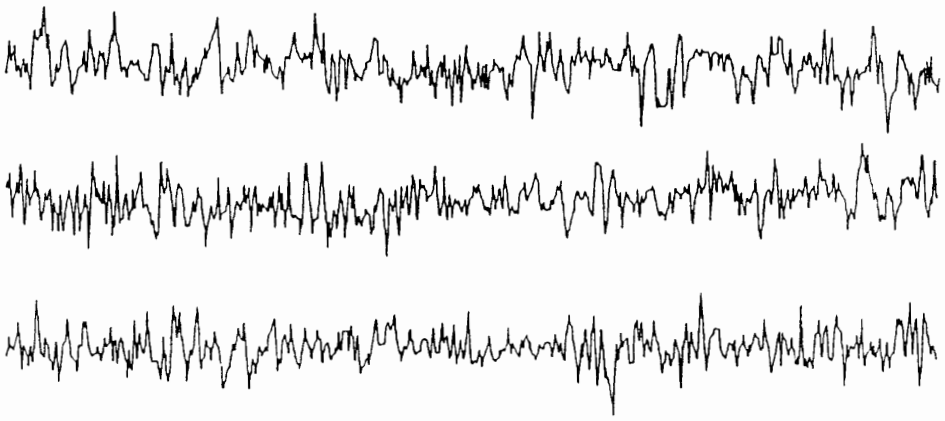

7

P'_w AT SEQUENTIAL STATIONS

u'/Uo = Ø.18%

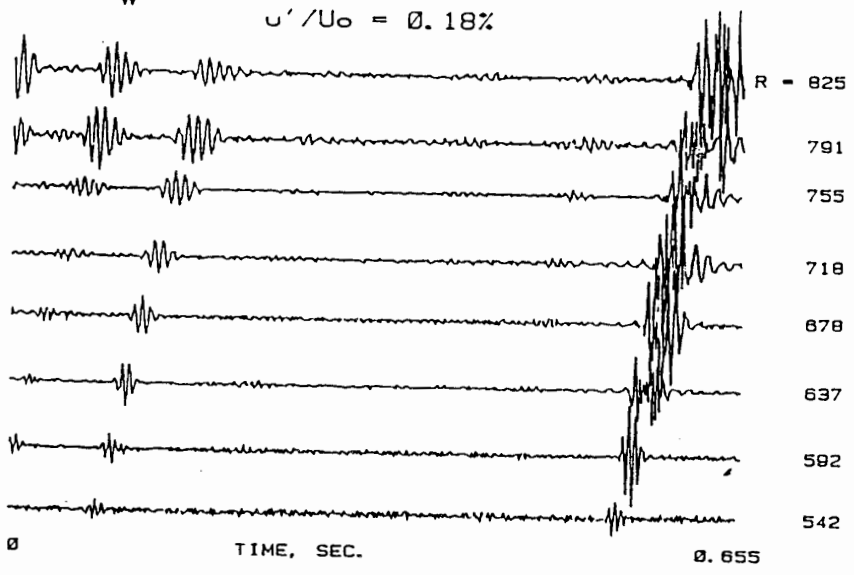

8

EXAMPLE OF

LONG-AVERAGE POWER SPECTRA

STATIONS R = 494 and 519

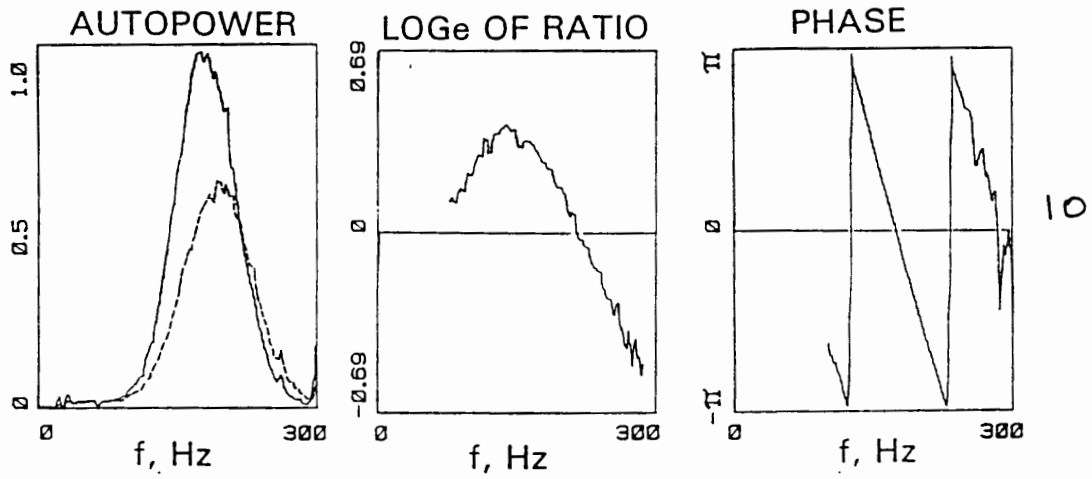

10

IN COMPARISON WITH STABILITY THEORY RESULTS,
FST-INDUCED PACKETS POSSESS SIMILAR:

* Propagation Speed
* Frequency Content
* Growth Rate
* Amplitude Distribution thru Layer

11

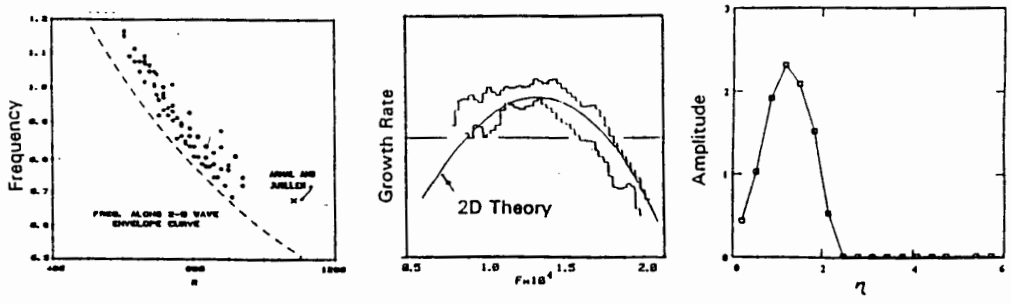

Comparing to Gaster Packets, FST-Induced Ones Are:

Narrower

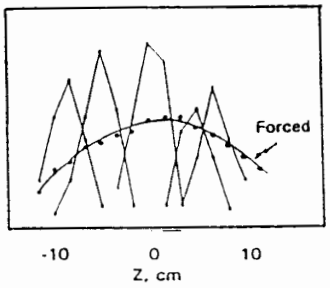

Longer

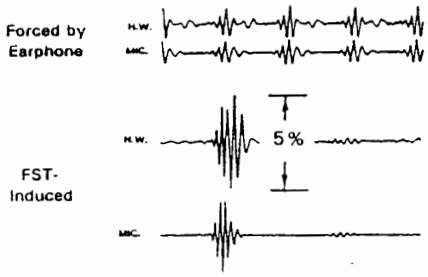

14

. . . and, sometimes, *STRONGER!*

SIMULTANEOUS RECORDS: MICROPHONES AND HOT-WIRE RAKE

FST LEVEL: u'/Uo 0.2 % 0.65 SEC. OF DATA

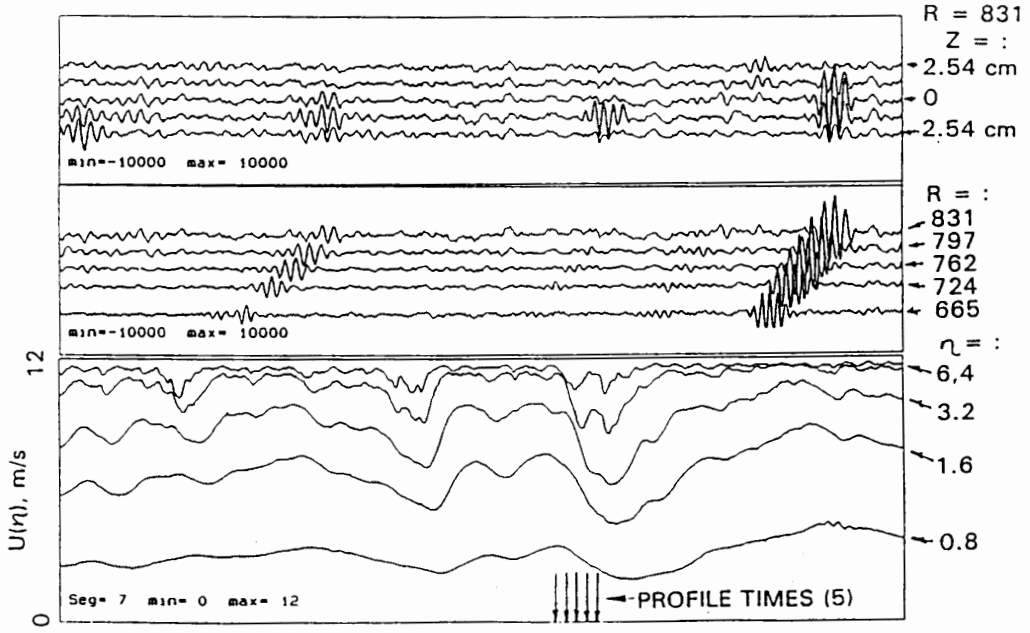

15

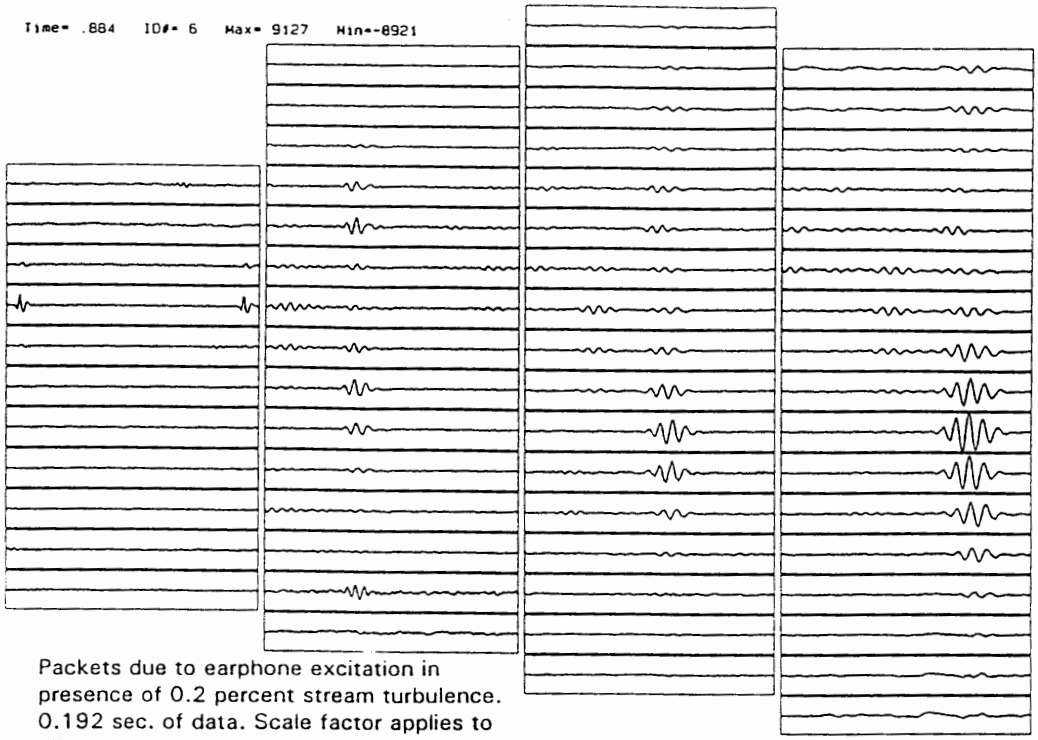

18.

Packets due to earphone excitation in presence of 0.2 percent stream turbulence. 0.192 sec. of data. Scale factor applies to all traces.

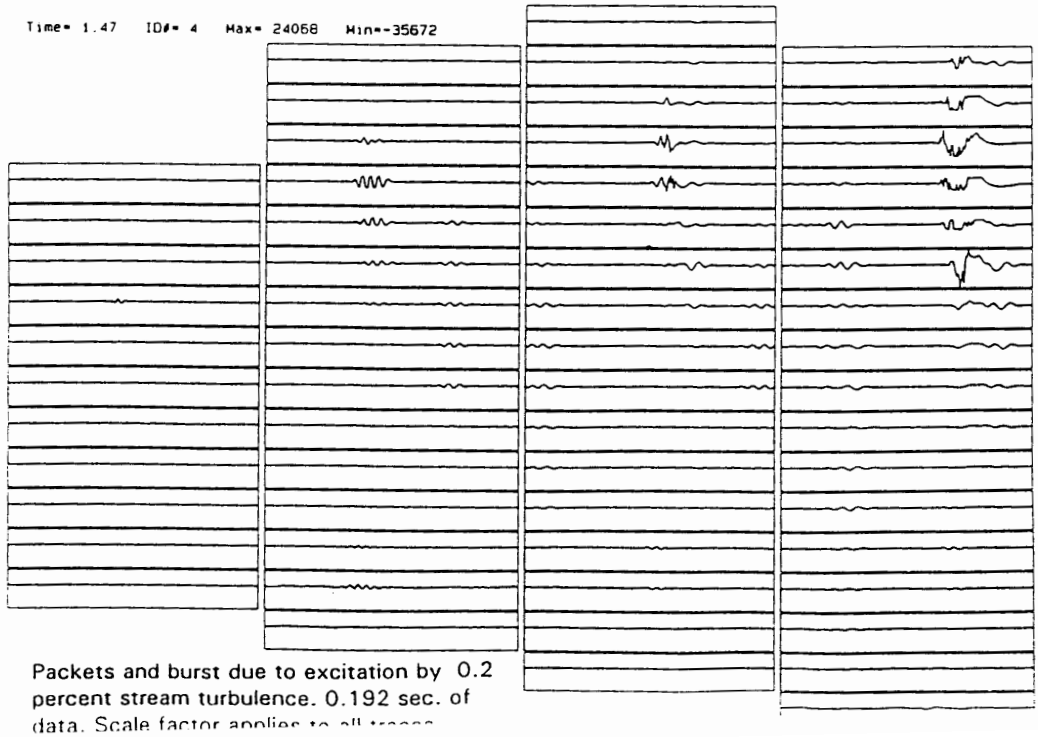

19.

Packets and burst due to excitation by 0.2 percent stream turbulence. 0.192 sec. of data. Scale factor applies to all traces.

The Evolution of Modulated Wavetrains into Turbulent Spots

M. Gaster
Department of Engineering
Cambridge University, U.K.

Experiments are being carried out to study the process by which the almost periodic disturbance waves generated naturally by the freestream evolve into turbulence. The boundary layer on a flat plate has been used for this study. The novelty of the approach is in the form of artificial excitation that is used.

Although we know, through many experimental and theoretical studies, something about the development of regular Tollmien-Schlichting waves, we know very little about the evolution of naturally excited waves. Indeed, if one carries out an experiment on a plate in a wind tunnel without any controlled excitation, it appears that bursts of turbulence appear spontaneously and one has to look very hard for any wavy precursor.

In this work the flow is excited artificially by deterministic white noise. The weak T-S wave created develops down stream, becomes nonlinear and blows up locally into a highly distorted flow. These large local distortions of the mean flow allow very high frequency disturbances to grow and form into small turbulent spots. The spots arise from the excitation, and if the same noise sequence is repeated a spot will form at the same position and time instant relative to the excitation. Of course the details of the high frequency oscillations within the spot will inevitably vary from realisation to realisation, but the overall structure is maintained. The probe may be moved around so that the structure and development of these artificially excited spots can be measured. Also the nonlinear wavy flow that causes the spot can be examined prior to breakdown.

Wavelet transform and SVD (Singular Value Decomposition) have been used as tools to examine different regions of the signals of interest. In particular these techniques enable the fine structure of the breakdown to be filtered out from the signal.

Recent work on the use of a dynamical system approach to spatial chaos will also be discussed.

1/

Transition from laminar to turbulent flow in the boundary Layer of a plate

British Maritime Technology
[BMT]

A typical wind tunnel experiment.

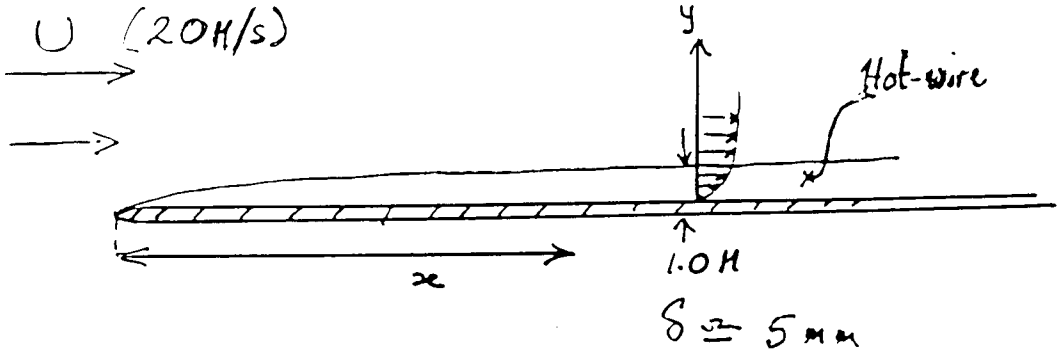

Typical fluctuations in the oncoming flow $\sqrt{u^2} < 0.01\% U_\infty$

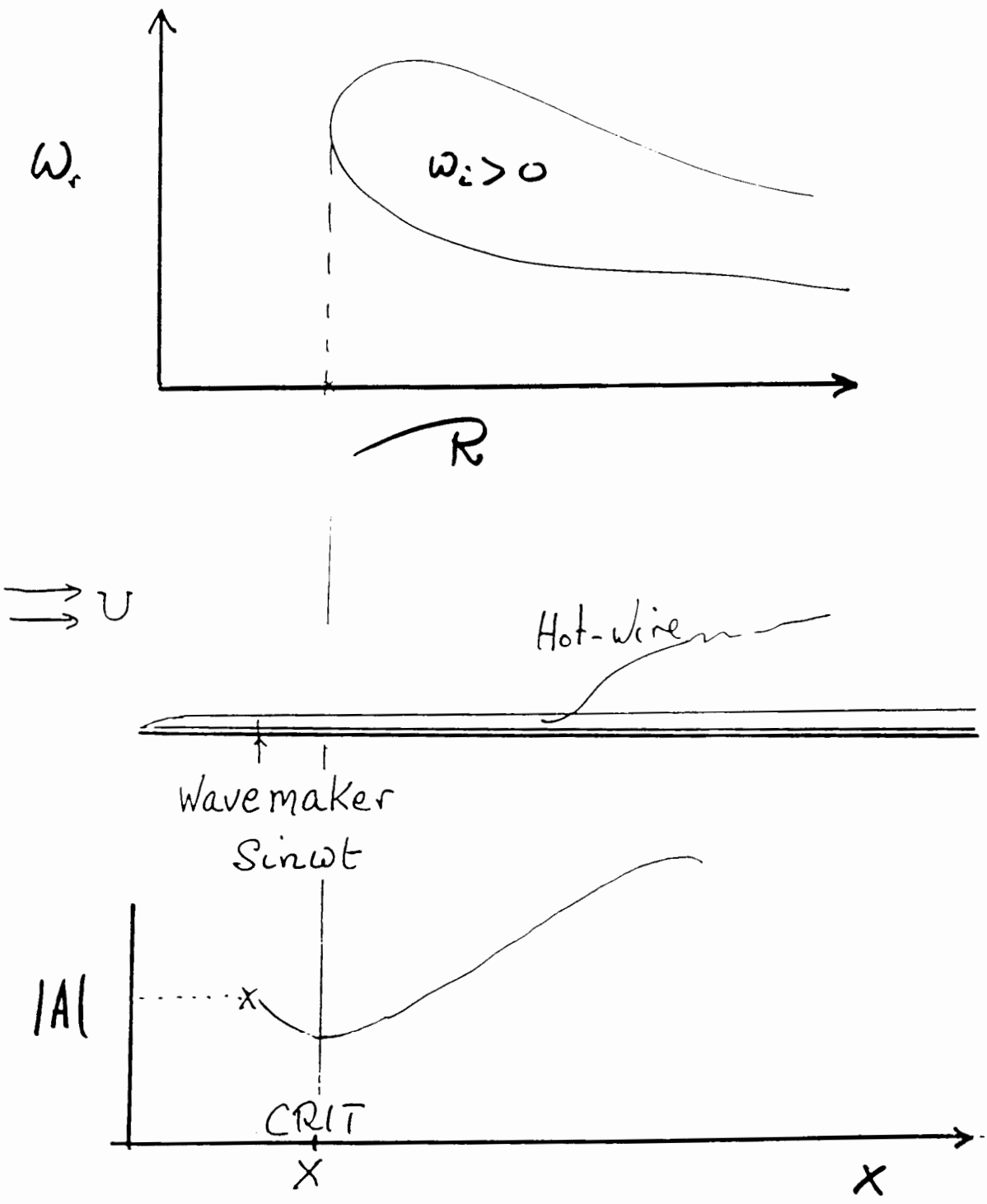
ω_r
$\omega_i > 0$
R
U
Hot-wire
Wavemaker
Sinωt
|A|
CRIT
X
X

3/

1075mm

1100mm

1125 mm

1150 mm

1175 mm

1200mm

1225mm

1250 mm

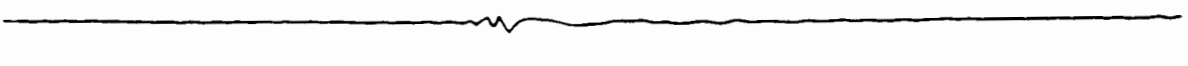

1275 mm

1300 mm

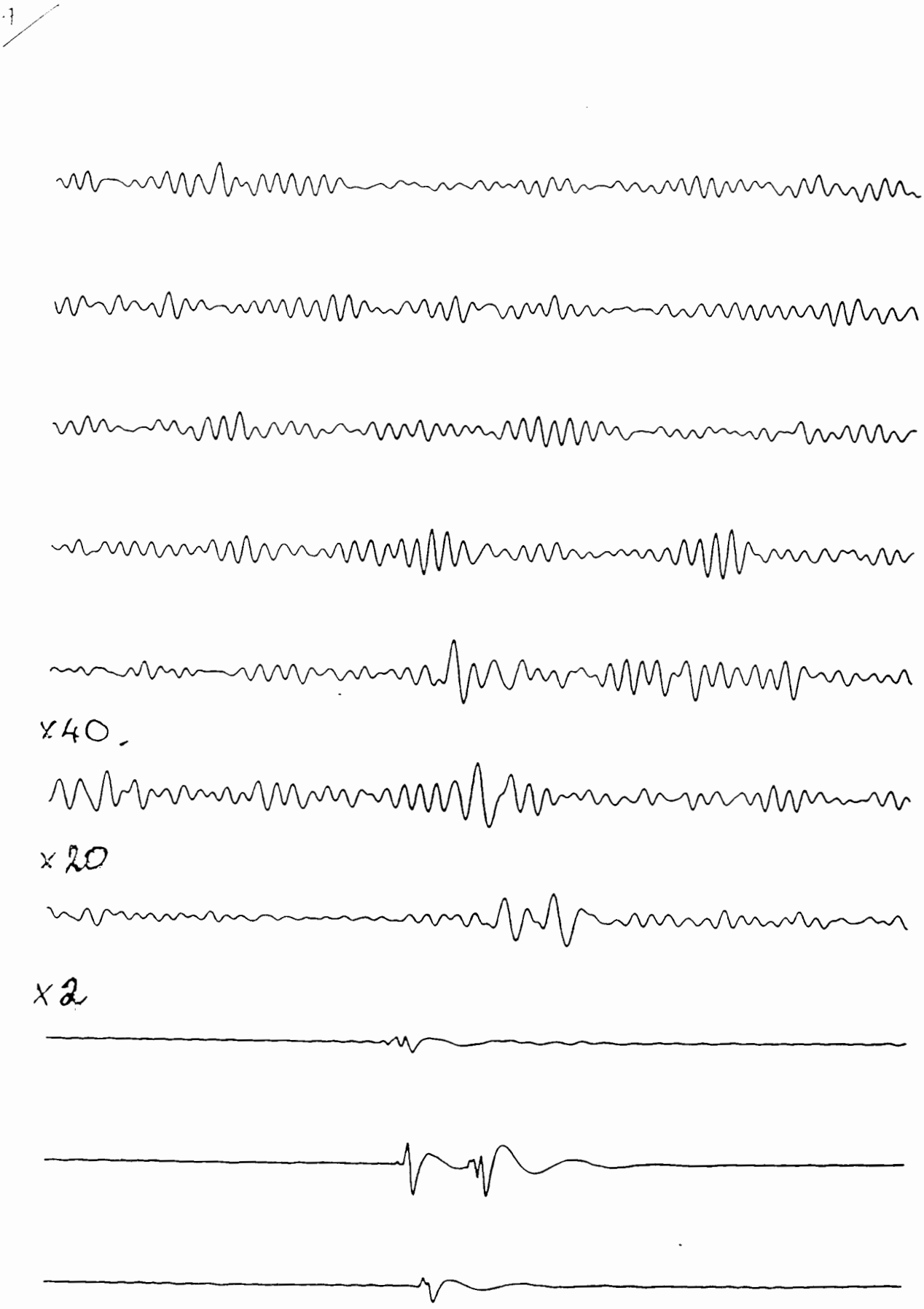
x40.
x20
x2

5/

X (mm) = 400.00

0.04 % FREE STREAM

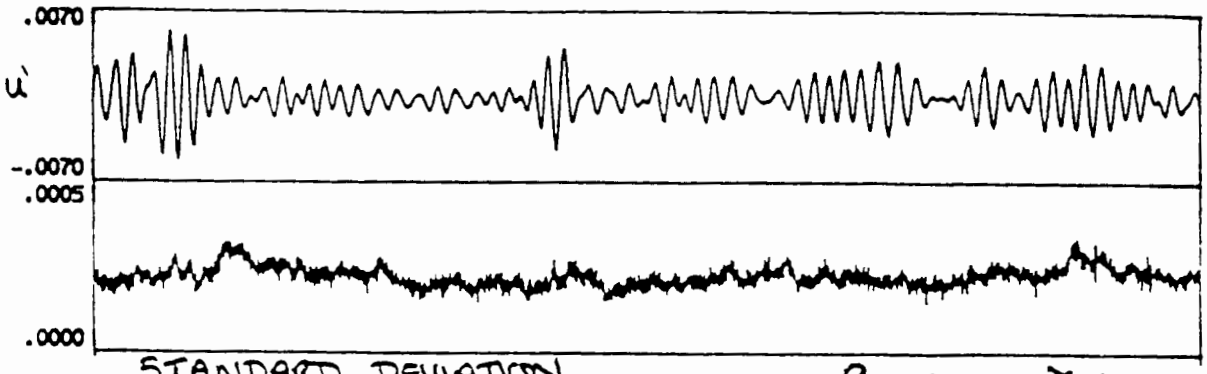

STANDARD DEVIATION

RATIO = 7 %

ETA = 4.24

0.2% FREE STREAM

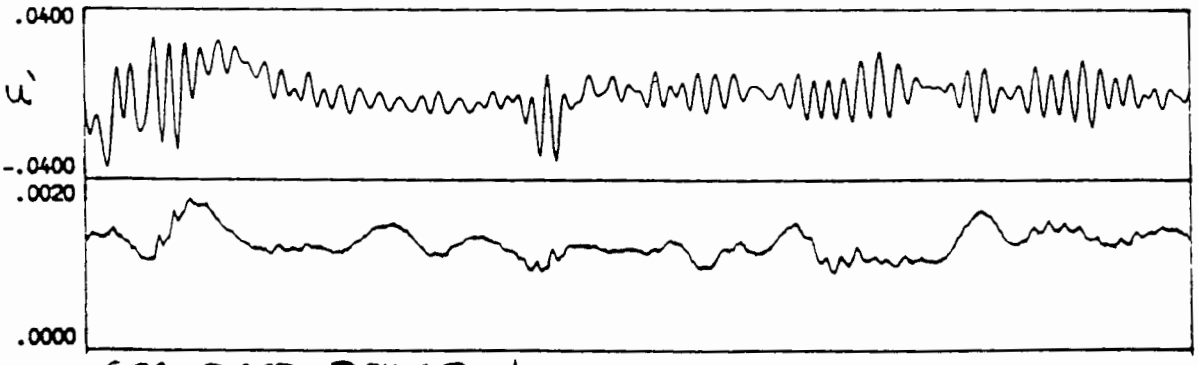

STANDARD DEVIATION.

RATIO = 5 %

ETA = 0.75

- NOTE DIFFERENT SCALES.

ETA = 0.75

8 % F.S

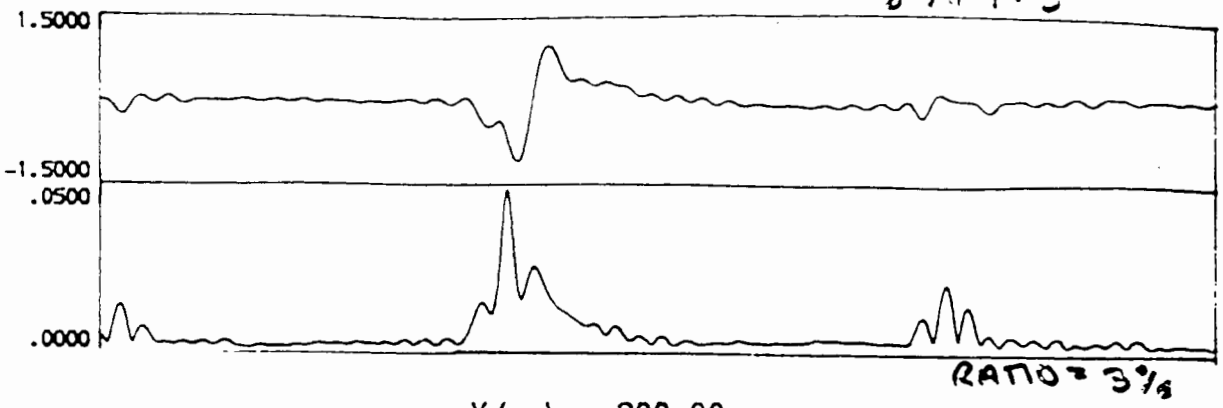

RATIO = 3%

X (mm) = 900.00

8% F.S.

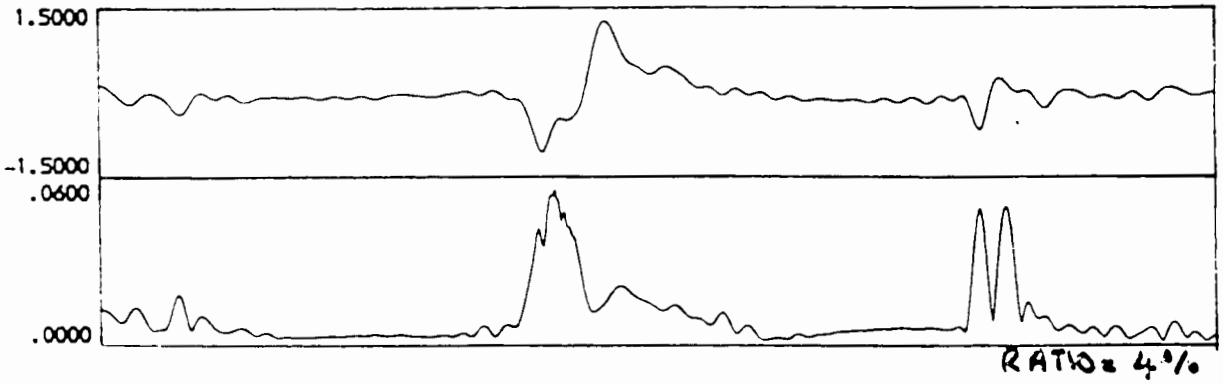

RATIO = 4%

X (mm) = 975.00

10 % F.S

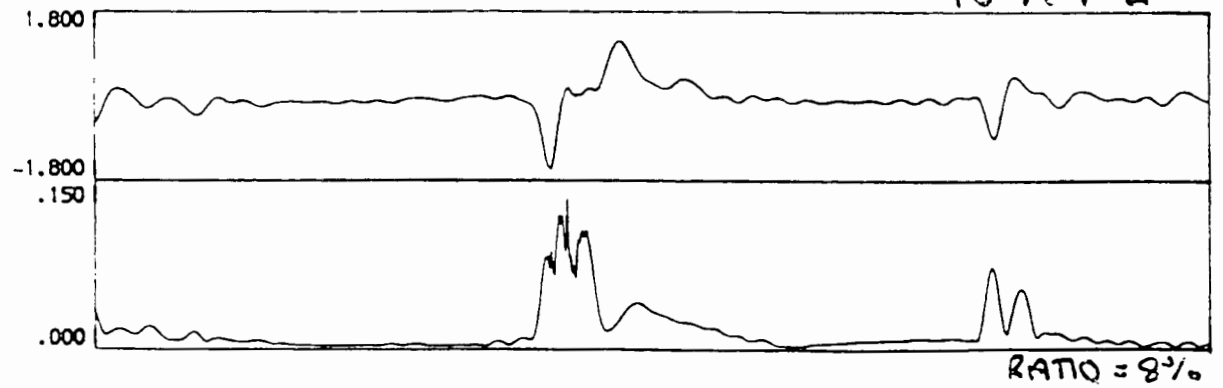

RATIO = 8%

X (mm) = 1000.0

33% F.S.

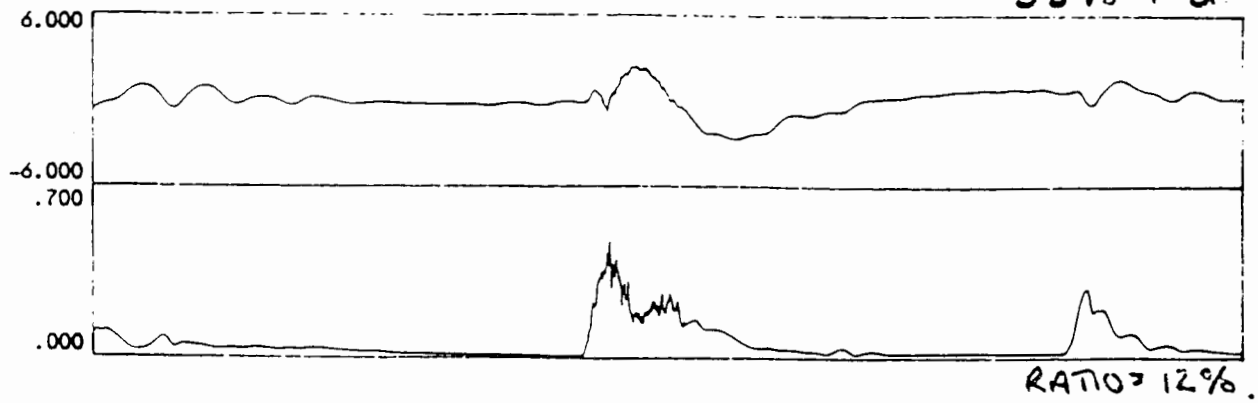

RATIO = 12%.

X (mm) = 1100.0

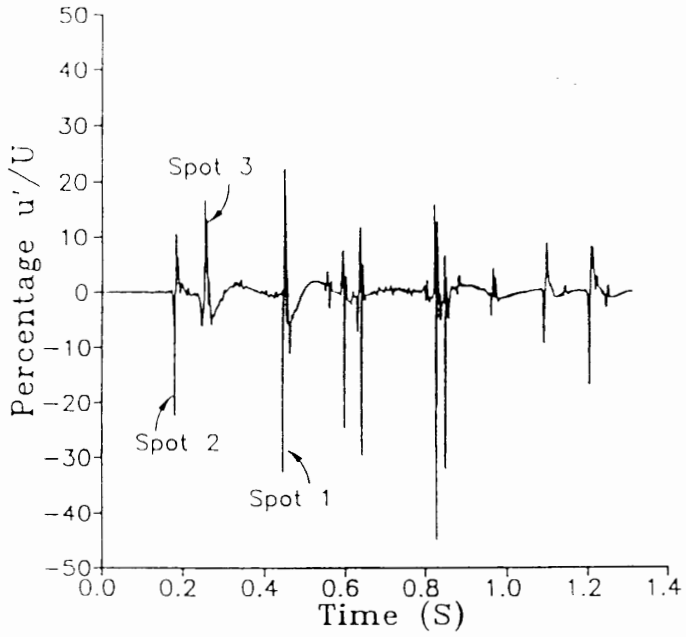

Figure 5

Fluctuating streamwise velocity signal showing incipient spots, X = 1.1 m, Z = 0.02 m.

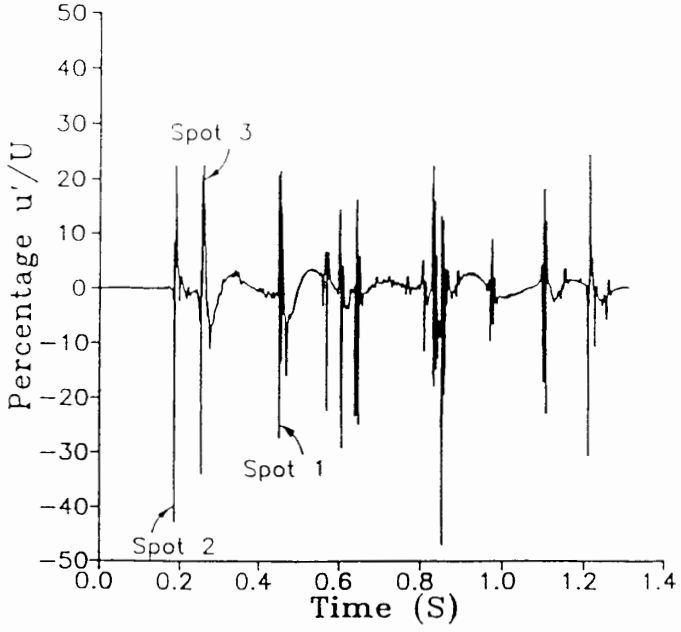

Figure 6

Fluctuating streamwise velocity signal showing incipient spots, X = 1.15 m, Z = 0.02 m.

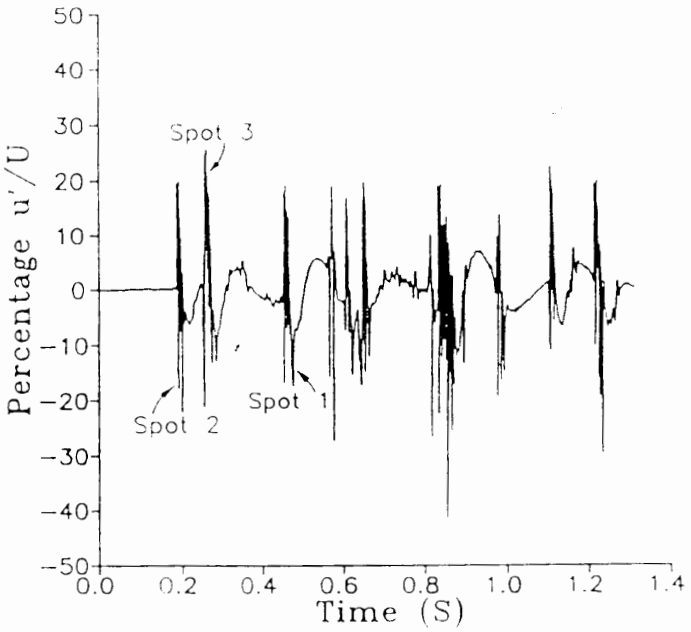

Figure 7

Fluctuating streamwise velocity signal showing incipient spots, X = 1.20 m, Z = 0.02 m.

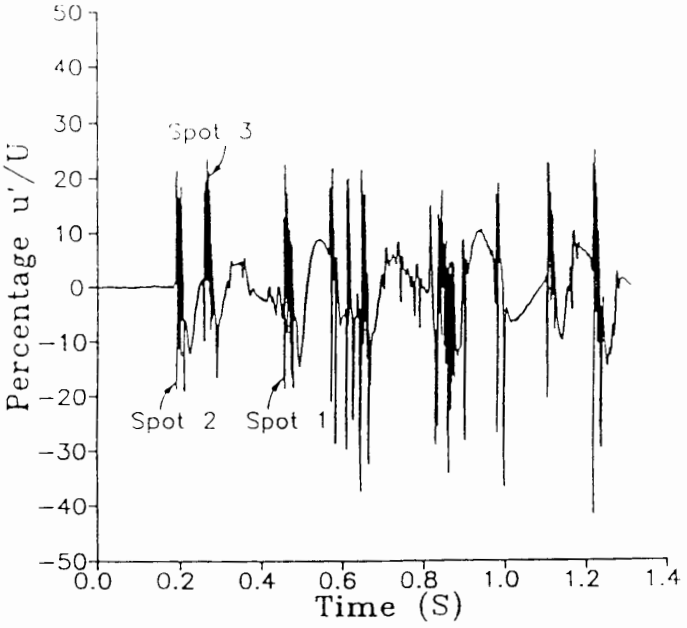

Figure 8

Fluctuating streamwise velocity signal showing incipient spots, X = 1.25 m, Z = 0.02 m.

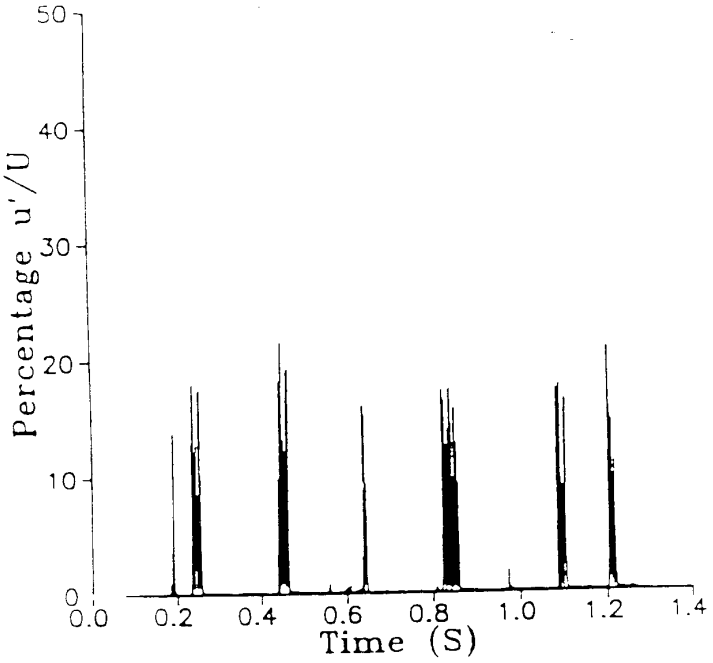

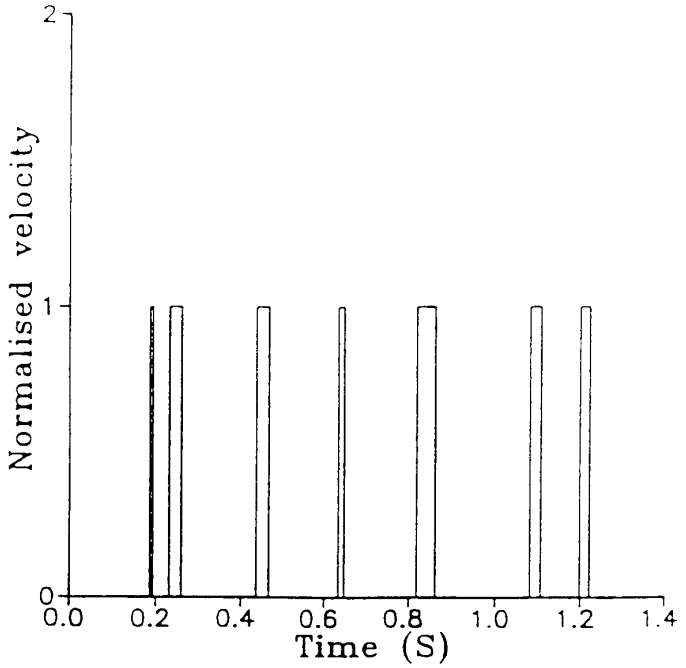

The processed signal from which the intermittency is estimated

Active Control of Transition Using the Lorentz Force

D. Nosenchuck and G. Brown
Department of Mechanical and Aerospace Engineering
Princeton University
Princeton, NJ 08544

Abstract

A new concept and technique has been developed to directly control boundary-layer transition and turbulence. Near-wall vertical motions are directly suppressed through the application of a Lorentz force. Current (j) and magnetic (B) fields are applied parallel to the boundary and normal to each other to produce a Lorentz force ($j \times B$) normal to the boundary. This approach is called magnetic turbulence control (MTC). Experiments have been performed on flat-plate transitional and turbulent boundary layers in water seeded with a weak electrolyte, at $Re_\theta \simeq 1700$. With the application of modest field densities (eg. $|B| < 1{,}000$ gauss and $|j| < 10$ mA/cm^2), measured reductions in mean and fluctuating turbulent stresses within the control region are seen to exceed 90%. Laser-sheet flow visualization confirms the substantial reductions in turbulent motion at $y^+ \lesssim 15$. The talk will present some theoretical considerations and initial experimental findings. Experiments with arrays of MTC 'tiles' will also be discussed.

Princeton University

Active Control of Transition Using the Lorentz Force

Daniel Nosenchuck and Garry Brown

Syracuse University/Minnowbrook End-Stage Transition Workshop

15 - 18 August 1993

Department of
Mechanical and
Aerospace Engineering

Control of Transition and Turbulence

- The end-stage of transition and turbulence are characterized by:
  - periodic eruptions of unstable, low-momentum 'near-wall' fluid
  - subsequent inrush of high-speed 'outer-flow' fluid
  - resultant large skin-friction drag
- Lorentz force easily generated:
  - surface electrodes produce electric field with current density j
  - magnetic field B is generated parallel to surface and normal to electric field
  - resultant normal force is $j \times B$
- Direct application of wall-normal force could prohibit lift-up and bursting of near-wall fluid
- Exploit three-dimensional Lorentz force in fluids of uniform conductivity

Key Results

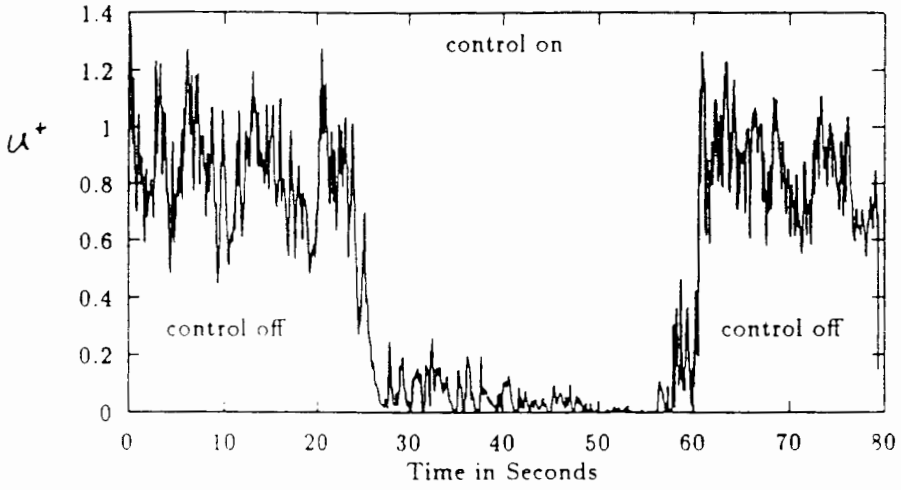

a: Control Sequence: Off-On-Off

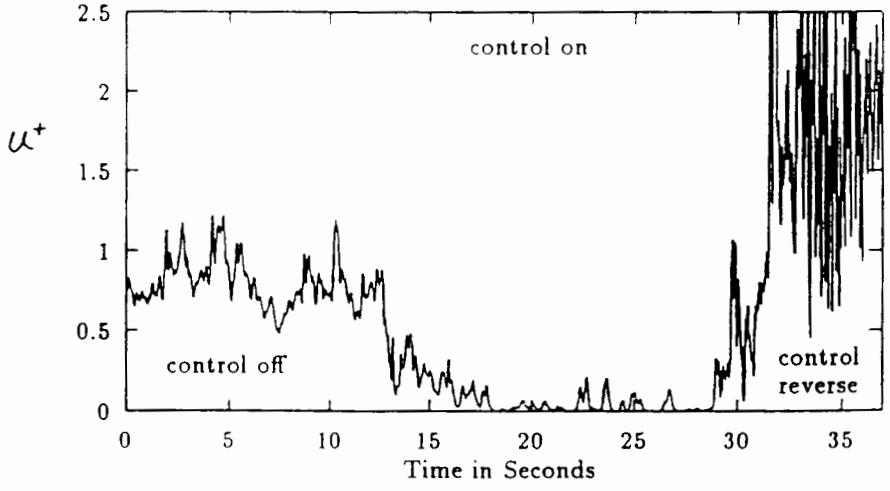

b: Control Sequence: Off-On-Reverse

MTC on Centerline at $y^+ \sim 1$
Velocity vs Time

Theoretical Considerations

- MOMENTUM

$$\rho\frac{D\mathbf{u}}{Dt} = -\nabla p + \mathbf{L} + \mu\nabla^2\mathbf{u}$$

where $\mathbf{L} = \mathbf{j} \times \mathbf{B}$ (Lorentz force)

- VORTICITY

$$\rho\frac{D\omega}{Dt} = \rho\omega \cdot \nabla\mathbf{u} + \nabla \times \mathbf{L} + \mu\nabla^2\omega$$

If $\mathbf{L} = L_y e_j$:

$$\rho\frac{D\omega_x}{Dt} = \rho\omega \cdot \nabla\mathbf{u} - \frac{\partial L_y}{\partial z} + \mu\nabla^2\omega_x$$

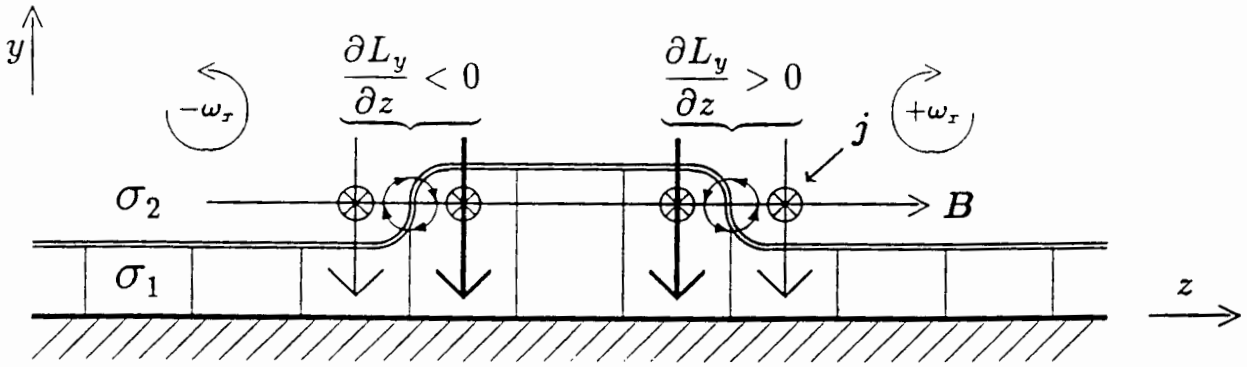

- Conductivity Gradient Controls Stability

$$\frac{\partial L_y}{\partial z} \approx \frac{\partial}{\partial z}\sigma e_z B_x \approx e_z B_x \frac{\partial\sigma}{\partial y}\frac{\partial y}{\partial z}$$

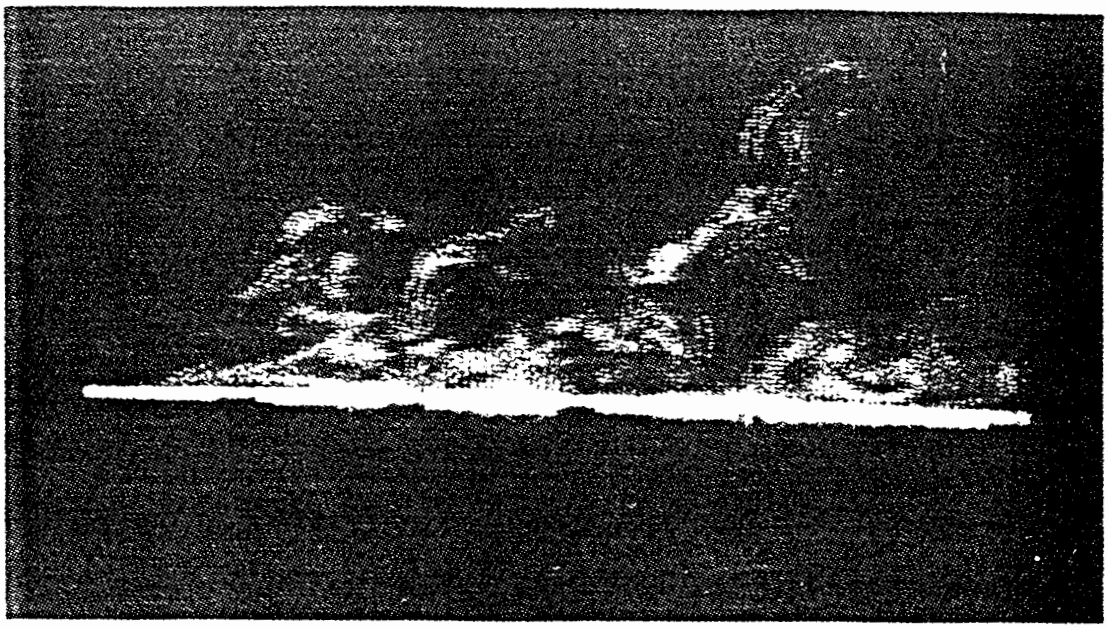

Control Off

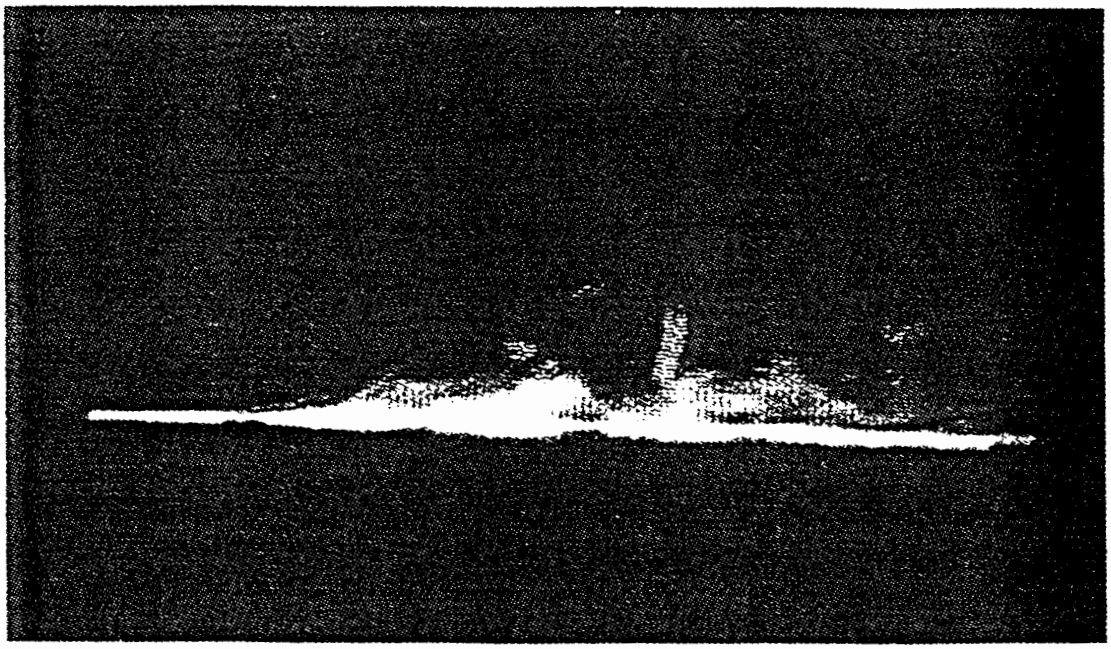

Control On

MTC Control of Turbulent Spots

NaOH throughout Boundary Layer

($Ø_1$, $Ø_2$, $Ø_3$ Active)

TILING

- Concentrate Lorentz force in near-wall region
- Large area coverage requires 'tiles'
- A TFM (turbulent flow modulation) tile is defined as that region on the wall bounded by two electrodes and two magnet poles
- Globally-uniform electric field established by phased operation and alternating electrode polarities
- Tile arrays formed with modular building blocks:

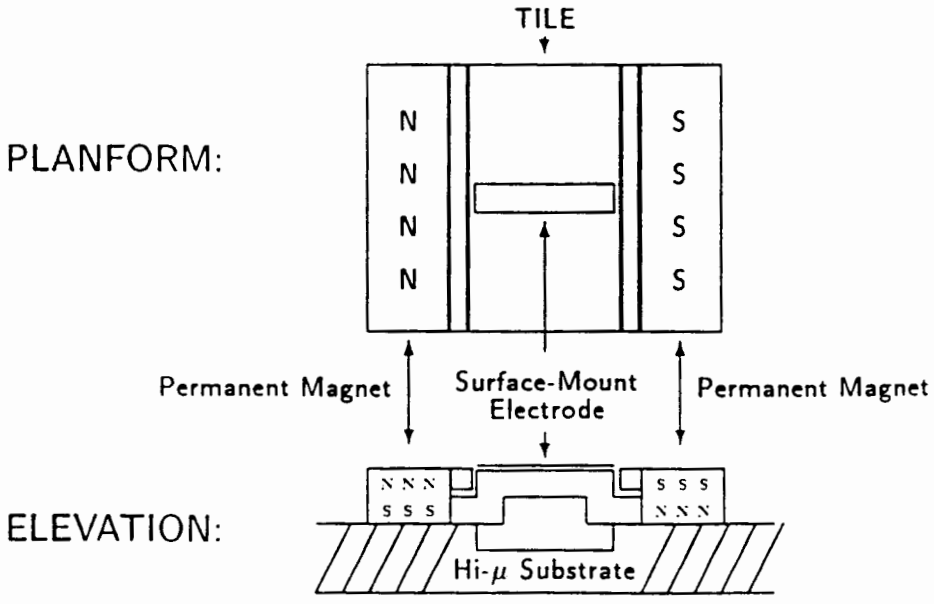

Three-Dimensional Theoretical Considerations

- VORTICITY

$$\rho\left[\frac{\partial \omega_i}{dt} + \frac{\partial}{\partial x_k}\left(u_k\omega_i - \omega_k u_i - \nu\frac{\partial \omega_i}{dx_k}\right)\right] = \epsilon_{ijk}\frac{\partial L_i}{\partial x_k}$$

  where $\epsilon_{ijk}\frac{\partial L_i}{\partial x_k}$ may be viewed as a vorticity source term

- Three-dimensional TFM electric and magnetic field lines can produce a Lorentz force-field that generates vorticity to 'capture' near-wall fluid

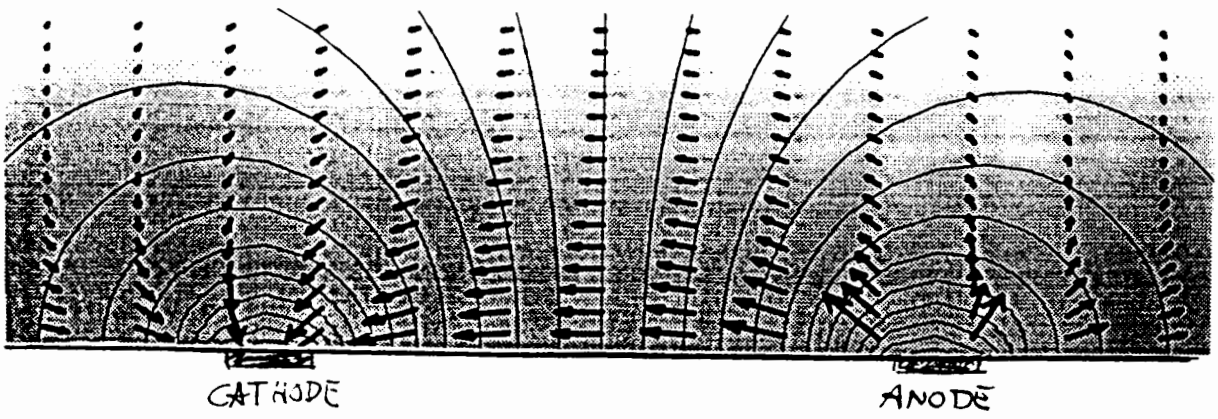

Grey-level indicates B-field strength
Contours indicate electric-field potential
Arrows denote current density j.

Role of Detuning in the Final Stage of Subharmonic Mode Transition in Boundary Layers

Thomas C. Corke
Illinois Institute of Technology
Mechanical & Aerospace Engineering Department
Fluid Dynamics Research Center
Chicago, IL 60616

This work involves mechanisms for transition to turbulence in a Blasius boundary layer through resonant interactions between a plane Tollmien-Schlichting Wave and pairs of oblique waves with equal-but-opposite wave angles. When the frequency of the TS wave is exactly twice that of the oblique waves, we have a "tuned" subharmonic resonance. This leads to the enhanced growth of the oblique modes. Following this, other nonlinear interactions lead to the the growth of other 3-D modes which are harmonically based, along with a 3-D mean flow distortion (for example see Corke and Mangano [1]). In the final stage of this process, a gradual spectral filling occurs which we have traced to the growth of fundamental and subharmonic side-band modes. To simulate this with controlled inputs, we introduced the oblique wave pairs at the same conditions, but shifted the frequency of the plane TS mode (by as much as 12%) so that it was not exactly twice that of the 3-D modes. These "detuned" conditions also lead to the enhanced growth of the oblique modes, as well as discrete side-band modes which come about through sum and difference interactions. Other interactions quickly lead to a broad band of discrete modes. Of particular importance is the lowest difference frequency which produces a low frequency modulation similar to what has been seen in past experiments with natural 3-D mode input (Kachanov and Levchenko [2]). Cross-bispectral analysis of time series allow us to trace the origin and development of the different modes. Following these leads to a scenario which we believe is more relevant to conditions of "natural" transition, where low amplitude background disturbances either lead to the gradual detuning of exact fundamental/subharmonic resonance, or in which 3-D mode resonance is detuned from the onset. The results contrast the two conditions, and document the propensity of the 2-D/3-D mode interactions to become detuned.

---

[1] *J. Fluid Mech.*, 209, 93-150.

[2] *J. Fluid Mech.*, 138, 209.

Role of Detuning in the Final Stage of Subharmonic Mode Transition in Boundary Layers

by

Thomas C. Corke

Illinois Institute of Technology
Mechanical and Aerospace Engineering Department
Fluid Dynamics Research Center

Chicago, IL

End Stage Transition Workshop
Syracuse University /Minnowbrook
August 1993

(a)
(b)
(c)
(d)
$(U - U_{mean})/u_{rms}$ (m/s)
Time (s)
0.150
0.075
0
−0.075
−0.150
0.30
0.15
−0.15
−0.30
1.50
0.75
−0.75
−1.50
1.4
0.7
−0.7
−1.4
0
0.075
0.150
0.225
0.300

Downstream evolution of u-spectra for 16/35.8 detuning

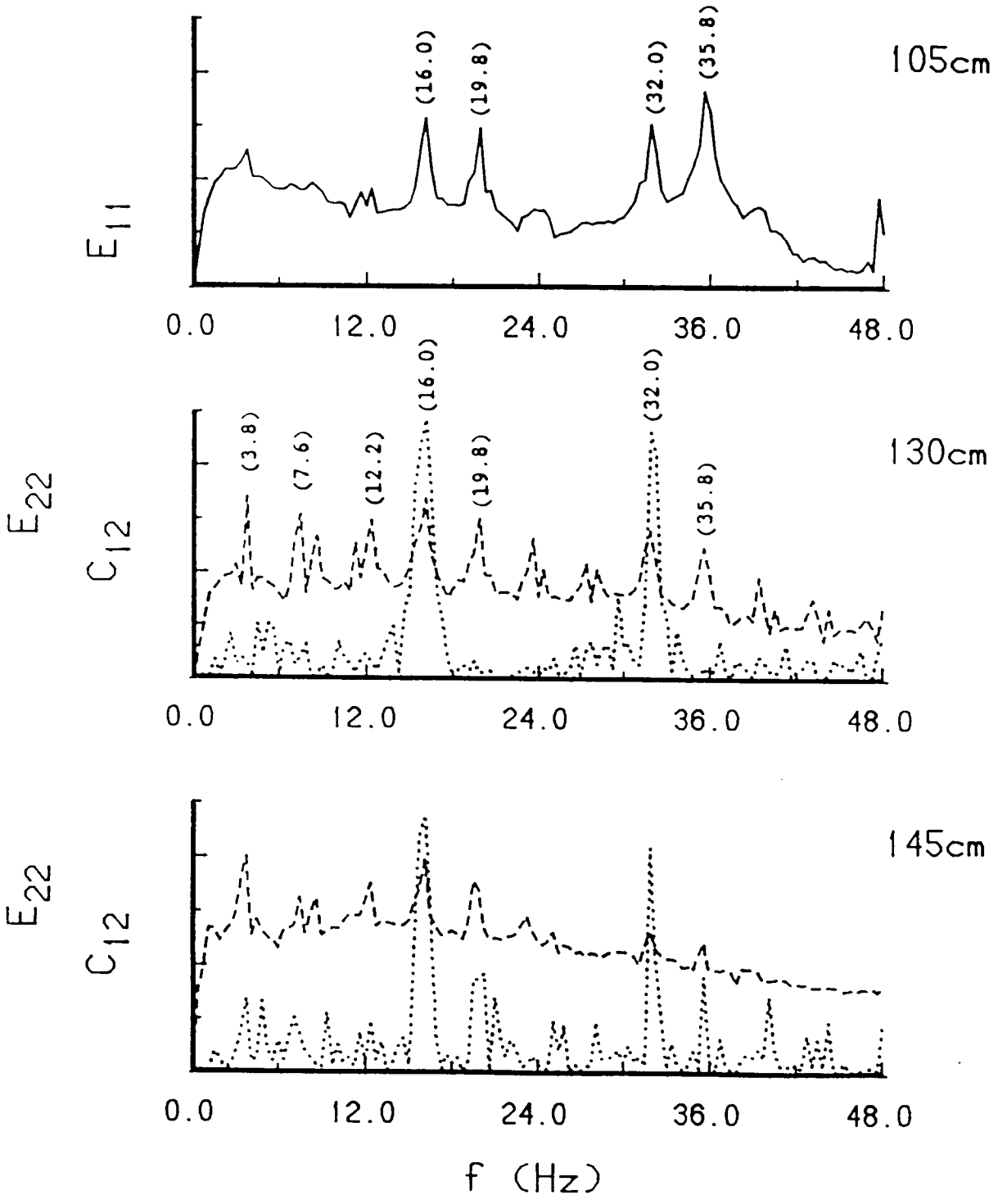

Summary:

- We observe a scenario in which 3-D modes develop by an interaction with an amplified plane TS mode through a **"tuned" or "detuned"** fundamental/ subharmonic resonance.

- With increased detuning (up to 13%), we observed **an increased sensitivity** of 3-D mode growth to the 2-D mode initial amplitude, consisting of:

  1. A decrease in the 2-D threshold amplitude necessary for resonance.

  2. An increase in the output response of the 3-D mode to the 2-D amplitude.

  3. Combined, there is a **propensity to detune.**

- Mankbadi (1993) performed a critical layer asymptotic analysis for a fully nonlinear interaction of frequency detuned modes in a 2-D bl.
  He shows that:
  - Contrary to a "tuned" parametric growth, with "detuning" the parametric growth rate is dependent not only on the initial amplitude of the plane wave, but also on the initial amplitudes of both 3-D wave pairs.
  - For a given frequency detuning, there is an *optimum angle* of oblique modes, **which is dependent on the amount of detuning and initial amplitudes**, at which the parametric growth rate equals that of the "tuned" resonance.
  - In an adverse p-grad, "detuning" could result in higher growth than with a "tuned" resonance.
- In a limited investigation, these results are consistent with those from PSE calculations by Bertolotti at ICASE.

Nonlinear Theory and Breakdown

Frank Smith
University College-London
Department of Mathematics
Gower Street
England, London WC1E6BT

Abstract

The main points of recent theoretical and computational studies on boundary-layer transition and turbulence are to be highlighted. The work is based on high Reynolds numbers and attention is drawn to nonlinear interactions, breakdowns and scales. The research focusses in particular on truly nonlinear theories, i.e. those for which the mean-flow profile is completely altered from its original state. There appear to be three such theories, dealing with unsteady nonlinear pressure-displacement interactions (I), with vortex/wave interactions (II), and with Euler-scale flows (III). Specific recent findings noted for these three, and in quantitative agreement with experiments, are the following. Nonlinear finite-time break-ups occur in I, leading to sublayer eruption and vortex formation; here the theory agrees with experiments (Nishioka) regarding the first spike. II gives rise to finite-distance blowup of displacement thickness, then interaction and break-up as above; this theory agrees with experiments (Klebanoff, Nishioka) on the formation of three-dimensional streets. III leads to the prediction of turbulent boundary-layer micro-scale, displacement - and stress-sublayer-thicknesses.

R I Bowles and F T Smith

INTRODUCTION

This article summarizes nonlinear theory and computations on end-game transition, and in particular on the development of spikes. There are three main nonlinear regimes I-III as indicated on page 2.

Pages 3, 4 concern nonlinear theory on input wave amplitudes that are initially low. These can provoke vortex-wave interactions (I), which in turn lead to close comparisons with experiments in boundary-layer and channel-flow transition as shown.

Pages 5-7 address pressure-displacement interactions (II), produced at higher amplitudes, eg following I. Comparisons with channel-flow experiments (page 6) and with boundary-layer computations (page 7) are included, especially on the first spike, for which the theory yields an integral transition criterion (page 5).

Pages 7 (lower half)-8 describe the subsequent stages (nearer Euler scales III) effectively at still higher amplitudes, eg following II. Shorter scales and significant normal pressure gradients come into the reckoning within the spike. These lead to local vortex roll-ups whether in two or three spatial dimensions.

Relevant papers during 1990-93 are in the A I A A Jnl, Jnl of Fluid Mechs, Proc Roy Soc A, European Jnl of Mechs, Computat Phys Commns.

NONLINEAR THEORY / COMPUTATION / SPIKES (R.I.B.,F.T.S., UCI

Aims at physical understanding (scales), numerical aids, exper: links, parameter dependence —— at medium-to-large Re .

THREE MAIN NONLINEAR INTERACTIONS (⟶ END-GAME, via events in 3I

I. VORTEX-WAVE INTERACTIONS, at low input wave amplitudes

$$(u,v) = (u_o, \epsilon v_o)(x,\bar{y},\bar{z}) + \epsilon (u_1, v_1)(\bar{x},\bar{y},\bar{z}) + \ldots,$$

$$(x, y, z) = \epsilon (\bar{x}, \bar{y}, \bar{z}), \quad \epsilon \equiv Re^{-1/2} .$$

⇒ u_o-vortex eqs. are nonlinearly coupled with u_1-wave eq..

II. PRESSURE-DISPLACEMENT INTERACTIONS, at medium input

⇒ Interacting-boundary-layer eqs (e.g. nonlinear T.S. evolut

III. EULER-SCALE MOTION, at high input

⇒ Unsteady Euler eqs. (e.g. by-pass) .

Aside (on start-game) : stability at sub- & super-critical R_δ ($= \sqrt{2}$

[J.F.M. 1984]

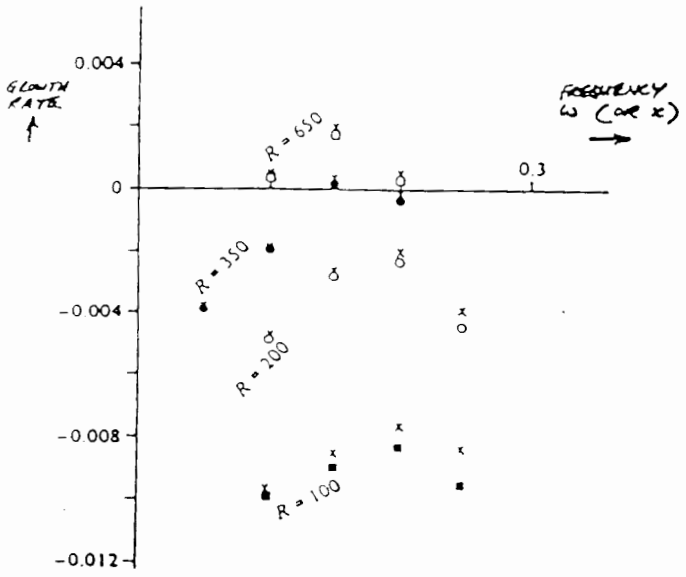

Comparisons between interactive and full solutions in the linear Blasius boundary layer.

Full solutions at R = 650, 350, 200, 100 are o , • , respectively, with × giving the corresponding interac results.

I. Stage I : 3D nonlinear evolution from near-2D input .

B. L.

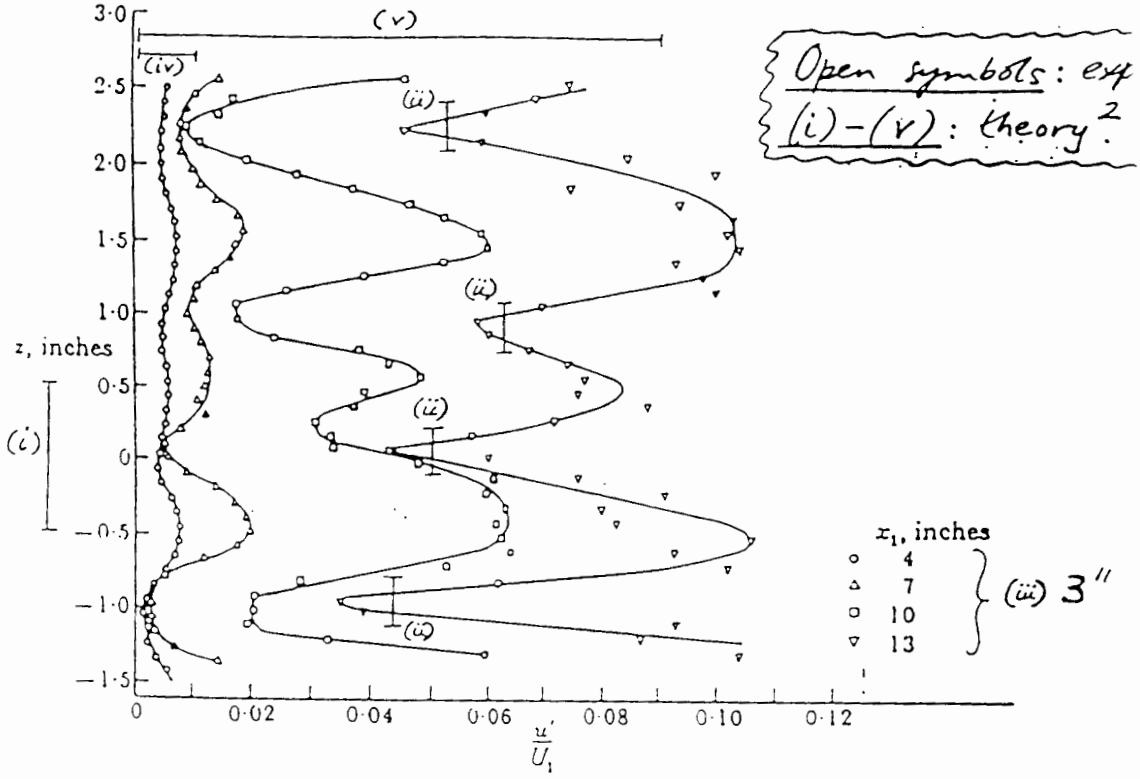

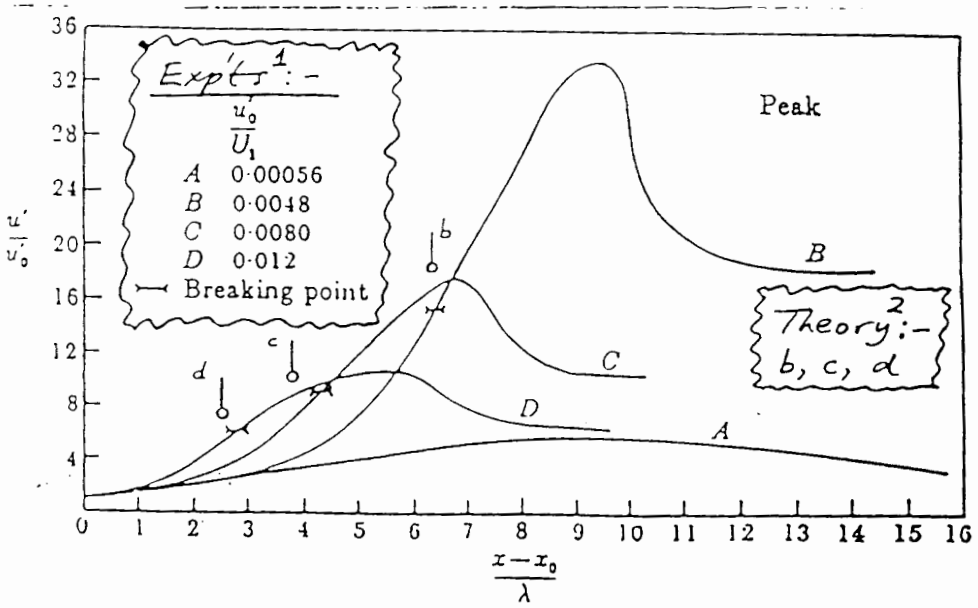

1. Klebanoff & Tidstrom '59 (e.g. ch. IX of "Lam. BL's")

2. Stewart & Smith '92 (JFM.)

$\Downarrow$ $p_x - i p_{zz} = p - i p Q$ & $Q_{xx} = (|p|^2)_{zz}$.

FTS, RIB '92 (Proc.Roy.Soc.)

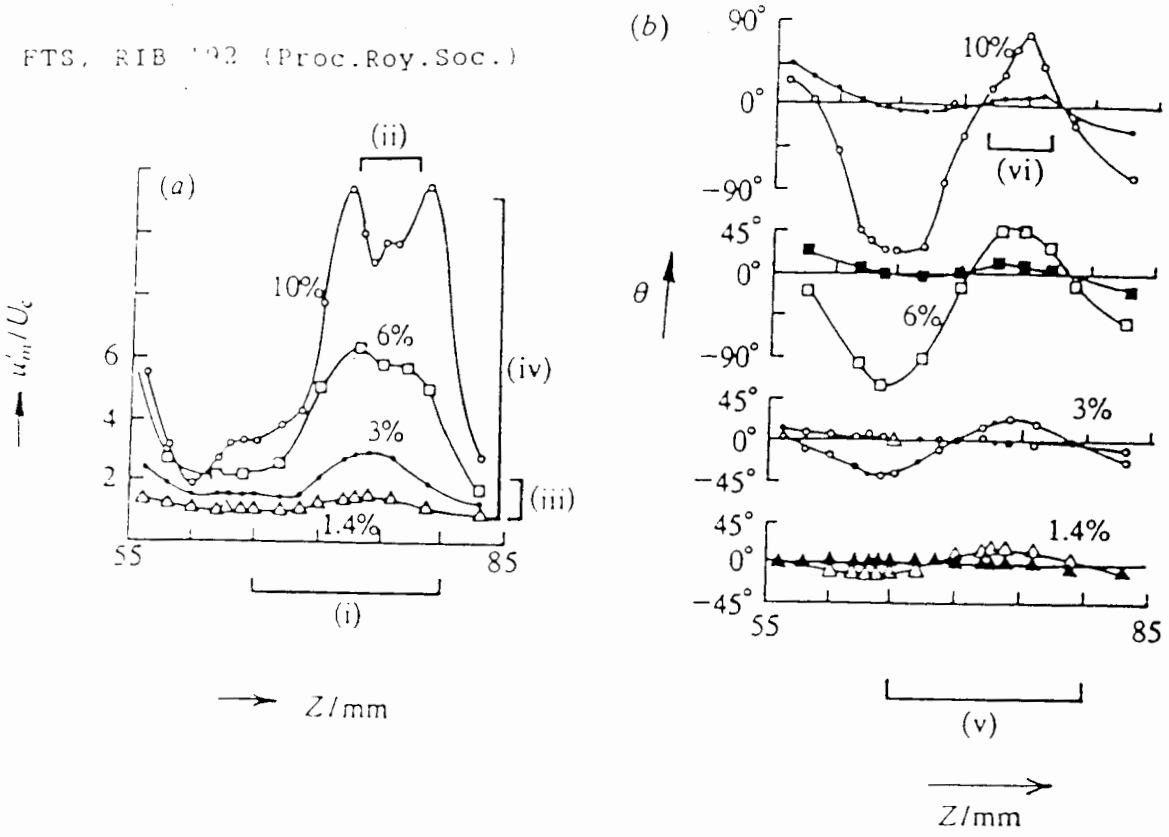

Comparisons with the experiments of Nishioka *et al.* (1979), on stage

II. 2nd stage : 3D, strongly nonlinear

→ "finite-time break-up" (CRITERION

As $t \to t_s-$, near $x = x_s$, in 2D,

$$\begin{cases} p \sim p_0 + (t_s - t)^{1/2}\,\tilde{p}(\tilde{x}) + \cdots, \\ u \sim u_0(y) + O(t_s - t)^{1/2}, \quad x - x_s = c(t - t_s) + (t_s - t)^{3/2} \end{cases}$$

FT S., MATHEMATIKA 1988

$$\Rightarrow \text{need } \int_0^\infty (u_0 - c)^{-2}\,dy = 0, \quad (*)$$

& hence $\left(\frac{3\tilde{x}}{2} + \tilde{p}\right)\tilde{p}_{\tilde{x}} - \frac{1}{2}\tilde{p} = 0.$

NISHIOKA ET AL EXPERIMENTS :-

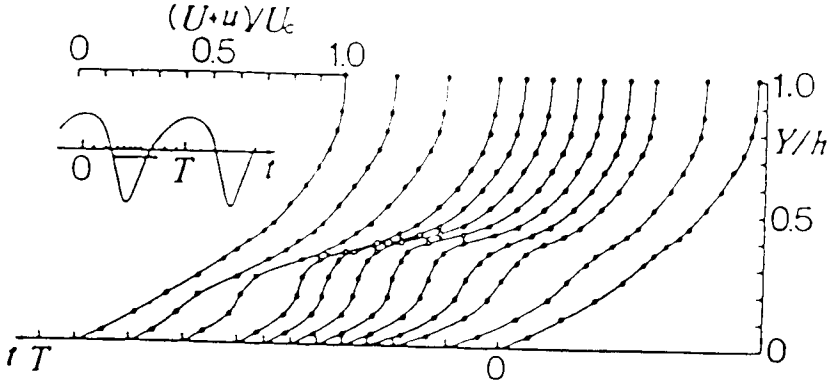

Fig. 5. Instantaneous velocity distributions at peak, at 9.4 % stage.

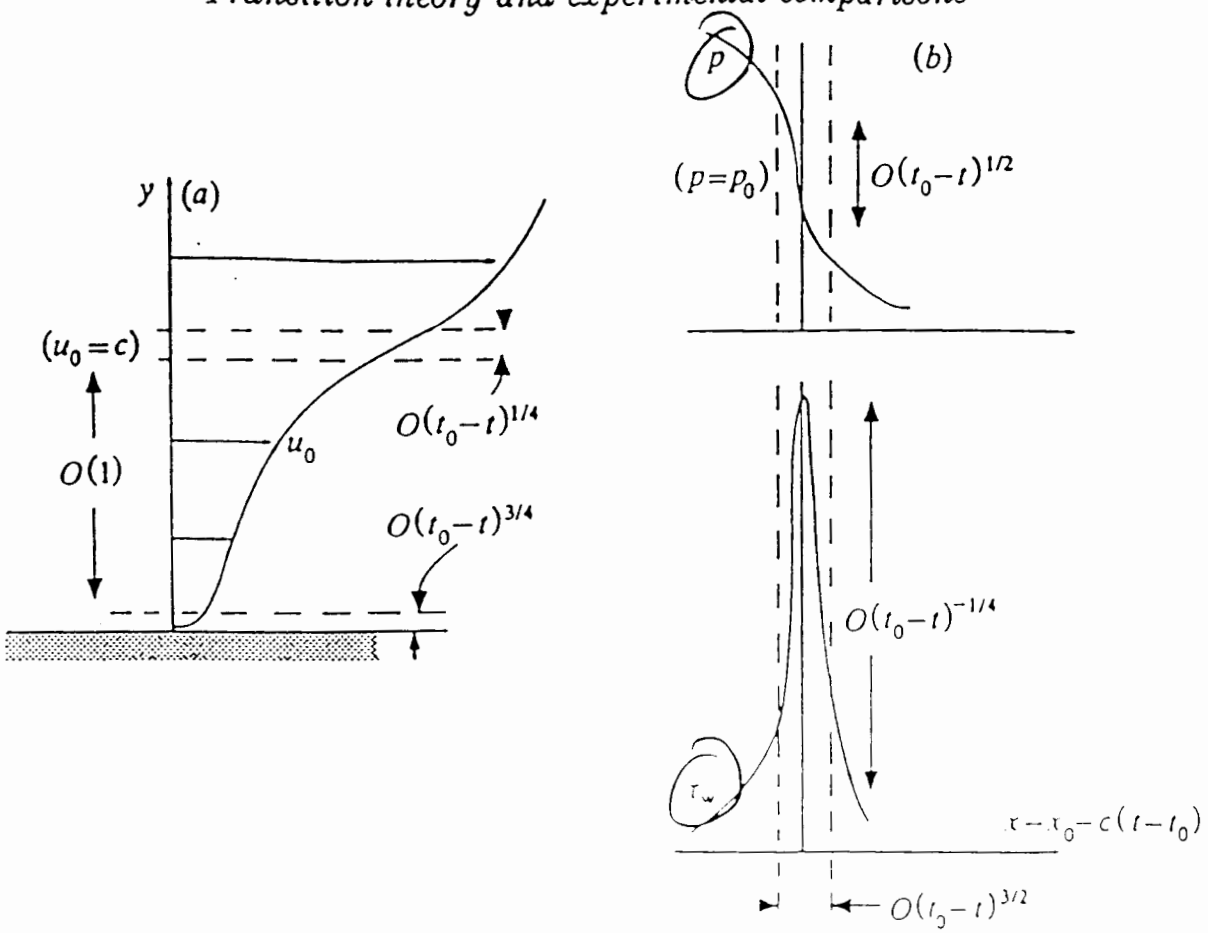

Figure . Schematic diagram for the transition stage II (strongly nonlinear).

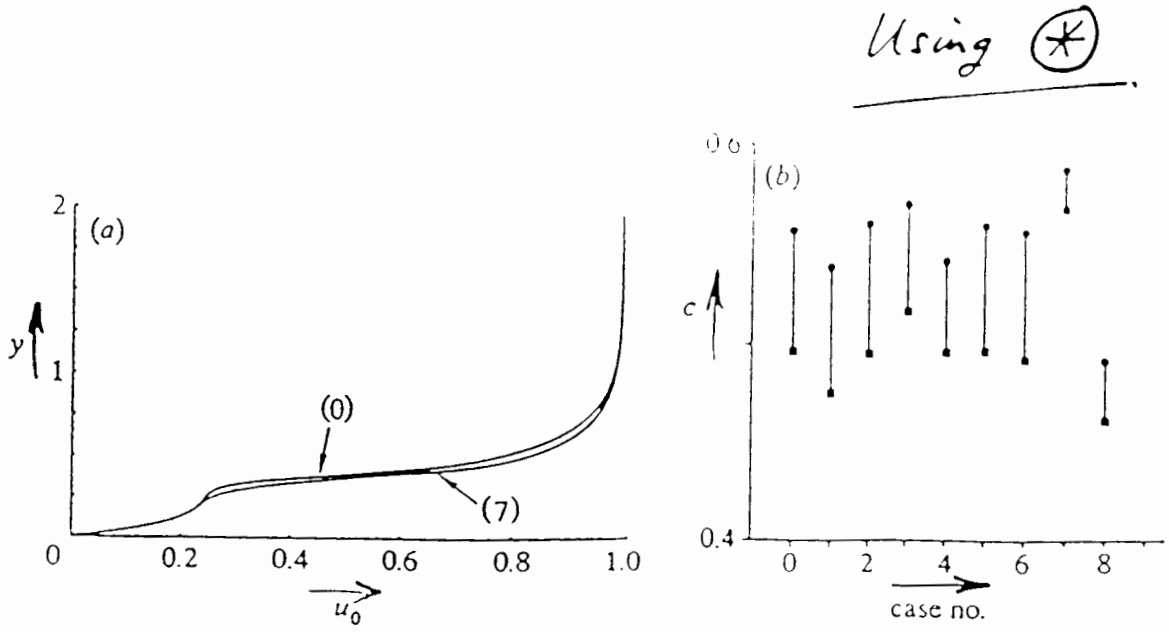

Figure . Comparisons with Nishioka *et al.*'s (1979) experiments, concerning the strongly nonlinear transition stage II.

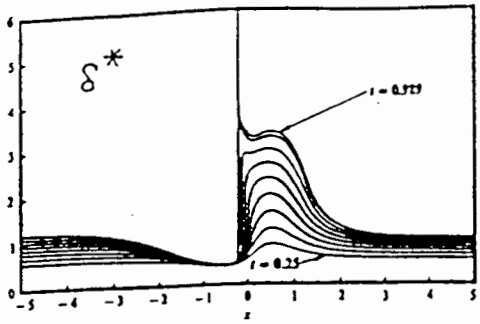

FIGURE 4. Temporal development of the displacement thickness; plotted curves are at $t = 0.25$ (0.10) 0.95 and $t_s = 0.959$.

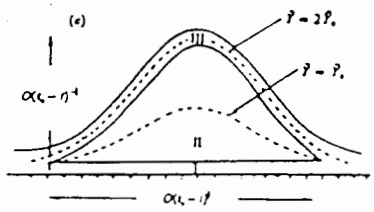

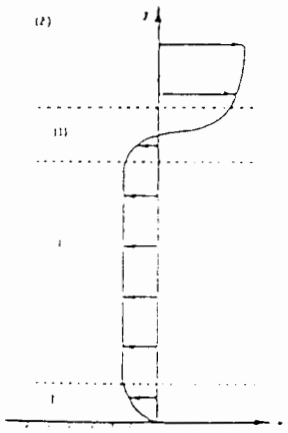

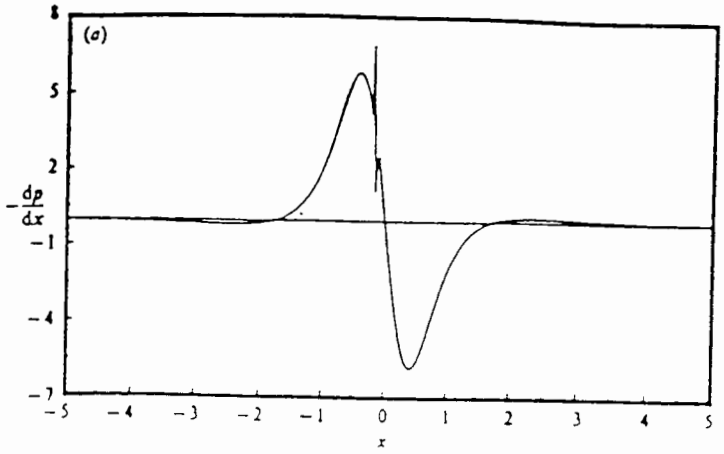

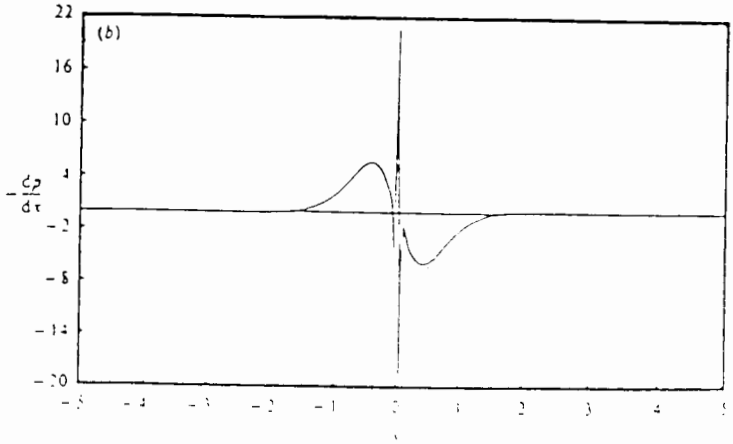

FIGURE 10. Mainstream pressure gradient at t_s (a) $Re = 10^4$; (b) $Re = 10^6$

(III) Subsequent stages in spike development

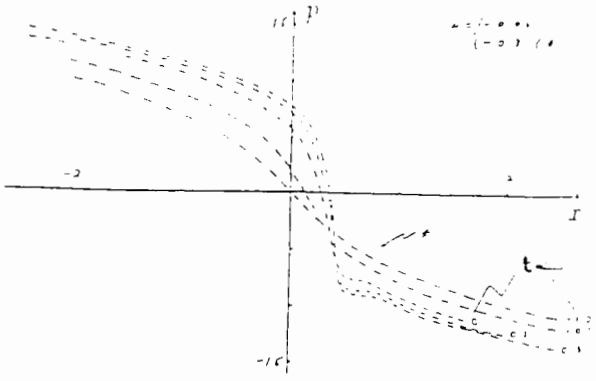

Inclusion of normal pressure gradient. (Hoyle et al 91-93)

$$p_t + pp_x = p_{xxx} + \mu p_x \int_{-\infty}^{\infty} \frac{p_t(s,t)}{p(x,t) - p(s,t)}\, ds$$

Work in Progress

Local vortex formation and rollup (Hoyle et al 91-93) : –

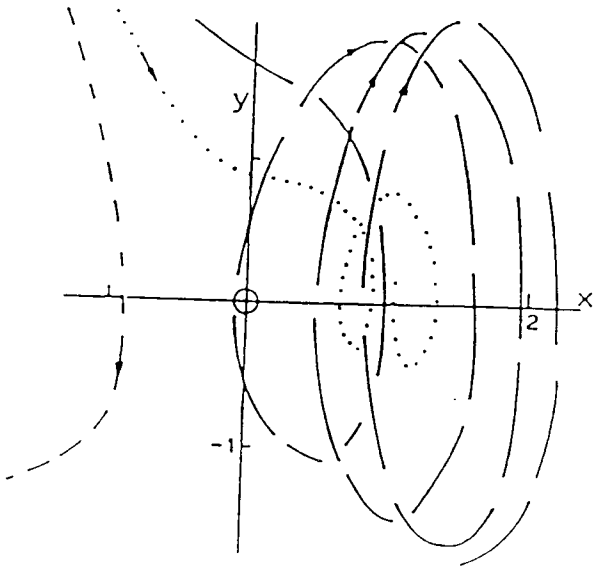

Compressibility : –

$$\int_0^\infty \frac{\mathrm{d}y}{\rho_0(u_0 - c)^2} = 0 \ .$$

3-D.
Pressure at breakdown
(Hoyle et al 91-93) : –

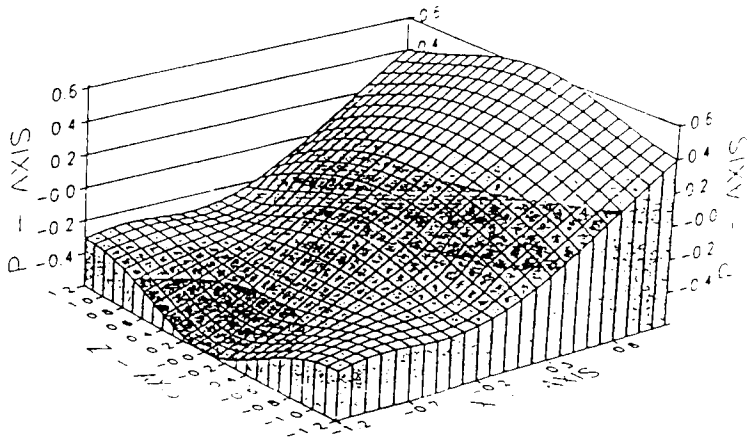

Professor Charles R. Smith
Department of Mechanical Engineering and Mechanics
Building No. 19
Lehigh University
Bethlehem, PA 18015
FAX: (215) 758-4116 EMAIL: crs1@lehigh.edu

Development of Hairpin Vortices in Turbulent Spots and End-Wall Transition

The end-stage phase of boundary layer transition is characterized by the development of hairpin-like vortices which evolve rapidly into patches of turbulent behavior. In general, the characteristics of the evolution from this hairpin stage to the turbulent stage is poorly understood, which has prompted the present experimental examination of hairpin vortex development and growth processes. Two topics of particular relevance to the workshop focus will be covered: 1) the growth of turbulent spots through the generation and amalgamation of hairpin-like vortices, and 2) the development of hairpin vortices during transition in an end-wall junction flow. Brief summaries of these studies are described below.

Using controlled generation of hairpin vortices by surface injection in a critical laminar boundary layer, detailed flow visualization studies have been done of the phases of growth of single hairpin vortices, from the initial hairpin generation, through the systematic generation of secondary hairpin-like flow structures, culminating in the evolution to a turbulent spot. The key to the growth process is strong vortex-surface interactions, which give rise to strong eruptive events adjacent to the surface, which results in the generation of subsequent hairpin vortex structures due to inviscid-viscous interactions between the eruptive events and the free stream fluid. The general process of vortex-surface fluid interaction, coupled with subsequent interactions and amalgamation of the generated multiple hairpin-type vortices, is demonstrated as a physical mechanism for the growth and development of turbulent spots.

When a boundary layer flow along a surface encounters a bluff body obstruction extending from the surface (such as a cylinder or wing), the strong adverse pressure gradients generated by these types of flows result in the concentration of the impinging vorticity into a system of discrete vortices near the end-wall juncture of the obstruction, with the extensions of the vortices engirdling the obstruction to form "necklace" or "horseshoe" vortices. Recent hydrogen bubble and particle image visualization have shown that as Reynolds number is increased for a laminar approach flow, the flow will become critical, and a destabilization of the necklace vortices results in the development of an azimuthal waviness, or "kinks," in the vortices. These vortex kinks are accentuated by Biot-Savart effects, causing portions of a distorted necklace vortex to make a rapid approach to the surface, precipitating processes of localized, three-dimensional surface interactions. These interactions result in the rapid generation, focussing, and ejection of thin tongues of surface fluid, which rapidly roll-over and appear as hairpin vortices in the junction region. Subsequent amalgamation of these hairpin vortices with the necklace vortices produces a complex transitional-type flow.

A presentation of key results from both these studies will be done, emphasizing both the ubiquity of such hairpin-type flow structures in manifold transitional-type flows, and the importance of vortex-surface interactions in the development of hairpin vortices.

Development of Hairpin Vortices in Turbulent Spots and End-Wall Transition

C. R. Smith
Department of Mechanical Engineering and Mechanics
Lehigh University
Bethlehem, PA 18015

Supported by AFOSR

Topics :

- Growth of a turbulent spot from a single hairpin vortex
  - ➡ generation by slot injection in laminar BL
  - ➡ evolution via vortex-surface interaction
- Development of hairpin-like vortices during transition in an end-wall junction flow.
  - ➡ transition in a strong pressure gradient environment

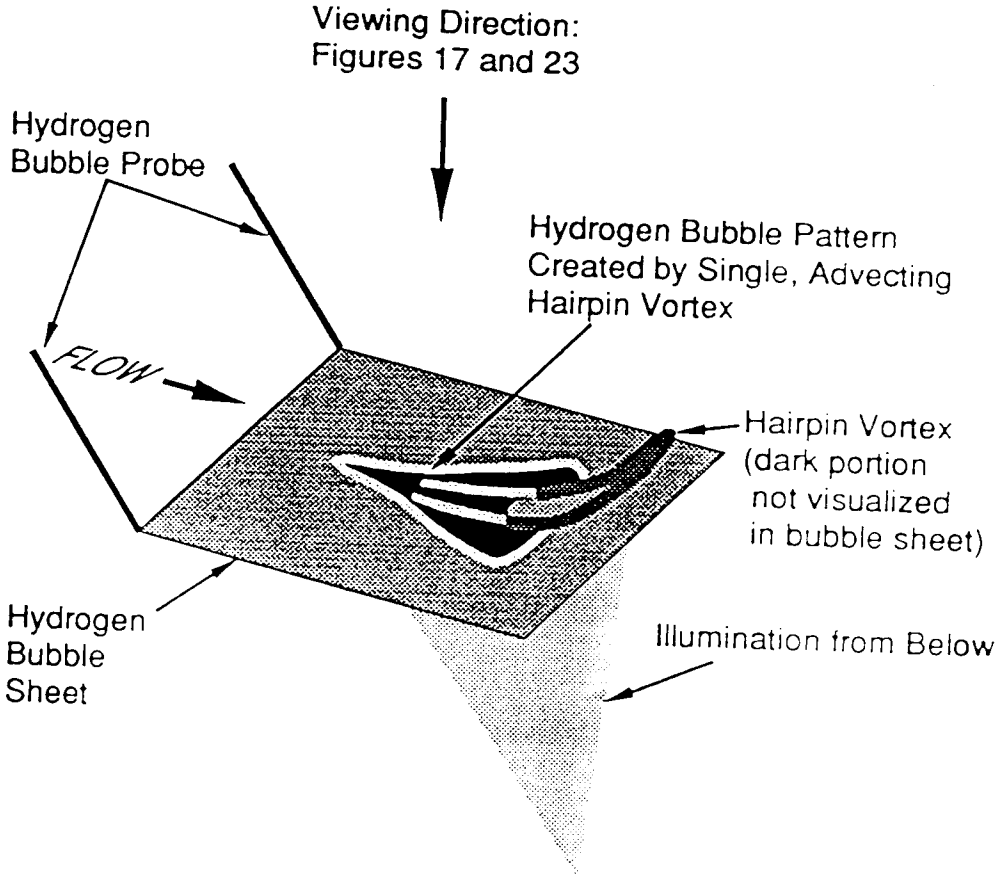

Schematic diagram of technique employed to visualize flow development associated with a single hairpin vortex

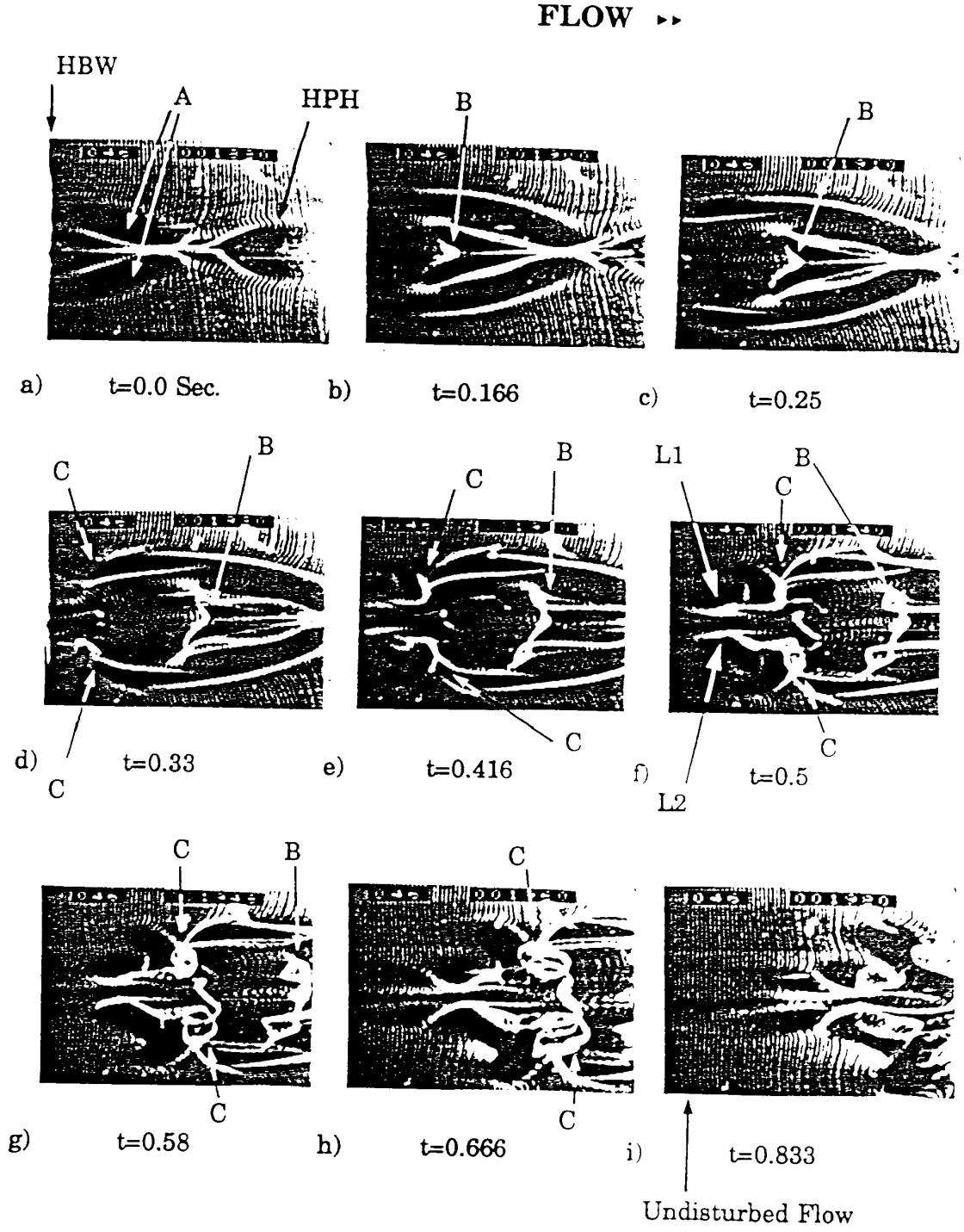

Plan-view hydrogen bubble wire visualization sequence illustrating the development of secondary vortices near the surface as a primary hairpin vortex passes a fixed streamwise location. HBW denotes the position of the hydrogen bubble wire, HPH is the location of head of primary vortex, A the location of the trailing legs of primary vortex, B the development of a secondary vortex behind head of primary, C the development of secondary vortices adjacent to the legs of the primary vortex, and L1,L2 the legs nearest the symmetry plane for the secondary vortices indicated by C.

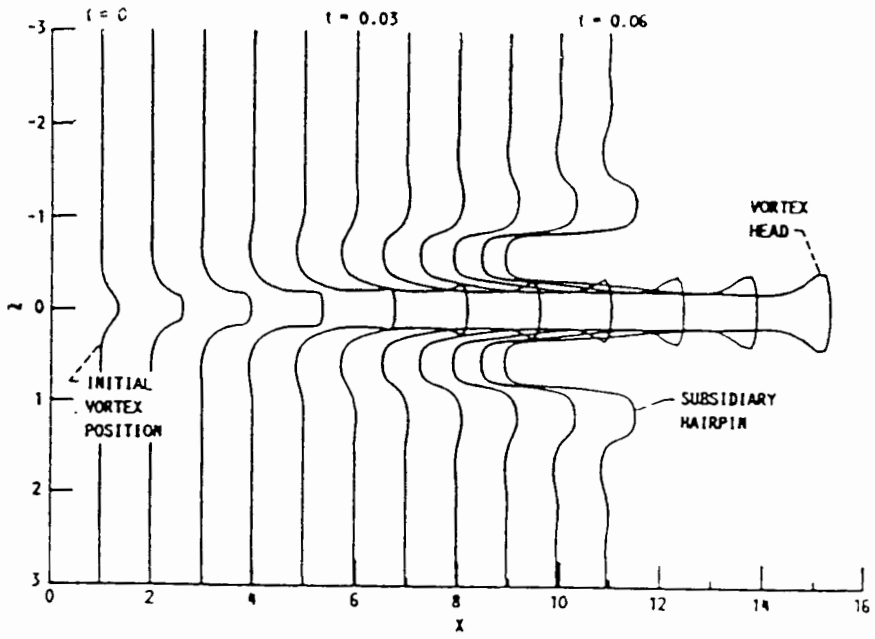

(a) TOP VIEW.

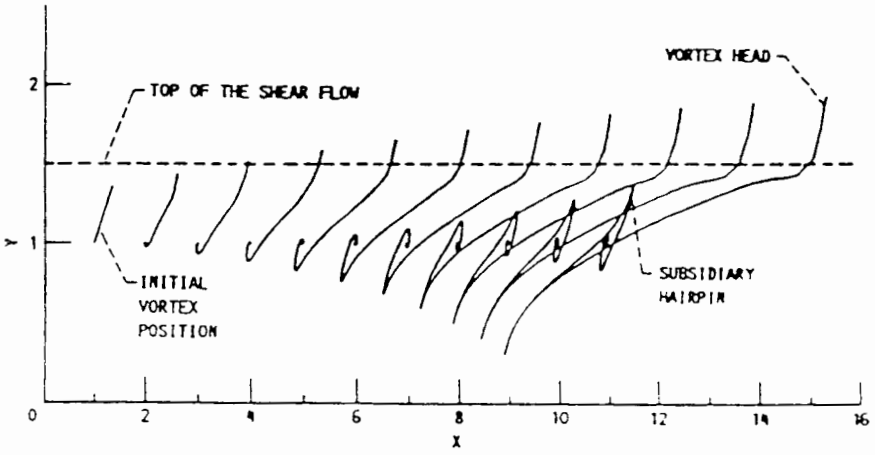

(b) SIDE VIEW.

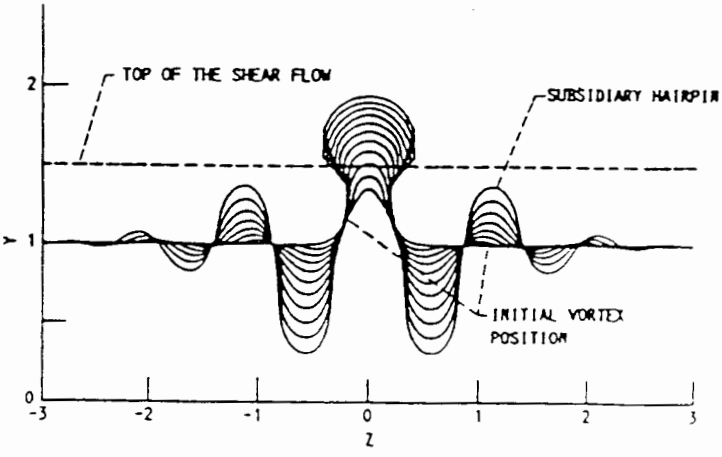

(c) END VIEW.

FIGURE 4. - TEMPORAL DEVELOPMENT FOR A HAIRPIN VORTEX IN A SHEAR FLOW; THE VORTEX POSITION IS PLOTTED EVERY 30 TIME STEPS ($\Delta t = 0.0002$).

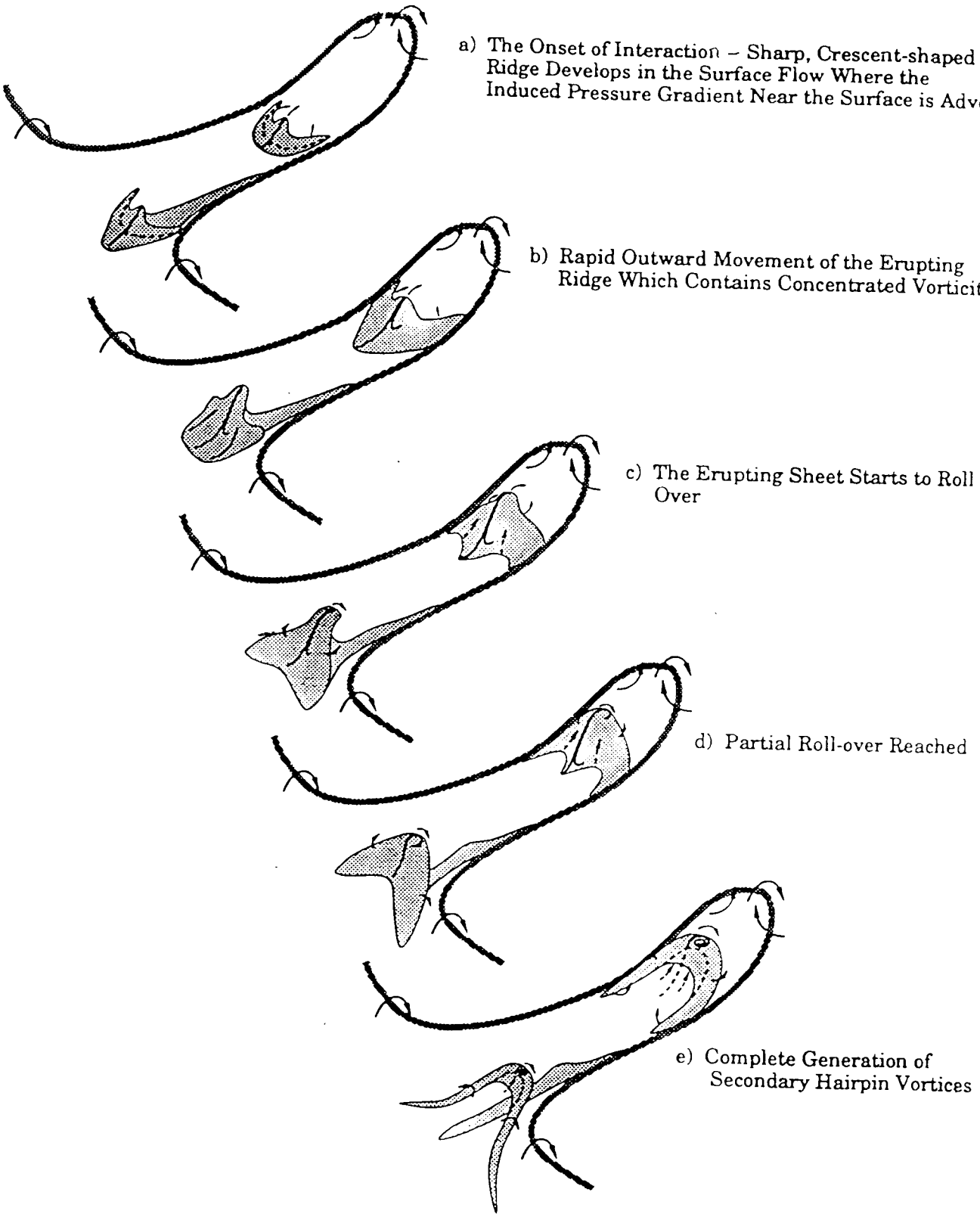

The generation of secondary vortices via surface interaction for a symmetric hairpin vortex

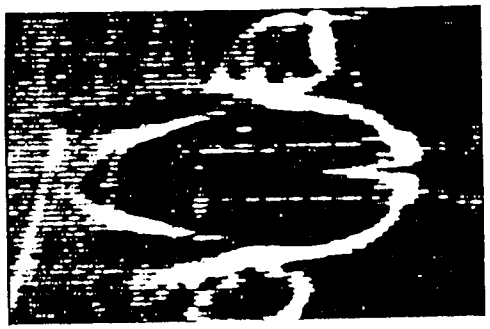

b') x=7.0 cm
y=0.25 cm

Turb. Spot (T.E.)

b) x=1.0 cm
y=0.39 cm

Single Hairpin Vortex

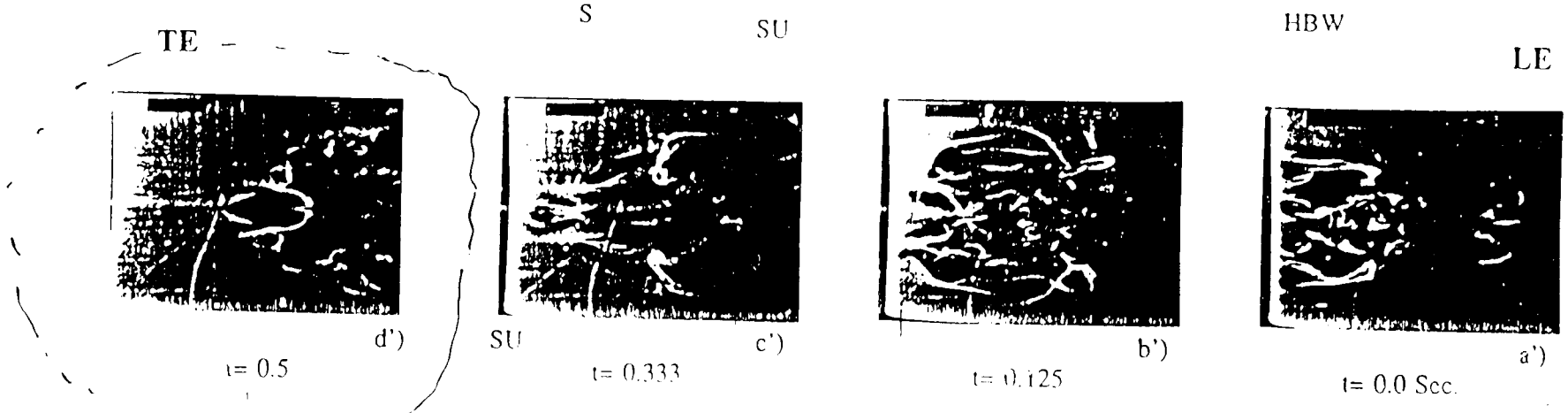

Effect of Reynolds number on the growth to a turbulent spot, as visualized by hydrogen bubbles. a) through d) $Re_{\delta 1}^{*}$=440, a') through d') $Re_{\delta 2}^{*}$=530.

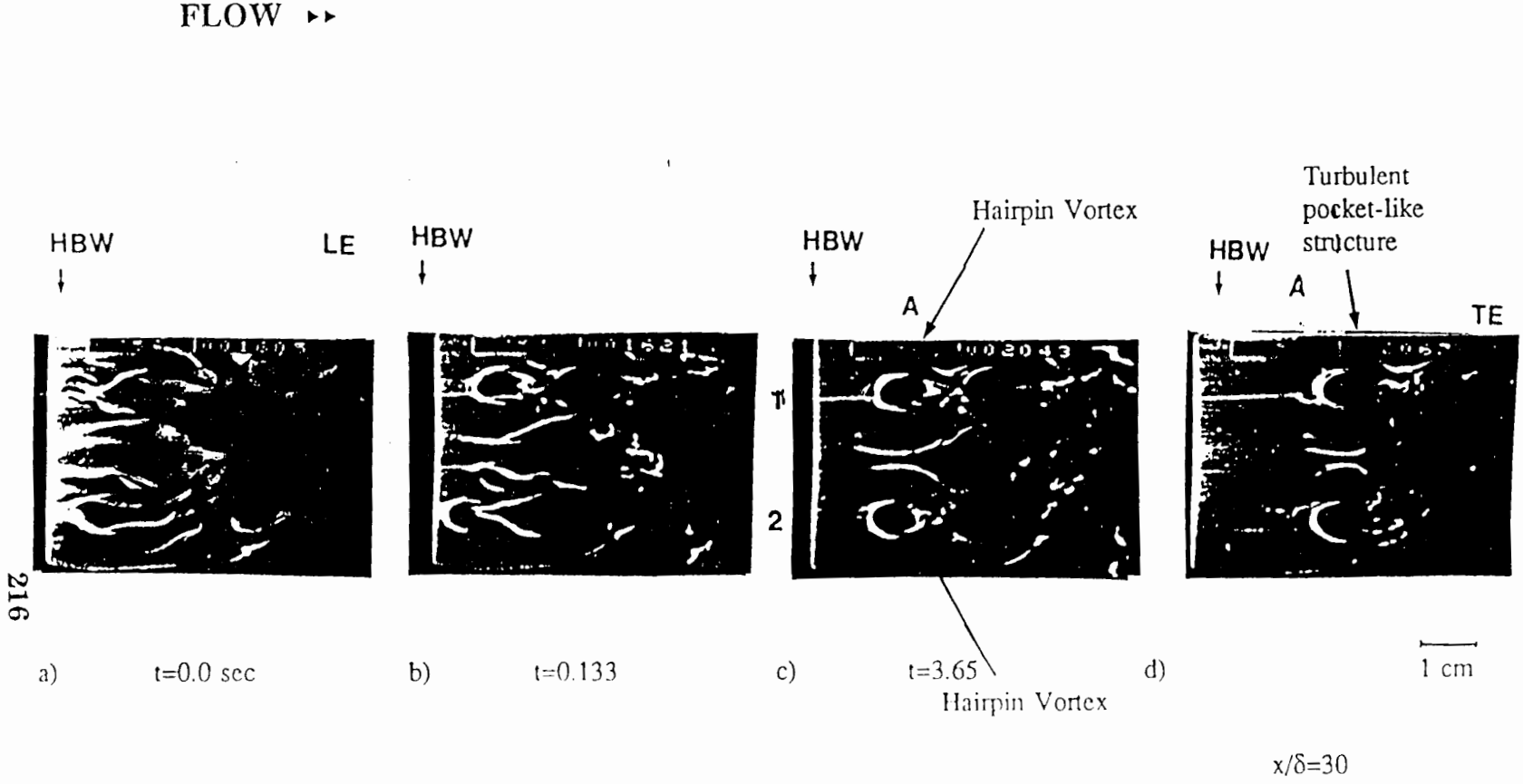

Plan-view sequence of hydrogen bubble visualization within a turbulent spot structure, illustrating the existence of hairpin vortices. Re_{δ}^{*}=440, Re_{Vw}=10.5, x_{wire}= 30 cm, y_{wire}= 0.635 cm.

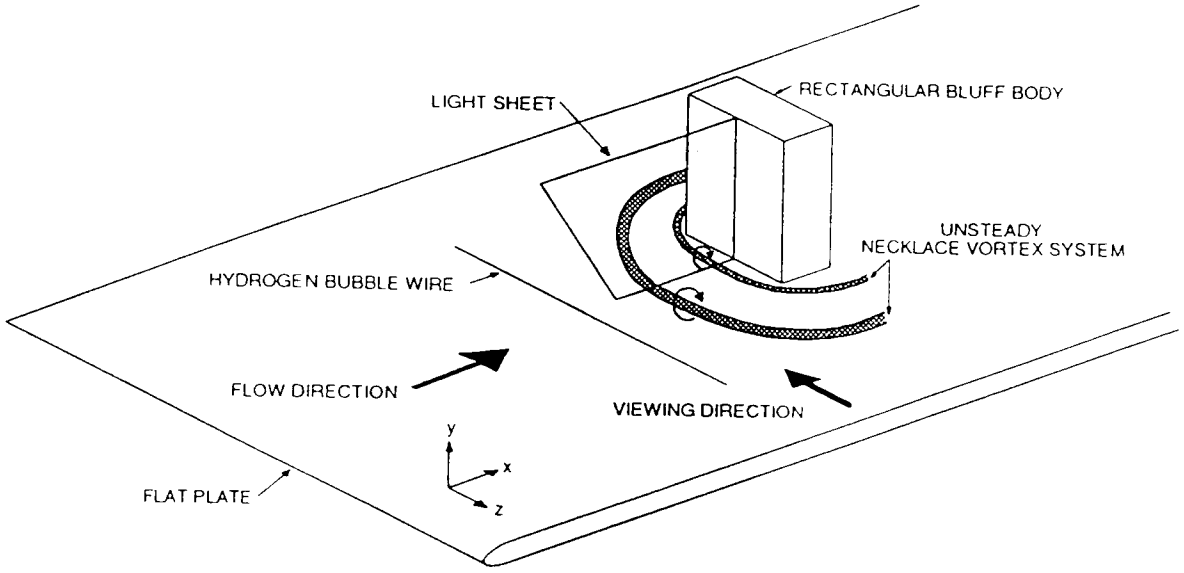

Schematic of experimental configuration

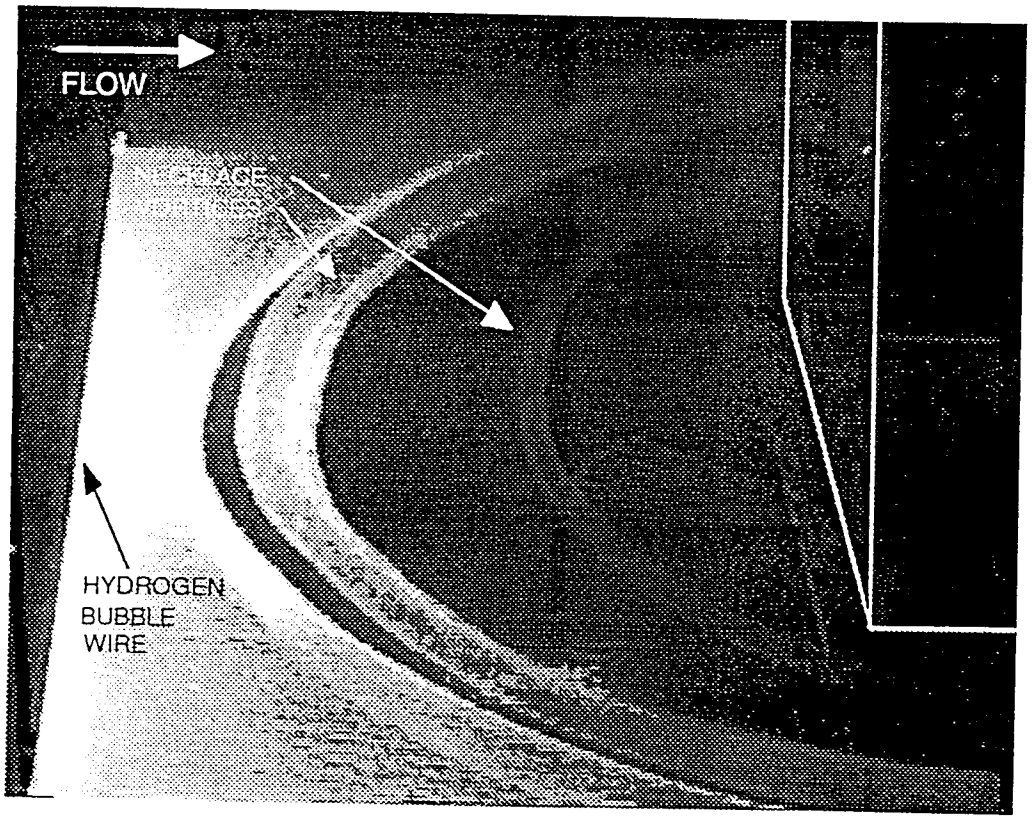

Hydrogen bubble visualization of the necklace vortex system formed at the junction of a rectangular bluff body and flat plate

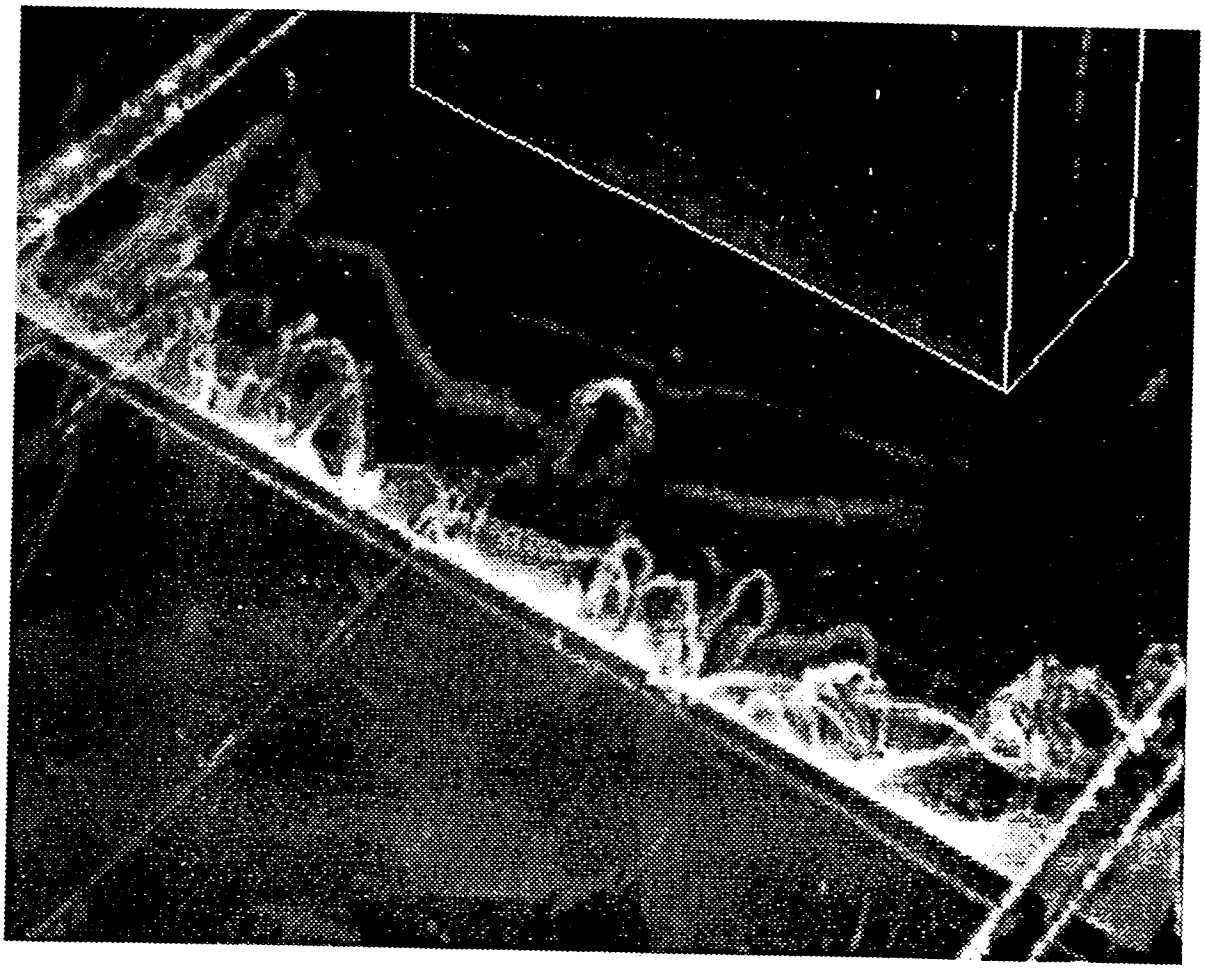

TRANSITIONAL

Revised Abstract for
End-Stage Transition Workshop
15-18 August 1993

Hairpin Vortices and the Final Stages of Transition

Abstract

A spatially developing direct numerical simulation has been performed for flow over a flat plate that is subjected to a one-time fluid injection through an elongated slit in the wall. The flow parameters have been chosen to closely approximate the experimental conditions of Haidari, Taylor, and Smith (AIAA-89-0964). A hairpin vortex quickly develops near the upstream end of the slit, and a pair of necklace vortices form around the slow-moving injected fluid. As seen in the experiments and reported in Haidari and Smith (in review, *JFM*), the hairpin vortex spawns both in-line and sidelobe secondary vortices. However, no subsidiary vortices (those formed by the inviscid deformation of a vortex-line bundle) are observed. At later times, a set of three different types of vortices are identified: hairpin vortex structures with heads that rise away from the wall, horseshoe-shaped vortices that do not rise out of the boundary layer, and quasi-streamwise vortices. These structures interact with each other and with the wall layer to generate new vortices that are similar in structure to those mentioned above, although a particular parent vortex may have an offspring that more nearly resembles another member of the set. Perturbation velocity and vertical vorticity contours reveal an arrowhead shape of the highly disturbed region that is reminiscent of a turbulent spot. Spatially averaged velocity profiles in the highly disturbed area are nonlaminar, but as yet do not show typical law-of-the-wall behavior.

Bart Singer
Fax: (804) 864-6134
E-mail: b.a.singer@larc.nasa.gov

NASA/CP—2007-214667

HAIRPIN VORTICES
and the
FINAL STAGES OF TRANSITION

Bart A. Singer

Acknowledgments

Ron Joslin,
Surya Dinavahi, Craig Streett,
Mary Adams

NUMERICS

- **Main Points**
  - Spatially developing direct numerical simulation
  - Buffer domain technique used for outflow conditions
  - Stretched vertical and streamwise grid
- **Other Details**
  - Compact differences for velocity in streamwise direction
  - Chebyshev series expansion in wall-normal direction
    - Gauss-Lobatto pts. for *u*, *v*, *w* and 2D *p*
    - Gauss pts. for 3D *p* component
  - Fourier cosine/sine series in spanwise direction
  - Fractional time-step splitting
    - Crank-Nicolson implicit for normal diffusion terms
    - Runge-Kutta explicit for all other terms
    - Influence-matrix technique for the 2D pressure component
    - Direct solves for the 3D pressure component

SUMMARY

- What's Old?
  - Injection produces hairpin vortex
  - Additional vortex heads appear where legs converge
  - Necklace vortex develops around injected flow
  - Flow becomes increasingly complex
  - Disturbed region takes on arrowhead shape like turbulent spot

- What's New?
  - Regenerative processes
    * New hairpin vortices appear
    * Subsidiary horseshoe vortices form under other vortices
    * Quasi-streamwise vortices form under other vortices
  - Turbulent spot development length is long
    * Highly intermittent (large velocity gradients) from start
    * Fully turbulent characteristics require more distance

Figure 1: Schematic of computational domain and injection slot. The solid black region along the symmetry line shows the location of the injection slot. The schematic in (b) shows the vertical velocity distribution along the symmetry line during times of maximum injection ($0.5 \leq t \leq 4.5$). The view on the lower left illustrates the spanwise distribution of vertical velocity. The Reynolds numbers are based on the local displacement thickness. Lengths are nondimensionalized on the displacement thickness at $Re_{\delta^*} = 530$.

Figure 2: Side view of isopressure surfaces at $t = 15.0$. Total velocity vectors on the centerline upstream of the injection slot are illustrated on the left. The thin black horizontal line represents the region over which fluid injection occurred. A streamline starting just upstream of the injection region spirals around a streamwise elongated low pressure region.

Figure 3: Looking downstream at primary and secondary high-pressure regions at $t = 21.75$. Cross-stream velocity vectors at $x = 55.4$.

Figure 4: Streamwise velocity profile at $x = 65.2$, $t = 15.0$. The Blasius profile at the same location is included for comparison.

Figure 5: Side view of high- and low-pressure regions ($p = \pm 0.035$) at $t = 35.70$. The low-pressure region resembles a hairpin vortex. The Blasius velocity profile is shown on the left. The downstream end of the hairpin vortex is at $x = 65.7$; the velocity profile is at $x = 56.9$.

Figure 6: Side view of high- and low-pressure regions ($p = \pm 0.035$) at $t = 50.25$. The Blasius velocity profile is shown on the left. The low-pressure zones show the primary hairpin vortex, a secondary vortex head, and a subsidiary vortex forming underneath each vortex leg. The downstream end of the hairpin vortex is at $x = 76.5$; the velocity profile is at $x = 64.3$.

Figure 7: Downstream view of low-pressure regions ($p = -0.035$) at $t = 50.25$. The surfaces are somewhat transparent so that perturbation velocity vectors at $x = 71.8$ can be seen.

Figure 8: Downstream view of high- and low-pressure regions ($p = \pm 0.035$) at $t = 50.25$. Perturbation velocity vectors at $x = 67.3$ are shown.

Figure 9: Plan view of high- ($p = 0.03$) and low-pressure ($p = -0.035$) regions at $t = 80.70$. The downstream edge of the vortex head is at $x = 94.0$. The upstream end of the high-pressure region is at $x = 80.5$.

Figure 10: Plan view of high- ($p = 0.02$) and low-pressure ($p = -0.035$) regions at $t = 97.20$. The downstream edge of the vortex head is at $x = 103.6$. The upstream end of the high-pressure region is at $x = 88.6$.

Figure 11: Side view of high- ($p = 0.02$) and low-pressure ($p = -0.035$) regions at $t = 97.20$. The Blasius profile is shown at the left at $x = 86.9$.

Figure 12: Plan view of high- ($p = 0.02$) and low-pressure ($p = -0.035$) regions at $t = 153.10$. The downstream edge of the vortex is at $x = 147.7$. The upstream end of the high-pressure region is at $x = 120.2$. The numbers indicate the order of appearance of the quasi-streamwise vortices.

Figure 13: Side view of low-pressure ($p = -0.035$) regions at $t = 153.10$. The Blasius profile is shown at the left at $x = 120.7$.

Figure 14: Plan view of the magnitude of perturbation streamwise velocity (bottom) and vertical vorticity (top) at $t = 150.10$, $y = 2.41$. The enveloping contours are $0.02U_0$ and $0.02U_0/\delta_0^*$ respectively. Contour increments are $0.05U_0$ for the velocity and $0.10U_0/\delta_0^*$ for the vorticity. The horizontal lines indicate the locations where $z = \pm 0.25$, i.e. the locations for the side views in the following figure.

Figure 15: Side view of the magnitude of perturbation streamwise velocity (bottom) and vertical vorticity (top) along $z = 0.25$ at $t = 150.10$. The enveloping contours are $0.02U_0$ and $0.02U_0/\delta_0^*$ respectively. Contour increments are $0.05U_0$ for the velocity and $0.10U_0/\delta_0^*$ for the vorticity. The horizontal lines on the bottoms indicate the wall locations. Velocity vectors appear at the left. The horizontal line extending beyond the velocity vectors indicates the position where $y = 2.41$, i.e. the location for the plan views in the previous figures.

Figure 16: Locally averaged ($120 \leq x \leq 132$, $|z| \leq 3.0$) profile in wall units at $t = 158.30$.

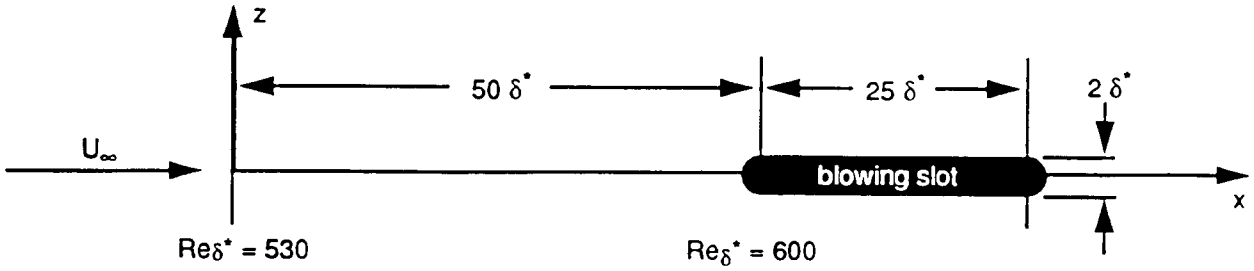

(a)

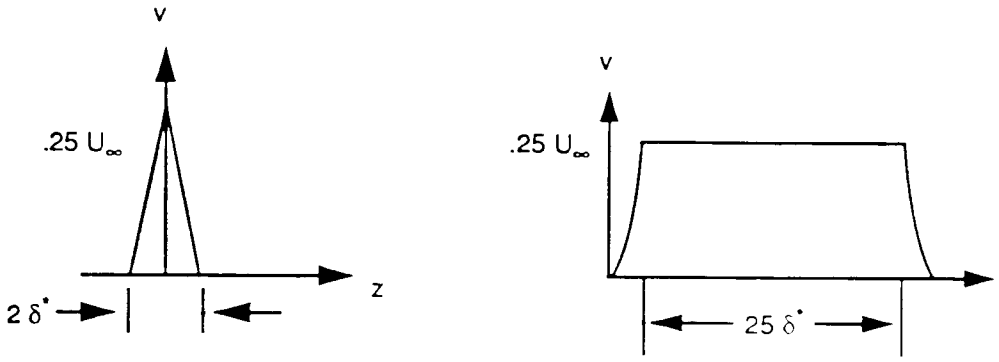

(b)

Fig 1

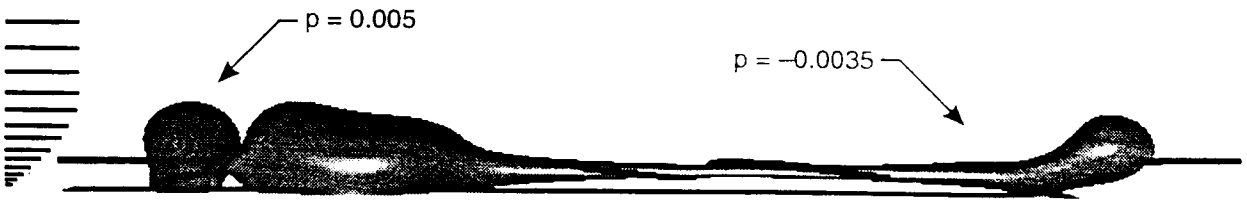
p = 0.005
p = –0.0035

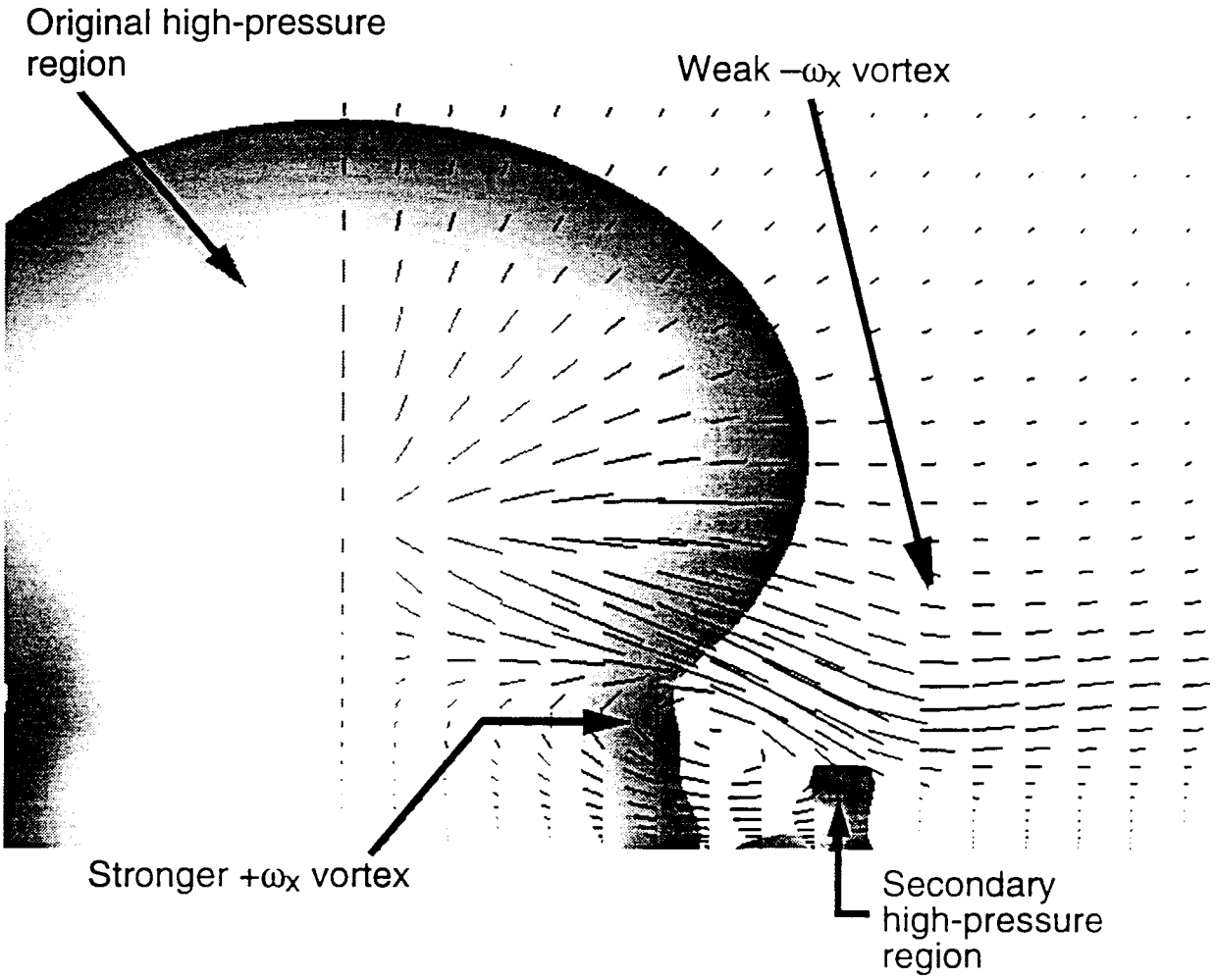
Original high-pressure region
Weak $-\omega_x$ vortex
Stronger $+\omega_x$ vortex
Secondary high-pressure region

Fig 3

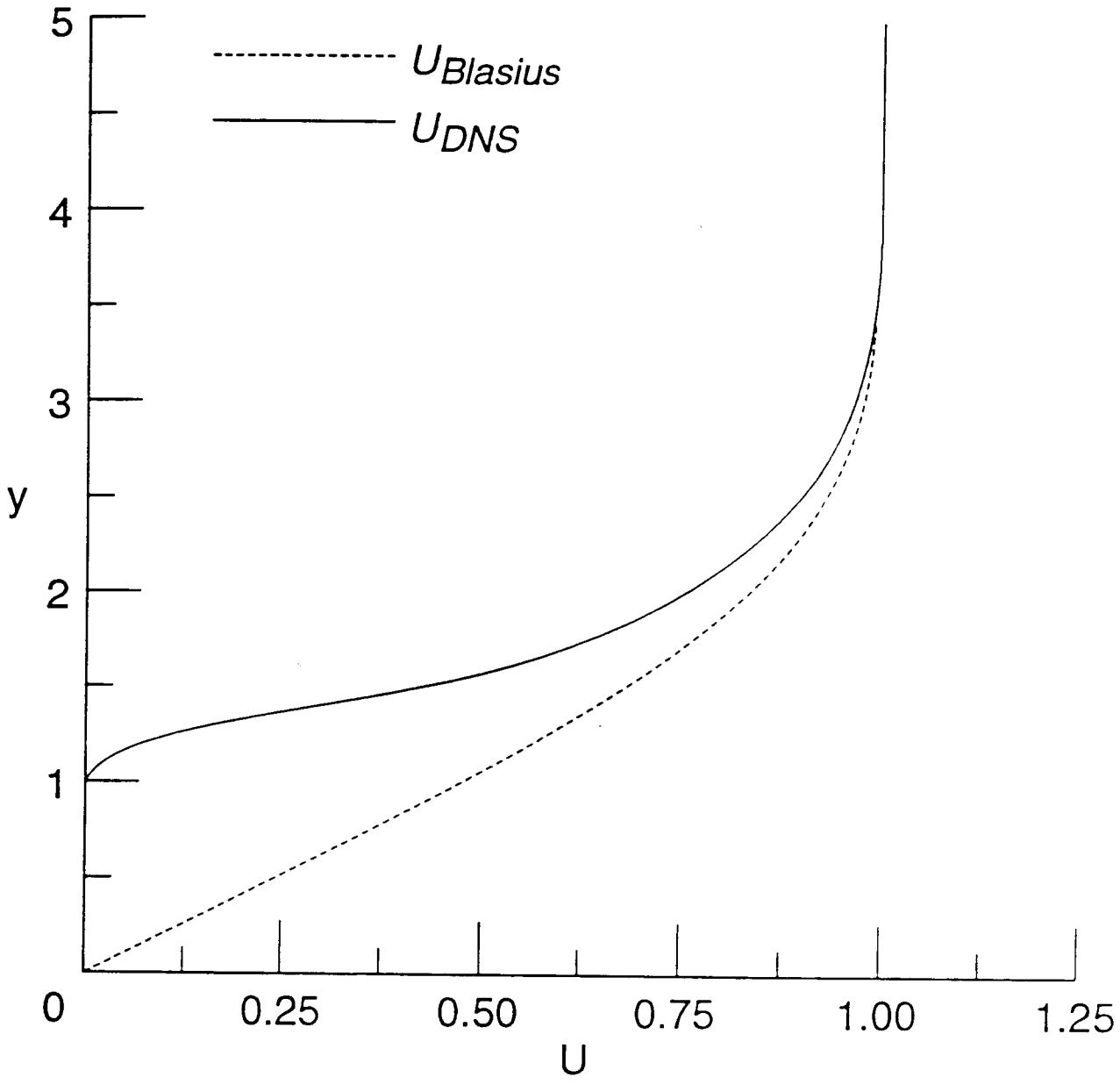

fig 4

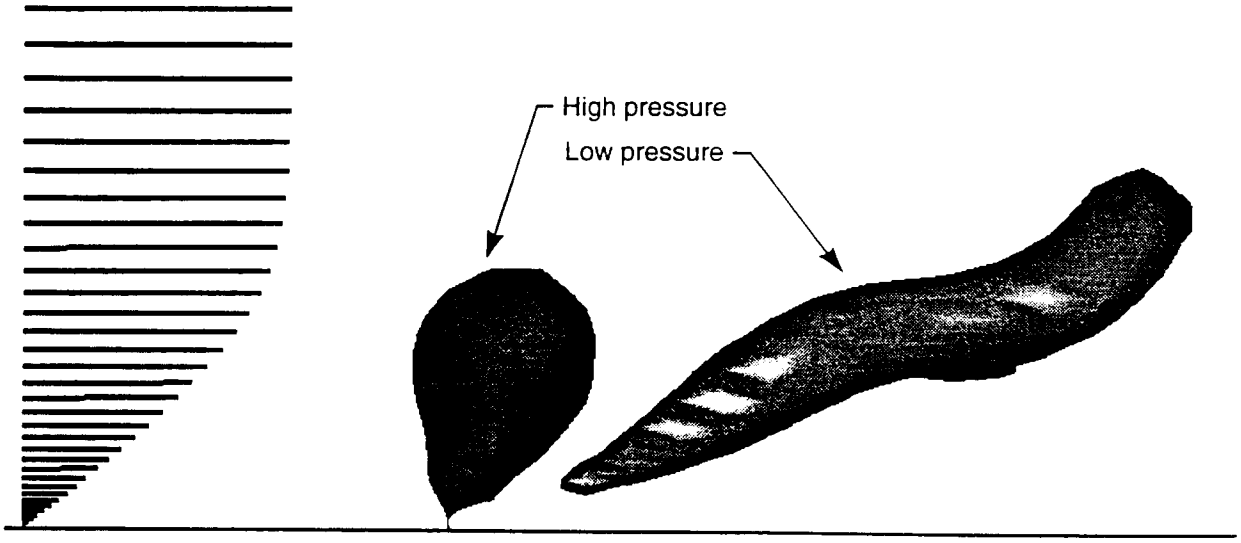

fig 5

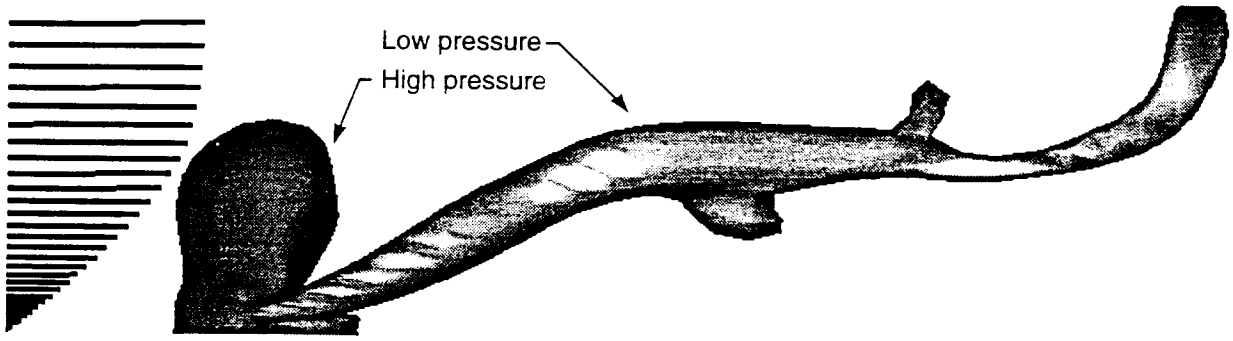
Low pressure
High pressure

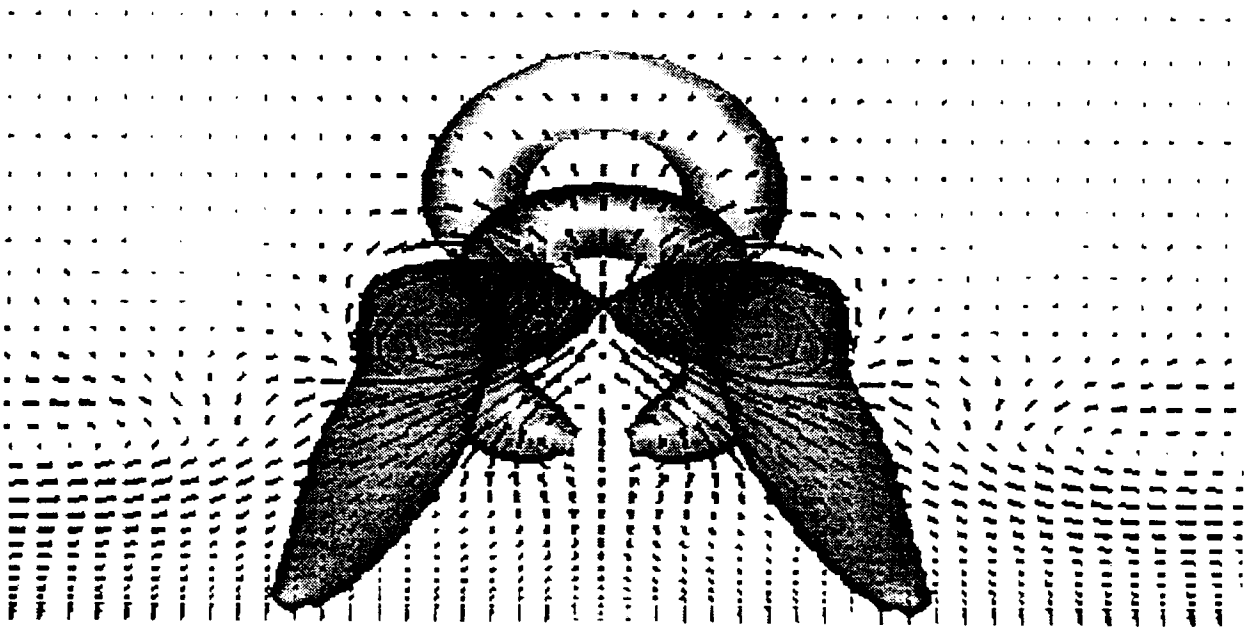

fig 7

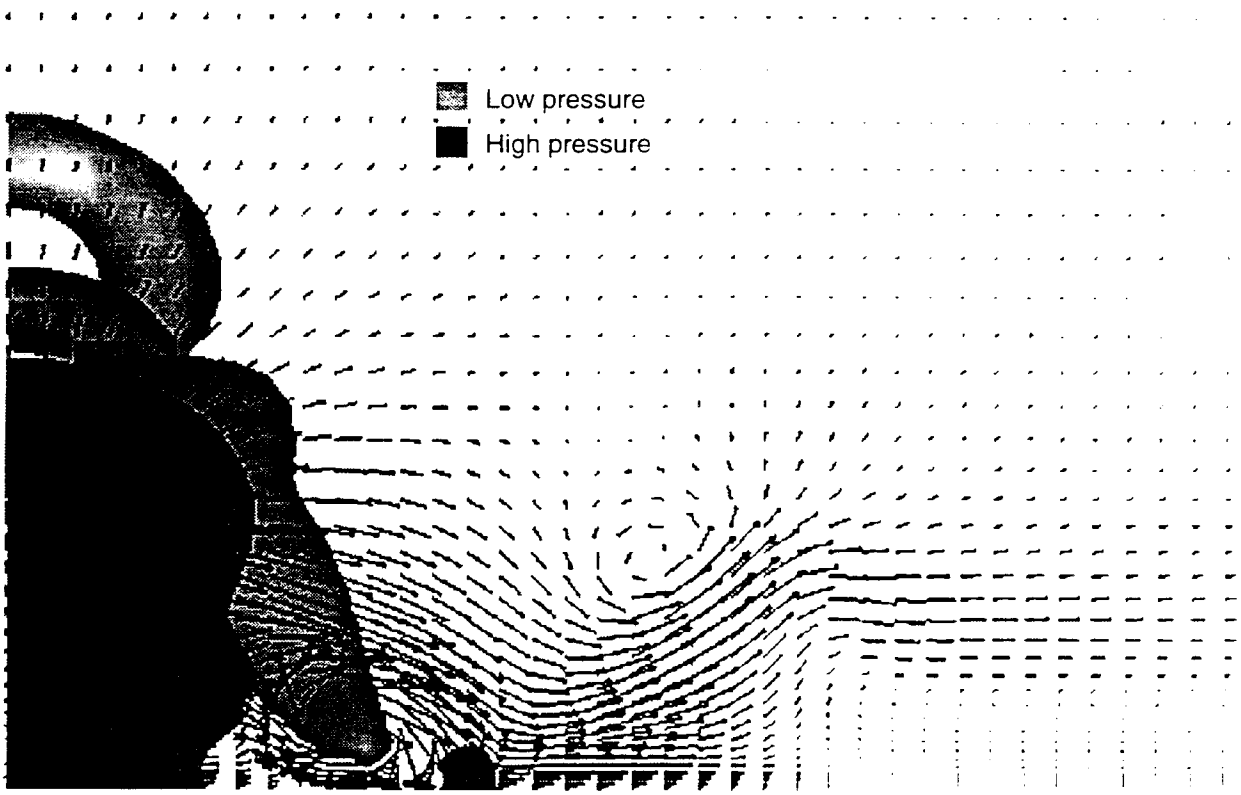

fig 8

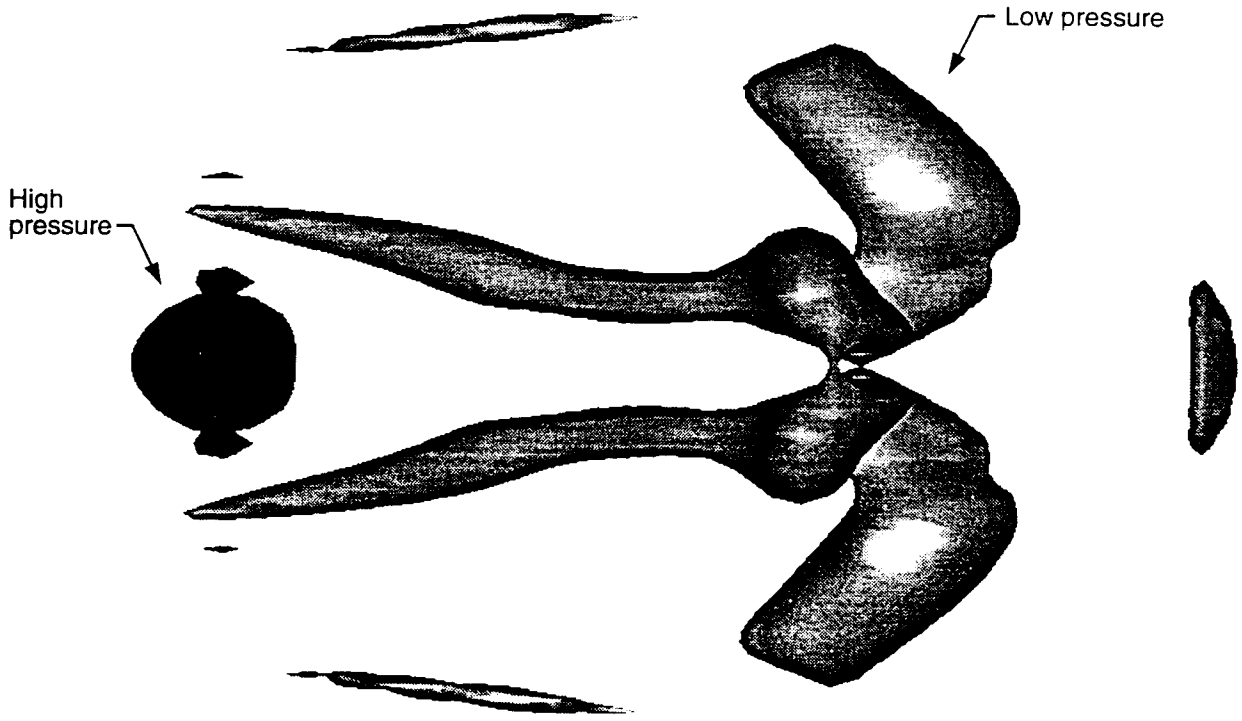

fig9

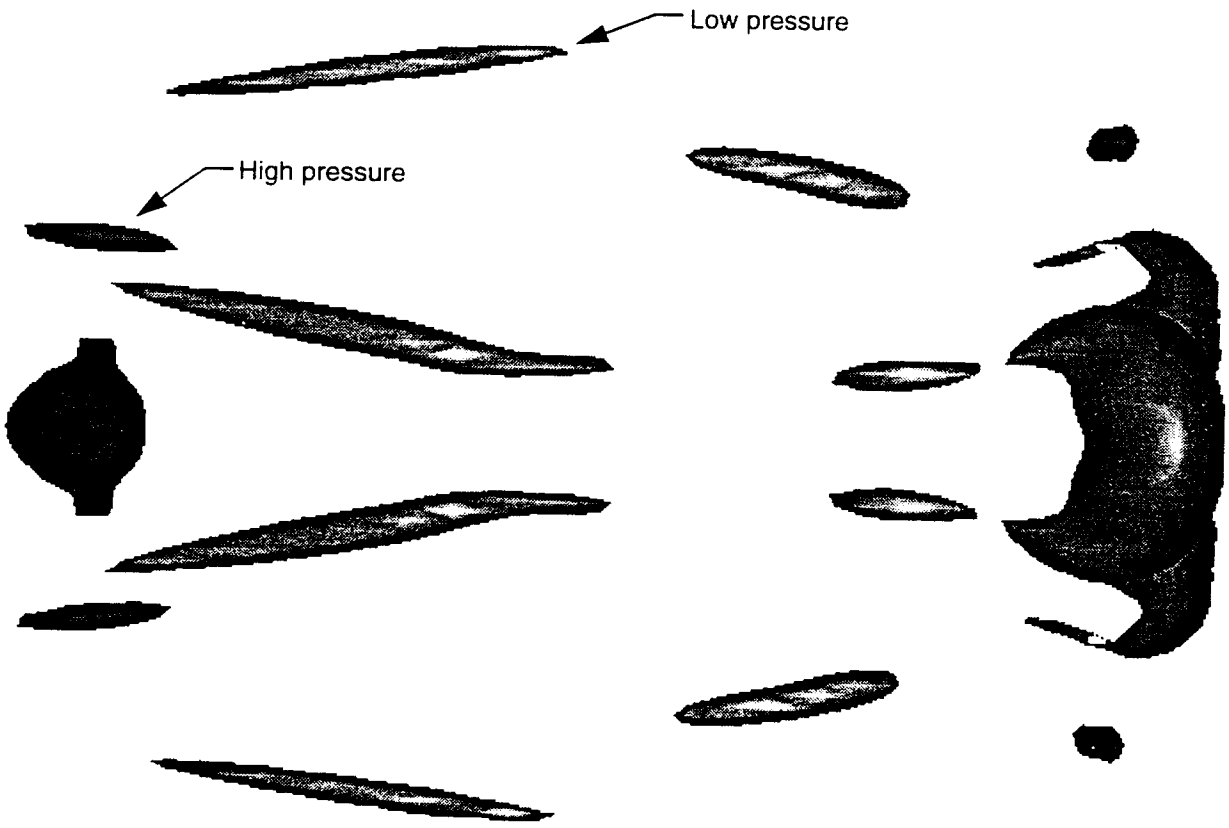

fig10

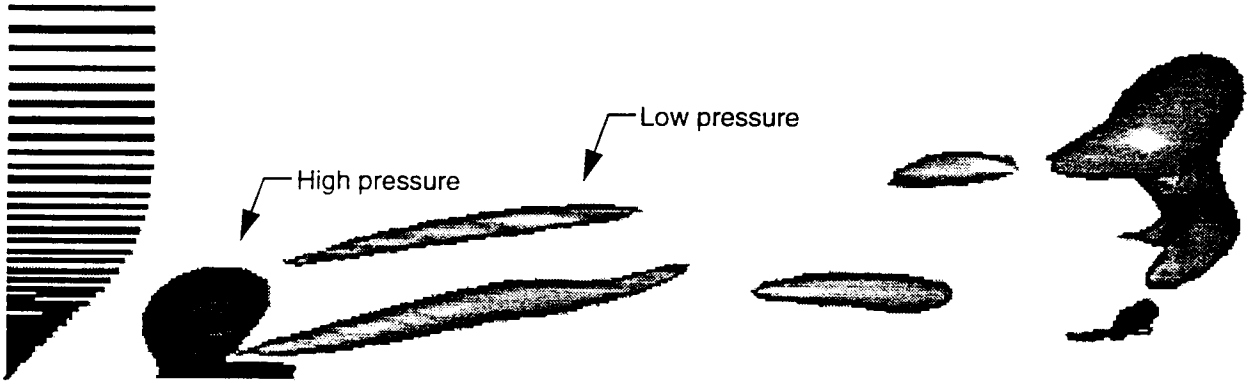

fig11

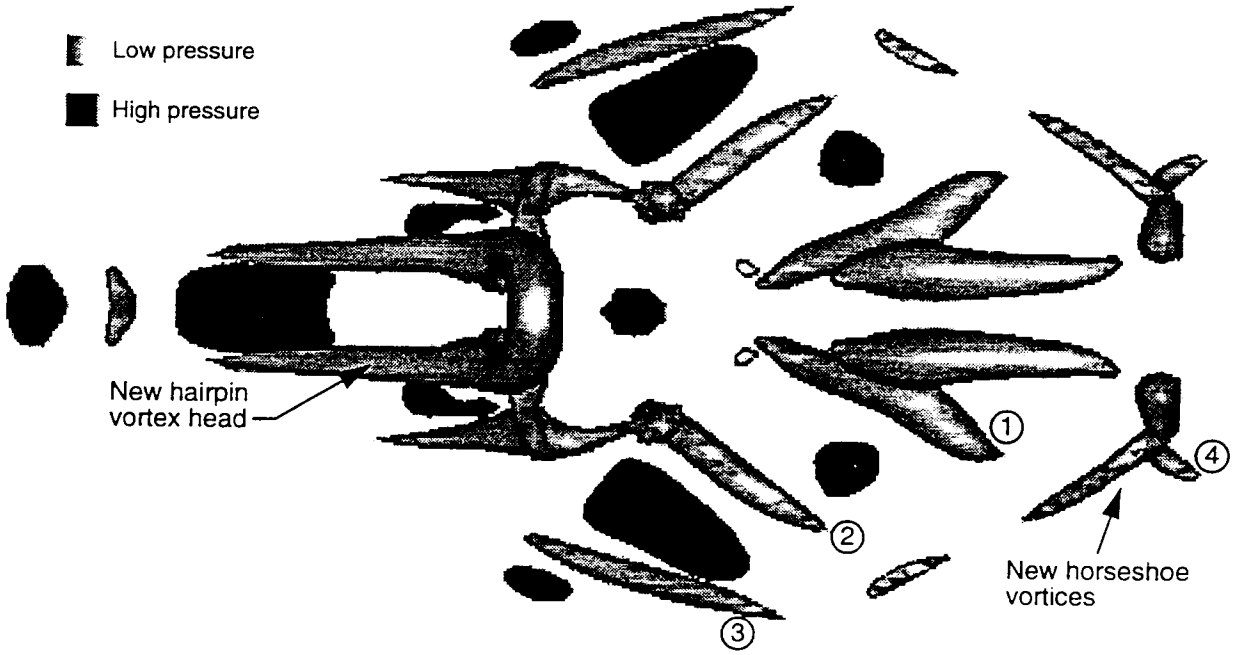
Low pressure
High pressure
New hairpin
vortex head
1
2
3
4
New horseshoe
vortices

fig 12

fig 13

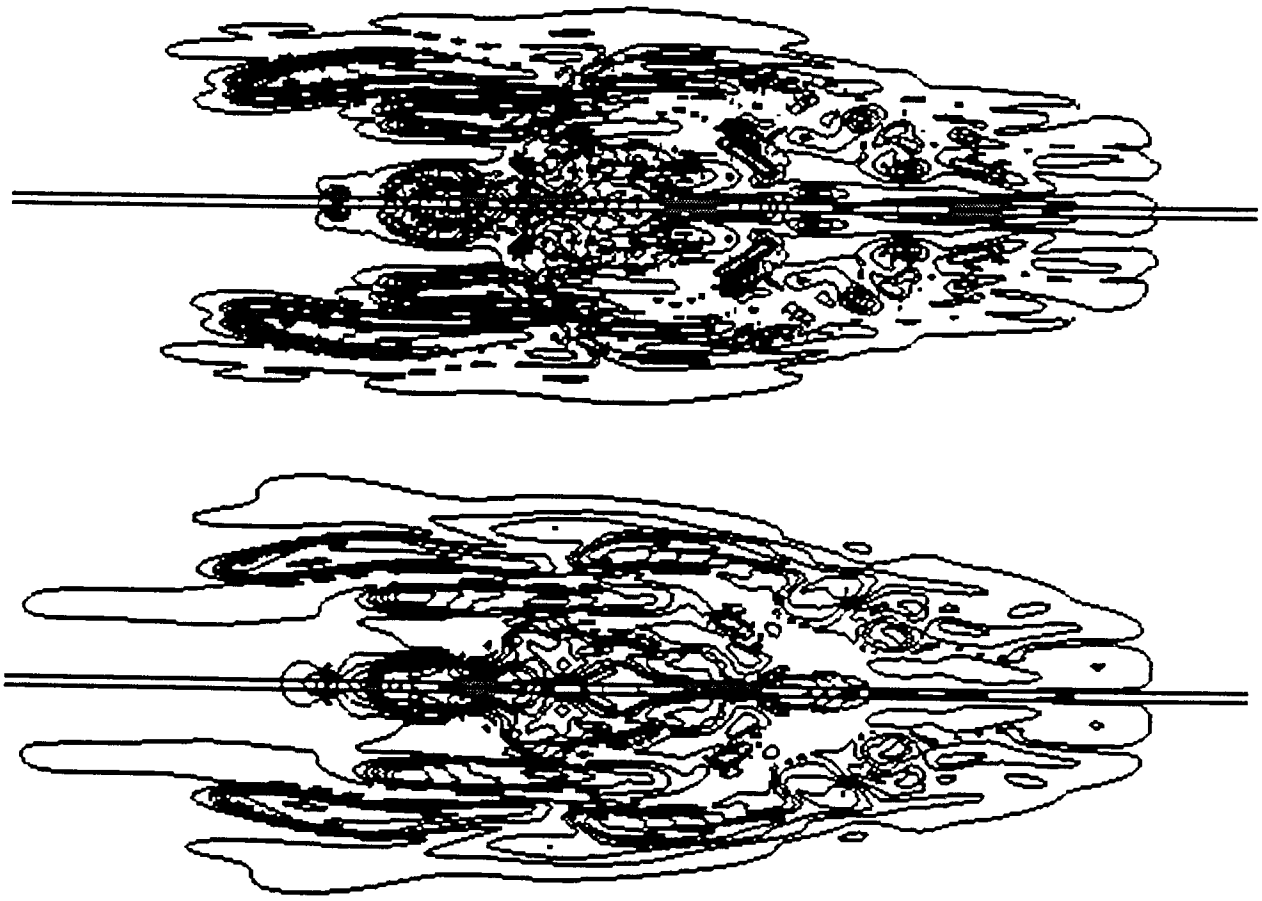

fig 14

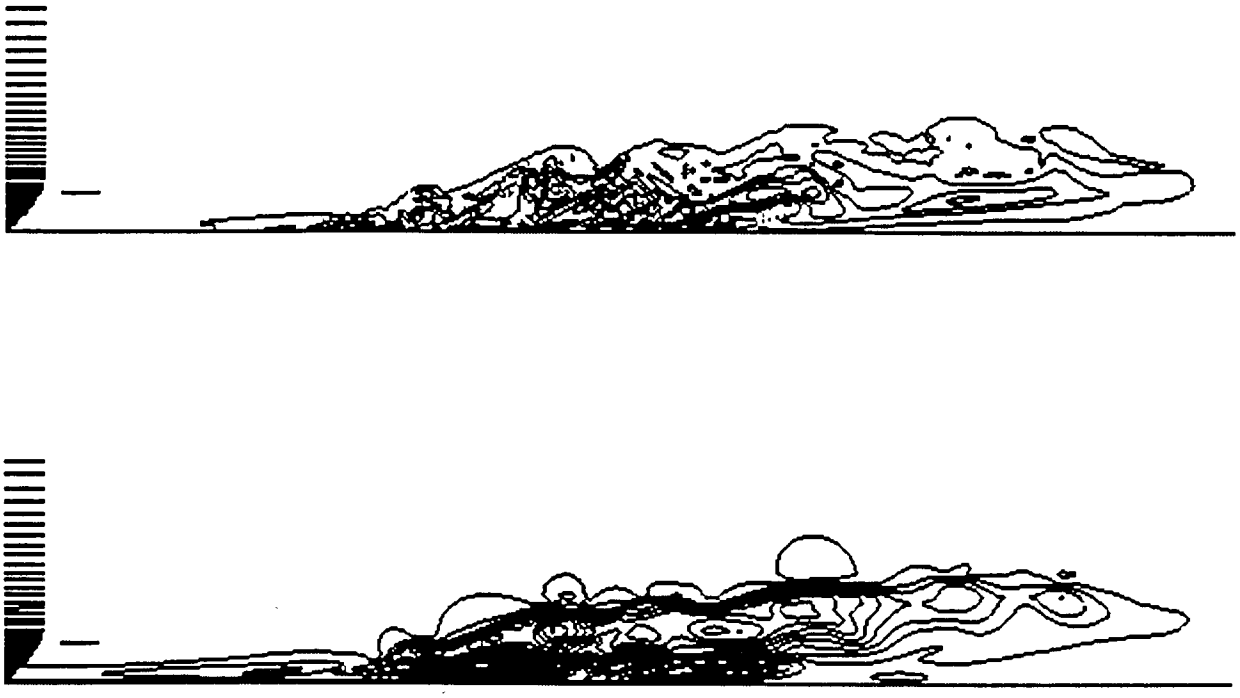

fig 15

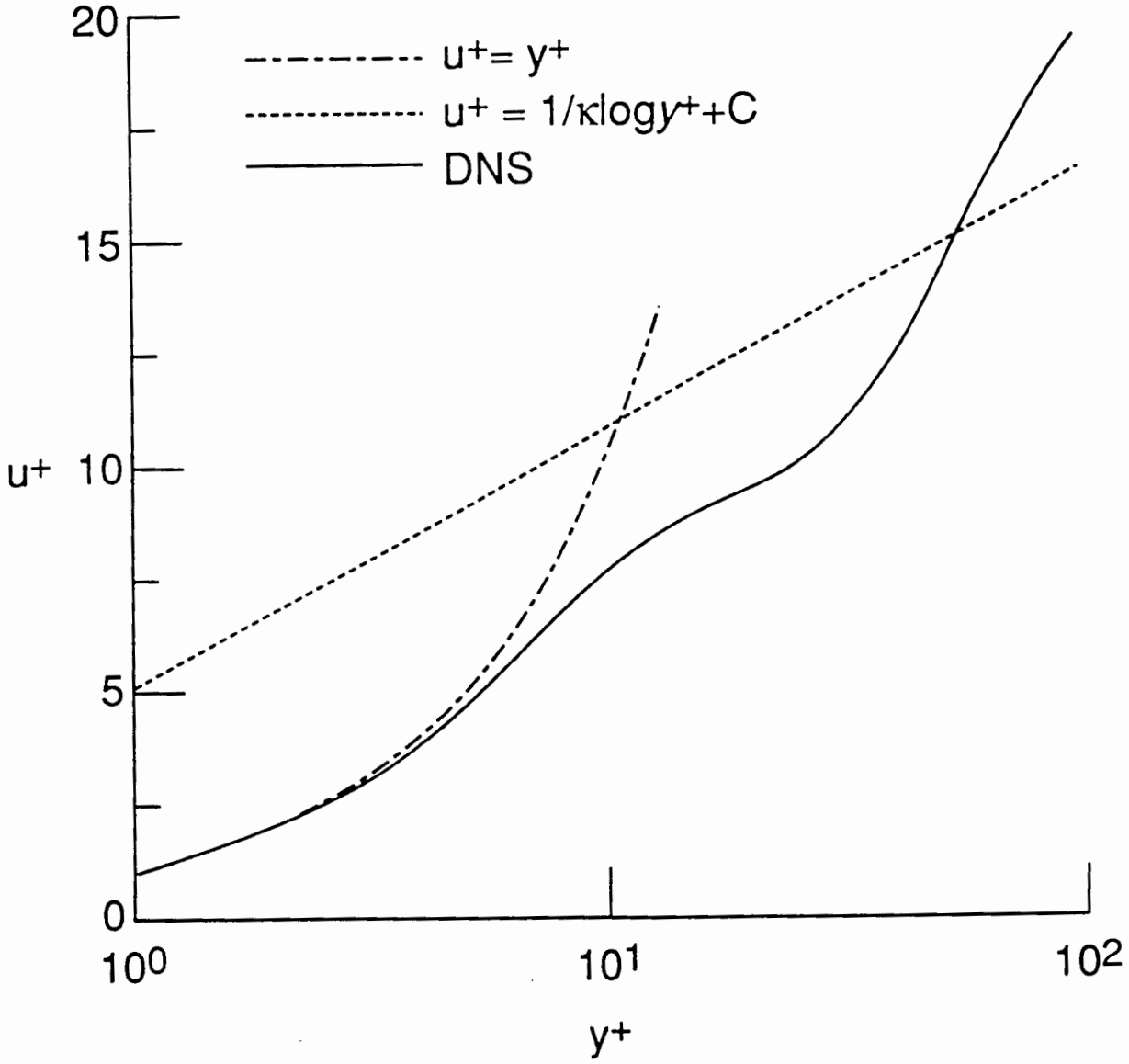

fig 16

ASPECTS OF TRANSITION IN TURBOMACHINES*

H.P. Hodson
Whittle Laboratory
University of Cambridge
UK

ABSTRACT

This talk provides a description several types of transition encountered in turbomachines. It is based largely on personal experience of the detection of transition in turbomachines. Examples are taken from axial compressors, axial turbines and radial turbines. The illustrations are concerned with transition in steady and unsteady boundary layers that develop under the influence of two-dimensional and three-dimensional flow fields.

Studies of transition in turbomachines are usually compromised since they are difficult to conduct in realistic environments. The physical size of the airfoils, the time-scales of phenomena, problems of accessibility and cost all conspire against the experimentalist. Yet, transition is known to be affected by many parameters and several causes may simultaneously compete to bring about transition in any one given situation in a turbomachine. In addition, the same apparent cause can give rise to different modes. Uncertainty therefore surrounds the measurement of transition onset and the measurement of the transition zone. This undoubtedly hinders the continuing search for improved turbomachine designs. Furthermore, it is argued that while less complex simulations must continue to be used to further understanding and knowledge of transition in turbomachines, experiments must be conducted in realistic environments. Such studies should include investigations of the nature of transition and of the various causes. Once the nature of the processes is better understood, specific problems regarding the origin of the transitional flow and its development may be addressed with confidence. One of the most important outcomes of this research should be the implementation of appropriate physical models of transition in current and future numerical calculation schemes.

---

* Presented at Workshop on "End stage boundary layer transition", Syracuse University, Aug. 1993

REFERENCES

Addison, J.S., 1990, "Wake-boundary layer interaction in axial turbomachinery", Ph.D. Thesis, Cambridge University

Arndt, N., 1991, "Blade row interaction in a multistage low-pressure turbine", ASME paper 91-GT-283.

Banieghbal, R. and Hodson, H.P., 1991, to be published

Dong, Y. and Cumpsty, N.A., 1989, "Compressor Blade Boundary Layers: Part I; Test Facility and Measurements with No Incident Wakes; Part II; Measurements with Incident Wakes," ASME Papers 89-GT-50 and 89-GT-51.

Harrison, S., 1989, "Secondary loss generation in a linear cascade of high-turning turbine blades", ASME paper 89-GT-47

Hodson, H.P., Banieghbal, M.R., and Dailey, G.M., "3-Dimensional Interactions in the Rotor of an Axial Turbine", Paper AIAA-93-2255, AIAA/SAE/ASME/ASEE 29th Joint Propulsion Conference & Exhibit, Monterey Ca, 1993

Hodson, HP, and Dominy RG, 1987, "The Off-Design of a Low Pressure Turbine Cascade", ASME Jnl Turbomachinery, April 1987, pp 201-209

Hodson, HP, Addison, JS and Shepherdson, C.A., 1992, "Models for Unsteady Wake-Induced Transition in Axial Turbomachines", Jnl de Physique, Vol. 2, No. 4, Apr, pp 545-574

Hodson, H.P., 1985, "Boundary Layer Transition and Separation near the Leading Edge of a High Speed Turbine Blade", ASME Jnl. Engineering for Gas Turbines and Power, Vol. 107, January 1985.

Hodson, H.P., 1989, "Modelling Unsteady Transition and Its Effects on Profile Loss", Proceedings, AGARD Conf. PEP 74a on Unsteady Flows in Turbomachines, AGARD CP 468

Hourmouziadis, J., 1989, "Aerodynamic Design of Low Pressure Turbines," AGARD Lecture Series, 167

Huntsman, I., and Hodson, H.P. "A Laminar Flow Rotor for a Radial Inflow Turbine", Paper AIAA-93-1796 AIAA/SAE/ASME/ASEE 29th Joint Propulsion Conference & Exhibit, Monterey Ca, 1993

Pfeil, H., and Herbst, R., "Transition Procedure of Instationary Boundary Layers," ASME Paper 79-GT-128, 1979.

Pfeil, H., Herbst, R. and Schröder, T., 1982, "Investigation of Laminar-Turbulent transition of boundary layers disturbed by wakes", ASME paper No. 82-GT-124.

Schubauer, G.B., and Klebanoff, P.S., "Contributions on the Mechanics of Boundary Layer Transition," NACA TN 3489 (1955) and NACA Rep. 1289 (1956)

Speidel, L., "Beeinflussung der laminaren Grezschicht durch periodische Strörungen der Zuströmung," Z. Flugwiss. 5, Vol. 9, 1957.

GENERAL OBSERVATIONS

Studies of transition in turbomachines compromised since

- difficult to conduct in realistic environments
- often limited to less complex simulations

In turbomachines, transition

- influenced by many parameters
- may be due to one or more competing causes in a given situation

Uncertainty

- surrounds predictions of transition onset and development of transition zone
- limits improvements in technology

REYNOLDS NUMBERS IN AXIAL TURBOMACHINES

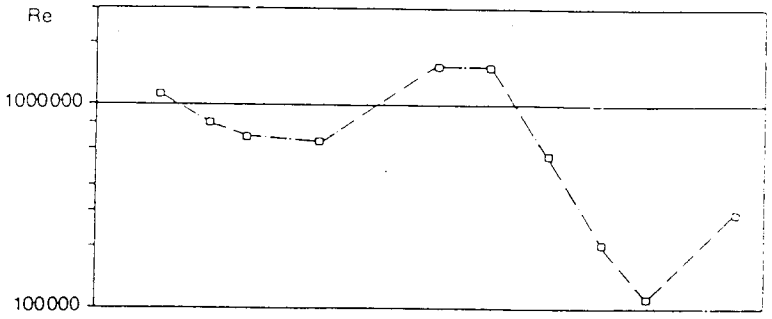

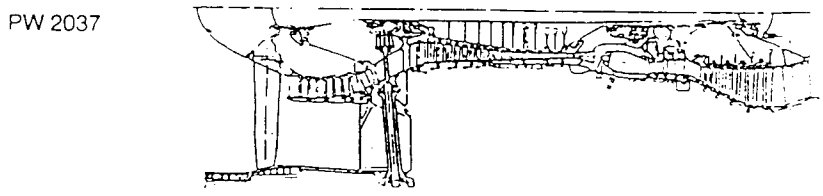

VARIATION OF REYNOLDS NUMBER IN BY-PASS ENGINE AT CRUISE
(HOURMOUZIADIS, 1989)

OBJECTIVES

- Introduce particular aspects of turbomachine transition
- Highlight some of the problems by use of examples
- Set scene for remainder of session

MOTIVATION

Problems

- Where does transition/separation occur?
- How can we model these phenomena?

Answers affect

- design of bladerow
- efficiency
- heat transfer & cooling requirements

INFLUENCES ON TRANSITION IN TURBOMACHINES

- free stream turbulence (magnitude/scale/homogeneity)
- pressure gradients
- fast (e.g., shocks) and slow (e.g., wakes) fluctuations of free stream pressure, temperature, velocity, turbulence
- separation
- film cooling
- laminarization
- rotation (Coriolis & centripetal accelerations)
- curvature
- quasi 3D effects - divergence/convergence of stream-lines
- 3-D effects - e.g., skew

WAKE INDUCED TRANSITION IN TURBOMACHINES

Wakes represent perturbations in

- Velocity
- Turbulence (typ. 3-5% max)
- Pressure .....etc.

Wakes give rise to

- premature transition

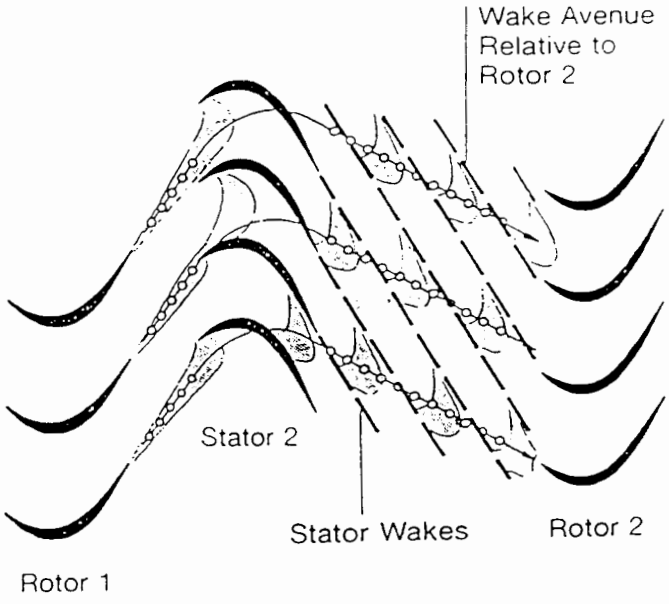

WAKES IN MULTISTAGE LP TURBINE (ARNDT)

Affects can extend beyond next bladerow

WAKE INDUCED TRANSITION IN WHITTLE LAB AXIAL TURBINE

- Turbulent 'events' more probable when wake present
- $U_{LE} \approx 0.88$xfree-stream
- $U_{TE} \approx 0.50$xfree-stream
- Like turbulent spots - but are they?

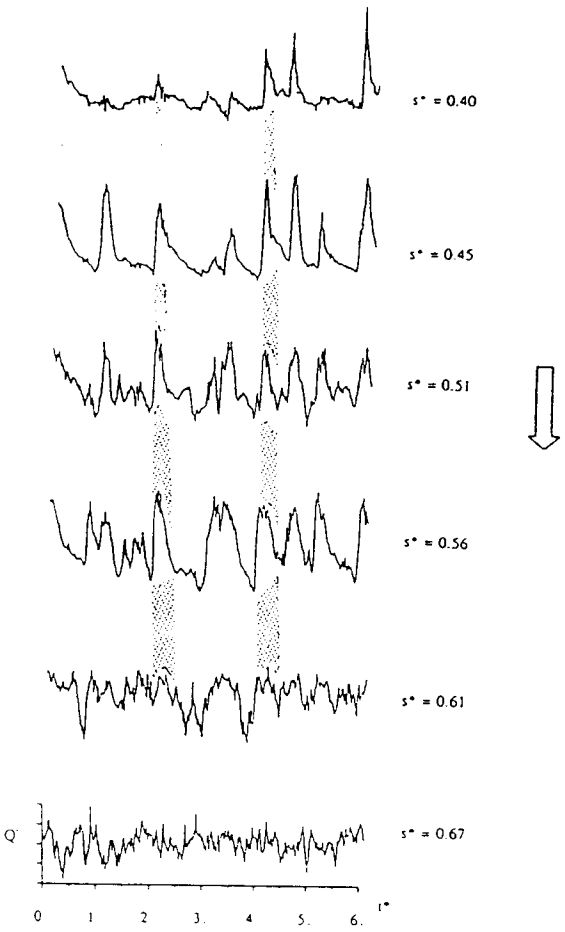

SURFACE-MOUNTED HOT-FILM SIGNALS FROM ROTOR SUCTION SURFACE (ADDISON, 1990)

SIMPLE DESCRIPTION OF 2-D WAKE-INDUCED TRANSITION

- periodic
- caused by turbulence(?) in wakes
- similar to steady transition

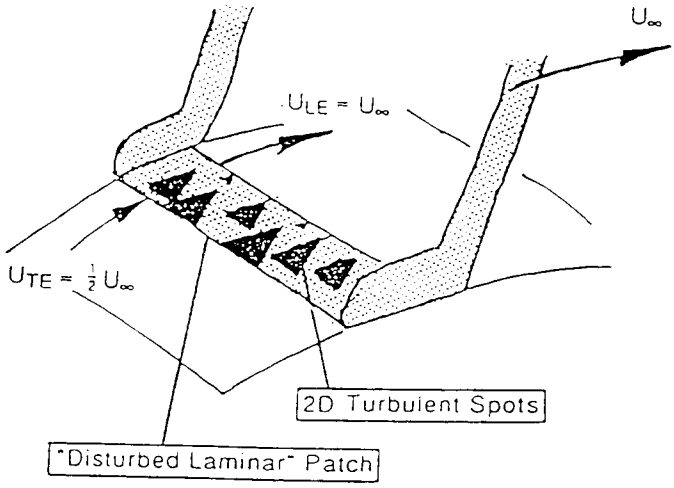

UNSTEADY 2-D TRANSITION MODEL

DATA FROM THE WHITTLE LAB. AXIAL TURBINE

- Single stage
- Re = 3.5×10^5
- $\frac{f \Delta s}{U} = 0.86$
- Onset based on experimental observation
- Spot Production: $\frac{n \sigma \theta_{tr}^3}{\upsilon} = \text{const.}$

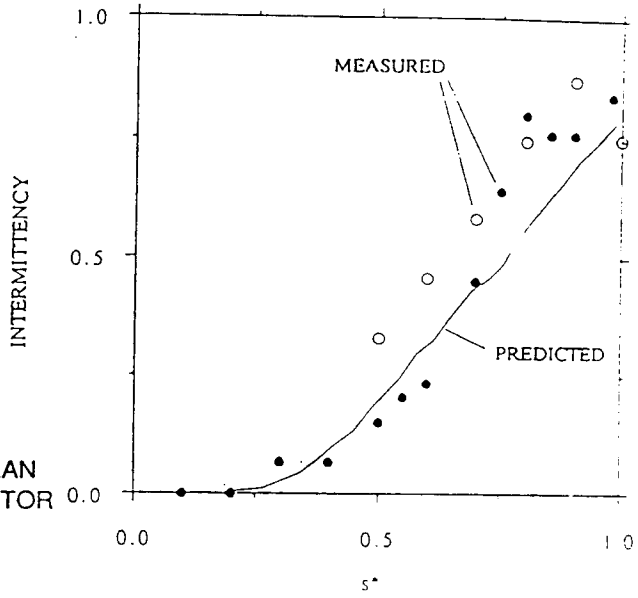

PREDICTED AND MEASURED TIME-MEAN INTERMITTENCY $\bar{\gamma}(S)$ FOR TURBINE ROTOR MID-SPAN SUCTION SURFACE (HODSON ET AL 1992)

EFFECT OF WAKE-PASSING FREQUENCY ON LOSS

Assume wake-affected zone is turbulent

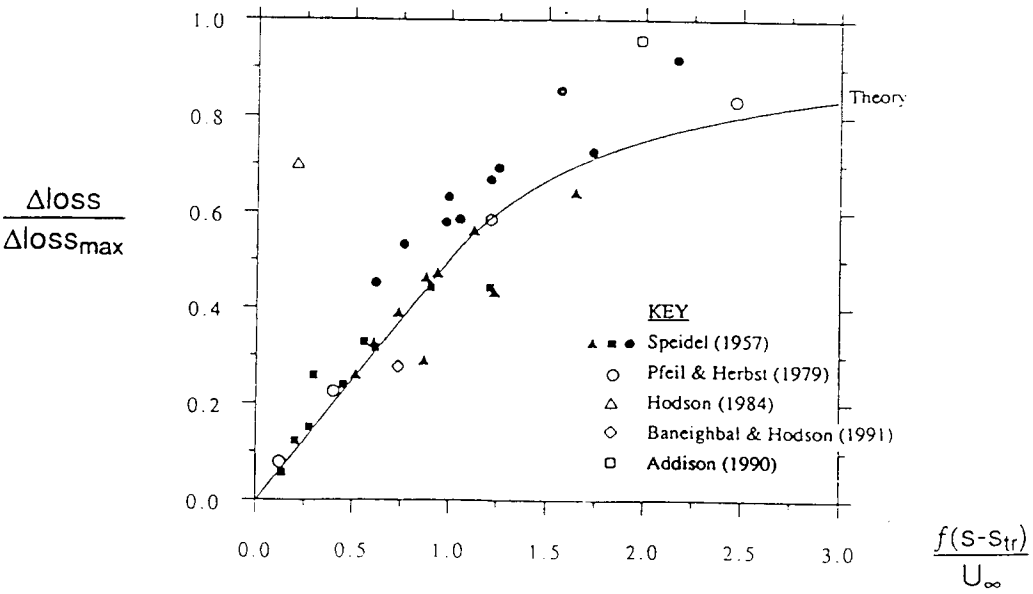

EFFECTS OF UNSTEADINESS ON PROFILE LOSS SHOWING COMPARISON BETWEEN SIMPLE MODEL AND EXPERIMENTS (HODSON, 1989)

S-T DIAGRAM FOR WAKE-INDUCED TRANSITION

Analogy with turbulent spot

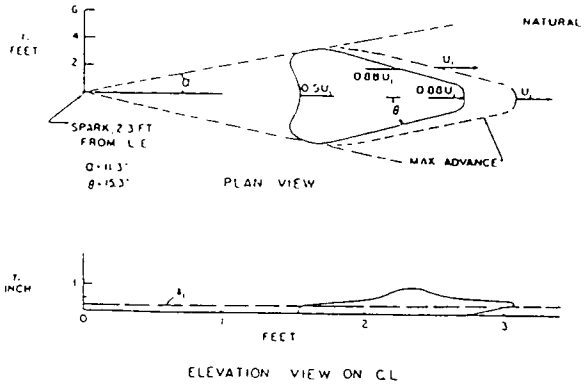

GEOMETRY AND GROWTH OF SPOT

$\overline{U_e}$ (time mean freestream velocity)

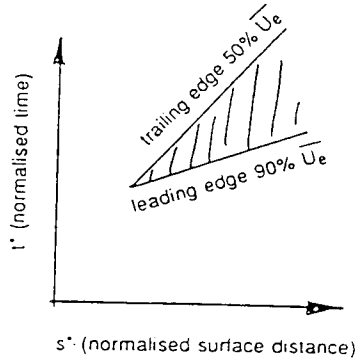

S-T DIAGRAM OF SPOT

EXTENDED TRANSITION ZONES

Calmed region behind turbulent 'events' can extend transition zone (Schubauer & Klebanoff, 1955)

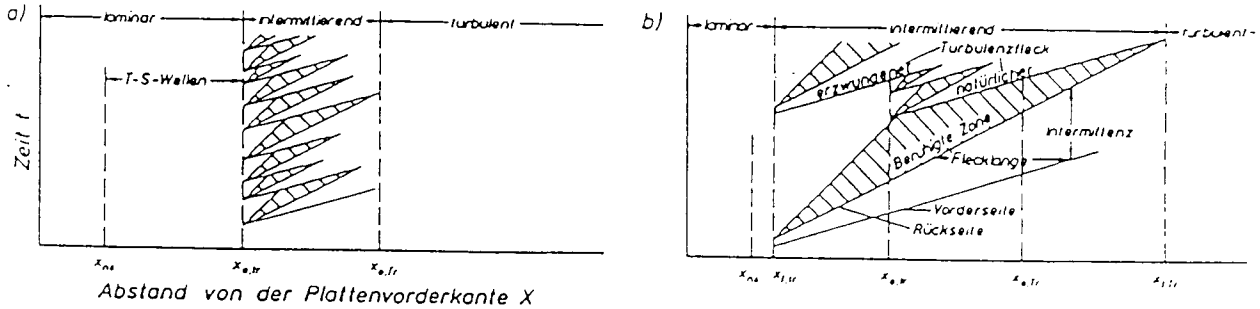

SCHEMATIC INTERPRETATION OF TRANSITION ON A FLAT PLATE: (A) NATURAL TRANSITION; (B) WAKE-INDUCED AND NATURAL TRANSITION (PFEIL, HERBST AND SCHRÖDER, 1982)

MULTI-MODE TRANSITION IN AN LP TURBINE

If steady flow transition occurred at 0.4s

- correlations predict 50% intermittency γ at 0.75s

For wake-affected flow,

- $\gamma_{max} \leq$ steady flow value
- limits calming effect
- separation possible when not instantaneously turbulent

ENSEMBLE-SKEW MEASURED BY SURFACE HOT-FILMS, RE = 1.3X10^5 (HODSON ET AL, 1993)

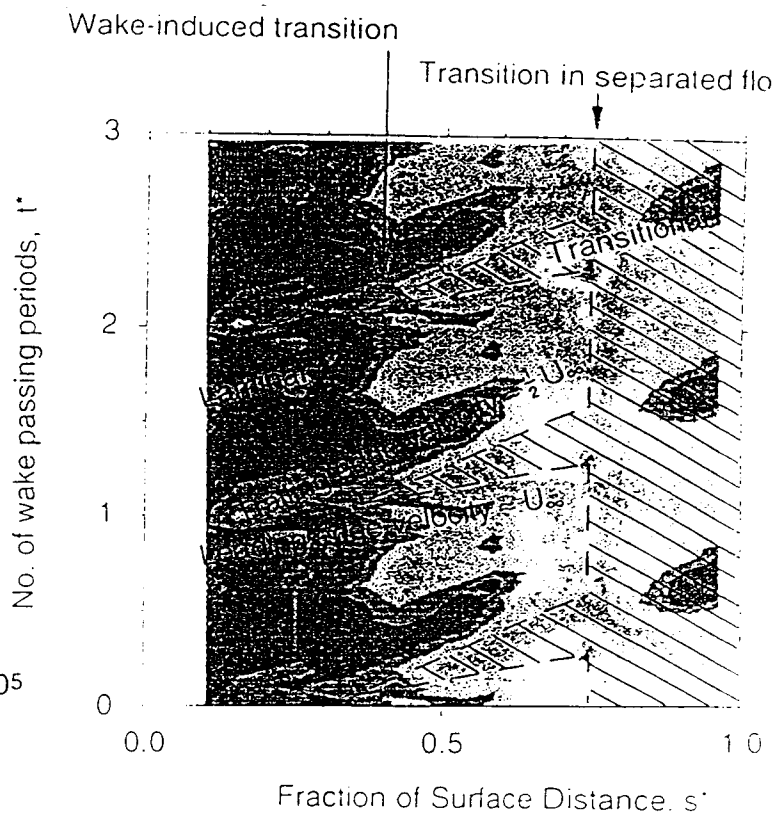

DELAYED SEPARATION/TRANSITION

Calmed region behind turbulent 'events' delays separation/transition

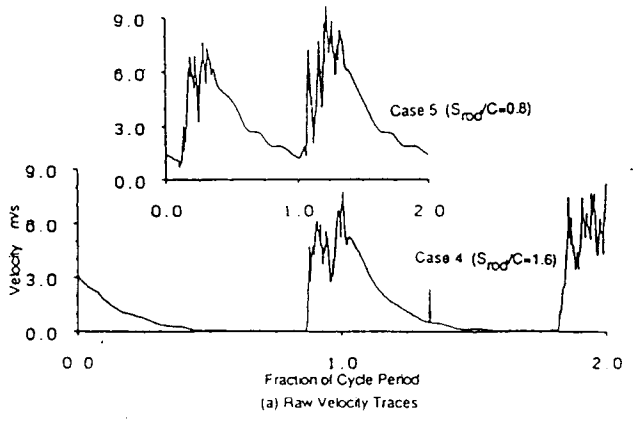

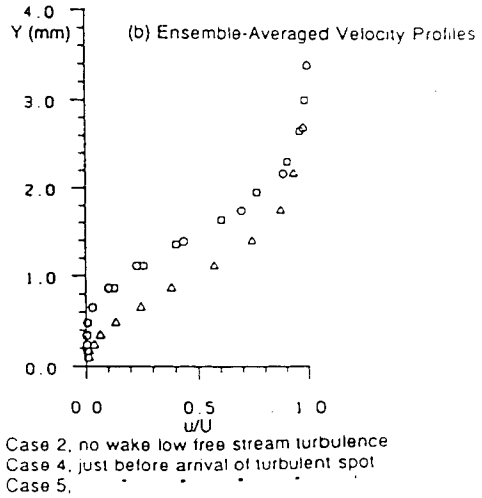

WAKE-INDUCED TRANSITION IN A COMPRESSOR CASCADE (A) INSTANTANEOUS VELOCITIES NEAR SUCTION SURFACE AND (B) ENSEMBLE-AVERAGED VELOCITY PROFILES FOR DIFFERENT UPSTREAM WAKE PITCHES (DONG & CUMPSTY, 1989)

MULTI-MODE TRANSITION IN 2-STAGE TURBINE

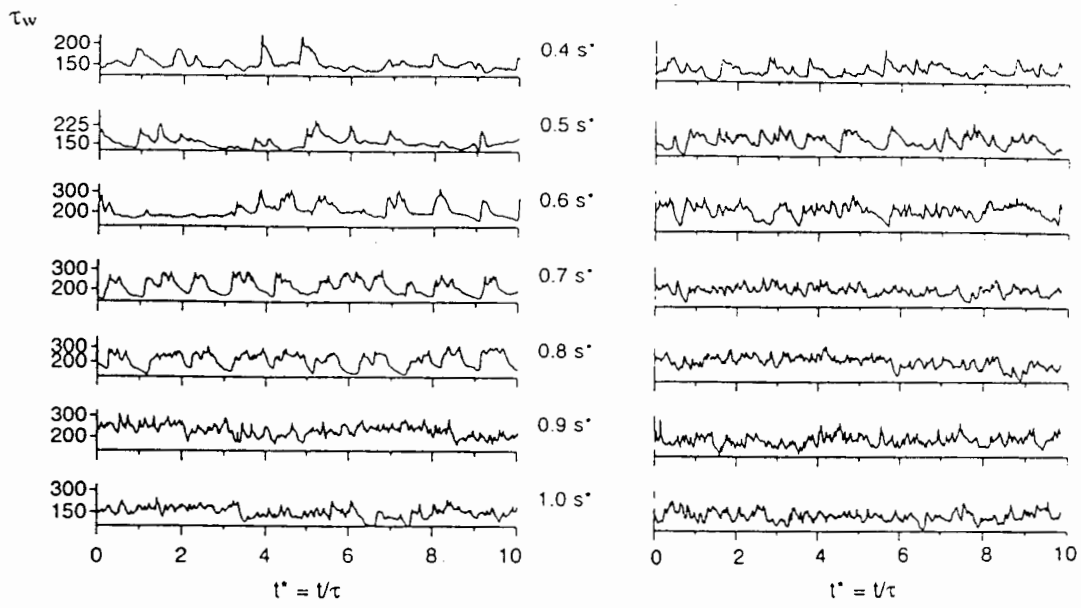

HOT-FILM OUTPUT SIGNALS ON TURBINE ROTOR MID-SPAN SUCTION SURFACE
(A) 1ST STAGE - LOW TU BETWEEN WAKES (FROM HODSON ET AL 1993)
(B) 2ND STAGE: DISTURBANCES PRESENT BETWEEN WAKES

MULTI-MODE TRANSITION IN 2-STAGE TURBINE

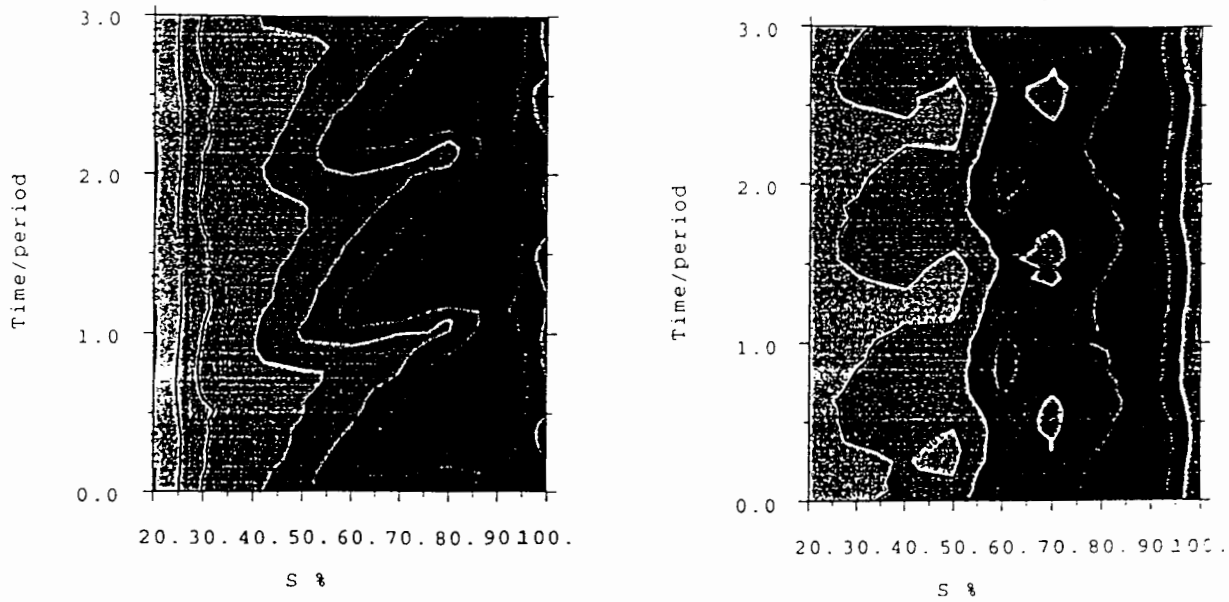

DISTANCE TIME-DIAGRAMS OF ENSEMBLE-MEAN WALL SHEAR STRESS ON TURBINE ROTOR MID-SPAN SUCTION SURFACE
(A) 1ST STAGE - LOW TU BETWEEN WAKES (FROM HODSON ET AL 1993)
(B) 2ND STAGE: DISTURBANCES PRESENT BETWEEN WAKES

SUMMARY OF WAKE-INDUCED TRANSITION

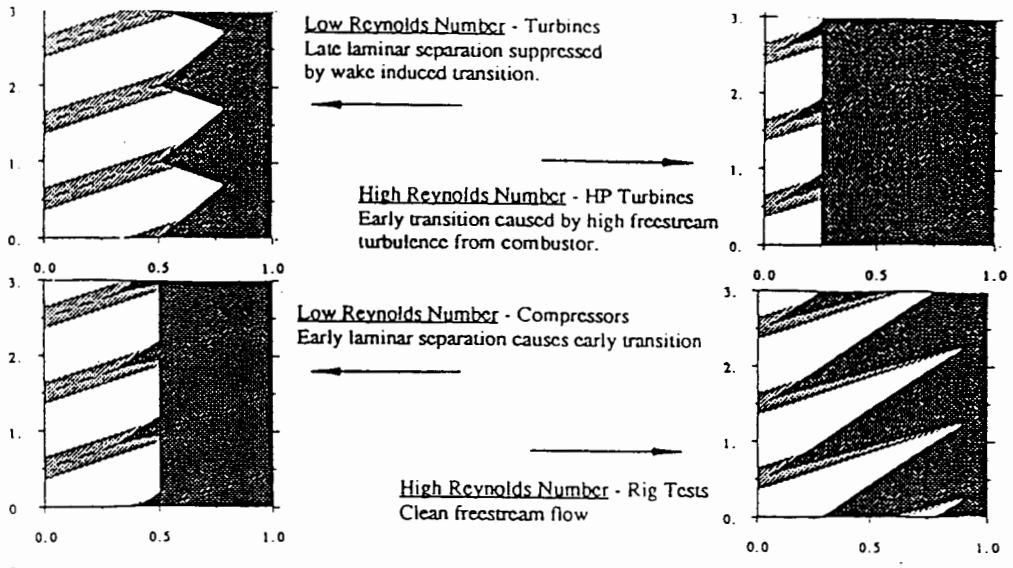

S-T DIAGRAMS SHOWING START OF TRANSITION TRENDS FOR LOW AND HIGH REYNOLD NUMBER FLOWS IN TURBINES AND COMPRESSORS (ADDISON, 1990)

WAKE-INDUCED TRANSITION

What really causes it - turbulence, velocity, pressure fluctuations ?

Where do spots/turbulent 'events' really form/how is this affected by changes in free-stream?

Why do some see wake-affected intermittent flow while others see turbulent flow?

What are the implications of existence of calmed region
(a) at rear of spots inside wake-affected zone?
(b) at rear of fully turbulent wake-affected zones?

What happens when wakes traverse a separation zone/how do free-stream conditions affect transition in separated flows?

ENDWALL TRANSITION IN AXIAL FLOW TURBINES

Secondary flow leads to

- 3-d boundary layers
- new, accelerating laminar flow behind lift-off line
- intermittent flow in rear of blade passage

How do we model 3-D transition?

HOT-FILM OUTPUT SIGNALS FROM ENDWALL OF A 2-D TURBINE CASCADE (HARRISON, 1989)

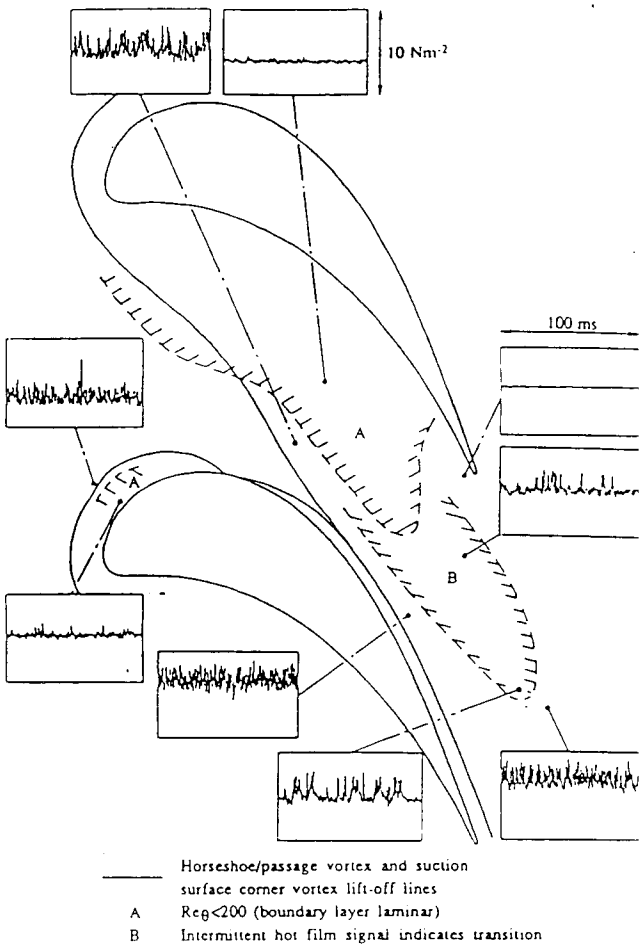

RADIAL INFLOW TURBINES

- significant skew/secondary flows on blade surfaces
- $Re_s \approx 10^6$
- Continuous acceleration over much of surface
- High values of acceleration parameter

$$k = \frac{\nu}{w^2} \nabla(w)$$

especially in secondary flow direction

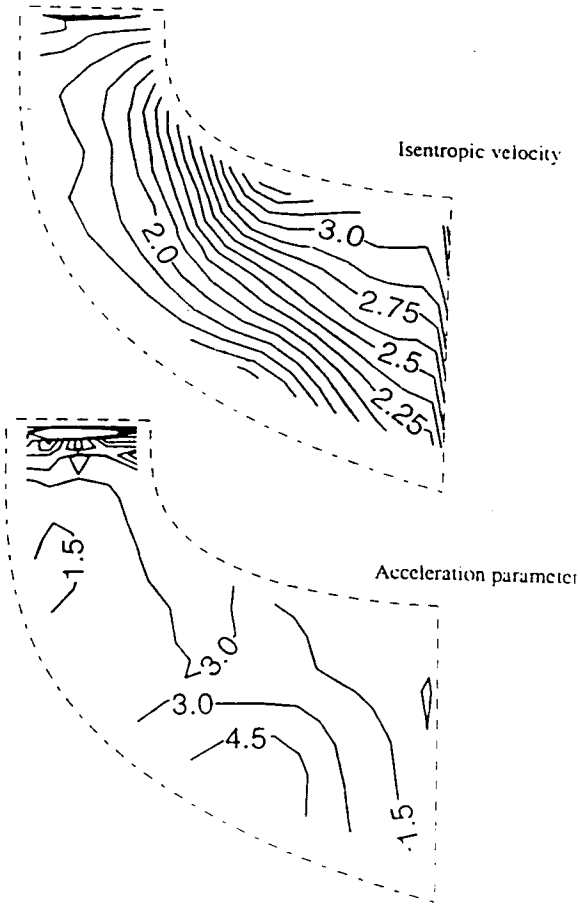

CONTOURS OF VELOCITY $W/W_{RADIAL,IN}$ AND ACCELERATION $|K|X10^6$ ON SUCTION SURFACE OF ROTOR OF A RADIAL INFLOW TURBINE (HUNTSMAN & HODSON, 1993)

RADIAL INFLOW TURBINES

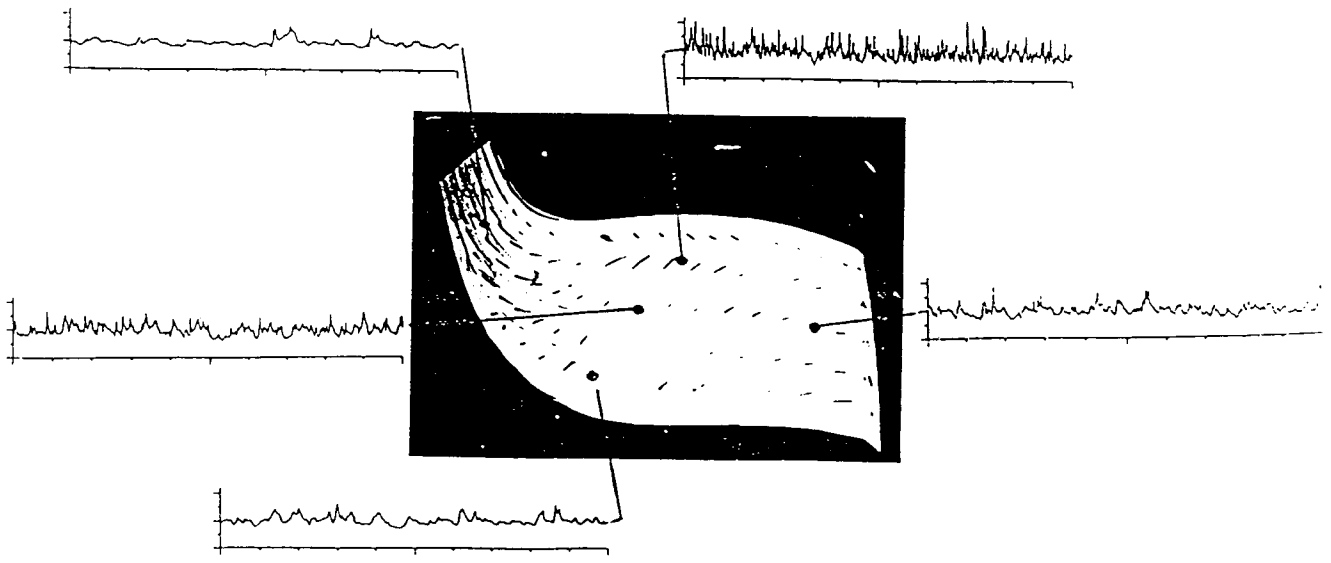

HOT-FILM OUTPUT SIGNALS AND SURFACE FLOW VISUALISATION FROM SUCTION SURFACE OF ROTOR OF A RADIAL INFLOW TURBINE (HUNTSMAN & HODSON, 1993)

INVESTIGATION OF TURBULENT SPOT FORMATION & TRANSITION USING THERMOCHROMIC LIQUID CRYSTALS

PROBLEMS

Existing database insufficient to answer important questions

- Where and when do turbulent spots form?
- How is their formation and growth affected by free-stream conditions?

SOLUTION

- Investigate development of transitional flow using fast-response instrumentation with full surface coverage, i.e. thermochromic liquid crystals

ADVERTISEMENT

- A opportunity exists for a Post-Doc to work on this project at Oxford then Cambridge University

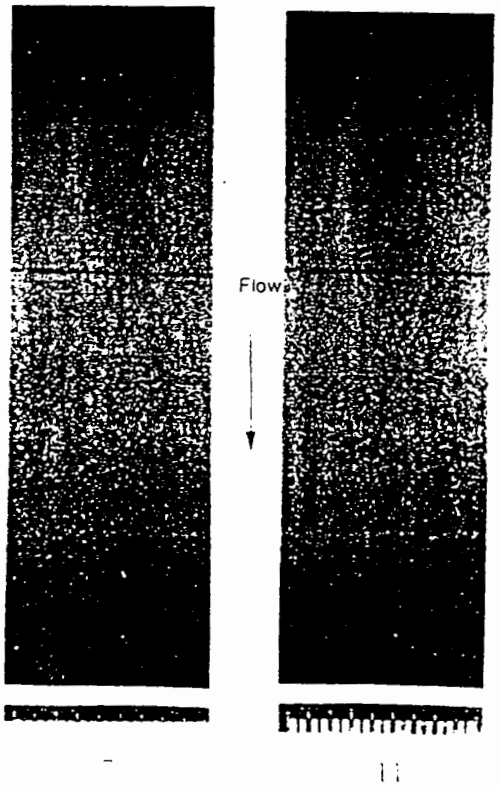

HOT FILM OUTPUT TRACES

SEPARATION/TRANSITION/LAMINARIZATION

Sharp leading edges can cause separation on both surfaces near l.e.

Flow separates at low Re

Questions:

- where does it reattach?
- why does it reattach - acceleration/transition?
- what happens after reattachment?

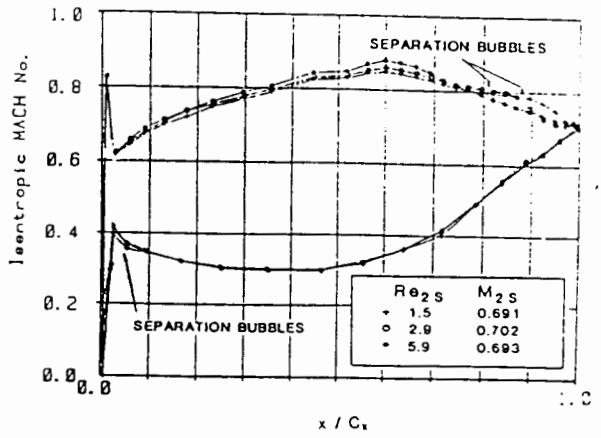

MACH NUMBERS AROUND AN LP TURBINE BLADE (HODSON, 1985)

EFFECT OF PRESSURE GRADIENT/REYNOLDS NUMBER ON SEPARATION/TRANSITION/LAMINARIZATION

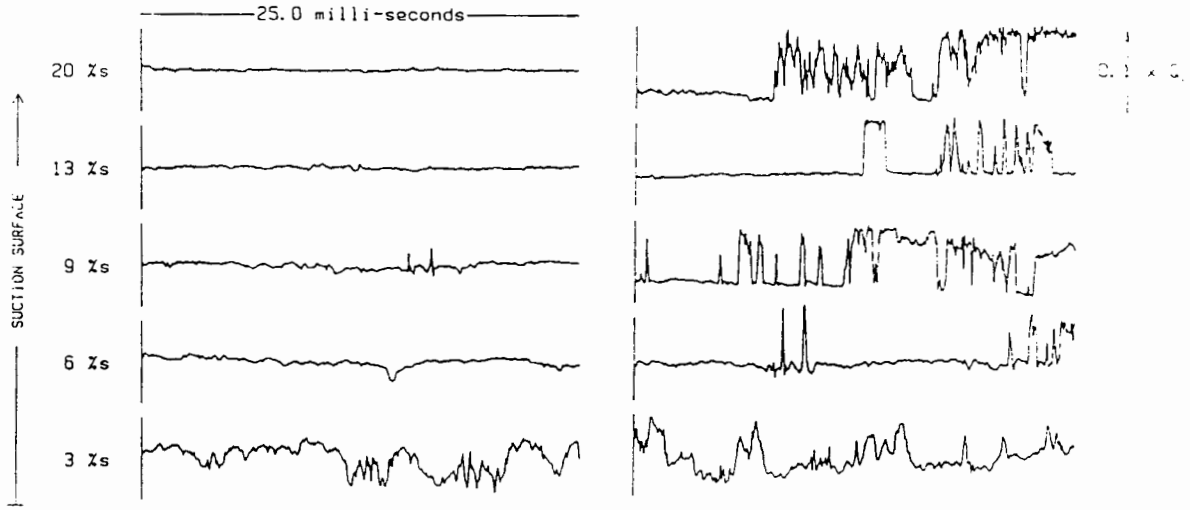

(A) RE ≈ 3X10^5 (B) RE ≈ 9X10^5

SURFACE-MOUNTED HOT-FILM OUTPUT SIGNALS FROM AROUND LEADING EDGE OF AN LP TURBINE BLADE, TU=0.5% (HODSON, 1985):

MODELLING TRANSITION IN TURBOMACHINES

Various approaches used in design

- Integral B.L. codes
- Differential codes + algebraic transition/turbulence models
- Differential codes + differential transition/turbulence models

B.L. codes may be coupled to inviscid solvers or stand-alone

Differential codes based on 2-D or 3-D forms of Navier-Stokes or B.L. equations

Transition is modelled using either intermittency or turbulence models

INTERMITTENCY

$$\gamma(P) = 1 - \exp\left[-\int_V g(P_0)\, dV_0\right]$$

- applicable to all flows providing spot production rate $g(P_0)$ and dependence volume V are known - these have never been measured
- 'natural companion' to 2-D integral solutions (linear combination)
- difficult to use correctly with algebraic turbulence models (profile switching)
- exclude effect of changing free-stream conditions - existing correlations based on conditions up to start of transition only

How do we prescribe spot production rate $g(P_0)$ and dependence volume V for general problems (unsteady, 3-D, variable free-stream conditions .....)?

TRANSITION VIA TURBULENCE MODELS

Solutions (e.g., via k-ε equations)

- rely on same boundary layer test data as other correlations for validation
- can account for effects of changing free-stream conditions
- can give development of free-stream turbulence etc.
- not limited to boundary layers
- computationally efficient when y+ hard to find, e.g. unstructured 3-D codes
- do not contain all physics - e.g. influence zones in unsteady flow, intermittent separation

FINAL REMARKS (1)

We know

- some parameters are significant (e.g., pressure grad., Tu intensity, history)
- some parameters may be significant (e.g., curvature, Tu scale, skew)

In many cases, we do not know

- the nature of transition
- the magnitude/significance of the various parameters

We need

- more systematic studies of transition - must be applicable to turbomachines

FINAL REMARKS (2)

Various numerical approaches/codes used in design

Whatever the approach, majority of transition models

- rely on same experiments for validation/correlation

To be effective in design, we need

- integral 2-D steady B.L. methods ..... 3-D unsteady N-S codes
- consistent hierarchical models of transition based on physics

Transition Models for Engineering Calculations

C. J. Fraser
Dundee Institute of Technology

Abstract :- While future theoretical and conceptual developments may promote a better understanding of the physical processes involved in the latter stages of boundary layer transition, the designers of rotodynamic machinery and other fluid dynamic devices need effective transition models now. This presentation will therefore centre round the development of some transition models which have been developed as design aids to improve the prediction codes used in the performance evaluation of gas turbine blading. All models are based on Narasimha's concentrated breakdown and spot growth hypothesis

The first model uses a correlation of the non-dimensional spot source rate density as a function of the local pressure gradient parameter and the freestream turbulence level at the onset of transition. Even although quite reasonable agreement is observed for a significant number of transitional flows, the rigidity of a correlation based on onset parameters leaves a lot to be desired. For gas turbine blade flows in particular, the pressure gradient may not only change rapidly in magnitude, but can also change in sign during transition. Since it was thought that this could have significant influence on the turbulent spot seeding rates, an alternative transition model was postulated in the differential form of a first order system. In the differential model the transition length parameter, λ, is left as a limited function of the streamwise distance, x.

ie. $$d\gamma/dx = \{2Ax_t/\lambda_{av}^2\}[1 - (x_t/\lambda_{av})(d\lambda/dx)]\exp(-Ax_t^2/\lambda_{av}^2)$$

where $$\lambda_{av} = [1/x_t]\int_{x_\lambda=0}^{x_\lambda=0.25} \lambda\, dxt \quad ; \quad A = 0.411 \quad \text{and} \quad x_t = (x - x_{tran})$$

Preliminary studies have indicated that $d\lambda/dx$ may in some circumstances vary significantly at the start of transition, but usually tends to zero for $\lambda > 0.2$. Equally good agreement with the experimental data is therefore found by simply using the original Narasimha intermittency function with λ_{av} as defined above. These two latter empirical forms however, impart the required dynamical flexibility on the intermittency characteristics and uncouples the predicted distributions from the start of transition parameters.

Comparisons of the boundary layer integral parameters using intermittency weighted predictions and measured data are used as a basis for assessment and evaluation of the transition models developed.

Transition Models for Engineering Calculations

C J Fraser

Department of Mechanical Engineering

Dundee Institute of Technology

Dundee

Scotland

UK

Zero Pressure Gradient Correlations

$$[R_\theta]_{tran} = 0.85 [163 + e^{(6.91 - t)}]$$

$$R_\lambda = 2.947 [10 - e^{(1.7 - t/2)}] (R_\theta)^{3/2}$$

$$\text{also } R_\lambda = \sqrt{[0.411 . (R_\theta)^3 / N_o]}$$

$$\therefore N_o \times 10^3 = 47.324 / [10 - e^{(1.7 - t/2)}]^2$$

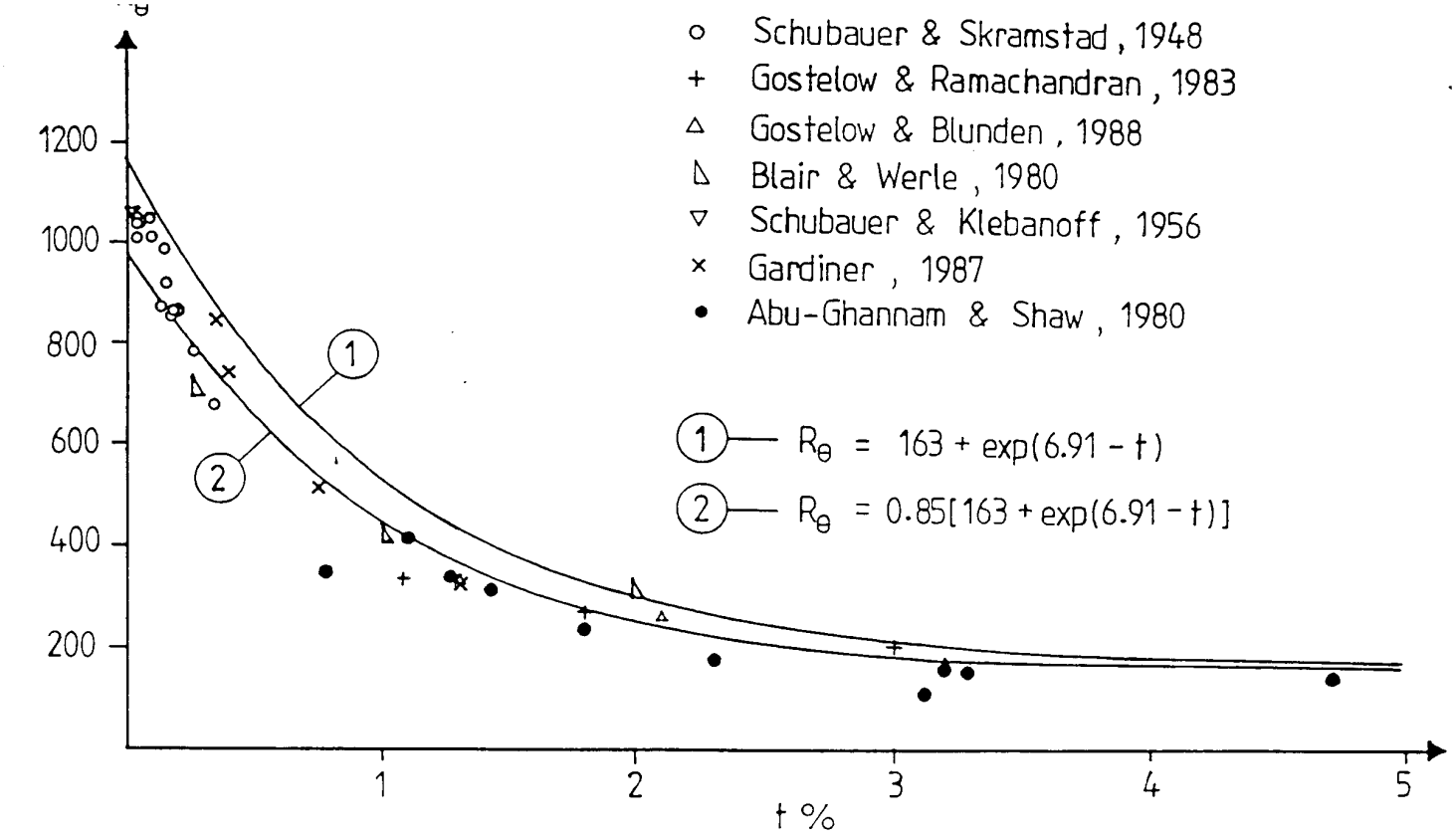
Schubauer & Skramstad , 1948
Gostelow & Ramachandran , 1983
Gostelow & Blunden , 1988
Blair & Werle , 1980
Schubauer & Klebanoff , 1956
Gardiner , 1987
Abu-Ghannam & Shaw , 1980
1 — $R_\theta = 163 + \exp(6.91 - t)$
2 — $R_\theta = 0.85[163 + \exp(6.91 - t)]$
1200
1000
800
600
400
200
1
2
3
4
5
t %

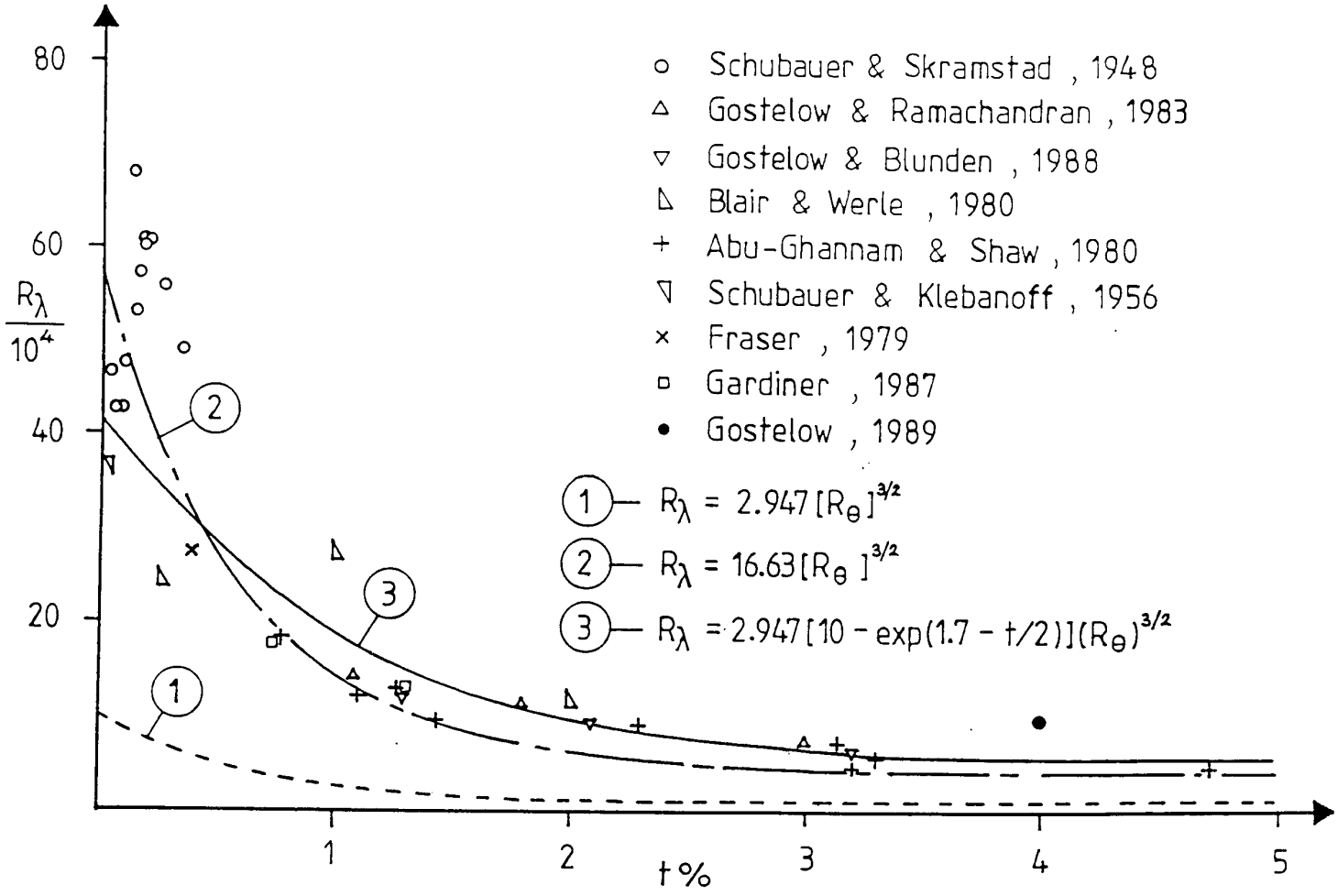
Schubauer & Skramstad , 1948
Gostelow & Ramachandran , 1983
Gostelow & Blunden , 1988
Blair & Werle , 1980
Abu-Ghannam & Shaw , 1980
Schubauer & Klebanoff , 1956
Fraser , 1979
Gardiner , 1987
Gostelow , 1989
1 — $R_\lambda = 2.947[R_\theta]^{3/2}$
2 — $R_\lambda = 16.63[R_\theta]^{3/2}$
3 — $R_\lambda = 2.947[10 - \exp(1.7 - t/2)](R_\theta)^{3/2}$
$R_\lambda / 10^4$
80
60
40
20
1
2
3
4
5
t %

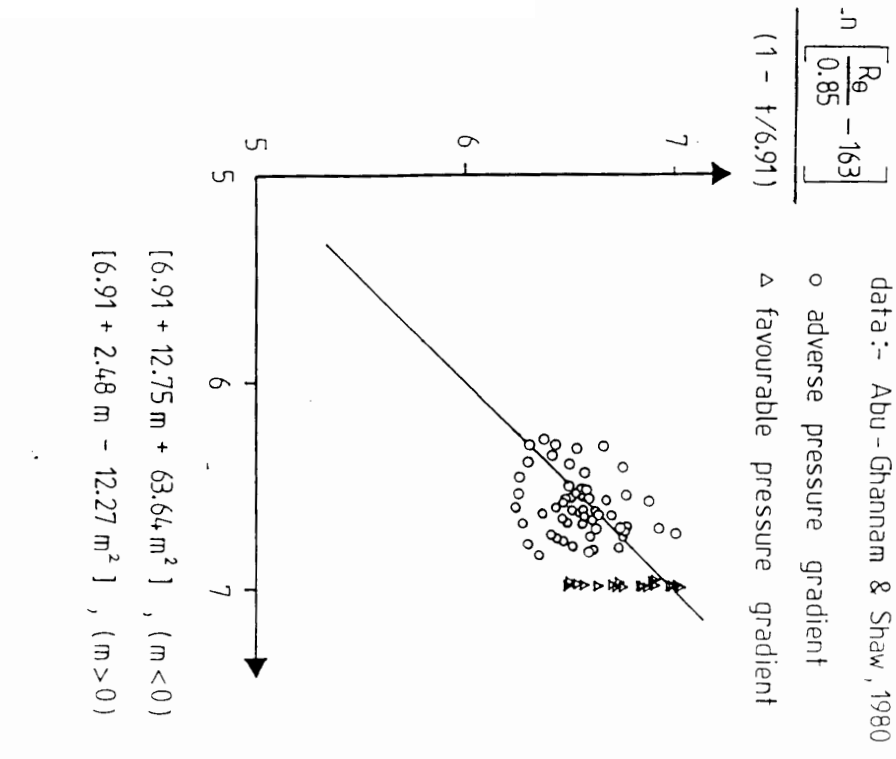
data :- Abu-Ghannam & Shaw, 1980
o adverse pressure gradient
Δ favourable pressure gradient
[6.91 + 12.75 m + 63.64 m²] , (m < 0)
[6.91 + 2.48 m - 12.27 m²] , (m > 0)
5
6
7

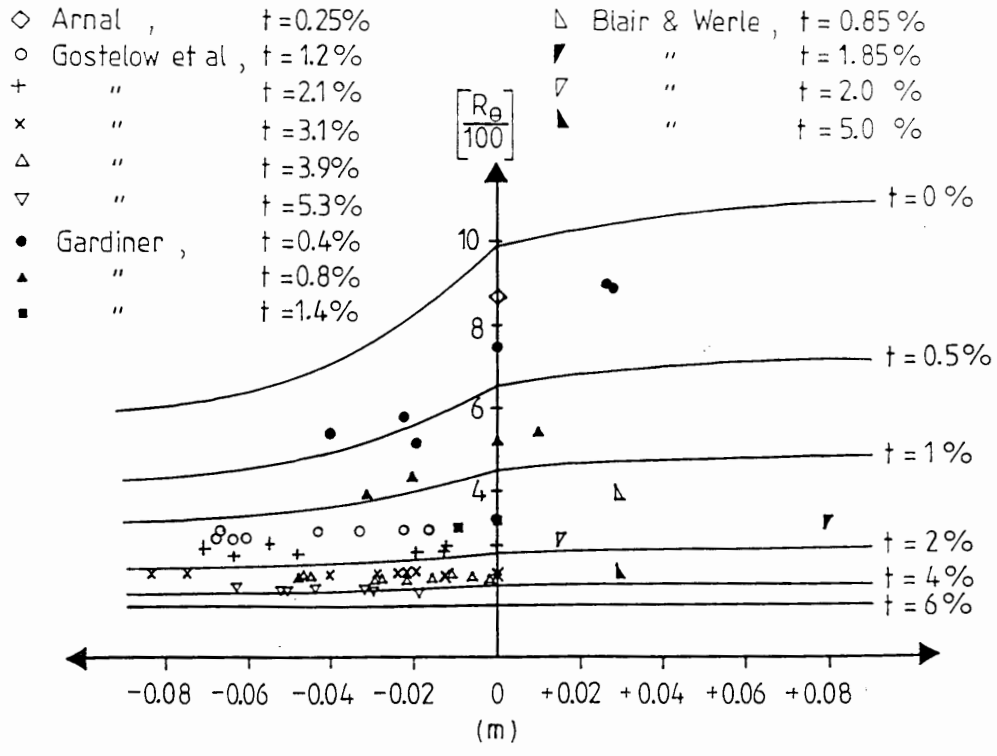
◇ Arnal , t = 0.25%
○ Gostelow et al , t = 1.2%
+ " t = 2.1%
× " t = 3.1%
Δ " t = 3.9%
▽ " t = 5.3%
● Gardiner , t = 0.4%
▲ " t = 0.8%
■ " t = 1.4%
Δ Blair & Werle , t = 0.85%
▼ " t = 1.85%
▽ " t = 2.0 %
▲ " t = 5.0 %
[Rθ/100]
10
8
6
4
t = 0 %
t = 0.5%
t = 1 %
t = 2%
t = 4%
t = 6%
-0.08 -0.06 -0.04 -0.02 0 +0.02 +0.04 +0.06 +0.08
(m)

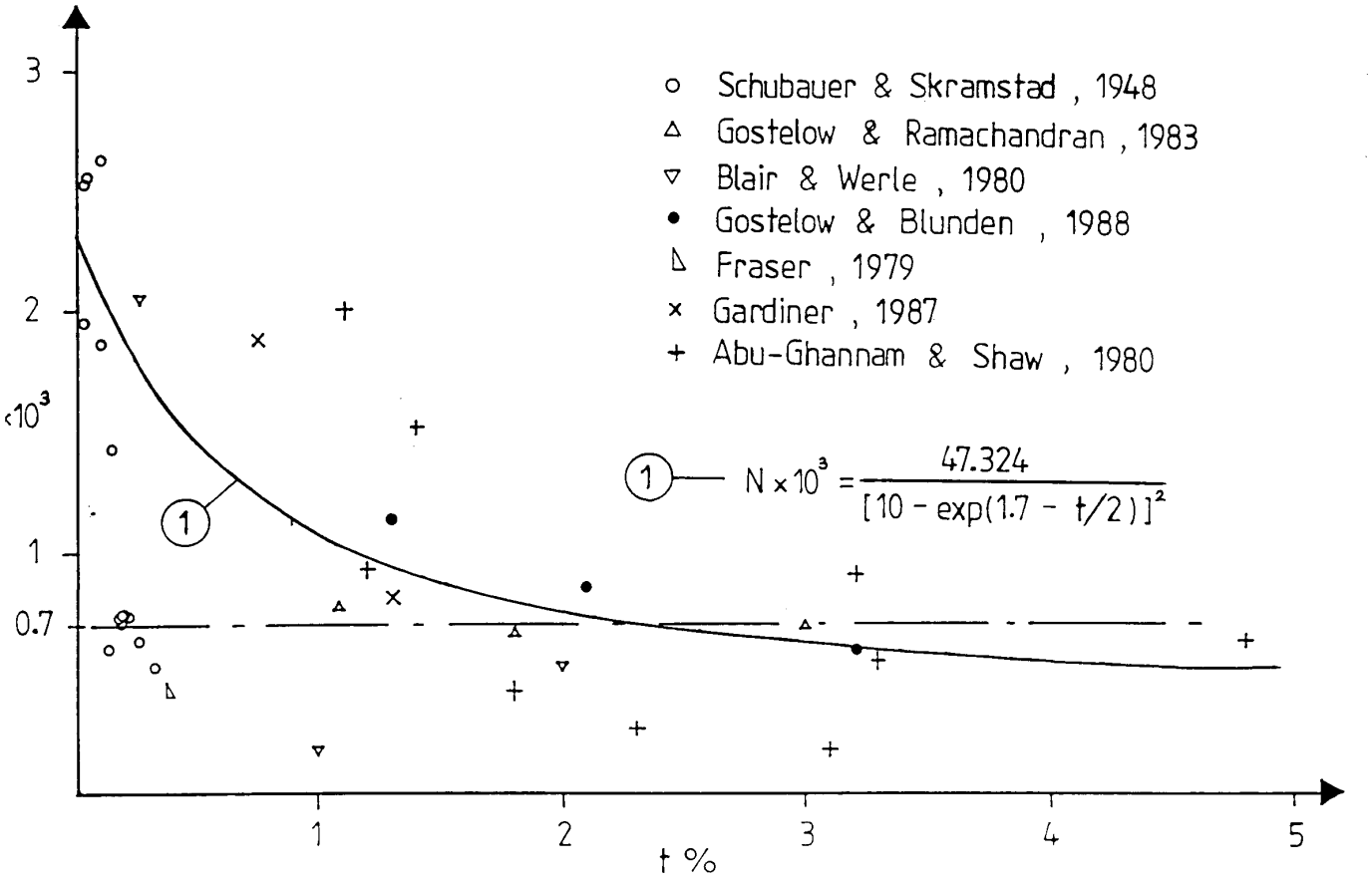

Non-zero Pressure Gradient Correlations

$$[R_\theta]_{tran} = 0.85 \left| 163 + e^{g(m)(1 - t/6.91)} \right|$$

$$g(m) = 6.91 + 12.75\ m + 63.64\ m^2 \quad \text{for } \{ m<0 \}$$

$$g(m) = 6.91 + 2.48\ m - 12.27\ m^2 \quad \text{for } \{ m>0 \}$$

$$\text{and} \quad m = (\theta^2/\nu)\ [dU/dx]$$

$$\text{for } \{m<0\}$$

$$N = N_o \cdot e^{\{f(m).f(t)\}}$$

$$f(m) = m\ (1 - 55\ m^2)$$

$$f(t) = 2.6\ t + 3.6\ \sqrt{(t)} - 86$$

$$\text{for } \{m>0\}$$

$$N = N_o \cdot e^{(t - 10\sqrt{(m)})} + 300\ m^4$$

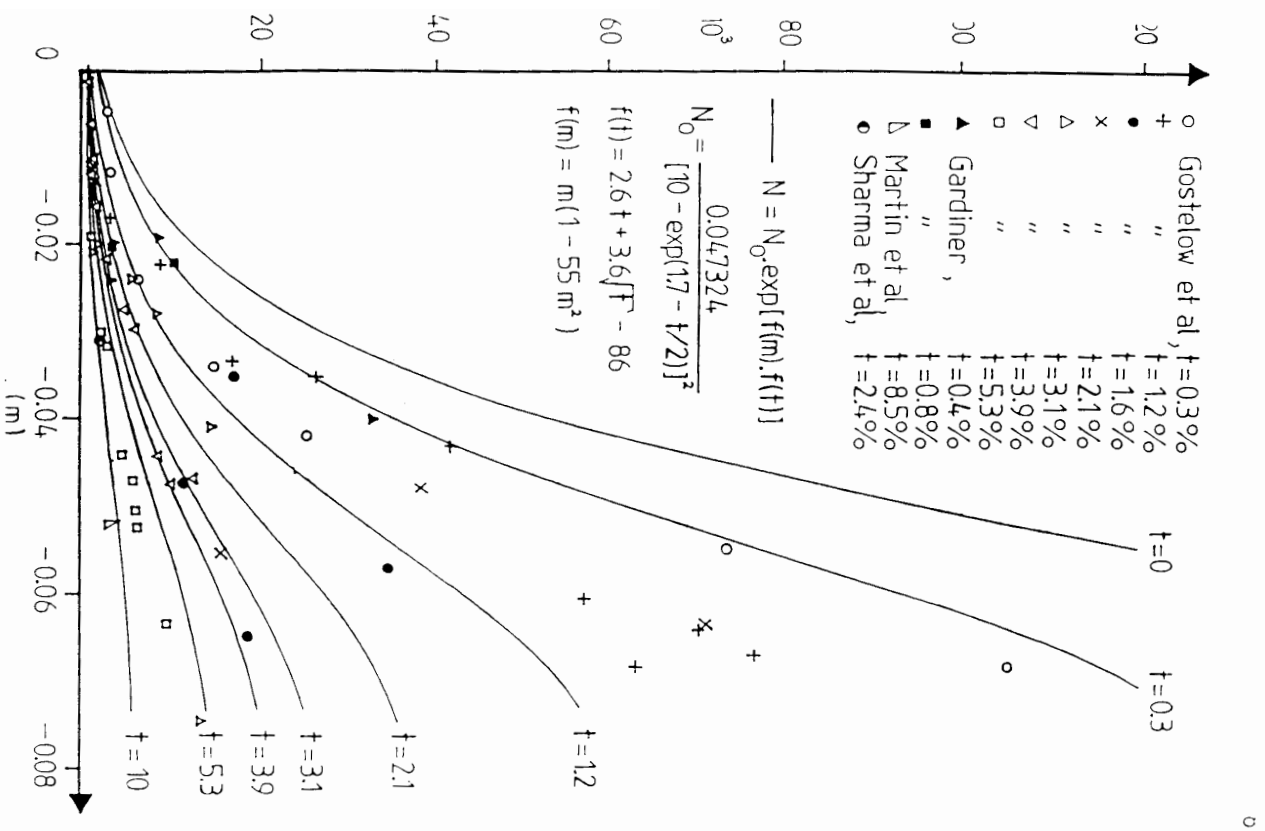
Gostelow et al, t=0.3%
" t=1.2%
" t=1.6%
" t=2.1%
" t=3.1%
" t=3.9%
" t=5.3%
Gardiner, t=0.4%
" t=0.8%
Martin et al, t=8.5%
Sharma et al, t=2.4%
N = N0.exp[f(m).f(t)]
N0 = 0.047324 / [10 - exp(1.7 - t/2)]²
f(t) = 2.6 t + 3.6√t - 86
f(m) = m(1 - 55 m²)
t=0
t=0.3
t=1.2
t=2.1
t=3.1
t=3.9
t=5.3
t=10
(m)
0
- 0.02
- 0.04
- 0.06
- 0.08
20
40
60
80
10³
20

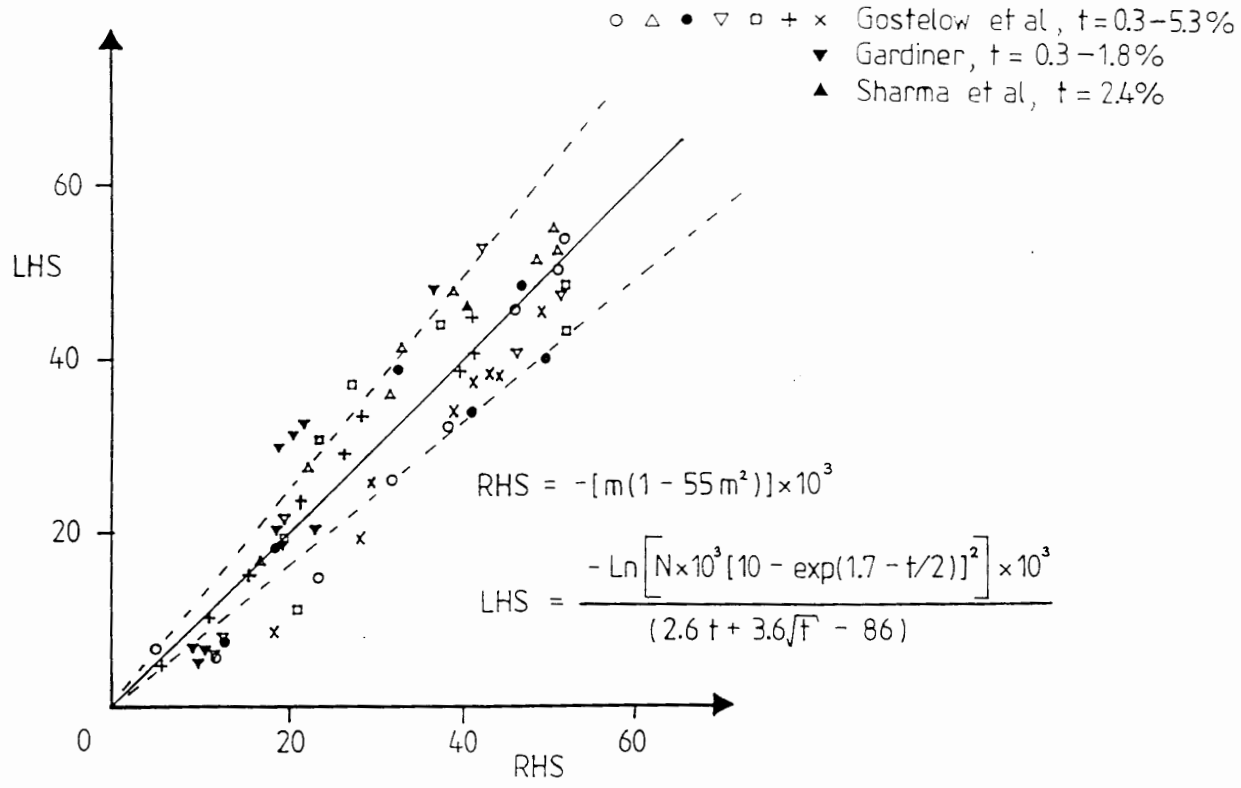
Gostelow et al, t = 0.3 – 5.3%
Gardiner, t = 0.3 – 1.8%
Sharma et al, t = 2.4%
RHS = -[m(1 - 55 m²)] × 10³
LHS = - Ln[N × 10³ [10 - exp(1.7 - t/2)]²] × 10³ / (2.6 t + 3.6√t - 86)
LHS
RHS
0
20
40
60

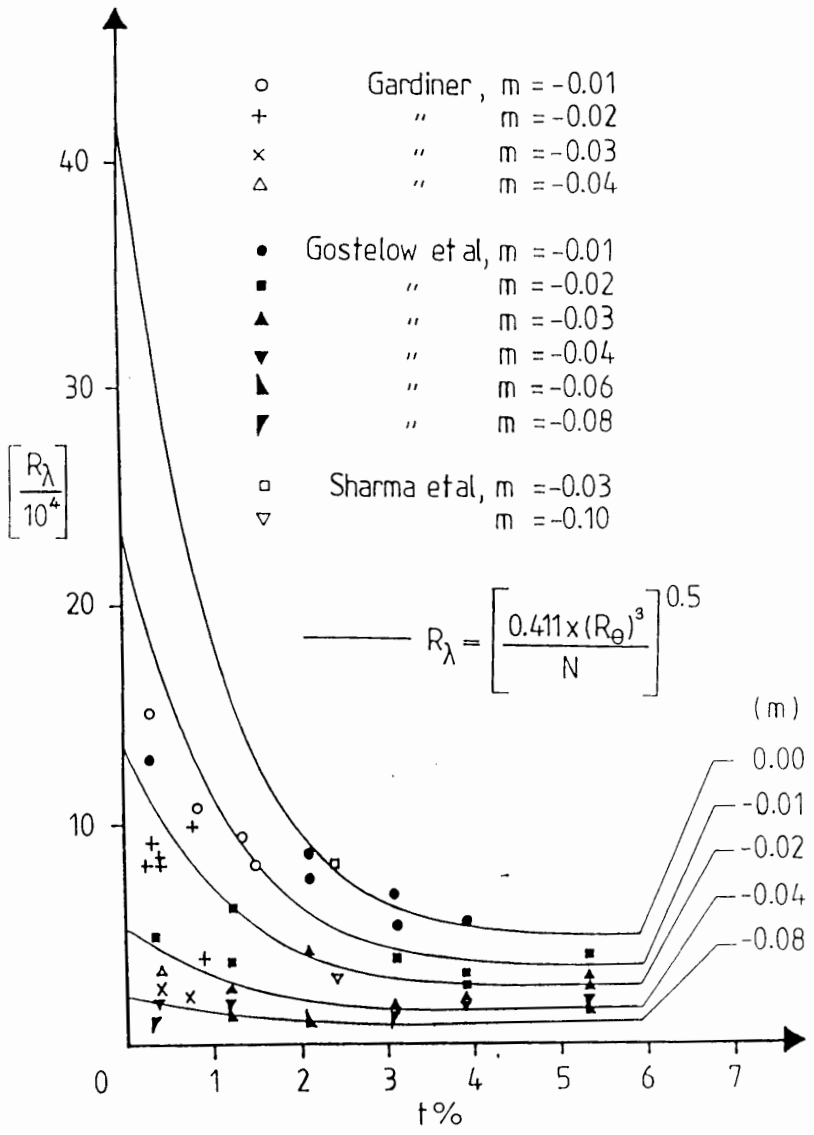
Gardiner, m = -0.01
" m = -0.02
" m = -0.03
" m = -0.04
Gostelow et al, m = -0.01
" m = -0.02
" m = -0.03
" m = -0.04
" m = -0.06
" m = -0.08
Sharma et al, m = -0.03
m = -0.10
$R_\lambda = \left[\frac{0.411 \times (R_\theta)^3}{N}\right]^{0.5}$
$\left[\frac{R_\lambda}{10^4}\right]$
(m)
0.00
-0.01
-0.02
-0.04
-0.08
t%

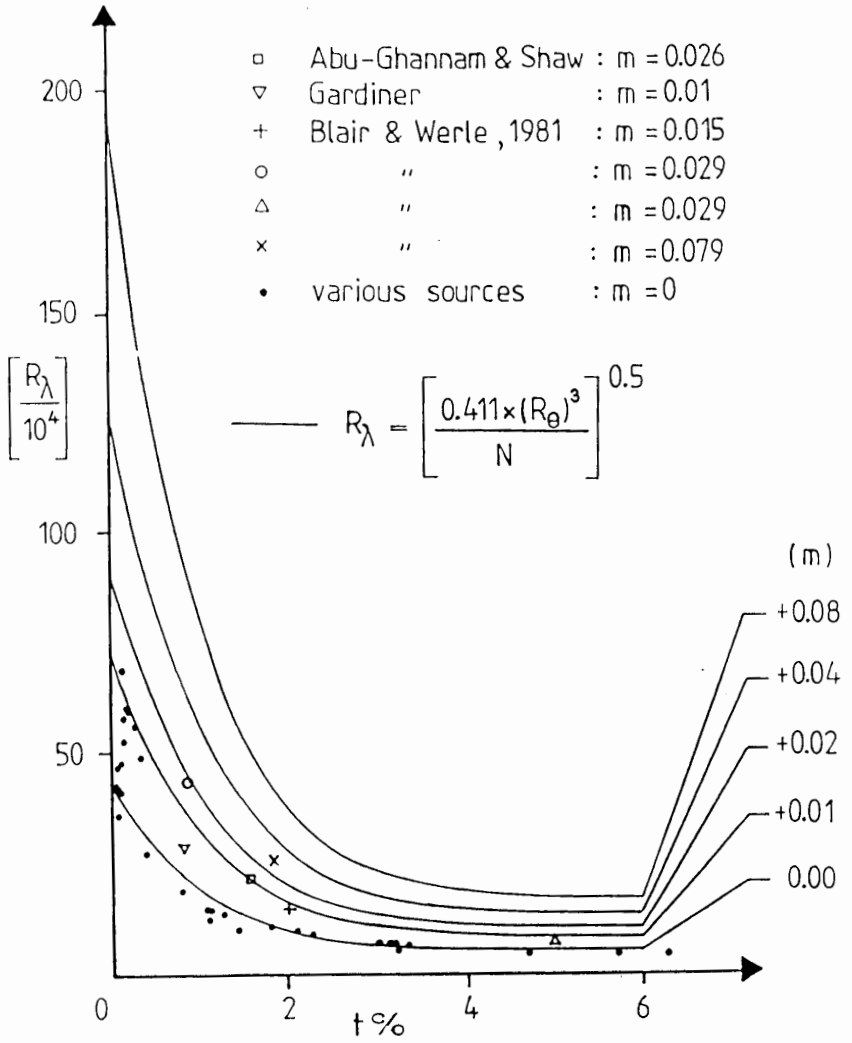
Abu-Ghannam & Shaw : m = 0.026
Gardiner : m = 0.01
Blair & Werle, 1981 : m = 0.015
" : m = 0.029
" : m = 0.029
" : m = 0.079
various sources : m = 0
$R_\lambda = \left[\frac{0.411 \times (R_\theta)^3}{N}\right]^{0.5}$
$\left[\frac{R_\lambda}{10^4}\right]$
(m)
+0.08
+0.04
+0.02
+0.01
0.00
t%

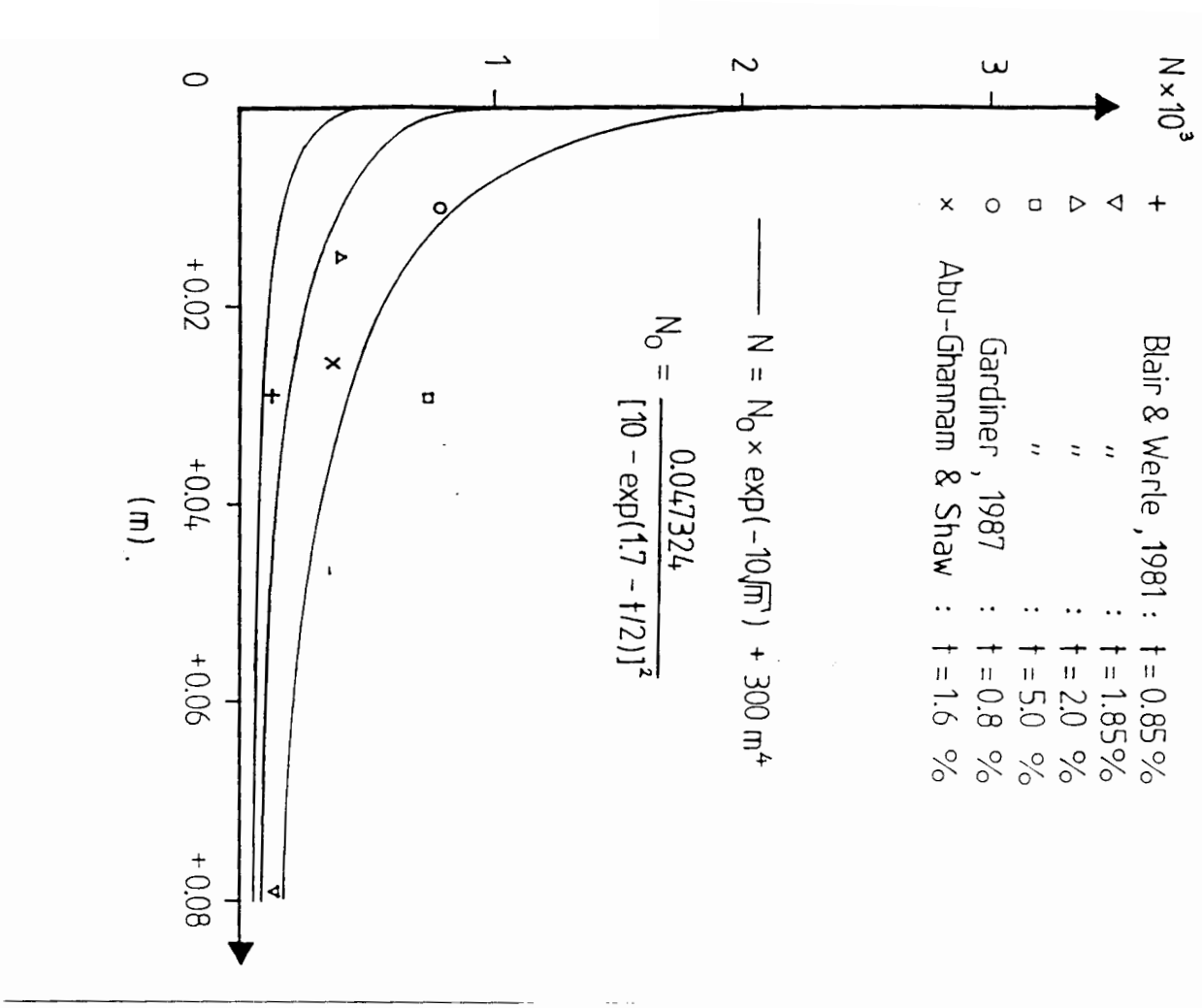
N × 10³
0
1
2
3
+0.02
+0.04
+0.06
+0.08
(m)
+ Blair & Werle, 1981 : t = 0.85 %
∇ " : t = 1.85%
△ " : t = 2.0 %
□ " : t = 5.0 %
○ Gardiner, 1987 : t = 0.8 %
× Abu-Ghannam & Shaw : t = 1.6 %
N = N0 × exp(-10√m) + 300 m⁴
N0 = 0.047324 / [10 - exp(1.7 - t/2)]²

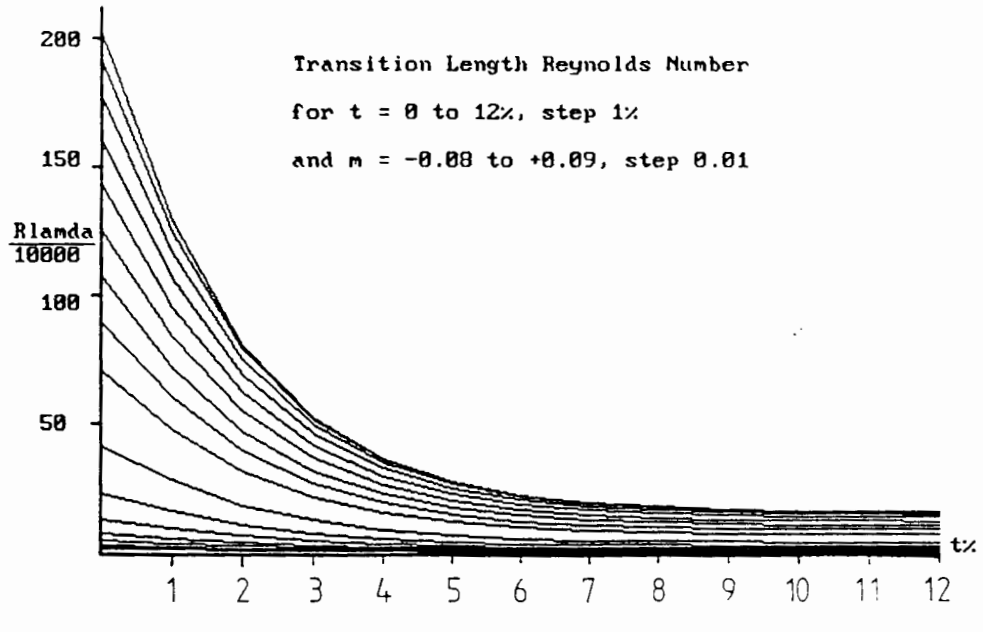
Transition Length Reynolds Number
for t = 0 to 12%, step 1%
and m = -0.08 to +0.09, step 0.01
Rlamda / 10000
200
150
100
50
t%
1
2
3
4
5
6
7
8
9
10
11
12

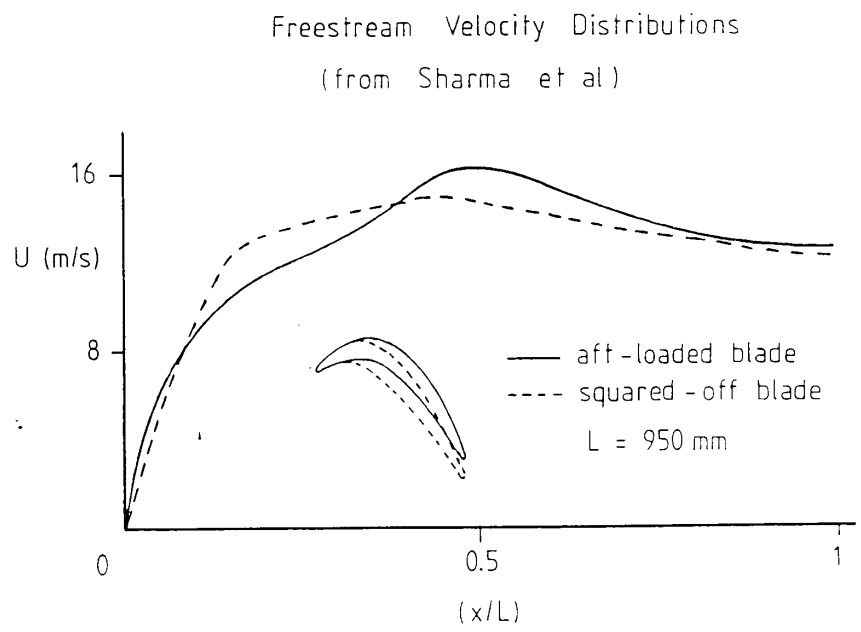
Freestream Velocity Distributions
(from Sharma et al)
16
U (m/s)
8
0
0.5
1
(x/L)
aft-loaded blade
squared-off blade
L = 950 mm

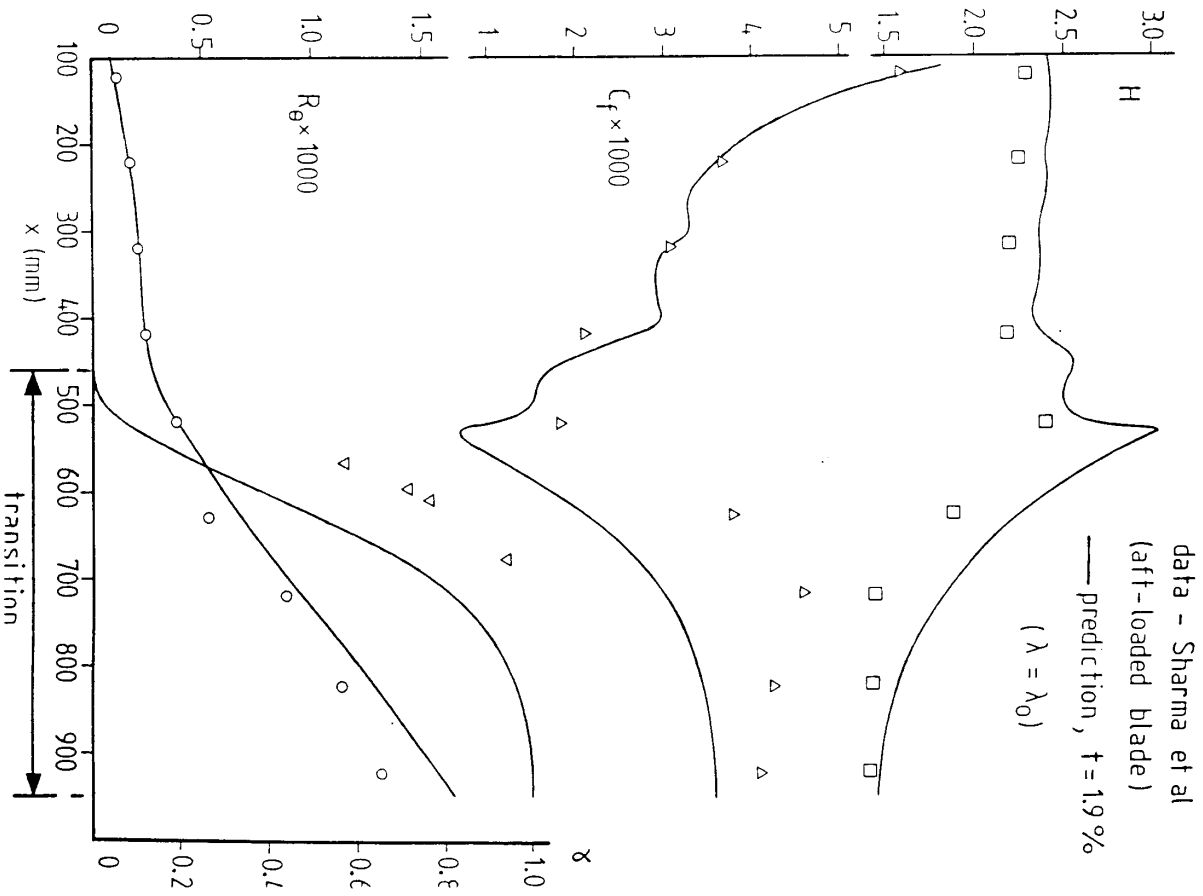
H
$C_f \times 1000$
$R_\theta \times 1000$
x (mm)
transition
α
data - Sharma et al
(aft-loaded blade)
prediction, t = 1.9 %
(λ = λ0)

Intermittency Functions

$\gamma = 1 - \exp(-Ax_t^2/\lambda^2)$

where $A = 0.411$ and $x_t = (x - x_{tran})$

Differential forms

$d\gamma/dx = \{2Ax_t/\lambda^2\}\,[1 - (x_t/\lambda)(d\lambda/dx)]\exp(-Ax_t^2/\lambda^2)$

$d\gamma/dx = \{2Ax_t/\lambda_{av}^2\}\,[1 - (x_t/\lambda_{av})(d\lambda/dx)]\exp(-Ax_t^2/\lambda_{av}^2)$

where $\lambda_{av} = [1/x_t]\int_{x_{\gamma=0}}^{x_{\gamma=1}} \lambda\, dx_t$

$\gamma = 1 - \exp(-Ax_t^2/\lambda_{av}^2)$

where $\lambda_{av} = [1/x_t]\int_{x_{\gamma=0}}^{x_{\gamma=0.25}} \lambda\, dx_t$

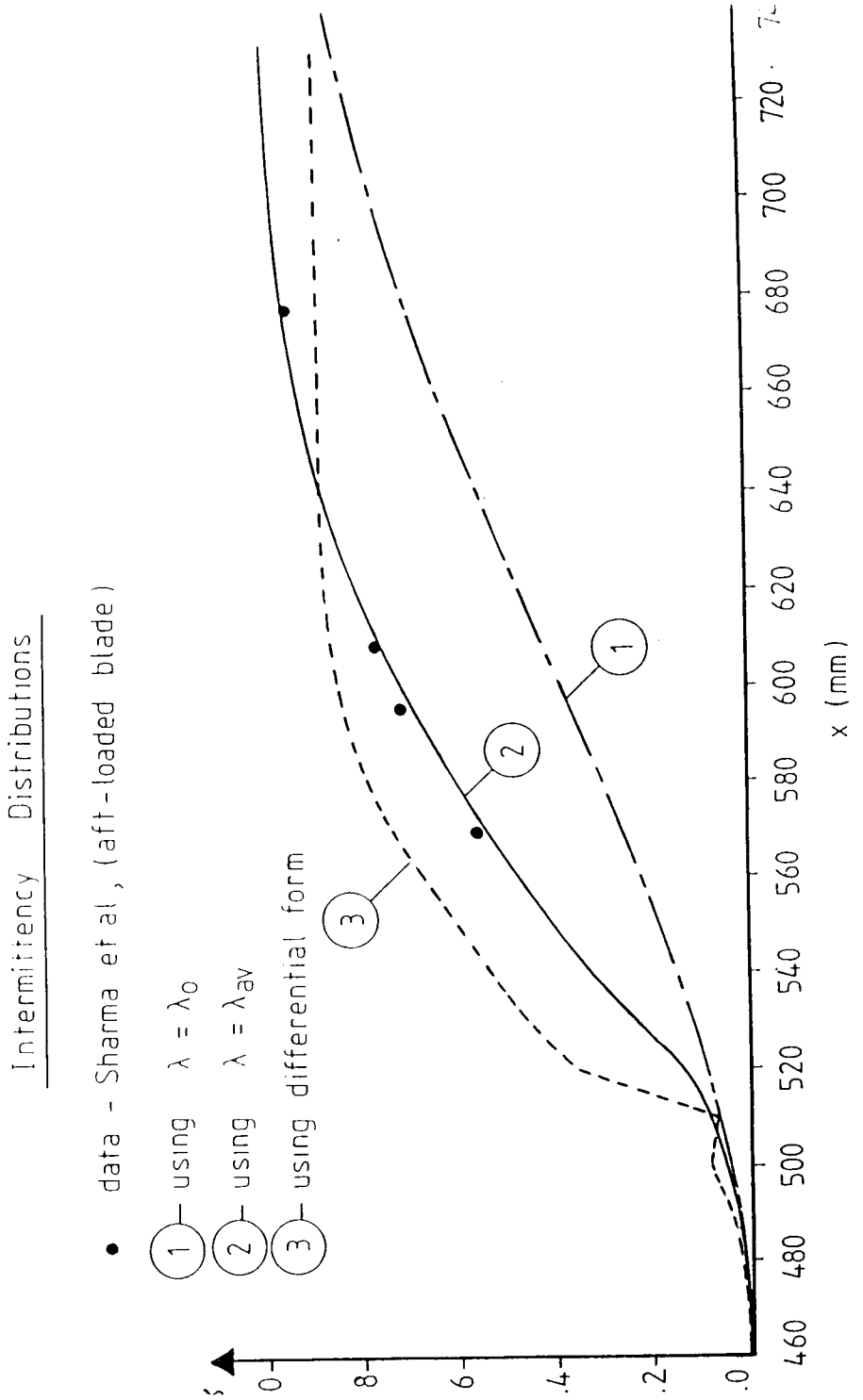

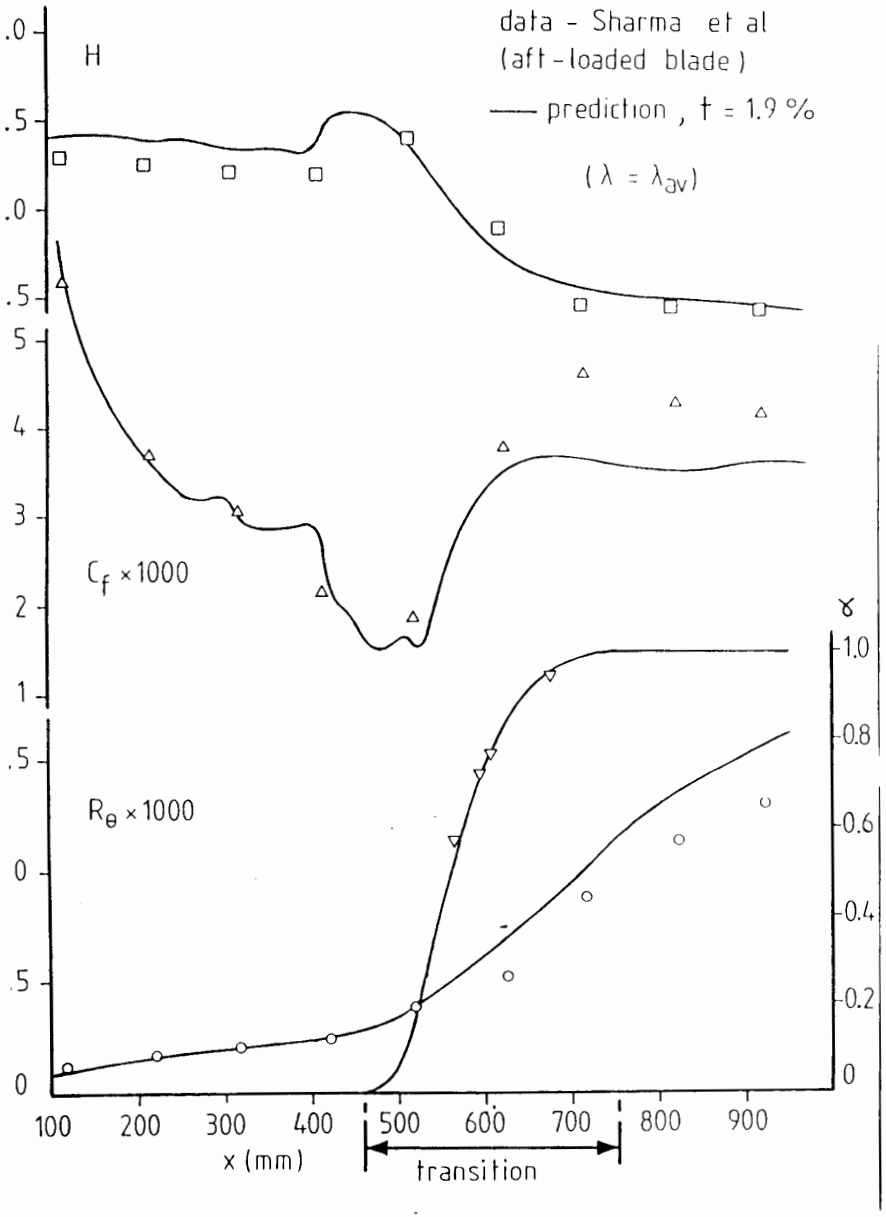
data - Sharma et al
(aft-loaded blade)
prediction , t = 1.9 %
(λ = λav)
H
Cf × 1000
Rθ × 1000
γ
x (mm)
transition

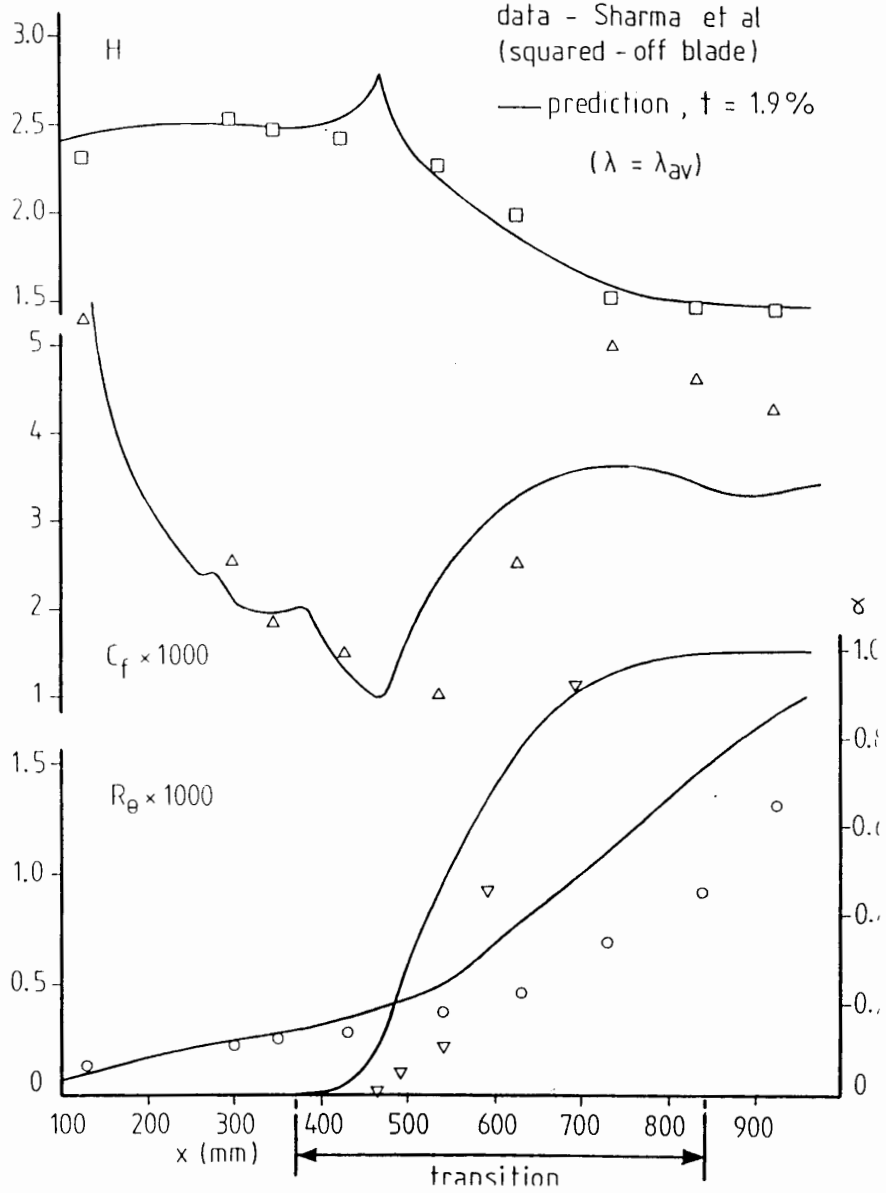
data - Sharma et al
(squared-off blade)
prediction , t = 1.9 %
(λ = λav)
H
Cf × 1000
Rθ × 1000
γ
x (mm)
transition

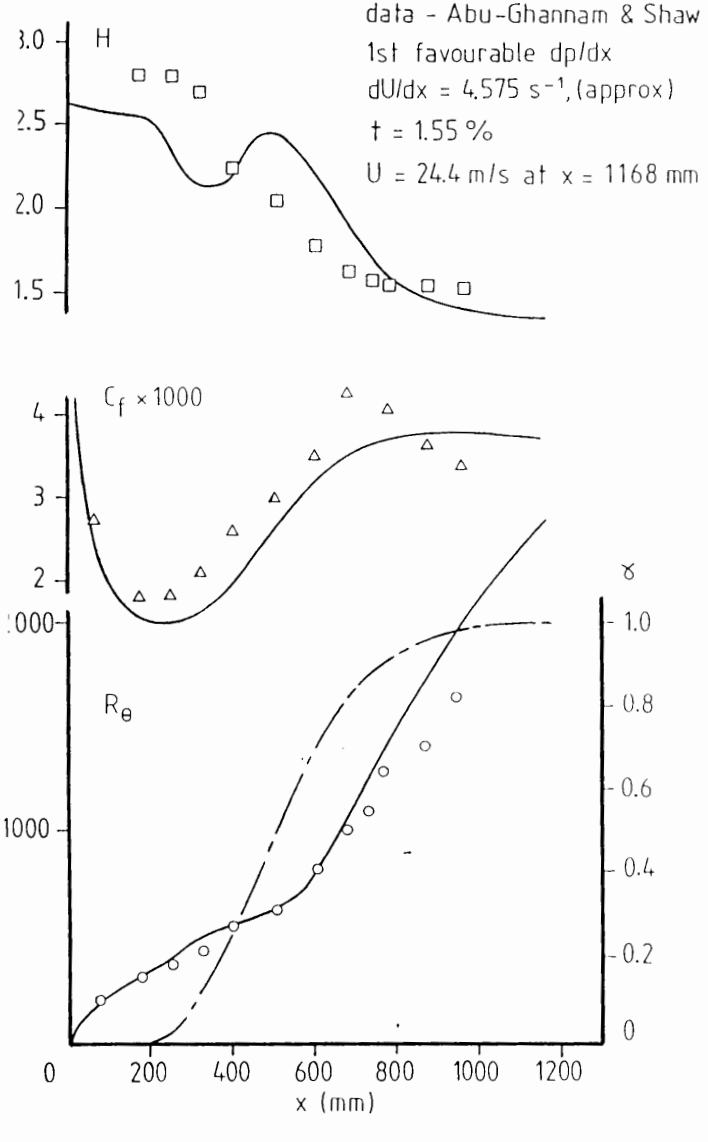
data - Abu-Ghannam & Shaw
1st favourable dp/dx
dU/dx = 4.575 s⁻¹, (approx)
t = 1.55 %
U = 24.4 m/s at x = 1168 mm
H
3.0
2.5
2.0
1.5
Cf × 1000
4
3
2
1000
Rθ
γ
1.0
0.8
0.6
0.4
0.2
0
0
200
400
600
800
1000
1200
x (mm)

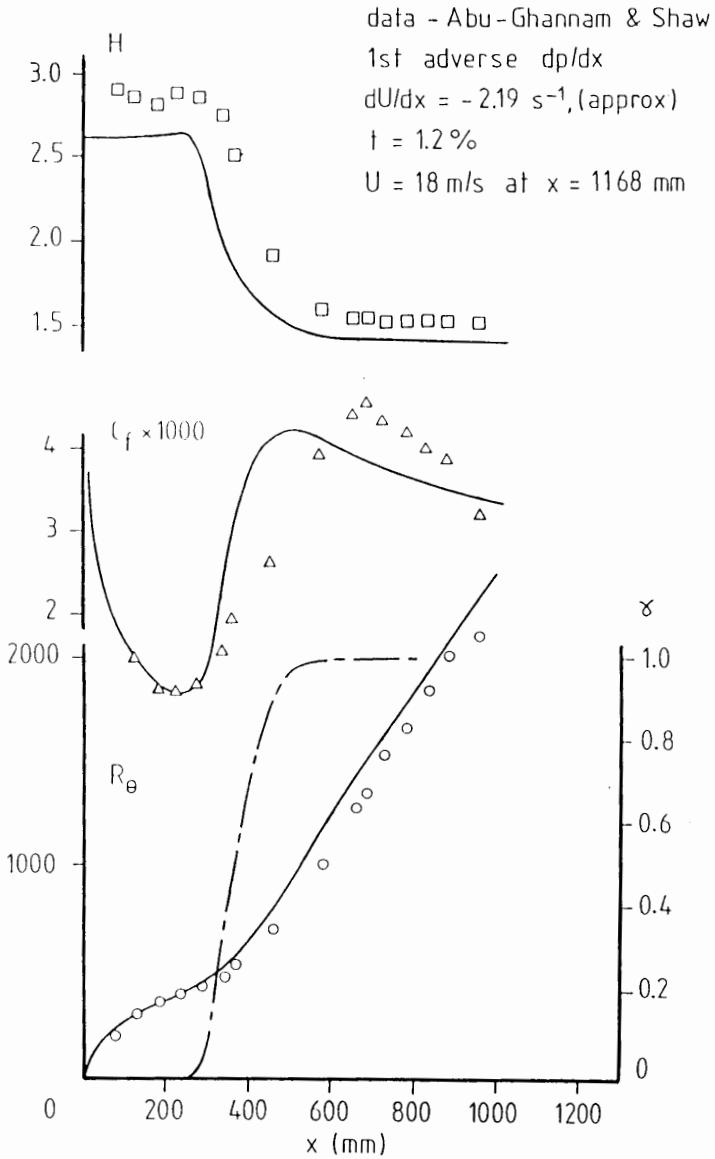
data - Abu-Ghannam & Shaw
1st adverse dp/dx
dU/dx = - 2.19 s⁻¹, (approx)
t = 1.2 %
U = 18 m/s at x = 1168 mm
H
3.0
2.5
2.0
1.5
Cf × 1000
4
3
2
2000
1000
Rθ
γ
1.0
0.8
0.6
0.4
0.2
0
0
200
400
600
800
1000
1200
x (mm)

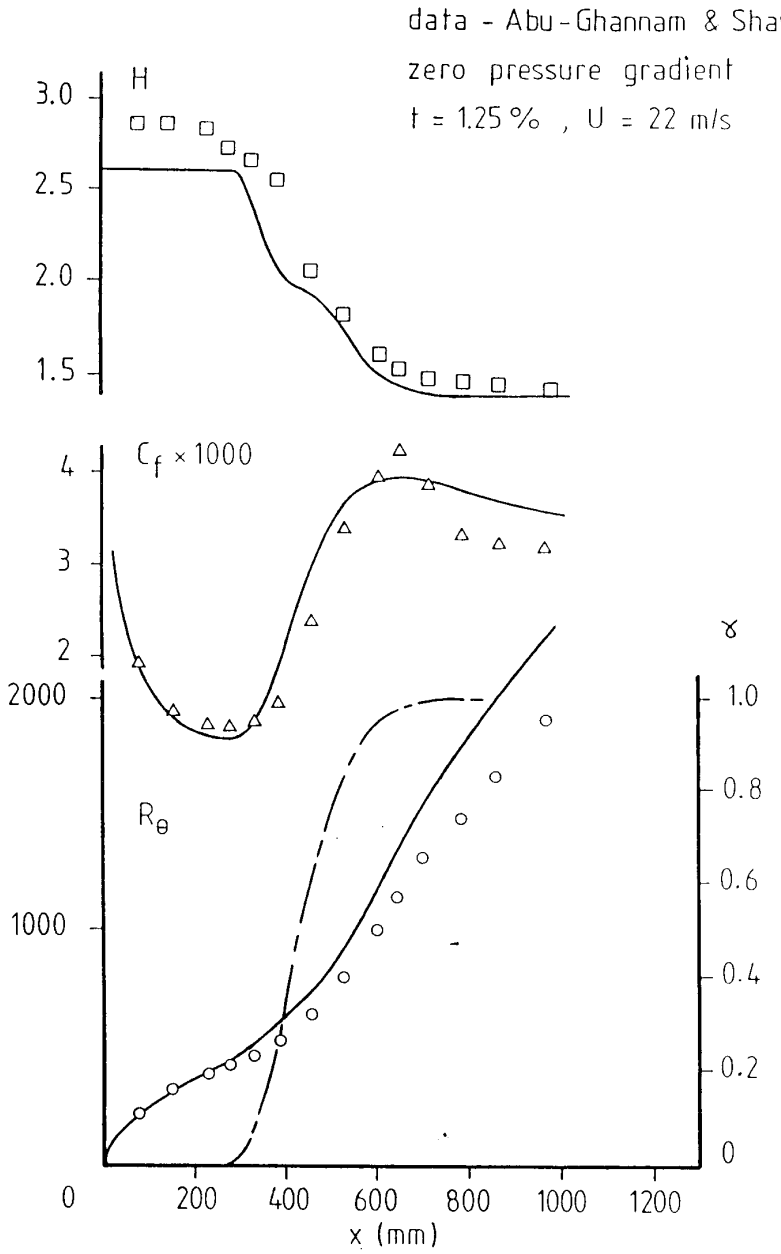
data - Abu-Ghannam & Shaw
zero pressure gradient
t = 1.25 % , U = 22 m/s
H
3.0
2.5
2.0
1.5
$C_f \times 1000$
4
3
2
2000
1000
R_θ
γ
1.0
0.8
0.6
0.4
0.2
0
0
200
400
600
800
1000
1200
x (mm)

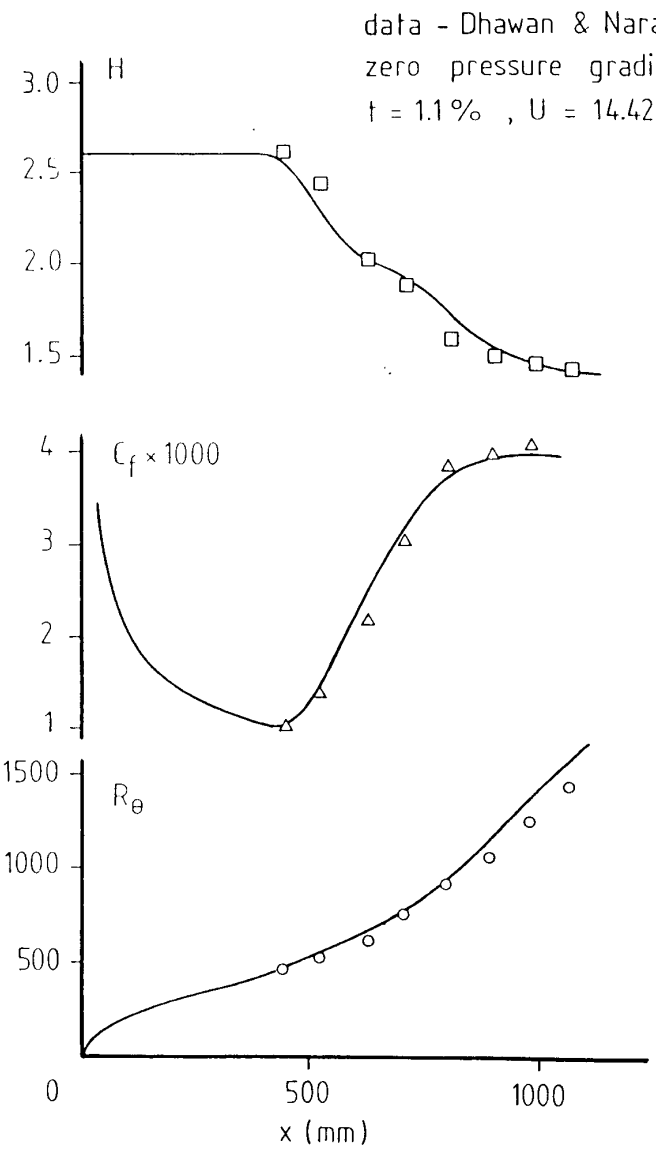
data - Dhawan & Narasimha
zero pressure gradient
t = 1.1 % , U = 14.42 m/s
H
3.0
2.5
2.0
1.5
$C_f \times 1000$
4
3
2
1
1500
1000
500
R_θ
0
500
1000
x (mm)

Superimpose blades y/n ? y

Press return to start computation? ▌

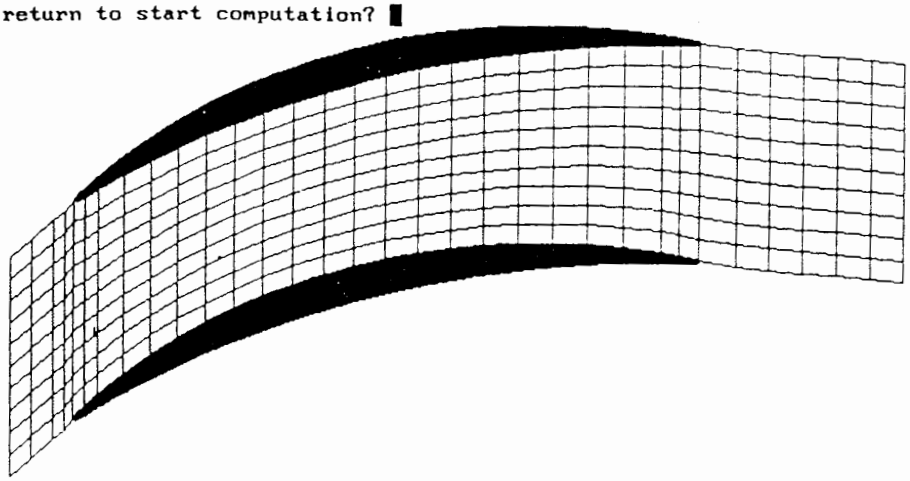

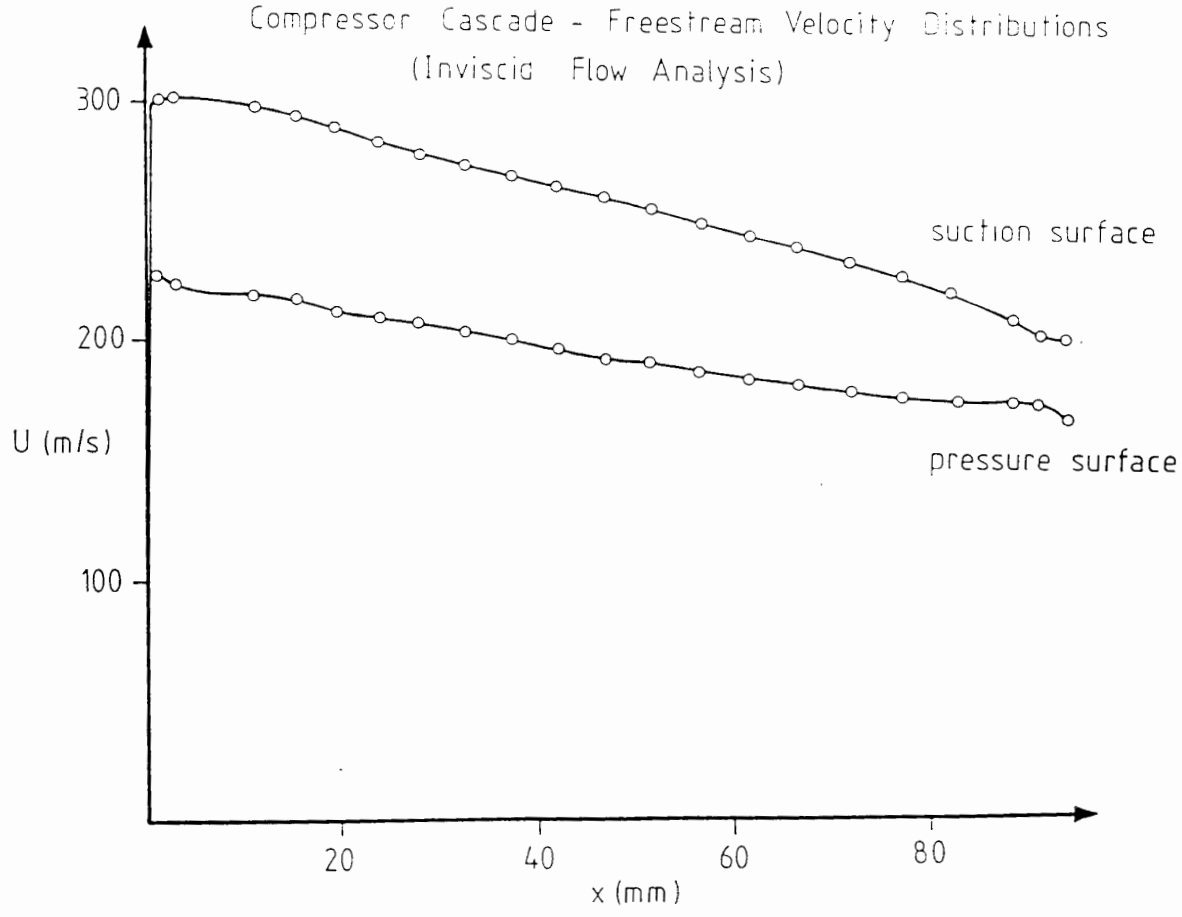

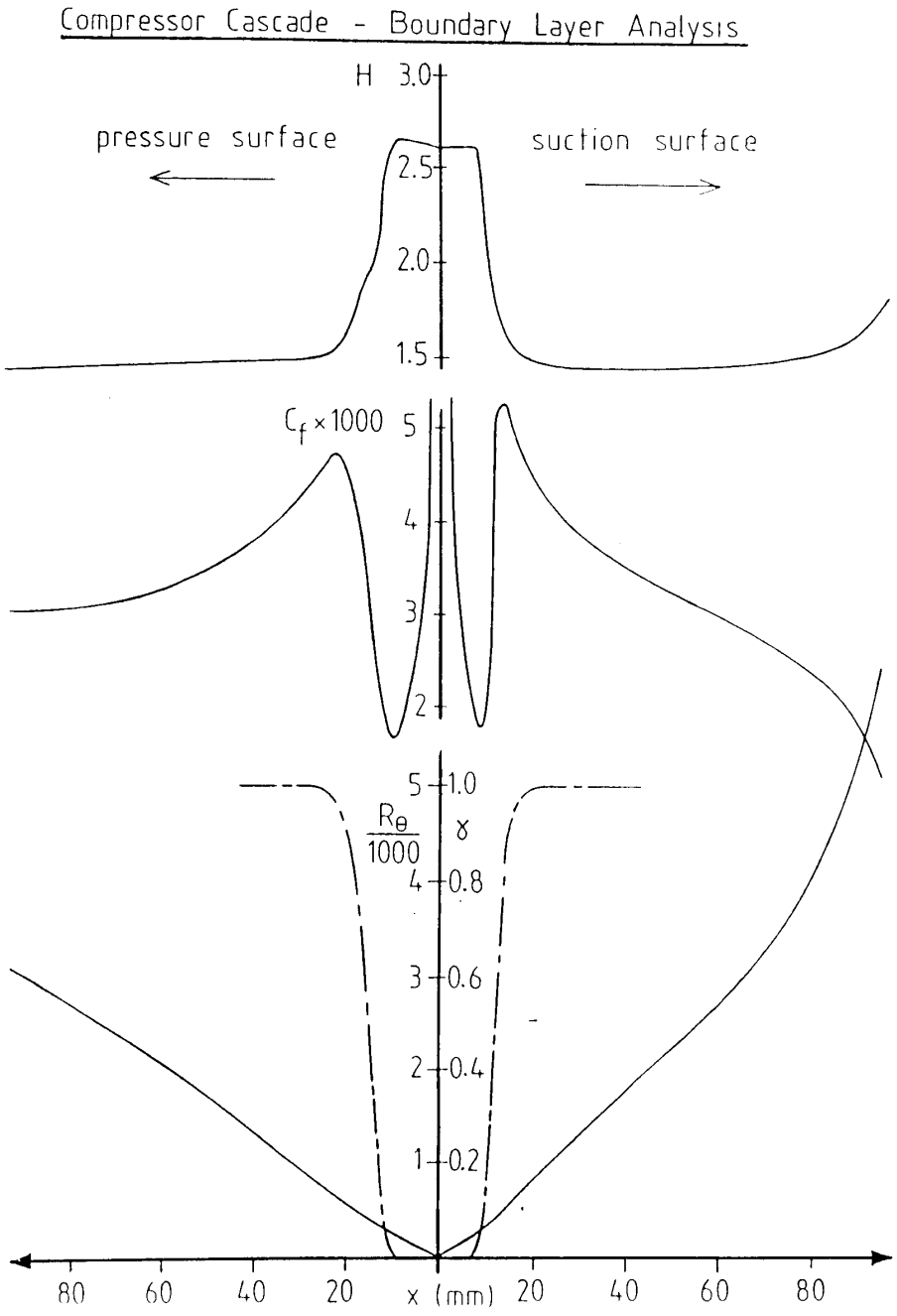
Compressor Cascade - Boundary Layer Analysis
H
3.0
2.5
2.0
1.5
pressure surface
suction surface
$C_f \times 1000$
5
4
3
2
$\frac{R_\theta}{1000}$
5
4
3
2
1
1.0
0.8
0.6
0.4
0.2
γ
80
60
40
20
x (mm)
20
40
60
80

Intermittency Models and Spot Measurements

D.A. Ashworth
Rolls Royce Plc.
P.O. Box 3 Fiton
Bristol, England

ABSTRACT

Experimental work at the University of Oxford Osney Laboratory has demonstrated characteristics of the late-stage transition process by the use of thin-film heat transfer gauges. The development of turbulent spots has been observed in a range of-environments, including flat plates, turbine blade cascade tests and wake-passing experiments.

These results were taken at Mach / Reynolds Numbers and gas-to-wall temperature ratios representative of gas turbines. Analyses of the spot characteristics are consistent with measurements taken in low speed experiments, and support the Schubauer and Klebanoff type of turbulent spots. The addition of simulated wakes from upstream stages has been observed to be primarily superpositional for these tests.

Intermittency models have been developed which can simulate the development of turbulent spots based on input of spot generation rates. As reliable methods become available to predict the streamwise distribution of spot generation rates, such models will provide a better separation of transitional influences, such as pressure gradient on spreading angle. These models can be used in a time-averaged form (by numerical integration) or in time-resolved methods.

It is possible to adapt such intermittency models to perform transitional boundary-layer calculations in conjunction with existing flowfield CFD techniques. There are many instances where the application of these models is appropriate to the analysis of fluid dynamic environments, such as during the design evaluation process or for simplified flowfield solvers. Time-resolved models are particularly useful in support of data analysis and interpretation. It is expected that further experimental work and analysis underway at the Osney Laboratory will help to develop practical applications for these techniques.

NASA/CP—2007-214667

Intermittency Models and Spot Measurements

D A Ashworth August 1993

Contents

- Spot Measurements
- Modelling Principles
- Results
- Applications/Future Work

Spot Measurements

- Measurements taken with Thin Film Heat Transfer Gauges are sensitive to laminar-turbulent transition and allow for high frequency resolution of turbulent spots

- Turbulent spots have been observed using TFGs on flat plates and a variety of 2D cascades. These have been taken at Mach numbers, Reynolds numbers and Tg/Tw consistent with gas turbine operating conditions.

- Initial results allowed for tracking of individual spots, and led to calculations of trajectories and growth rates consistent with low-speed spot measurements

- Analysis of data suggested modelling techniques based on the Emmons' principles.

Applications and Future Work

- Choice of model needs to suit application
- Process enables a better separation of variables
- Simulations provide a useful analysis tool
- Better predictions of inputs can feed common models
- Ability to apply to calculations involving time dependent phenomena, history effects, varying pressure gradients, 3-D flows, ...
- Better resolution of spots and effects of input parameters required for improved models

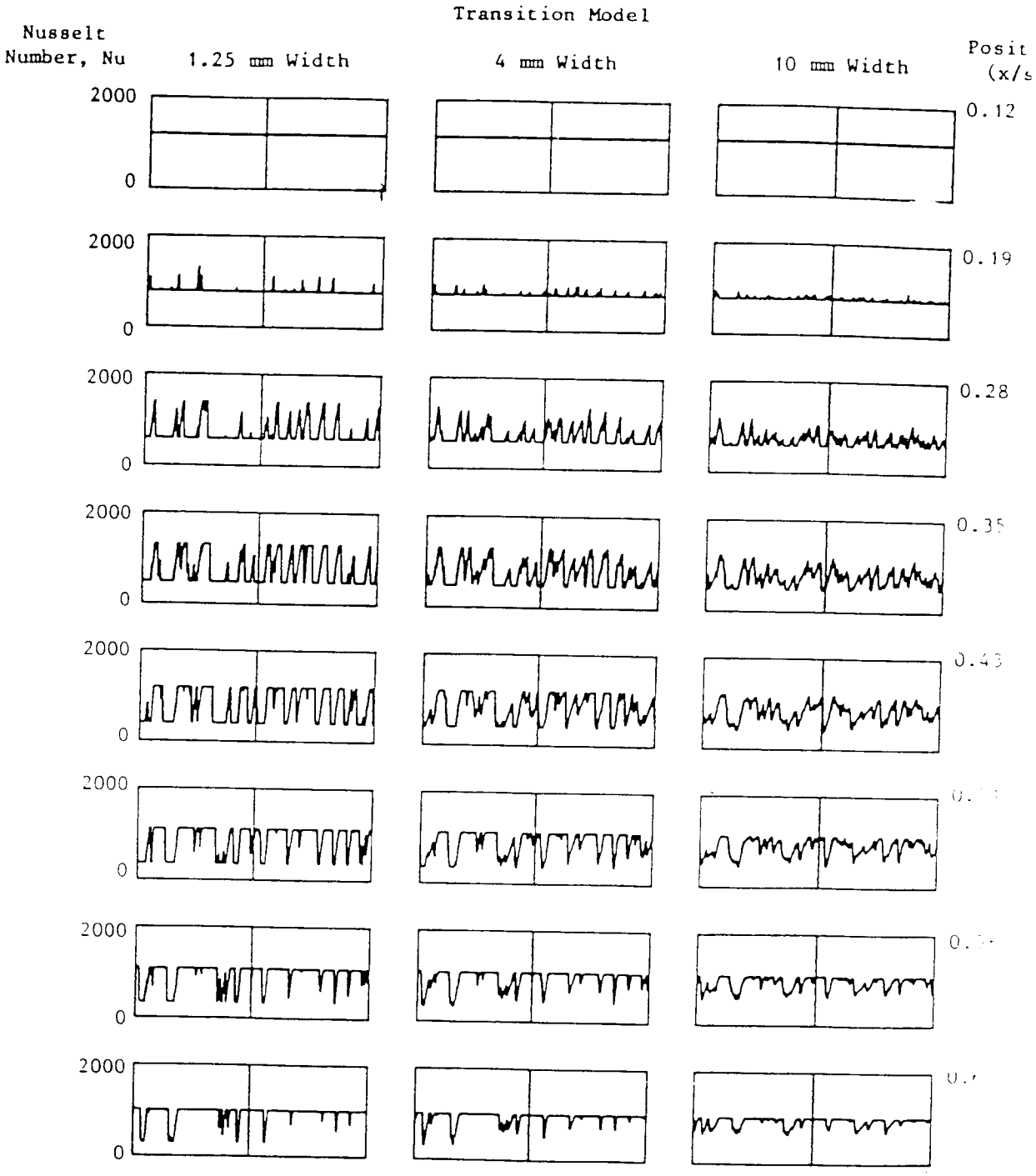

Effect of Variation in Spanwise Gauge Width on the Predicted Instantaneous Values of Nusselt Number through Transition. Even the 'noise-less' Intermittency Signals Become Difficult to Interpret as the Gauge Width Increases to 10 mm due to the Effects of Spanwise Averaging.

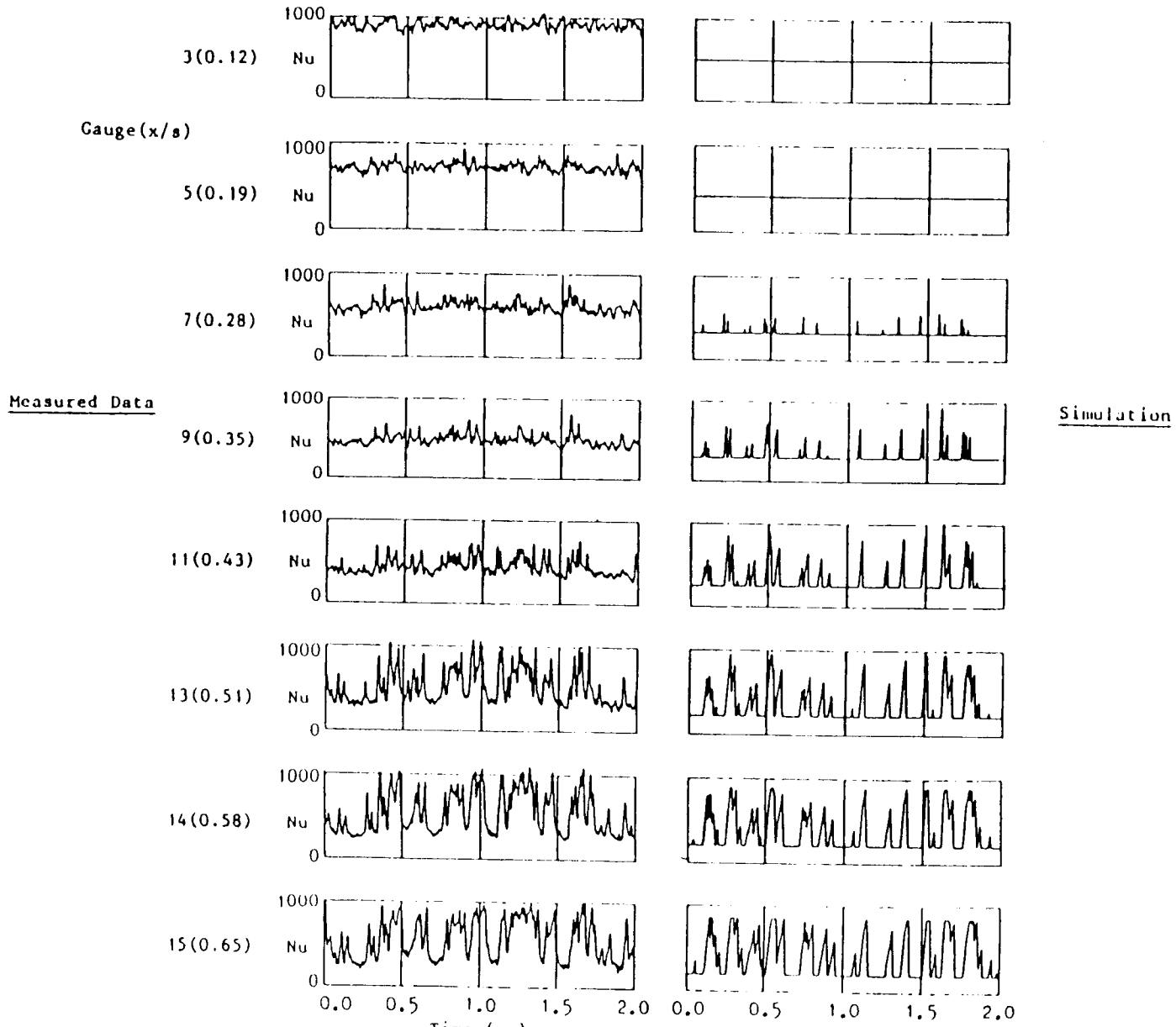

Comparison of transition simulation model predictions of instantaneous surface heat transfer rates with observed data.

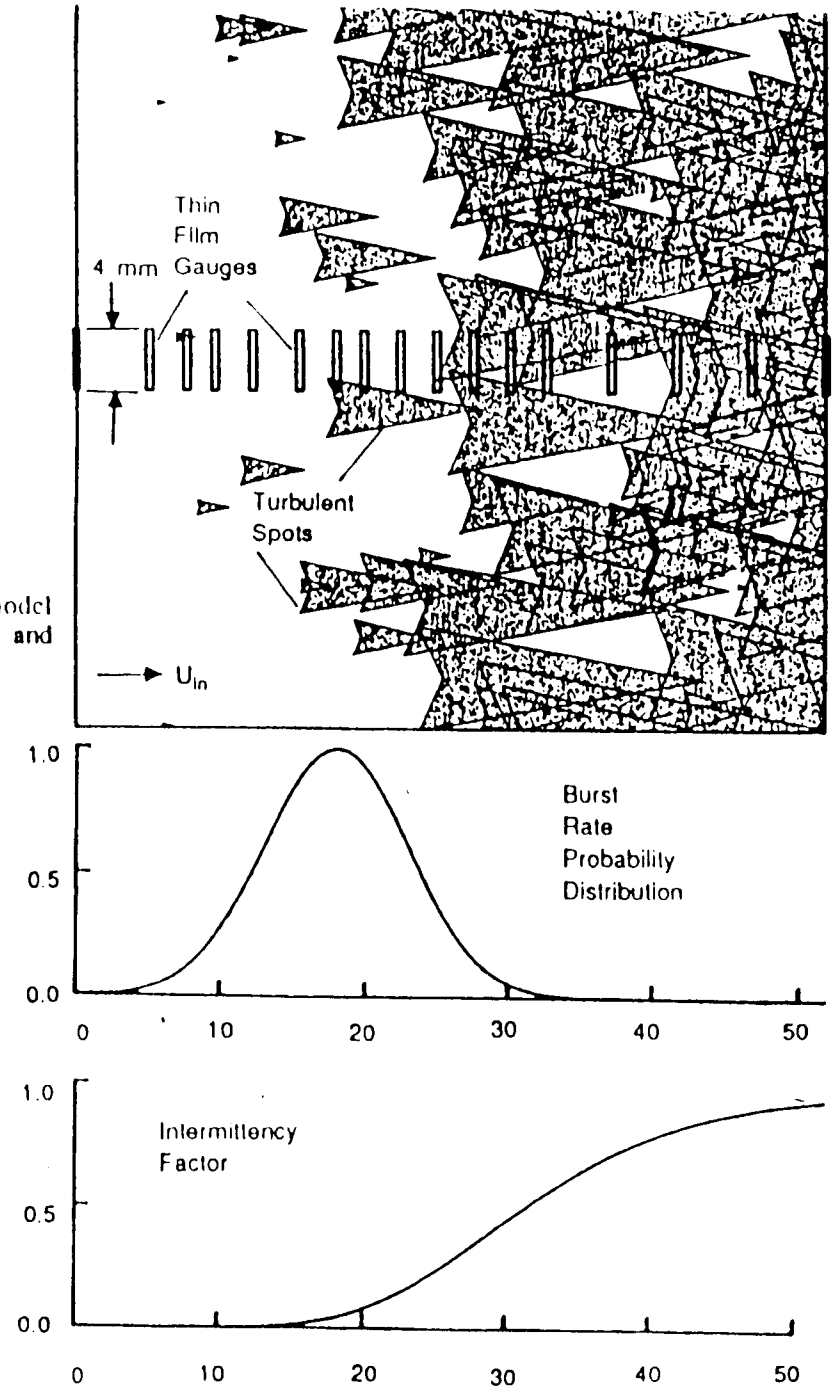

Plan view of simulation of transition on model surface with assumed burst rate distribution and resulting intermittency.

Modelling Principles

Several approaches can be made to the development of the Emmons model depending on the application:

- Analytical solutions for straightforward spot sources
- Numerical integration for steady calculations
- Spot simulations for unsteady calculations and analysis

These can be patched into flowfield or boundary-layer models

The models give an increasing amount of flexibility based on an input of spot generation rates, trajectories and spreading rates

	MODE	DESCRIPTION	TYPICAL γ	APPLICABILITY	PREDICTION TYPE
1.	NATURAL TRANSITION	T-S WAVE AMPLIFY, DEVELOP 3-D DISTURBANCES -> TURBULENT SPOTS	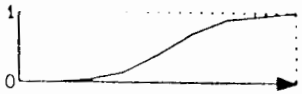	MILD ADVERSE -> FAVOURABLE dp/dx, CONVEX -> FLAT, ISOTROPIC DISTURBANCES	STABILITY CALC.-> ONSET Re, INTERMITTENCY MODEL
2.	WAKE PASSING	TURBULENT PATCHES DUE TO WAKE PRESENCE	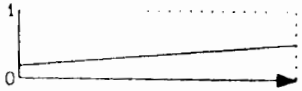	TIME AND SPACE AVERAGED (~2-D), REAL TURBINES	STRIPED-AIR CALC. -> DURATION + LAG EFFECTS
3.	GOERTLER VORTICITY	LONGITUDINAL VORTICITY INDUCED BY CONCAVE SURFACES -> INSTABILITY	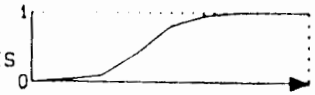	CONCAVE SURFACES, OR REGIONS WITH CONCAVE STREAMLINES	CORRELATIONS, TURBULENT VISCOSITY MODELS
4.	INTERMITTENT SEPARATION	MOMENTARY FLOW REVERSAL, DUE TO FLOW UNSTEADINESS	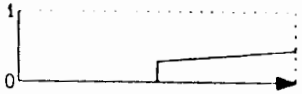	MILD ADVERSE dp/dx, PERIODIC EFFECTS, SHOCK/B.L. INTERACTIONS	CORRELATIONS BASED ON CRITICAL POHLHAUSEN PARAMETER
5.	STEADY SEPARATION	STRONG ADVERSE dp/dx, TURBULENT RE-ATTACHMENT	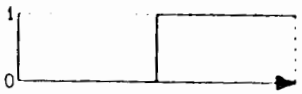	DIFFUSION REGIONS, NEAR CHANGE IN SIGN OF dp/dx -ve TO +ve	CORRELATION FOR CRITICAL POHLHAUSEN PARAMETER

Description of Some of the Competing Modes of Transition from Laminar to Turbulent Flow.

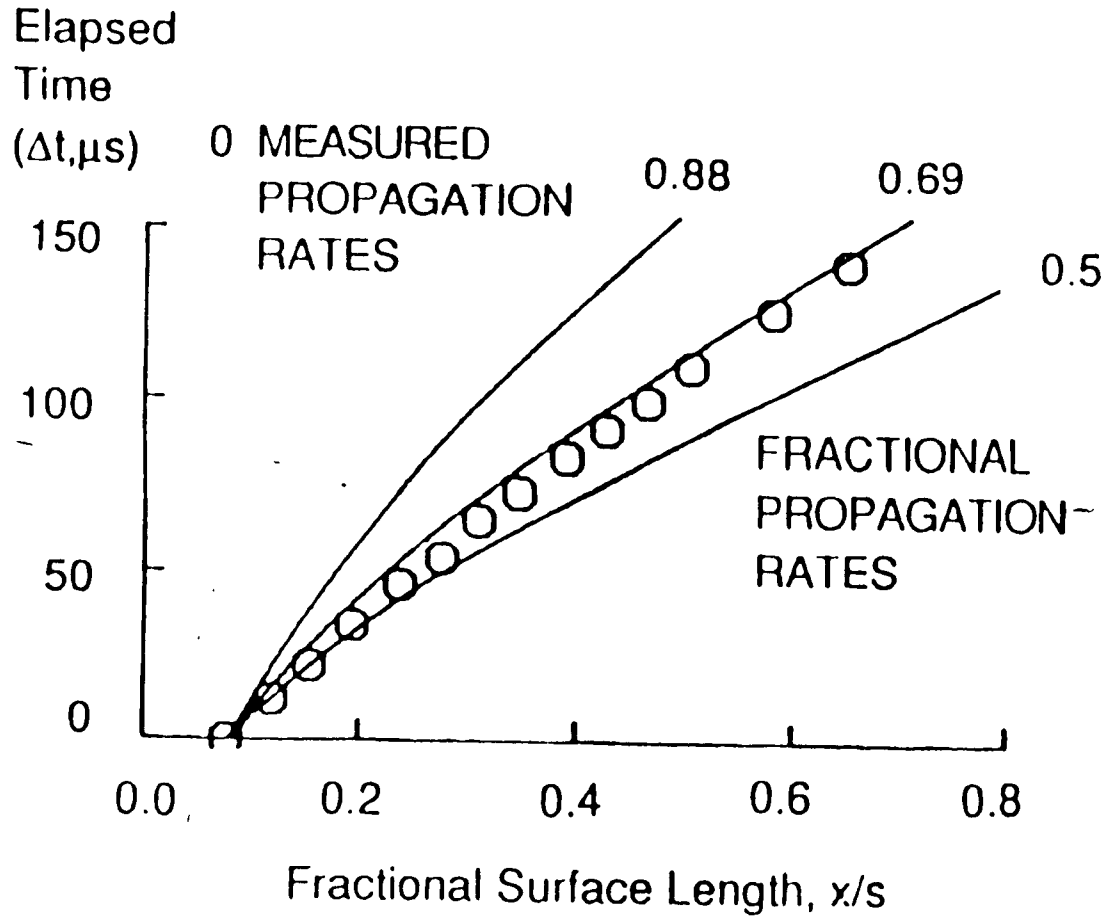

Turbulent spot trajectories along model surface.

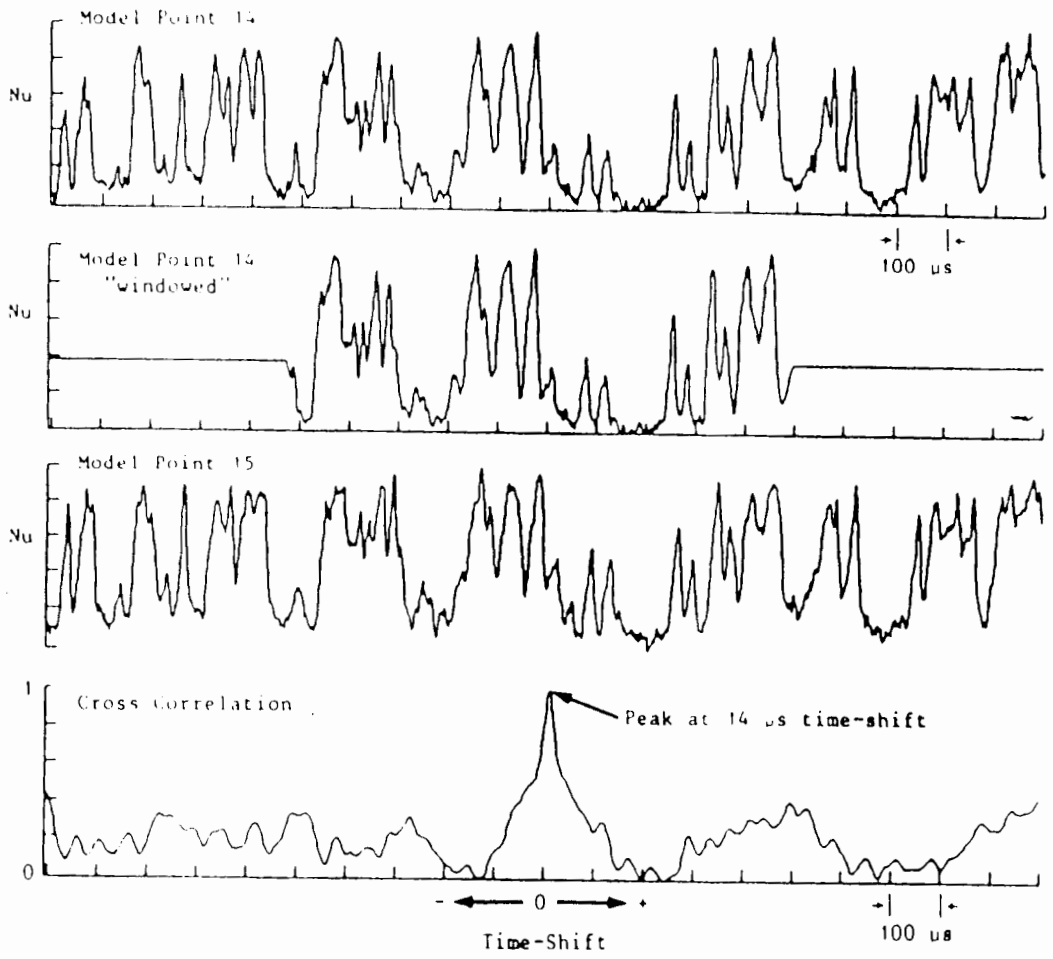

Example of Cross-Correlation Analysis of Adjacent Heat Transfer Signals in a Transitional Boundary Layer.

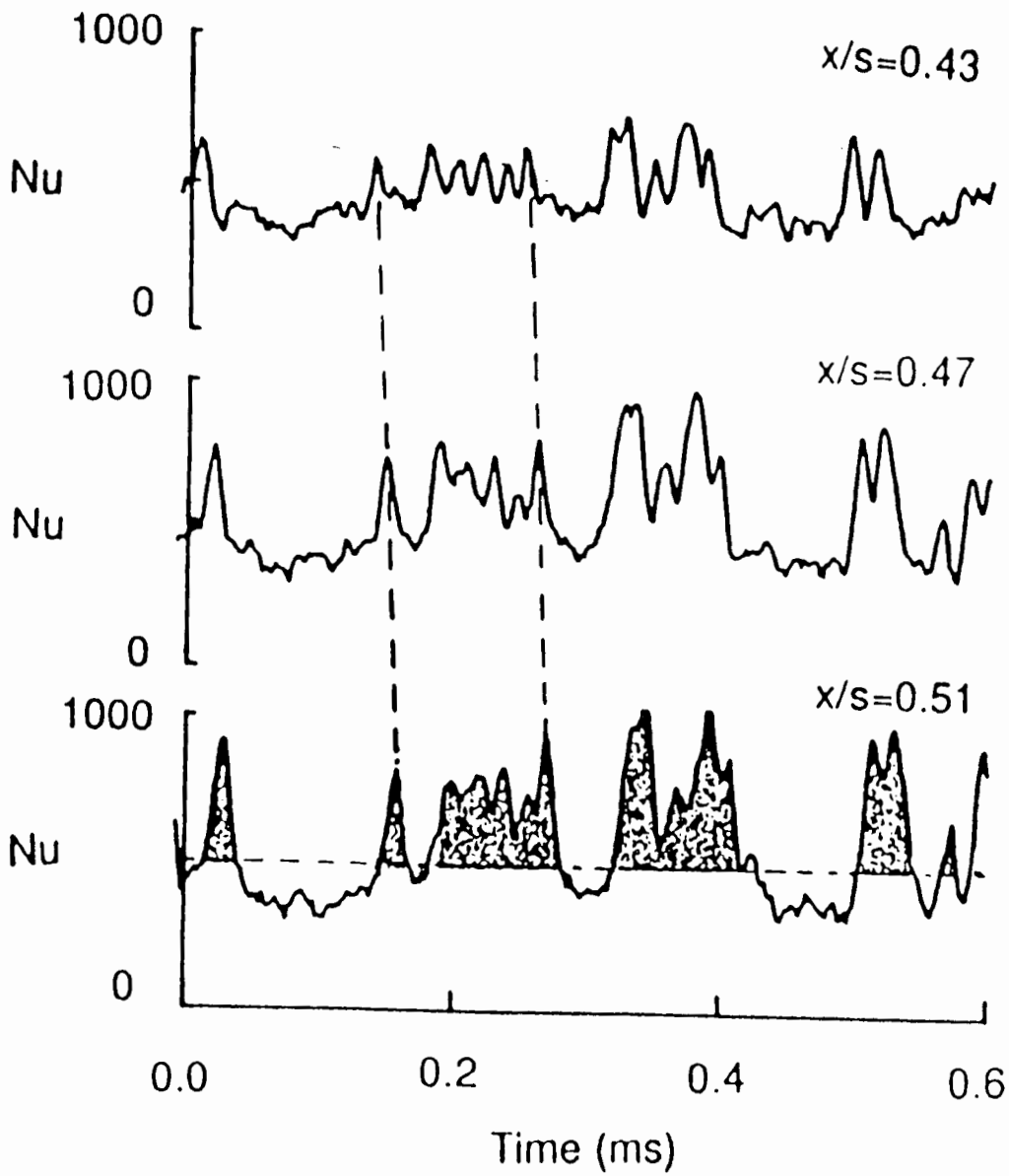

Time resolved surface heat transfer rates on successive gauge positions showing convection rate and intermittency estimation procedure

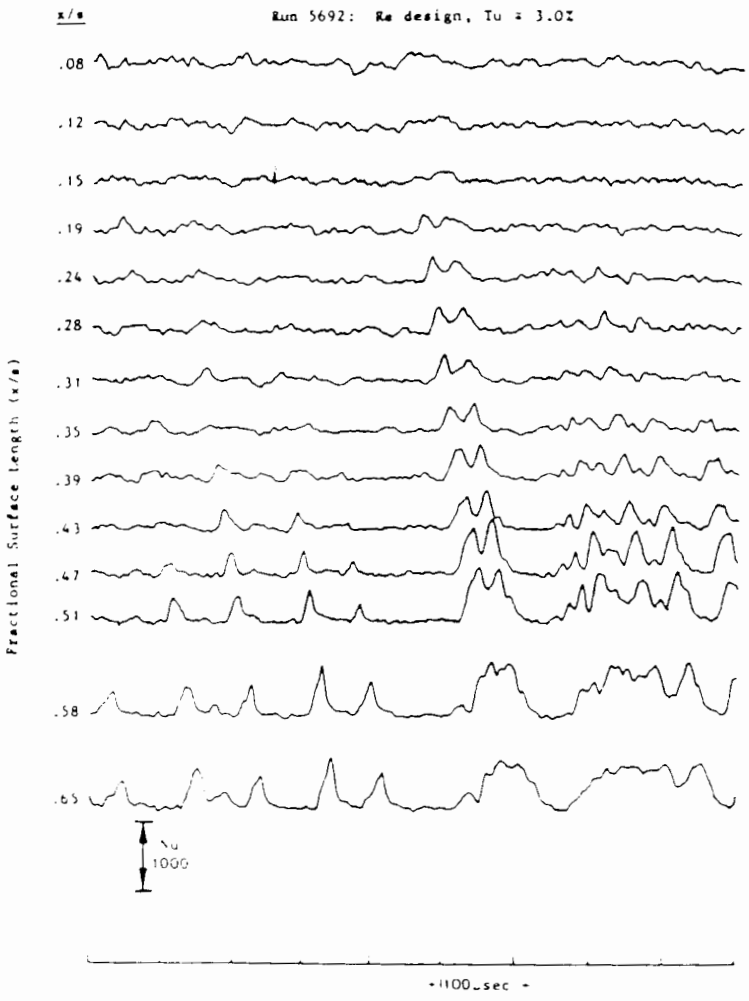

Heat Transfer Measurements (as defined in Fig. 5.1) Drawn to an Expanded Time-Scale. By Closely Spacing Adjacent Traces the Degree of Similarity between Neighbouring Gauge Measurements is Evident. A Pair of Disturbances Occurring at about x/s 0.15 - 0.19 can be Tracked Along the Surface until they Merge by x/s = 0.65.

BOUNDARY LAYER TRANSITION ON AN AXIAL COMPRESSOR STATOR BLADE - WAKE PASSING AND FREESTREAM TURBULENCE EFFECTS

G.J. Walker and W.J.Solomon
Department of Civil & Mechanical Engineering
University of Tasmania
Hobart, Tasmania
Australia

ABSTRACT

Quantitative observations of transitional boundary layers in regions of strong flow deceleration on an axial compressor stator blade are reported. Measurements were obtained at a fixed chordwise position, and the blade incidence was varied by changing the compressor throughflow so as to move the transition region relative to the stationary probe. It was thus possible to observe typical boundary layer behavior at various stages of transition in the turbomachine environment. The range of observations covers separating laminar flow at transition onset, and reattachment of intermittently turbulent periodically separated shear layers.

Transition was characterised by the regular appearance of turbulent spots in association with disturbances from the passing wakes of upstream rotor blades. However, the initial breakdown did not coincide with the wake passage as has usually been observed by other workers. The spots rather evolved from the growth of instability wave packets which lagged the wake passage. This behavior is quite similar to that observed by other workers in the wind tunnel studies of artificially generated turbulent spots.

Data presented from the compressor blade measurements include : mean and ensemble-average velocity distributions and associated integral parameters; distributions of total, periodic and random disturbance components; typical individual velocity fluctuation records; contours of ensemble-average random disturbance level; and boundary layer intermittency distributions.

The transitional flow behavior is compared for two characteristically different types of freestream disturbance environment:
(a) isolated rotor wake disturbances interspersed with regions of relatively low freestream turbulence level; and
(b) isolated rotor wake disturbances with a continuous, relatively high freestream turbulence level superimposed.
In the latter case there is a noticeable increase in random velocity fluctuations within the boundary layer and a slight decrease in unsteadiness (i.e. amplitude of ensemble-average velocity variations with time). Transition onset is a little earlier, but the essential character of the turbulent breakdown (with spots appearing regularly in association with the rotor wake passage) remains unchanged. It is concluded that freestream turbulence is not the dominant factor promoting transition in this particular case.

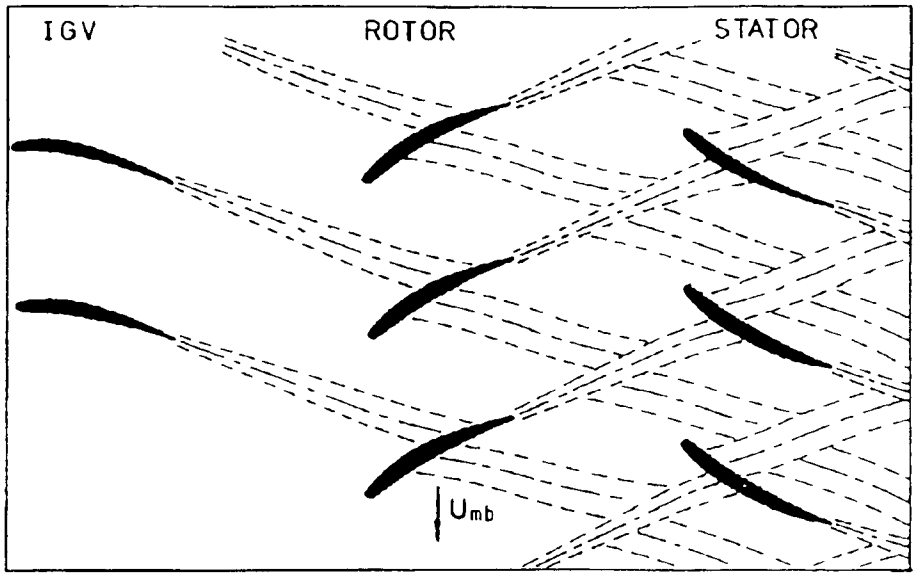

Fig. 1 Cross-section of compressor blading, showing typical instantaneous wake dispersion

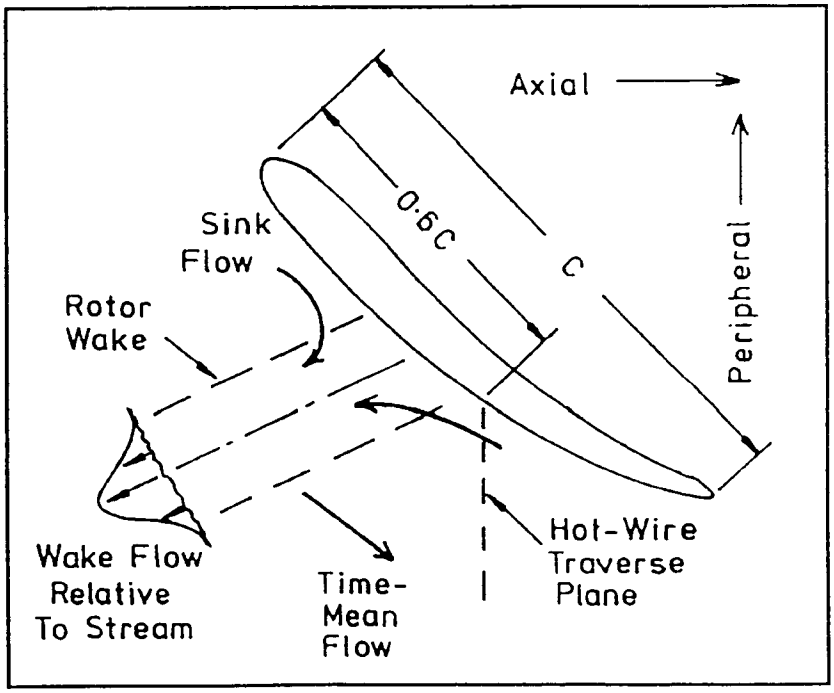

Fig. 2 Stator blade boundary layer - hot wire traverse detail

Table 1 Test Parameters (time-mean values)

Case	1	2	3	4	5
ϕ	0.726	0.704	0.609	0.752	0.791
i (°)	-3.1	-2.0	2.3	-4.5	-6.3
U_{std} (ms^{-1})	20.3	19.8	17.6	20.8	21.4
$Tu_{D,\infty}$	0.029	0.033	0.050	0.034	0.026
δ (mm)	1.44	1.44	2.80	1.15	1.11
θ (mm)	0.157	0.167	0.287	0.136	0.137
Re_θ	186	197	339	160	161
H	3.77	3.37	2.17	3.92	3.70
$C_f \times 10^3$	0.39	0.70	1.73	0.42	0.59

Case	8	9	10	11	12
ϕ	0.785	0.755	0.732	0.700	0.607
i (°)	-6.1	-4.6	-3.4	-1.9	2.3
U_{std} (ms^{-1})	21.8	20.7	20.2	19.6	17.6
δ (mm)	1.19	1.28	1.44	1.52	2.74
θ (mm)	0.138	0.148	0.158	0.175	0.266
Re_θ	163	175	187	207	314
H	4.04	4.04	3.98	3.61	2.29
$C_f \times 10^3$	0.42	0.37	0.37	0.52	1.47

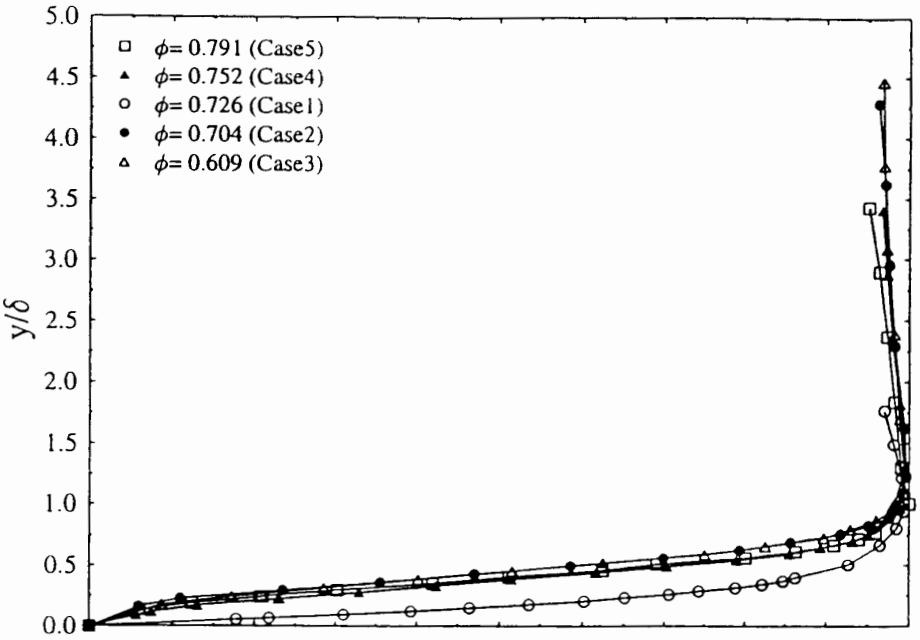

a. Stator blade suction surface clear of IGV wake street

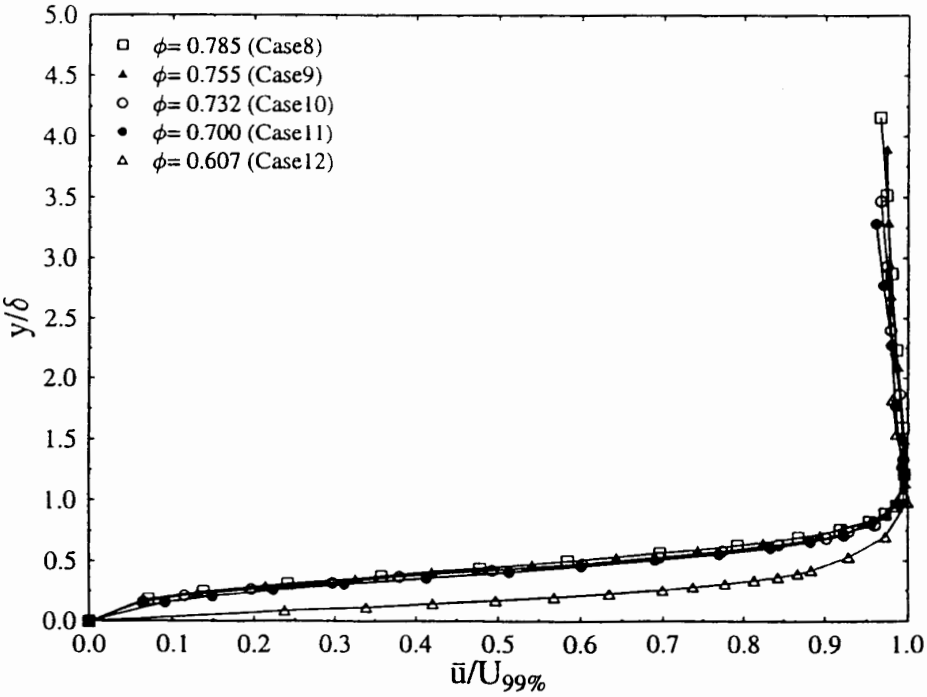

b. Stator blade suction surface in IGV wake street

Fig. 4 Mean velocity variation near stator suction surface, x/c = 0.60

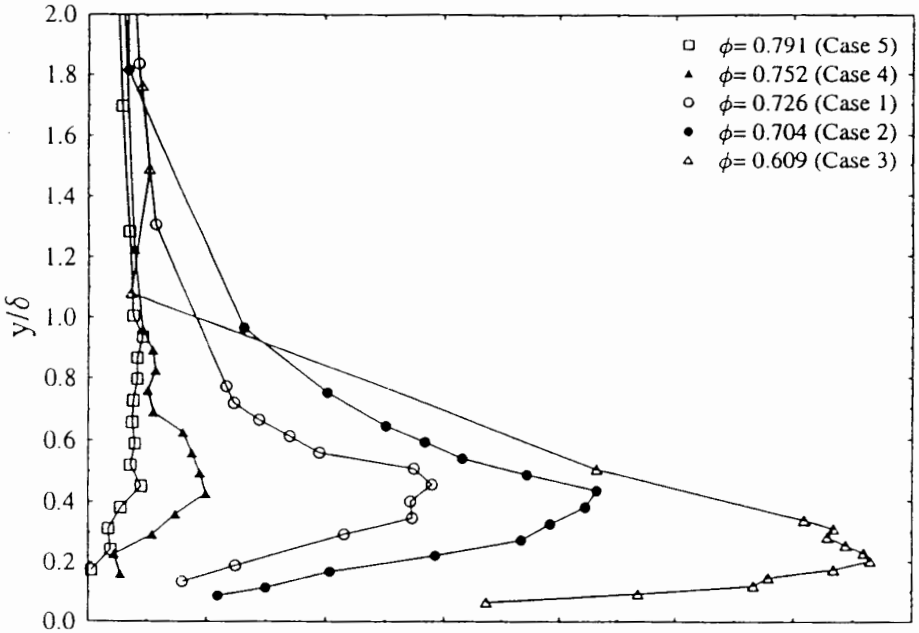

a. Stator blade suction surface clear of IGV wake street

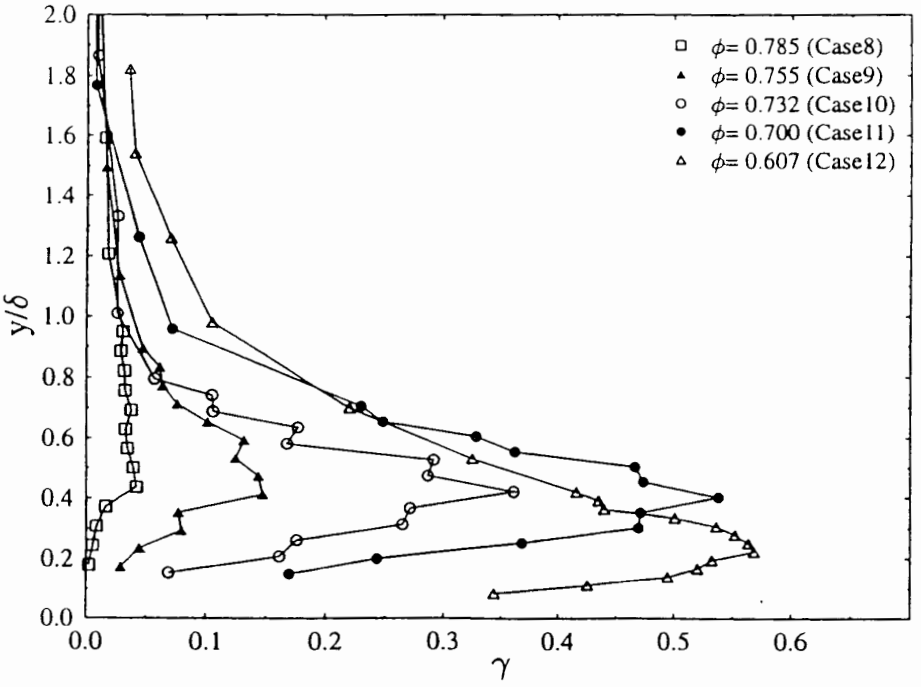

b. Stator blade suction surface in IGV wake street

Fig. 6 Intermittency distributions for boundary layers at different stages of transition, stator suction surface, x/c = 0.60

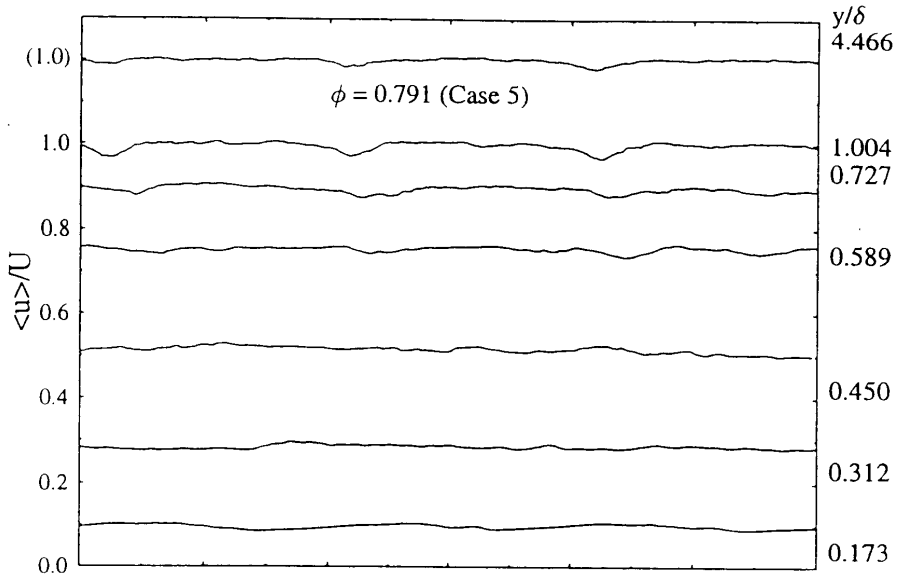

a. Stator blade suction surface clear of IGV wake street

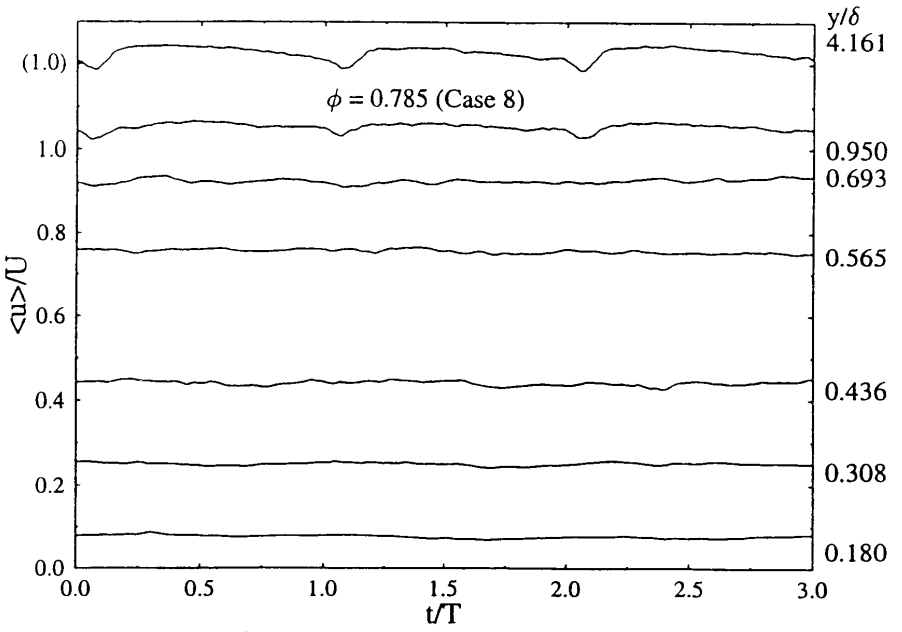

b. Stator blade suction surface in IGV wake street

Fig. 8 Ensemble-averaged velocity variation with time, stator suction surface, x/c = 0.60

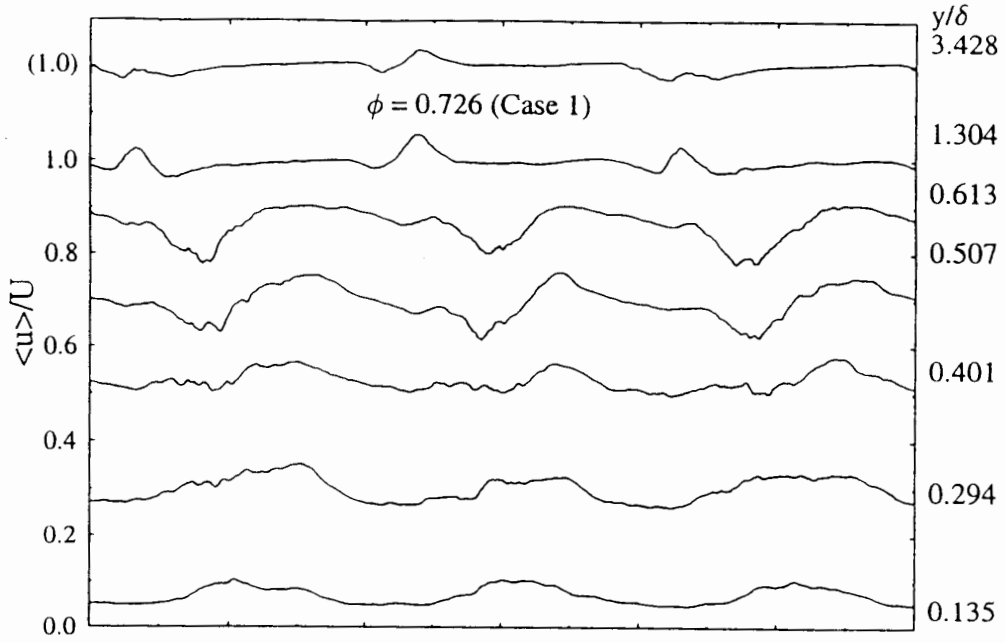

a. Stator blade suction surface clear of IGV wake street

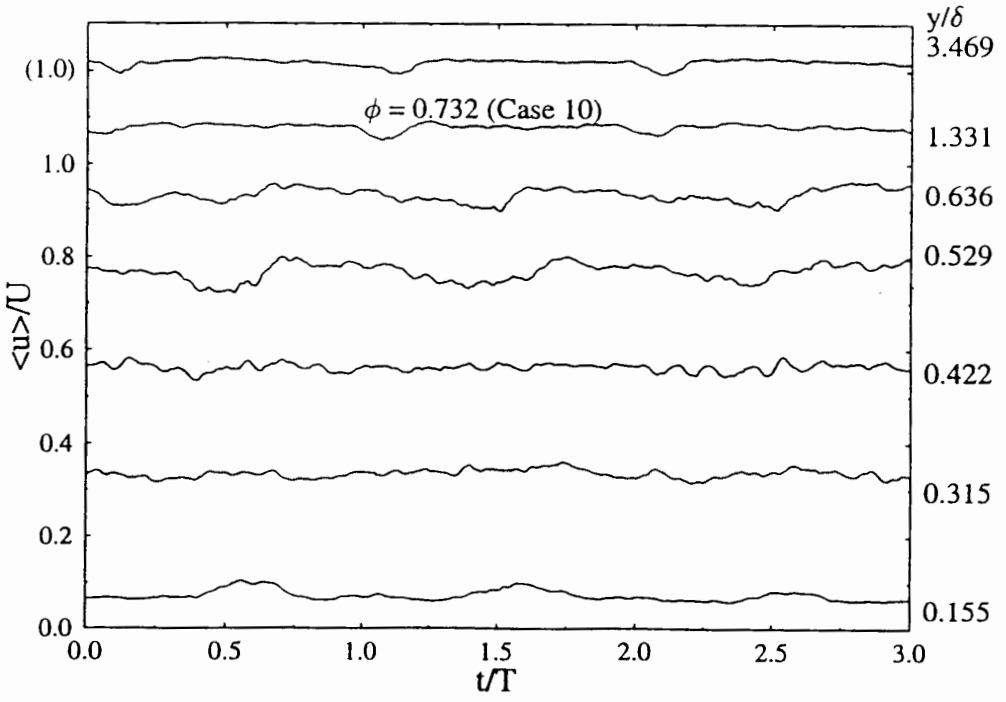

b. Stator blade suction surface in IGV wake street

Fig. 10 Ensemble-averaged velocity variation with time, stator suction surface, x/c = 0.60

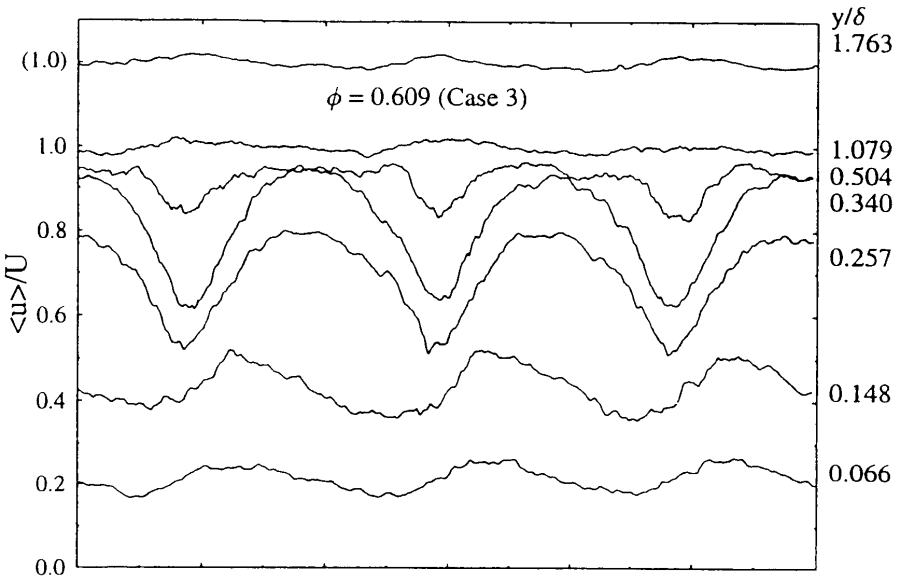

a. Stator blade suction surface clear of IGV wake street

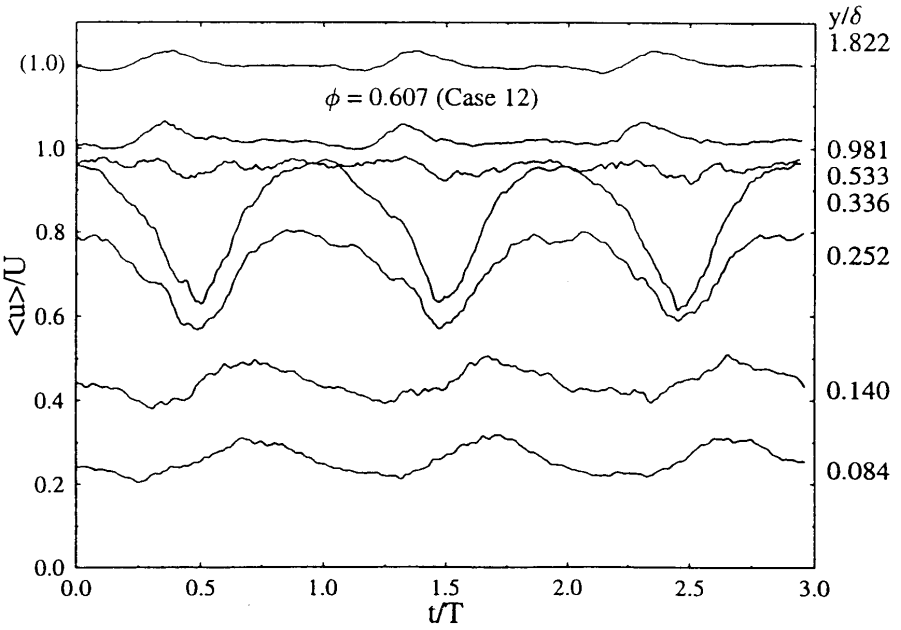

b. Stator blade suction surface in IGV wake street

Fig. 12 Ensemble-averaged velocity variation with time, stator suction surface,

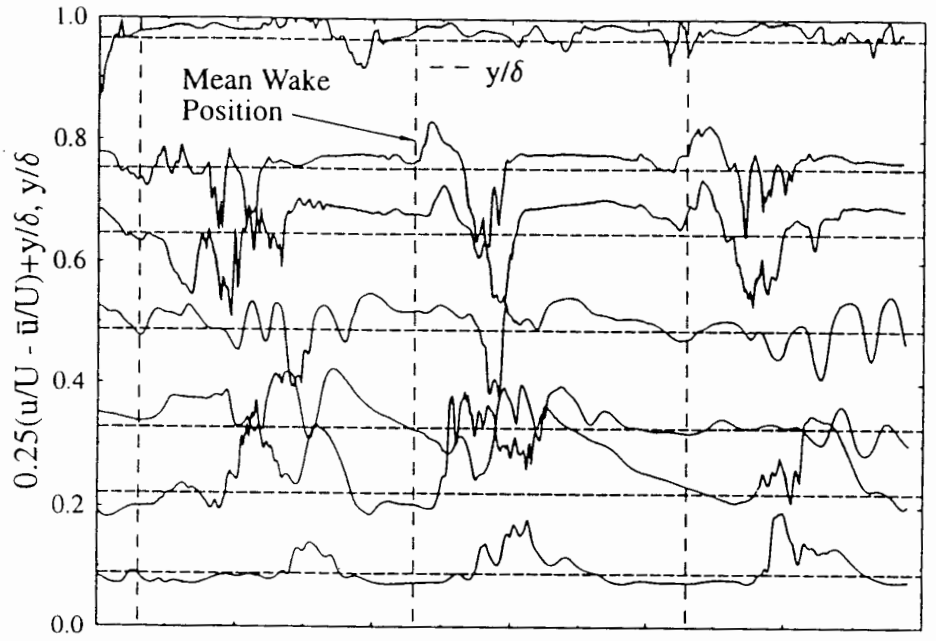

a. Stator blade suction surface clear of IGV wake street (Case 2)

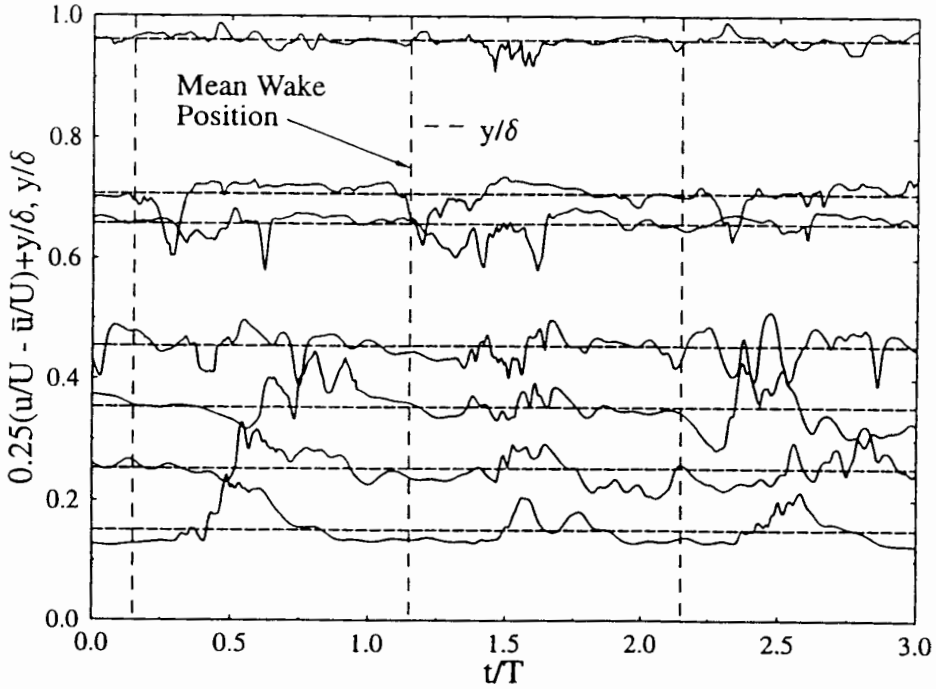

b. Stator blade suction surface in IGV wake street (Case 11)

Fig. 14 Set of typical individual u(t) records for different y, stator suction surface, x/c = 0.60

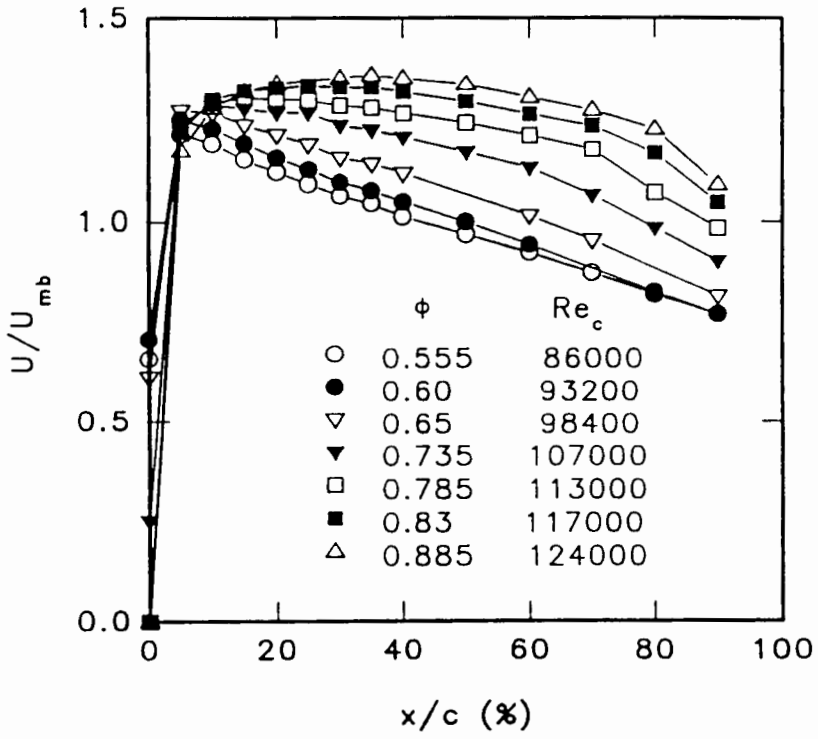

Fig. 16 Stator suction surface velocity distributions at mid-blade height (Compressor speed 500rpm, $Re_{ref} \approx 120000$)

Heat Transfer in Boundary Layer Transition

Ting Wang
Clemson University
Mechanical Engineering
109 Riggs Hall
Clemson, SC 29634

Experiments have been performed to investigate the effects of elevated free-stream turbulence and streamwise acceleration on flow and thermal structures in transitional boundary layers. The free-stream turbulence ranges from 0.5 to 6.4 % and the streamwise acceleration ranges from K= 0 to 0.8×10^{-6}. The onset of transition, transition length and the turbulent spot formation rate are determined. The statistical results and conditionally sampled results of the streamwise and cross-stream velocity fluctuations, temperature fluctuations, Reynolds stress and Reynolds heat fluxes are presented. The eddy viscosity, turbulent thermal diffusivity and the turbulent Prandtl number are calculated. Different distributions of eddy viscosity and turbulent thermal diffusivity across the boundary layer reflect the apparent disparity between the momentum and thermal transports in the transitional boundary layer. Very mild acceleration ($K=0.07\times10^{-6}$) can significantly delay the onset and length of transition, while a further increase of acceleration to $k=0.25\times10^{-6}$ only slightly changes the onset of transition. In comparison with the acceleration, elevated free-stream turbulence is dominant in advancing the onset of transition. Acceleration only slightly delays the transition but significantly extends the length of transition at highly elevated free-stream turbulence levels. In terms of conditional sampling techniques, nine separate criterion functions are investigated. The results indicate that using a criterion function based on Reynolds shear stress for turbulent/nonturbulent discrimination in a heated transitional boundary layer is superior to a single velocity or temperature scheme. To match the universal intermittency distribution of Dhawan and Narasimha, the minimum values of intermittency at about $y/\delta=0.1$ should be used as the representative "near-wall" value.

FLUID MECHANICS AND HEAT TRASFER IN TRANSITIONAL BOUNDARY LAYERS

TING WANG

Department of Mechanical Engineering
Clemson University
Clemson, SC 29634-0921

Phone: (803) 656-5630
Fax: (803) 656-4435

Presentation at the
End-Stage Boundary Layer Transition Workshop

15-18 August , 1993

Blue Mountain Lake, New York

On-going projects related to boundary layer transition at Clemson University

1. Baseline: Natural transition
2. Effects of favorable streamwise pressure gradients
3. Effects of Free-stream turbulence intensity (FSTI)
4. Combined effects of favorable gradients and FSTI.
5. Effects of roughness
6. Effects of adverse pressure gradients

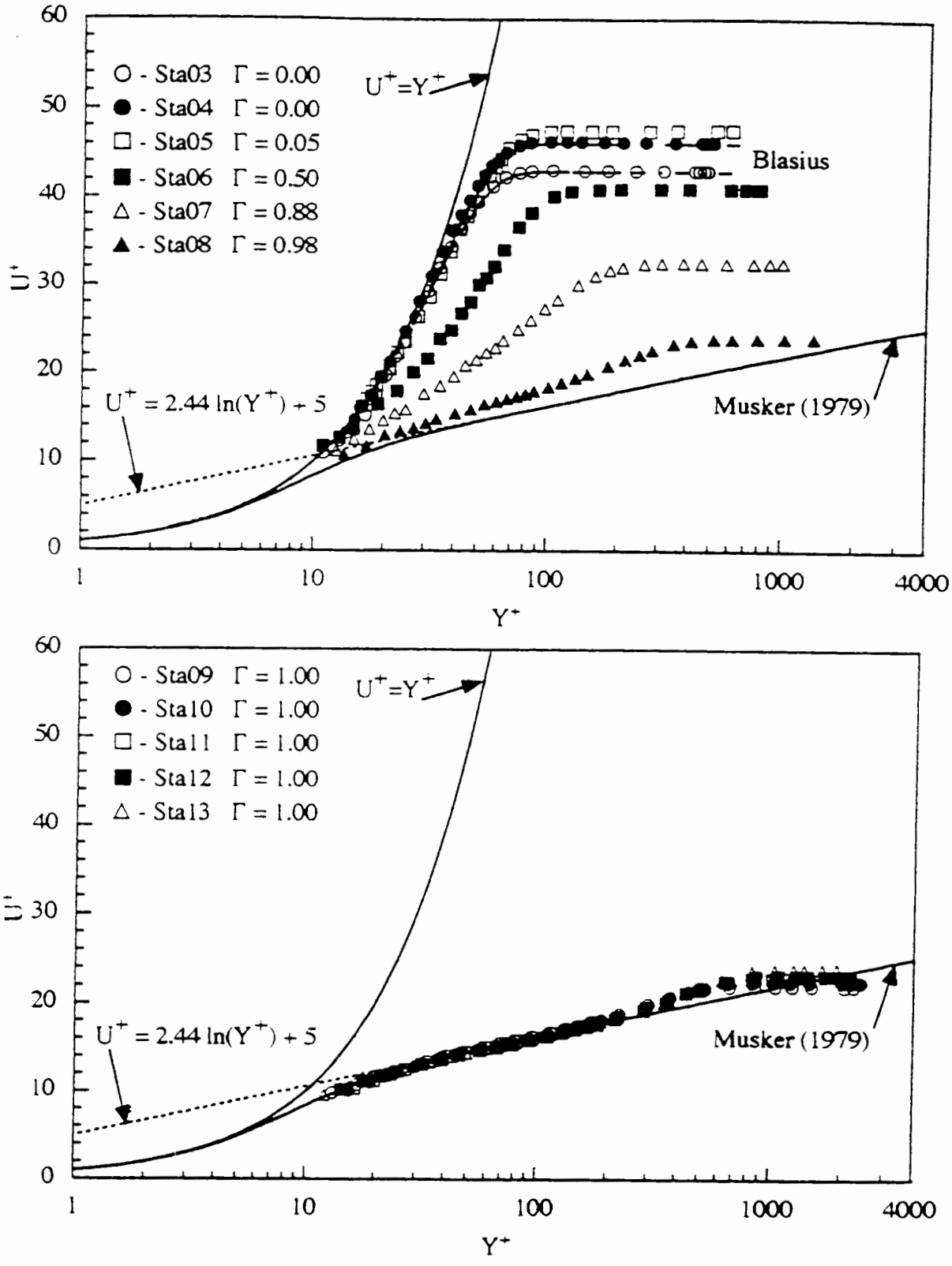

Figure 4.4 Mean velocity profiles for the baseline case in wall coordinates measured by the three-wire probe.

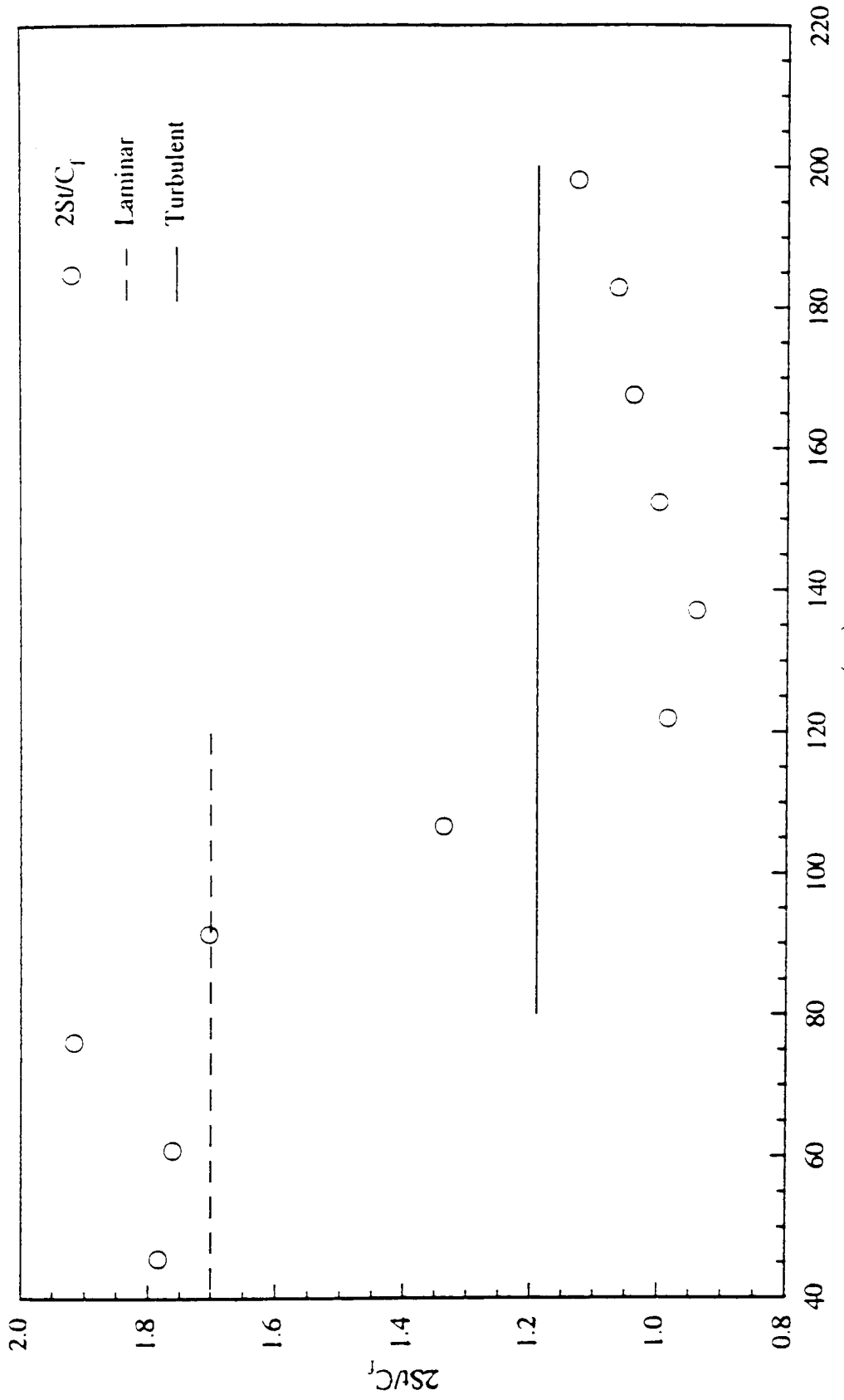

Figure 4.10 Reynolds analogy factor, $2St/C_f$, for the baseline case.

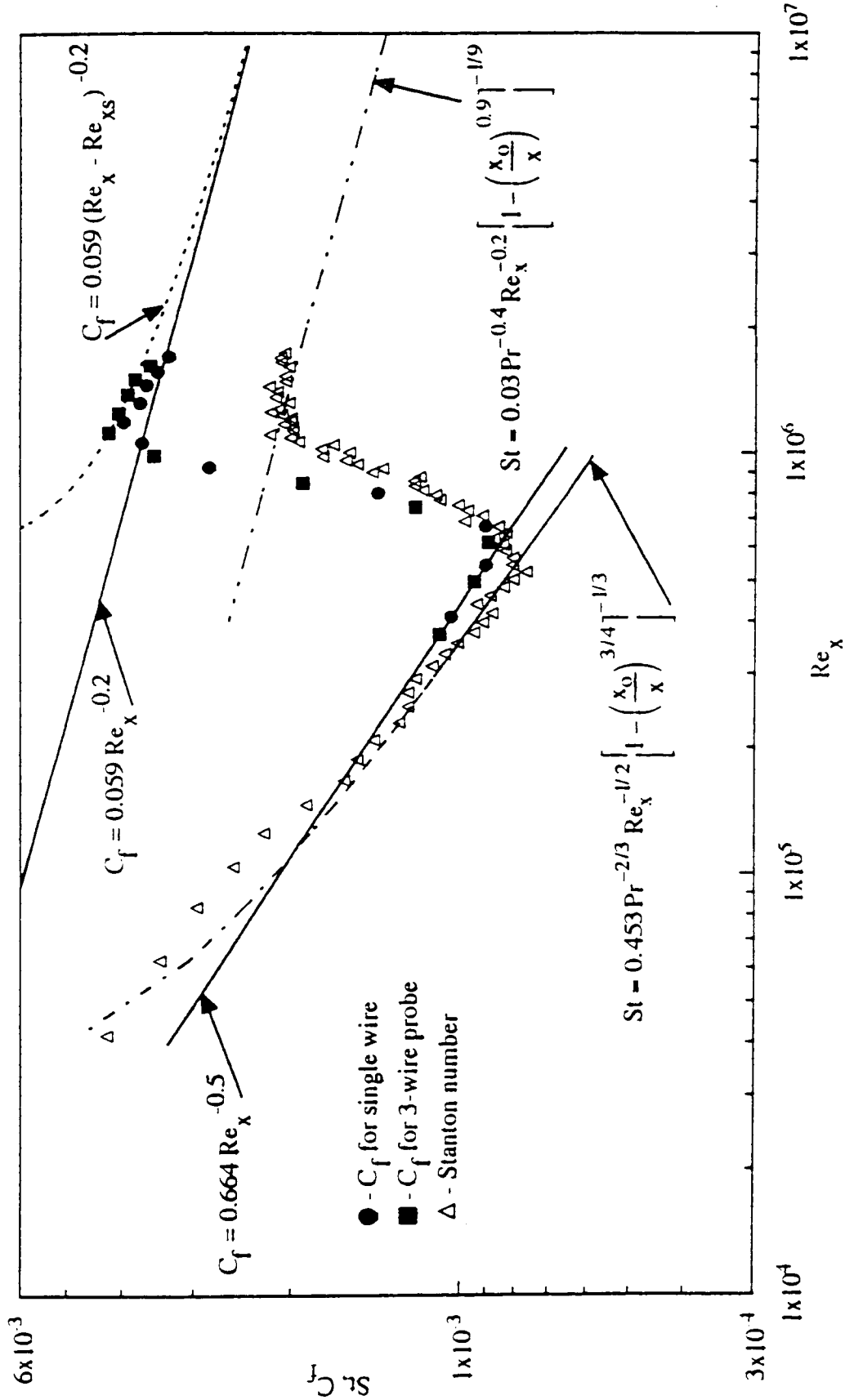

Figure 4.7 Centerline Stanton number and skin friction coefficient distributions for the baseline case.

3-WIRE BOUNDARY LAYER SENSOR

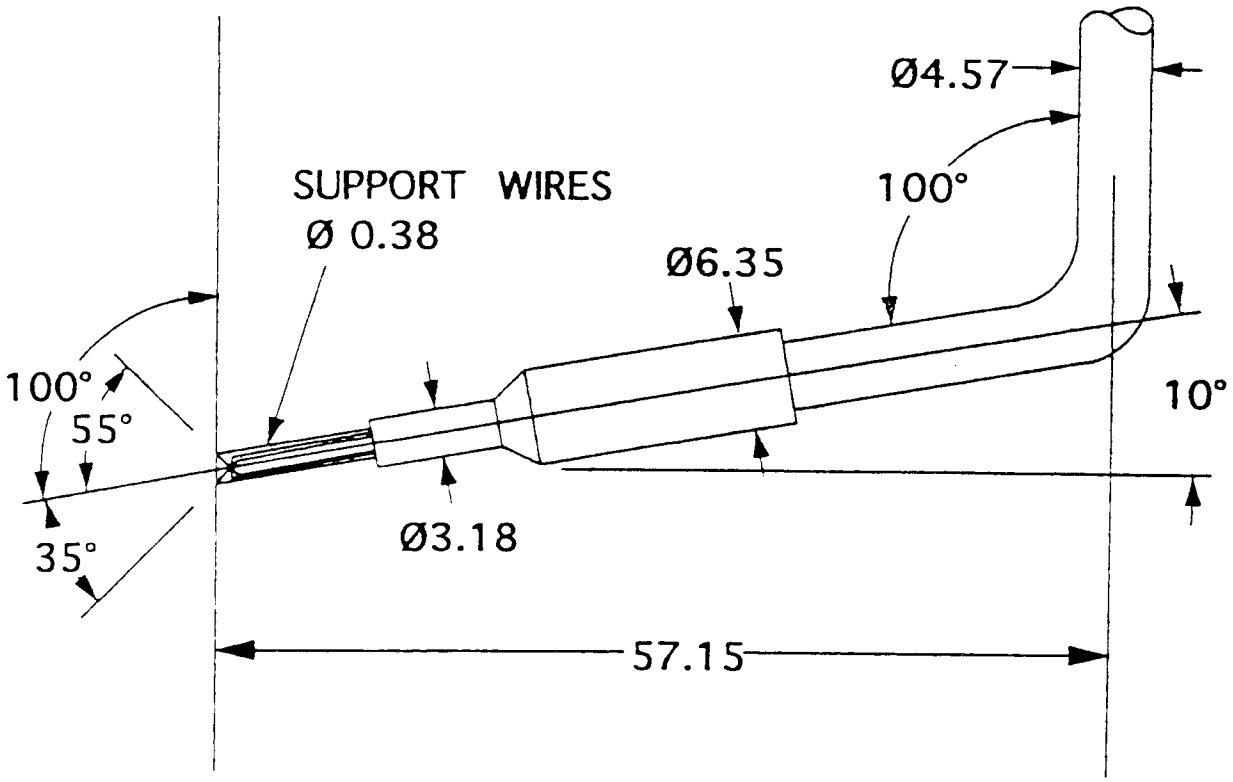

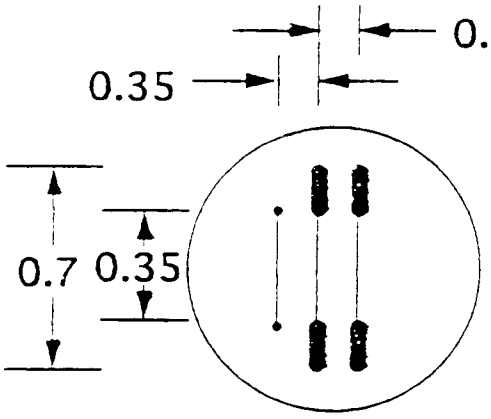

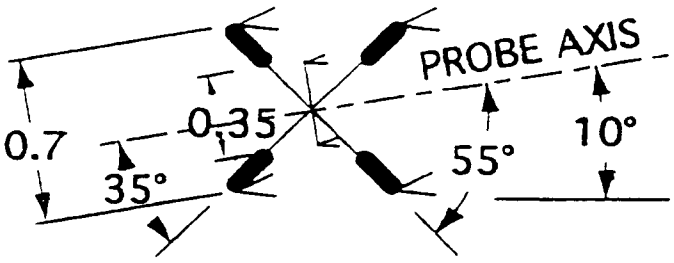

SIDE VIEW PLANE VIEW

DIMENSIONS IN mm

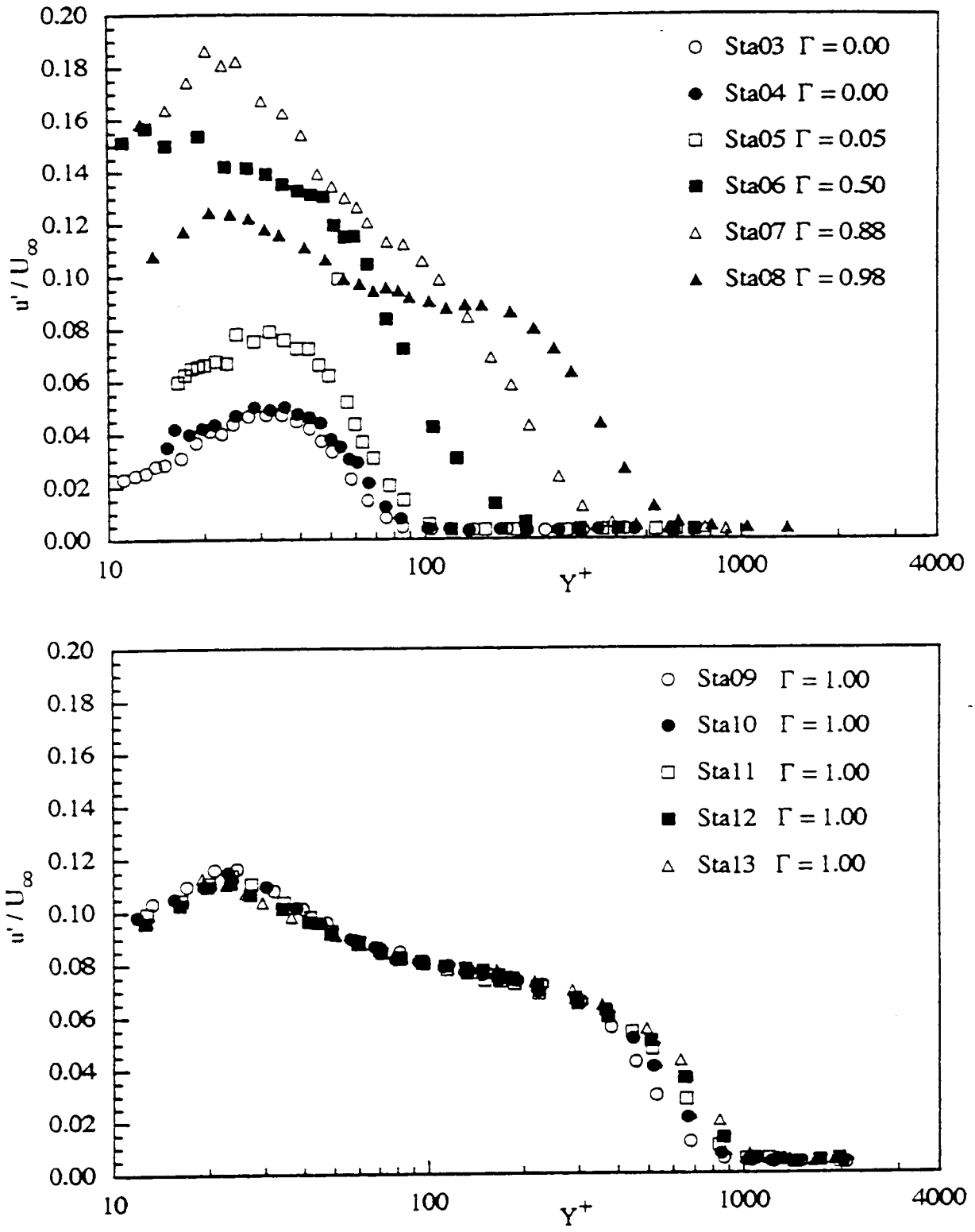

Figure 4.13 Streamwise Reynolds normal stress distribution for the baseline case in wall units.

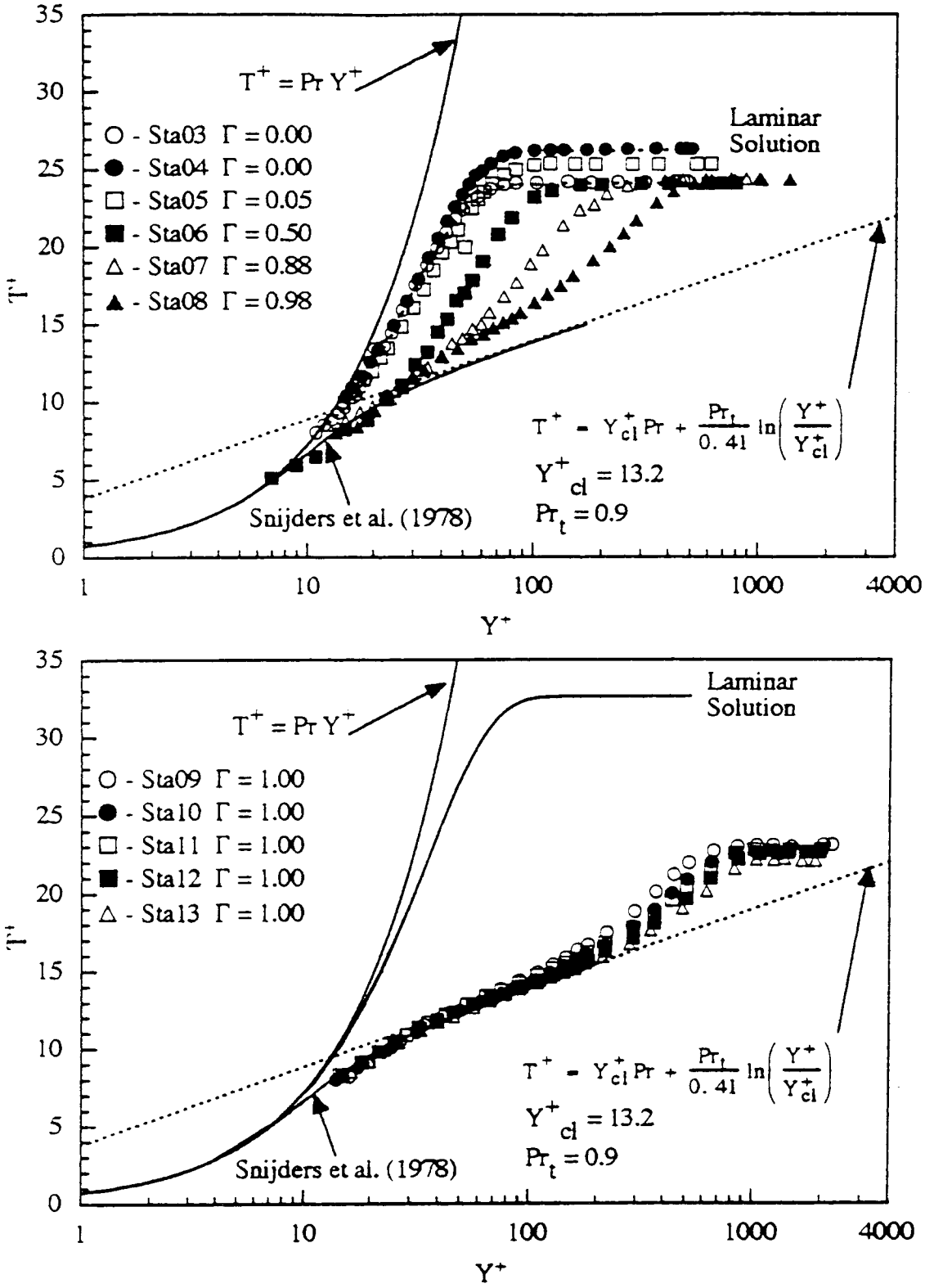

Figure 4.22 Mean temperature profiles for the baseline case in wall coordinates measured by the three-wire probe.

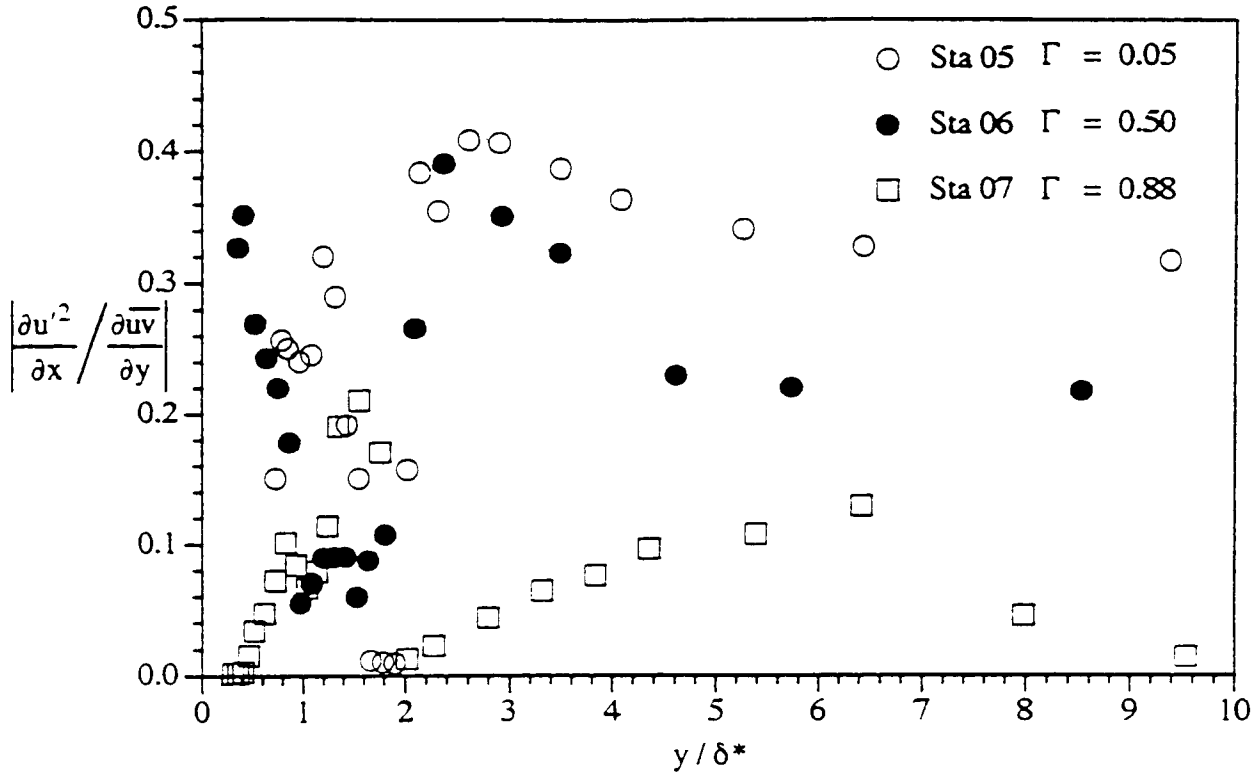

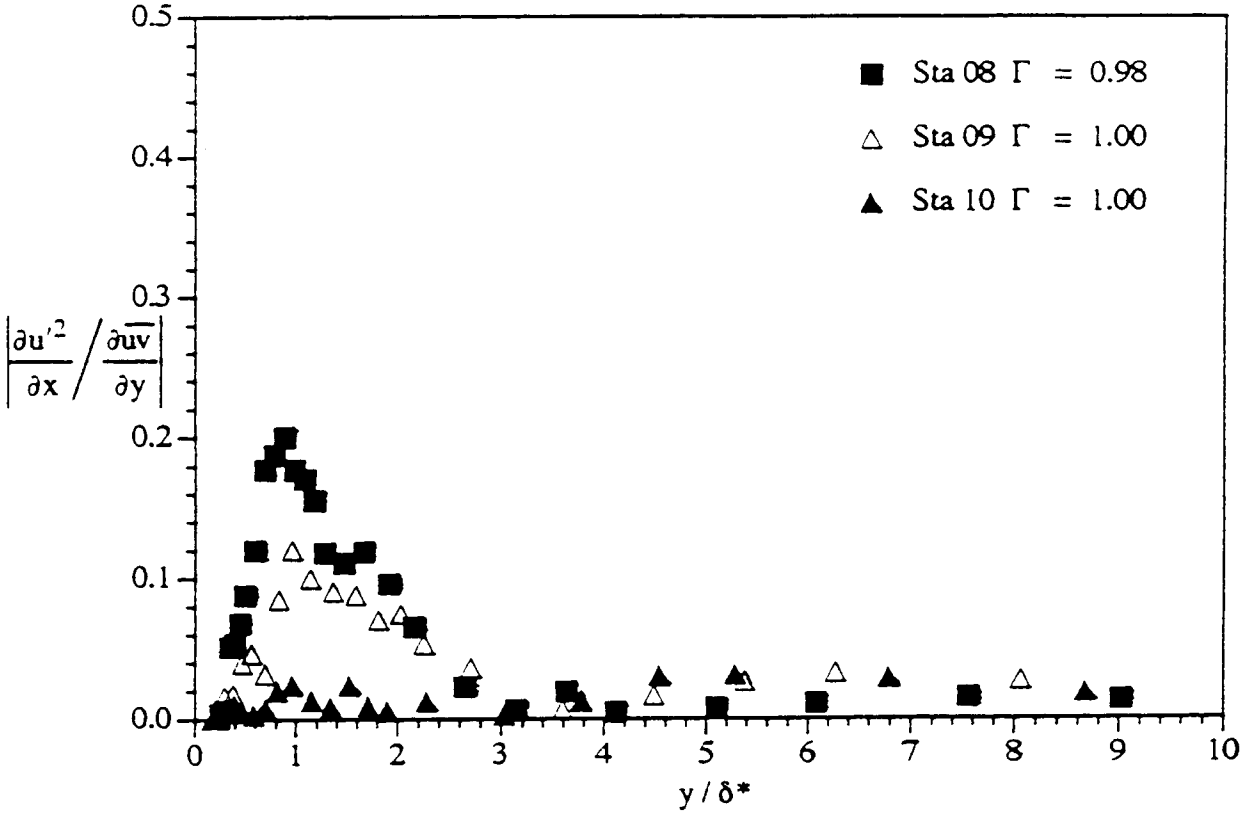

Figure 4.15 Ratio of streamwise gradient of Reynolds normal stress to cross-stream gradient of Reynolds shear stress for the baseline case.

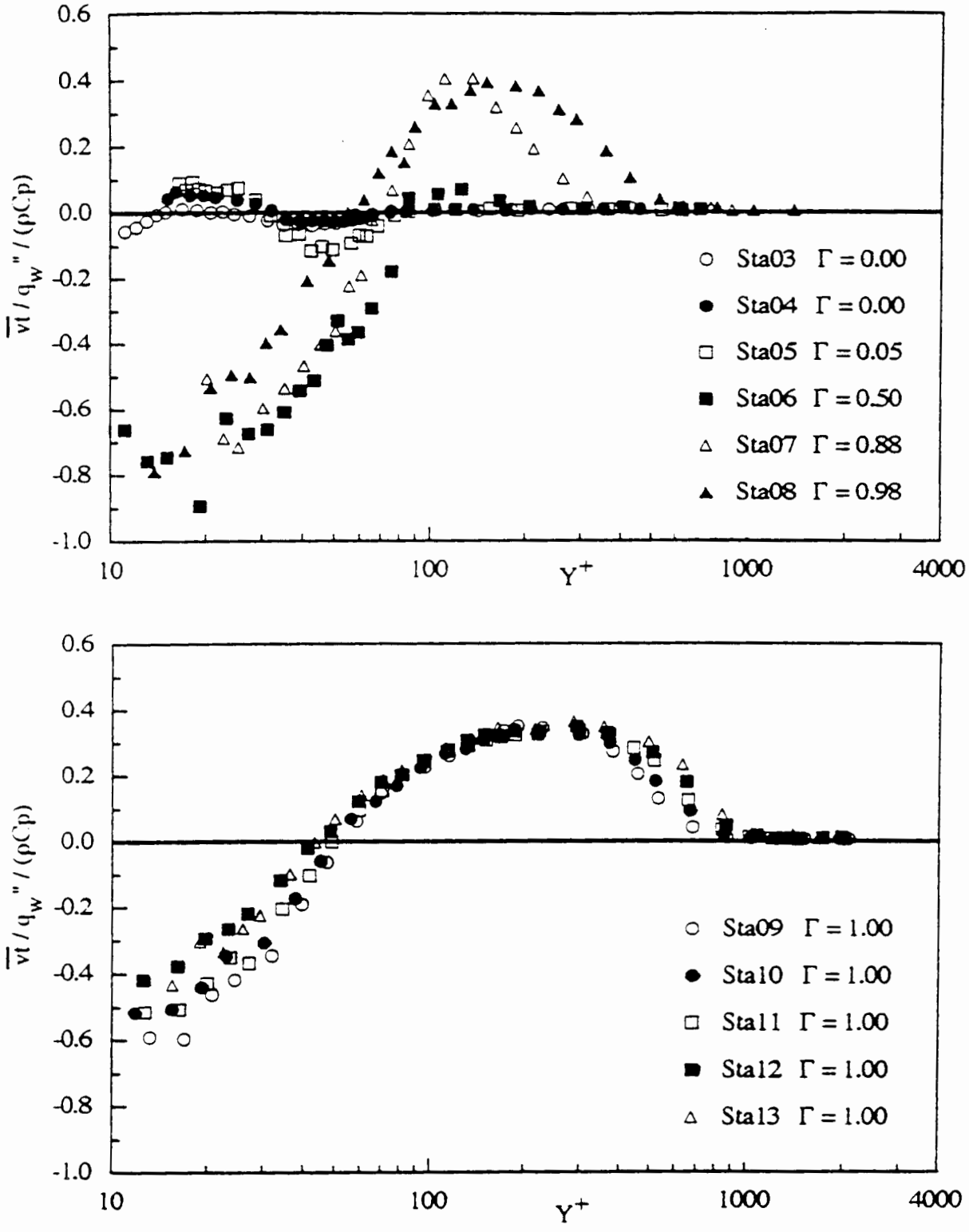

Figure 4.25 Reynolds cross-stream heat flux distribution for the baseline case in wall units.

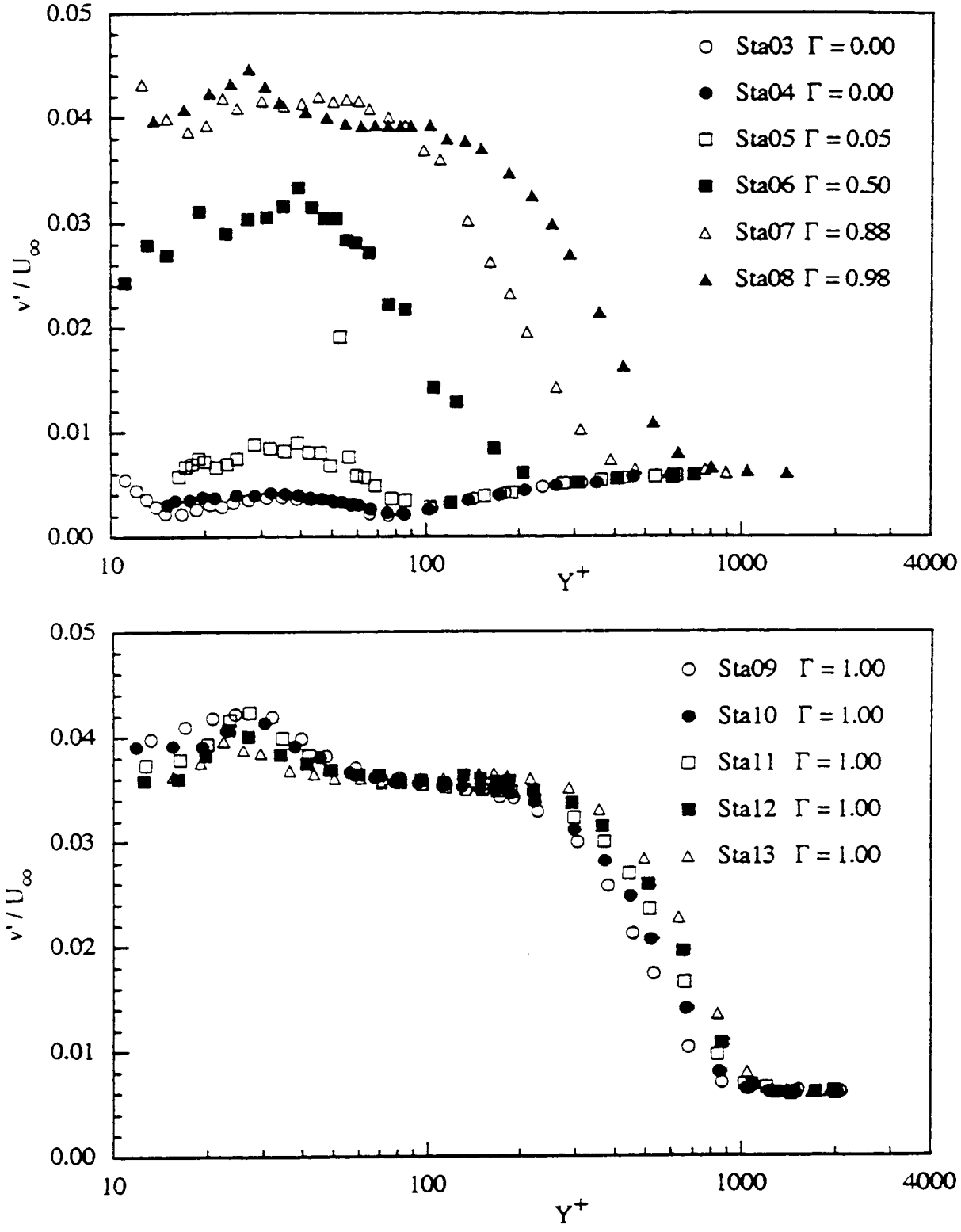

Figure 4.16 Reynolds cross-stream stress distribution for the baseline case in wall units.

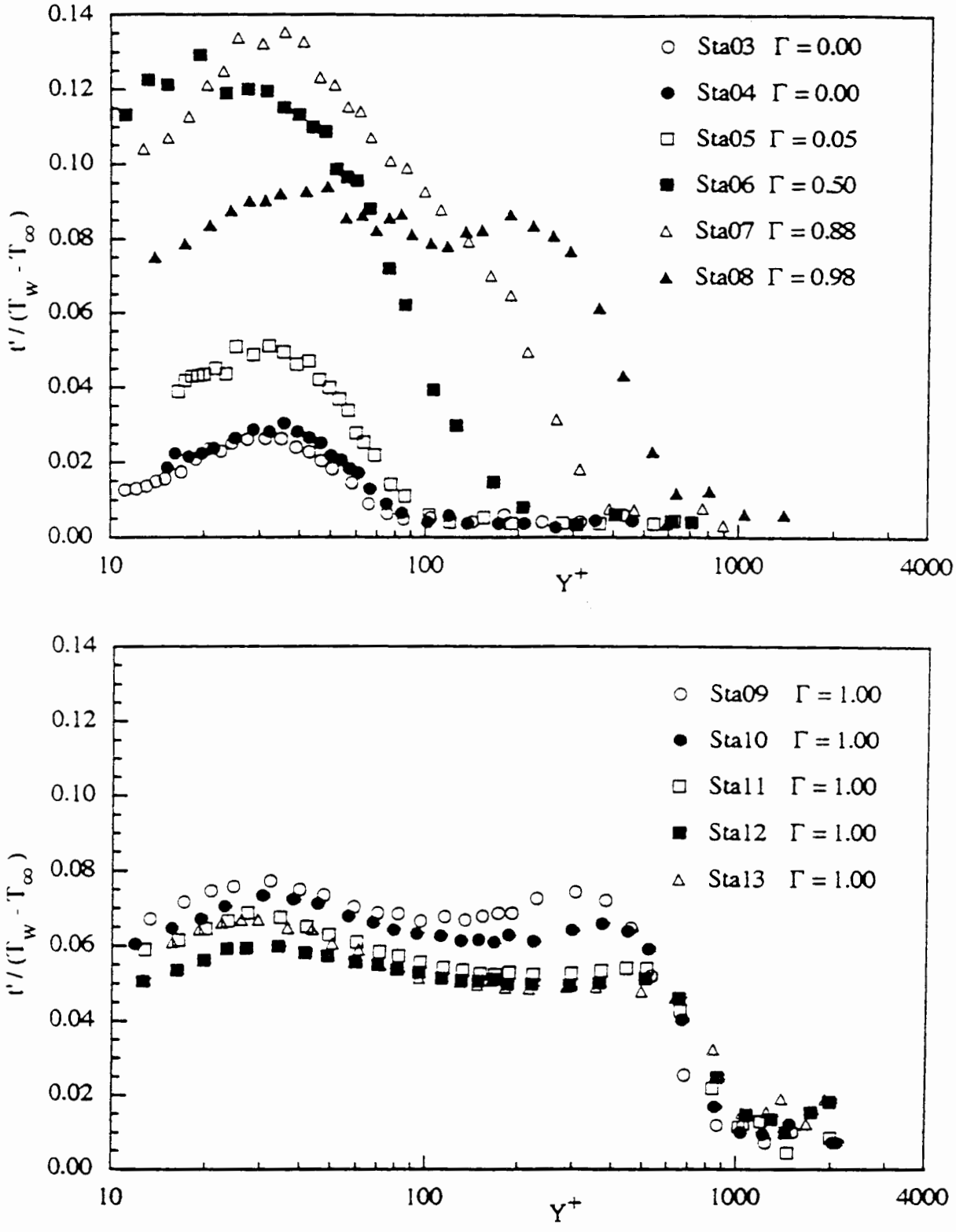

Figure 4.23 RMS temperature distribution for the baseline case in wall units.

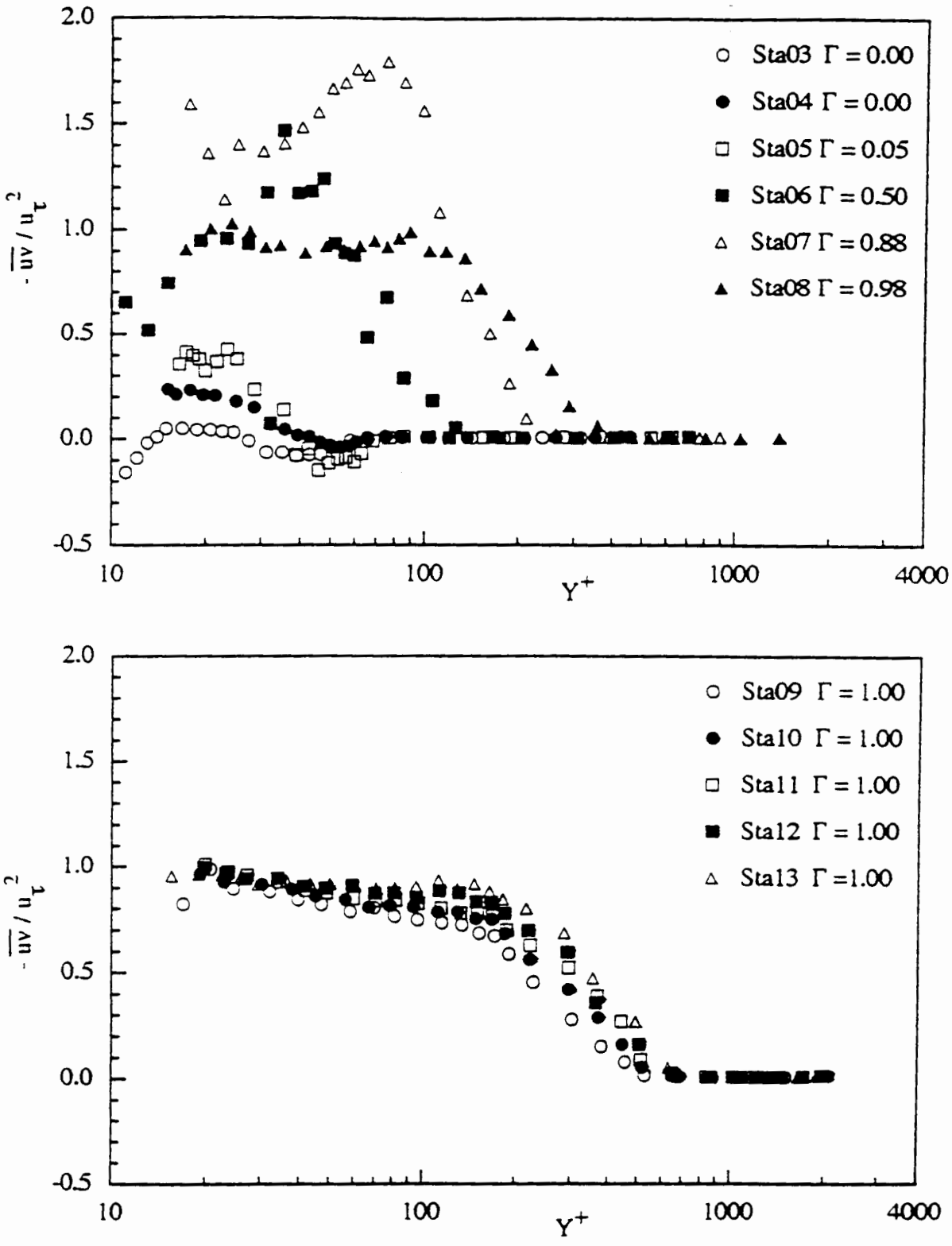

Figure 4.19 Reynolds shear stress distribution for the baseline case in wall units.

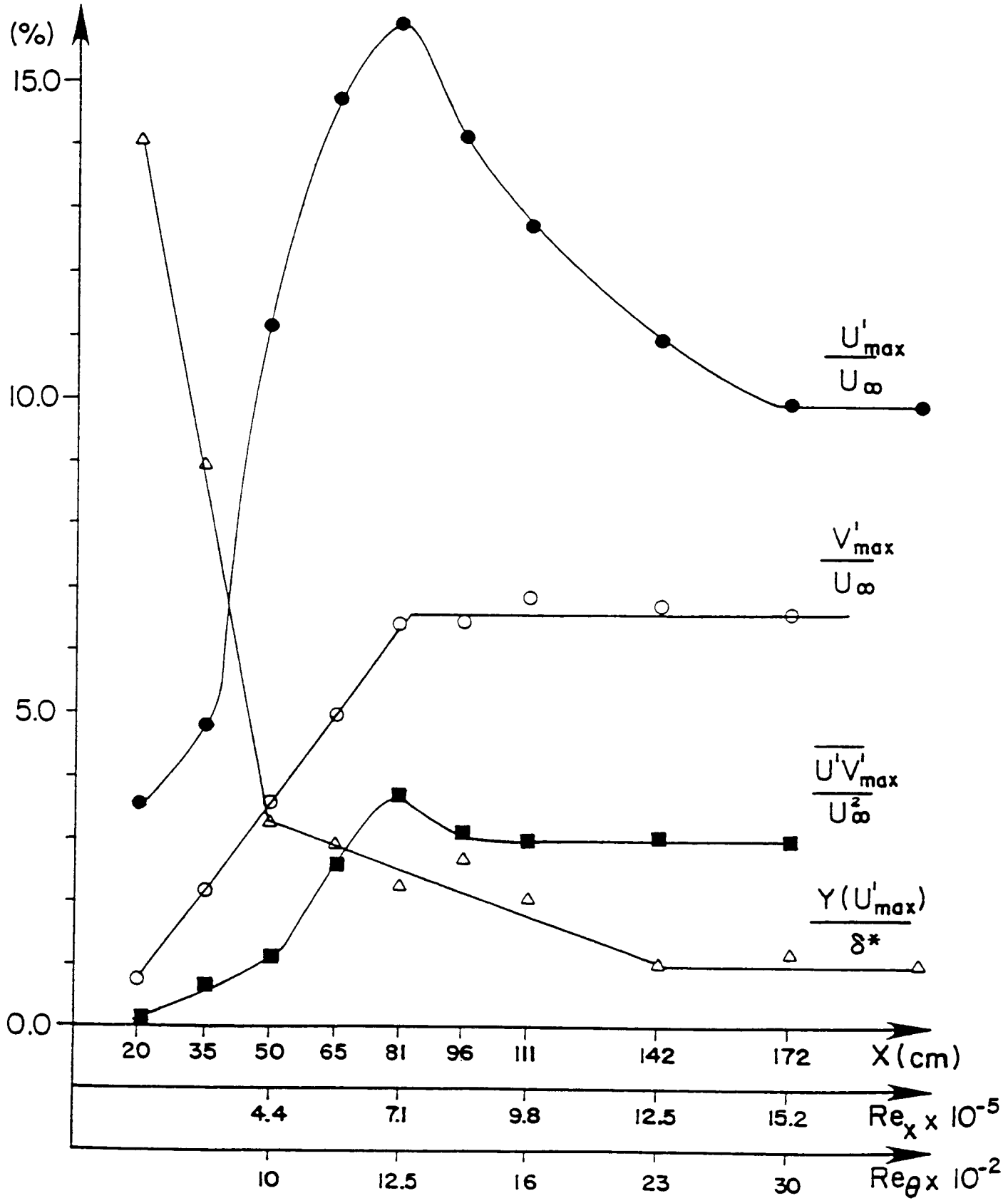

Distribution of maximum Reynolds normal stress and the corresponding y-position in the streamwise direction.

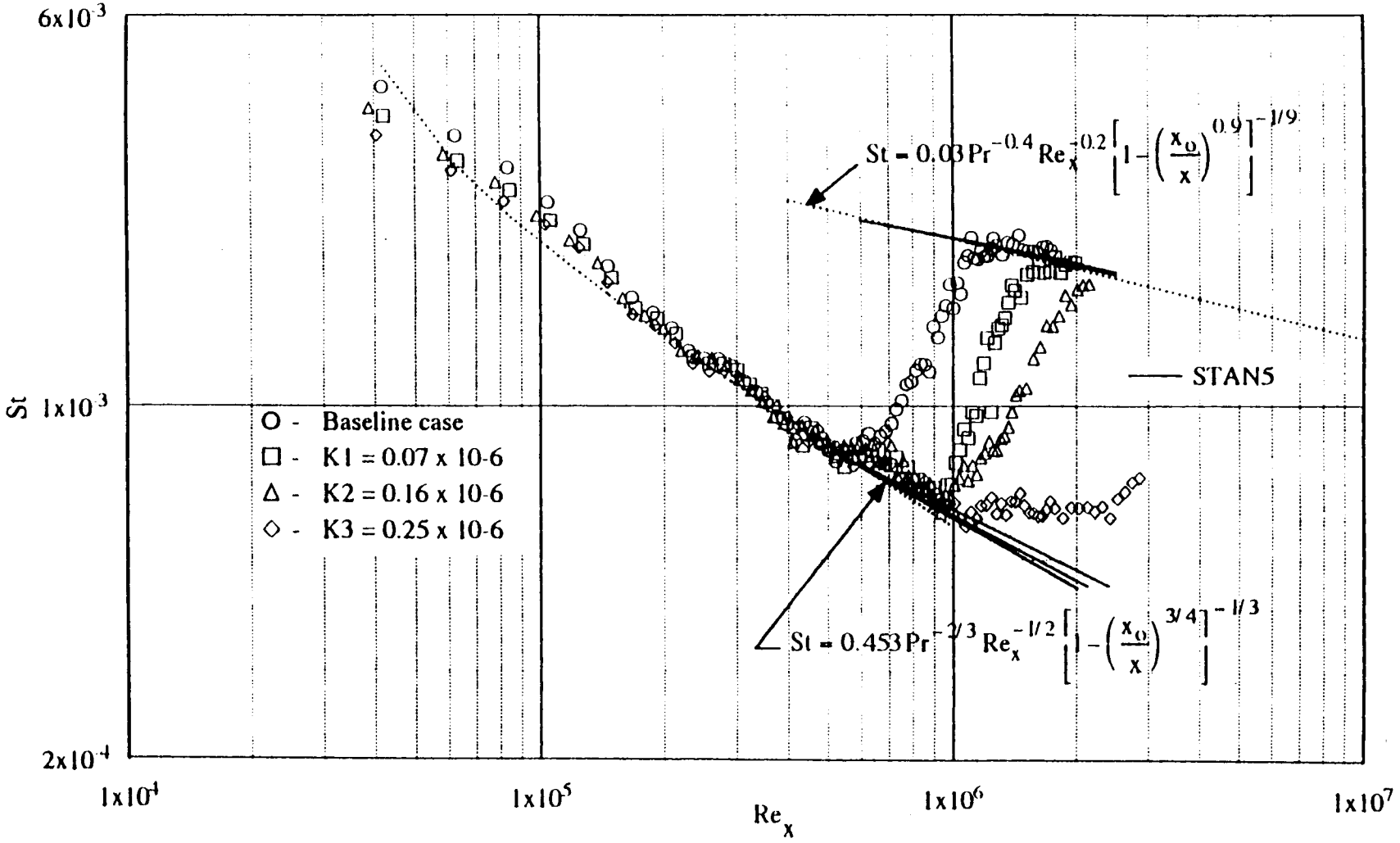

Figure 5.4 Centerline stanton number distribution for all cases.

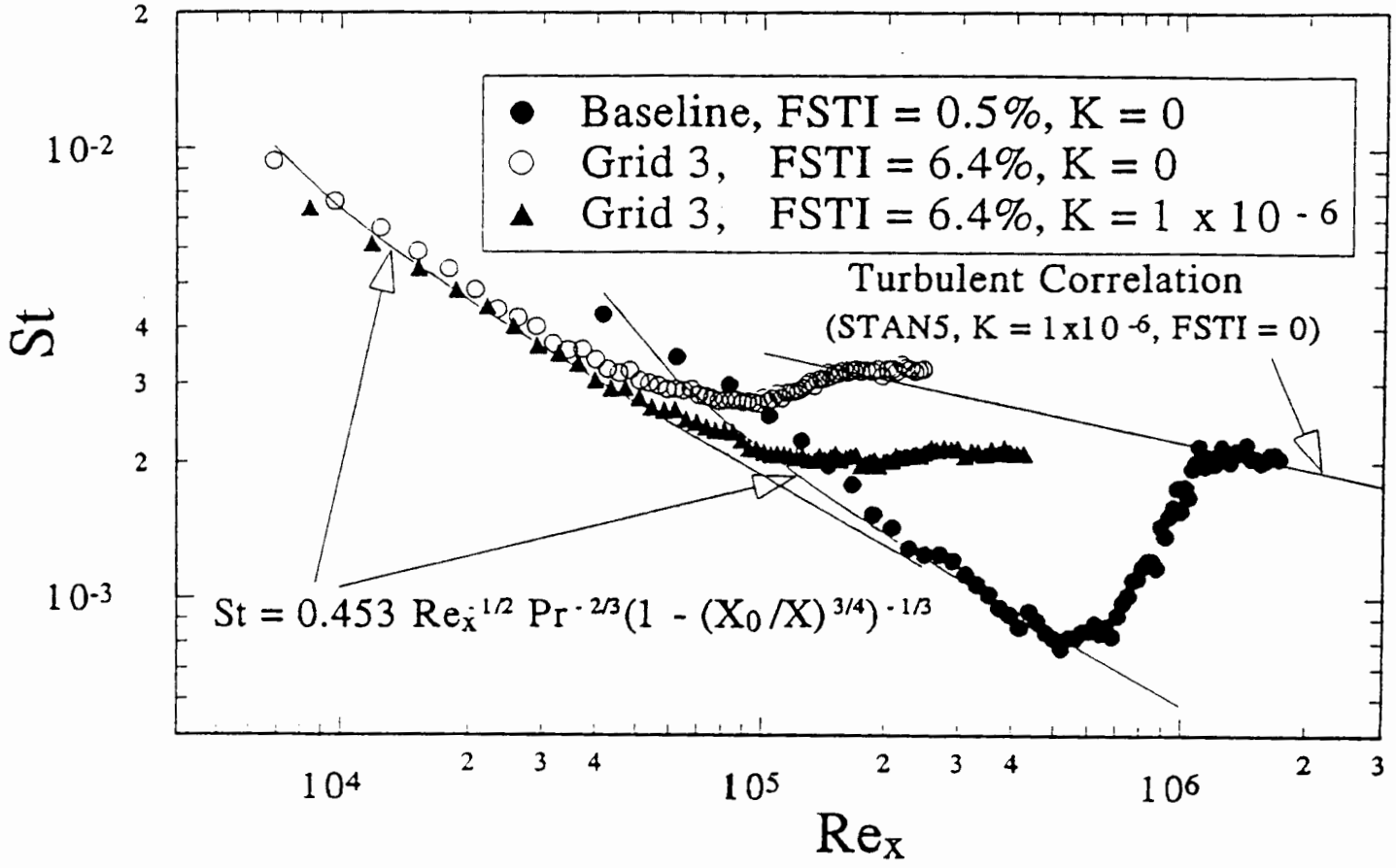
Baseline, FSTI = 0.5%, K = 0
Grid 3, FSTI = 6.4%, K = 0
Grid 3, FSTI = 6.4%, K = 1 x 10 - 6
Turbulent Correlation
(STAN5, K = 1x10 -6, FSTI = 0)
St = 0.453 Rex 1/2 Pr - 2/3(1 - (X0 /X) 3/4) - 1/3
St
Rex
10-2
10-3
10 4
10 5
10 6

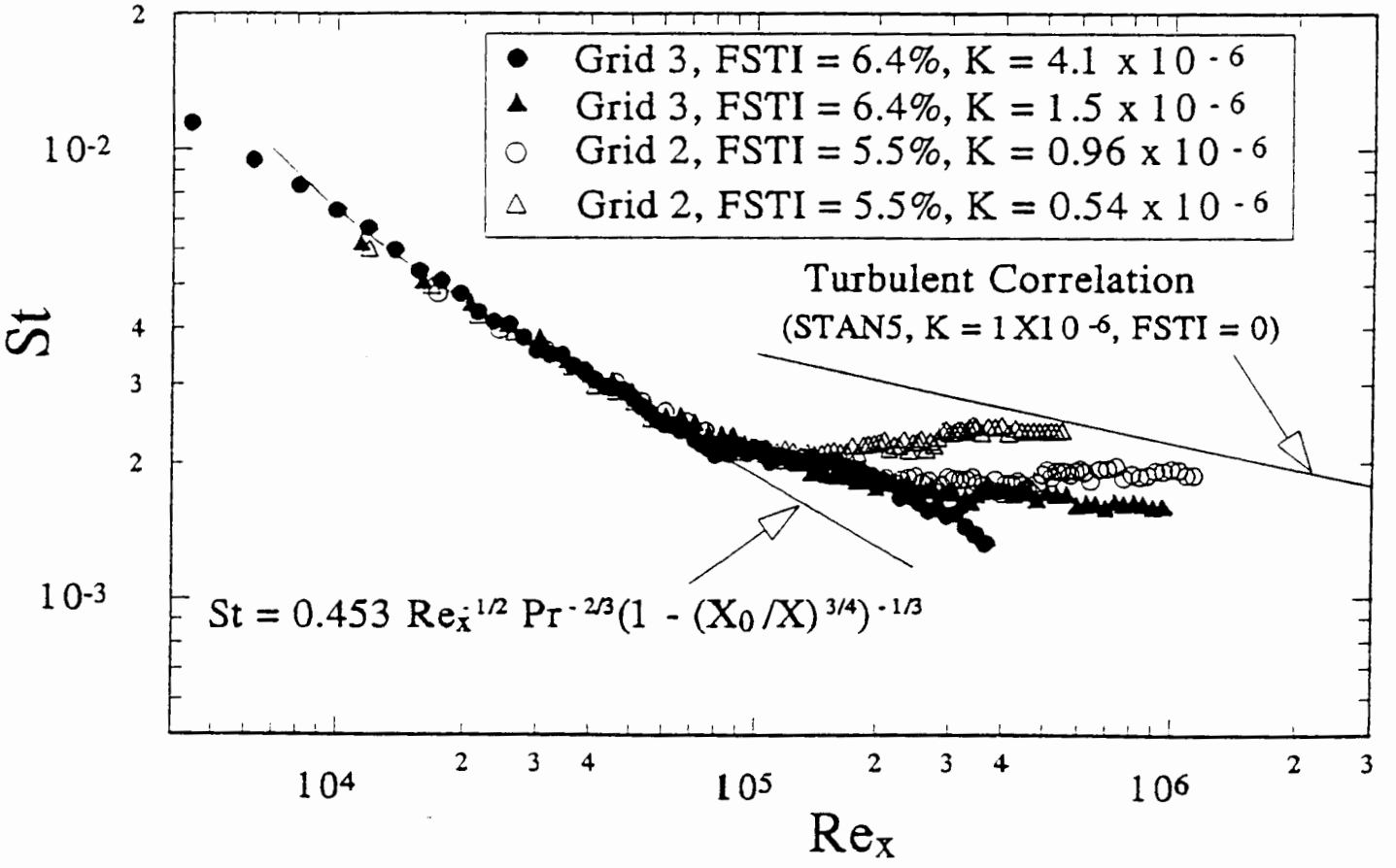
Grid 3, FSTI = 6.4%, K = 4.1 x 10 - 6
Grid 3, FSTI = 6.4%, K = 1.5 x 10 - 6
Grid 2, FSTI = 5.5%, K = 0.96 x 10 - 6
Grid 2, FSTI = 5.5%, K = 0.54 x 10 - 6
Turbulent Correlation
(STAN5, K = 1X10 -6, FSTI = 0)
St = 0.453 Rex 1/2 Pr - 2/3(1 - (X0 /X) 3/4) - 1/3
St
Rex
10-2
10-3
10 4
10 5
10 6

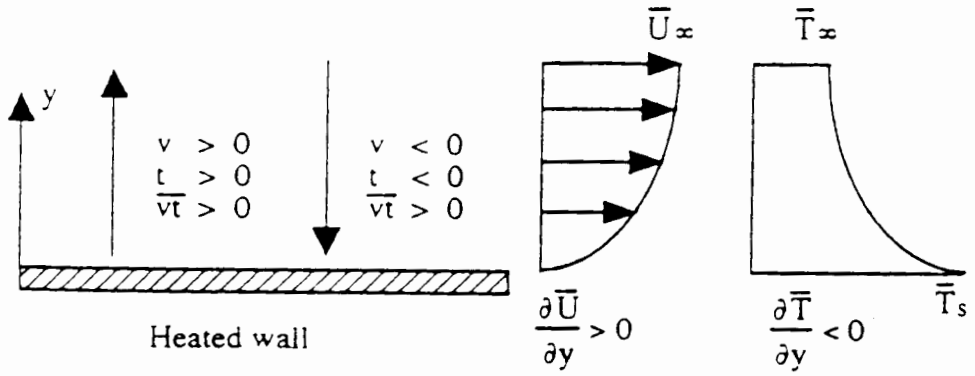

(a)

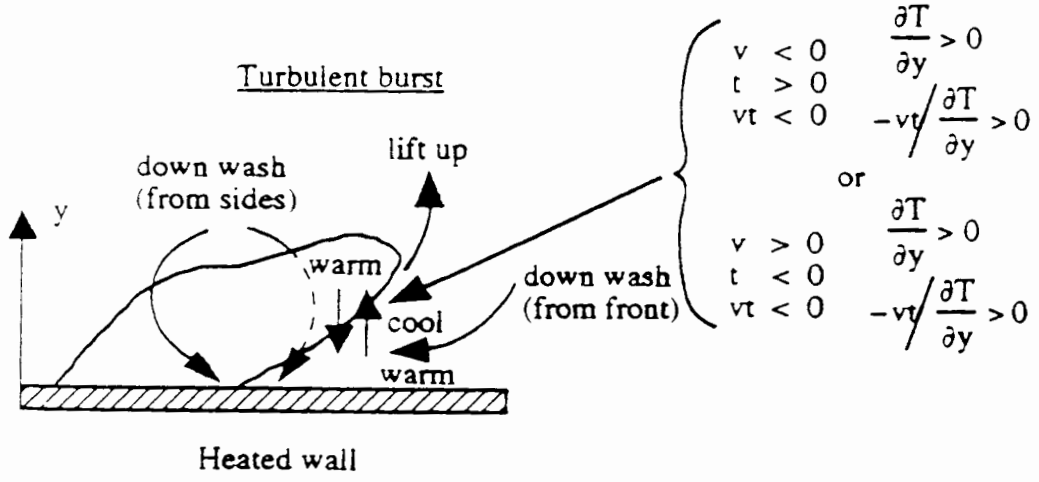

(b)

Figure 4.26 (a) Scenario of statistical transport correlation between v' and t' and (b) Scenario of instantaneous view of cross-stream Reynolds heat flux distibution.

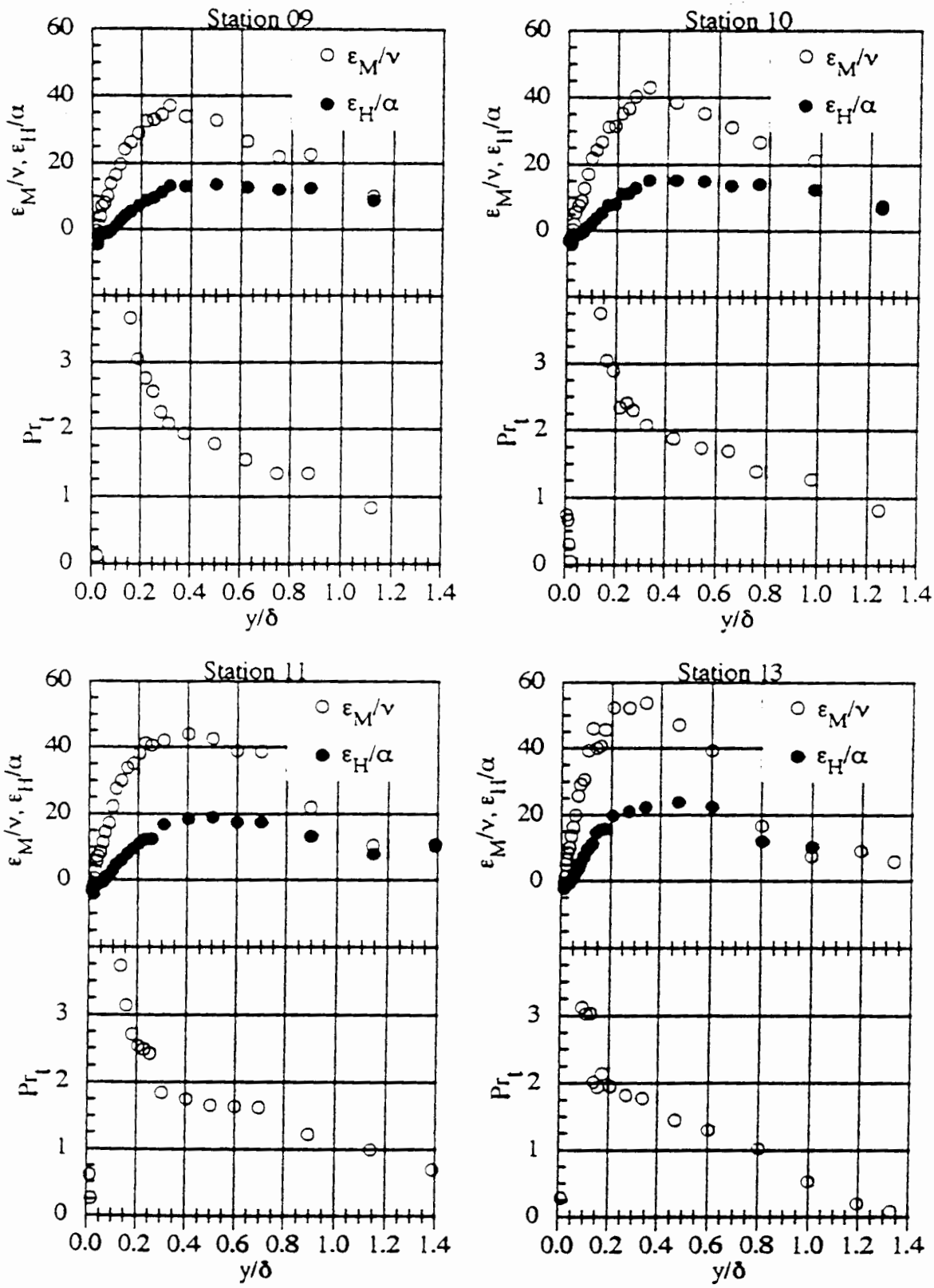

Figure 4.31 Distribution of eddy viscosity, turbulent thermal diffusivity and turbulent Prandtl number for baseline case (stations 9-11,13).

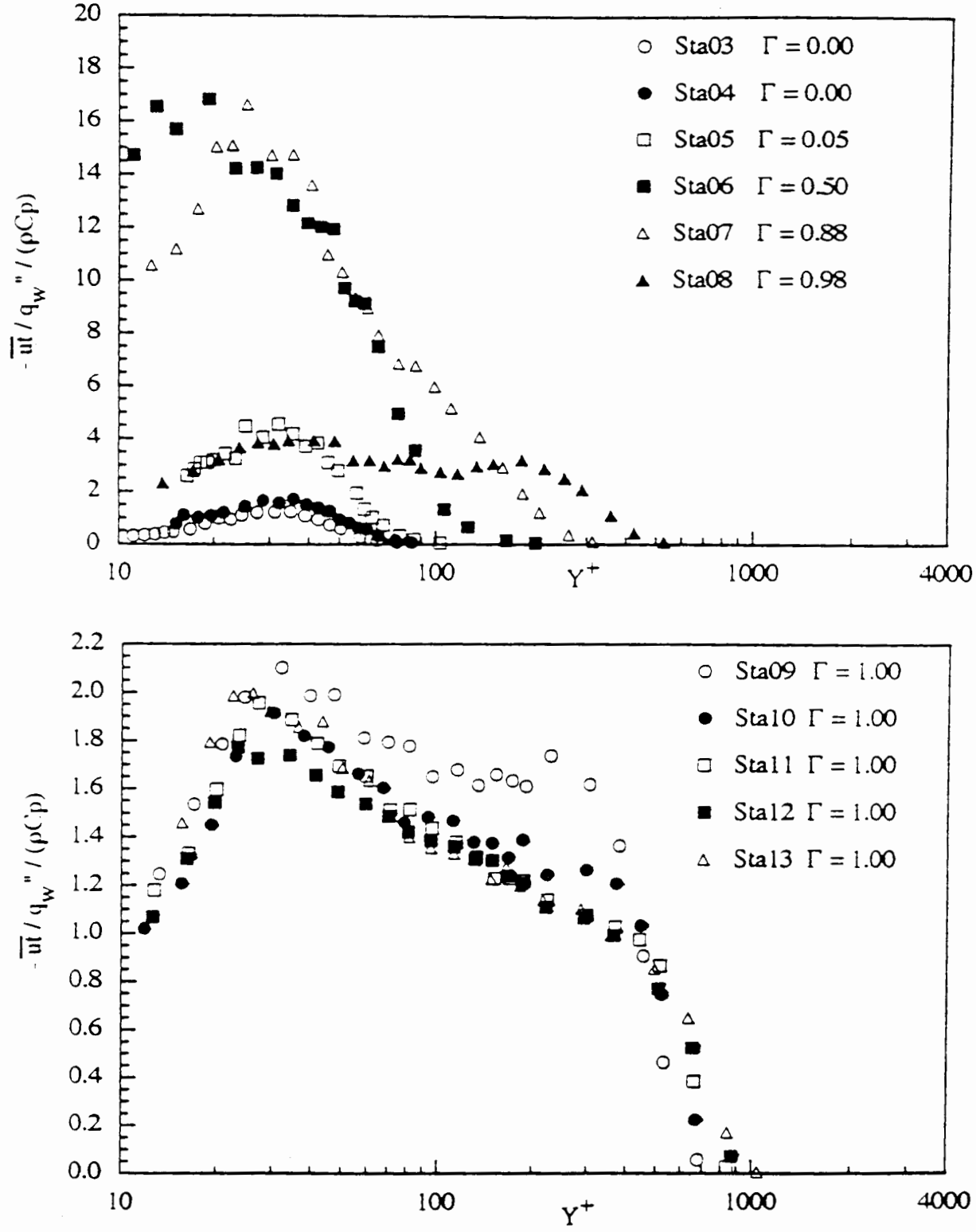

Figure 4.28 Reynolds streamwise heat flux distribution for the baseline case in wall units.

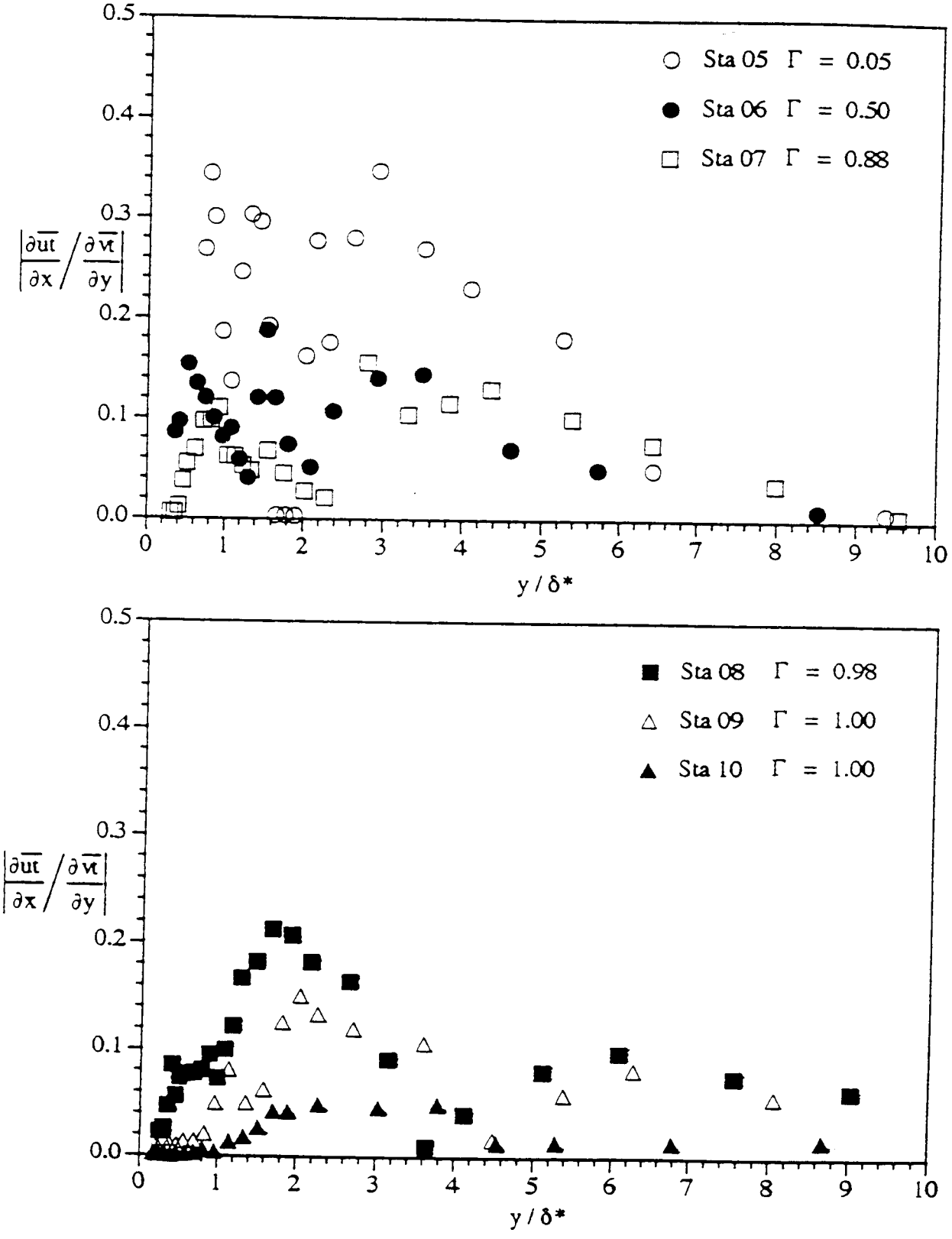

Figure 4.29 Ratio of gradient of Reynolds streamwise heat flux to gradient of Reynolds cross-stream heat flux for the baseline case.

CORRESPONDING CRITERION FUNCTIONS FOR $\Gamma = 0.5$, $y/\delta^* = 1.1$ (BASELINE CASE)

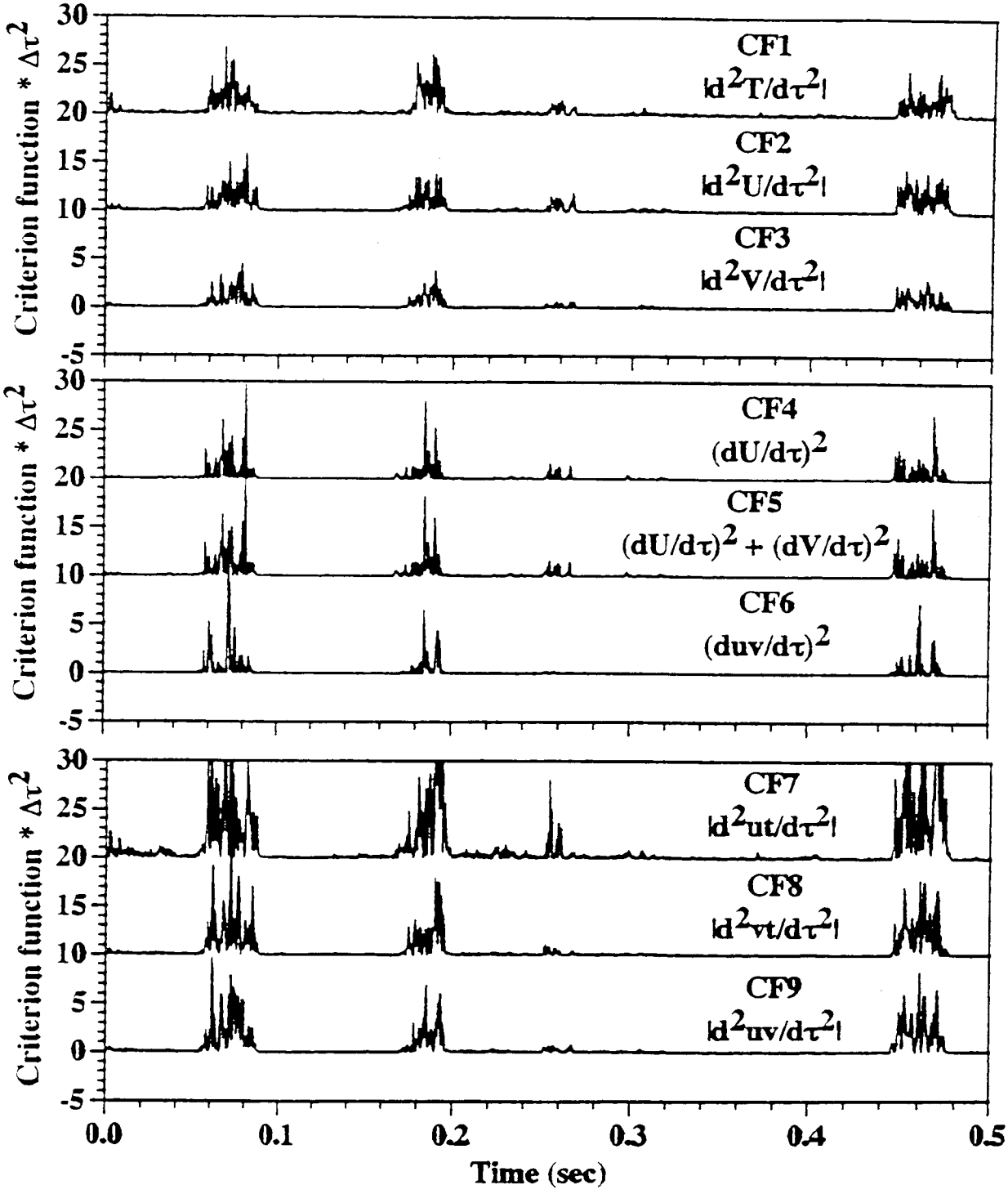

FACTORS FOR DETERMINING WHICH CRITERION FUNCTION IS "BEST"

- SHARPNESS IN DEMARCATION BETWEEN TURBULENT AND NON-TURBULENT PORTIONS OF THE FLOW
- SMALL VARIATION OF THRESHOLD VALUE THROUGHOUT TRANSITION REGION
- LOW UNCERTAINTY IN DETERMINING THRESHOLD VALUE
- LOW SENSITIVITY OF RESULTED INTERMITTENCY TO UNCERTAINTY IN CHOOSING THRESHOLD

COMPARISON OF TWO CRITERION FUNCTIONS AND CORRESPONDING INTERMITTENCY FUNCTIONS FOR $\Gamma = 0.5$, $y/\delta^* = 1.1$ (baseline case)

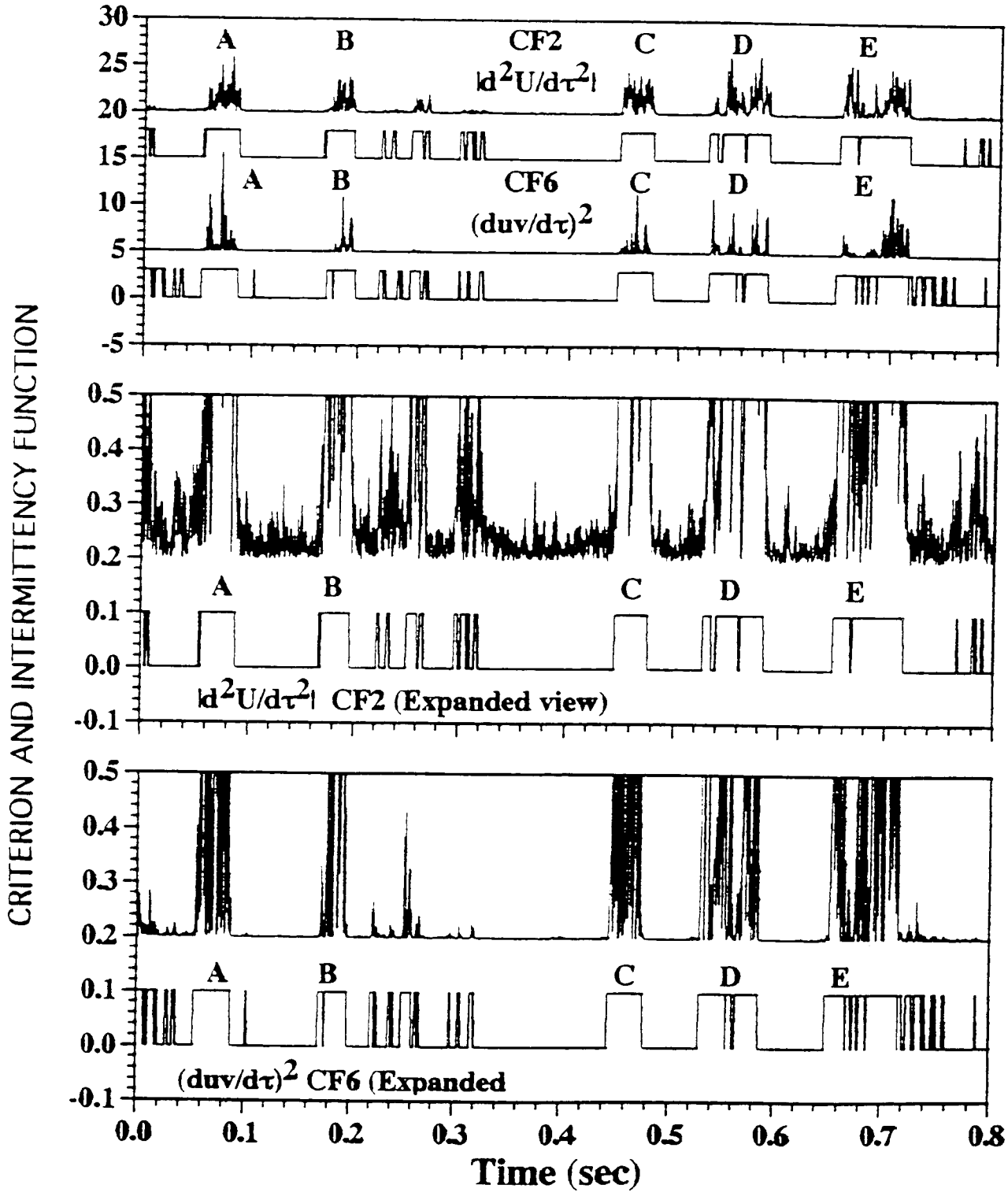

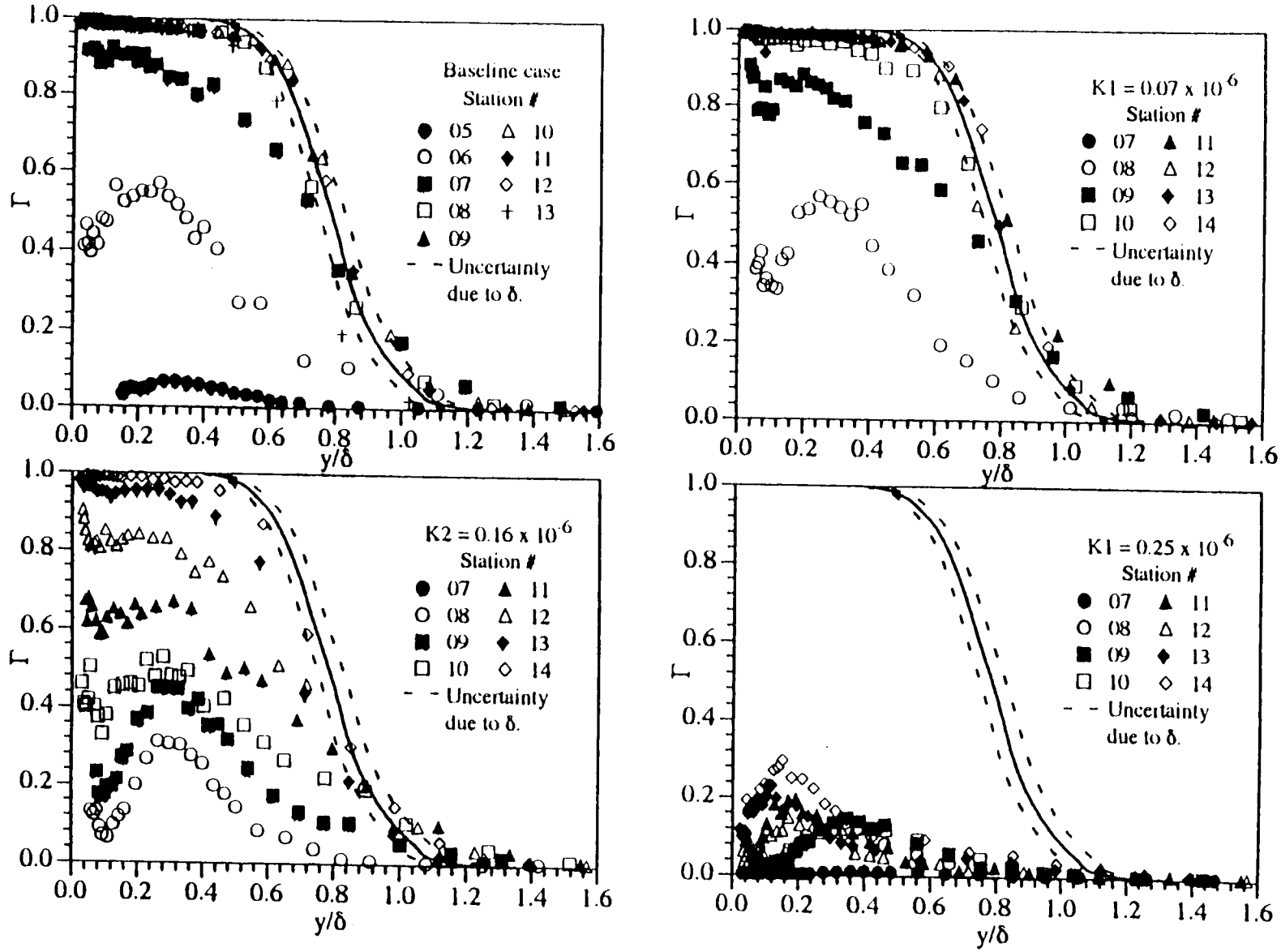

Figure 6.12 Intermittency distribution through boundary layer using $(duv/d\tau)^2$.

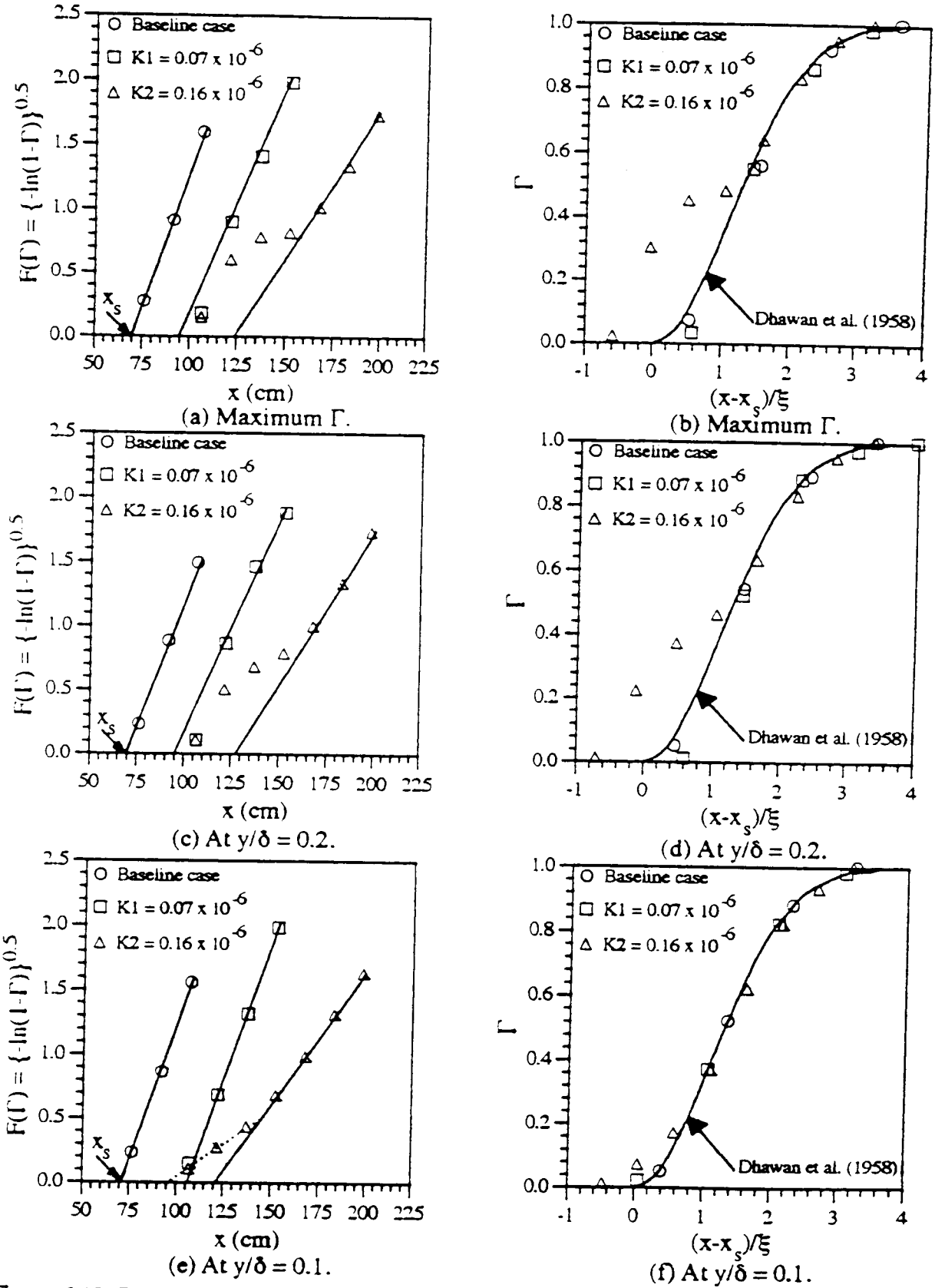

Figure 6.13 Determination of x_s and corresponding representative near-wall intermittency in Γ versus x coordinates using the value of Γ at different y/δ locations as the representative intermittency.

DETERMINATION OF NEAR-WALL INTERMITTENCY

- THREE LOCATION CONSIDERED FOR REPRESENTATIVE NEAR-WALL INTERMITTENCY
  - (1) LOCATION OF INTERMITTENCY PEAK ($y/\delta \sim 0.3$)
  - (2) VALUE AT $y/\delta = 0.2$ (MOST COMMONLY USED)
  - (3) LOCAL MINIMUM VALUE NEAR THE WALL ($y/\delta \sim 0.1$)
- BOTH (1) AND (2) RESULT IN TOO LARGE A DEVIATION FROM UNIVERSAL DISTRIBUTION
- USING (3) MATCHES UNIVERSAL DISTRIBUTIONS AND IS CONSIDERED APPROPRIATE FOR NEAR-WALL INTERMITTENCY VALUE

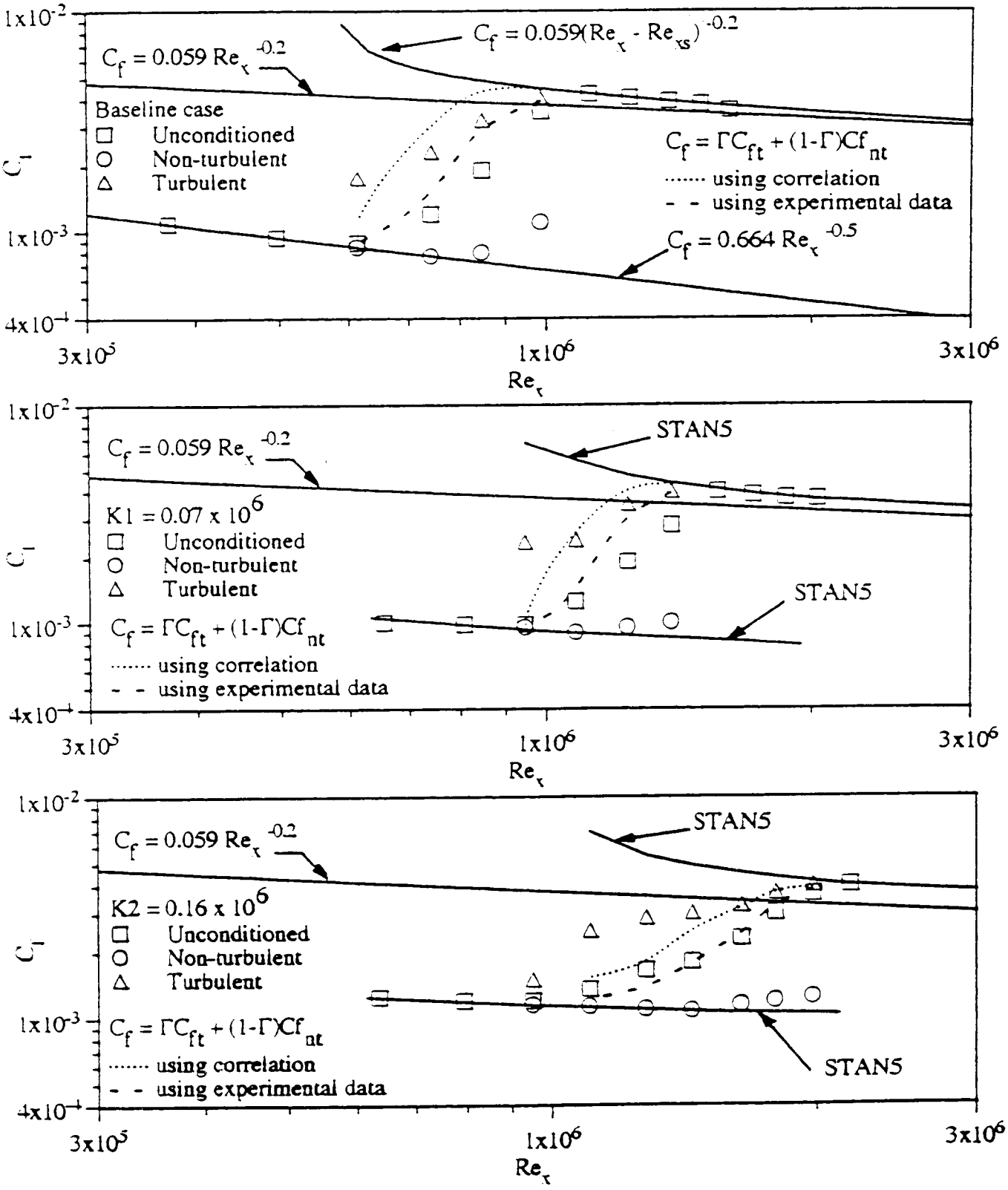

Figure 7.1 Conditionally sampled skin friction coefficient.

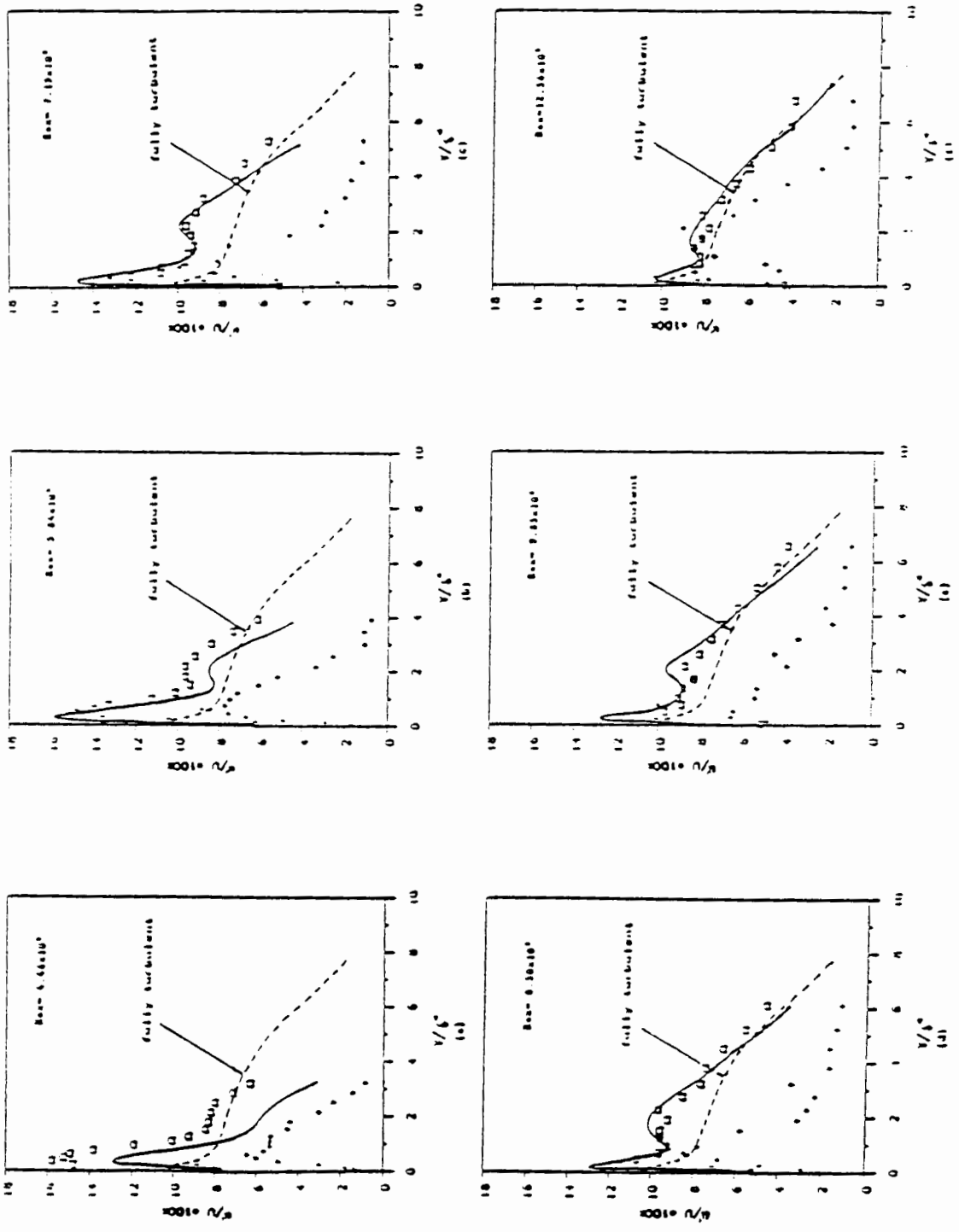

Figure 3.25. Conditionally Sampled Result of Reynolds Normal Stress Distribution
(—— - total part; □ - turbulent part; * - non-turbulent part)

PUBLICATIONS

"Combined Effects of Elevated Free-Stream Turbulence and Streamwise Acceleration on Flow and Thermal Structures in Transitional Boundary Layers," Zhou, D., and Wang, T., to be presented at the 1993 National Heat Transfer Conference at Atlanta, Georgia. ASME HTD-Vol. 242, pp. 41~52.

"Effects of Elevated Free-Stream Turbulence on Flow and Thermal Structures in Transitional Boundary Layers," Zhou, D., and Wang, T., presented at the 1993 ASME International Gas Turbine and Aeroengine Congress and Exposition, Cincinnati, Ohio. ASME paper 93-GT-66.

"Effects of Different Criterion Functions on Intermittency in Heated Transitional Boundary Layers with and without Streamwise Accelerations," Keller, F.J., and Wang, T., presented at the 1993 ASME International Gas Turbine and Aeroengine Congress and Exposition, Cincinnati, Ohio. ASME paper 93-GT-67.

"Experimental Investigation of Reynolds Shear Stresses and Heat Fluxes in a Transitional Boundary Layer," Wang, T., Keller, F.J., and Zhou, D., ASME HTD-Vol. 226, Fundamental and Applied Heat Transfer Research for Gas Turbine Engine, pp. 61-70, 1992.

"Laminar Boundary Layer Flow and Heat Transfer with Favorable Pressure Gradient at Constant K Values," Zhou, D., and Wang T., presented at the 1992 ASME International Gas Turbine and Aeroengine Congress and Exposition. ASME paper 92-GT-246.

Keller, F.J., 1993, "Flow and Thermal Structures in Heated Transitional Boundary Layers with and without Streamwise Acceleration," Ph.D. Dissertation, Dept. of Mech. Engr., Clemson University, Clemson, SC.

Kuan, C.L., 1987, "An Experimental Investigation of Intermittent Behavior in the Transitional Boundary Layer," M.S Thesis, Dept. of Mech. Engr., Clemson University, Clemson, SC.

Kuan, C.L and Wang, T., 1990, "Investigation of Intermittent Behavior of Transitional Boundary Layer Using a Conditional Averaging Technique," *Experimental Thermal and Fluid Science*, Vol. 3, pp.157-170.

Boundary Layer Development on a Turbine Blade in a Linear Cascade

Dave Halstead and Ted Okiishi, Iowa State University

Dave Wisler, GE Aircraft Engines

ABSTRACT

Several different boundary–layer development patterns for flow over the suction surface of a turbine airfoil in a linear cascade were studied and documented using a sliding surface hot–film sensor. The state of the boundary layer, whether laminar, transitional or turbulent, was determined at numerous locations along the airfoil suction surface from leading to trailing edge. Boundary–layer transition from laminar to turbulent flow through laminar separation and turbulent reattachment, or through a combination of bypass transition and strong and weak separation and turbulent reattachment, or through solely bypass transition without separation, was observed and benchmark data were recorded. Surface flow visualization and numerical boundary–layer analysis results are consistent with the hot–film data. Flow and geometry information necessary for numerical code operation is available.

Boundary Layer Development on a Turbine Blade in a Linear Cascade

Dave Wisler
GE Aircraft Engines

Dave Halstead
Ted Okiishi
Iowa State University

- Objectives
- Test Facility and Instrumentation
- Measurement Characteristics of Surface Hot–Films
- Hot–Film Boundary Layer Measurements
- Boundary Layer Calculations
- Observations / Conclusions

Objectives

- Determine boundary layer characteristics along a turbine airfoil using
  - surface–mounted hot–films
  - flow visualization
  - computational analysis.
- Assess consistency of experimental measurements and boundary layer computations.
- Develop a reliable measurement technique for multistage turbomachines.

Turbine Cascade Facility

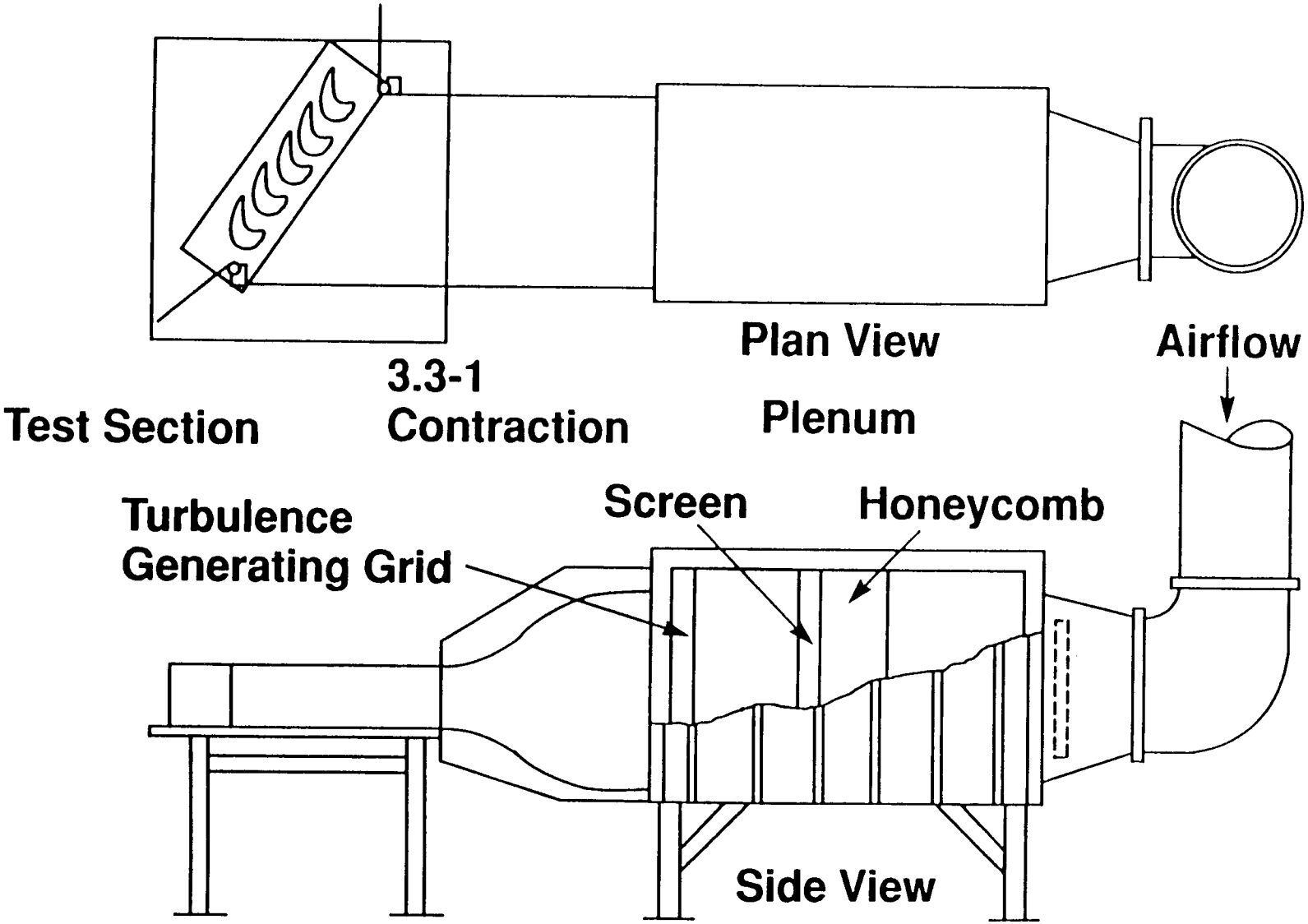

Turbine Cascade Blading

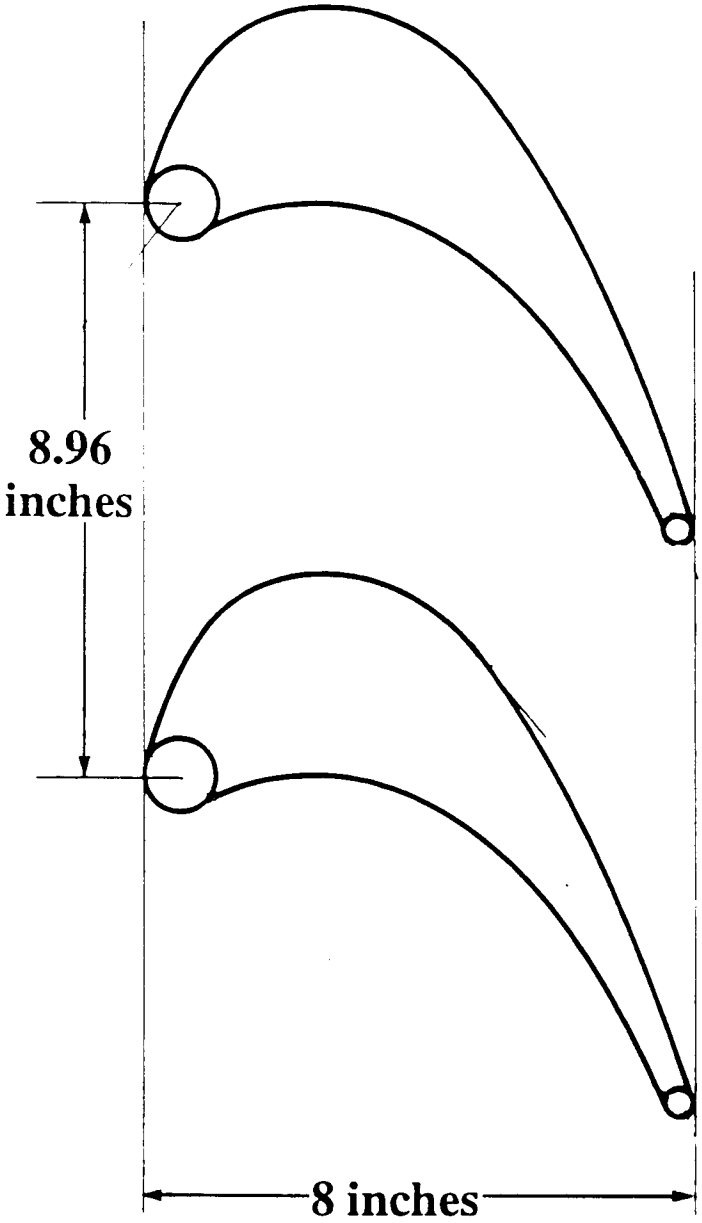

Suction Surface Velocity Distributions

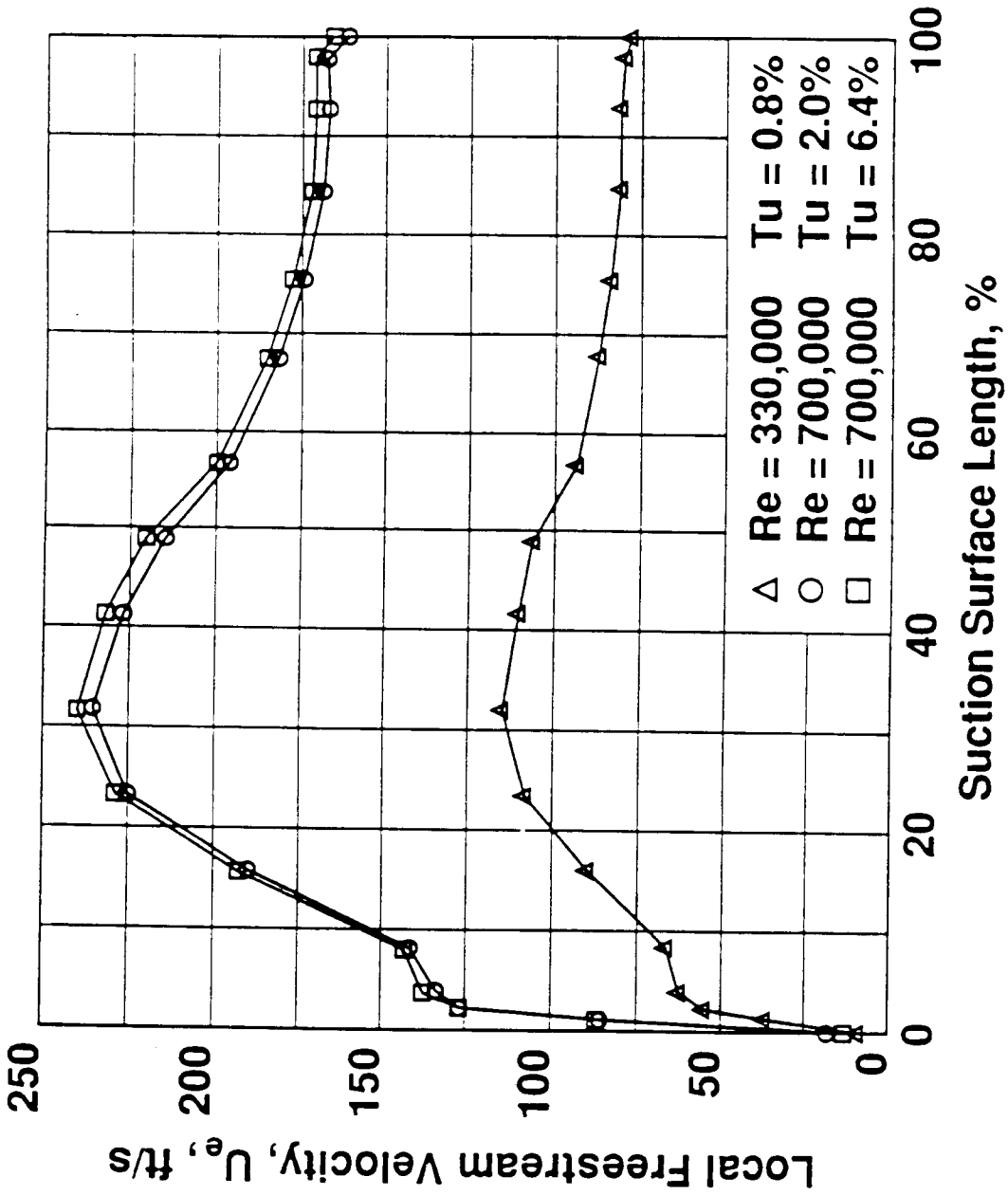

Single-Sensor Hot-Film Gage

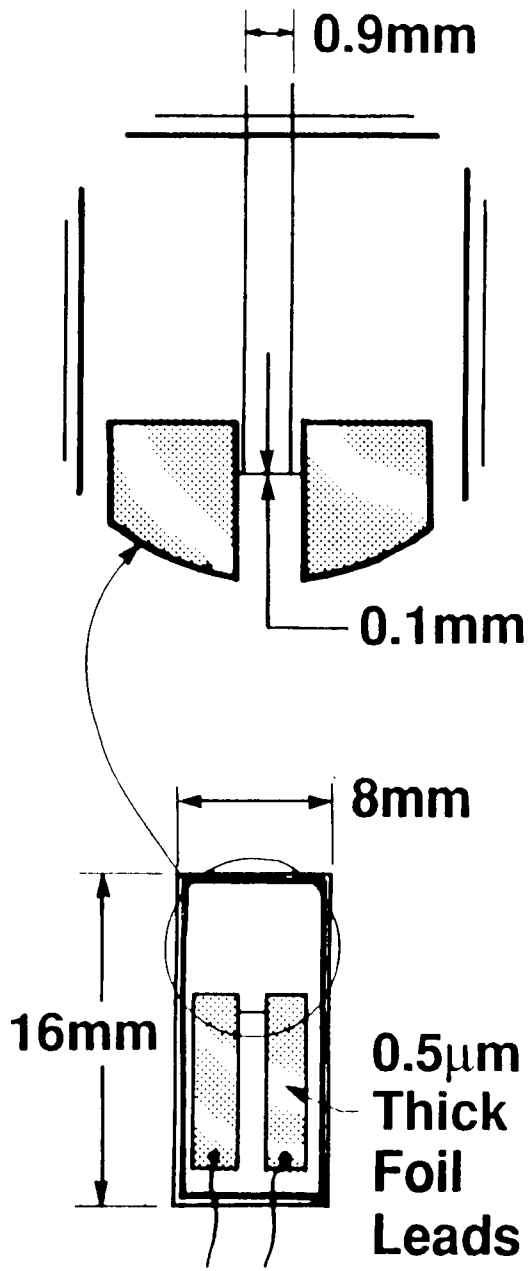

Surface Hot-Film Gage Mounting Technique

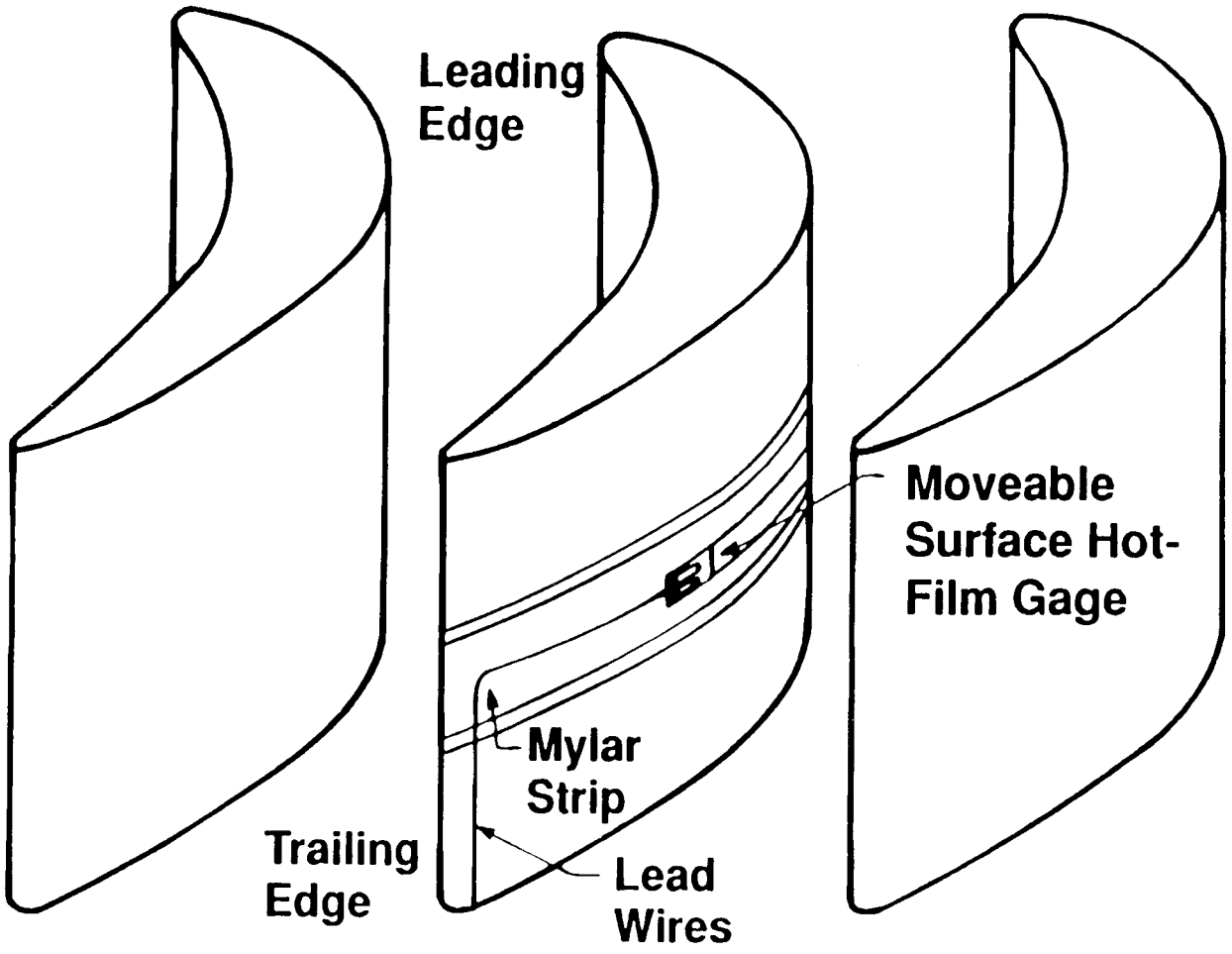

Measurement Characteristics of a Hot–Film Sensor

(Bellhouse and Schultz, 1966)

$$\tau_w^{1/3} = a\ E^2 + b$$

$$\tau_w^{1/3} \propto Q \qquad Q^{1/2} \propto \frac{E-E_0}{E_0}$$

$$\tau_w^{1/6} \propto \frac{E - E_0}{E_0}$$

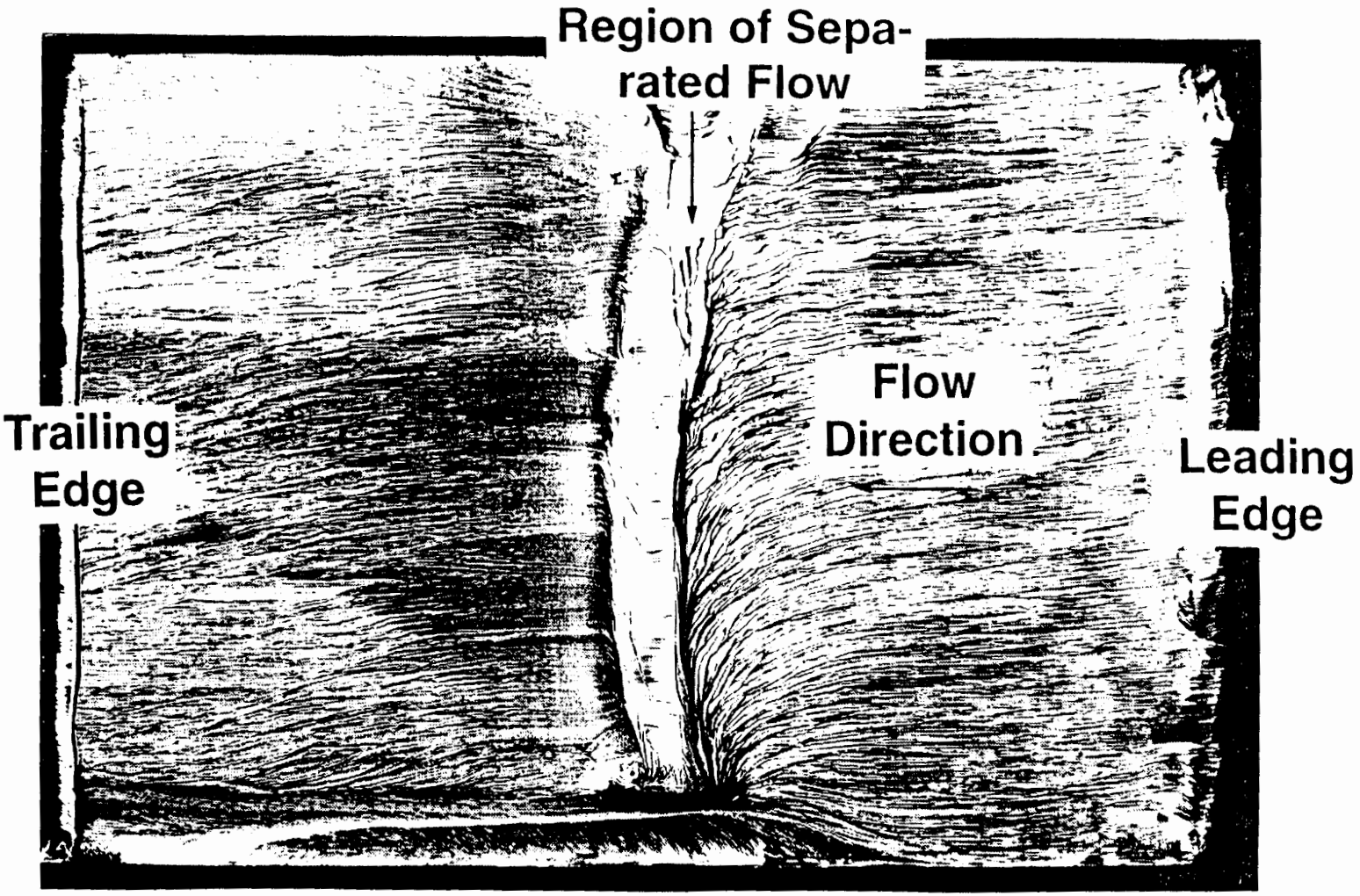

Suction–Surface Flow Visualization

Re = 330,000 Tu_0 = 0.8%

Selected Hot–Film Traces

Re = 330,000 Tu = 0.8%

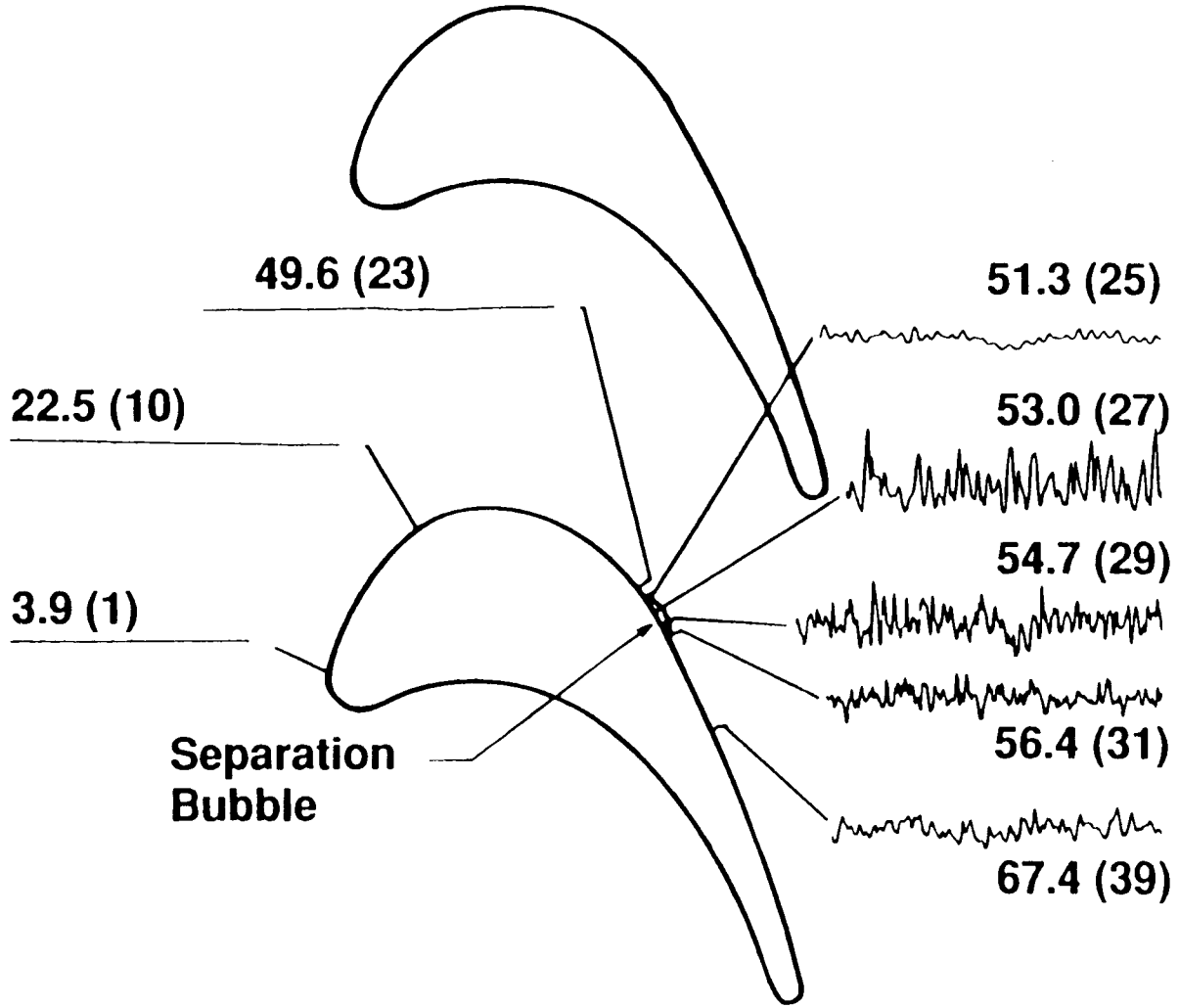

Instantaneous Hot–Film Traces

Re = 330,000 Tu = 0.8%

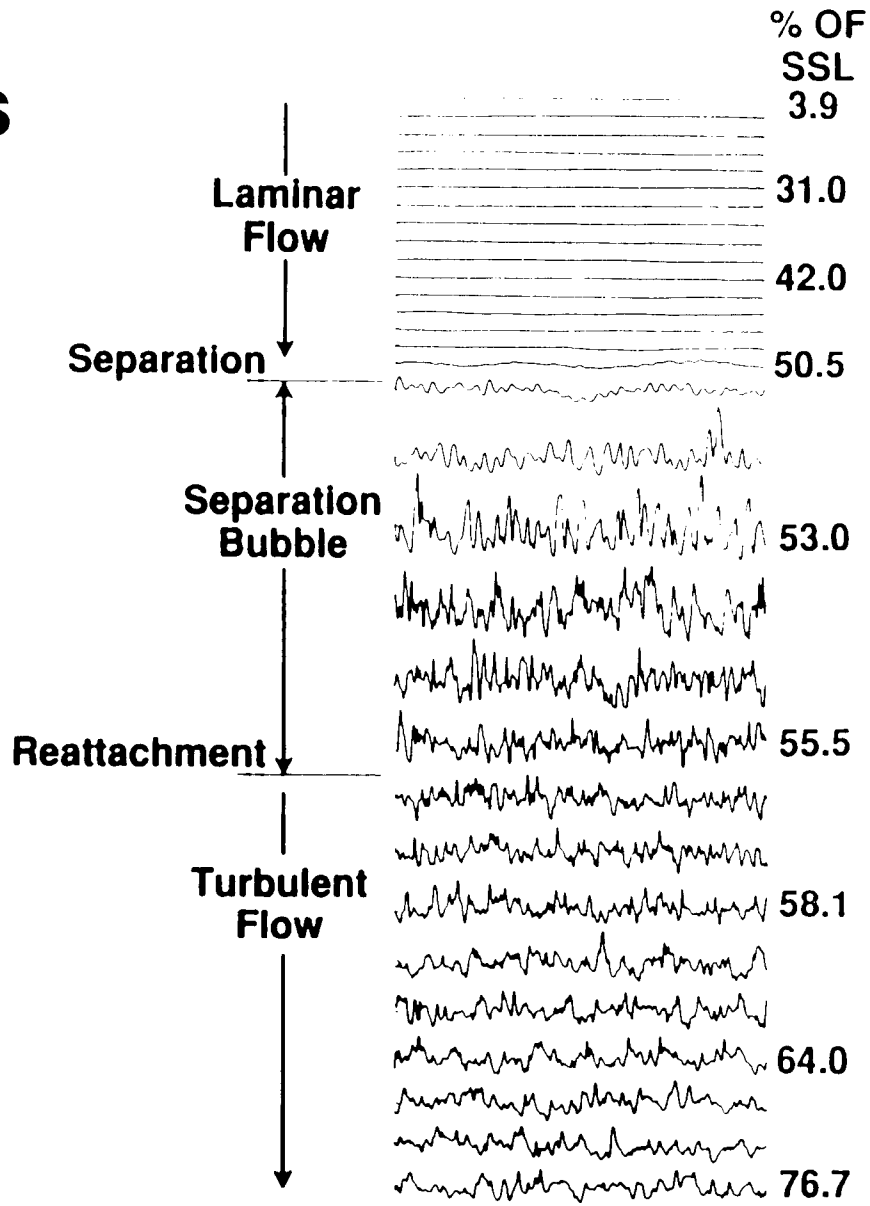

Time–Averaged Measurements

Re = 330,000 Tu = 0.8%

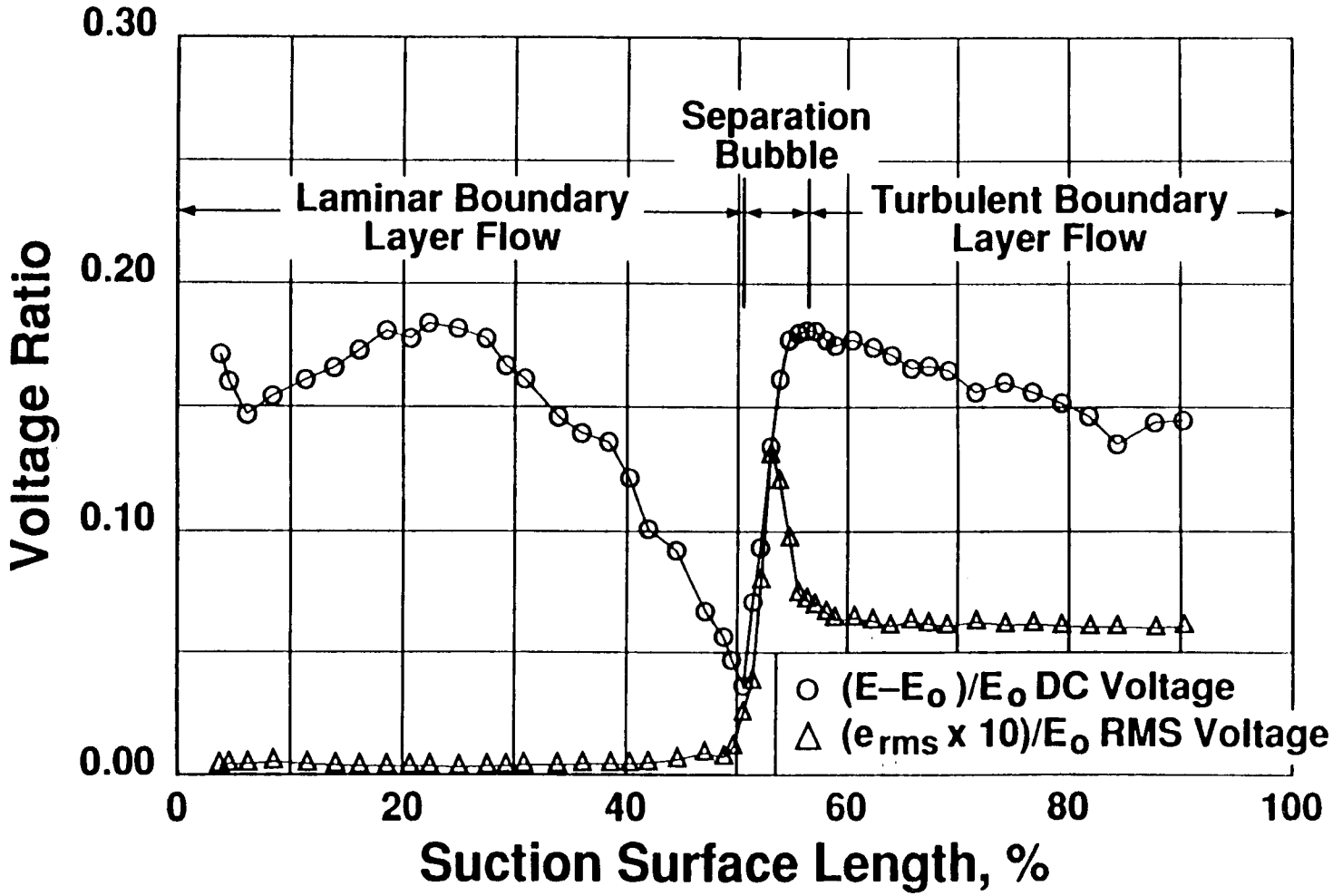

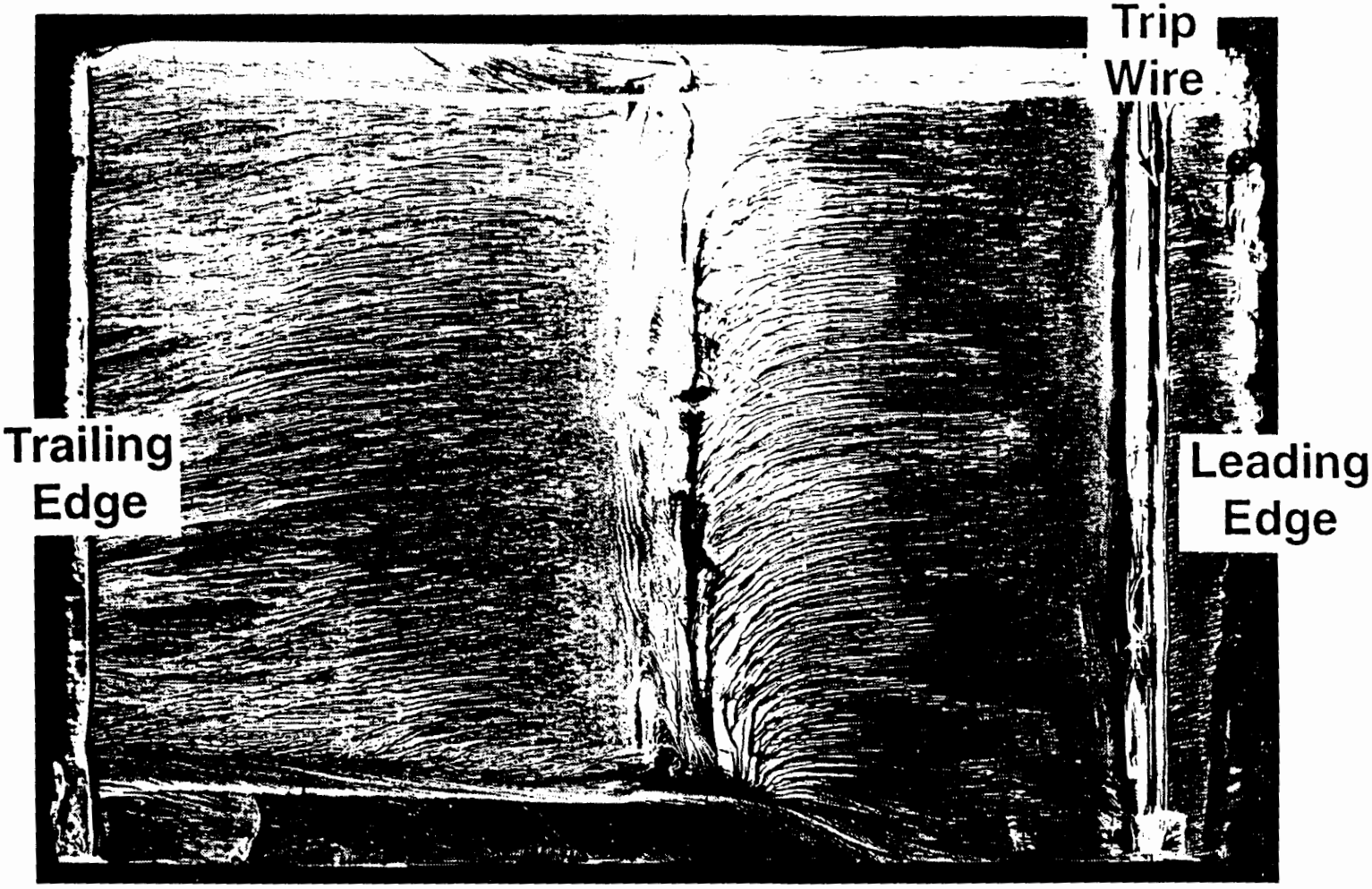

Suction–Surface Flow Visualization

Re = 330,000 Tu_0 = 0.8% with Tripwire

Selected Hot–Film Traces

Re = 330,000 Tu = 0.8% With Tripwire

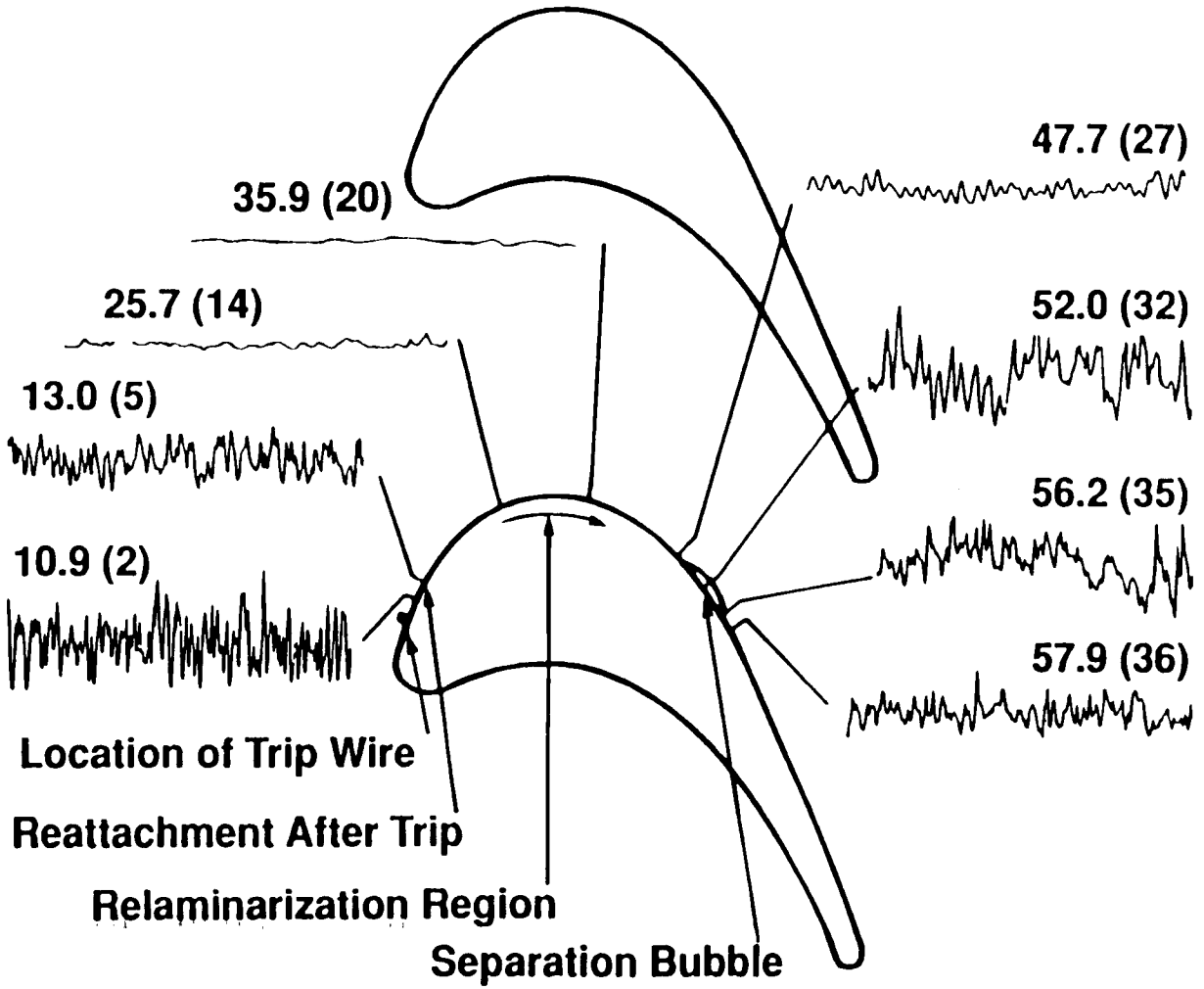

Instantaneous Hot–Film Traces

Re = 330,000 Tu = 0.8%
With Tripwire

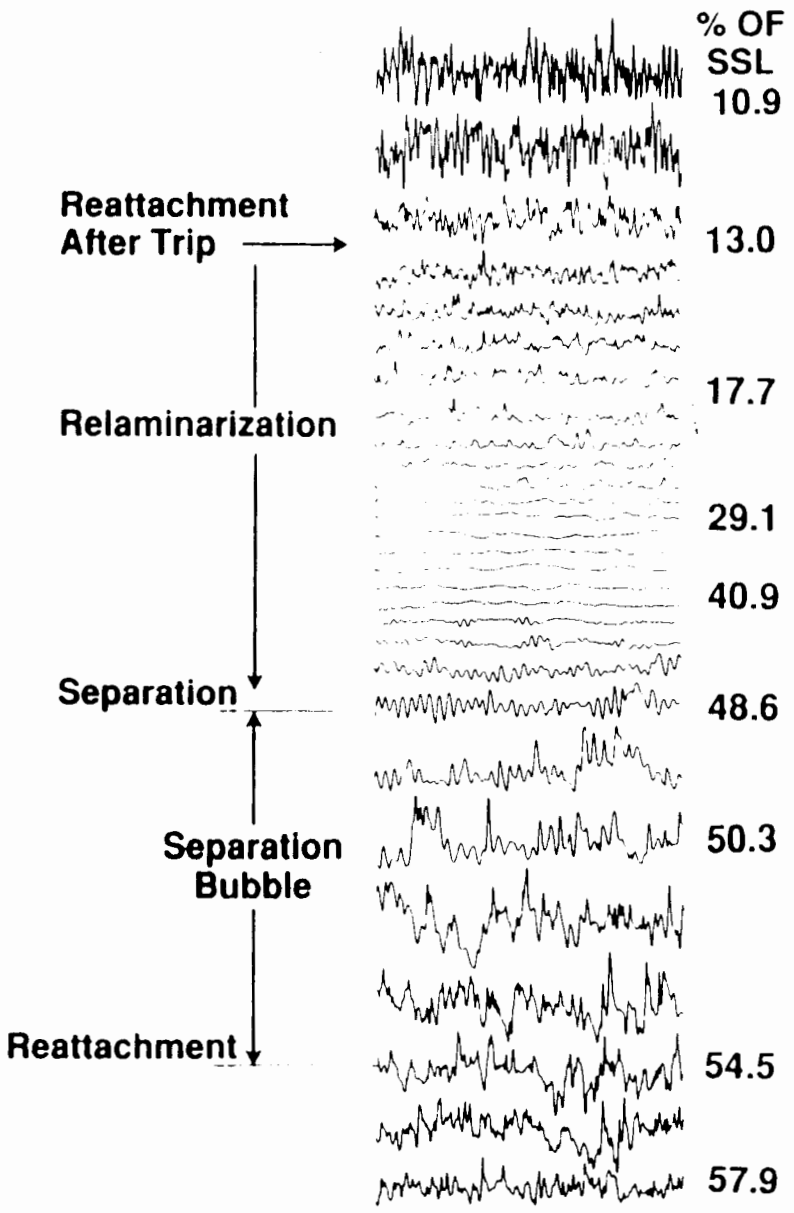

Time–Averaged Measurements

Re = 330,000 Tu = 0.8% With Tripwire

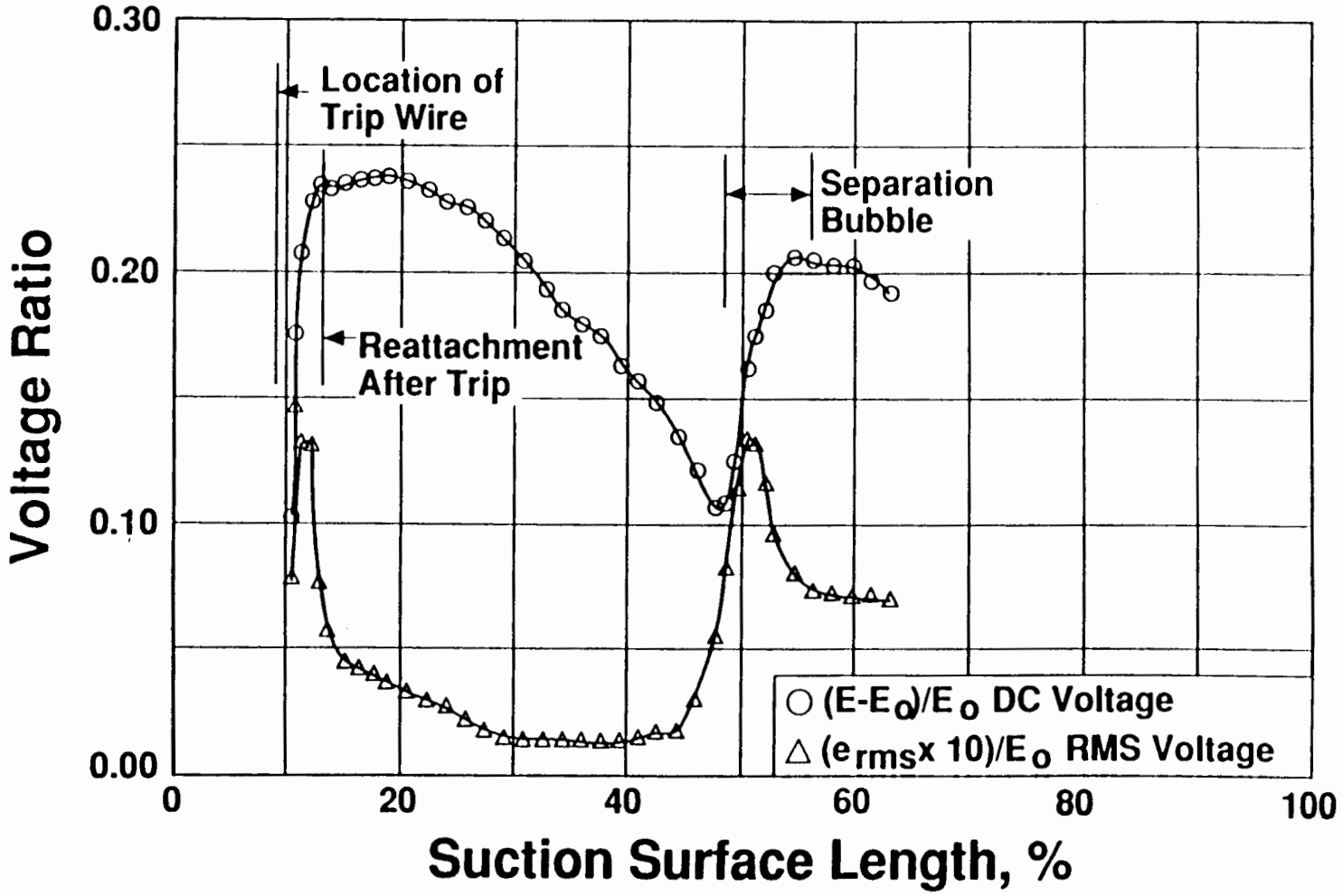

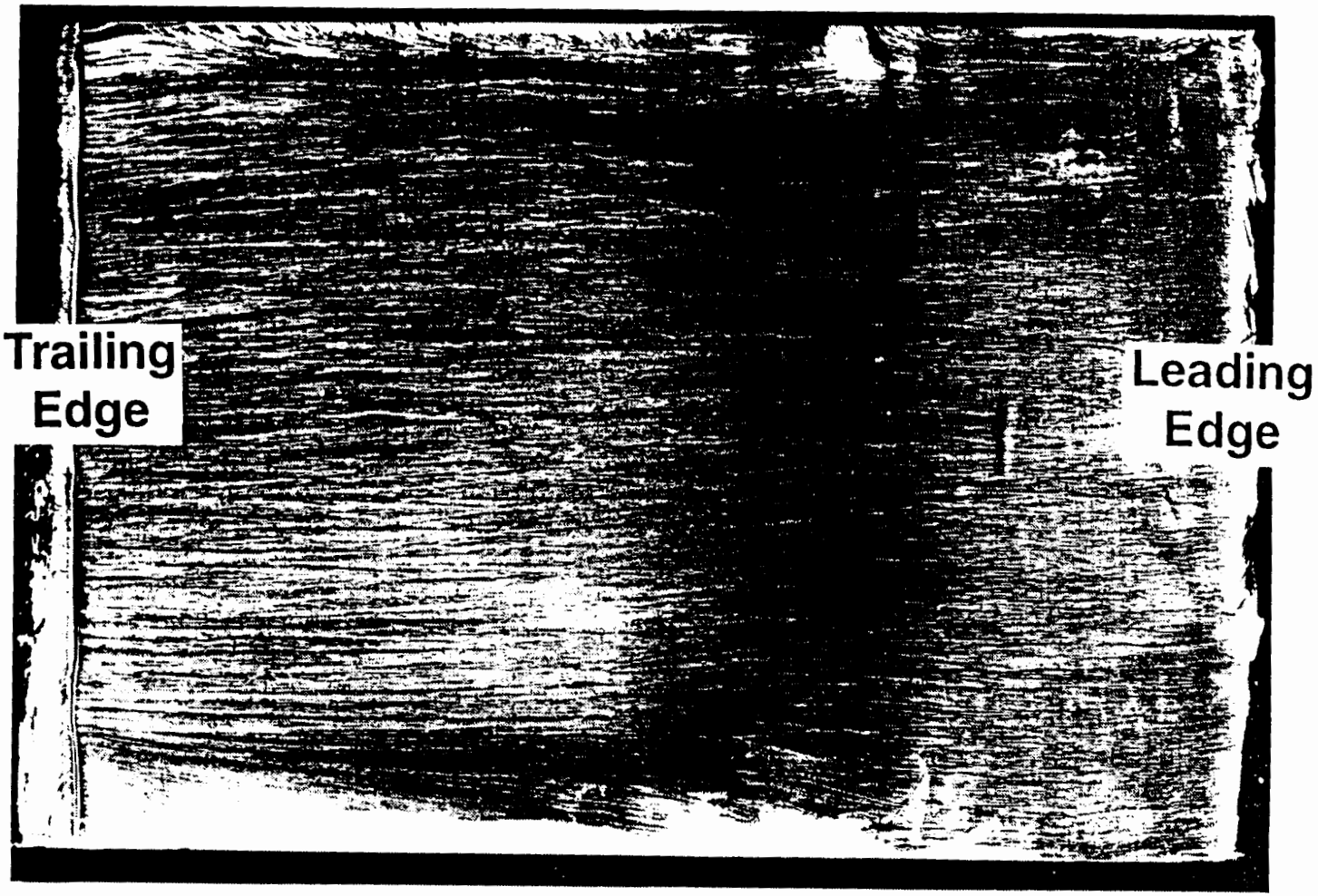

Suction–Surface Flow Visualization

Re = 700,000 Tu_0 = 6.4%

Selected Hot–Film Traces

Re = 700,000 Tu = 6.4%

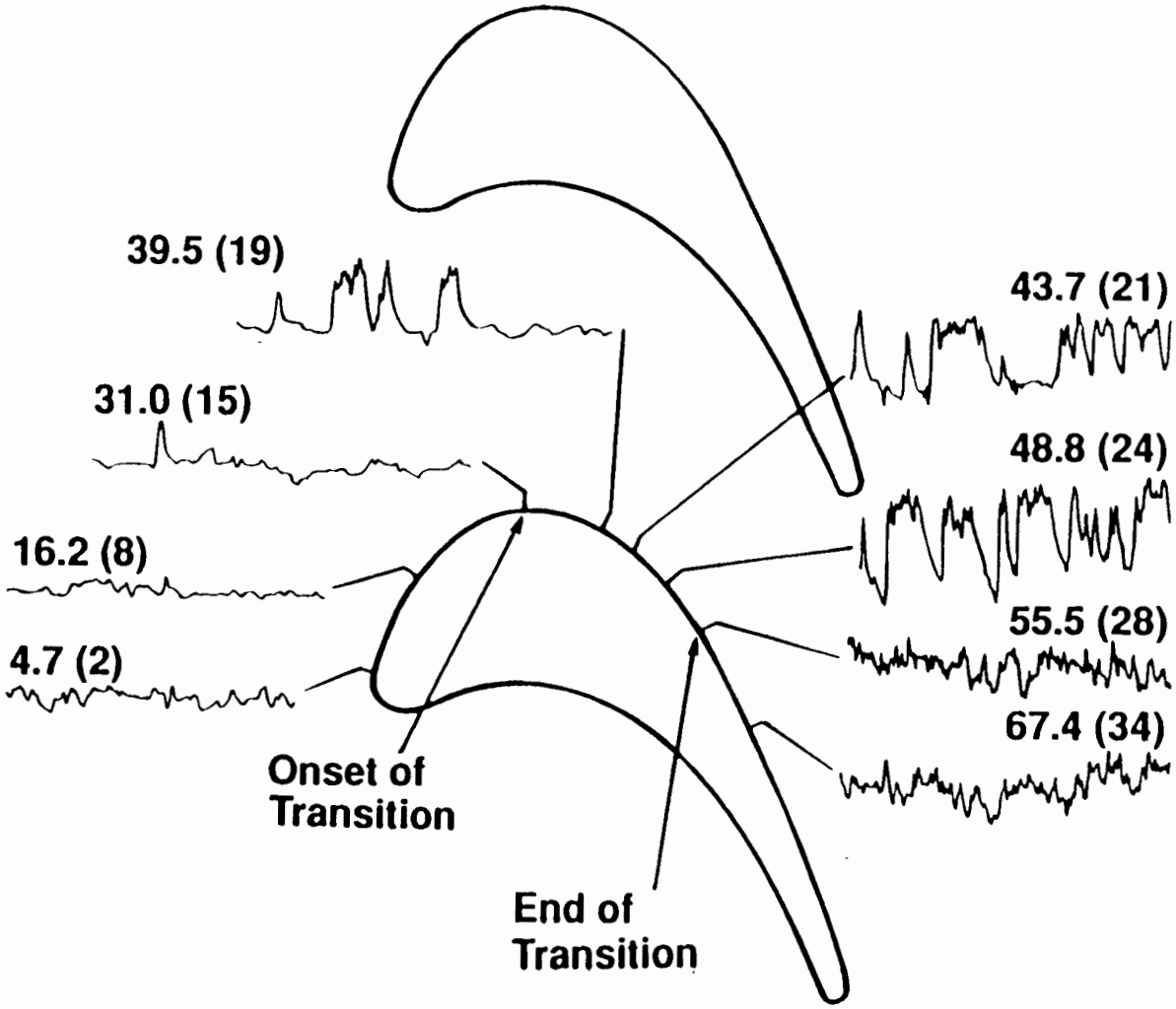

Instantaneous Hot–Film Traces

Re = 700,000 Tu = 6.4%

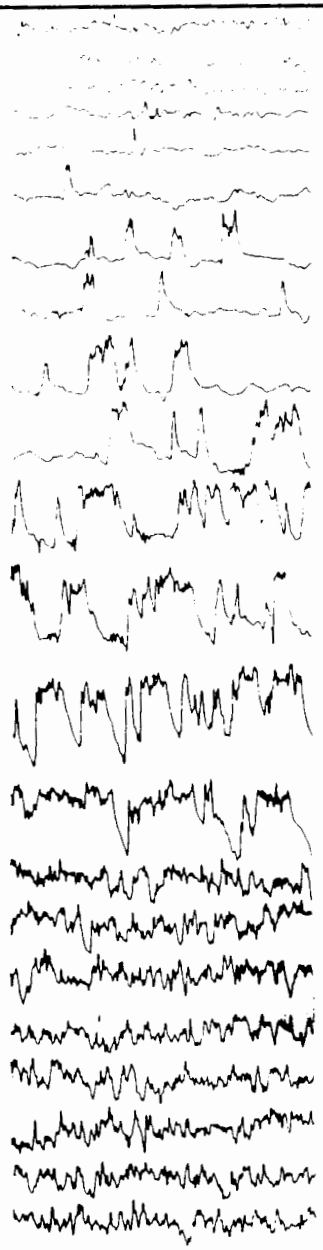

Time–Averaged Measurements

Re = 700,000 Tu = 6.4%

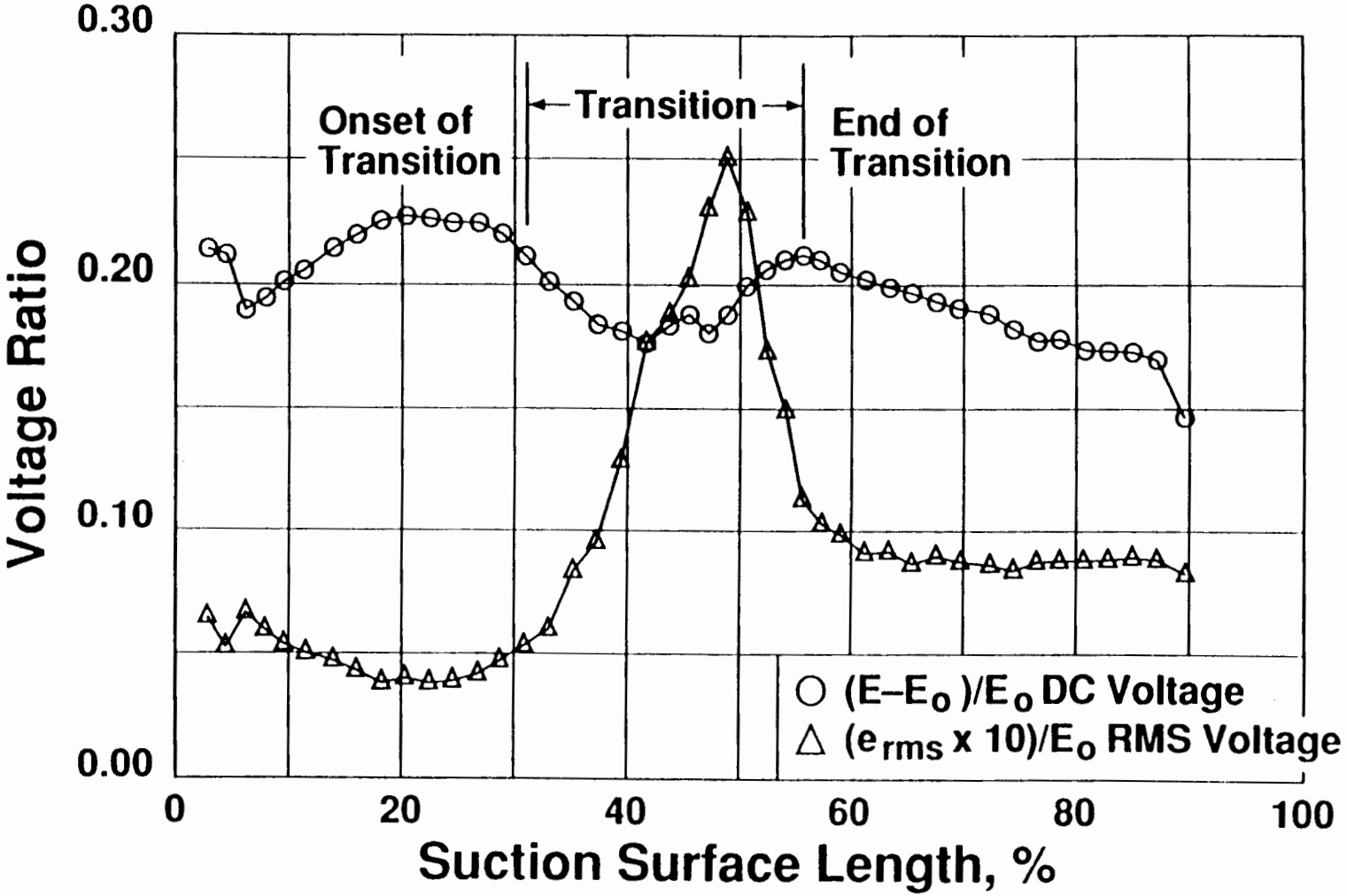

Boundary Layer Calculations

Re = 330,000 Tu = 0.8%

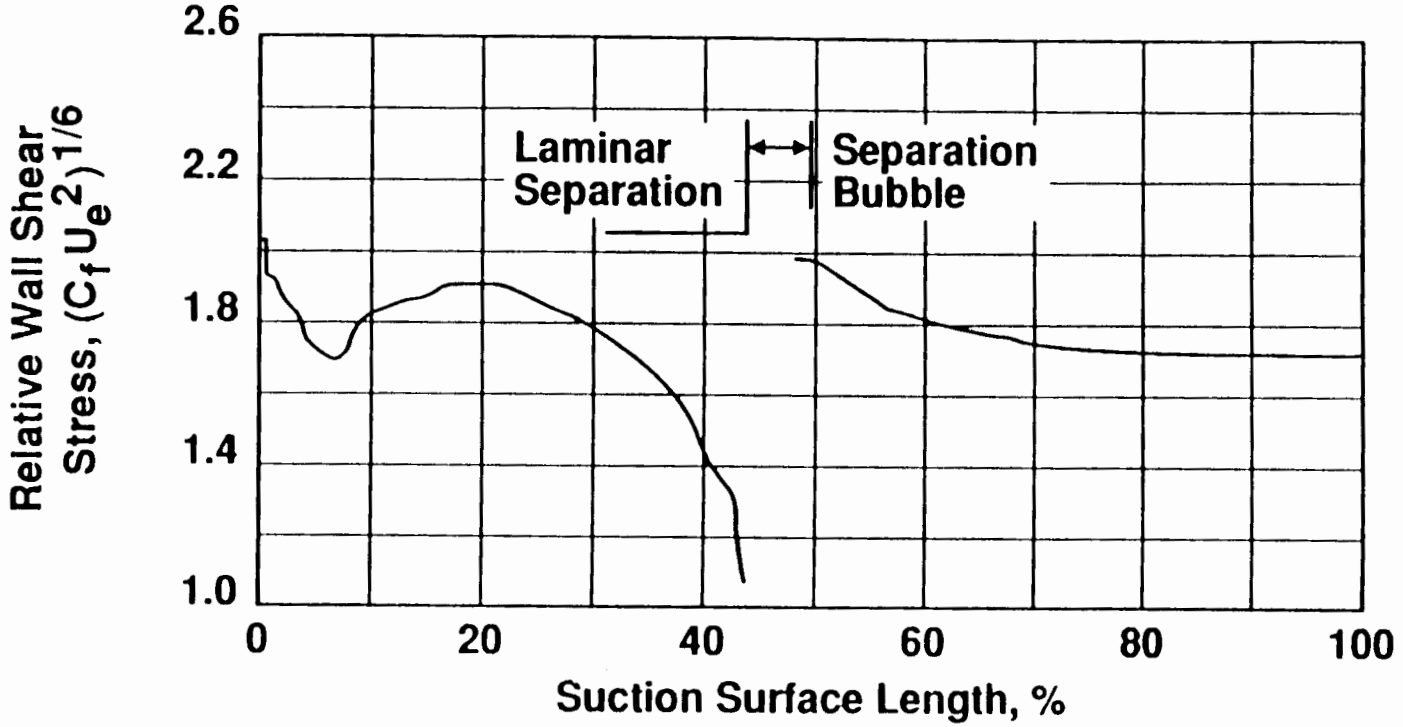

Comparison of Calculations and Measurements

Measurements

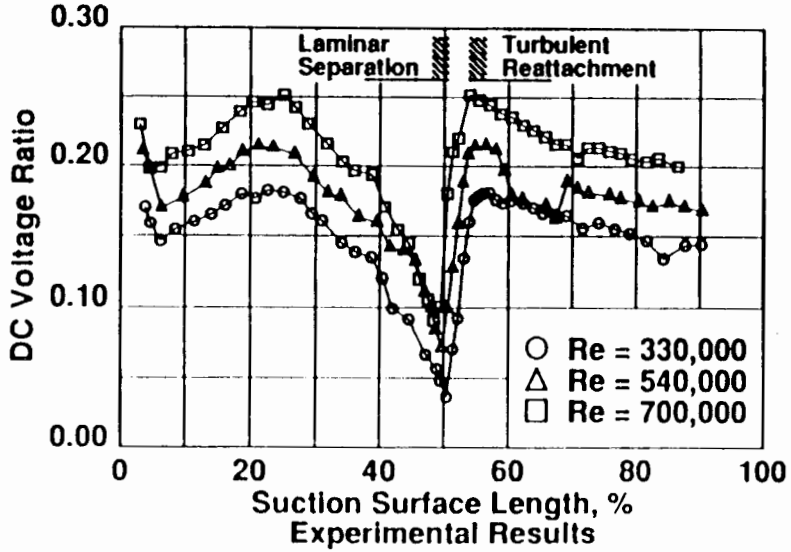

Calculations

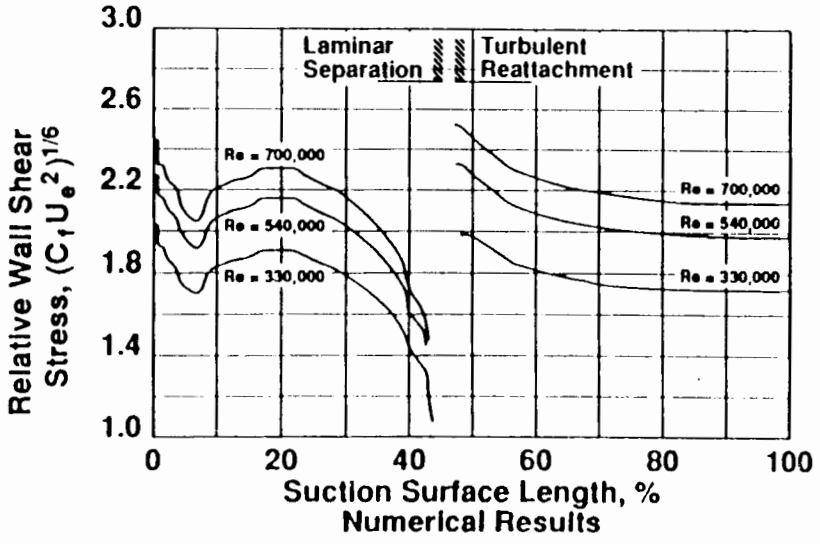

Observations / Conclusions

- Measurements from surface hot–film sensors provide details of principal features of boundary layer development
  - laminar
  - separated
  - relaminarized
  - transitional
  - turbulent.
- Comparison of experimental measurements and boundary layer calculations indicate consistent relationship between wall shear stress and anemometer output voltage.
- Direct calibration of hot–film sensor output with wall shear stress is not required to discern boundary layer development features.

Characteristics of Boundary Layer Transition in a Multi-Stage Low-Pressure Turbine

Dave Wisler, David E. Halstead and Ted Okiishi
General Electric Company
PO Box 156301
One Neumann Way,
Mail Drop H92
Cincinnati, OH 45212-6301

An experimental investigation of boundary layer transition in a multi-stage turbine has been completed using surface-mounted hot-film sensors. Tests were carried out using the two-stage Low Speed Research Turbine of the Aerodynamics Research Laboratory of GE Aircraft Engines. Blading in this facility models current, state-of-the-art low pressure turbine configurations. The instrumentation technique involved arrays of densely-packed hot-film sensors on the surfaces of second stage rotor and nozzle blades. The arrays were located at mid-span on both the suction and pressure surfaces.

Boundary layer measurements were acquired over a complete range of relevant Reynolds numbers. Data acquisition capabilities provided means for detailed data interrogation in both time and frequency domains. Data indicate that significant regions of laminar and transitional boundary layer flow exist on the rotor and nozzle suction surfaces. Evidence of relaminarization both near the leading edge of the suction surface and along much of the pressure surface was observed. Measurements also reveal the nature of the turbulent bursts occurring within and between the wake segments convecting through the blade row. The complex character of boundary layer transition resulting from flow unsteadiness due to nozzle/nozzle, rotor/nozzle, and nozzle/rotor wake interactions are elucidated using these data. These measurements underscore the need to provide turbomachinery designers with models of boundary layer transition to facilitate accurate prediction of aerodynamic loss and heat transfer.

No figures available.

A RESEARCH PROGRAM FOR IMPROVING HEAT TRANSFER PREDICTION CAPABILITY FOR THE LAMINAR TO TURBULENT TRANSITION REGION OF TURBINE VANES/BLADES

Frederick F. Simon
National Aeronautics and Space Administration
Lewis Research Center
Cleveland, Ohio 44135

SUMMARY

A program sponsored by the National Aeronautics and Space Administration (NASA) for the investigation of the heat transfer in the transition region of turbine vanes and blades with the objective of improving the capability for predicting heat transfer is described. The accurate prediction of gas-side heat transfer is important to the determination of turbine longevity, engine performance, and developmental costs. The need for accurate predictions will become greater as the operating temperatures and stage loading levels of advanced turbine engines increase. The present methods for predicting transition shear stress and heat transfer on turbine blades are based on incomplete knowledge and are largely empirical. To meet the objective of the NASA program, a team approach consisting of researchers from government, universities, a research institute, and a Small Business is presented. The research is divided into the areas of experiments, direct numerical simulations (DNS), and turbulence modeling. A summary of the results to date is given for the above research areas in a high-disturbance environment (bypass transition) with a discussion of the model development necessary for use in numerical codes.

INTRODUCTION

A NASA program is described and a progress report is given for the investigation of the heat transfer in the transition region of turbine vanes and blades. The objective of the program is to improve the capability for predicting the gas-side heat transfer for turbine vanes and blades. An improvement in the present predictive accuracy for the heat transfer coefficient from ±35 to ±10 percent would significantly improve the ability to predict blade metal temperatures (Stepka, 1980). According to Graham (1979) an error of 35 percent in the heat transfer coefficient is equivalent to about a 100 °F error in wall temperature prediction which can result in an order of magnitude error in the estimated life of a turbine blade. In addition, an inability to accurately predict gas-side heat transfer often leads to an over-design for thermal protection with an increase in the use of coolant air which penalizes propulsion efficiency.

The prediction of heat transfer on a turbine blade or vane is a formidable task due to the flow of high temperature combustion gases with turbulence intensities that range from 10 to 20 percent over curved surfaces that experience favorable and adverse pressure gradients. A research program in transition must consider and evaluate the effects of free-stream turbulence, convex and concave curvature, favorable and adverse pressure gradient, roughness, wake passing, and the stagnation region (fig. 1). A significant portion of the turbine blade/vane may be in a transitional flow between laminar and turbulent boundary layer states. Heat transfer levels in the turbulent flow region of the blade/vane can be as high as three times that of the laminar flow region. Because of the complexity of the problem a program plan was developed at NASA Lewis in 1986 with emphasis on subsonic flows. The NASA Transition Workshop of 1984 (Graham, 1985) formed the basis for the development of this plan. The plan took the approach of initiating the experimental and analytical research with a simple geometry of a flat plate at a zero pressure gradient and systematically increasing the geometry and flow complexities with an eventual effort of a turbine vane in an environment of high turbulence with and without wakes.

The knowledge base is limited for the situation of transition in an engine environment where disturbance levels are initially large. In such a large disturbance environment, traditional linear mechanisms are bypassed and finite nonlinear effects must be considered. This is demonstrated by using the work of Suder, O'Brien, and Reshotko (1988) to make a comparison between the onset of transition for a linear and a nonlinear path (fig. 2). In figure 2, time traces of flush-mounted hot films are shown for cases of low and higher free-stream turbulence intensities. The low free-stream turbulence case shows the presence and amplification of Tollmien-Schlichting (T-S) waves as the path to the onset of transition. The higher free-stream turbulence case shows the sudden appearance of turbulence spots without a sign of linear disturbance growth (although they may be present). As first indicated by Morkovin (1978) the linear stability mechanisms are bypassed and finite nonlinear instabilities occur. Morkovin labels this path to transition as bypass transition. In the bypass model, amplification of Tollmien-Schlichting waves may still be present, but at a much slower rate than the bypass mechanism, and, thus, is of little effect.

The present paper presents the approach in which the NASA Bypass Transition Program proposes to accomplish the stated objective of improved heat transfer prediction capability for the transition region of turbine vanes/blades and a status report of some of the results to date with recommendations for future work. To meet the objective requires that the physics associated with bypass transition heat transfer be investigated, identified, and modeled. The results obtained to date are given in terms of their application to the prediction of transition onset and transition path, as well as through transition skin-friction and heat transfer predictions. Research results are presented in the three areas of experiments, direct numerical simulation (DNS), and turbulence modeling.

NOMENCLATURE

C_f	skin friction coefficient
H	boundary layer shape factor
h	heat transfer coefficient, W/m^2, K
K	pressure gradient parameter, $(\nu/U_e)\partial U_e/\partial x$
L_{tr}	transition length
N	nondimensional spot formation rate
Re_x	Reynolds number based on distance x from leading edge
Re_θ	momentum thickness Reynolds number
$Re_{\Delta 2}$	enthalpy thickness Reynolds number
St	Stanton number
Tu	turbulence intensity at free-stream
U_e	free-stream velocity
U_τ	friction velocity

u',v',w'	fluctuating velocities in x,y,z directions
u^+	streamwise mean velocity in wall units
x	distance from leading edge
y^+	normalized y distance in wall units
α	spreading angle of spot
β	velocity of center of spot divided by free-stream velocity
γ	intermittency
δ	boundary layer thickness
δ^*	displacement thickness
η	Blasius similarity variable
θ	boundary layer momentum thickness
ν	kinematic viscosity

Subscripts:

tr	transition onset
E	transition end

APPROACH

It is believed that a team approach will best meet the needs of a fundamental investigation into bypass transition. Simoneau (1986) states that research of a complex nature requires focus and organization and recommends the use of research technology teams. The team members outlined in figure 3 consists of researchers from NASA Lewis, the Center for Modeling of Turbulence and Transition (CMOTT), NASA Ames, NASA Langley, The University of Minnesota, The University of Texas at Austin, Texas A&M, Case Western Reserve University, The University of Toledo, and Dynaflow, Inc. The results of the team efforts in the three areas of experiments, DNS and turbulence modeling are reviewed at annual contractor/grantee workshops sponsored by NASA Lewis.

Experiments on flat surfaces, curved surfaces, and airfoil shapes with and without simulated rotor wakes are being carried out in a number of facilities (figs. 4 to 7). Figure 4 shows the NASA Lewis closed circuit wind tunnel for flat surfaces with variable free-stream turbulence levels and pressure gradient. Measurement systems for this facility allow for characterization of the free-stream intensity and length scale, boundary layer mean temperature and velocity measurements, boundary layer temperature and velocity fluctuations, boundary layer turbulent streamwise and cross-stream stresses and heat fluxes, intermittency and mean surface heat transfer. These same measurements are made for a curved surface in the University of Minnesota test facility (fig. 5). Details of these facilities and measurement approaches may be found in the references of Suder, O'Brien, and

Reshotko (1988); Sohn and Reshotko (1991); Kim and Simon (1991); and in an excellent summary of bypass transition experimental results by Volino and Simon (1991). Measurements of the effects of wakes on transition is being accomplished by using a squirrel cage wake generator at Texas A&M (fig. 6(a)) and the Spoked Wheel Rotor Simulator at NASA Lewis (fig. 6(b)). Transition heat transfer measurements are being made at NASA Lewis on a large blade sprayed with liquid crystals to obtain temperature distributions (fig. 7). Measurements from the above experiments are providing benchmark data for investigation of fundamental mechanisms for model development, and to check numerical predictions.

DNS analyses of a flat surface and an airfoil shape are being made at NASA Ames, NASA Langley, and NASA Lewis. The resulting information provides a numerical data base for modeling and investigating mechanisms. The experimental data generated in the program help to validate the DNS results. Parabolized Stability Equations (PSE) methods are being developed by Dynaflow, Inc. to analyze transition and heat transfer in flows over gas turbine blades.

Turbulence models are being developed at The University of Texas at Austin, Case Western Reserve University, and NASA Lewis for the numerical prediction of transition heat transfer. The development and assessment of these models are being guided by the experimental and DNS results.

RESULTS

A summary of the results to date are presented with emphasis on their application to the understanding and prediction of transition onset and the transition region and the comparison of predictions with benchmark experimental data.

TRANSITION ONSET

Fundamentally, the onset of the transition region is characterized by the intermittent appearance of turbulent spots. These spots grow as they move downstream and eventually merge to form the turbulent boundary layer. This event will have a different observed effect on the physics of flow, the skin friction, and the heat transfer, resulting in different definitions for transition onset. Suder, O'Brien, and Reshotko (1988) experimentally investigated several methods for determining the onset of transition on flat unheated surfaces for a range of free-stream turbulence from 0.3 to 5 percent. The methods for determining transition may be classified into two categories; (1) those based on the physics of flow dynamics and (2) those which result from measurements of skin friction or heat transfer. Methods which fall into the category of flow dynamics are the mean profiles, shape factor, RMS profiles, and the intermittency. Table I lists the five methods (according to the parameters interrogated) employed with a comparison of distances from the leading edge to onset of transition. Mean boundary layer velocity profiles were measured and compared to classical laminar and turbulent profiles. A comparison of the mean profiles with the Blasius profile for a laminar boundary layer (fig. 8(a)) allows one to determine deviation from the Blasius profile as one means of identifying transition onset. For the grid 1 case of figure 8(a), deviation has already begun at 10 in. Another means of onset determination is the deviation of the shape factor from its Blasius value of 2.59 to a decreasing value as the boundary layer becomes more turbulent. A comparison of the boundary layer shape factor variation for four turbulence generating grids is shown in figure 8(b). For the grid 1 case deviation of the shape factor from the traditional laminar value begins at a distance of about 11 in. A more traditional approach for determining onset is based on the distribution of skin friction versus distance as shown in figure 8(c). A comparison of the skin friction coefficient with its theoretical laminar value as shown in figure 8(c) allowed a determination of onset as departure from the laminar line, which for grid 1 is about 9 in. from the plate leading edge. The rms of longitudinal velocity fluctuations is another indicator of transition onset since the velocity fluctuations in a laminar boundary layer are much less

than those obtained for a turbulent boundary layer. The rms profiles of the longitudinal velocity fluctuations (fig. 8(d)) indicate that as the flow begins to transition, the rms values of the velocity fluctuations begin to increase rapidly. In the case of grid 1 (fig. 8(d)) onset begins at approximately 9 in.

The intermittency factor is defined as the percent of time the boundary layer is turbulent and is therefore a measure of the passage of turbulent spots. Therefore, measurement of the intermittency factor should produce the most definitive indication of transition onset. The results presented by Suder, O'Brien, and Reshotko (1988) of flush-mounted hot-films permitted a determination of the intermittency factor as a function of Reynolds number (fig. 8(e)). Transition onset was determined by the location of the hot-film which first recorded intermittency. For grids 0.5 and 1, onset positions of 6.2 and 4.2 in., respectively, were obtained. In the case of grids 2 and 3, transition onset occurred before the location of the first hot-film (4.22 in.). Based on a comparison of the above methods, Suder, O'Brien, and Reshotko (1988) concluded that the intermittency approach gave the earliest indication of transition (table I), suggesting that the other approaches, given above, are not affected by the presence of small amounts of turbulent spots. The five methods of table I show general agreement with each other and show reasonable comparison with the empirical correlations of Van Driest and Blumer (1963), Seyb (1972), Abu-Ghannam and Shaw (1980) and Dunham (1972). Suder, O'Brien, and Reshotko (1988) also noted that, in addition to the influence of free-stream turbulence on transition, there may also be an influence of the frequency distribution (or, alternatively, length scale distribution) of the free-stream disturbances.

As indicated above, onset of transition as determined by the first appearance of turbulent spots is best described by intermittency measurements. An accurate measurement for small values of intermittency is not practical so that use of the extrapolation method of Narashimha (1957) is recommended. Simon and Stephens (1991) used this method to determine the zero intermittency point and the transition length (fig. 9) for the experimental data of Sohn and Reshotko (1991). Volino and Simon (1991) used this approach on the accelerated transition flow data of Blair and Anderson (1987). The results (fig. 10) indicate a change in slope at the lower free-stream turbulence for a value of the function plotted on the ordinate of figure 10 of less than 0.3. Narasimha (1985) and Blair and Anderson (1987) referred to this change in slope as a "subtransition."

Stuckert and Herbert (1992) compared their Parabolized Stability Equations (PSE) approach with the experimental data of Sohn and Reshotko (1991) as shown in figure 11. The onset of transition as defined by the minimum Stanton number is predicted very well by the PSE method. Volino and Simon (1991) compared the zero intermittency point with the minimum Stanton number (used by some as a definition for transition onset) and determined that the minimum Stanton number is located somewhat downstream of the zero intermittency point. This was also noted by Simon and Stephens (1991).

Use of two-equation near-wall turbulence models has in general been successful in the prediction of bypass transition onset. Simon and Stephens (1991) used the Jones-Launder turbulence model to predict onset and compared their results with experimental data and the correlation of Abu-Ghannan and Shaw (1980). The comparison of their results with the correlation of Abu-Ghannan and Shaw is good as shown in figure 12. Simon and Stephens (1991) assumed the transition onset to occur when the numerical computations indicated a rapid increase in turbulence kinetic energy, indicating a nonzero intermittency. This assumption was confirmed (Simoneau and Simon, 1993) by comparison with the DNS calculations of Rai and Moin (1991) shown in figure 13 for the case of zero pressure gradient and 2.6 percent free-stream turbulence. Figure 13 shows how the two-equation turbulence model captures the nonlinear disturbance growth which leads to the first sign of turbulent spot formation. Suder, O'Brien, and Reshotko's (1988) single-wire measurements within the boundary layer indicated spot initiation at a boundary layer turbulence level of 3.5 percent regardless of the path to transition (high or low free-stream turbulence). This experimental result appears consistent with the calculations of Simon and Stephens (1991) and Rai and Moin (1991) shown in figure 13.

Figure 13 suggests that, below a certain critical Reynolds number, amplification of disturbances is not significant. This was the basis for the assumption made by Schmidt and Patankar (1988) in their development of a turbulence model for transition and the basis used by Simon and Stephens (1991) for initializing the calculations for disturbance energy shown in figure 13. The assumption made by the above authors was that this critical Reynolds number is close to the critical Reynolds number for linear instability. To help establish the credibility of this assumption, DNS studies of controlled disturbances in a Blasius boundary layer are being performed at NASA Lewis using Spalart's fringe code (Ashpis and Spalart, 1992, and Ashpis and Spalart, 1993). The objective of these studies is to simulate bypass mechanisms by introducing into the boundary layer controlled discrete disturbances and computing the space-time evolution of the resulting disturbances and their spectra. The input disturbances are of linear and nonlinear amplitudes, and are introduced at subcritical and supercritical Reynolds numbers. An example of a response to a pulsed disturbance is given in figure 14, which shows a structure composed of a nonlinearly distorted wave packet superposed on a narrow, streamwise elongated, structure. Wave packets may develop in various routes, one of which is into turbulent spots.

Other experimental and analytical values for transition onset are given in figure 12. Figure 12 shows some experimental transition onset results given in the survey report of Volino and Simon (1991) and some examples of the result of transition onset calculations utilizing a number of turbulence models developed at the University of Texas at Austin. Figure 12 shows the general applicability of turbulence models for predicting transition onset.. Turbulence models developed at the University of Texas at Austin (Crawford, 1991) called the Texas model (TXM) and the Multi-Time-Scale (MTS) model have the potential of improved simulation of the transition region.

The K.Y. Chien turbulence model (1982) results shown in figure 12 were found by Stephens and Crawford (1990) to give a premature value for transition onset. They explained that this is because the damping function of the Chien model is dependent only on the boundary layer normal distance and that an improved onset prediction is obtained when the damping function is dependent on the turbulent Reynolds number. The inability of the K.Y. Chien model to simulate transition onset was also found by the heat transfer Navier-Stokes calculations of a turbine blade by Ameri and Arnone (1992).

The effect of curvature on transition onset at low free-stream turbulence is summarized from the experimental work of Wang (1984) and Kim and Simon (1991) in figure 15. As indicated in figure 15, a convex surface when compared to a flat surface will delay transition onset and a concave surface compared to a flat surface will shift transition onset upstream. The differences in onset location, based on the minimum in the Stanton number, for a convex surface and a flat surface diminish as the free-stream turbulence increases (fig. 16).

TRANSITION REGION

This section describes the relevant physical characteristics of the transition region required for the understanding and modeling of the region. Figure 17 shows conditionally sampled velocity profiles in the transition region of a flat plate as reported by Sohn, Reshotko, and Zaman (1991). Figure 17 shows the departure from a Blasius profile as an indication of the transition region which occurs after transition onset. The nonturbulent profiles increase in their deviation from the Blasius curve with increases in intermittency. With increase in intermittency the turbulent part of each profile is seen to become more like that of a fully-turbulent boundary layer. The effect of the nonturbulent profiles showing increased deviation from a Blasius profile with increased intermittency is attributed by Kim and Simon (1991) and Sohn and Reshotko (1991) to a post-burst relaxation period required for a disturbance in the nonturbulent part of the flow to damp-out. With an increase in the number of turbulent spots, or increased intermittency, there are more post-burst relaxation periods included in the nonturbulent part of the flow. Figure 17 demonstrates that the transition region cannot be accurately

described by a combination of Blasius and fully turbulent boundary layer profiles as proposed by Dhawan and Narasimha (1958) by using an intermittency weighting approach.

As can be observed in figure 8(d), the streamwise component of turbulence intensity measurements will, under certain conditions, exhibit a double hump. The observance of a double hump in the data is attributed to the switching between laminar and turbulent boundary layer flows as a turbulent spot goes by a hot-wire probe. Confirmation of this switching explanation is seen in the DNS calculations of the streamwise fluctuation of Rai and Moin (1991) which do not exhibit a double hump (fig. 18). This switching effect gives rise to a velocity fluctuation level which is higher than that obtained in either the laminar or the turbulent regions and affects the experimental shear stress profile (Kim and Simon, 1991).

It is generally known that a concave curvature has a destabilizing effect on flow, with transition occurring earlier than on a flat plate. Görtler vortices are the primary mode of instability. Kim and Simon (1991) established the existence of stable vortices on a concave surface for low free-stream turbulence, but found no stable vortices for a higher turbulence intensity case (8.3 percent). Figure 19 displays Stanton number results obtained at the University of Minnesota (Volino and Simon, 1993). They show the effects of concave curvature and acceleration as compared to unaccelerated flow on a flat plate. The unaccelerated, flat plate, 8 percent free-stream turbulence data (Kim and Simon, 1991) are only slightly above a standard, fully-turbulent flow, flat-plate, low turbulence intensity correlation, which is shown in figure 19 for reference. Unaccelerated flow, concave wall data taken at 8 percent free-stream turbulence intensity lie well above this correlation. Accelerated concave wall data fall below the correlation as do accelerated flat plate data of Blair and Anderson (1987). The accelerated flat plate data taken at 5 percent turbulence intensity show a transition from the laminar to turbulent flow; however, there is no sign of transition for any of 8 percent turbulence intensity cases, even the accelerated-flow cases. On the concave surface, acceleration lowers the Stanton number in opposition to the curvature effect. This countering of the curvature effect by acceleration was also seen in the measurements of the shear stress profiles obtained at the University of Minnesota, figure 20, where acceleration counteracts the concave curvature effects, reducing the shear stress profile to unaccelerated flat-wall levels. Increasing the acceleration is expected to further reduce the level of shear stress. The above mentioned effects of free-stream turbulence, curvature, and acceleration lend further understanding of the highly-disturbed flow and will play an important role in the development of predictive models.

Experimental and calculated values of the momentum thickness Reynolds number at the onset and end of transition, as compared with the correlations of Abu-Ghannam and Shaw (1980), are given in figures 12 and 21. In these plots, the transition region may be defined as existing between an intermittency of 0 and 0.99 or between the points of minimum and maximum heat transfer. These curves present a good summary of the measurements and calculations for the transition region. These curves demonstrate the strong effect free-stream turbulence intensity plays, although it is expected that the spectra and length scale of the free-stream turbulence will be needed to further refine the turbulence effects.

As indicated above, the use of low Reynolds number, two-equation turbulence models (figs. 12 and 21) appears to have some success in simulating transition onset and end which is governed by the transport and production of turbulence in the boundary layer. Generally, as can be seen in figure 21, these models give an underprediction of transition length. A reason for this may be found in the work of Volino and Simon (1993). Volino and Simon (1993) applied an octant analysis to the experimental data to analyze the difference in structure between turbulent and transitional flows. They indicate that transitional boundary layers show incomplete mixing or incomplete development of turbulence with a domination of the large scale eddies. This is attributed to the incomplete development of the cascade of energy from large to small scales. Based on this observation, it is stated that the standard k-ε turbulence model does not comprehend the physics of the transition region and what is needed is a model that will comprehend both large and small scales separately. This would require a modified k-ε equation with perhaps two equations for the turbulent kinetic energy (k); one equation for

the large scale eddies and one for the small scale eddies. Such a multi-time-scale (MTS) model for application to transition flows has been implemented by Crawford (1992). This model is an evolution of two-scale k-ε models developed by Hanjalic, Launder, and Schiestel (1980) and Kim (1990). A preliminary result (fig. 21) shows promise for this MTS model's ability to simulate the transition region for turbulence levels greater than 2 percent.

Schmidt and Patankar (1988) attributed the underprediction of the transition length to the production term of the turbulent kinetic energy equation. They modified the production term to make predictions consistent with experimental results. Figure 22 shows the effect of the modification as compared with the Abu-Ghannam and Shaw (1980) correlations.

Simon and Stephens (1991), following the concept of Schmidt and Patankar, utilized stability considerations for determining the location of the initial profiles in the numerical calculations, and developed a basis for utilizing intermittency in transition calculations. They followed the method of Vancoille and Dick (1988) to develop conditional averaged turbulence model equations for heat transfer. This approach is felt to be better than a global time average approach which does not take into account a transition zone which consists of turbulent spots surrounded by laminar-like fluid. The method of Simon and Stephens (1991) assumes the universal intermittency relationship of Narasimha (1957) which compares favorably with the experimental data as presented by Volino and Simon (1991). As can be seen on figure 23 a determination of intermittency requires knowledge of the transition length. This was done by Simon and Stephens by utilizing the approach of Narasimha (1985) which expresses the transition length in terms of a nondimensional spot formation rate (N). Narasimha (1985) demonstrates that N reaches a constant value at the higher turbulence levels. Figure 24 gives the value of N used by Simon and Stephens which is based on experiment. The value of N given in figure 24 may be compared to the result of an analysis by Simon (1994). The analytical value of N reported by Simon is a constant of 0.00029, in agreement with the experimental data of figure 24 and in accordance with the analysis dependent on turbulent spot characteristics. The use of N permits a determination of transition length by means of the following equation reported by Simon and Stephens (1991):

$$Re_{L_{tr}} = \frac{2.15}{\sqrt{N}} Re_{\theta_{tr}}^{3/2} \tag{1}$$

Transition calculations were made by Simon and Stephens (1991) utilizing equation (1) and the intermittency path equation of Narasimha (1957) with the TEXSTAN code of Crawford (1985). Results of calculations employing equation (1) are compared to the experimental results of Volino and Simon (1991, table 5) in figure 25. The experimental data of Kim and Simon (1991), Suder et al. (1988), Sohn and Reshotko (1991), and Kuan and Wang (1990) are for zero-pressure-gradient flow on a flat plate. The data of Blair and Anderson (1987) is for two flat plate data sets with two values of acceleration. In general, there is a good relationship with equation (1) and the experimental data with the exception of the higher acceleration data. With an increase in flow acceleration there is an apparent increase in transition length. This increase in transition length is consistent with the characteristics of turbulent spots under accelerating conditions as shown by Simon (1994). Simon using the Narasimha (1985) reported results of Wyganaski (1981), which show a low turbulent spot spreading angle of 5 degrees for a favorable pressure gradient case, calculates a value of N given in figure 25. The results of the numerical calculations utilizing the TEXSTAN code are given in figure 26 for cases computed with and without intermittency. The value of using intermittency for improvement of the transition model is clearly demonstrated. It is interesting to note, according to the calculations, that the boundary layer acts as if it were a laminar boundary layer up to a significant value of the intermittency. This is consistent with the measured velocity profiles of Sohn, O'Brien, and Reshotko (1989) which showed a laminar-like overall profile in the transition region for intermittency value up to 0.34 at 1 percent free-stream turbulence.

EXAMPLES OF COMPUTATIONAL RESULTS

Some examples of computations compared to experimental data are presented here as a means of demonstrating "the bottom line" objective of successfully predicting bypass transition heat transfer.

A DNS calculation of transition on a flat plate, for a free-stream turbulence and velocity of 2.6 percent and 100 ft/s, was performed by Rai and Moin (1991). Rai and Moin use a high-order-accurate finite-difference approach for the direct numerical simulation of transition and turbulence. Figure 27 compares the experimental results of Suder, O'Brien, and Reshotko (1988) and Sohn and Reshotko (1991) with the numerical results for two computational grid distributions. Sufficient confidence has been established with the DNS approach that the resulting numerical base is seen as valuable for the development and testing of turbulence models applicable to bypass transition.

As explained above, Schmidt and Patankar (1988) modified the production term of the turbulent kinetic energy equation. They referred to this approach by the acronym PTM or Production Term Modification. Figure 28 demonstrates the improved prediction of transition as a result of using PTM. Examples of calculations comparisons with experimental data, as reported by Schmidt and Patankar, are given in figure 29. The comparison with the data of Wang (1984) for a flat plate at 2 percent free-stream turbulence is excellent (fig. 29(a)) and is an improvement over the mixing length approach of Park and Simon (1987). The use of the PTM approach for predicting the flat plate heat transfer data of Rued (1985) for a free-stream turbulence range of 1.7 to 10.8 percent is shown in figure 29(b). A comparison with the C3X blade results of Hylton et al. (1983) is given in figure 29(c). The calculations for figure 29(c) required the modification of the near-wall length scale due to the presence of an adverse pressure gradient on the suction side of the blade. The lower curve for each run shows the effect of the length scale modification. While there is a favorable comparison of the computations with experiment, the accuracy of the prediction in the fully turbulent region diminished as the blade Reynolds number increased.

The use of the intermittency computational approach of Simon and Stephens (1991) has promise for prediction of transitional flows. A comparison with the experimental data of Blair and Werle (1980) is given in figure 30. There is generally good agreement. Figure 30 contrasts the definition of transition onset based on intermittency and the minimum in heat transfer.

At the University of Texas at Austin, a number of turbulence models have been tested for their ability to simulate bypass transition. Examples of results of comparisons with the flat plate experimental heat transfer data of Sohn and Reshotko (1991) and the benchmark skin friction data set of the European ERCOFTAC conference, coordinated by Savill (1991), are given in figures 31 and 32. At a free-stream turbulence level of 3 percent, the experimental data of Sohn and Reshotko are best described by the Launder-Sharma (LS) and Texas (TXM) models (Crawford, 1993). There is some confirmation of this in the skin friction coefficient comparison of figure 32 (Crawford, 1992). The Nagano-Tagawa (NT) model also shows some promise. A more critical test of turbulence models for the prediction of the heat transfer on turbine blades was made by Sieger, Schulz, Crawford, and Wittig (1992). An example of their results is given in figure 33. Figure 33 shows that for a free-stream turbulence of 8.3 percent, the heat transfer experimental data of the pressure side of the Hylton et al. (1983) blade is reproduced well by all the models tested. The lowest heat transfer is given by the Launder-Sharma model. The pressure side has a transitional like behavior over the entire surface. For the prediction of transition on the suction side of the blade, figure 33 indicates that improvements are needed in the turbulence models. With the exception of the Launder-Sharma model, all the models give an early transition at the high free-stream turbulence intensity.

The potential of the Launder-Sharma model to simulate transition was further confirmed by the work of Wu and Reshotko (1991) as shown in figure 34. The work of Yang (1991) suggests an improvement over the

Launder-Sharma model by the use of a new low-Reynolds-number turbulence model (Yang and Shih, 1992) and an intermittency weighing factor. The intermittency weighing factor used by Yang is related to an intermittency factor defined by the variation of the boundary layer shape factor through the transition region. The intermittency weighing factor is used to modify the calculated eddy viscosity in the transition region. The result is an improvement over the Launder-Sharma model, as shown in figure 35. In addition, Yang and Shih point out that a drawback of the LS model is its inability to perform as well as other models for fully-developed turbulent boundary layers.

As indicated above a possible improvement to the k-ε turbulence model is the Multi-Time-Scale (MTS) model. A comparison of this model, developed at the University of Texas under the supervision of Crawford (1993), with data set T3A is given in figure 36. Comparing figure 36 with figure 32 shows the potential of the MTS model.

CONCLUDING REMARKS

This progress report of a NASA research program for the prediction of transition heat transfer on turbine vane and blades has demonstrated the value of a team approach with an appropriate experimental and analytical skill mix, as recommended by Simoneau (1986) for complex problems. The synergism resulting from a team of experimentalists, analysts, and modelers is required for the complex research area of bypass transition which requires an in-depth investigation of the effects of free-stream turbulence, convex and concave curvature, favorable and adverse pressure gradient, wakes, and the effect of the stagnation region of a blade or vane. The team effort has led to the following accomplishments:

1. An extensive experimental data base of bypass transition on flat and curved surfaces has been obtained. The detailed nature of the data base permits an investigation of the physics involved and is an aid in the development and testing of turbulence models. Conditional analyses have demonstrated that the transition region is not a simple combination of Blasius and turbulent boundary layer profiles.

2. Effects of convex and concave curvature on transition have been documented. When low free-stream turbulence level cases are compared to the results of transition on a flat surface at equivalent turbulence levels, convex curvature will delay transition onset and concave curvature will shift transition onset upstream.

3. The effect of acceleration and free-stream turbulence for a transitioning boundary layer on a concave surface is being documented. The existence of stable vortices on a concave-curved wall were found at low free-stream turbulence intensities. No coherent vortices were found at the higher free-stream turbulence intensities.

4. Two-equation turbulence models appear to capture the growth of nonlinear disturbances in bypass transition and are capable, with appropriate damping functions and constants, of predicting transition onset. These models under-predict the transition length, however, unless (1) provision is made for the intermittent nature of the transition region, (2) a modification is made for the rate of turbulence production, or (3) a multiscale model is used to account for the incomplete nature of the turbulent energy cascade in the transition region. The need for a multiscale turbulence model has been confirmed by an analysis of the experimental data. A number of low-Reynolds number turbulence models have been assessed. The Launder-Sharma, the Texas and the Yang and Shih turbulence models were found to be effective for simulating bypass transition, although improvements in these models, and all the models tested, are required.

5. Direct Numerical Simulation (DNS) has proven to be a very powerful tool for (1) understanding the physics, (2) supporting and guiding the experimental results, and (3) forming a data base for the development

and testing of transition turbulence models. Results obtained with DNS compare very well to the experimental results.

6. Transition onset was well predicted by the Parabolized Stability Equations (PSE) method. This method has the potential of predicting most of the transition region with reasonable computational requirements.

The following recommendations for future work are based on the annual NASA-Lewis bypass transition workshops:

1. There are indications that spectra and length scales of free-stream turbulence play a role in the transition process. These factors should be investigated. The use of laboratory and DNS numerical experiments would be useful here.

2. Future experiments should better document the free-stream turbulence by providing the three components of velocity fluctuations, the frequency range over which the free-stream turbulence was measured, and other turbulence characteristics.

3. DNS calculations with heat transfer and for a turbine blade geometry should be made. DNS calculations should be applied to the study of boundary layer receptivity to free-stream disturbances and their effect on stability. A DNS data base should be established.

4. A study on the effect of the leading edge geometry on transition, with use of experiments and DNS, should be initiated.

5. There needs to be an increase in the range of the turbulence levels studied (6 to 20 percent), which are more in line with the levels present in a combustor.

6. The community should continue to develop the use of the PSE approach as a design tool.

7. There should be an increase in the experimental Mach number to better simulate actual engine conditions and permit increased computational efficiency of the numerical codes for the purpose of comparison of numerical and experimental results. Also there should be transonic measurements with shock-boundary layer interactions to investigate this effect.

8. The community should continue the development of turbulence models which are more faithful to the physics of transition, as determined by DNS and experimental efforts. Development of multiscale, two-equation turbulence models should continue.

9. The application of Large Eddy Simulation (LES) to bypass transition should be investigated.

10. Spectral measurements within the late transitional boundary layer should be made to determine which wavelengths are amplified and the relationships of these wavelengths to the most unstable wavelengths computed from linear stability theory.

Some of the above recommendations are already being carried out by members of the NASA bypass transition team. In addition, the work on the effect of unsteady flows (e.g., wakes) has been initiated. Significant progress has been made in the understanding and improving predictive capability of heat transfer on turbine vanes and blades. This progress has, to date, been mostly limited to flat and curved surfaces with little work on actual vanes or blades. A key recommendation of the transition team is to increase the effort being made on

vanes and/or blades. This recommendation is consistent with the original plan of 1986 of increasing geometry and flow complexities. We believe we are on schedule.

REFERENCES

Abu-Ghannam, B.J.; and Shaw, R.: Natural Transition of Boundary Layers—The Effects of Turbulence, Pressure Gradient, and Flow History. J. Mech. Eng. Sci., vol. 22, no. 5, 1980, pp. 213–228

Ameri, A.A.; and Arnone, A.: Navier-Stokes Turbine Heat Transfer Predictions Using Two-Equation Turbulence Closures. NASA TM–105817, 1992.

Ashpis, D.E.; and Spalart, P.R.: Direct Numerical Simulation of Wall-Generated Disturbances in a Boundary Layer. Bull. Am. Phys. Soc., vol. 37, 1992, pp. 1813–1817.

Ashpis, D.E.; and Spalart, P.R.: Work in process, 1993.

Blair, M.F.: Influence of Free-Stream Turbulence on Turbulent Boundary Layer Heat Transfer and Mean Profile Development, Pt. I. Experimental Data. J. Heat Transfer, vol. 105, Feb. 1983, pp. 33–40.

Blair, M.F.; and Anderson, O.L.: Study of the Structure of Turbulence in Accelerating Transitional Boundary Layers. VTRC Report R87–956900–1, United Technologies Research Center, East Hartford, CT, 1987.

Blair, M.F.; and Werle, M.J.: The Influence of Free-Stream Turbulence on the Zero Pressure Gradient Fully Turbulent Boundary Layer. UTRC Report R80–914388–12, United Technologies Research Center, East Hartford, CT, 1980.

Chien, K.-Y.: Predictions of Channel and Boundary-Layer Flows with a Low-Reynolds-Number Turbulence Model. AIAA J., vol. 20, no. 1, 1982, pp. 33–38.

Coakley, T.J.: Turbulence Modeling Methods for the Compressible Navier-Stokes Equations. AIAA Paper 83–1693, 1983.

Crawford, M.E.: TEXSTAN Program. University of Texas at Austin, 1985.

Crawford, M.E.; and Simon, F.F.: Turbulence Modeling for the Simulation of Transition in Wall Shear Flows. Progress Report, NASA Grant NAG3–864, 1991.

Crawford, M.E.; and Simon, F.F.: Progress Report, NASA Grant NAG3–864, 1992.

Crawford, M.E.; and Simon, F.F.: Progress Report, NASA Grant NAG3–864, 1993.

Dhawan, S.; and Narasimha, R.: Some Properties of Boundary Layer Flow During Transition From Laminar to Turbulent Motion. J. Fluid Mech., vol. 3, 1958, pp. 418–436.

Dunham, J.: Predictions of Boundary Layer Transition on Turbomachinery Blades. Boundary Layer Effects in Turbomachines, AGARD AG–164, J. Surugue, ed., 1972.

Graham, R.W.: Fundamental Mechanisms that Influence the Estimate of Heat Transfer to Gas Turbine Blades. NASA TM–79128, 1979.

Graham, R.W.: Transition In Turbines. NASA CP–2386, 1985.

Hanjalic, K.; Launder, B.E.; and Schiestel, R.: Multiple-Time-Scale Concepts in Turbulent Transport Modelling. Vol. 2: Turbulent Shear Flows. Springer-Verlag, New York, 1980.

Hylton, L.D., et al.: Analytical and Experimental Evaluation of the Heat Transfer Distribution Over the Surfaces of Turbine Vanes. NASA CR–168015, 1983.

Kuan, C.L.; and Wang, T.: Investigation of Intermittent Behavior of Transitional Boundary Layer Using a Conditional Averaging Technique. Exp. Thermal Fluid Sci., vol 103, 1990, pp. 157–173.

Kim, S.–W.: Numerical Investigation of Separated Transonic Turbulent Flows With a Multiple-Time-Scale Turbulence Model. NASA TM–102499, 1990.

Kim, J.; and Simon, T.W.: Free-Stream Turbulence and Concave Curvature Effects on Heated, Transitional Boundary Layers. NASA CR–187150, 1991.

Launder, B.E.; and Sharma, B.I.: Application of the Energy-Dissipation Model of Turbulence to the Calculation of Flow Near a Spinning Disc. Lett. Heat Mass Transfer, vol 1, 1974, pp. 131–138.

Morkovin, M.V.: Instability Transition to Turbulence and Predictability. AGARD AG–236, 1978.

Myong, H.K.; and Kasagi, N.: A New Approach to the Improvement of k-ε Turbulence Model for Wall-Bounded Shear Flows, JSME Int. J., Ser. II, vol 33, 1990, pp. 63–72.

Narasimha, R.: On the Distribution of Intermittency in the Transition Region of a Boundary Layer, J. Aeronaut. Sci., vol. 24, no. 9, 1957, pp 711–712.

Narasimha, R.: The Laminar-Turbulent Transition Zone in the Boundary Layer. Prog. Aerosp. Sci., vol. 22, 1985, pp 29–80.

Park, W.; and Simon, T.: Prediction of Convex-Curved Transitional Boundary Layer Heat Transfer Behavior Using MLH Models. Presented at the Joint ASME/JSME Thermal Engineering Conference, Honolulu, HI, March 22–27, 1987.

Rai, M.M.; and Moin, P.: Direct Numerical Simulation of Transition and Turbulence in a Spatially Evolving Boundary Layer. AIAA Paper 91–1607, 1991.

Rued, K.: Transitional Boundary Layers Under the Influence Of High Free Stream Turbulence, Intensive wall Cooling and High Pressure Gradients in Hot Gas Circulation. NASA TM–88524, 1985 (Translation of thesis submitted at the University of Karsruhe, West Germany).

Savill, A.M.: Turbulence Model Predictions for Transition under Free-Stream Turbulence. Presented at the RAeS Transition and Boundary Layer Conference, Cambridge, England, 1991.

Schmidt, R.C.; and Patankar, S.V.: Two-Equation Low-Reynolds-Number Turbulence Modeling of Transitional Boundary Layer Flows Characteristic of Gas Turbine Blades. NASA CR–4145, 1988.

Schubauer, G.B.; and Skramstad, H.K.: Laminar-Boundary Layer Oscillations and Transition on a Flat Plate. NACA Report 909, 1948.

Seyb, N.J.: The Role of Boundary Layers in Axial Flow Turbomachines and Prediction of Their Effects. Boundary Layer Effects in Turbomachines, AGARD AG–164, J. Surugue, ed., 1972, pp. 261–274.

Shih, T.H.: An Improved κ-ε Model for Near-Wall Turbulence and Comparison With Direct Simulation. NASA TM–103221, 1990.

Sieger, K., et al.: Comparative Study of Low-Reynolds Number k-ε Turbulence Models for Predicting Heat Transfer along Turbine Blades with Transition. Presented at: International Symposium on Heat Transfer in Turbomachinery, Athens, Greece, 1992.

Simon, F.: The Use of Transition Region Characteristics to Improve the Numerical Simulation of Heat Transfer in Bypass Transitional Flows. To be published in 1994.

Simon, F.F.; and Stephens, C.A.: Modeling of the Heat Transfer in Bypass Transitional Boundary-Layer Flows. NASA TP–3170, 1991.

Simoneau, R.J.: Opportunities and Challenges in Heat Transfer—From the Perspective of the Government Laboratory. Heat Transfer Eng., vol. 7, nos. 3–4, 1986, pp. 76–81.

Simoneau, R.J.; and Simon, F.F.: Progress Towards Understanding and Predicting Heat Transfer in the Turbine Gas Path, Int. J. Heat Fluid Flow, vol. 14, no. 2, 1993, pp. 106–128. (Also, NASA TM–105674, 1993.)

Sohn, K.H.; O'Brien J.E.; and Reshotko, E.: Some Characteristics of Bypass Transition in a Heated Boundary Layer. NASA TM–102126, 1989.

Sohn, K.H.; and Reshotko, E.: Experimental Study of Boundary Layer Transition With Elevated Freestream Turbulence on a Heated Flat Plate. NASA CR–187068, 1991.

Sohn, K.H.; Reshotko, E.; and Zaman, K.B.M.Q.: Experimental Study of Boundary Layer Transition on a Heated Flat Plate. NASA TM–103779, 1991.

Sohn, K.H.; Zaman, K.B.M.Q.; and Reshotko, E.: Turbulent Heat Flux Measurements in a Transitional Boundary Layer. NASA TM–105623, 1992.

Stephens, C.A.; and Crawford, M.E.: An Investigation into the Numerical Prediction of Boundary Layer Transition Using the K.Y. Chien Turbulence Model. NASA CR–185252, 1990.

Stepka, F.S.: Analysis of Uncertainties in Turbine Metal Temperature Predictions. NASA TP–1593, 1980.

Stuckert, G.K.; and Herbert, T.: Transition and Heat Transfer in Gas Turbines. Final Report. NASA Contract NAS3–26602, 1992.

Suder, K.L.; O'Brien, J.E.; and Reshotko, E.: Experimental Study of Bypass Transition in a Boundary Layer. NASA TM–100913, 1988.

Van Driest, E.R.; and Blumer, C.B.: Boundary Layer Transition: Free-stream Turbulence and Pressure Gradient Effects. AIAA J., vol. 1, no. 6, 1963, pp. 1303–1306.

Vancoillie, G.; and Dick, E.: A Turbulence Model for the Numerical Simulation of the Transition Zone in a Boundary Layer. Int, J. Eng. Fluid Mech., vol. 1, no. 1, 1988, pp. 28–49.

Volino, R.J.; and Simon, T.W.: Bypass Transition in Boundary Layers Including Curvature and Favorable Pressure Gradient Effects. NASA CR–187187, 1991.

Volino, R.J.; and Simon, T.W.: An Application of Octant Analysis to Turbulent and Transitional Flow Data. Presented at the International Symposium on Gas Turbines in Cogeneration, IGTI ASME TURBO EXPO, Cincinnati, OH, May 24–27, 1993.

Volino, R.J.; and Simon, T.W.: Measurements in a Transitional Boundary Layer on a Concave Surface. Progress Report, NASA Grant NAG3–1249, 1993.

Wang, T.: An Experimental Investigation of Curvature and Free-free-stream Turbulence Effects on Heat Transfer and Fluid Mechanics in Transitional Boundary Layers. PhD Thesis, Department of Mechanical Engineers, University of Minnesota, MN, 1984.

Wygnanski, I.: The Effects of Reynolds Number and Pressure Gradient on the Transitional Spot in a Laminar Boundary Layer. The Role of Coherent Structures in Modelling Turbulence and Mixing; Proceedings of the International Conference, T. Timencz, ed., Springer-Verlag, Berlin, 1981, pp. 304–332.

Wu, S.T.; and Reshotko, E.: Environmental Effects on Transition and the Control of Transition. Cooperative Agreement under contract NCC3–124, 1991.

Yang, Z.: Modeling of Near Wall Turbulence and Modeling of Bypass Transition. Center for Modeling of Turbulence and Transition (CMOTT): Research Briefs, W.W. Liou, ed., NASA TM–105834, pp. 83–94,

Yang, Z.; and Shih, T.H.: A k-ε Modeling of Near Wall Turbulence. NASA TM–105238, 1991.

Yang, Z.; and Shih, T.H.: A k-ε Calculation of Transitional Boundary Layers. NASA TM–105604, 1992.

TABLE I.–SUMMARY OF TRANSITION ONSET (SUDER, O'BRIEN, AND RESHOTKO, 1988)

Grid	Nominal free-stream turbulence, percent	Method	Onset, in., χ
0	0.3	Mean profiles	40.3
		Shape factor	40.3
		Skin friction	38.0
		RMS profiles	40.0
		Intermittency	38.3
0.5	0.7	Mean profiles	9.3
		Shape factor	9.3
		Skin friction	9.3
		RMS profiles	8-9
		Intermittency	6.2
1	1	Mean profiles	9-10
		Shape factor	11
		Skin friction	9
		RMS profiles	9
		Intermittency	4.2
2	2	Mean profiles	<5
		Shape factor	<5
		Skin friction	<5
		RMS profiles	<5
		Intermittency	<4

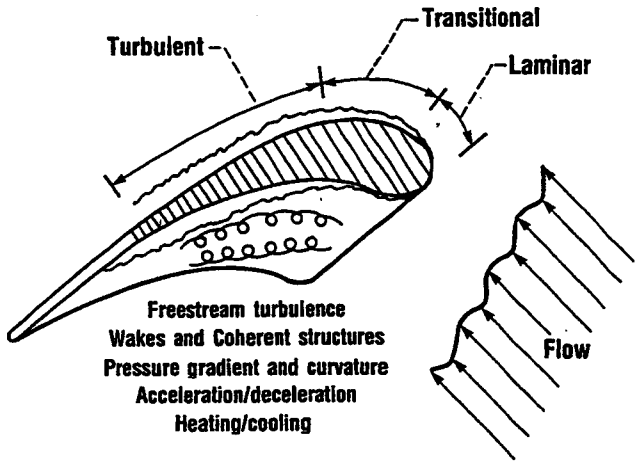

Figure 1.—Working environment of turbine vanes/blades.

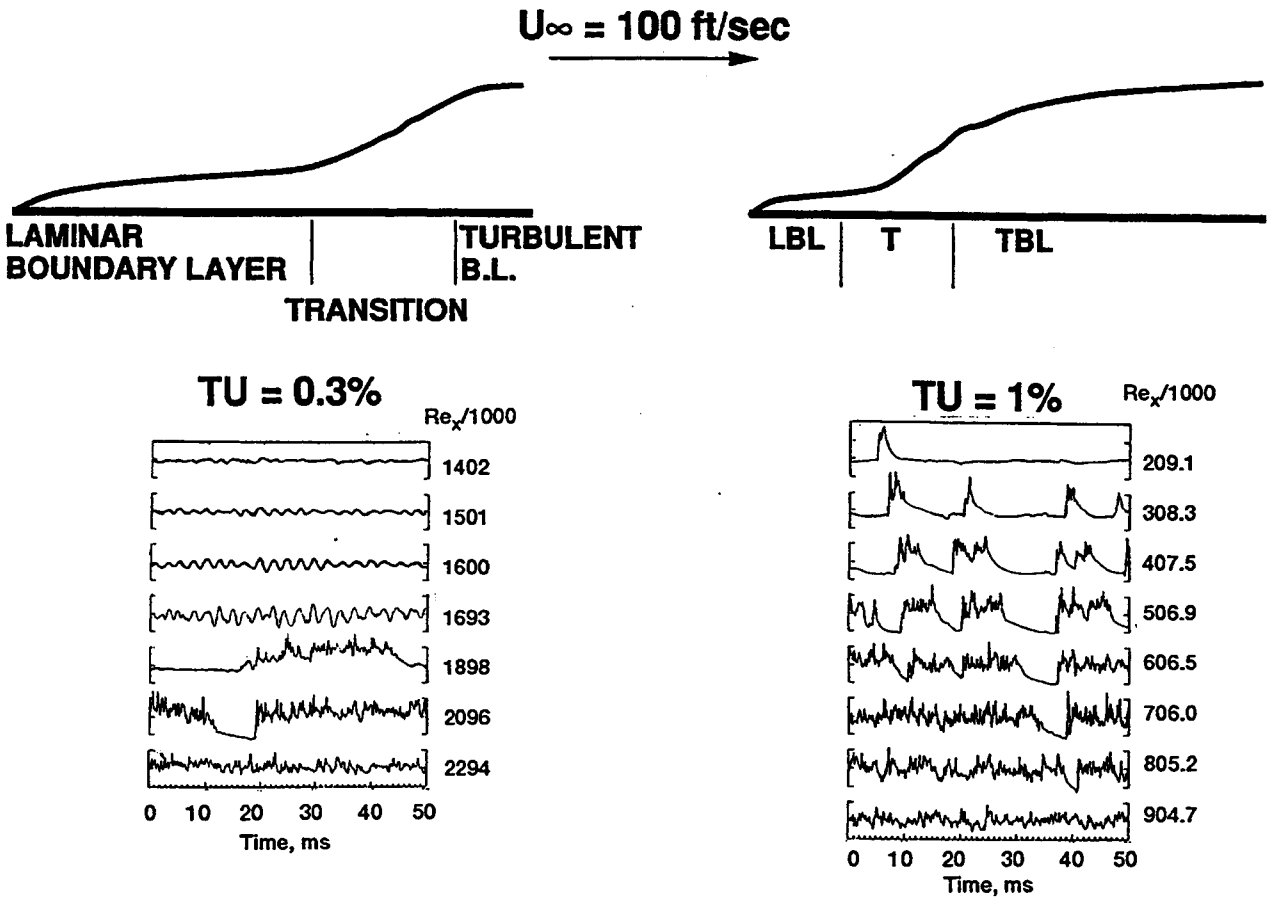

Figure 2.—Linear versus bypass path to transition. From Suder, O'Brien, Reshotko (1988).

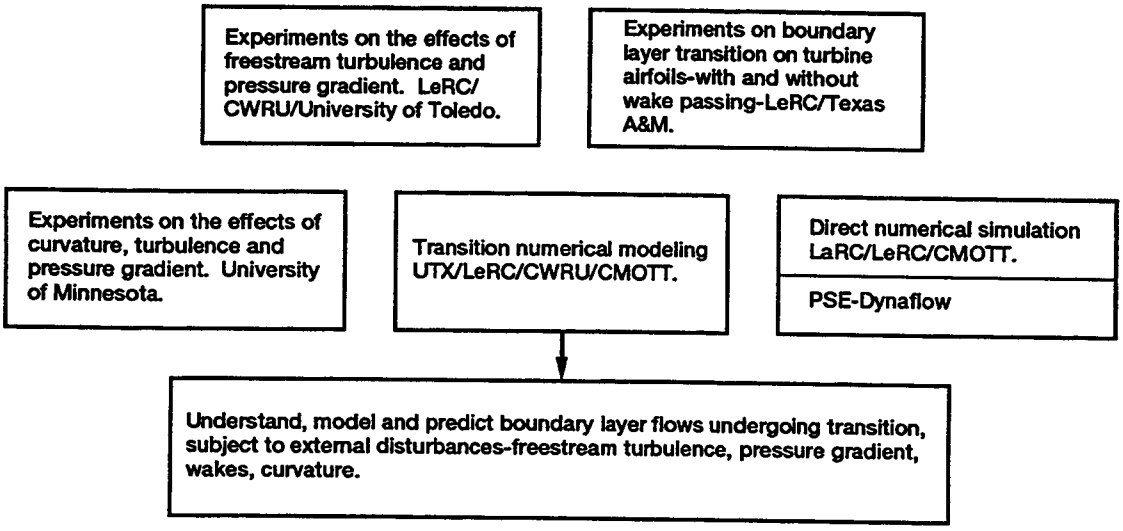

Figure 3.—By-pass transition research program.

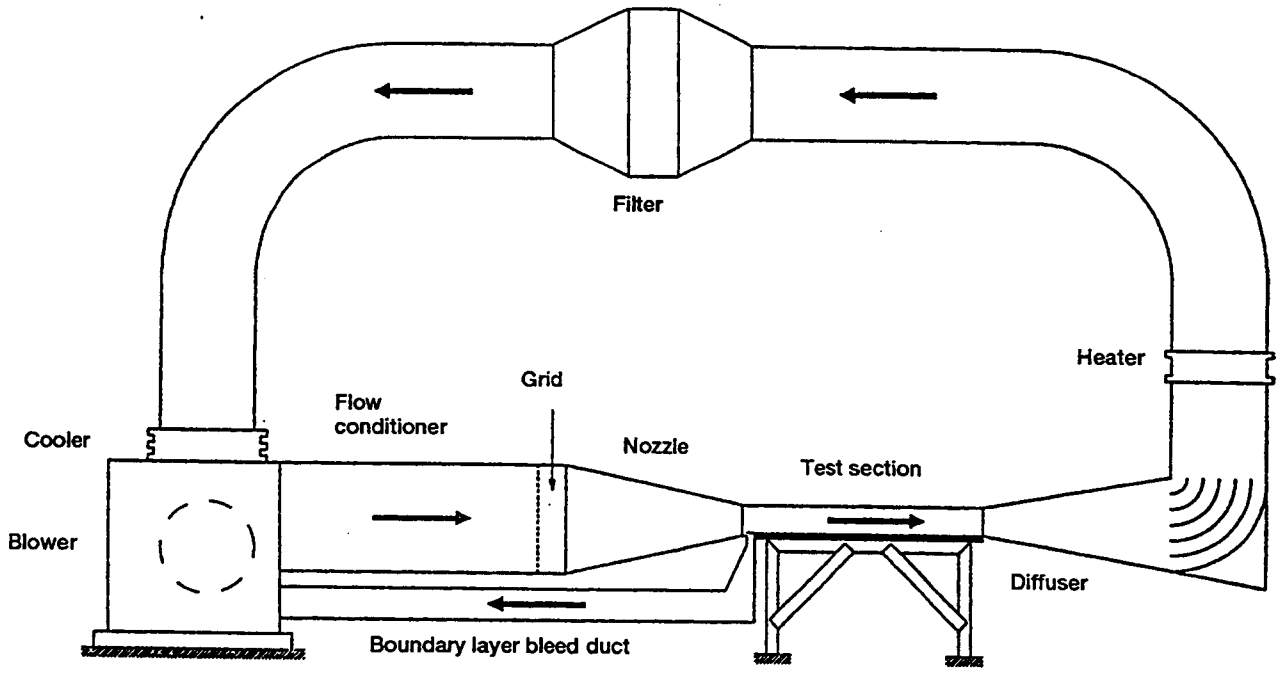

Figure 4.—Schematic diagram of the NASA/Lewis wind tunnel.

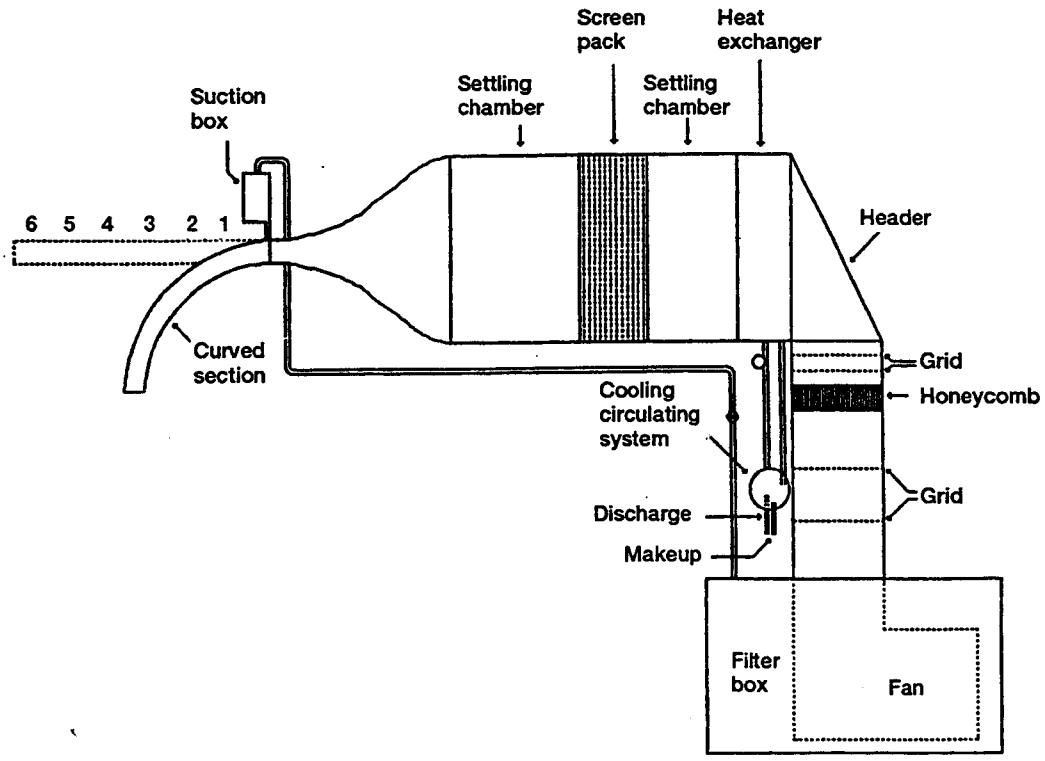

Figure 5.—Schematic diagram of the University of Minnesota test facility.

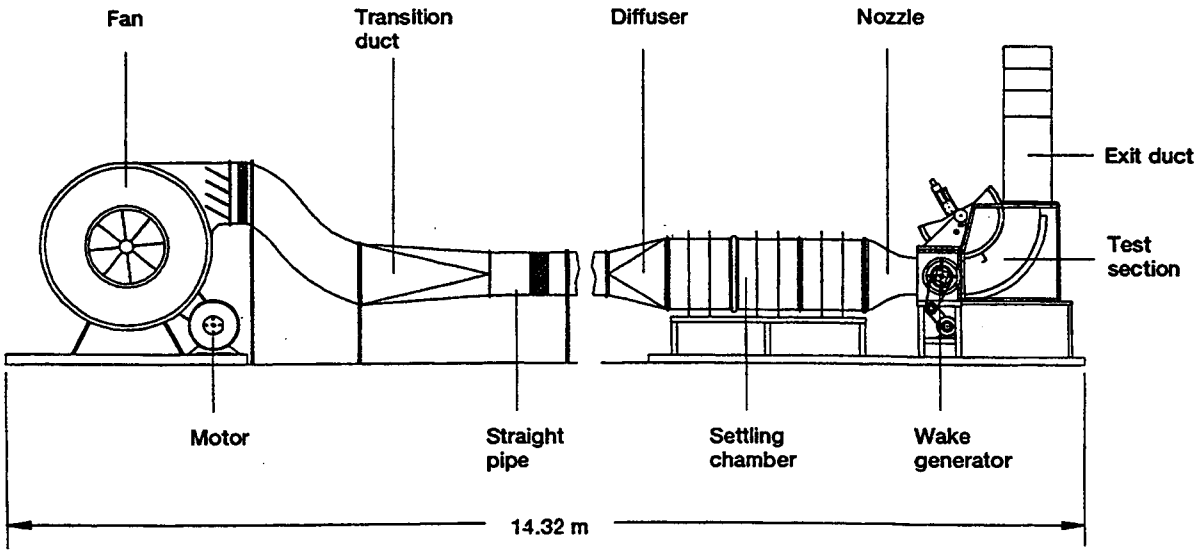

(a) Texas A&M "squirrel/cage" test facility.

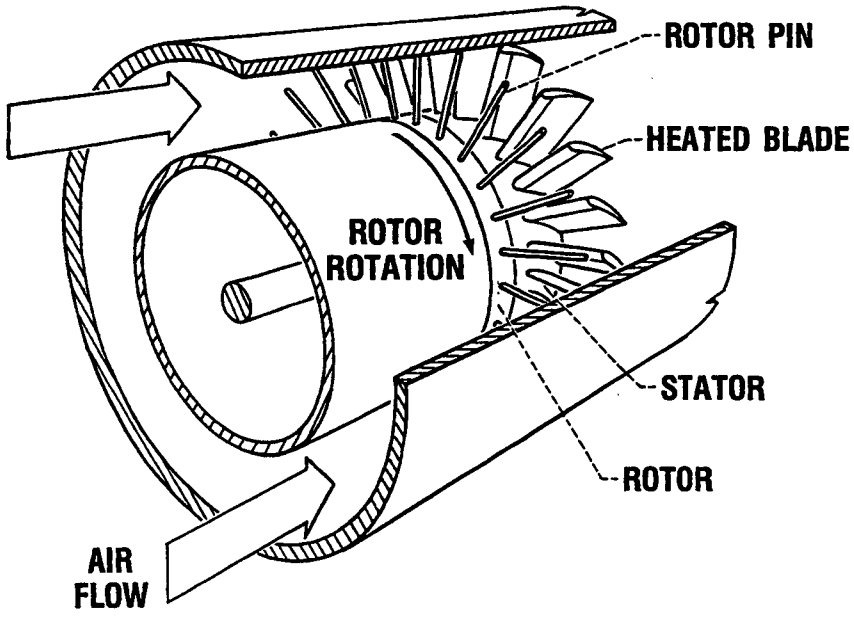

(b) Rotor-wake heat transfer rig (NASA/Lewis).

Figure 6.—Rotor-wake test facilities.

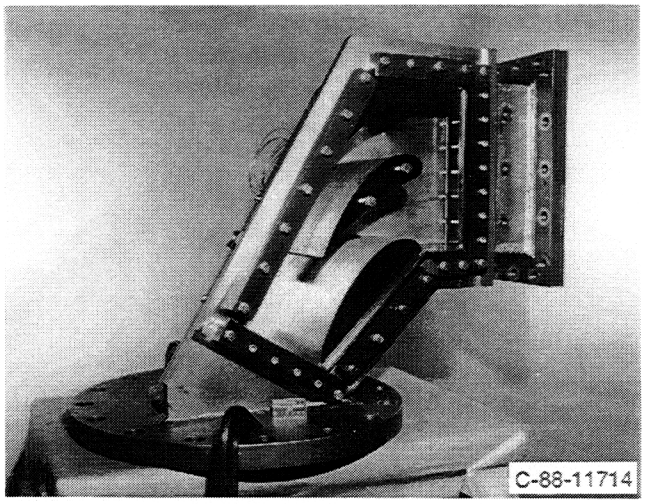

Figure 7.—Large blade test section (NASA/Lewis).

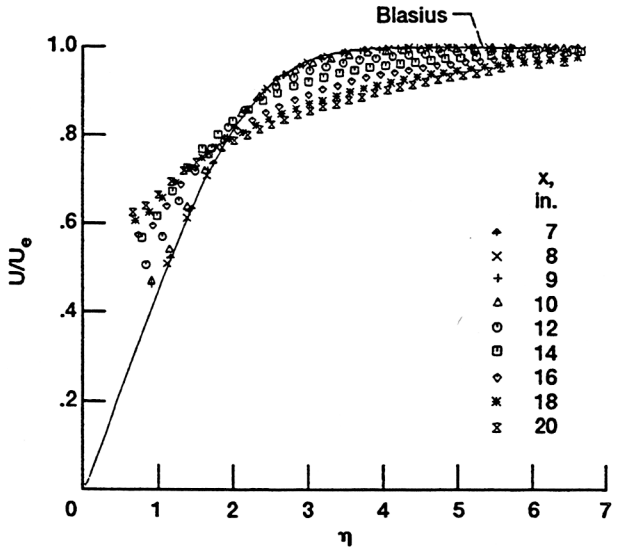

(a) Grid 1: plots of η versus $f'(\eta)$ overlaid.

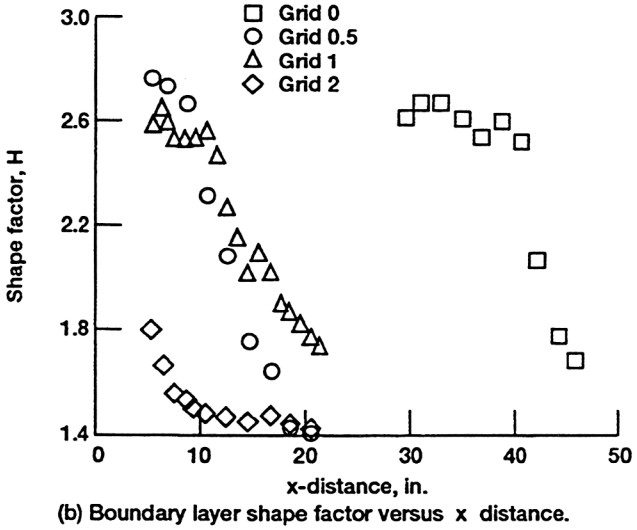

(b) Boundary layer shape factor versus x distance.

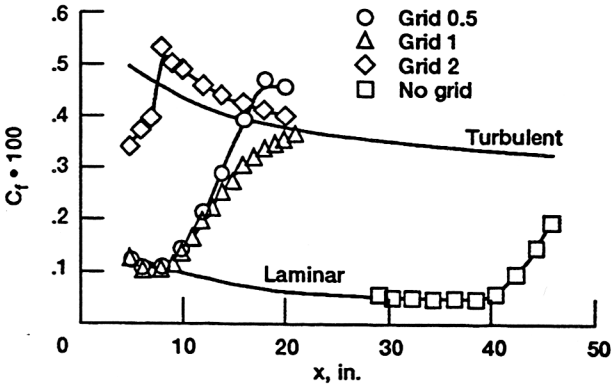

(c) Skin friction coefficient versus x distance.

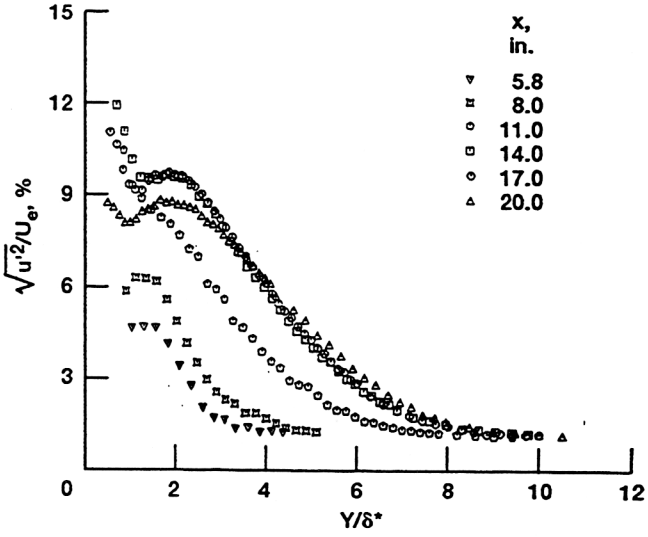

(d) Grid 1: Boundary layer profiles of the RMS of the velocity fluctuations within the boundary layer.

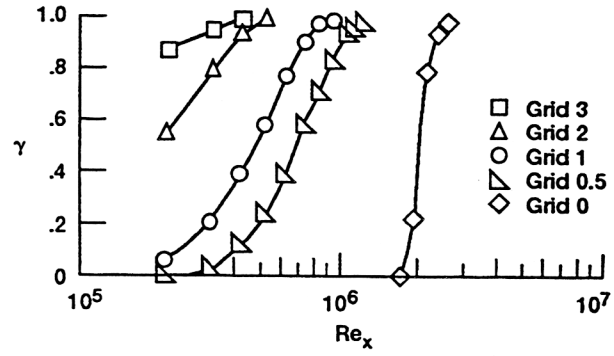

(e) Intermittency factor (γ) versus Reynolds number based on x distance.

Figure 8.—Experimental evidence of transition onset (Suder, O'Brien and Reshotko, 1988).

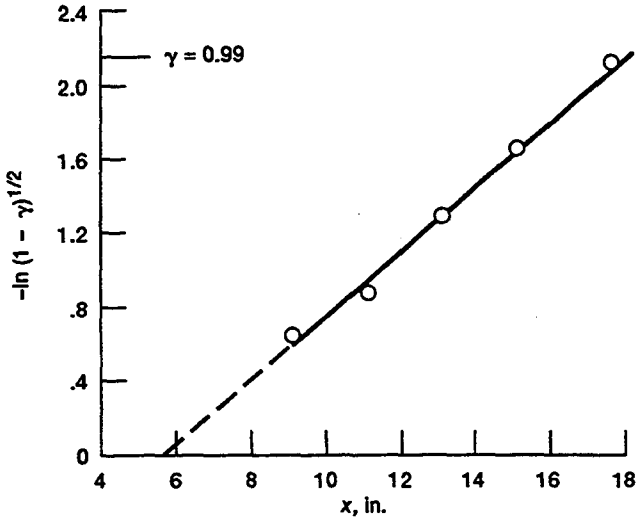

(a) Free-stream turbulence intensity, Tu_e, 1.1 percent: transition length. L_{tr} 1.03 ft; nondimensional spot formation rate, 0.53×10^{-3}; momentum thickness Reynolds number, $Re_{\theta,tr}$, 337.

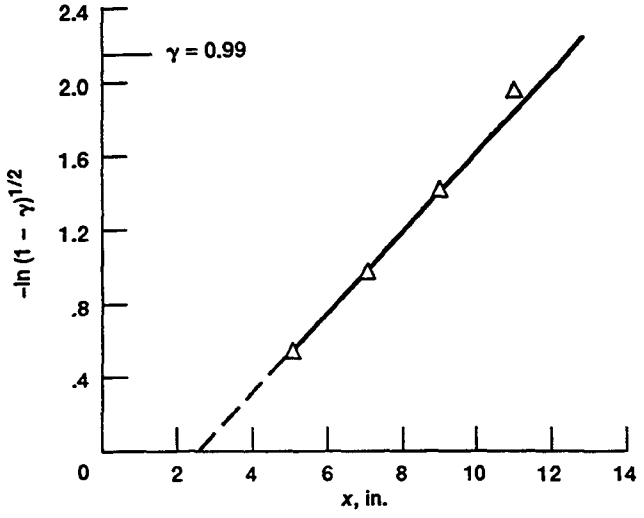

(b) Free-stream turbulence intensity. Tu_e, 2.4 percent: transition length. L_{tr} 0.81 ft; nondimensional spot formation rate, 0.26×10^{-3}; momentum thickness Reynolds number, $Re_{\theta,tr}$, 229.

Figure 9.—Method of Narasimha (1957) for transition onset and length (Simon & Stephens, 1991).

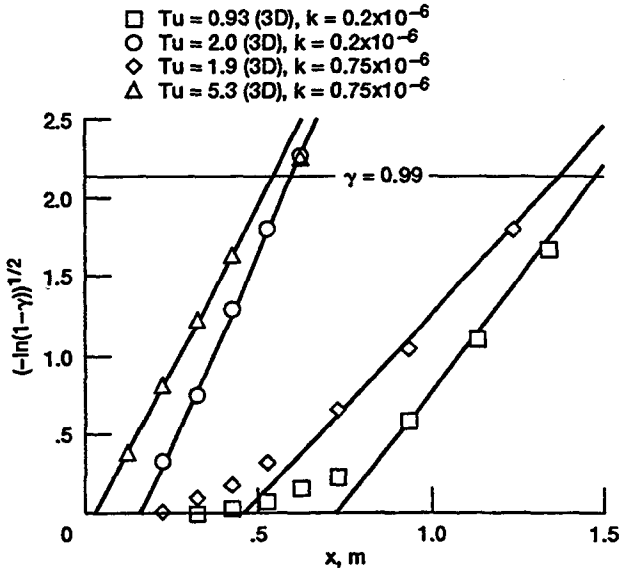

Figure 10.—Intermittency data for (data of Blair and Anderson, 1987) accelerated flow (Volino and Simon, 1991).

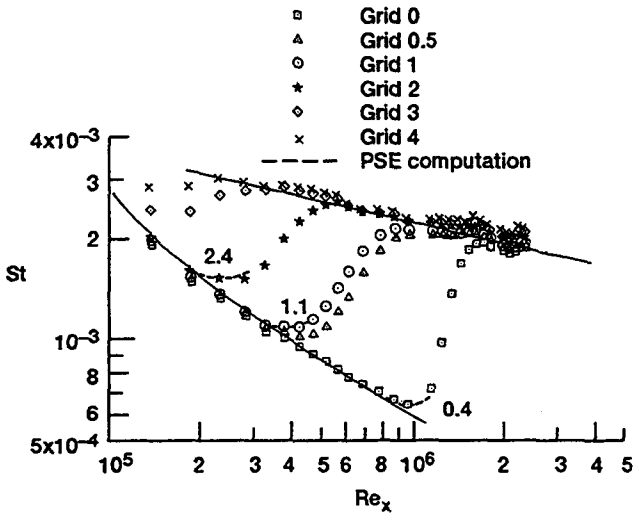

Figure 11.—Onset prediction using PSE approach (Stuckert & Herbert, 1992) Data of Sohn & Reshotko (1991).

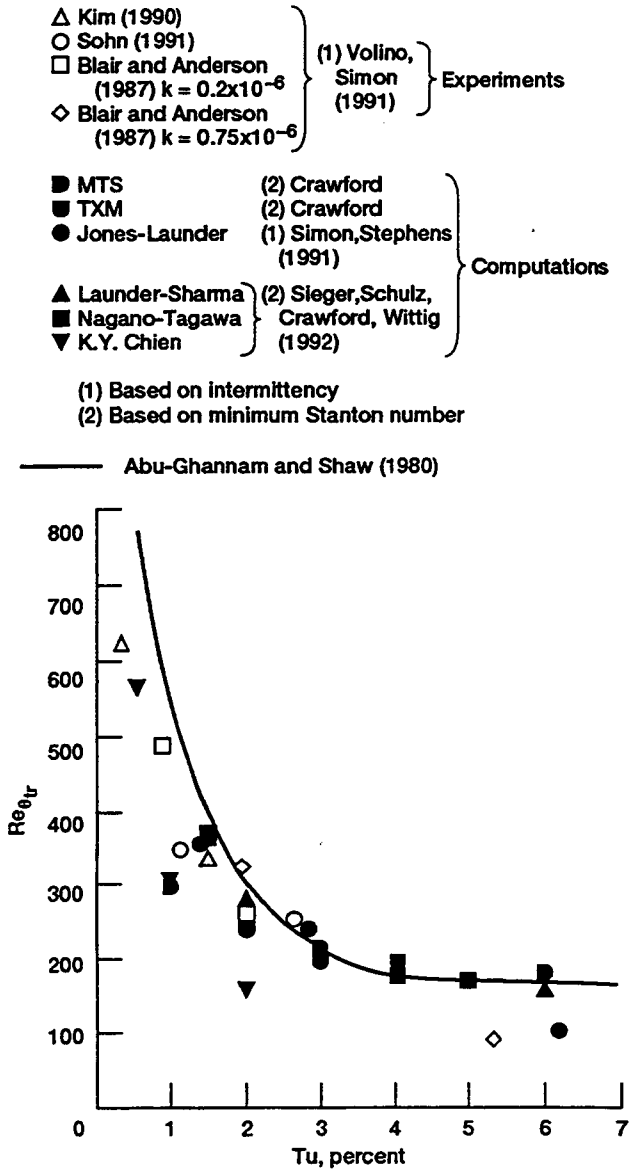

Figure 12.—Computed and experimental momentum thickness Reynolds number for transition onset.

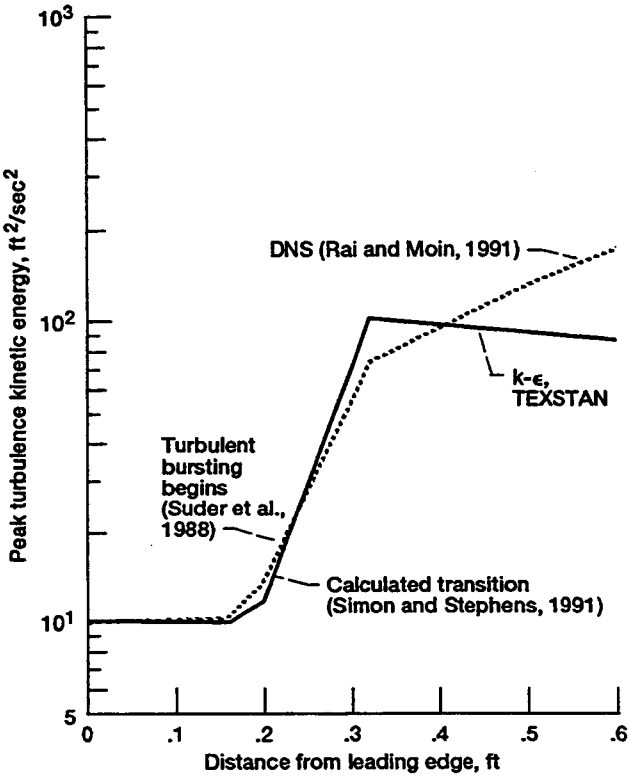

Figure 13.—Comparison of computed disturbance energy from computations based on a k-ϵ model and on direct numerical simulation (DNS) for bypass transition (Simoneau and Simon, 1993).

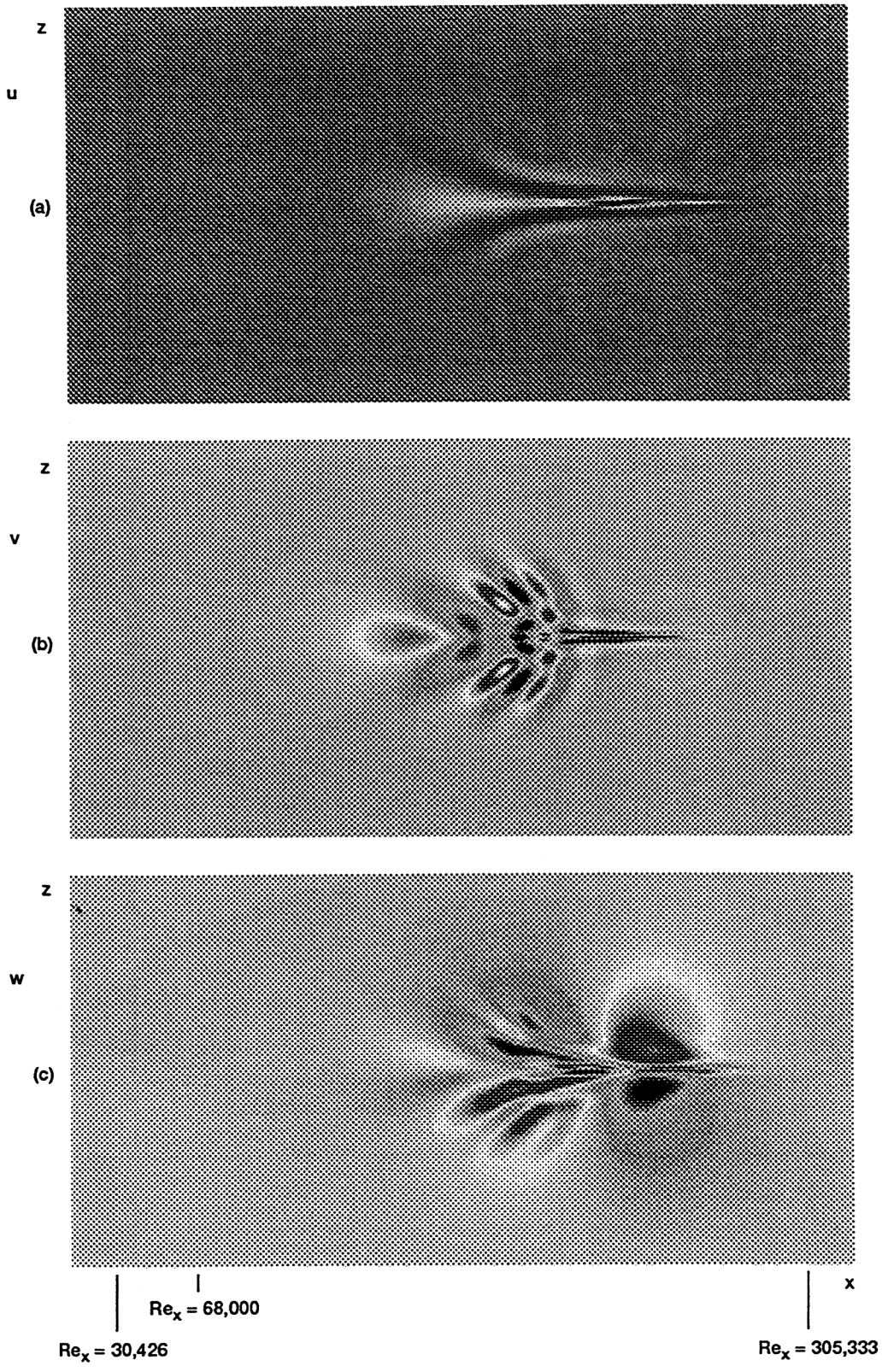

Figure 14.—Flow structure generated by a blowing pulse in Blasius boundary layer (Ashpis and Spalart, 1993) contours of velocity components are shown on a horizontal x-z plane at $y/\delta_o^* = 2.6$. The amplitude of the pulse is 0.01 U_e. The pulse is generated at $Re_{x_o} = 68{,}000$ where displacement thickness $\delta_o^* = 1.112$, $Re_{\delta_o^*} = 448.7$.

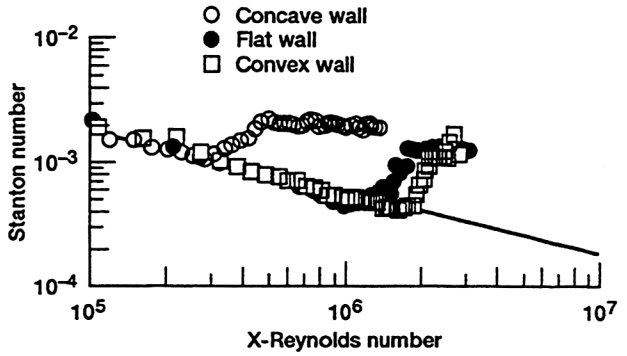

Figure 15.—Effect of streamwise curvature on bypass transition. Wall radii of curvature 90-100 CM; free-stream distribution level 0.6-0.7 percent. (Wang, 1984; Kim and Simon, 1991).

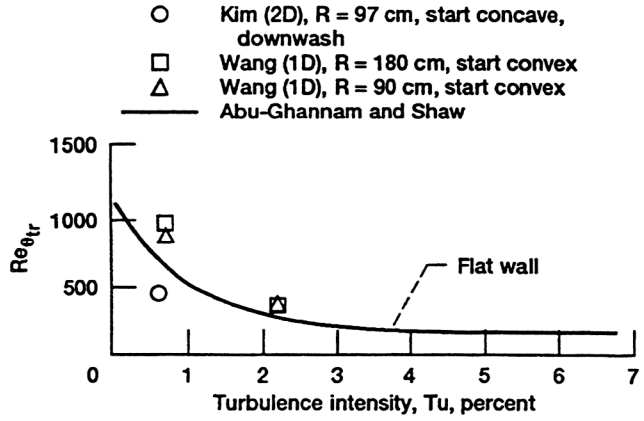

Figure 16.—Transition start based on St, curved wall cases. (Volino and Simon, 1991).

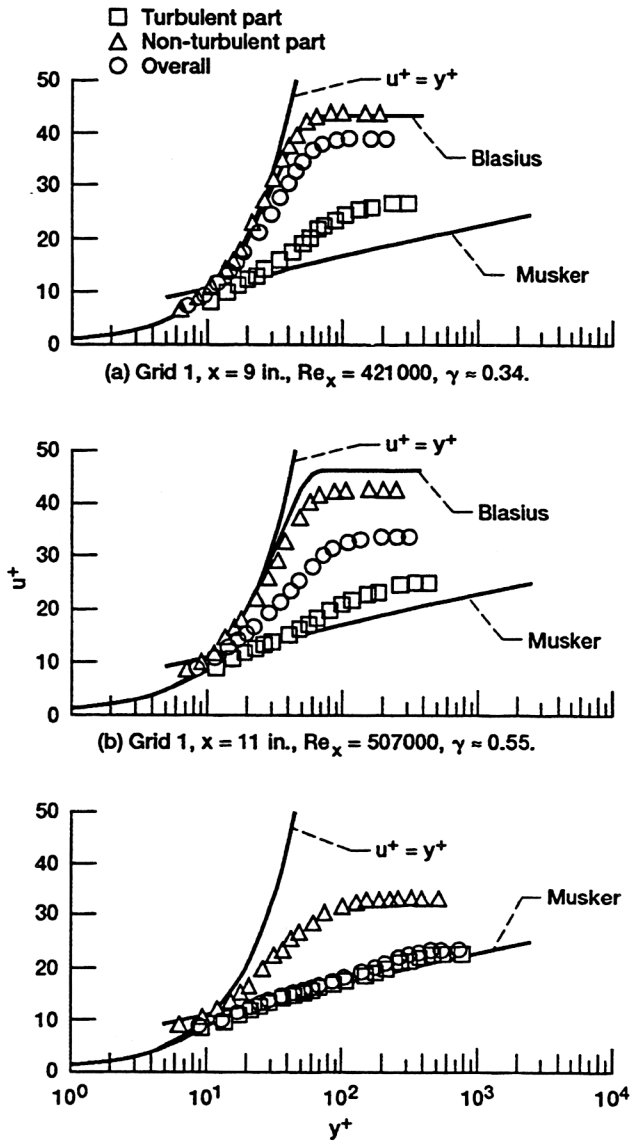

Figure 17.—Conditionally sampled mean velocity profiles in wall units. (Sohn, Reshotko and Zaman, 1991).

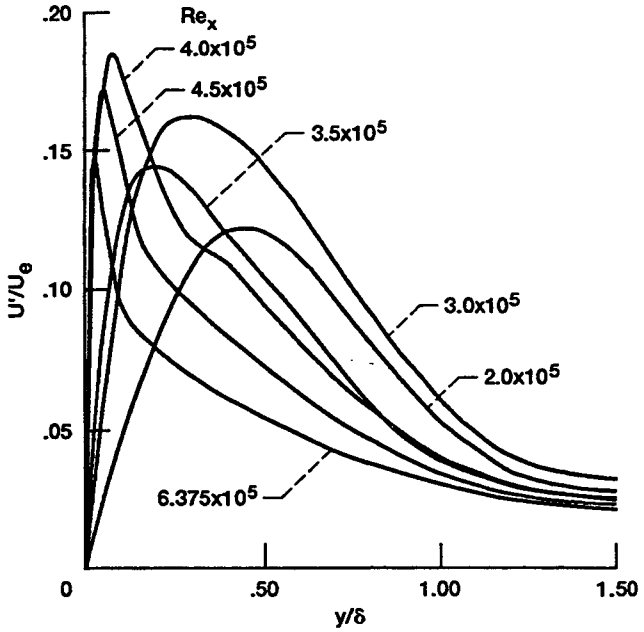

Figure 18.—DNS computed streamwise component of turbulence intensity (Rai and Moin, 1991).

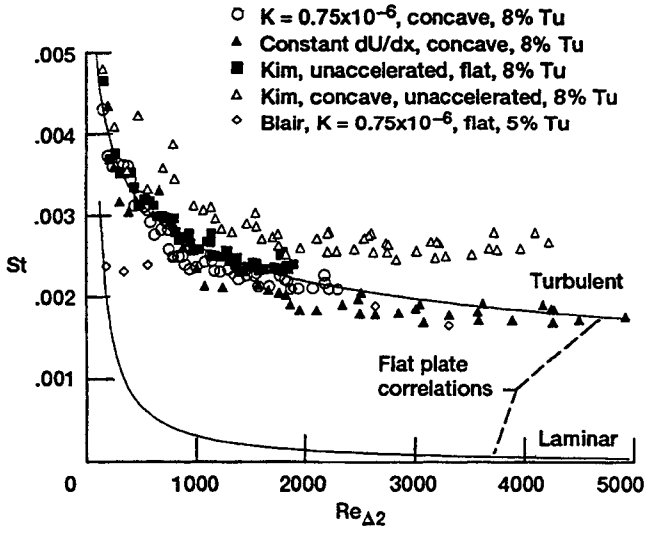

Figure 19.—Stanton numbers on concave and flat surfaces; unaccelerated and accelerated flow (Volino and Simon, 1993).

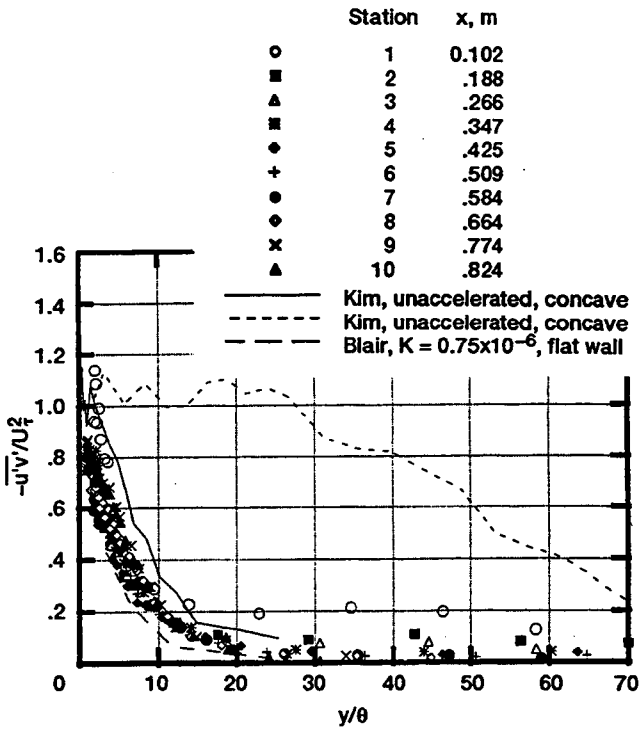

Figure 20.—Turbulent shear stress (concave surface), constant dU/dx case (Volino and Simon, 1993).

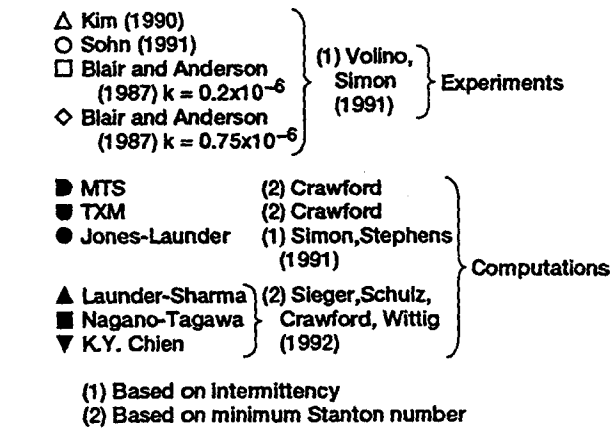

Figure 21.—Computed and experimental momentum thickness Reynolds number for transition onset.

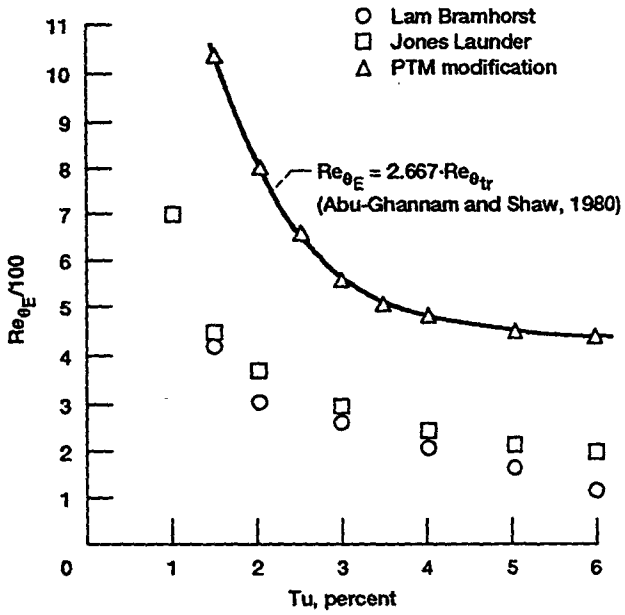

Figure 22.—Calculated momentum thickness Reynolds numbers at the end of transition using the "PTM" model (Schmidt and Patonkar, 1988).

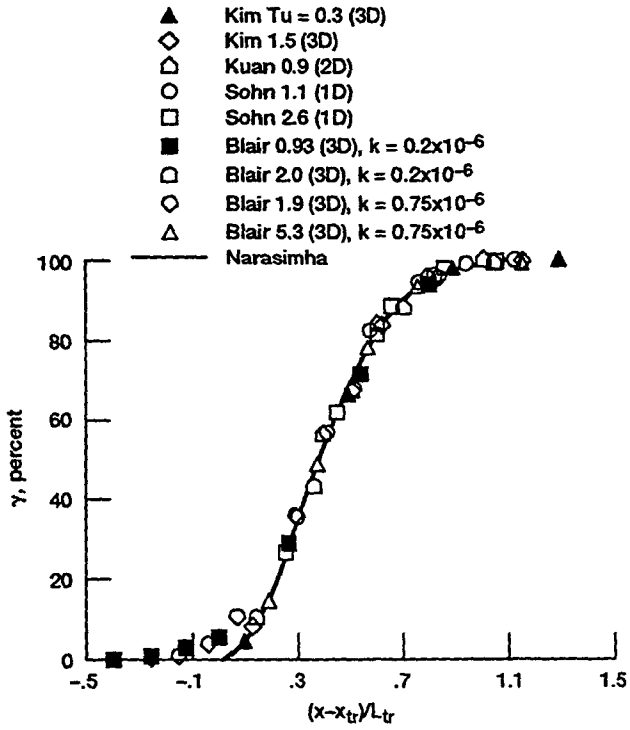

Figure 23.—Intermittency (Volino and Simon, 1991).

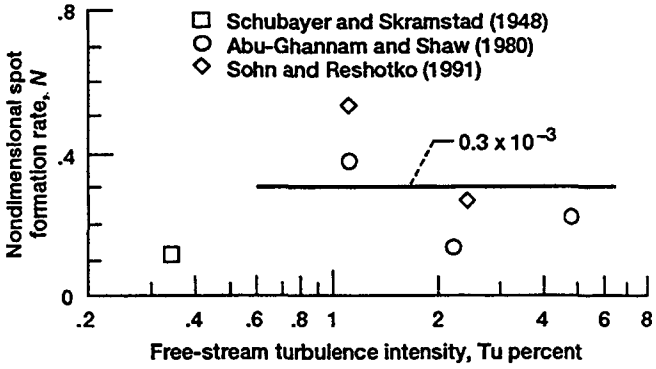

Figure 24.—Variation of nondimensional spot formation rate with free-stream turbulence (Narasimha (1985) method) (Simon and Stephens, 1991).

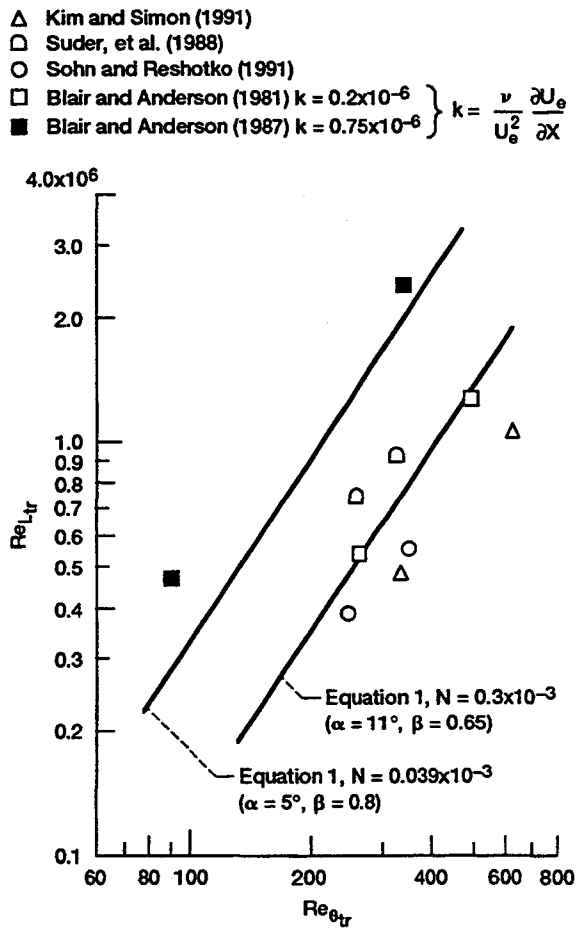

Figure 25.—Transition length correlation.

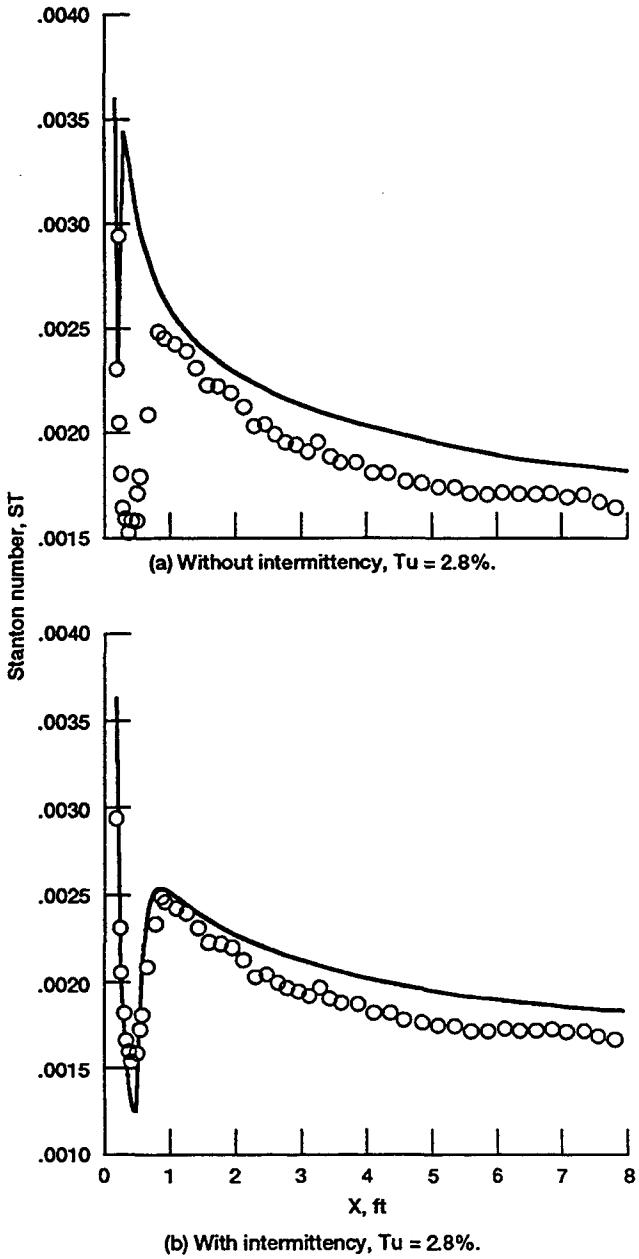

(a) Without intermittency, Tu = 2.8%.

(b) With intermittency, Tu = 2.8%.

Figure 26.—Use of intermittency to model transition region.

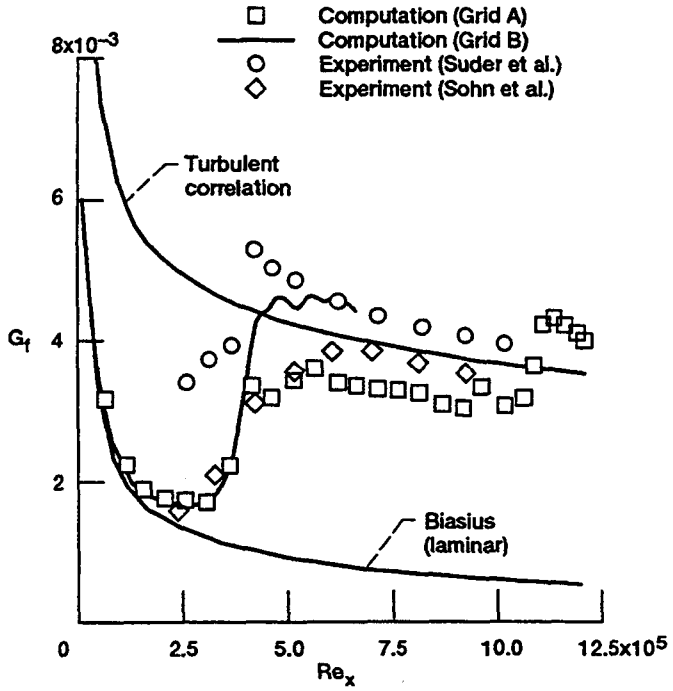

Figure 27.—Computed skin friction along the length of the flat plate (grids A and B). (Rai and Moin, 1991).

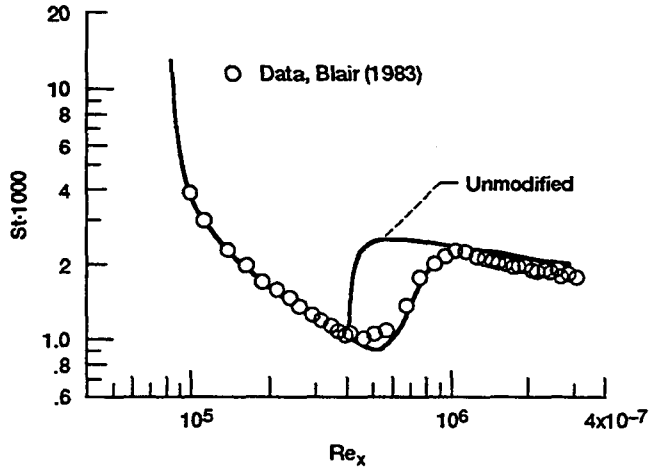

Figure 28.—Effect production term modification on the calculated Stanton number. Tu = 1.4% (Schmidt and Patankar, 1988).

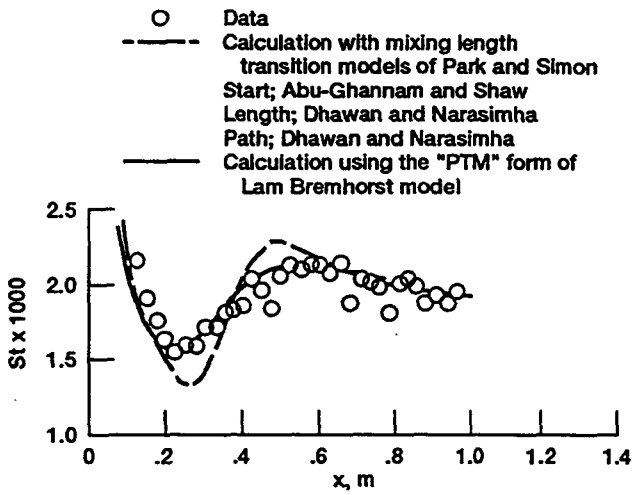

(a) Comparison of the predicted heat transfer during transition with the data of Wang (1984).

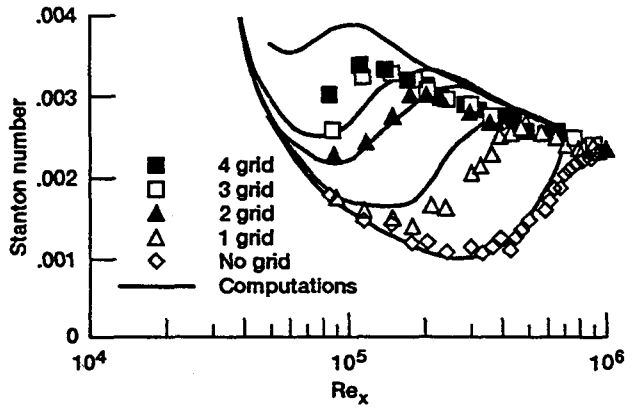

(b) Comparison of the predicted heat transfer during transition with the zero pressure gradient data of Rued (1985) for k based on Tu.

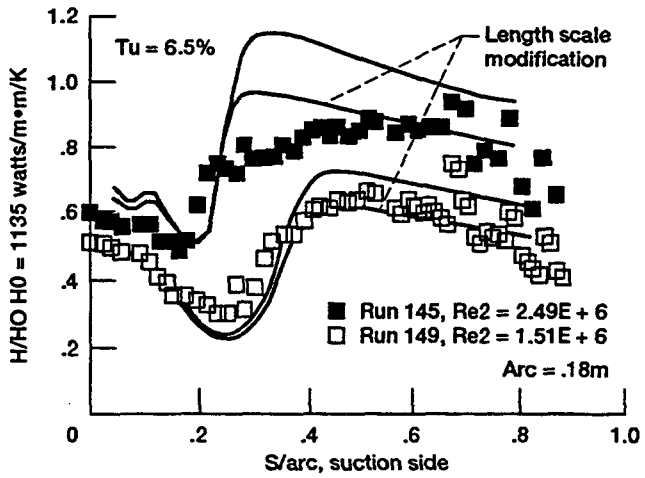

(c) Comparison of the predicted and experimental heat transfer around the suction side of Hylton et al.'s (1983) C3X blade.

Figure 29.—Computational results of PTM method (Schmidt and Patankar, 1988).

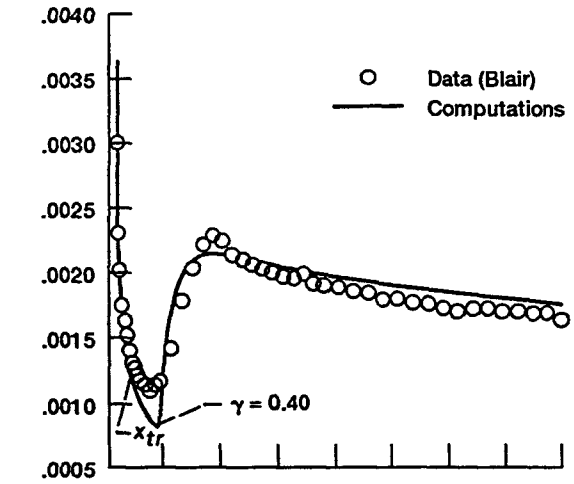

(a) Total turbulence intensity, Tu, 1.4 percent.

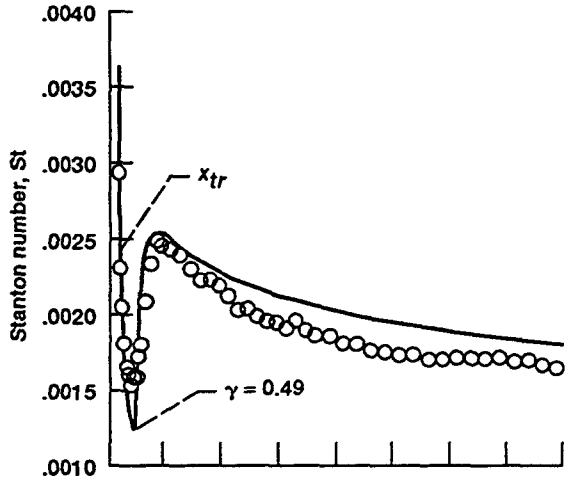

(b) Total turbulence intensity, Tu, 2.8 percent.

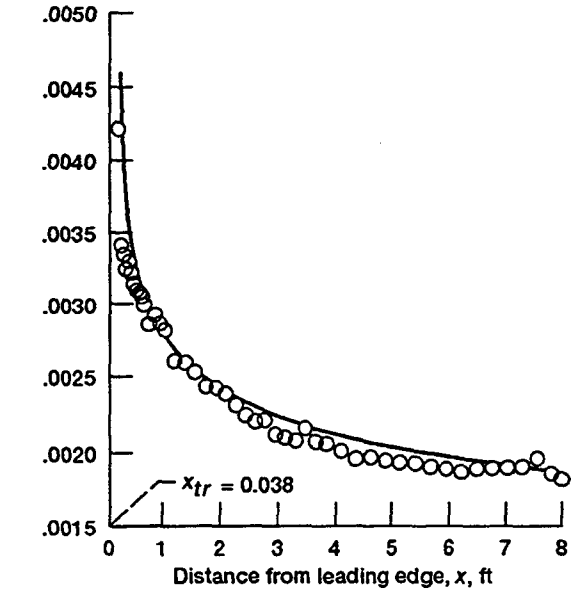

(c) Total turbulence intensity, Tu, 6.2 percent.

Figure 30.—Comparison of prediction with experiment (zero pressure gradient). (Simon & Stephens, 1991)

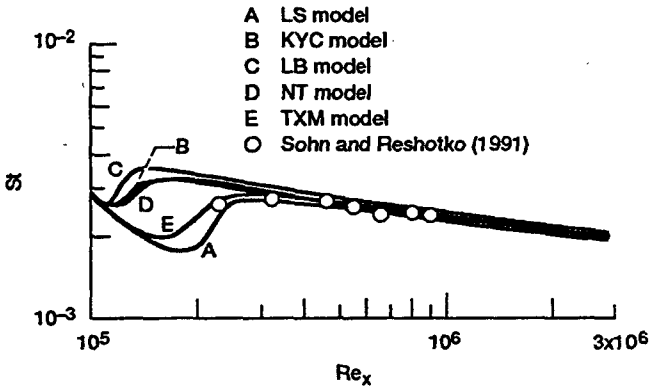

Figure 31.—The predictions of transition for flow over flat plate using different two-equation models compared with Sohn's data for grid 3 (Tu = 3%) (Crawford, 1993).

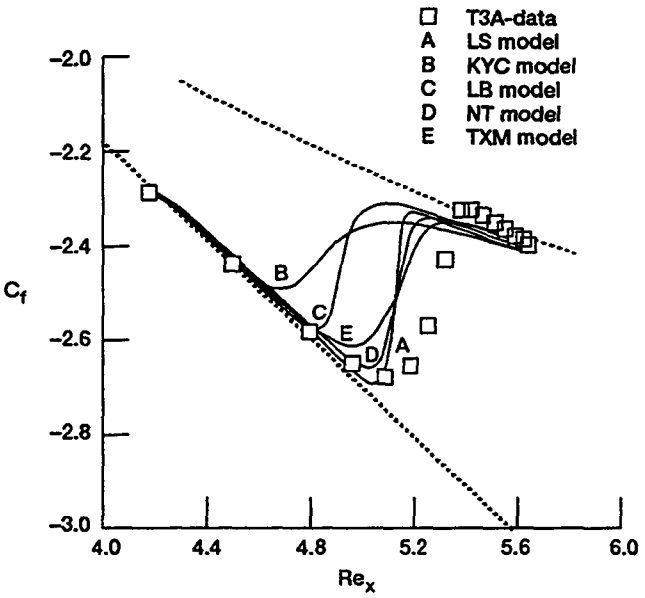

Figure 32.—Computational abilities of various turbulance models (Crawford, 1993). (T3A-data, Savill, 1991), Tu = 3 percent.

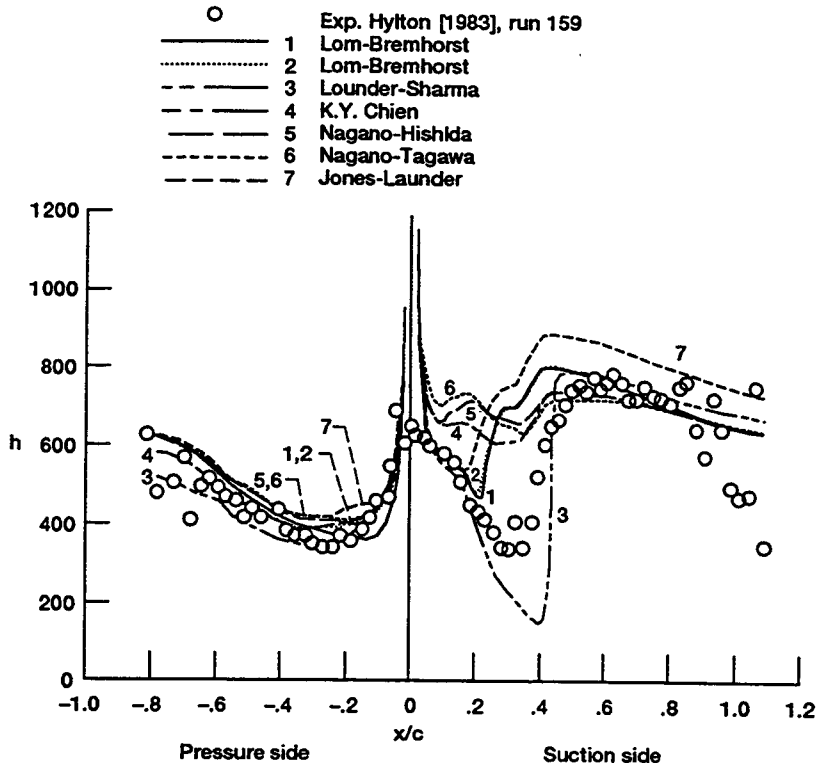

Figure 33.—Computational abilities of various turbulence models (Sieger, Schulz, Crawford and Wittig, 1992).

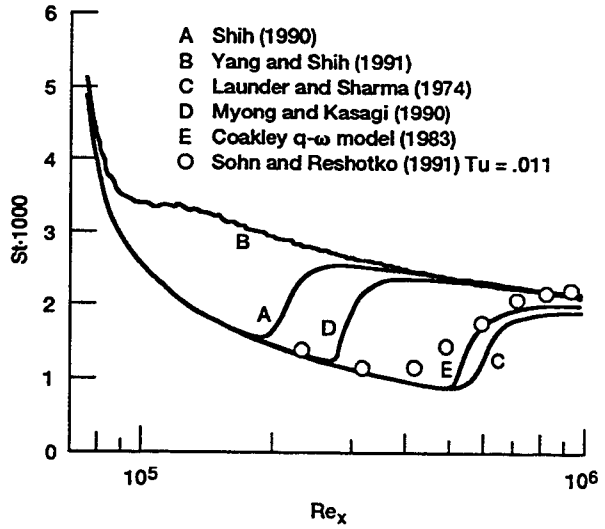

Figure 34.—Some computational comparisons with Sohn and Reshotko grid no. 1 (Wu and Reshotko, 1991).

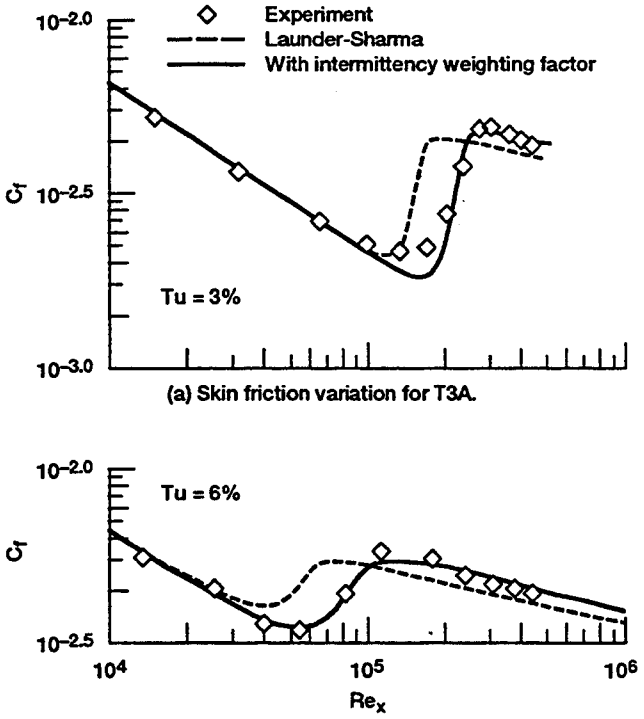

(a) Skin friction variation for T3A.

(b) Skin friction variation for T3B.

Figure 35.—Use of an intermittency weighting factor in computations (Yang, 1992; Yang and Shih, 1992).

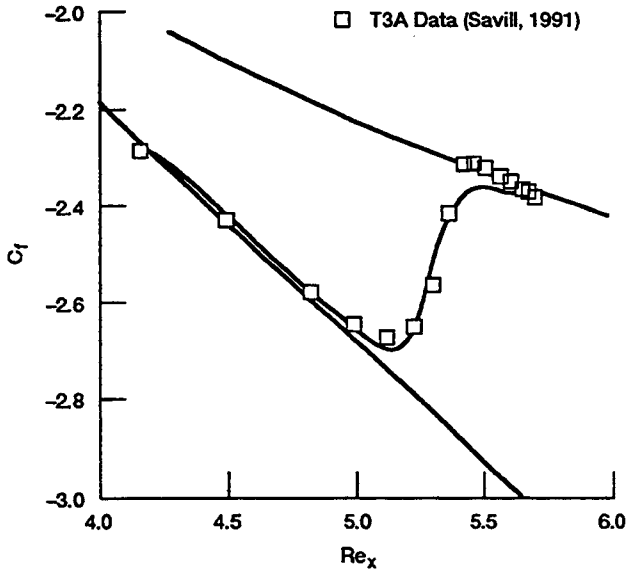

Figure 36.—The numerical prediction of transition flow using MTS model compared with experimental data of T3A (Crawford, 1993).

ON THE PREDICTION OF SEPARATION BUBBLES USING A MODIFIED CHEN-THYSON MODEL

by

Max F. PLATZER
John A. EKATERINARIS
M.S. CHANDRASEKHARA

Department of Aero/Astronautics
Naval Postgraduate School
Monterey, CA

End-Stage Transition Workshop
Syracuse University
16-18 August 1993

OUTLINE

BACKGROUND

ANALYSIS OF NACA 65–213 SEPARATION BUBBLE USING CEBECI'S VISCOUS–INVISCID INTERACTION METHOD

ANALYSIS OF NACA 0012 SEPARATION BUBBLE USING NAVIER–STOKES METHOD

COMPARISON WITH EXPERIMENT

SUMMARY

ANALYSIS

OF

NACA 65-213 AIRFOIL

USING

VISCOUS-INVISCID INTERACTION

METHOD

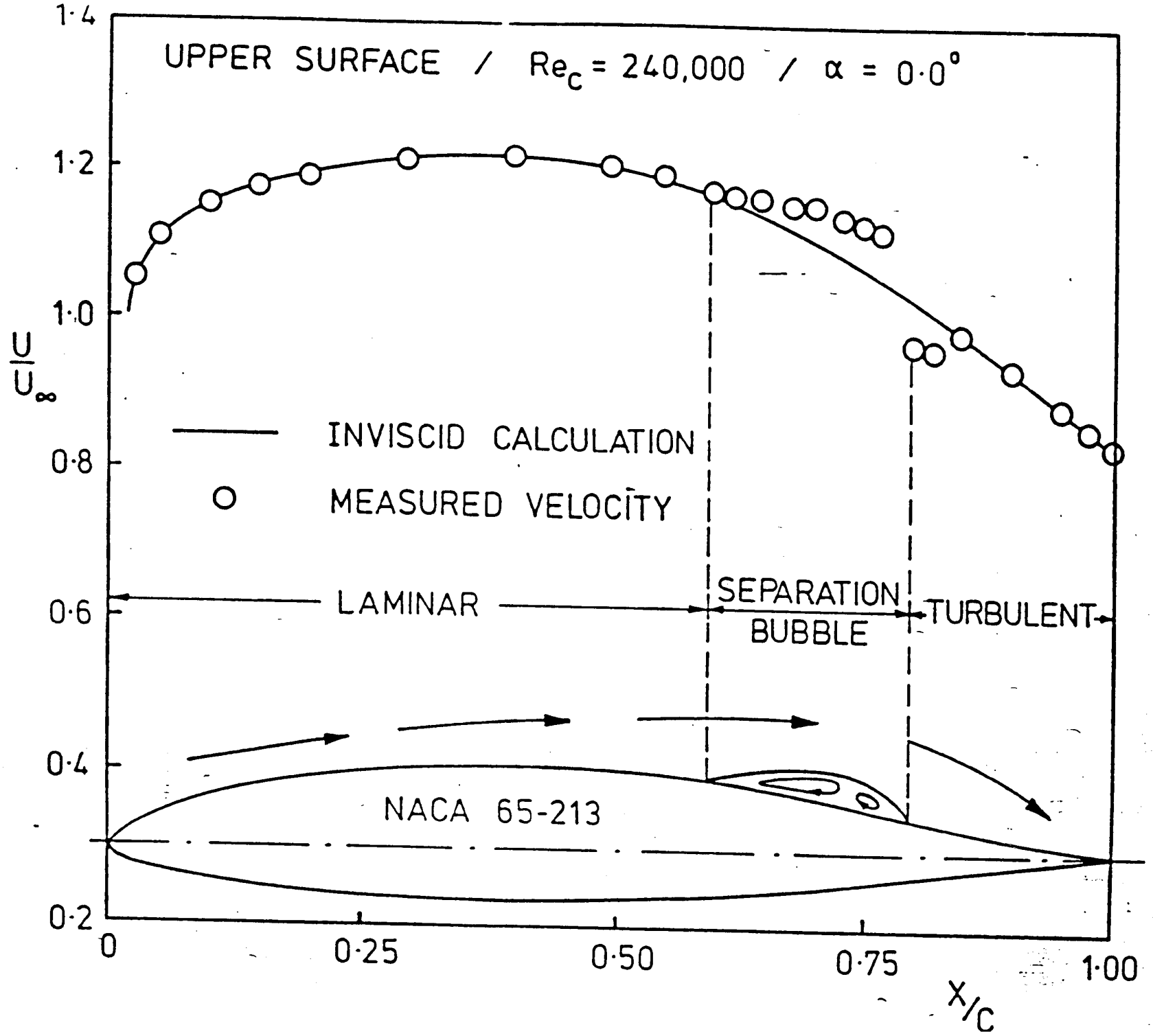
UPPER SURFACE / Re_c = 240,000 / α = 0·0°
1·4
1·2
1·0
0·8
0·6
0·4
0·2
U/U∞
INVISCID CALCULATION
MEASURED VELOCITY
LAMINAR
SEPARATION BUBBLE
TURBULENT
NACA 65-213
0
0·25
0·50
0·75
1·00
X/C

Chen and Thyson

$$\gamma_{tr} = 1 - \exp\left[-\frac{u_e^3}{G_{\gamma_{tr}} v^2} R_{x_{tr}}^{-1.34} (x - x_{tr}) \int_{x_{tr}}^{x} \frac{d\xi}{u_e} \right]$$

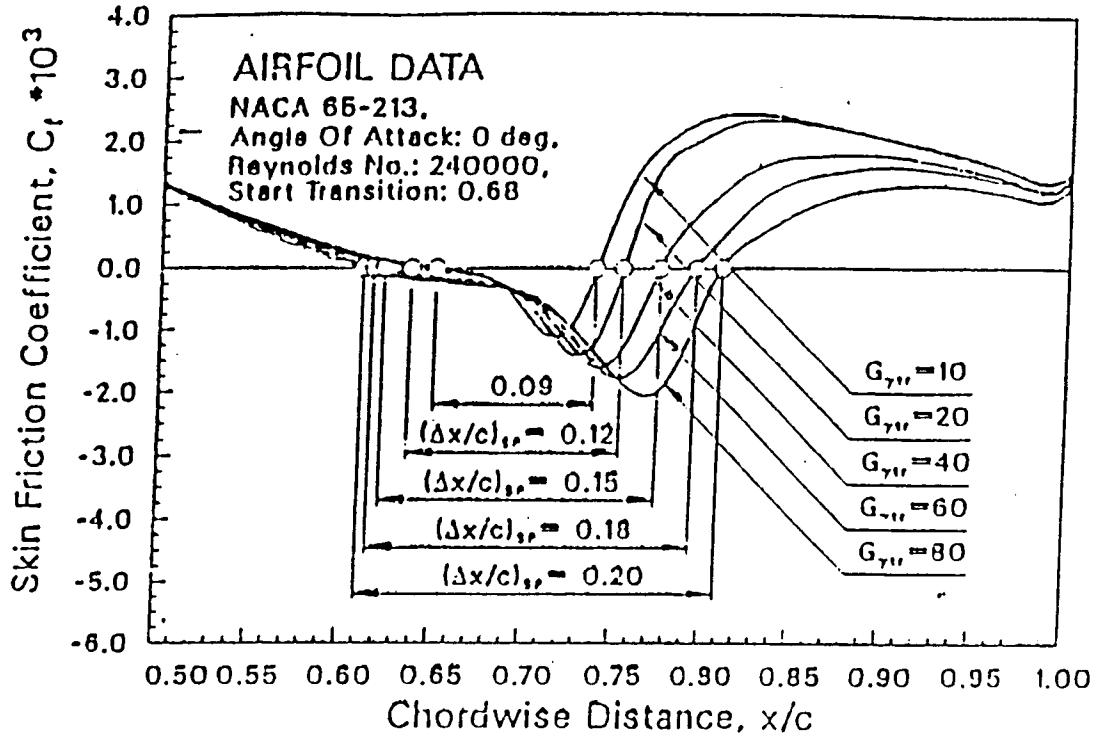
AIRFOIL DATA
NACA 65-213,
Angle Of Attack: 0 deg,
Reynolds No.: 240000,
Start Transition: 0.68
Skin Friction Coefficient, $C_f * 10^3$
4.0
3.0
2.0
1.0
0.0
-1.0
-2.0
-3.0
-4.0
-5.0
-6.0
0.09
$(\Delta x/c)_{ss}$ = 0.12
$(\Delta x/c)_{ss}$ = 0.15
$(\Delta x/c)_{ss}$ = 0.18
$(\Delta x/c)_{ss}$ = 0.20
$G_{\gamma\prime\prime}$=10
$G_{\gamma\prime\prime}$=20
$G_{\gamma\prime\prime}$=40
$G_{\gamma\prime\prime}$=60
$G_{\gamma\prime\prime}$=80
0.50 0.55 0.60 0.65 0.70 0.75 0.80 0.85 0.90 0.95 1.00
Chordwise Distance, x/c

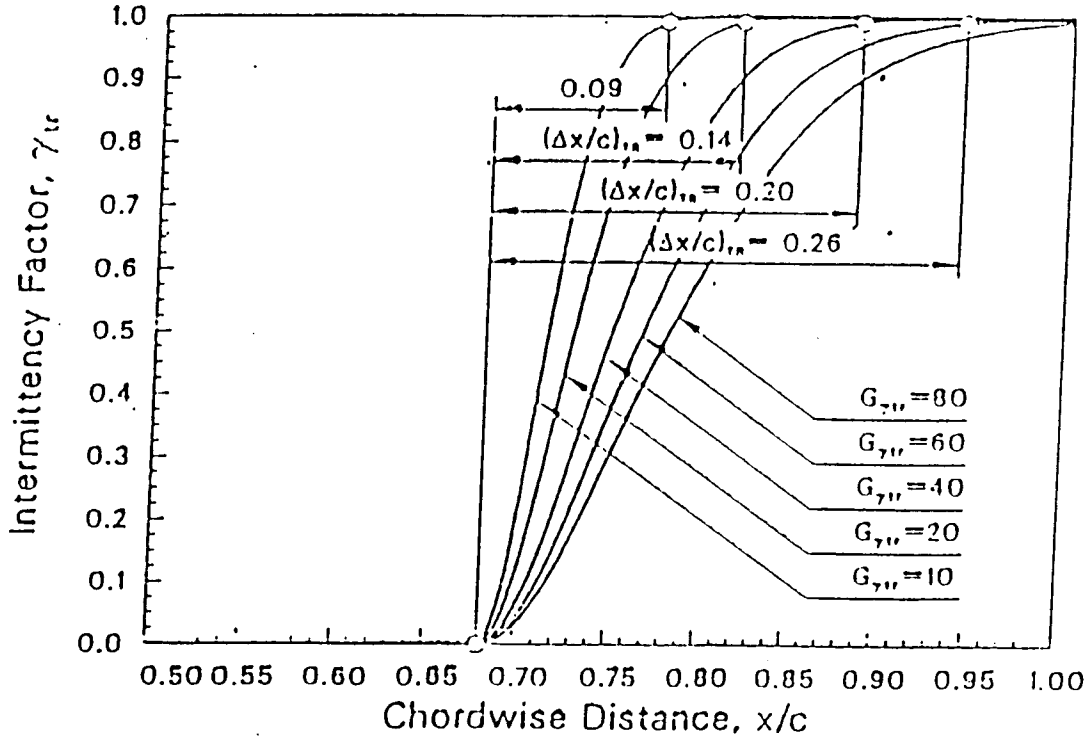
Intermittency Factor, γ_{tr}
1.0
0.9
0.8
0.7
0.6
0.5
0.4
0.3
0.2
0.1
0.0
0.09
$(\Delta x/c)_{tr}$ = 0.14
$(\Delta x/c)_{tr}$ = 0.20
$(\Delta x/c)_{tr}$ = 0.26
$G_{\gamma\prime\prime}$=80
$G_{\gamma\prime\prime}$=60
$G_{\gamma\prime\prime}$=40
$G_{\gamma\prime\prime}$=20
$G_{\gamma\prime\prime}$=10
0.50 0.55 0.60 0.65 0.70 0.75 0.80 0.85 0.90 0.95 1.00
Chordwise Distance, x/c

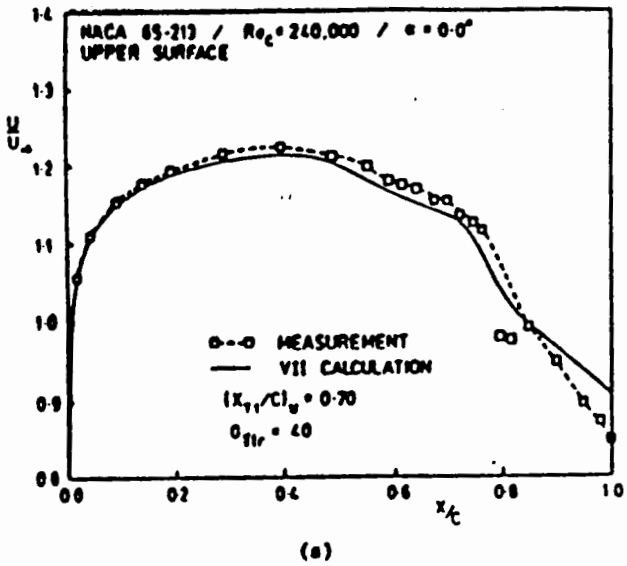

(a)

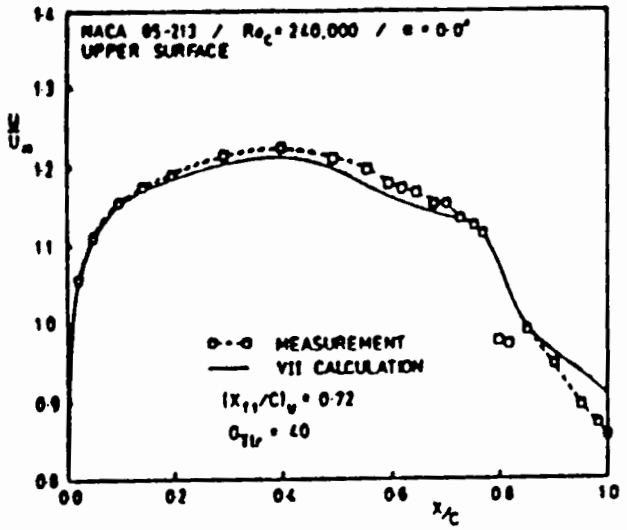

(b)

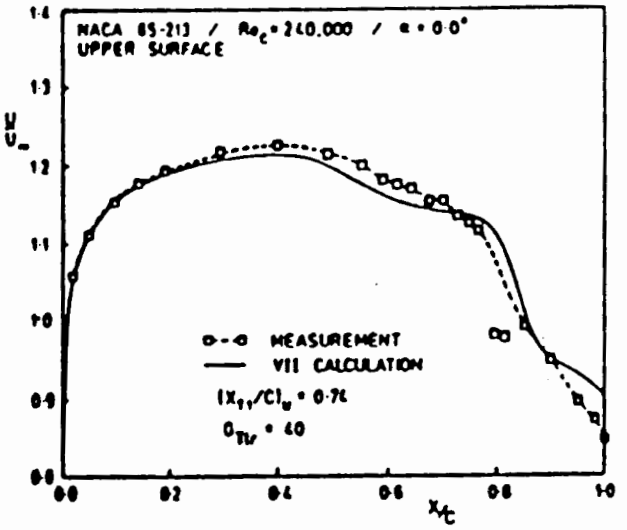

(c)

Calculated and measured inviscid surface velocity distributions: G_{ytr} fixed, varying $(x_{Tl}/c)_u$

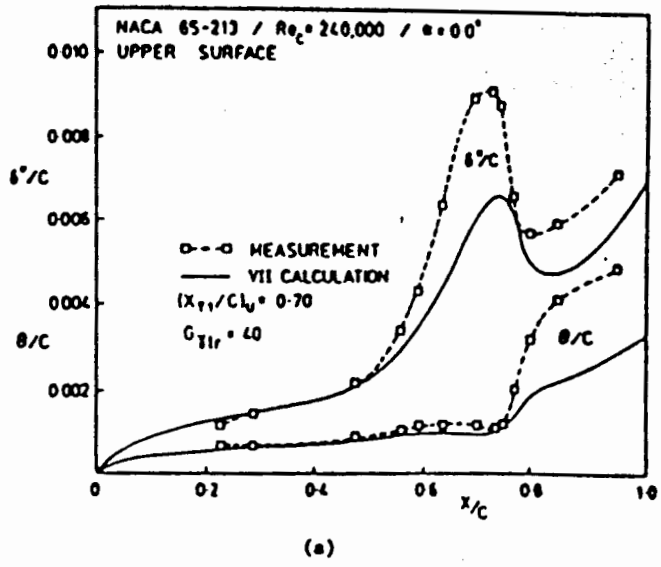

(a)

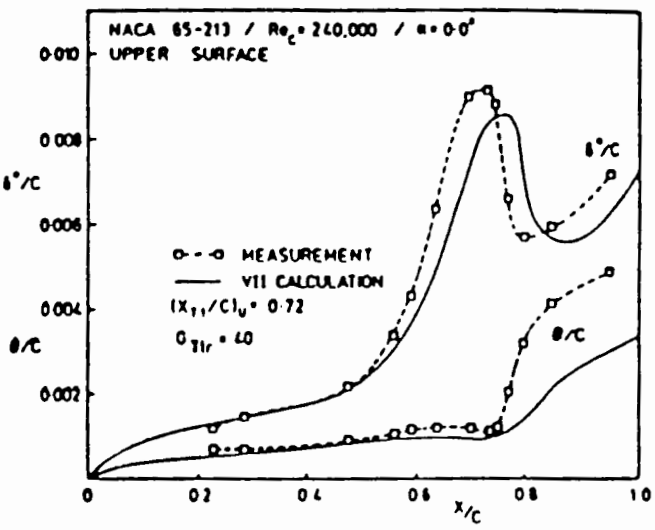

(b)

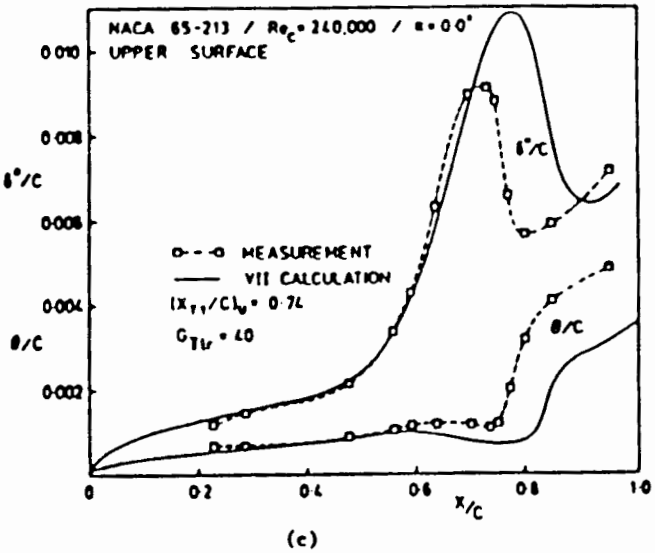

(c)

Calculated and measured displacement and momentum thicknesses of viscous layer: G_{ytr} fixed, varying $(x_{Tl}/c)_u$

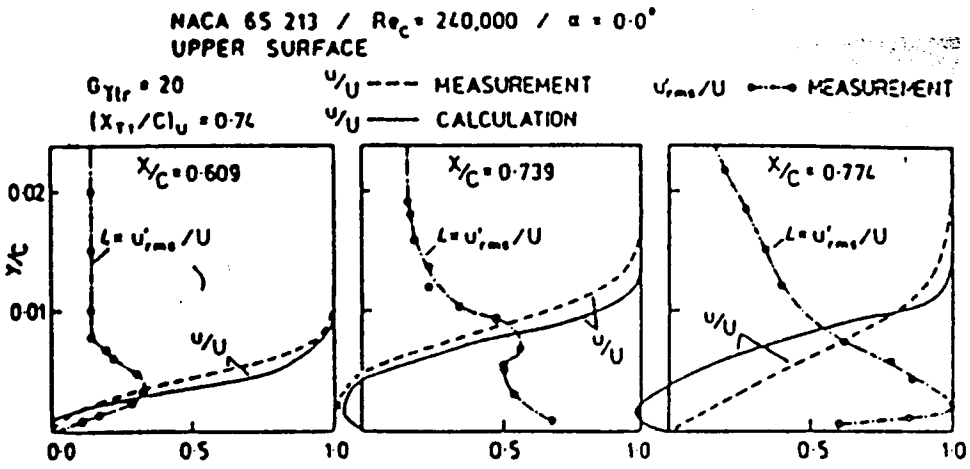

Velocity and turbulence intensity profiles in separation bubble region

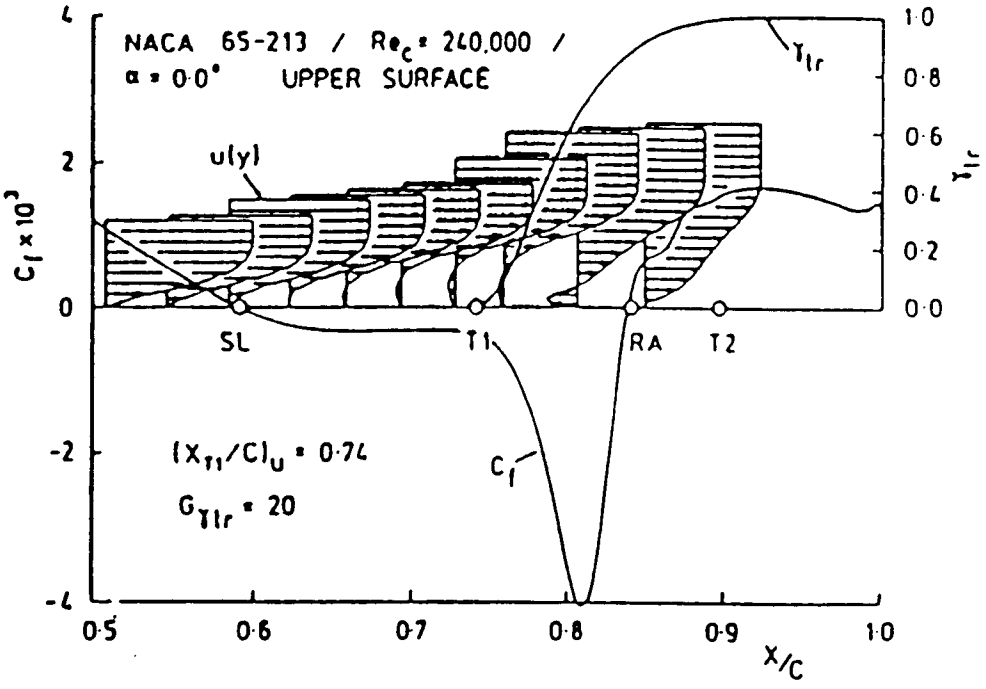

Typical computed separation bubble flow

ANALYSIS

OF

NACA 0012 AIRFOIL

USING

NAVIER–STOKES METHOD

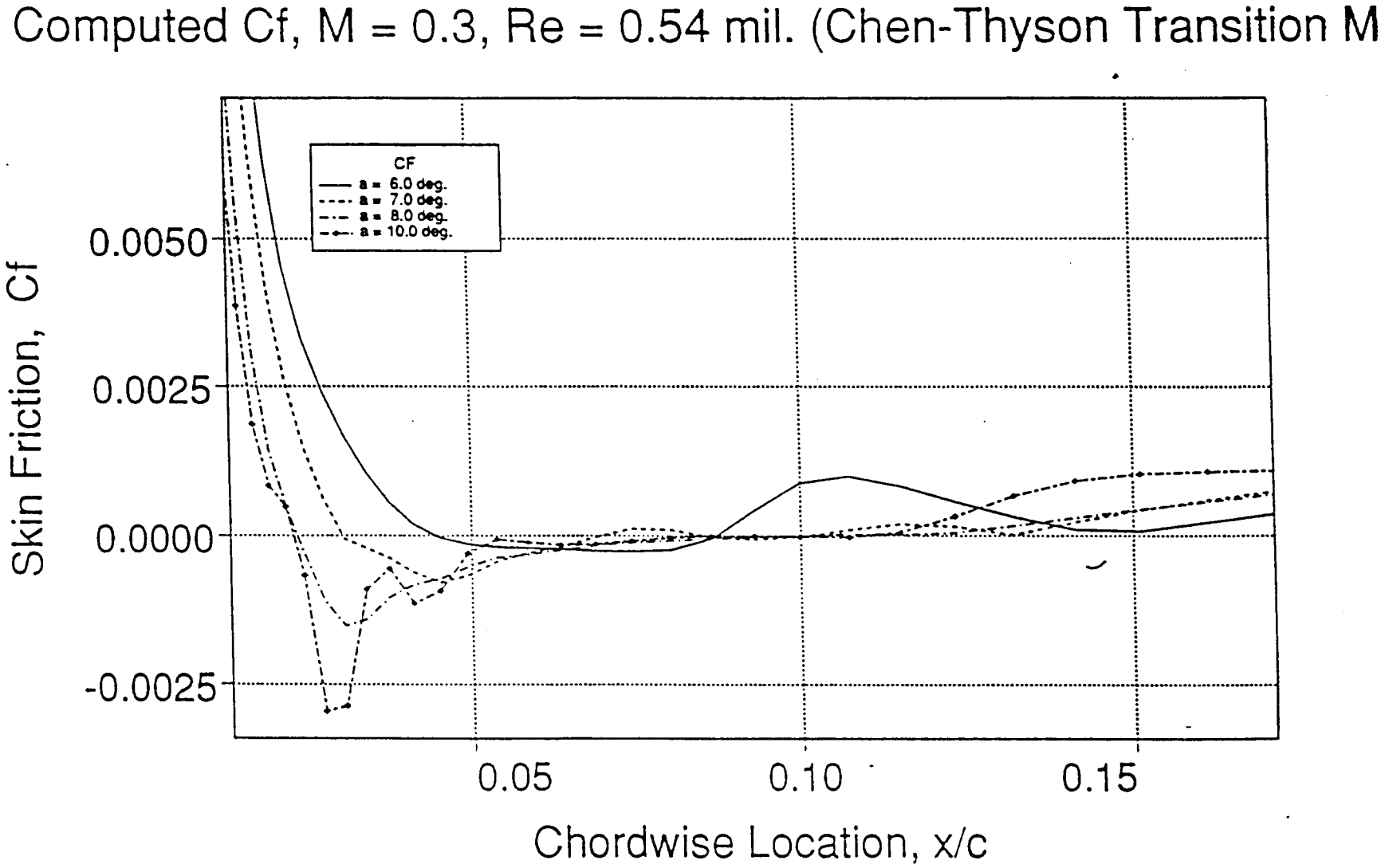
Computed Cf, M = 0.3, Re = 0.54 mil. (Chen-Thyson Transition M
CF
a = 6.0 deg.
a = 7.0 deg.
a = 8.0 deg.
a = 10.0 deg.
Skin Friction, Cf
0.0050
0.0025
0.0000
-0.0025
0.05
0.10
0.15
Chordwise Location, x/c

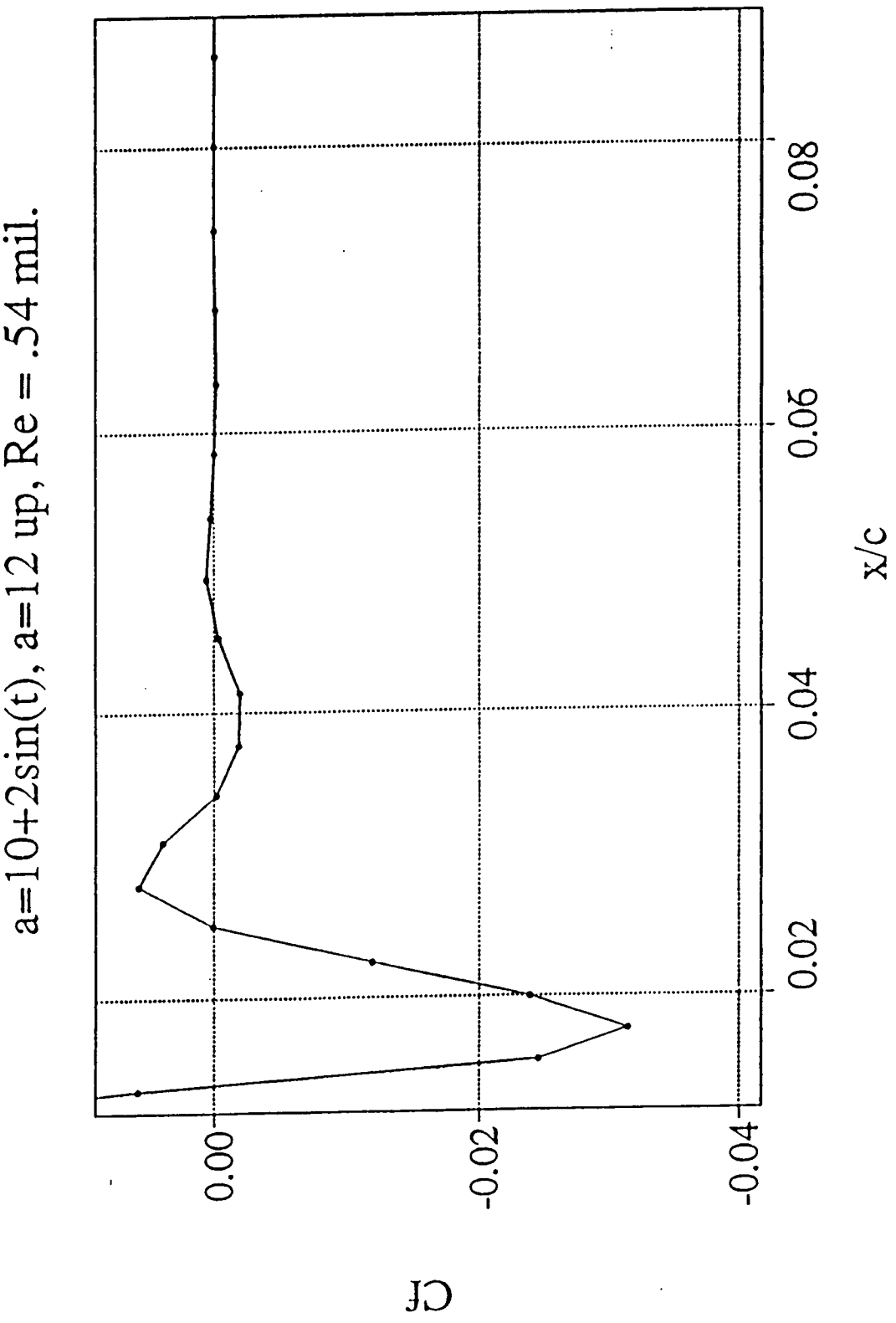
a=10+2sin(t), a=12 up, Re = .54 mil.
0.00
-0.02
-0.04
0.02
0.04
0.06
0.08
x/c
Cf

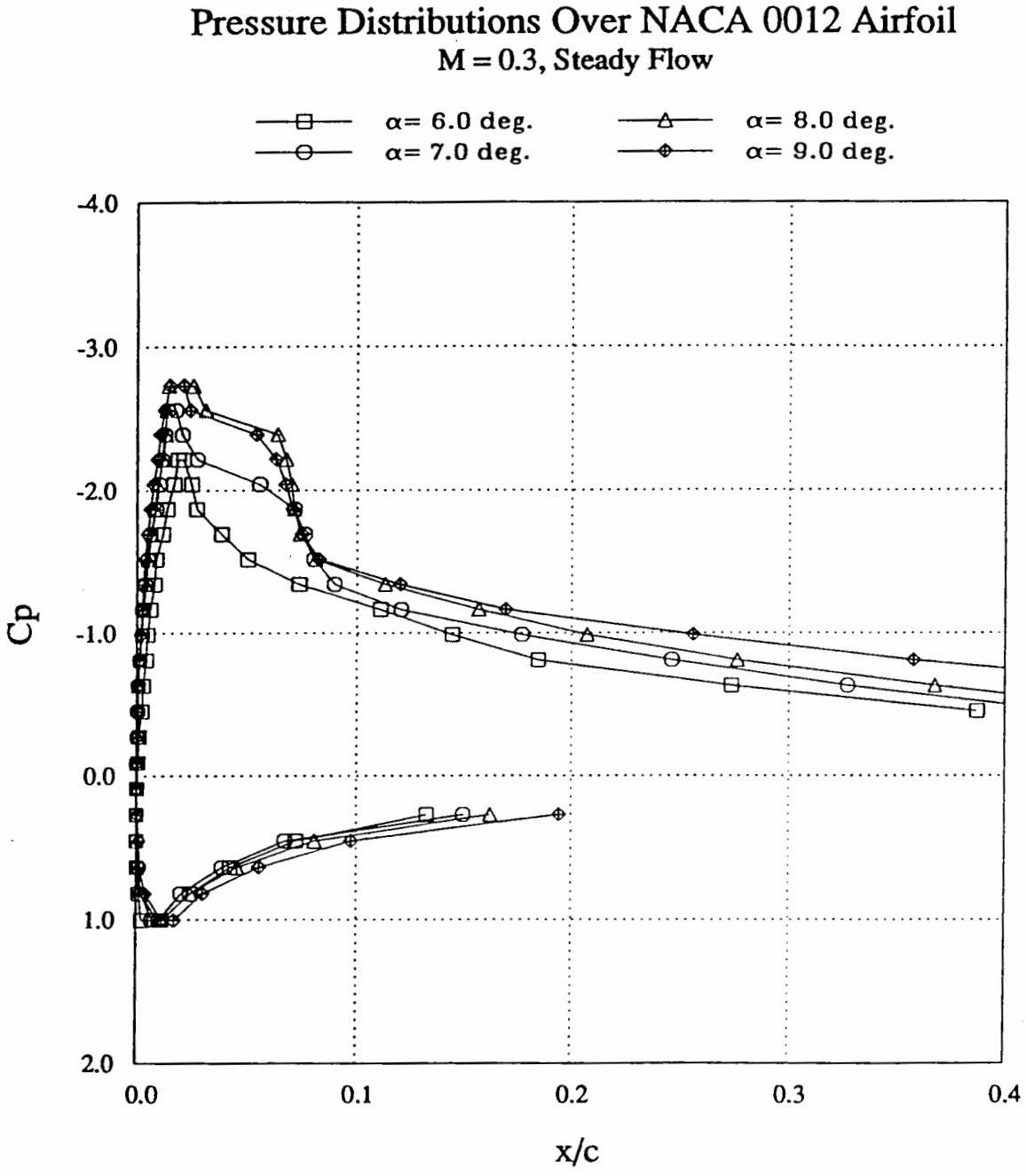
Pressure Distributions Over NACA 0012 Airfoil
M = 0.3, Steady Flow
α= 6.0 deg.
α= 7.0 deg.
α= 8.0 deg.
α= 9.0 deg.
-4.0
-3.0
-2.0
-1.0
0.0
1.0
2.0
Cp
0.0
0.1
0.2
0.3
0.4
x/c

SUMMARY

Separation Bubbles on NACA 65-213 and NACA 0012 could be predicted successfully with a modified Chen-Thyson transition model

The Stability of the Boundary Layer and the Spot
(the effects on its shape, rate of growth and internal structure)

I. Wygnanski
Department of Fluid Mechanics and Heat Transfer
Tel Aviv University
Ramat-Aviv, Israel 66978

Aerospace and Mechanical Engineering Department
University of Arizona
Tucson, AZ 85721

ABSTRACT

The similarity among turbulent spots observed in various transition experiments, and the rate in which they contaminate the surrounding laminar boundary layer is only cursory. The shape of the spot depends on the Reynolds number of the surrounding boundary layer and on the pressure gradient to which it and the surrounding laminar flow are exposed. The propagation speeds of the spot boundaries depend, in addition, on the location from which the spot originated and do not simply scale with the local free stream velocity. The understanding of the manner in which the turbulent spot destabilizes the surrounding, vortical fluid is a key to the understanding of the transition process. We therefore turned to detailed observations near the spot boundaries in

general and near the spanwise tip of the spot in particular.

Two, oblique wave packets of the Tollmien - Schlichting type, were observed beyond the tip of the spot. They passively trailed the spot when the surrounding boundary layer was marginally stable, but beyond the critical Re they amplified and broke down generating either new autonomous spots or coalescing with the "parent" spot and changing its shape and its rate of growth. When the boundary layer stability was enhanced by favorable pressure gradient the wave packets disappeared. Their absence is associated with the smaller rate of spread of the spot in a favorable pressure gradient.

Measurements of all three components of velocity in a turbulent spot are rare, particularly near the tip of the spot. A special hot-wire rake consisting of 8 "V" arrays was built in order to measure the spanwise and streamwise components of velocity simultaneously over a sizable fraction of the span of the spot. The data reveals the existence of a strong spanwise component of velocity which increases monotonically with increasing distance from the plane of symmetry and attains its maximum value near the tip. This perturbation velocity resembles a wave which follows the leading interface of the spot and looks like a single vortex near the tip. It also changes direction near the tip from having the dominant vorticity component parallel to the leading interface to a dominant, yet diffused vertical vorticity. A typical dimension of this vortex is comparable to 20% of the span of the spot at the location measured. This observation does not support the notion which is based on observations in a nascent spot that a spot may consist of an orderly formation of "Λ" vortices whose number is proportional to the size of the spot. No such vortices were observed near the tip of a fully aged (or developed) spot when they were analyzed by similar techniques.

THE STABILITY OF THE BOUNDARY LAYER AND THE SPOT

(the effects on its shape, rate of growth and internal structure)

I. Wygnanski

Department of Fluid Mechanics and heat Transfer, Tel Aviv University,
Ramat-Aviv, Israel 66978
Aerospace and Mechanical Engineering Department, University of Arizona,
Tucson AZ. 85721

ACKNOWLEDGEMENTS

M. Zilberman

R. E. Kaplan

J. Haritonidis

A. Glezer

Y. Katz

A. Seifert

The work was supported for many years by AFOSR


1
2

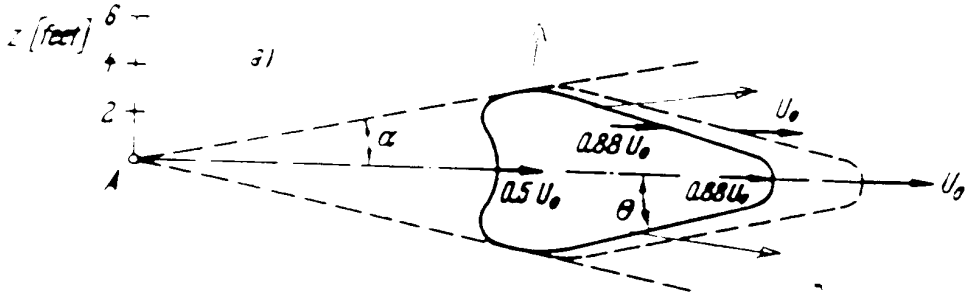
z [feet]
6
2
a)
A
α
0.88 U∞
U∞
0.5 U∞
θ
0.88U∞
U∞

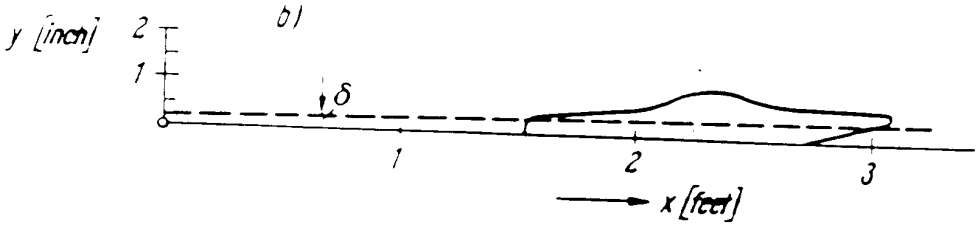
y [inch]
2
1
b)
δ
1
2
3
x [feet]

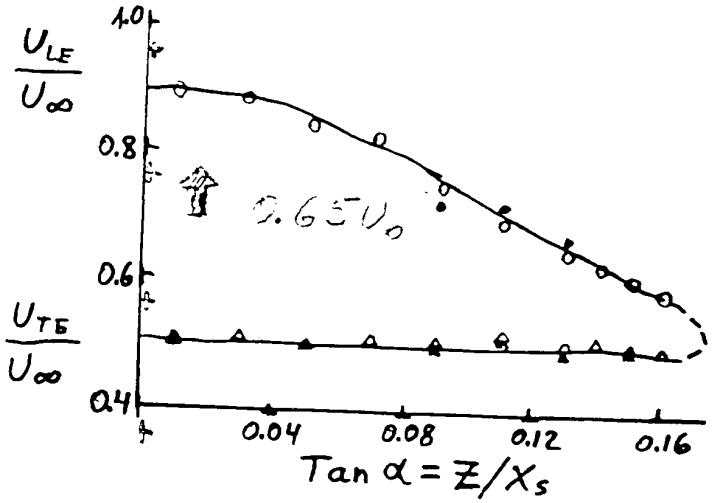
1.0
U_LE / U∞
0.8
0.65U∞
0.6
U_TE / U∞
0.4
0.04
0.08
0.12
0.16
Tan α = Z/Xs

WSF 1976

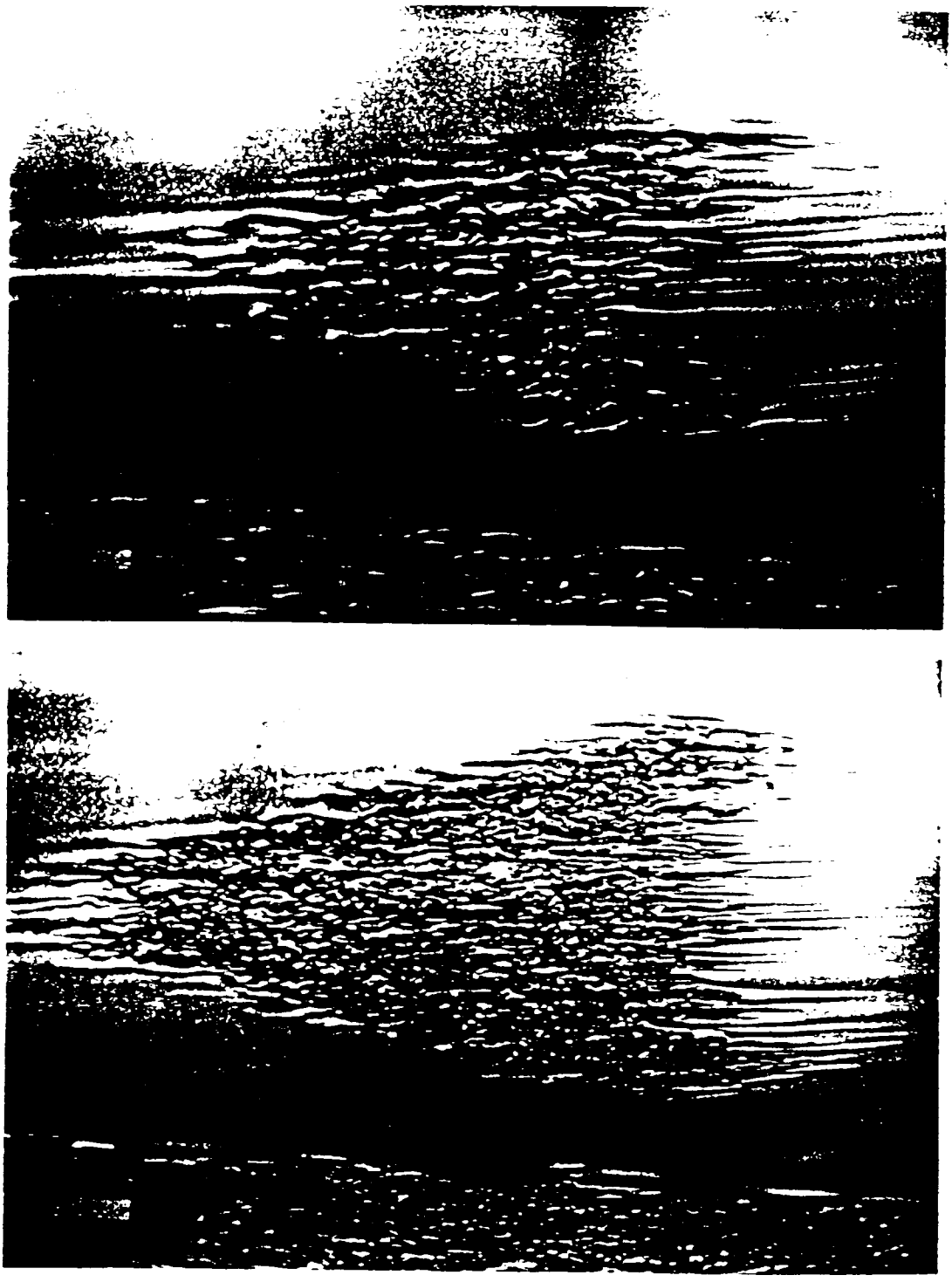

Cantwell Coles & Dimotakis 1978

Figure 6. Aluminum visualization of sublayer streaks for turbulent spots in water. (a) Low Reynolds number; U_∞ = 12 cm/sec. (b) Higher Reynolds number; U_∞ = 23 cm/sec. Note region of transverse contamination from channel bottom.

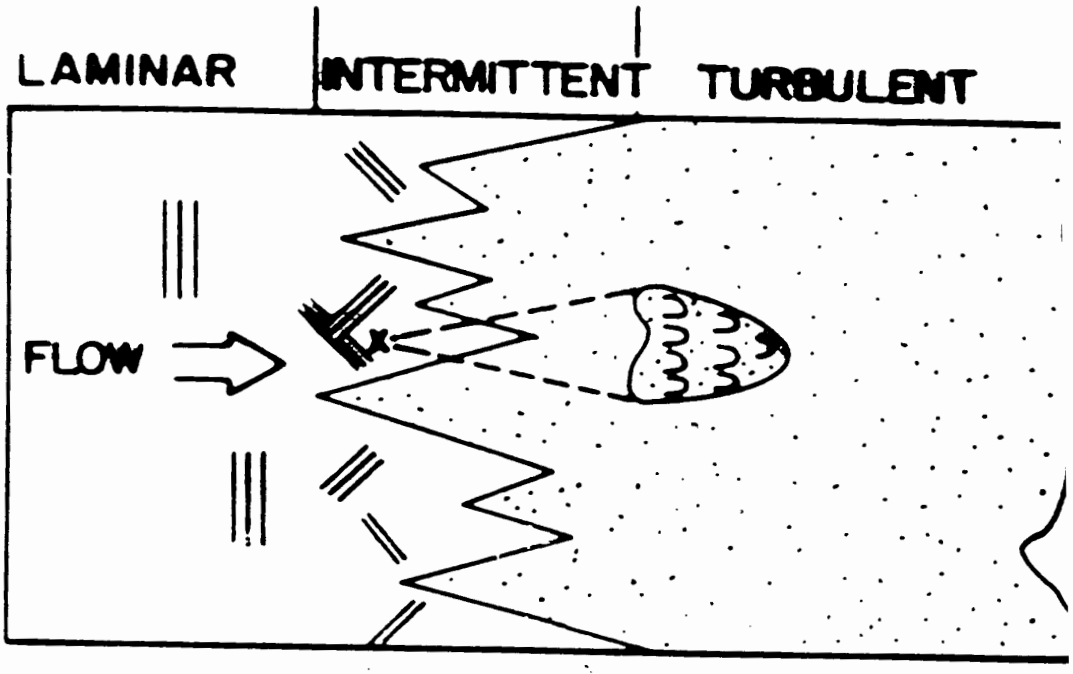

1. The spot represents the final recognizable stage in the transition process.

2. It provides a linkage to linear stability.

3. It generates large coherent structures in a fully turbulent boundary layer.

4. It has a higher internal degree of order than the turbulent boundary layer.

$\beta = 0.$

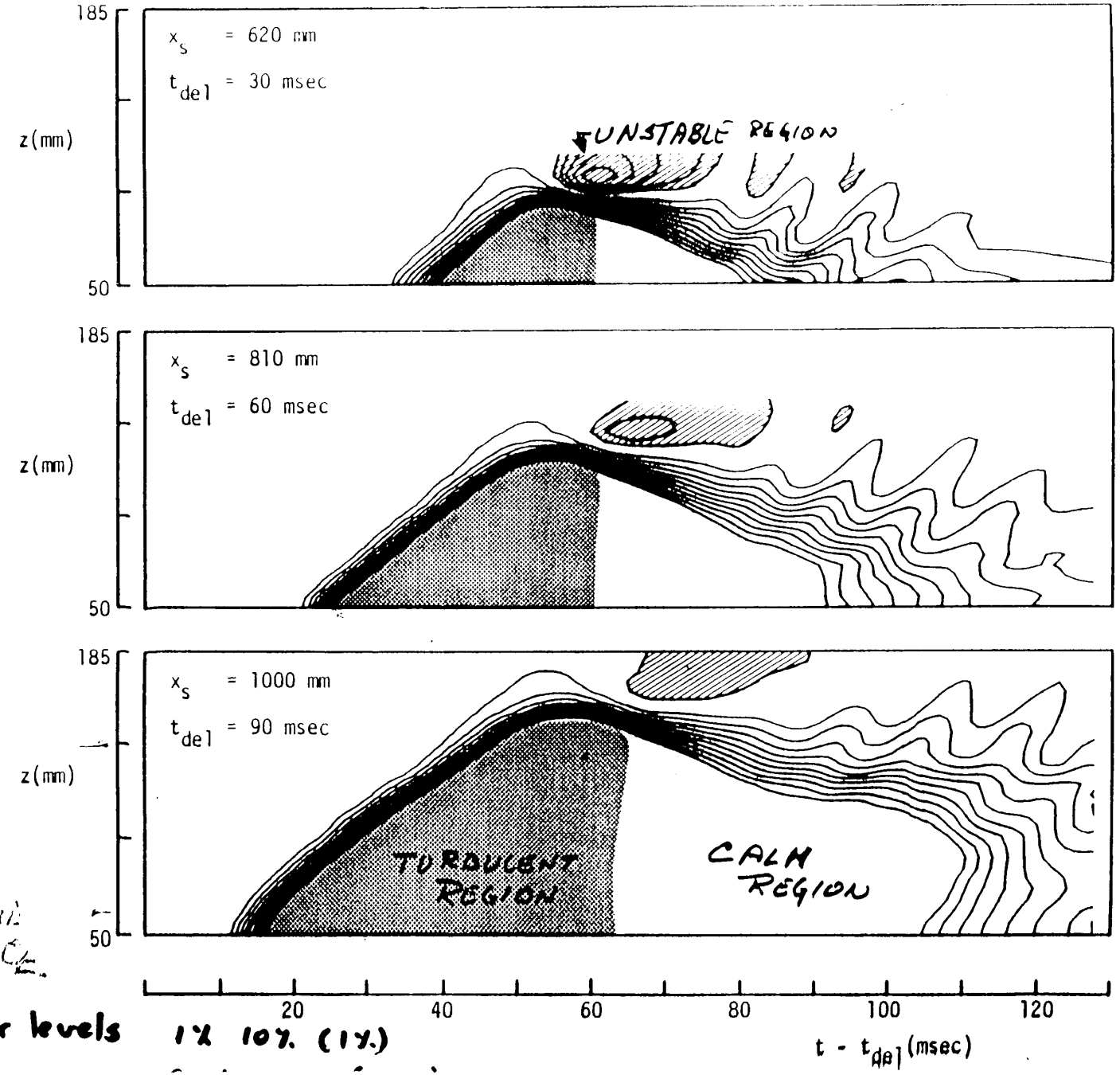

$\frac{\hat{u}}{u_\infty} \cdot \langle \hat{u}(x,t) \rangle = \langle u(x,t) \rangle - u_{bar}(x)$

$\frac{y}{\delta^*} \doteq 0.6$

Note: Hill is not C.

contour levels 1% 10% (1%)

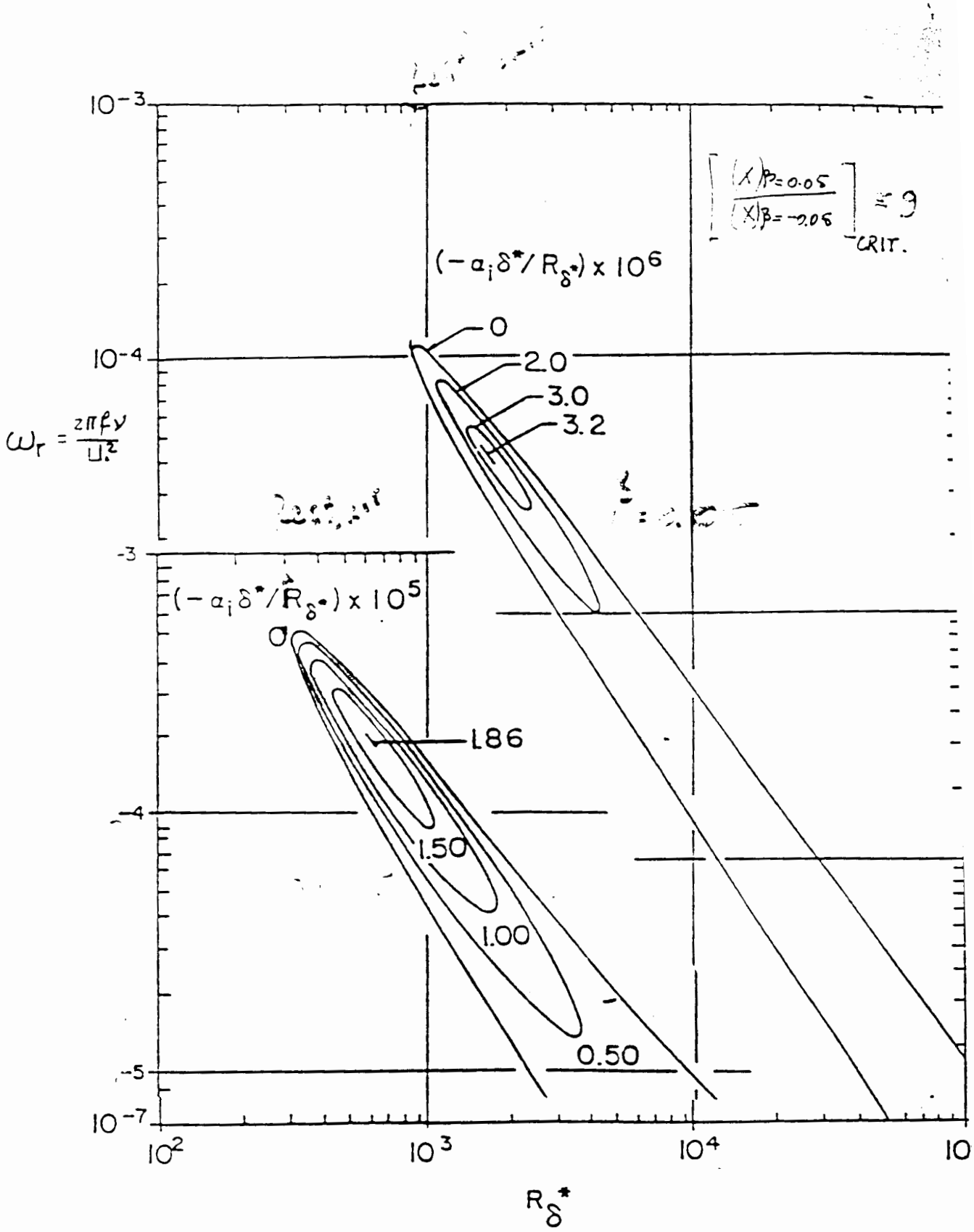

WAZZAN OKAMURA & SMITH (1968)

Figure 9. - Curves of constant spatial amplification rates ($\beta = 0.05$) (top β = Bottom

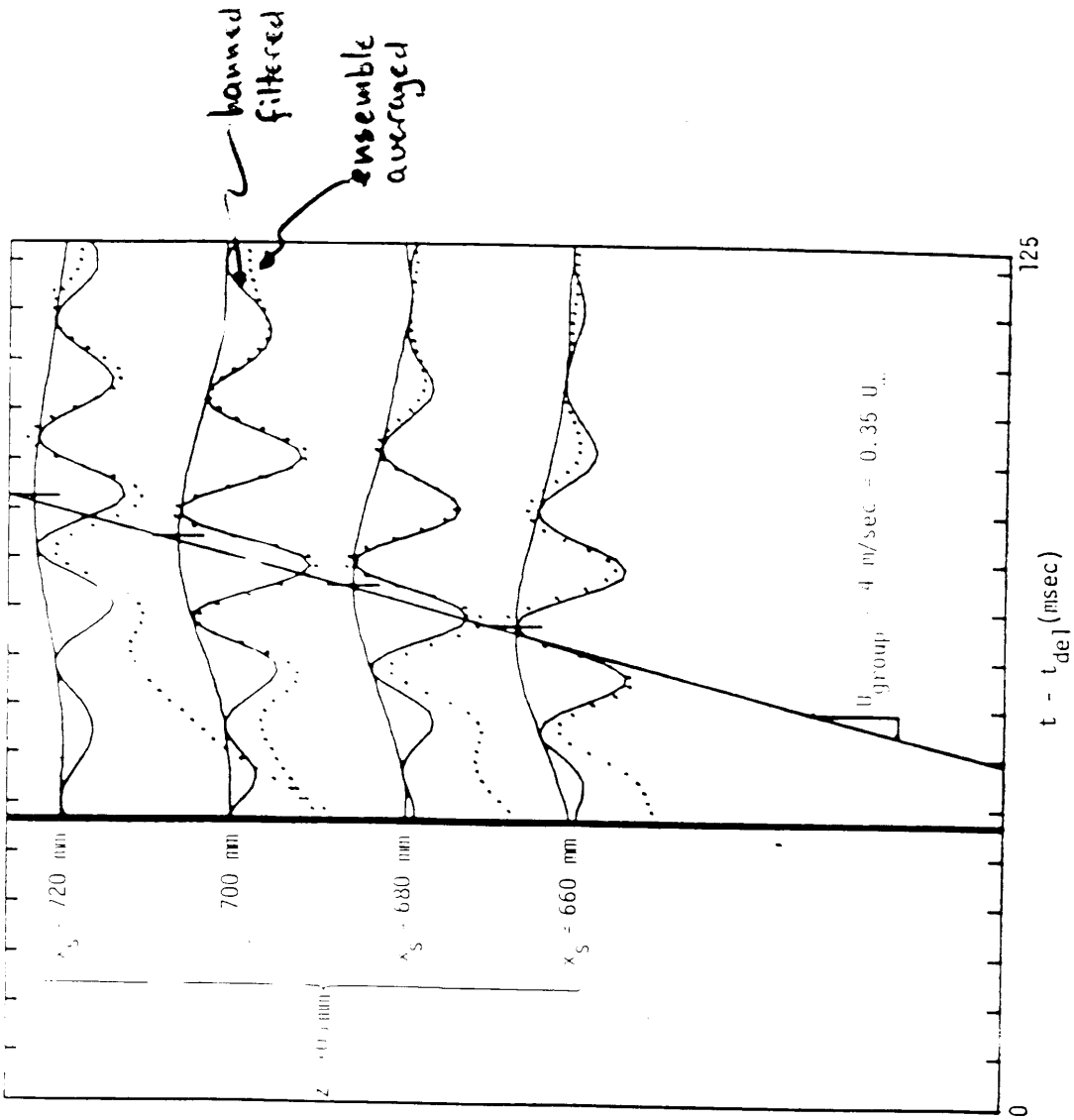

Chamber & Thoma 1995

$\langle u_c'^2(\bar{x},t)\rangle = \frac{1}{b(\bar{x},t)} \langle G(\bar{x},t)\cdot u_t'^2 \rangle$ $\beta = 0.0$

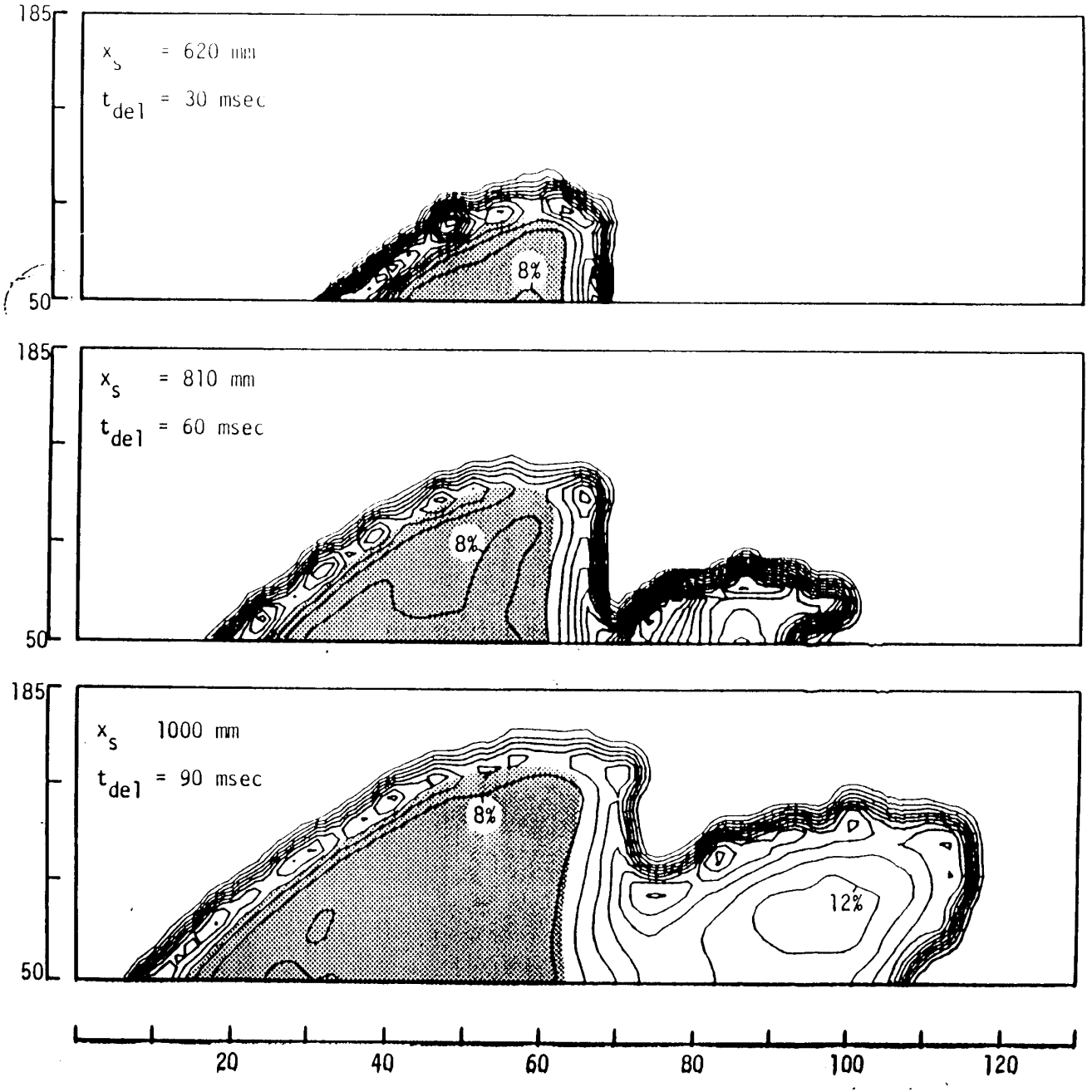

Note origin

$\frac{y}{\delta^*} = 0.6$

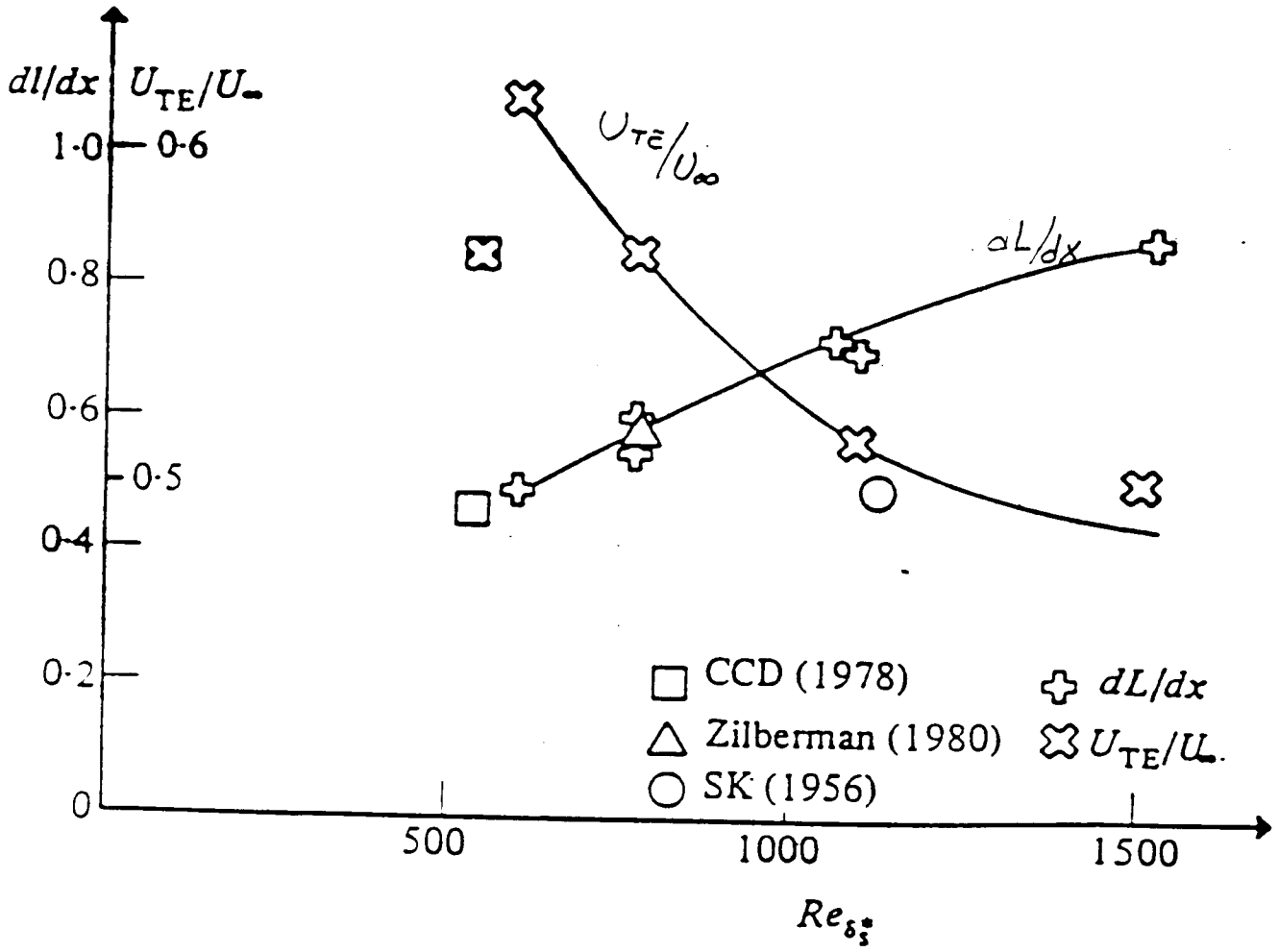
dl/dx
U_TE/U_∞
1·0
0·6
0·8
0·6
0·5
0·4
0·2
0
500
1000
1500
Re_δ*
U_TE/U_∞
dL/dx
CCD (1978)
Zilberman (1980)
SK (1956)
dL/dx
U_TE/U_∞

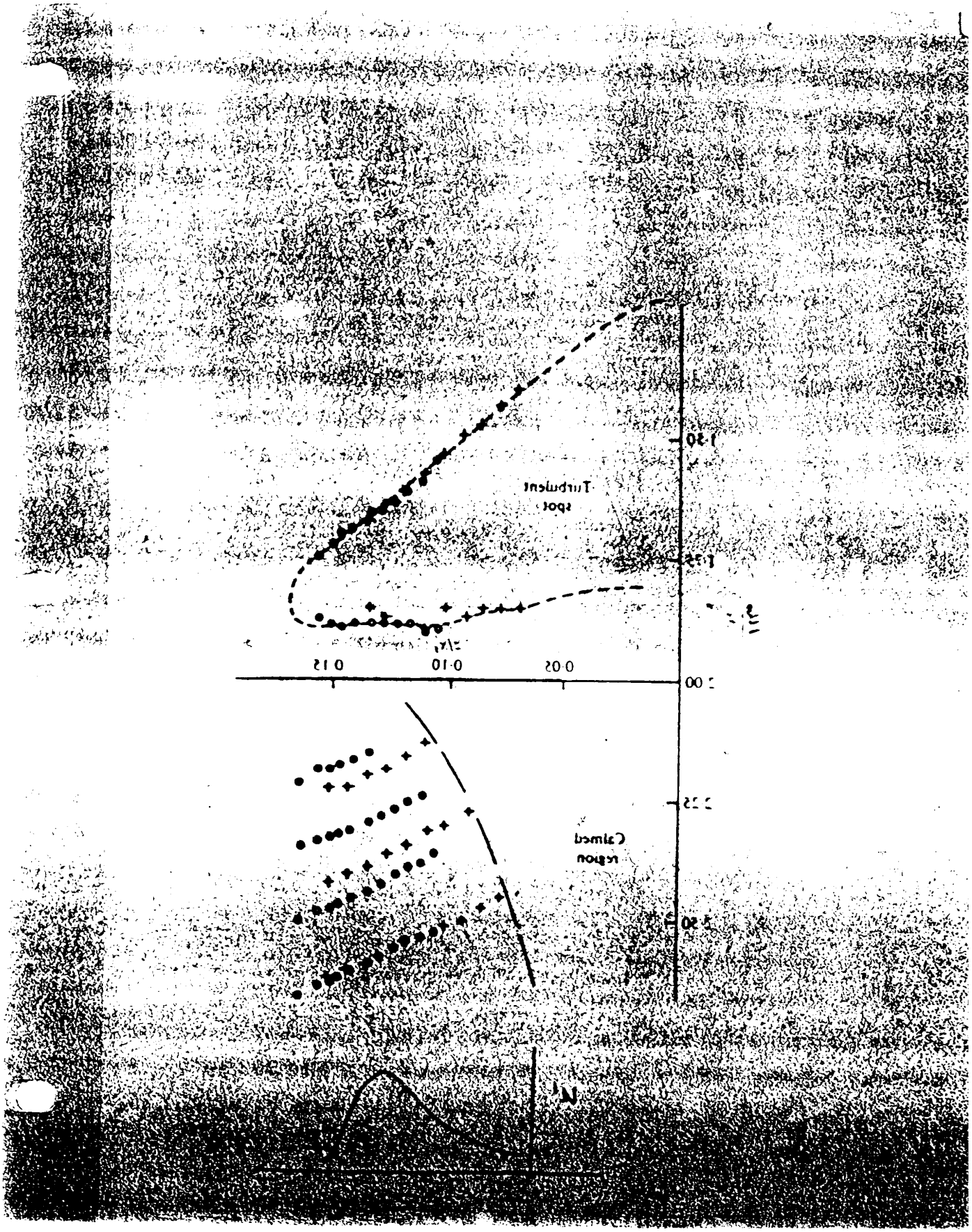
Turbulent
spot
Calmed
region

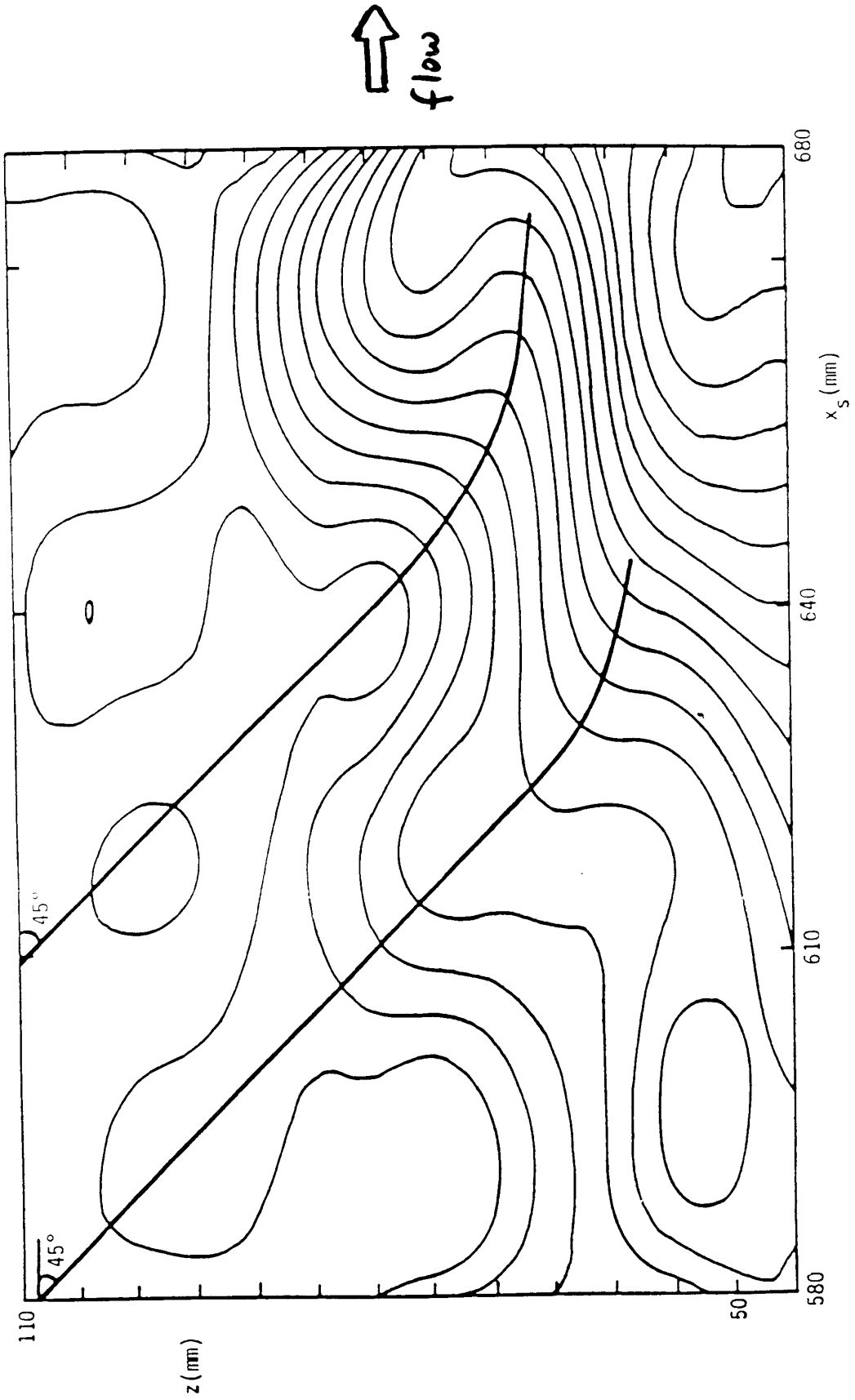
flow
45°
45°
110
50
z (mm)
580
610
640
680
x_s (mm)

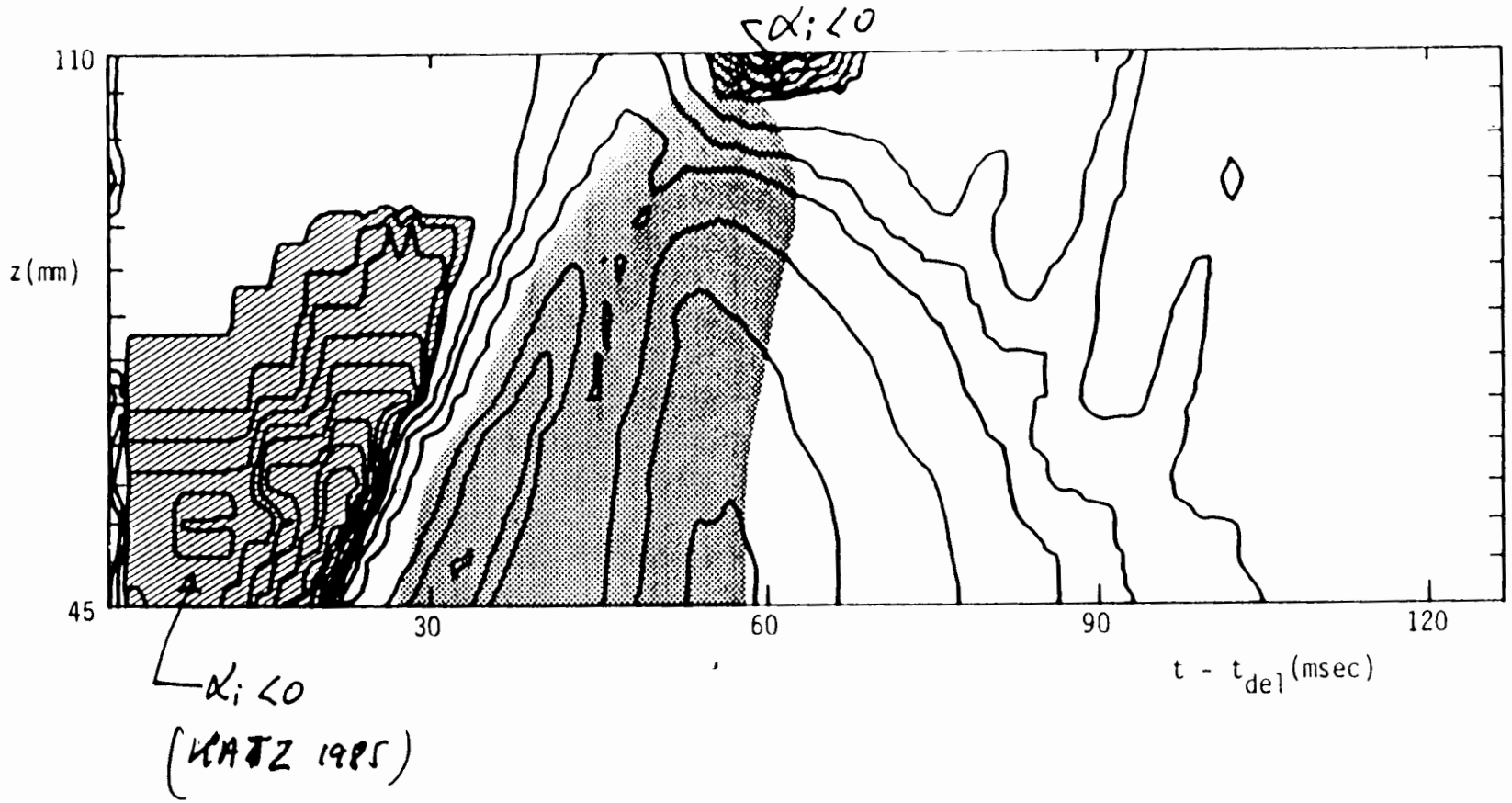
α_i < 0
110
z (mm)
45
30
60
90
120
t - t_del (msec)
α_i < 0
(KATZ 1985)

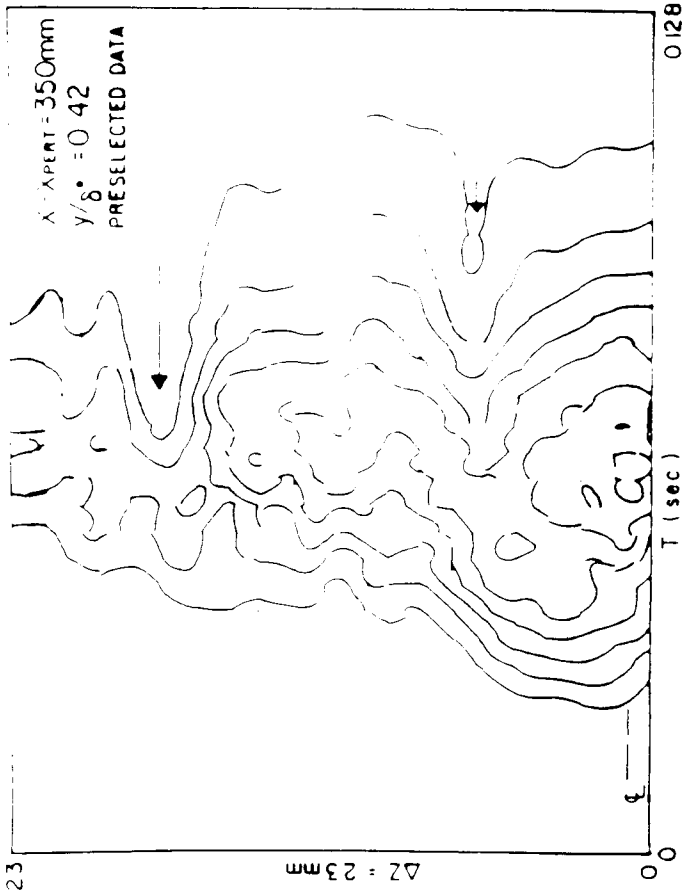
X-XPERT = 350mm
y/δ* = 0.42
PRESELECTED DATA
0.128
T (sec)
0
0
ΔZ = 23mm
23

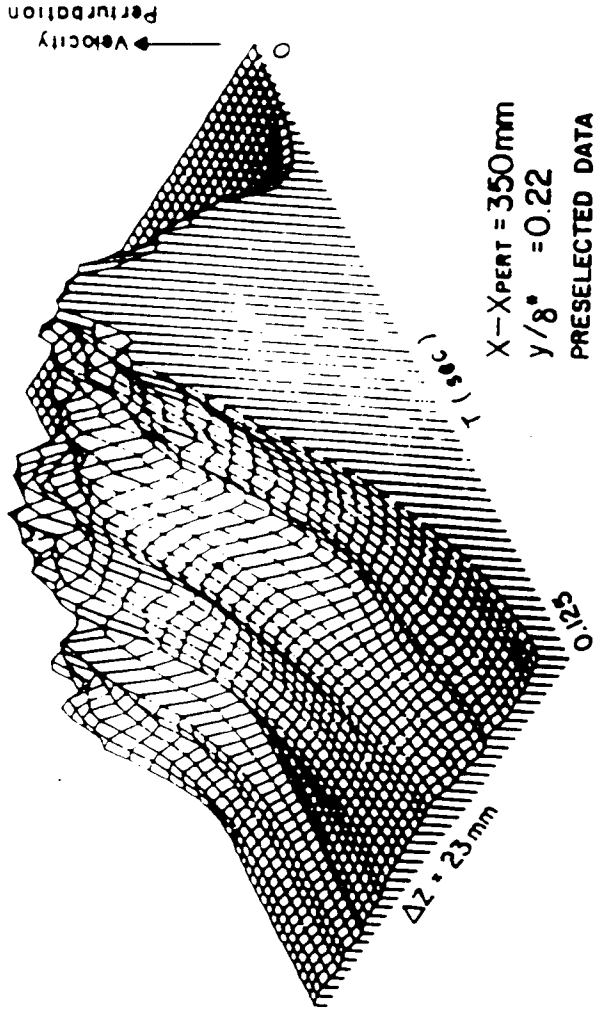
Velocity
Perturbation
0
X-XPERT = 350mm
y/δ* = 0.22
PRESELECTED DATA
T (sec)
0.125
ΔZ = 23mm

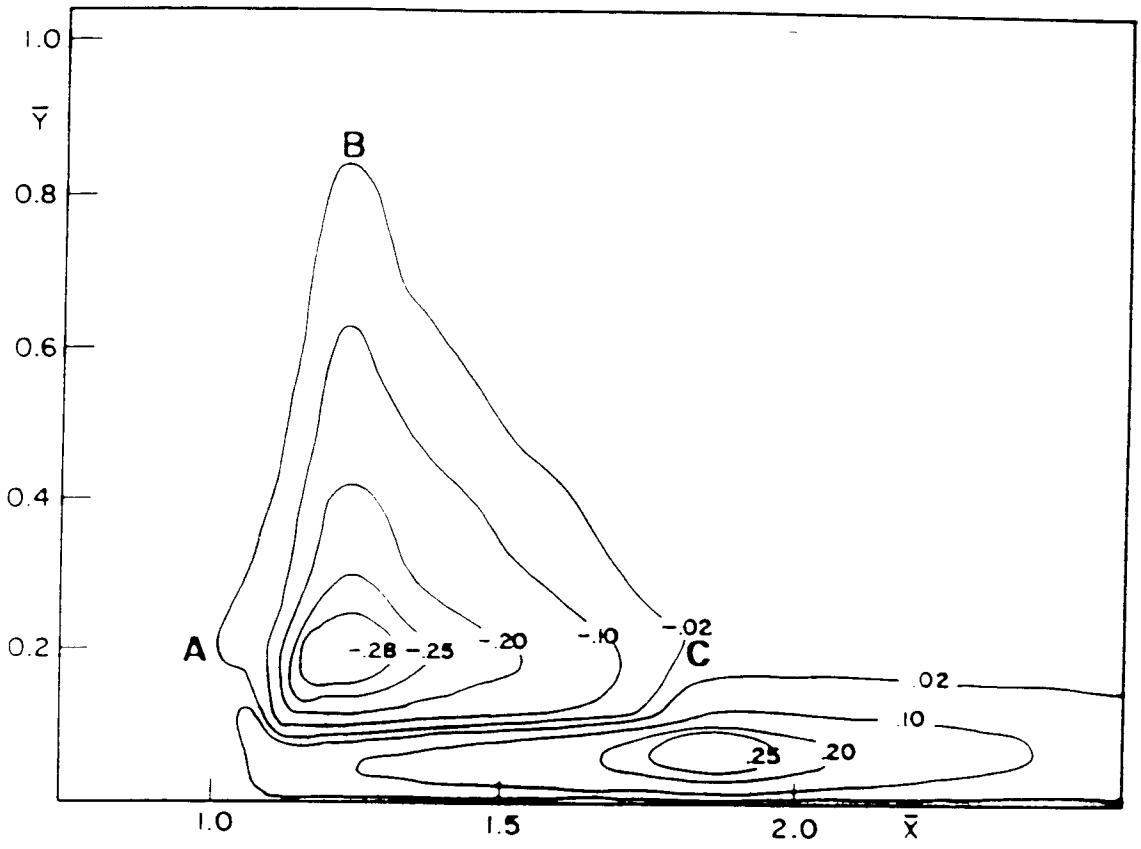
1.0
Ȳ
0.8
0.6
0.4
0.2
B
A
C
-.28 -.25
-.20
-.10
-.02
.02
.10
.25
.20
1.0
1.5
2.0
X̄

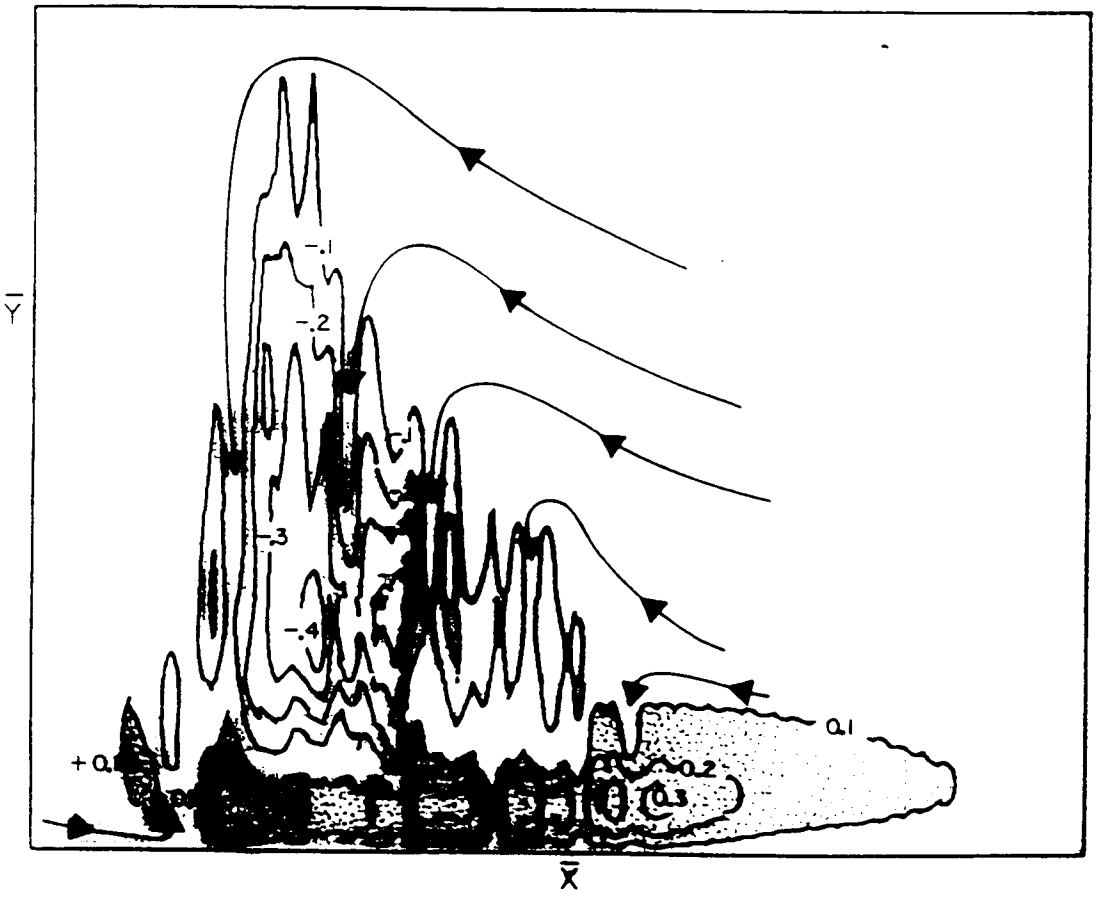
Ȳ
-.1
-.2
-.3
-.4
0.1
+0.1
0.2
0.3
X̄

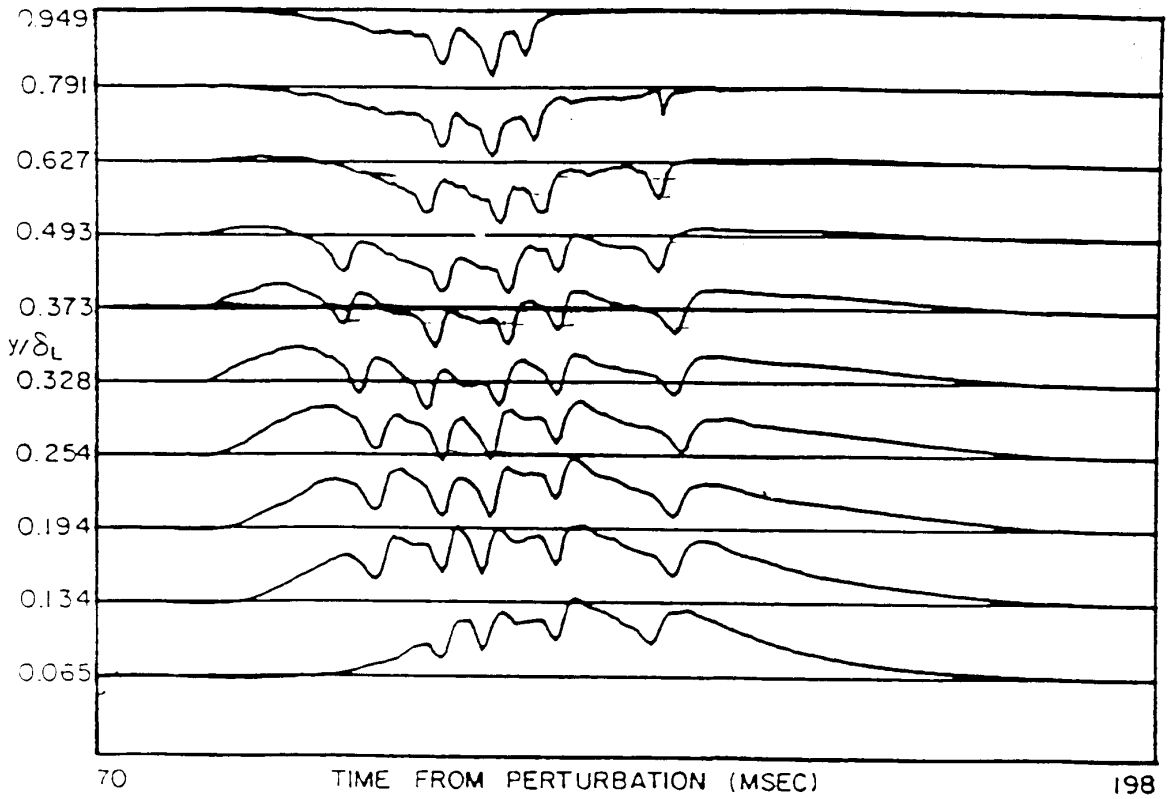
0.949
0.791
0.627
0.493
0.373
y/δL
0.328
0.254
0.194
0.134
0.065
70
TIME FROM PERTURBATION (MSEC)
198

FIG. 6 b

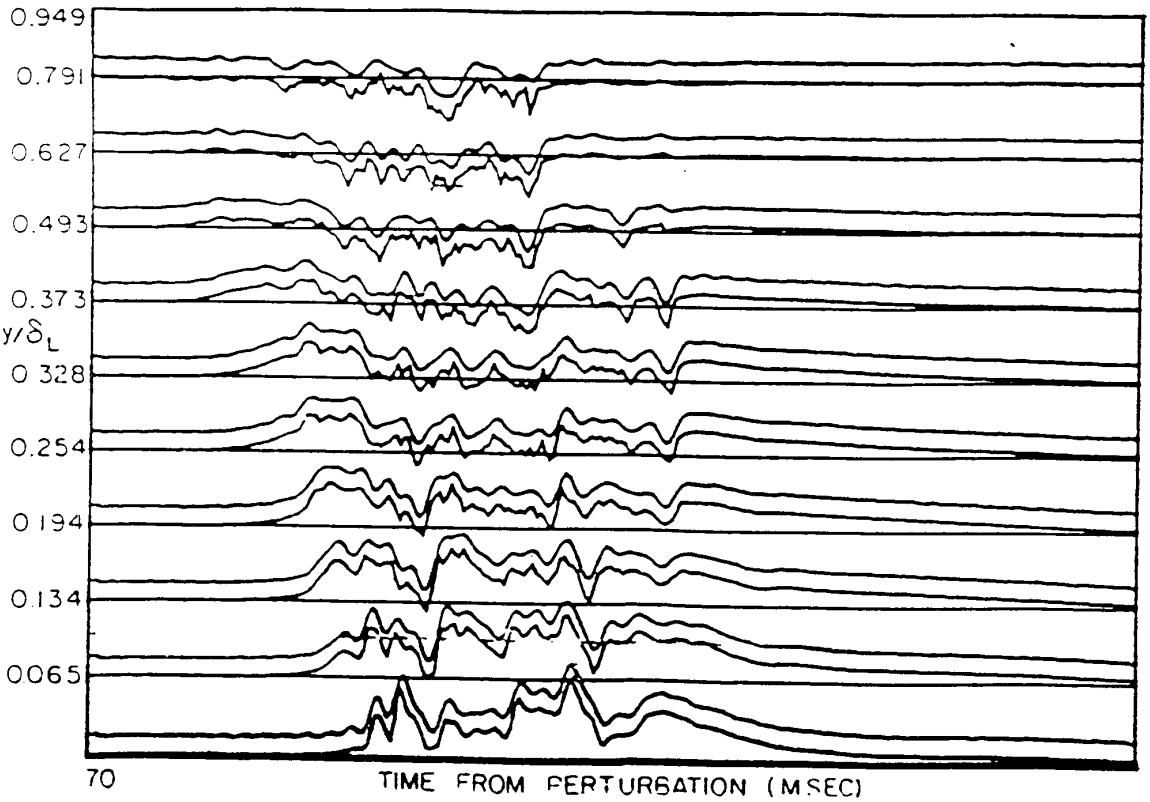
0.949
0.791
0.627
0.493
0.373
y/δL
0 328
0.254
0 194
0.134
0065
70
TIME FROM PERTURBATION (MSEC)

FIG 6 a

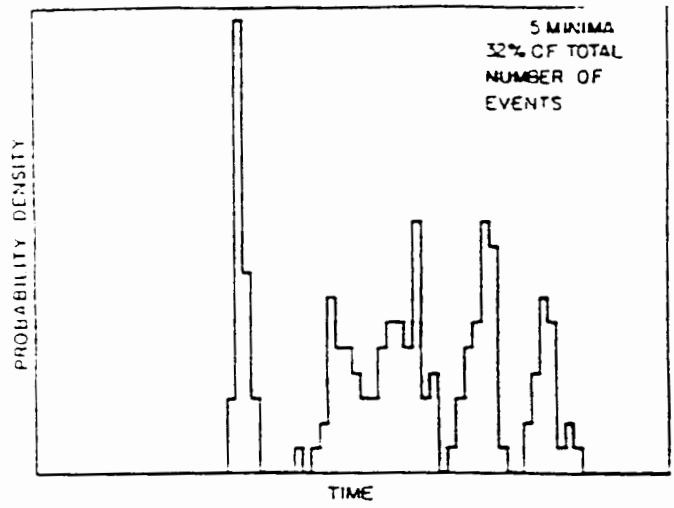

FIG. 7: HISTOGRAMS SHOWING THE PREFERRED TIME OF ARRIVAL OF EDDIES IN THE MOST PROBABLE SPOT AT A GIVEN LOCATION.

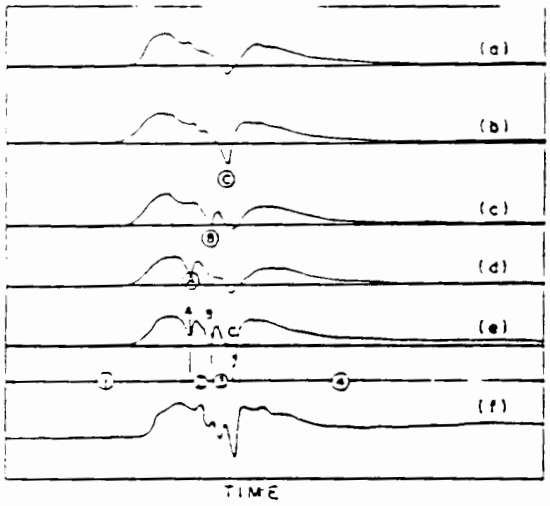

FIG. 8: A SCHEMATIC DIAGRAM SHOWING THE EDUCTION TECHNIQUE

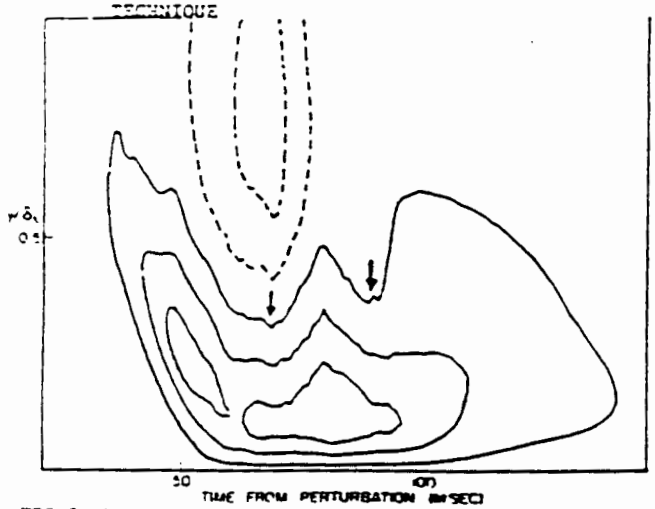

FIG.9: VELOCITY PERTURBATION CONTOURS RESULTING FROM A PASSAGE OF A SPOT a) simple ensemble average

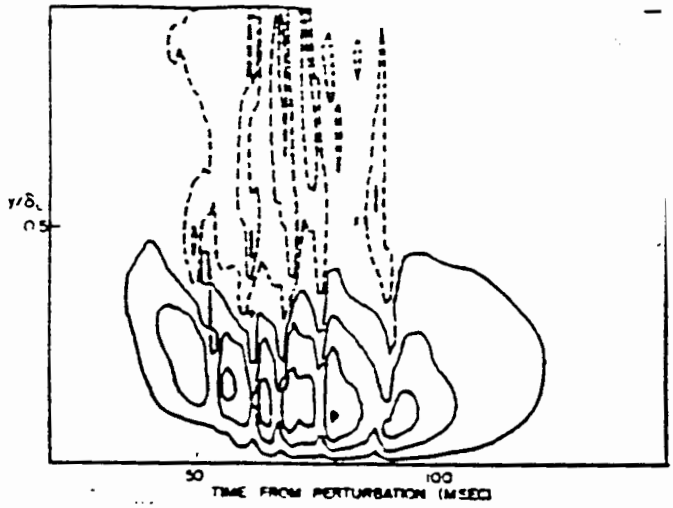

FIG. 9: b) the most probable realization

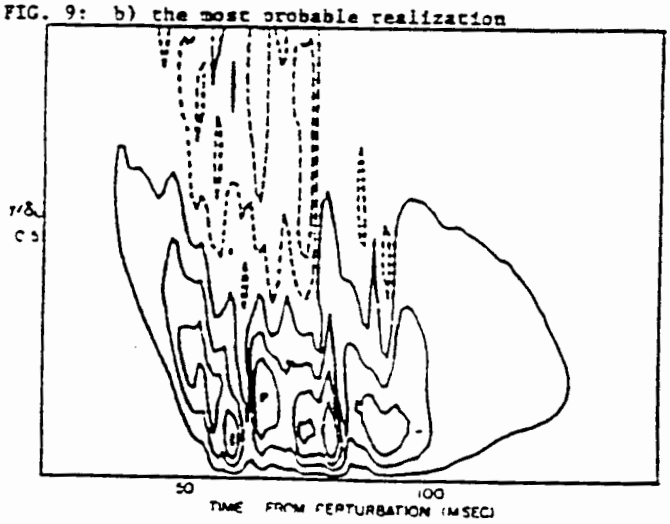

FIG. 9: c) a single realization

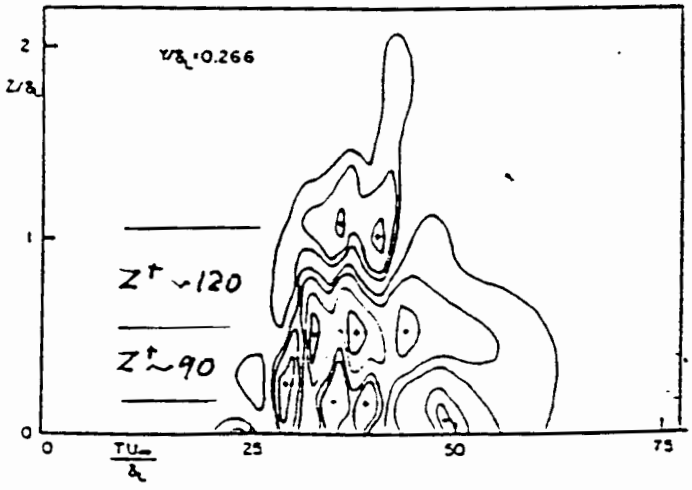

FIG. 10: PLAN VIEW OF A SPOT.

MOST PROBABLE REALIZATION

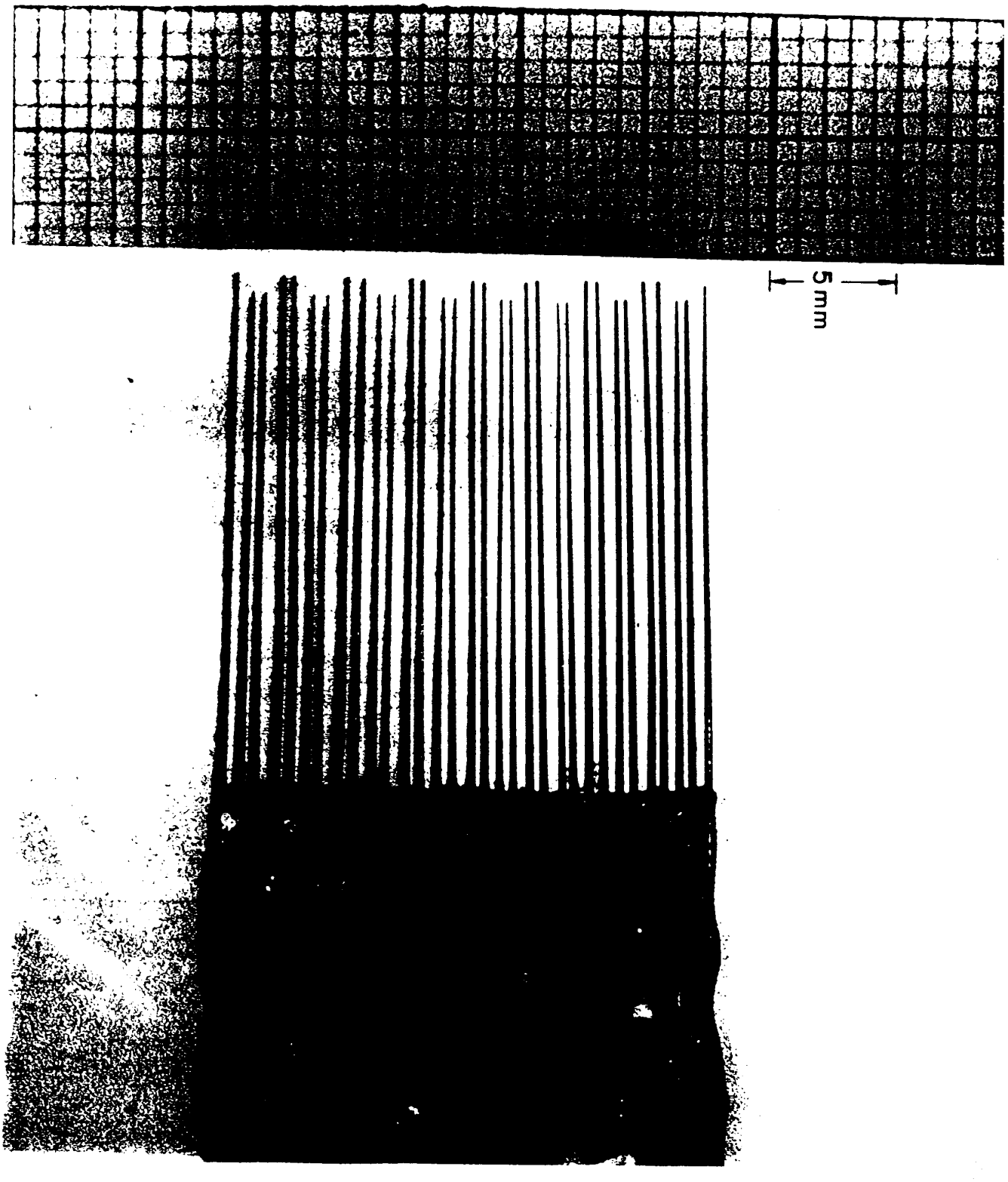
5 mm

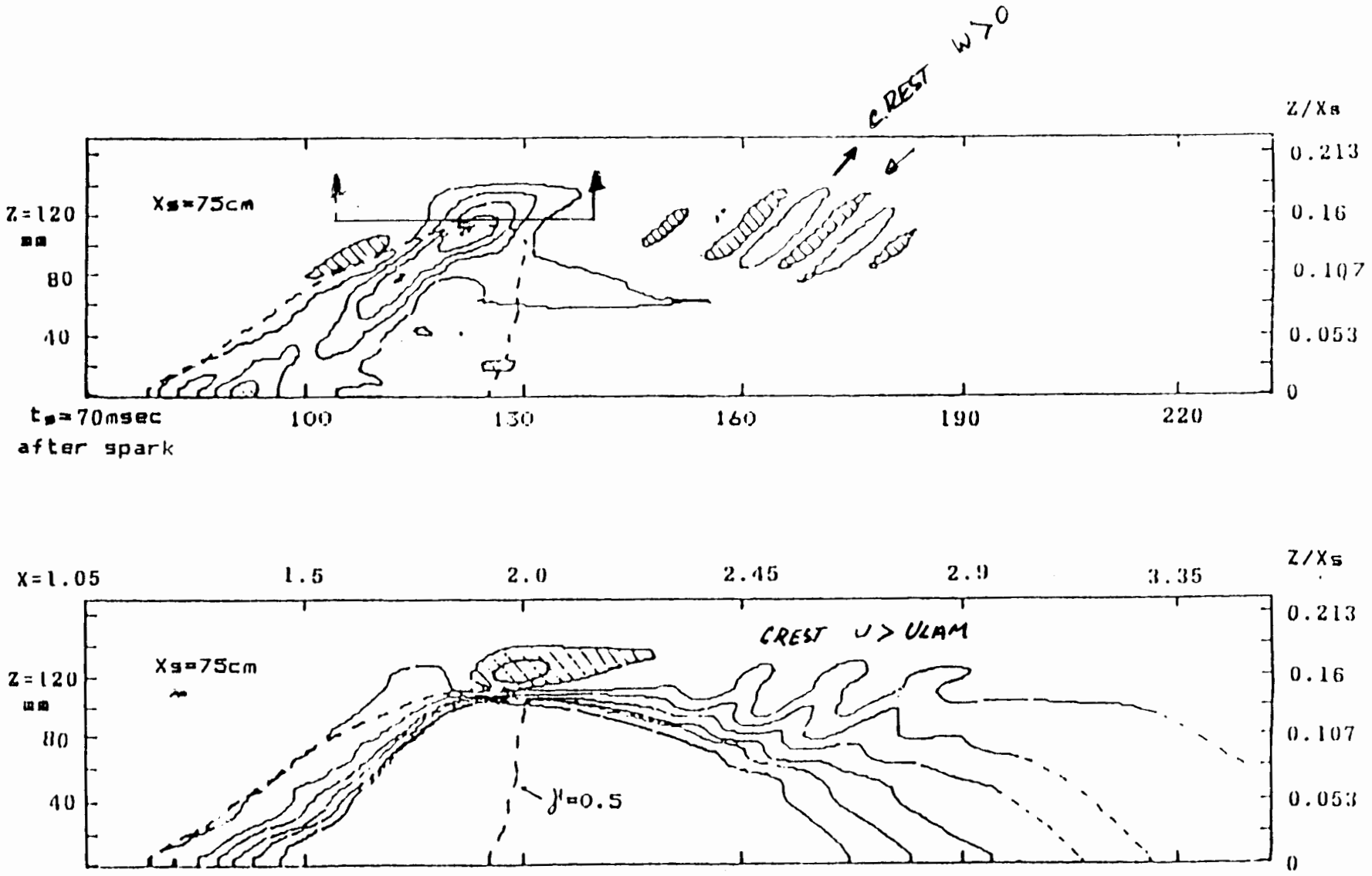

Fig. 4.2.4 comparison between Educed U pertubation (lower fig.) and Educed W (upper fig.) at Xs=75cm.

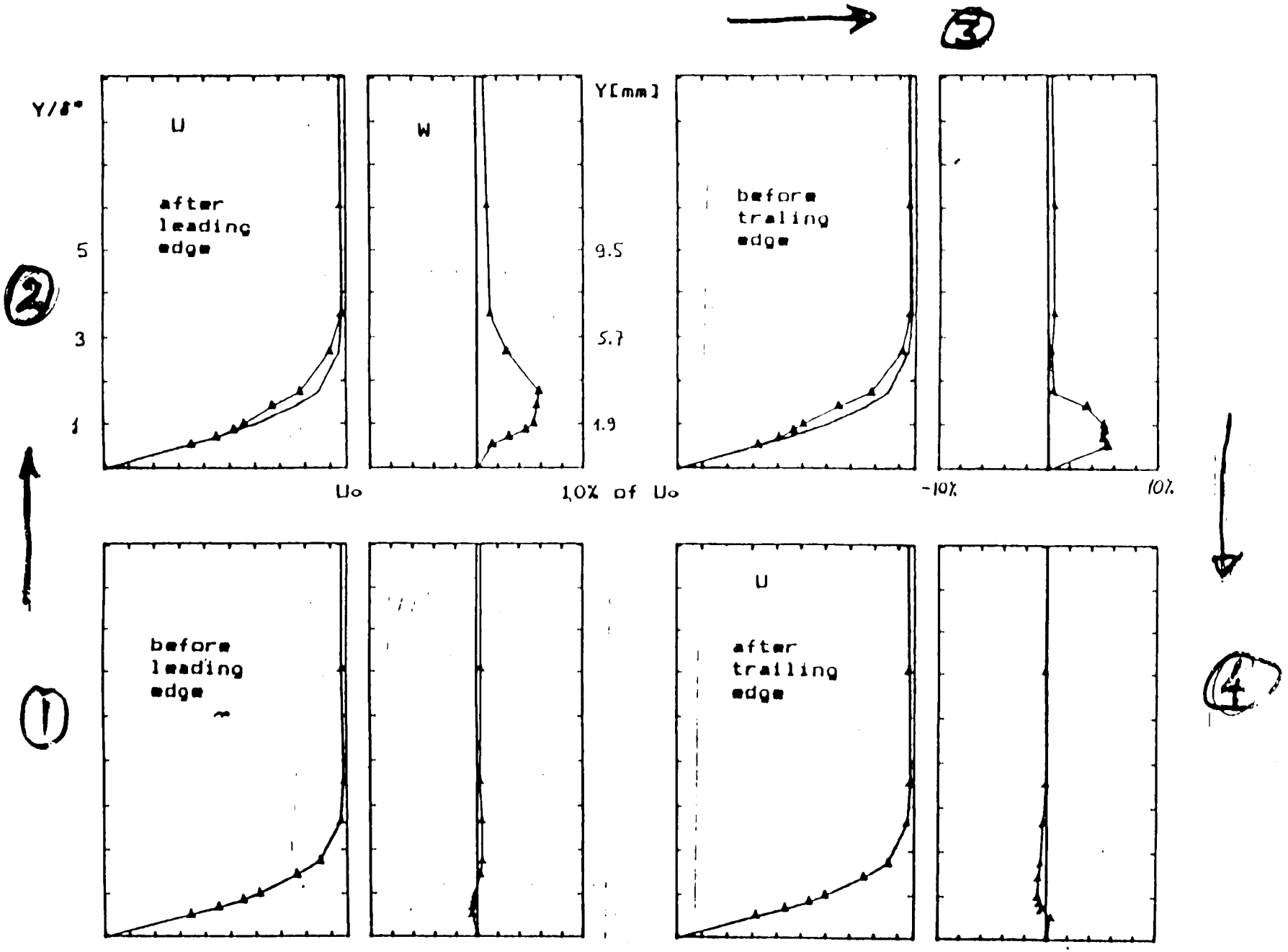

Fig. 6.7.5 Instantenous streamwise and spanwise velocity profiles on turbule laminar interface, in compare with laminar profiles. $Z/X_s=0.149$, for different times afetr spark. $\delta^* = 1.9$ mm

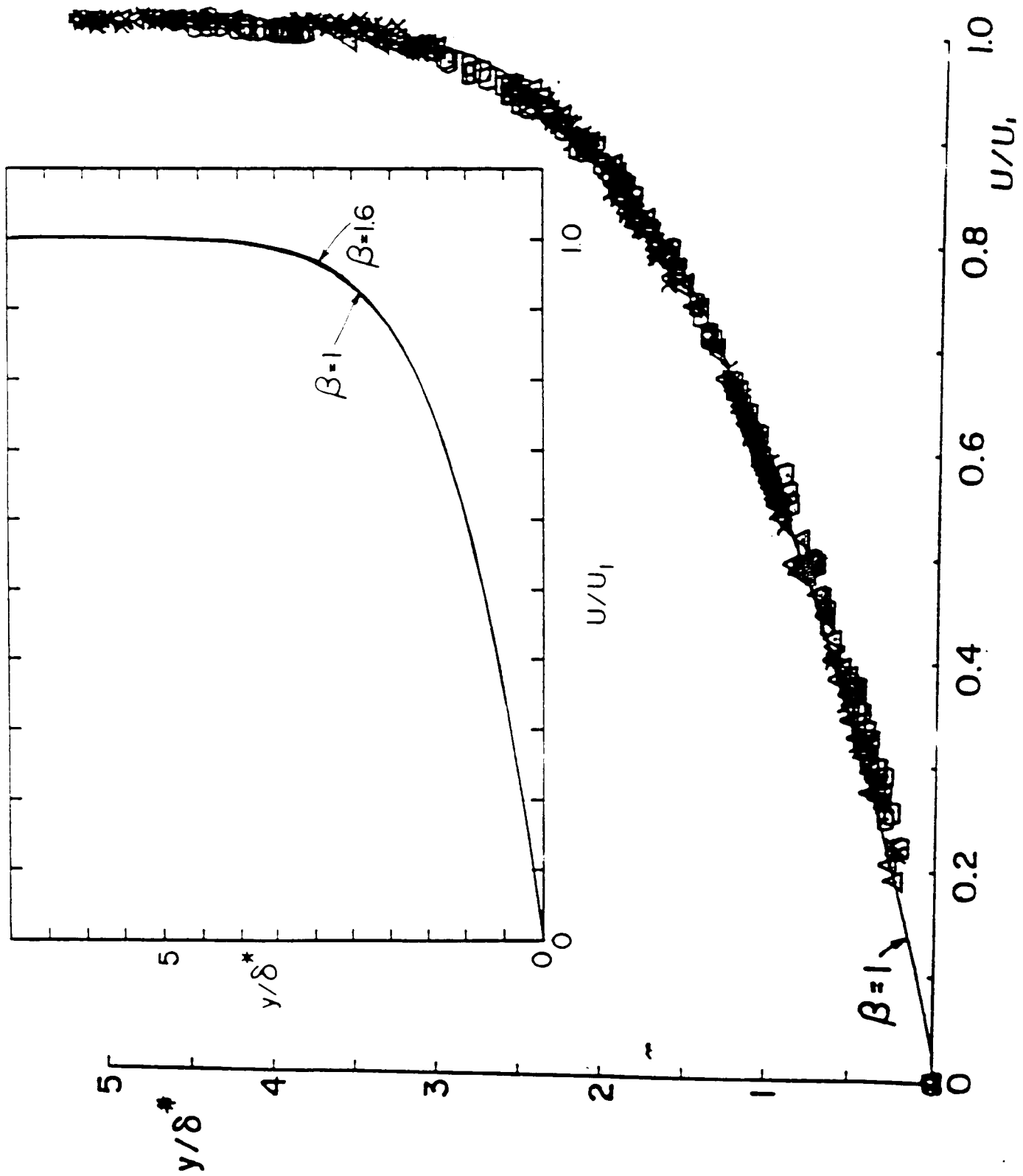
β=1.6
β=1
U/U1
y/δ*
β=1
U/U1
y/δ*

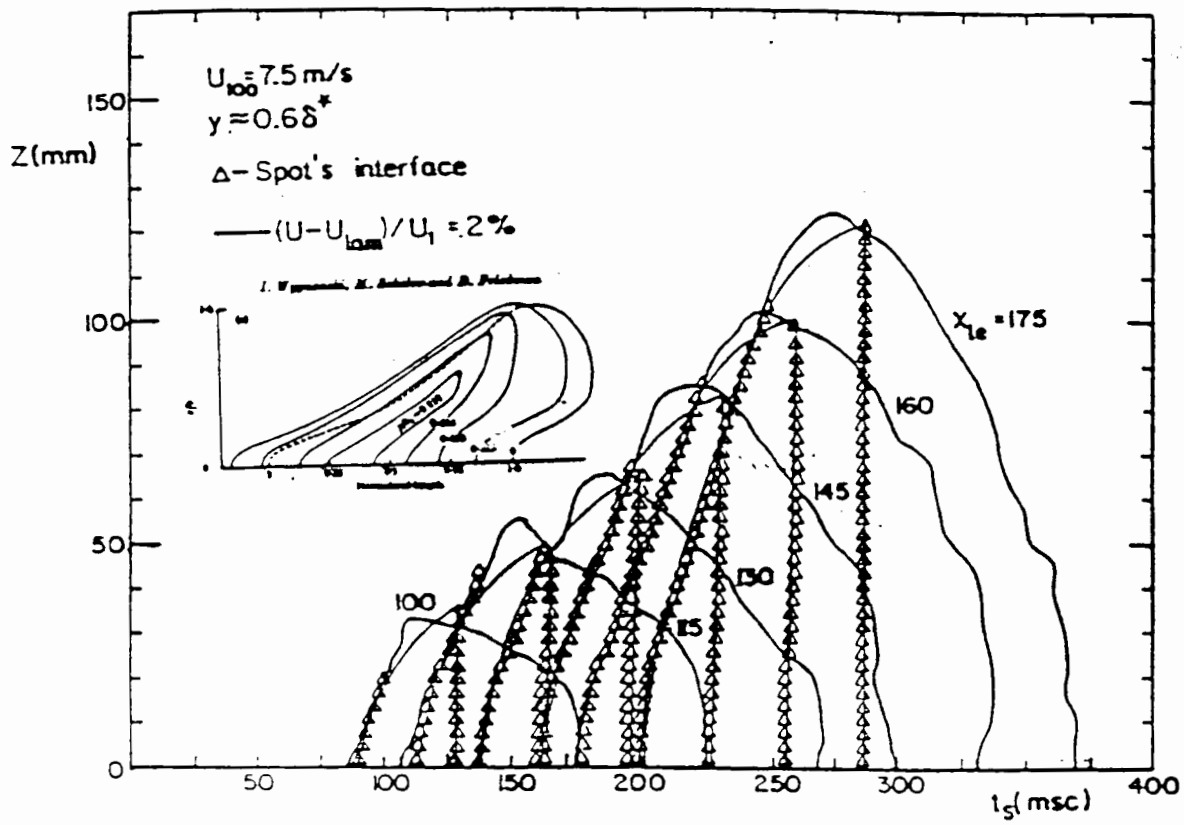
U_{100}=7.5 m/s
y ≈0.6δ*
Δ– Spot's interface
——(U–U_{100m})/U_1 =.2%
Z(mm)
150
100
50
0
50
100
150
200
250
300
400
t_5(msc)
X_{te}=175
160
145
130
115
100

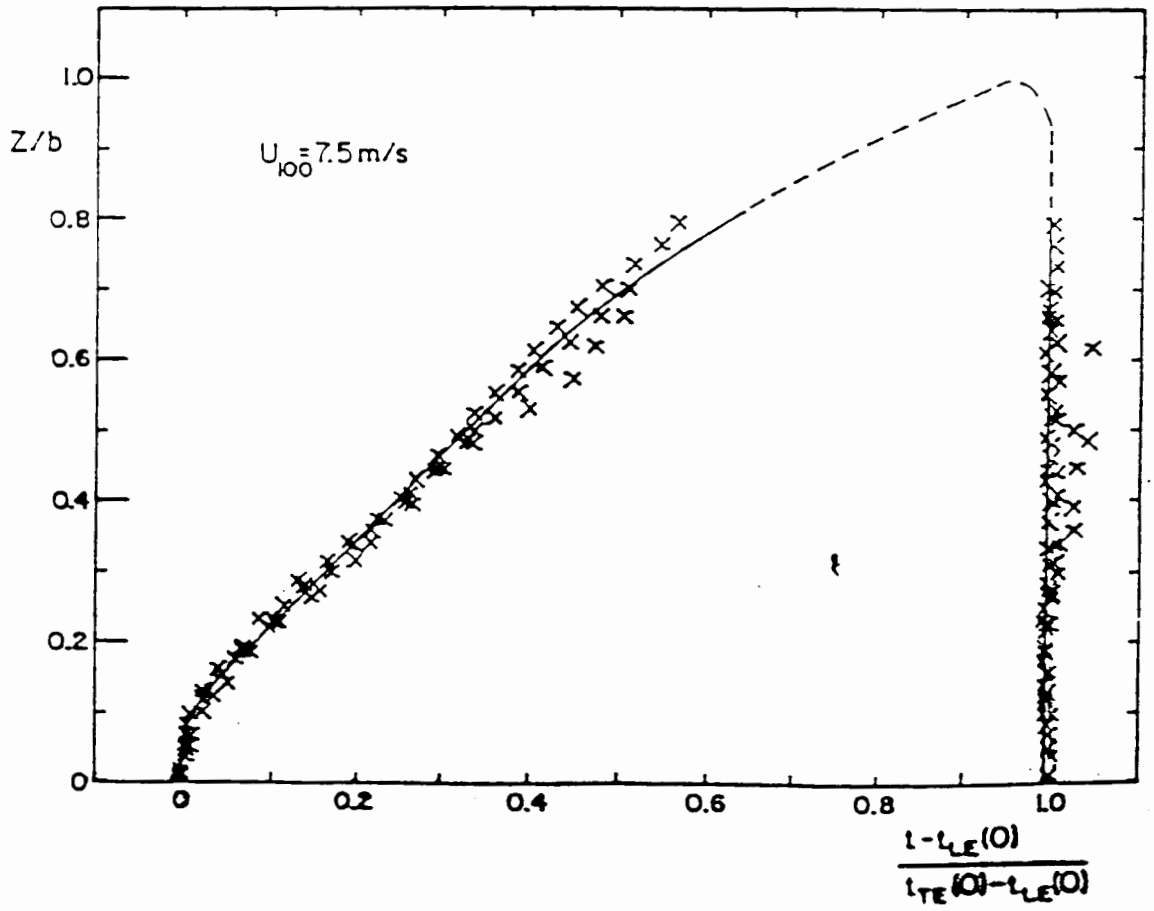
Z/b
U_{100}=7.5 m/s
1.0
0.8
0.6
0.4
0.2
0
0
0.2
0.4
0.6
0.8
1.0
$\frac{t-t_{LE}(0)}{t_{TE}(0)-t_{LE}(0)}$

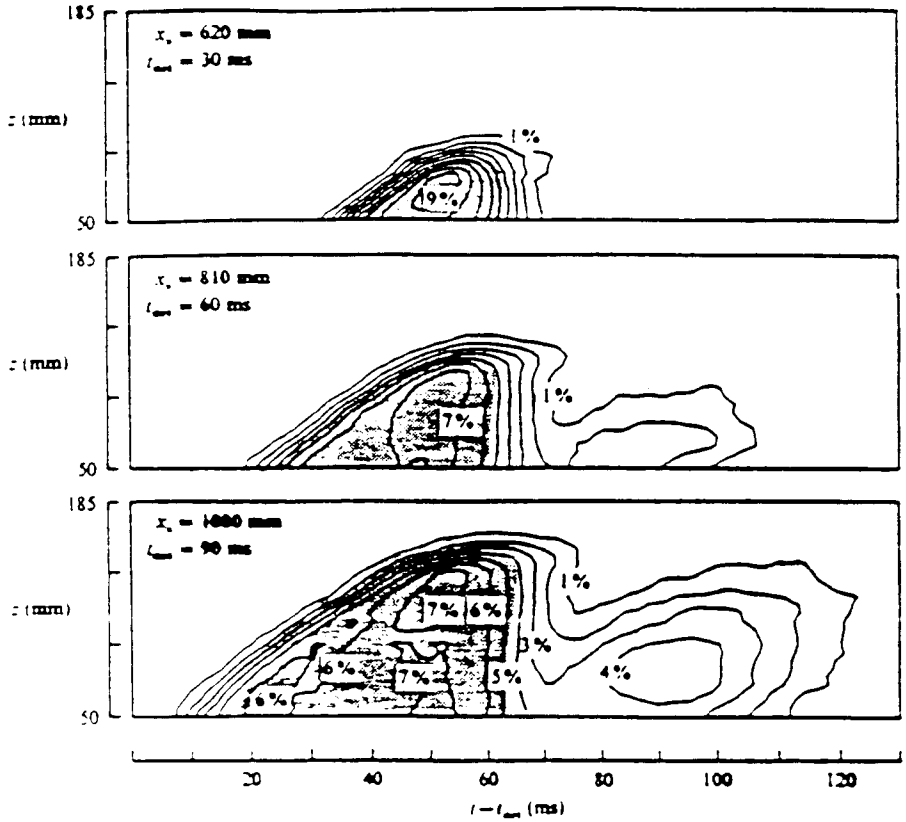

$\beta = 0$

FIGURE 6. Spanwise distribution of 'true' r.m.s. contours at the same locations as shown in figure 3. Contour levels are 1%–10% at intervals of 1%. The shaded area indicates $\gamma > 50\%$.

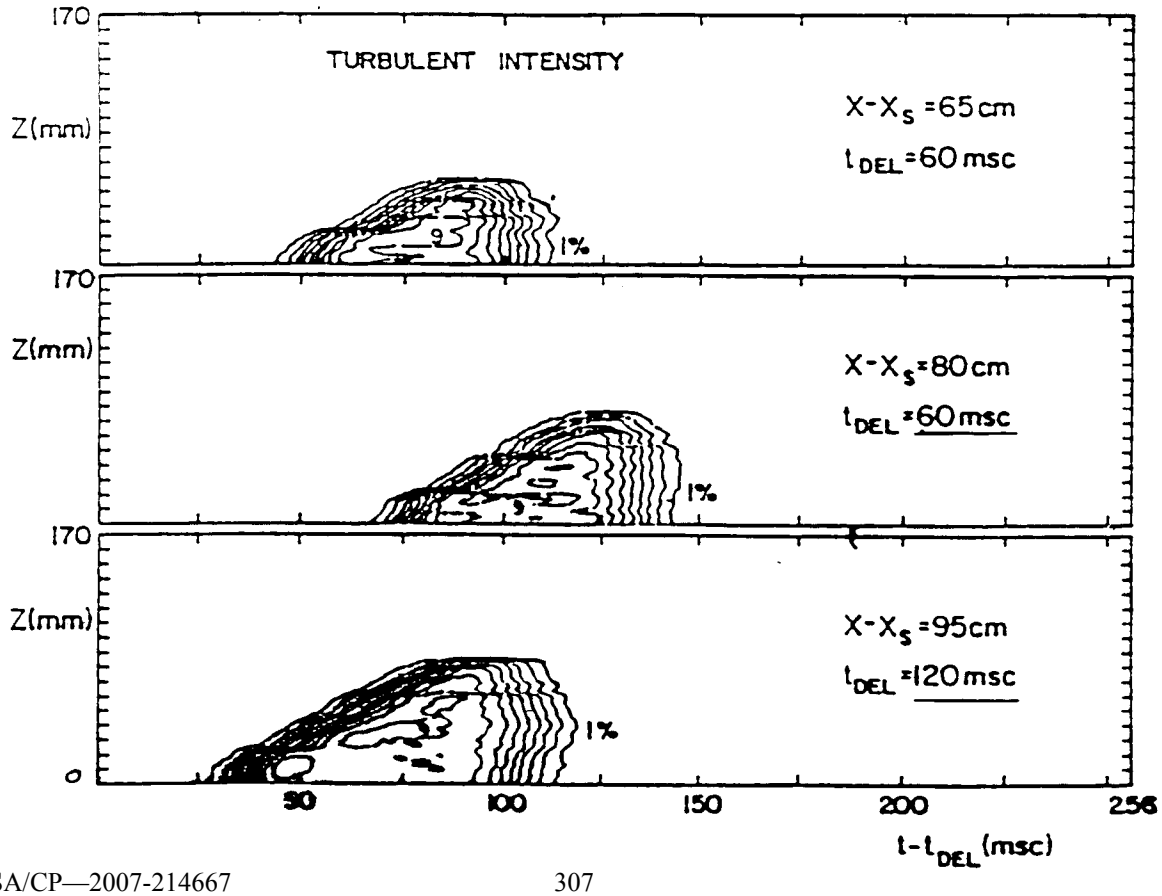

$\beta = 1.0$

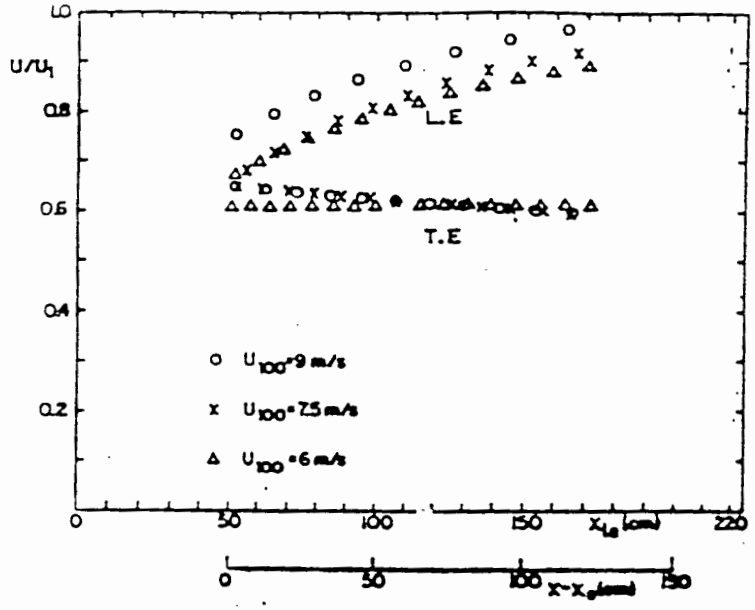

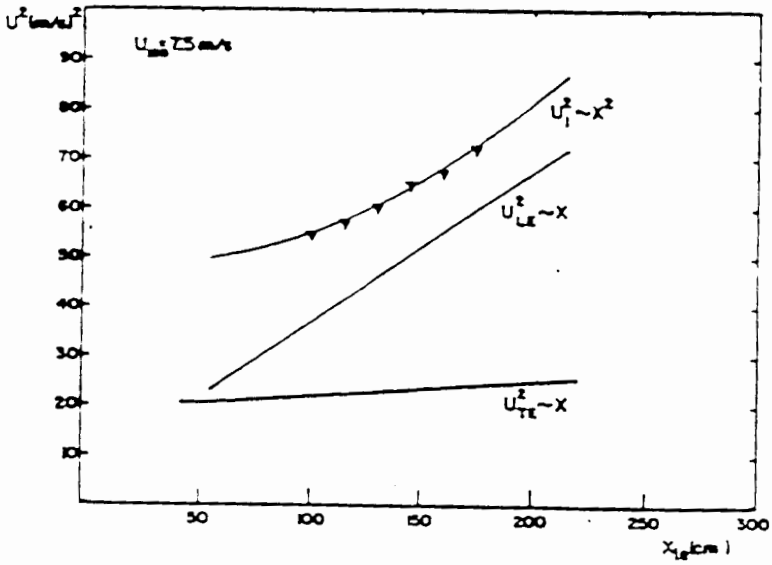

$$\frac{\delta_{INT.}}{U_r} = \frac{\rho}{\mu}\int \delta_j^{\beta} R_{e\delta_r^*j}^{\frac{x}{}}$$

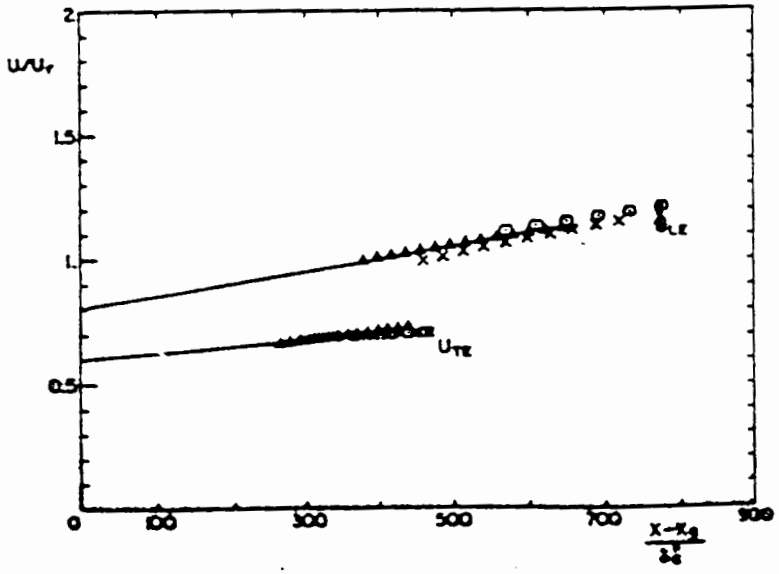

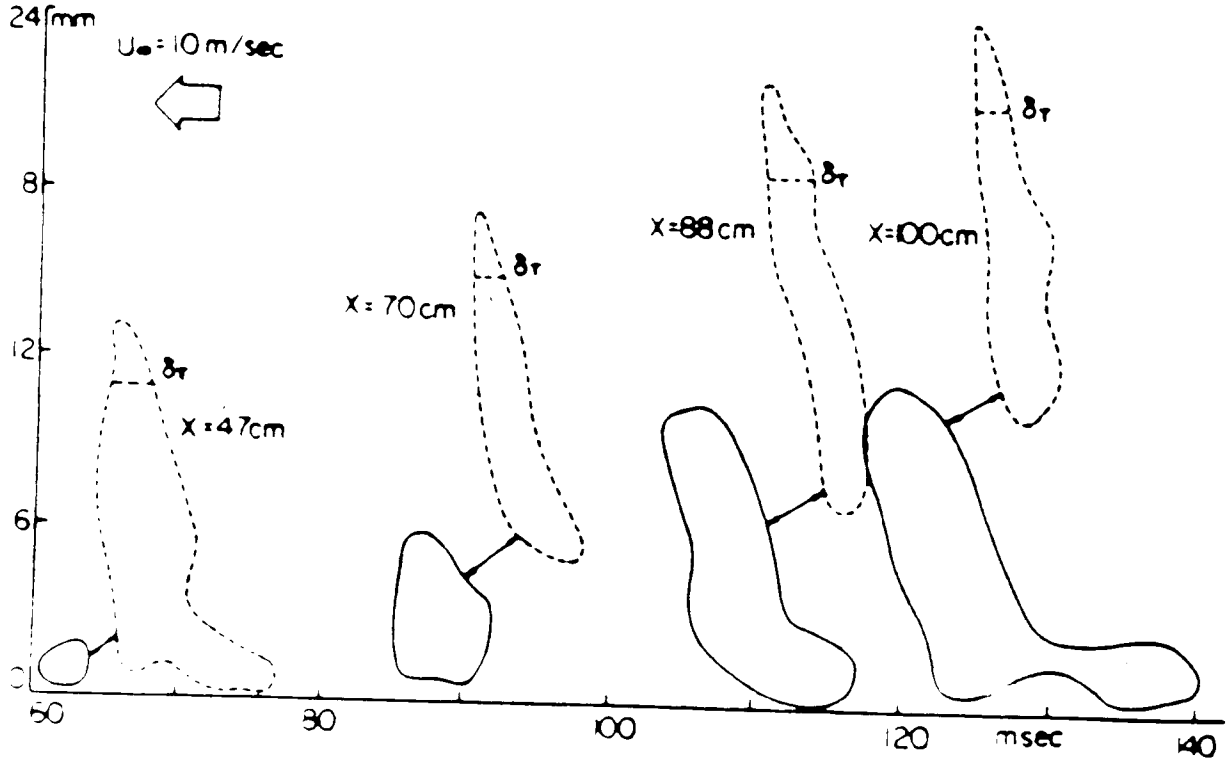
24 mm
U_∞ = 10 m/sec
8
12
6
0
δ_T
X = 47cm
X = 70cm
X=88cm
X=100cm
50
80
100
120
msec
140

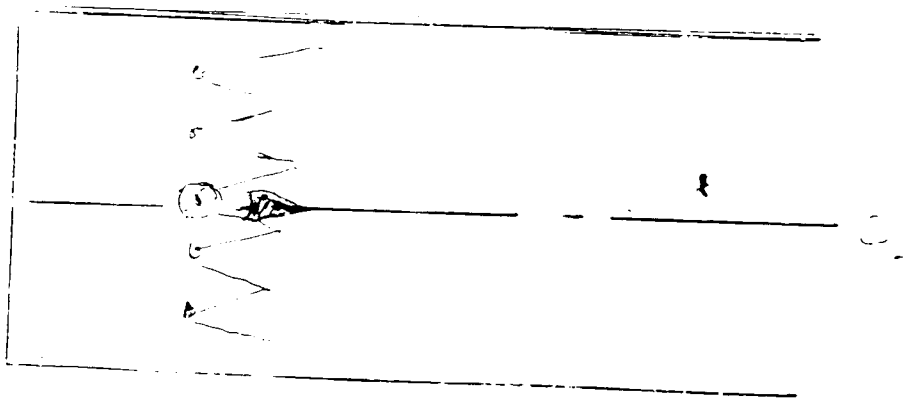

Some Scenarios for Transition on Turbomachinery Blading

J.P. Gostelow
University of Technology
Sydney, Australia

Abstract

Measurements on transition under different levels of adverse pressure gradient and free-stream turbulence level are described. This extensive series of investigations, which was predicated on intermittency measurement techniques, has resulted in correlations for transition length and turbulent spot formation rate. These correlations are intended to be used in conjunction with boundary layer prediction methods and examples are given of such predictions. More effective predictions of the transition region, especially under conditions of variable pressure gradient, are dependent on a more comprehensive understanding of transition and spot behavior. It is expected that this will result in improved transition modeling.

Measurements of natural and by-pass transition on a flat plate are described in which transition may occur by means of turbulent spots or alternatively by a subharmonic route having a low frequency cascading of discrete and periodic events. Breakdown mechanisms are discussed and evidence is presented on breakdown mechanisms within an incipient spot. Free-stream turbulence is presented as a by-pass inducing mechanism and work on spots resulting from such a by-pass is discussed. Insight on the structure of spots can be gleaned from such a study of these rather extensive by-pass spots. The work on spots extends to the adverse pressure gradient case and comparative information is provided on the growth and development of spots under zero and adverse pressure gradients.

SOME SCENARIOS FOR TRANSITION ON TURBOMACHINERY BLADING

J.P. GOSTELOW

A rather broad and grandiose title for what I now propose to do, which is to outline some of the work we have been doing in Sydney on transition under adverse pressure gradients. There have been three main phases so far:-

(i) **Transition length experiments** under linear adverse pressure gradients and varying free-stream turbulence levels.

(ii) **Work on triggered spots under moderate linear adverse pressure gradient.** Free stream turbulence level of 0.3% and comparison with zero pressure gradient.

(iii) **Work on triggered spots under controlled diffusion adverse pressure gradient.** Carefully selected critical conditions allowing comparison between different transition scenarios.

(i) **Transition Length Experiments.** Below is given the complete data set in one of the presentation formats we are using. Correlations of the data have been produced and published in ASME and other venues.

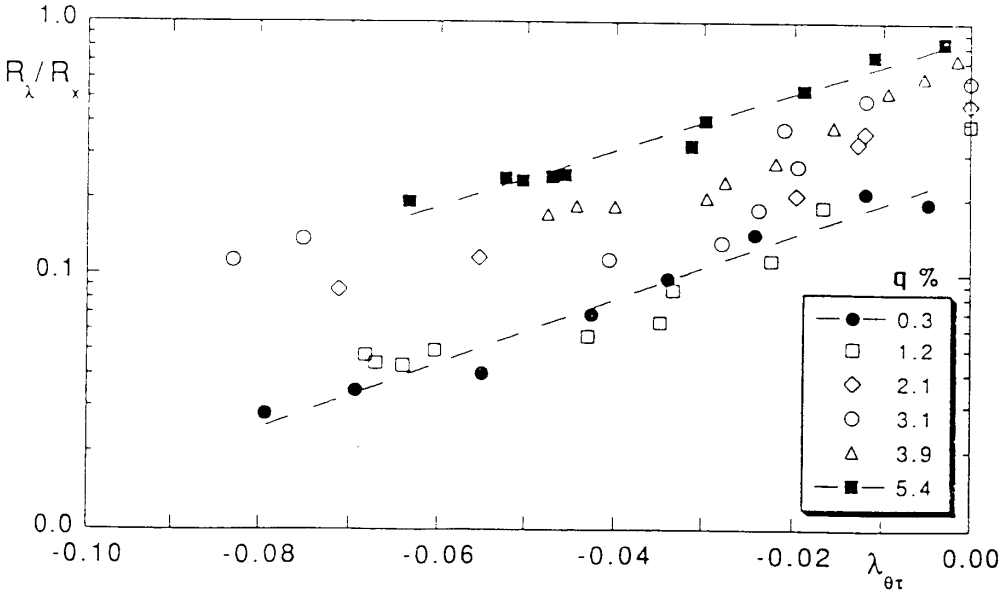

Transition length normalized by distance as a function of transition inception pressure gradient parameter.

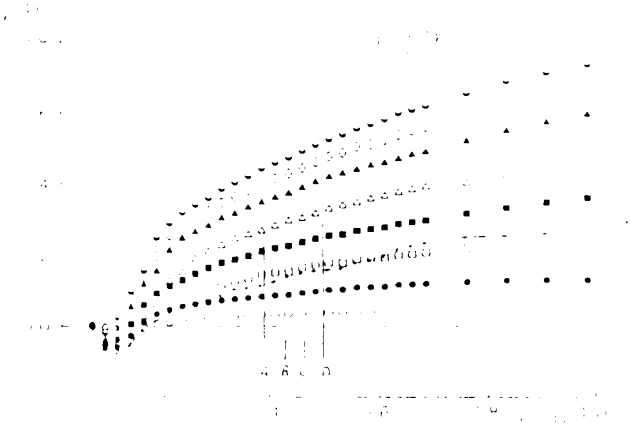

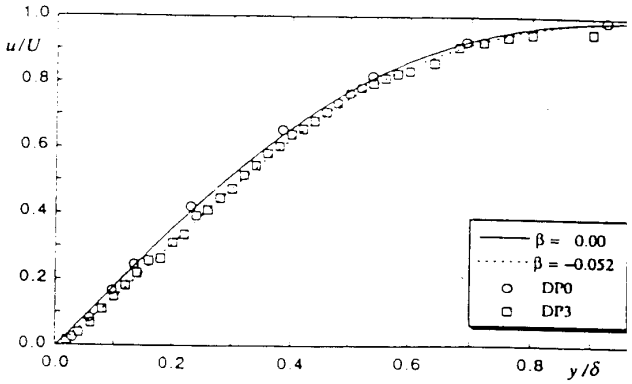

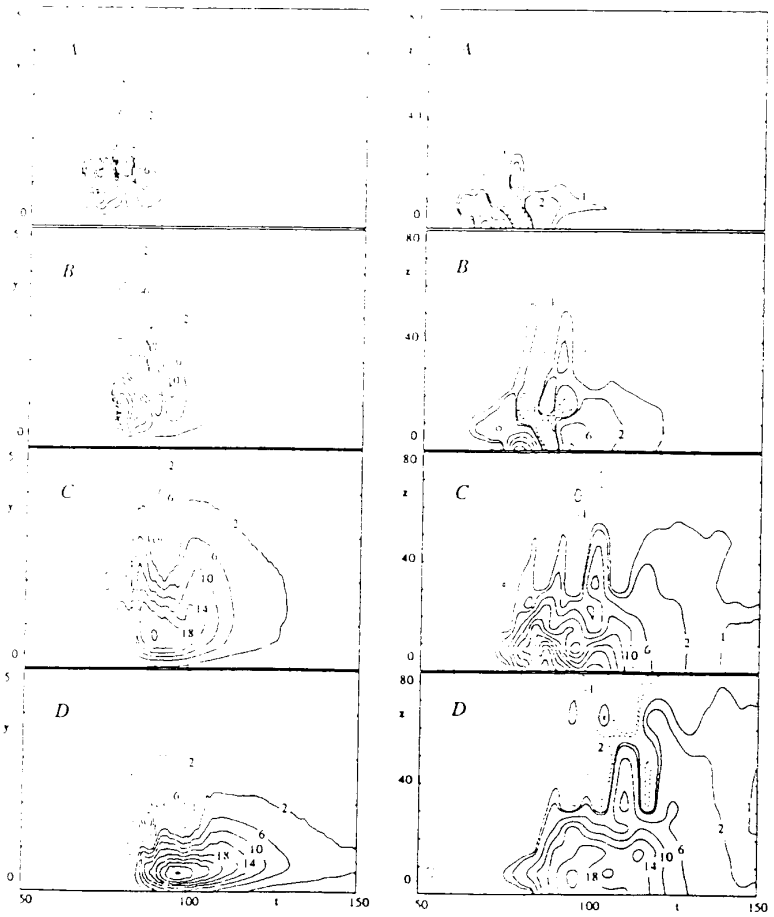

CONTOURS OF VELOCITY PERTURBATION $(u-u_0)/U$ ON THE CENTER-LINE IN THE y-t PLANE.

CONTOURS OF VELOCITY PERTURBATION $(u-u_0)/U$ AT A HEIGHT OF 1.2mm IN THE z-t PLANE.

(ii) Triggered Spots under Moderate Linear Adverse Pressure Gradient.

Above are given the pressure gradients used for phase (i), given as discrete points, and thatused for phase (ii), as a continuous line. Spots were measured at streamwise locations A,B,C,D. Also above is given the velocity profile comparison with appropriate Falkner -Skan parameters.

On the left are given the contours of velocity perurbation in the y-t and z-t planes.

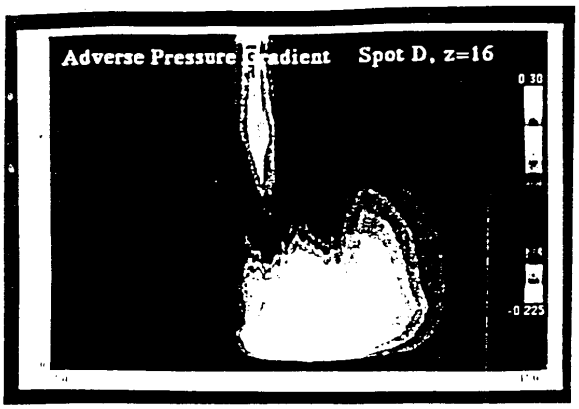

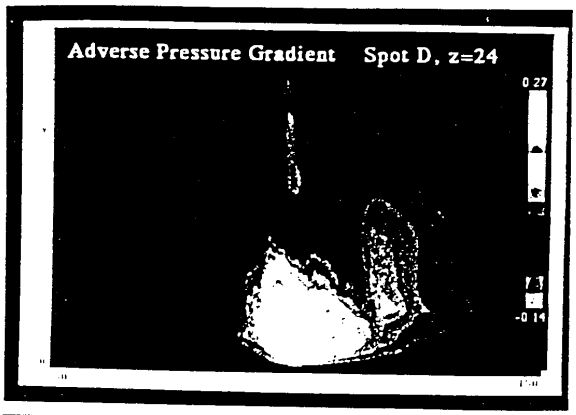

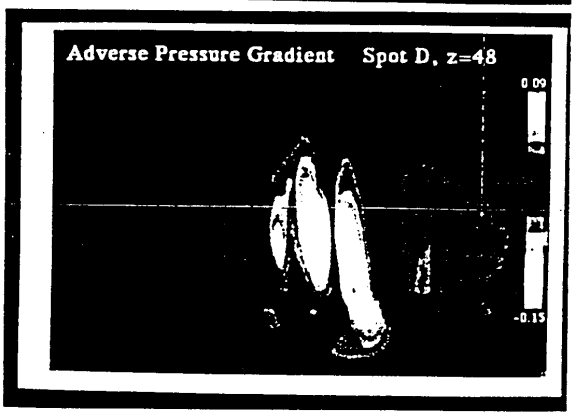

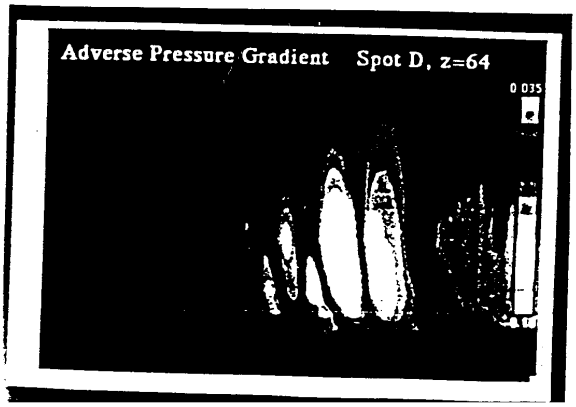

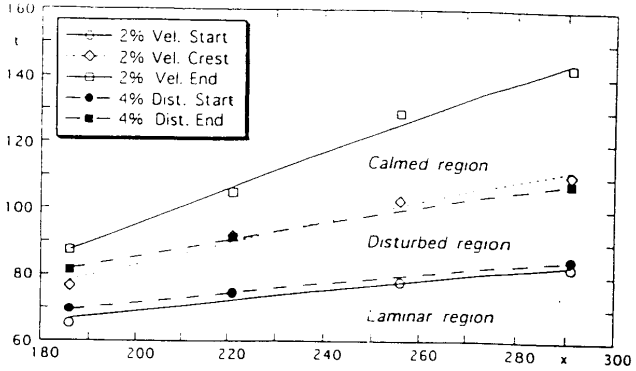

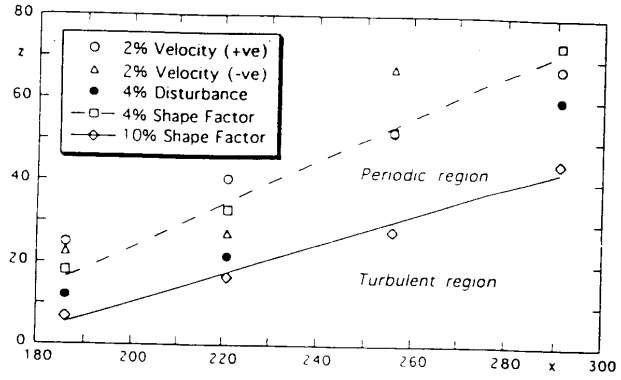

On the left hare are given velocity perturbation contours for the D spot at different z locations. Whilst near the center-line the differences from a zero pressure gradient spot are not profound, the outer region is not a turbulent spot. It is a highly amplified wave packet which has managed to keep abreast of the spot.

Above are given x-t and z-t plots. These enable celerity and spreading rate to be determined. On the basis of these results the leading edge of the adverse pressure gradient spot propagates at 80% of free stream velocity, the trailing edge of the turbulent region at 50% U and the trailing edge of the calmed region at 23% U. The attendant wave packet propagates at a somewhat familiar 39% U. The turbulent region of the spot spreads at a half angle of 20° and the wave packet has a detectable spreading half angle of 29°.

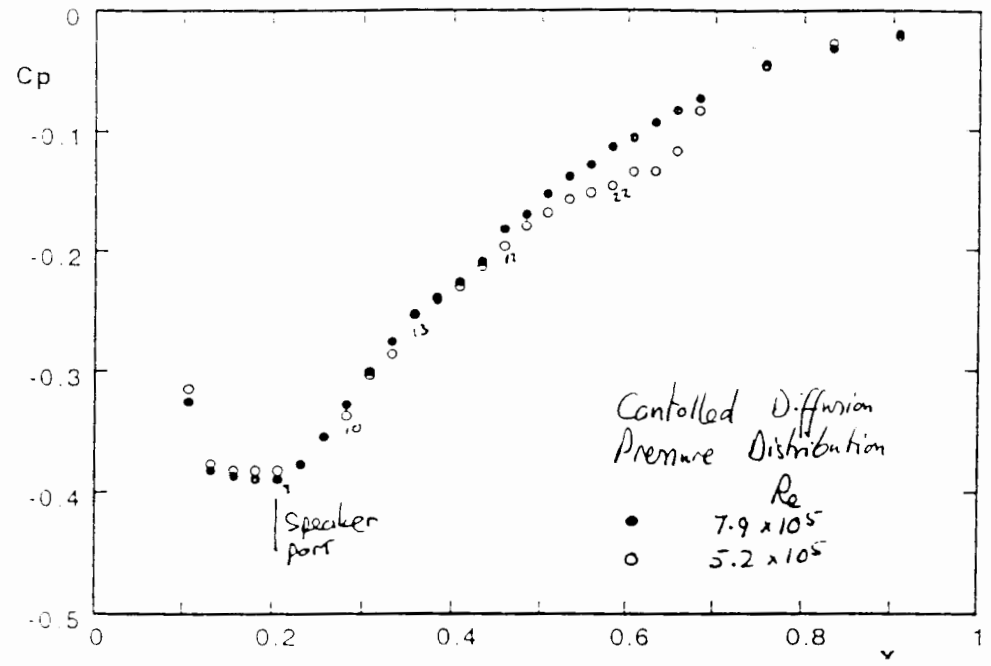

(iii) **Triggered Spots Under Controlled Diffusion Adverse Pressure Gradient.** Above is given the controlled diffusion pressure distribution being investigated; typical of a compressor stator. Initial tests reported here in preliminary form are for the higher Reynolds number (unseparated boundary layer). Triggering is such that the disturbance decays and then becomes amplified. The evolution from wave packet to spot is not by a by-pass mechanism.

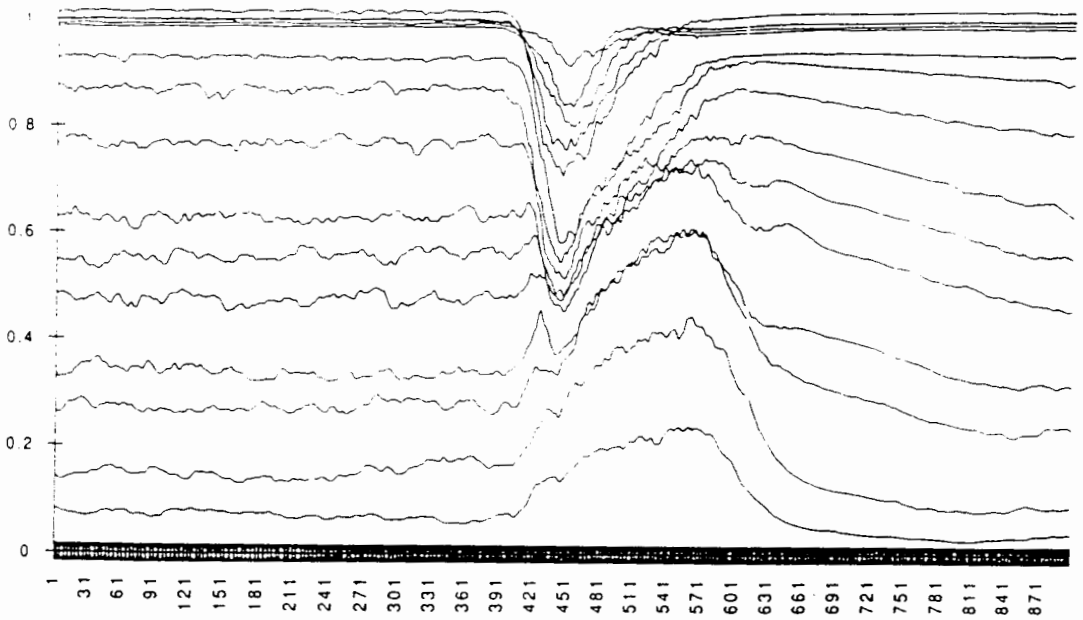

In these results it is possible to compare growth rates of the spot and the adjacent and competing natural transition of strongly amplified disturbances. Above are given some phase-averaged velocity traces for a situation where the surrounding boundary layer is in a transitional state.

These results are raw data for the spot as it develops in the streamwise direction. The station numbers are identified and stations are 50 mm apart in a streamwise direction.

Stations 19 and 20 are essentially "don't even think about it" territory. The ensemble of 30 raw traces in the lower figure was taken at station 19. The most recognisable feature of the spot remaining is the calmed region. This feature remains visible well into the turbulent layer. Phase averaging also reveals spot structure which remains well into the turbulent layer.

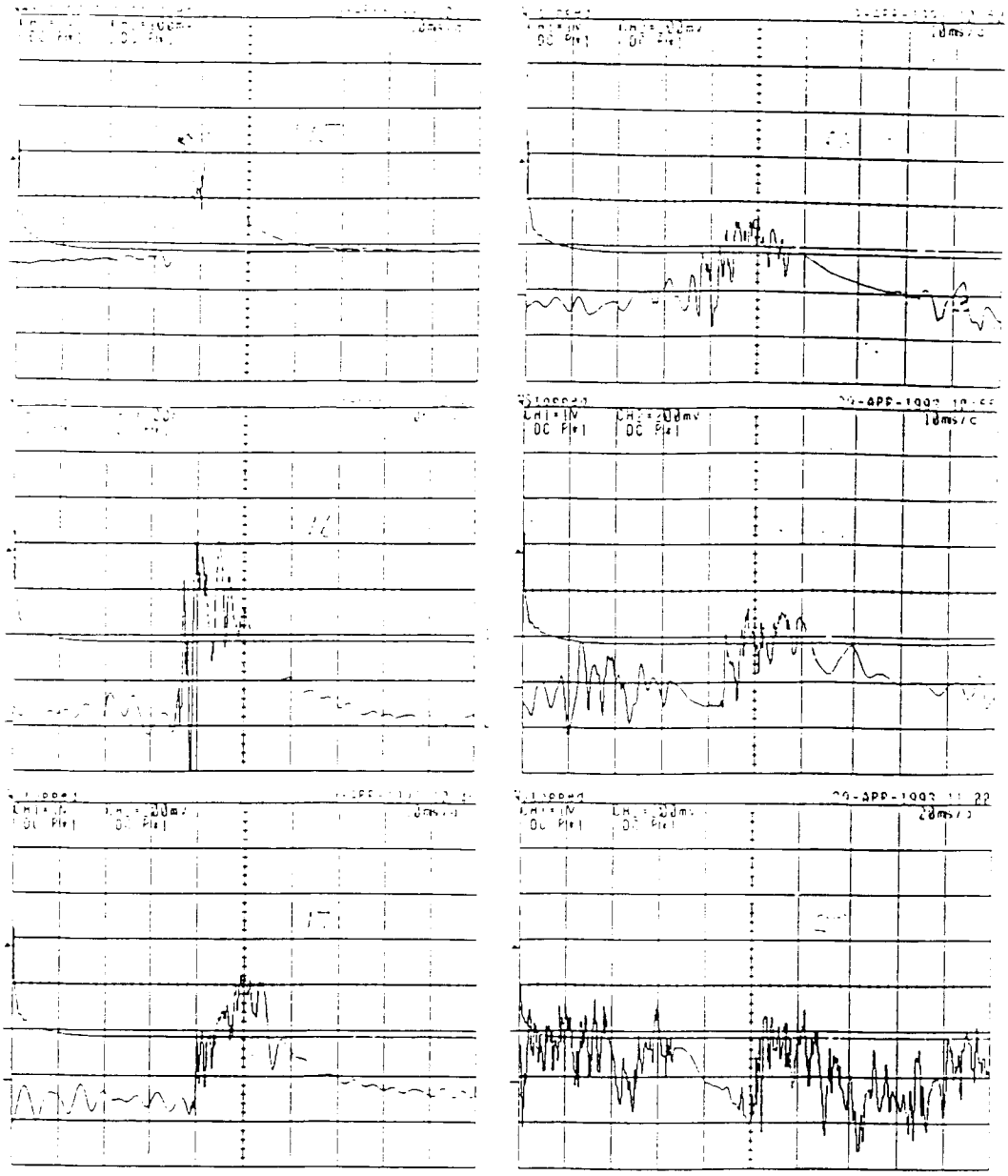

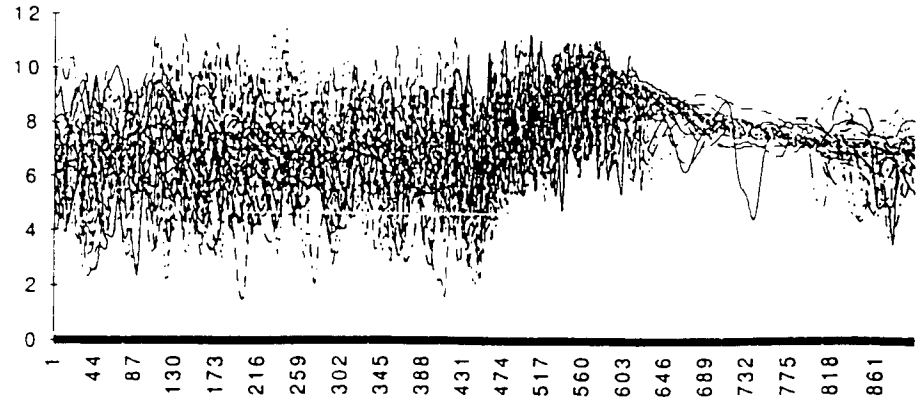

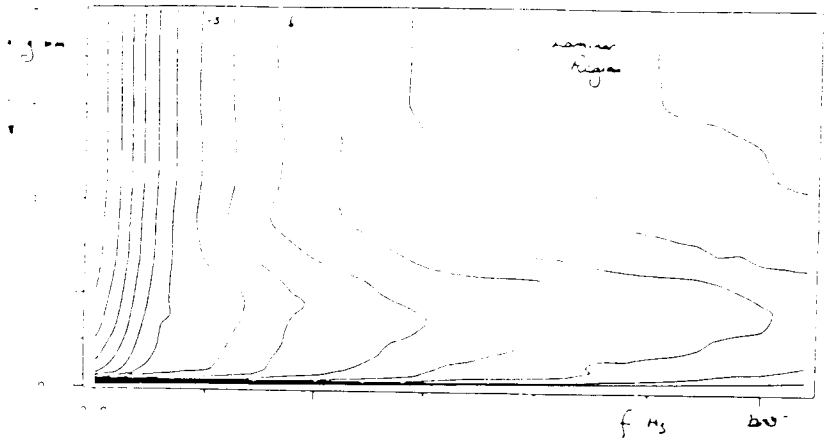

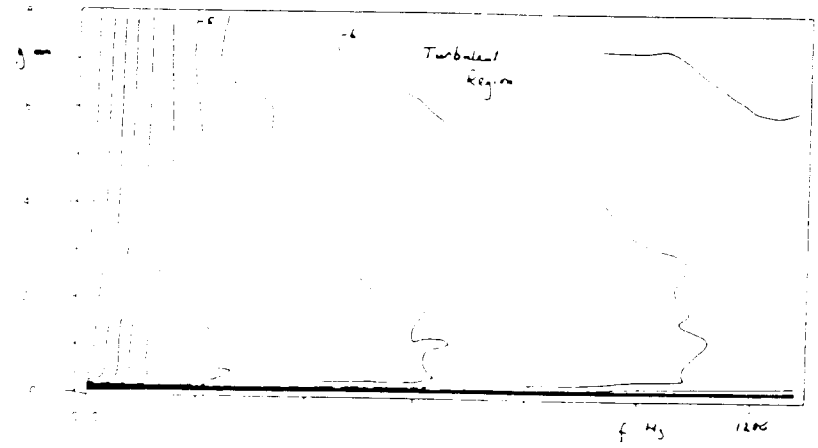

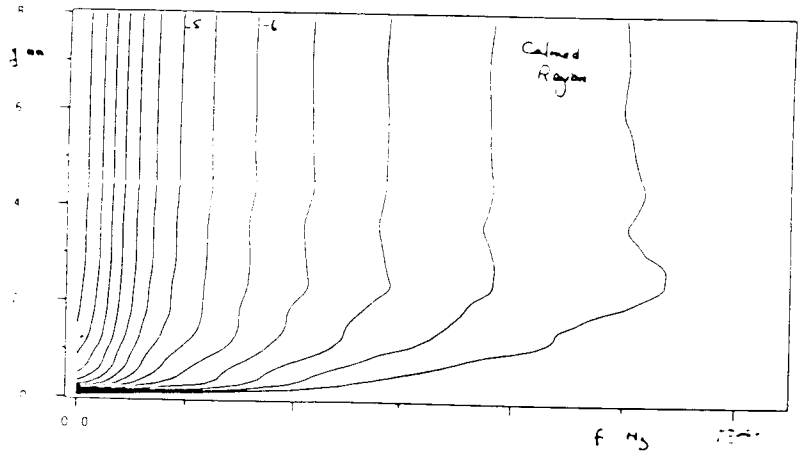

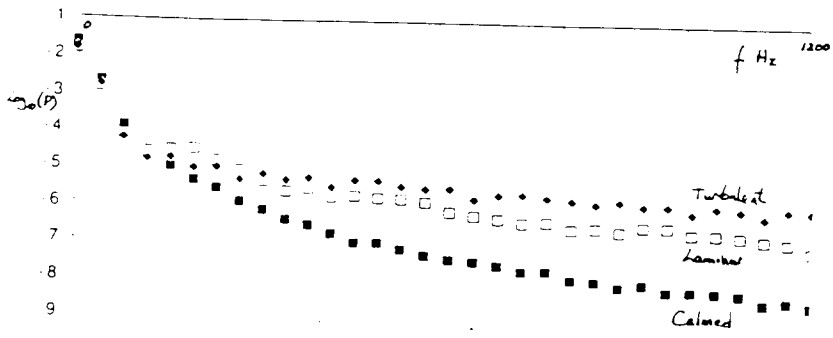

These power spectra have been presented in the form of y-f plots. The contours are of constant power density on a log basis. The lower of the four figures is a more conventional spectrum for the laminar, turbulent and calmed regions of a spot. The calmed region is obviously the most quiescent, the surrounding laminar layer shows the effects of strong disturbances at the fundamental frequency and higher, especially around a height of one displacement thickness. The turbulent region shows a filling in of the spectrum and a spreading of the higher turbulence components throughout the boundary layer.

These are only preliminary results and any suggestions for data analysis would be appreciated.

The important point is that this is an experiment which will permit a side-by-side comparison of most of the known transition scenarios which are relevant to turbomachinery blading. The value and importance of the adverse pressure gradient situation is that it presents a sounding board which enables us to probe and compa these different scenarios.

Turbulent-Spot Growth Characteristics : Wind-Tunnel and Flight Measurements of Natural Transition at High Reynolds and Mach Numbers

J.P. Clark, T.V. Jones
University of Oxford
Oxford, U.K.

J.E. LaGraff
Department of Mechanical, Aerospace and Manufacturing Engineering
Syracuse University
Syracuse, NY 13244

Abstract

A series of experiments are described which examine the growth of turbulent spots on a flat plate at Reynolds and Mach numbers typical of gas-turbine blading. A short-duration piston tunnel is employed and rapid-response miniature surface-heat-transfer gauges are used to assess the state of the boundary layer. The leading- and trailing-edge velocities of spots are reported for different external pressure gradients and Mach numbers. Also, the lateral spreading angle is determined from the heat-transfer signals which demonstrate dramatically the reduction in spot growth associated with favourable pressure gradients. An associated experiment on the development of turbulent wedges is also reported where liquid-crystal heat-transfer techniques are employed in low-speed wind tunnel to visualise and measure the wedge characteristics. Finally, both liquid crystal techniques and hot-film measurements from flight tests at Mach number of 0.6 are presented.

Turbulent-Spot Growth Characteristics : Wind-Tunnel and Flight Measurements of Natural Transition at High Reynolds and Mach Numbers

J.P. Clark and T.V. Jones, University of Oxford, Oxford, U.K.
J.E. LaGraff, Syracuse University.

A series of experiments are described which examine the growth of turbulent spots on a flat plate at Reynolds and Mach numbers typical of gas-turbine blading. A short duration piston tunnel is employed and rapid-response miniature surface-heat-transfer gauges are used to assess the state of the boundary layer. The leading- and trailing-edge velocities of spots are reported for different external pressure gradients and Mach numbers. Also, the lateral spreading angle is determined from the heat-transfer signals which demonstrate dramatically the reduction in spot growth associated with favourable pressure gradients. An associated experiment on the development of turbulent wedges is also reported where liquid crystal heat transfer techniques are employed in a low-speed wind tunnel to visualise and measure the wedge characteristics. Finally, both liquid-crystal techniques and hot-film measurements from flight tests at a Mach number of 0.6 are presented.

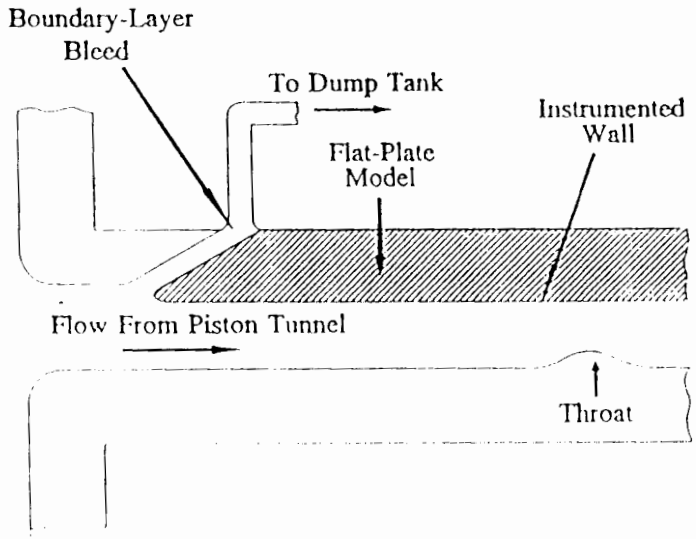

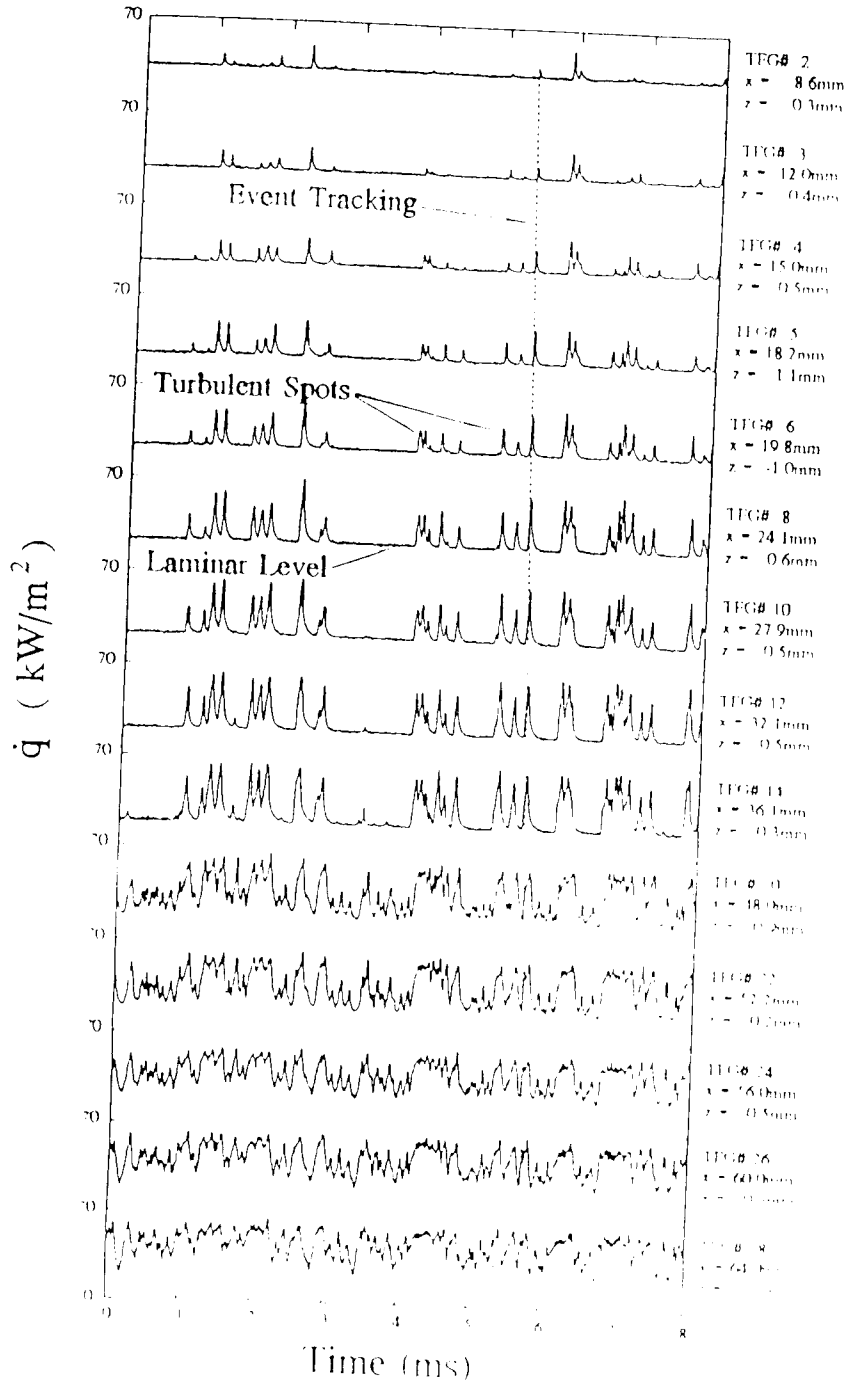
Event Tracking
Turbulent Spots
Laminar Level
q (kW/m 2)
Time (ms)

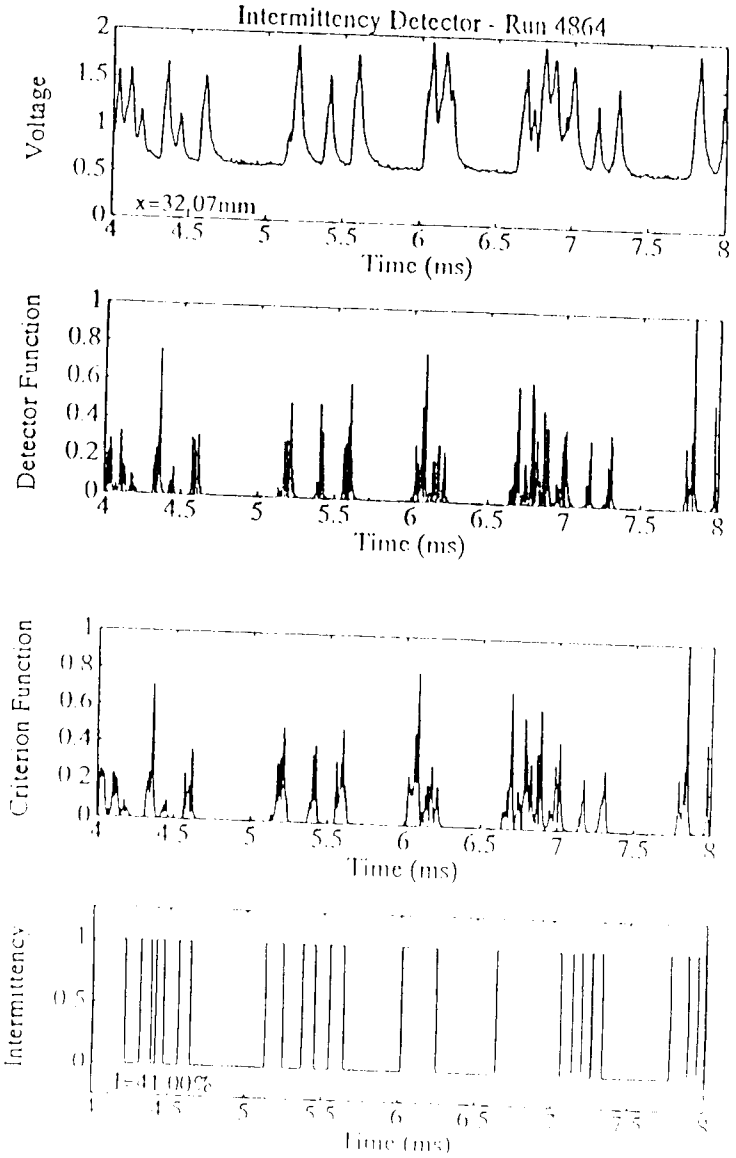
Intermittency Detector - Run 4864
Voltage
x=32.07mm
Time (ms)
Detector Function
Time (ms)
Criterion Function
Time (ms)
Intermittency
Time (ms)

o - dP/dx=MF (3.9+/-0.1 degrees)
x - dP/dx=SF (3.3+/-0.1 degrees)
dz (mm)
dx (mm)

Turbulent-Spot Trajectories
dP/dx = S F
Legend
Time
(μs)
x (mm)

Intermittency
Universal Curve
o - Mach 0.24 Flow
x - Mach 0.55 Flow
+ - Mach 1.32 Flow
* - Mach 1.86 Flow
(x-xt)/(x75-x25)

Intermittency
Universal Curve
o - dP/dx=MF
x - dP/dx=SF
+ - dP/dx=MA
(x-xt)/(x75-x25)

CONTOUR
h
W/m²K
1 59.9
2 66.6
3 81.1
4 84.9
5 95.5
6 105.8
7 117.9
8 122.1
9 131.2
10 147.3

CONTOUR
h
W/m²K
1 74.4
2 92.9
3 114.3
4 125.2
5 136.0

Intermittent Turbulence In the Attachment Line Flow Formed On An Infinite Swept Wing

Ian Poll
University of Manchester
Dept. of Engineering
Manchester, England M139PL

Abstract

The transition process which takes place in the attachment-line boundary layer in the presence of gross contamination is an issue of considerable interest to wing designers. It is well known that this flow is very sensitive to the presence of isolated roughness and that transition can be initiated at a very low value of the local momentum thickness Reynolds number. Moreover, once the attachment line is turbulent, the flow over the whole wing chord - top and bottom surface - will be turbulent and this has major implications for wing drag.

In order to investigate this phenomenon and produce a quantitative model of the development of intermittent turbulence with both Reynolds number and spanwise position, tests have been performed on a series of geometrically similar cylinder models. Data has been gathered on different sized models, in different low-speed wind-tunnels over a wide range of sweep angles (20° to 70°). A model of the transition process has been produced using Emmons' sport theory and the data have been used to determine the models' various unknown constants. Brief consideration is also given to the effects of high speed compressibility and heat transfer. The model provides a good description of the process over a very wide range of conditions.

Intermittent and Low Reynolds Number Turbulence In the Attachment Line Flow Formed On An Infinite Swept Wing

Ian Poll
University of Manchester
Dept. of Engineering
Manchester, England M13 9PL

The work which I presented related to the transition process which can occur on the leading edge of an infinite swept wing i.e. one in which the surface pressure field has no spanwise variation. To be more specific the transition which can occur in the attachment-line boundary layer. This is the boundary layer which forms on the line which divides the upper surface flow from the lower surface flow - see figure 1. The present study relates to two aspects of this problem.

a) The spanwise development of intermittent turbulence downstream of a large 2-D trip

and

b) The relaminarisation of the fully developed turbulent flow as the value of the characteristic Reynolds number, $\bar{R}$ (see figure 2) is progressively reduced.

Since item a) is a classic example of a by-pass transition process, the work is primarily experimental. However, the experiment is not easy for the following reasons.

1. The attachment line transition is a "high Reynolds number" phenomenon. There is no way that it can be investigated with bench top scale experiments. The achievement of the necessary conditions requires the use of large models in industrial scale wind tunnels. This makes the problem difficult to study in University laboratories. However at Manchester we are fortunate in having a large scale low speed wind tunnel (9' x 7' test section, maximum speed 250 ft/sec) which is suitable for the study.

and

2. Even with the necessary facilities the attachment line boundary layers are very thin with the turbulent flows being less than 5 mm thick. When this is coupled with the problem of the model being a large distance (2' to 3') from the tunnel wall or floor, it is apparent that conventional traversing of the boundary layer is impossible. Therefore, we have developed a novel and simple approach involving the use of a range of impact pressure probes mounted on the model at a fixed height above the surface. By measuring the indicated pressure over a wide range of tunnel speed, model leading-edge sweep-angle, probe size and probe spanwise location, it is possible to generate a matrix of data which can be interpolated to produce conventional velocity profile information with very high levels of accuracy.

Figures 1 to 16 describe in sequence the way in which the problem of describing the attachment line transition. By combining the data with a model developed from Emmons spot hypothesis an accurate, quantitative description of the process has been produced. A particularly interesting conclusion from this study has been that, whilst an infinite swept (spanwise invariant) laminar and fully turbulent attachment line boundary layers can be set up, the transitional case always exhibits spanwise variation - there is no physically realisable, spanwise invariant, transitional, attachment-line flow!

Figures 17 to 25 summarise our contribution to item b) - the relaminarisation of the fully turbulent attachment line boundary layer by reducing the characteristic Reynolds number. All the information shown corresponds to flows which are fully turbulent. This means that, if a hot wire anemometer is placed in the flow, the signal will be turbulent (no laminar gaps) the whole time. Nevertheless it is clear that the flow does not have the structure of a high Reynolds number turbulent boundary layer.

It is apparent from the velocity profiles that, at the highest Reynolds number conditions, the inner region of the boundary layer obeys the "universal law of the wall". However as the Reynolds number ($\bar{R}$) is reduced below 600, the profiles are shifting relative to the universal law in a way which is consistent with a Reynolds number variation in the additive constant (c). The shift in the inner region is monotonic with $\bar{R}$ and, at the lowest Reynolds number, the value of the additive constant is about 7.5 compared with 5.2 at large Reynolds number. By computing the velocity profile with a full field boundary layer code, it has been found that the observed changes in the profile are consistent with the following turbulence mode.

1. Von Karman's constant invariant at 0.41.

2. Van Driest's damping factor (A^+) rising rapidly as the Reynolds number falls.

and 3. The outer mixing length (Lo/δ) rising slowly with decreasing Reynolds number.

We have also observed that as the Reynolds number drops the shape factor H rises very rapidly, achieving a value of about 2 and that the skin friction coefficient goes through a maximum - all this occurring whilst the flow is still "fully turbulent".

Many (if not all) of these features have been observed in low Reynolds number pipe and channel flow. However, they have not been observed in 2-D flat plate, zero pressure gradient flow. This is because, at the Reynolds number which need to be achieved, flat plate flow is invariably contaminated by the disturbances introduced by the trip (needed to make the flow turbulent). Different tripping devices produce different flow fields at these conditions and the underlying behaviour of the turbulence cannot be separated out.

The most important conclusion of the work to date is that relaminarisation can be modelled by an appropriate variation A^+.

①

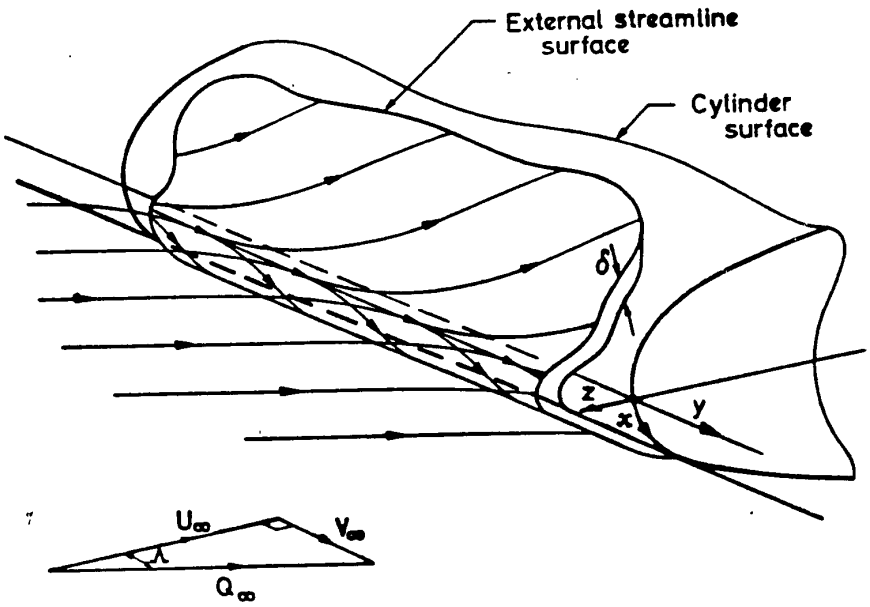

Fig. 1. Flow near the leading edge of a swept cylinder.

②

INFINITE SWEPT ATTACHMENT LINE PARAMETERS

LENGTH SCALE $V = \left\{ \frac{\nu_e}{(dU_e/dx)_{x=0}} \right\}^{1/2}$

REYNOLDS NUMBER $\overline{R} = \frac{V_e V}{\nu_e}$

TRIP-DETECTOR SEPARATION = S

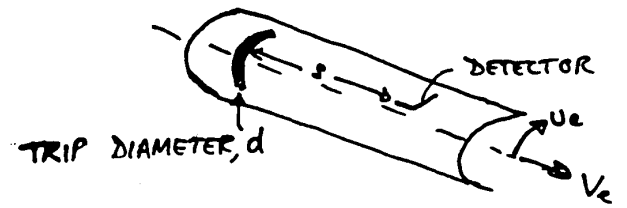

Figure 2

(3)

INTERMITTENCY DEFINED AS A WEIGHTING FUNCTION

SKIN FRICTION $\quad C_f = \gamma_1 (C_f)_T + (1-\gamma_1)(C_f)_L$

HEAT TRANSFER $\quad St = \gamma_2 (St)_T + (1-\gamma_2)(St)_L$

LOCAL DYNAMIC PRESSURE $\quad \frac{1}{2}\rho V^2 = \gamma_3 \left(\frac{1}{2}\rho V^2\right)_T + (1-\gamma_3)\left(\frac{1}{2}\rho V^2\right)_L$

<u>etc.</u>

IN GENERAL $\quad \gamma_3 = \gamma_3(z)$

BUT AS $z \to 0 \quad \gamma_3 \to \gamma_2 \simeq \gamma_1 = \gamma$

Figure 5

---

(4)

POLL (1983) PROPOSED, ON THE BASIS OF AN EXTREMELY LIMITED AMOUNT OF DATA, THAT FOR CONSTANT S

$$\gamma = 1 - EXP\left[-0.411\left(\frac{\bar{R} - \bar{R}_B}{\lambda}\right)^2\right]$$

WHERE $\bar{R}_B$ IS THE VALUE APPROPRIATE FOR THE ONSET OF TRANSITION AND

$$\lambda = \bar{R}\Big)_{\gamma=0.75} - \bar{R}\Big)_{\gamma=0.25}$$

$\lambda = \lambda\left(\bar{R}_B, S/\eta_0\right)$ ← NOT KNOWN

$\bar{R}_B = \bar{R}_B\left(S/\eta, d/\eta\right)$ ← KNOWN

Figure 6

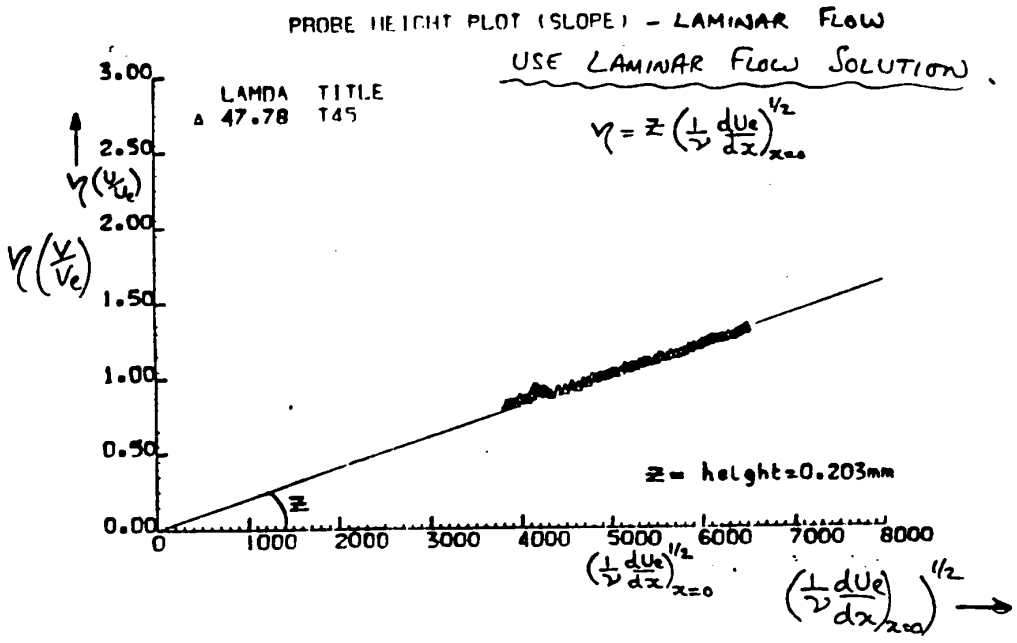

Figure 9

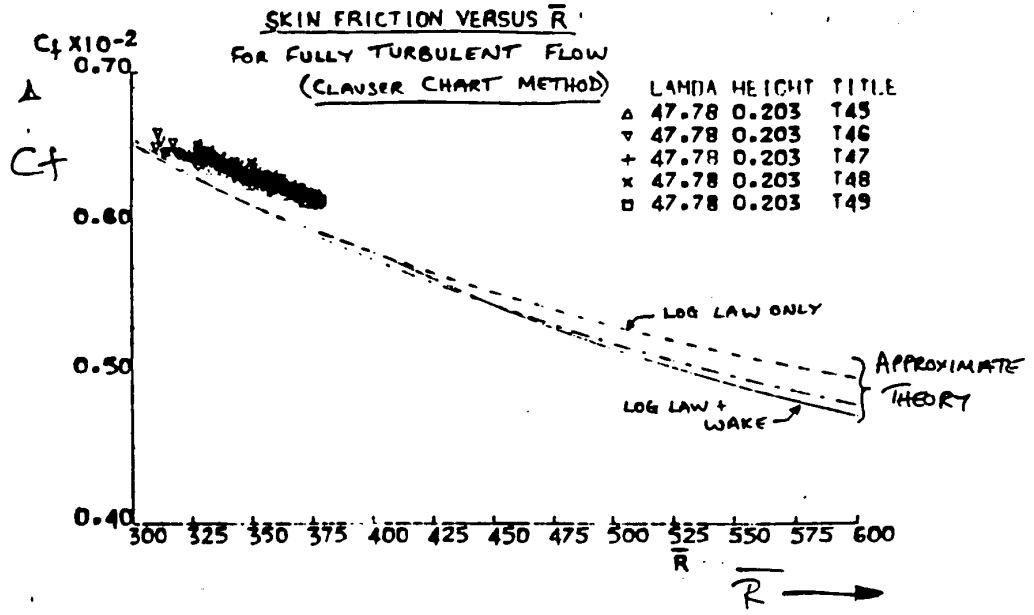

Figure 10

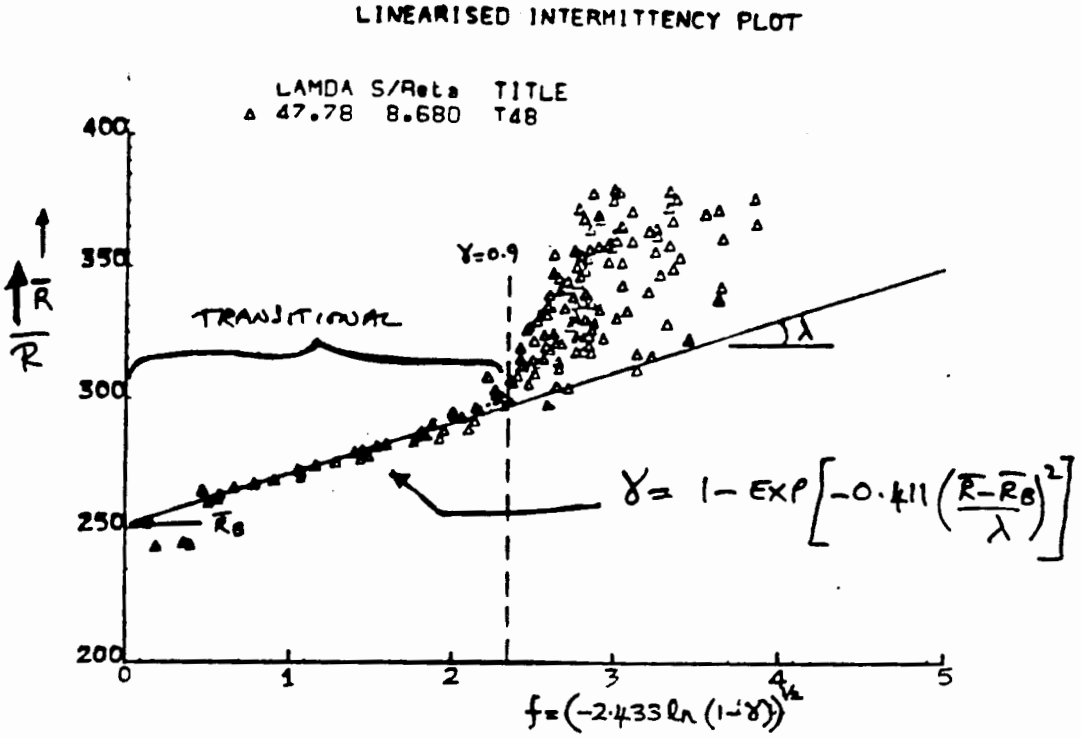

Figure 13

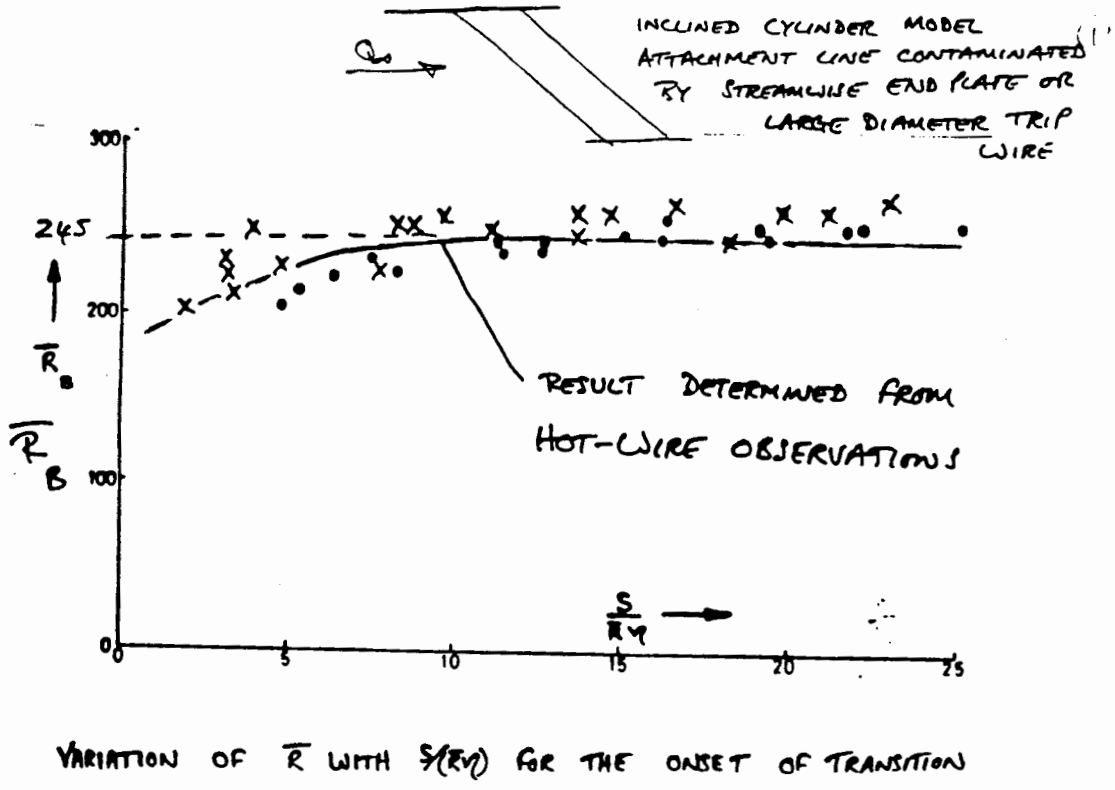

VARIATION OF $\bar{R}$ WITH $S/(R\gamma)$ FOR THE ONSET OF TRANSITION

Figure 14

VELOCITY PROFILES FOR VARIOUS RBAR

DANKS DATA

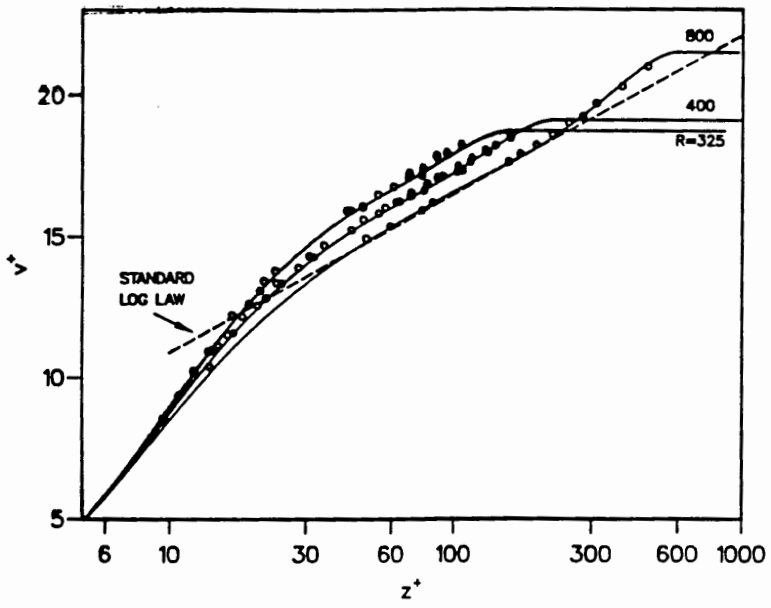

Figure 17

VELOCITY PROFILES FOR VARIOUS RBAR

CUMPSTY'S DATA

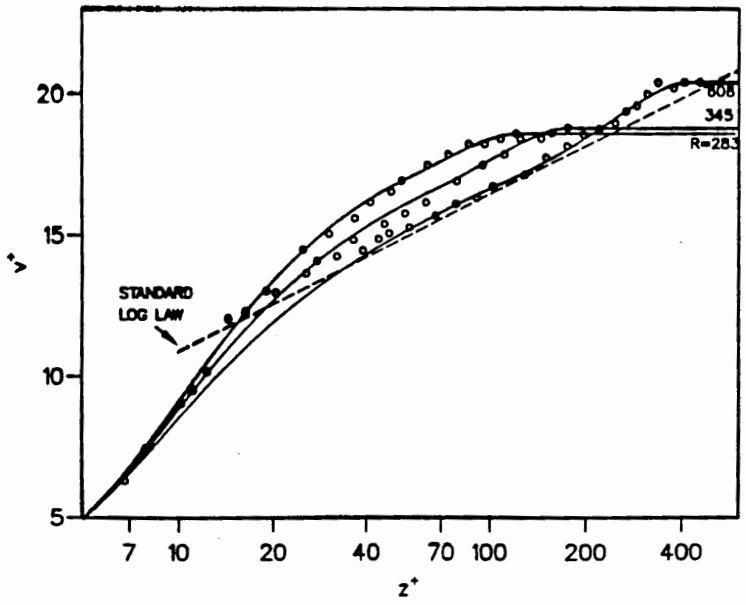

Figure 18

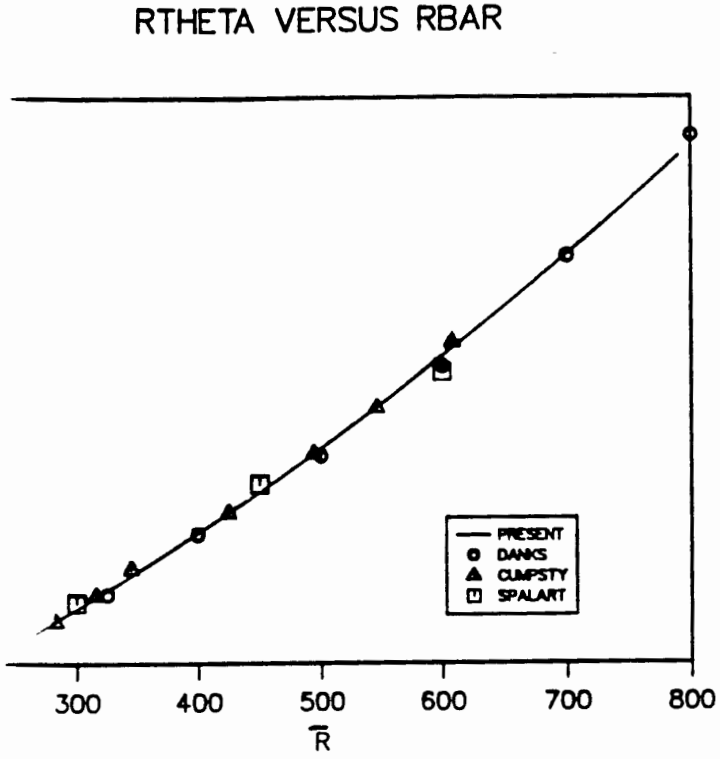

Figure 21

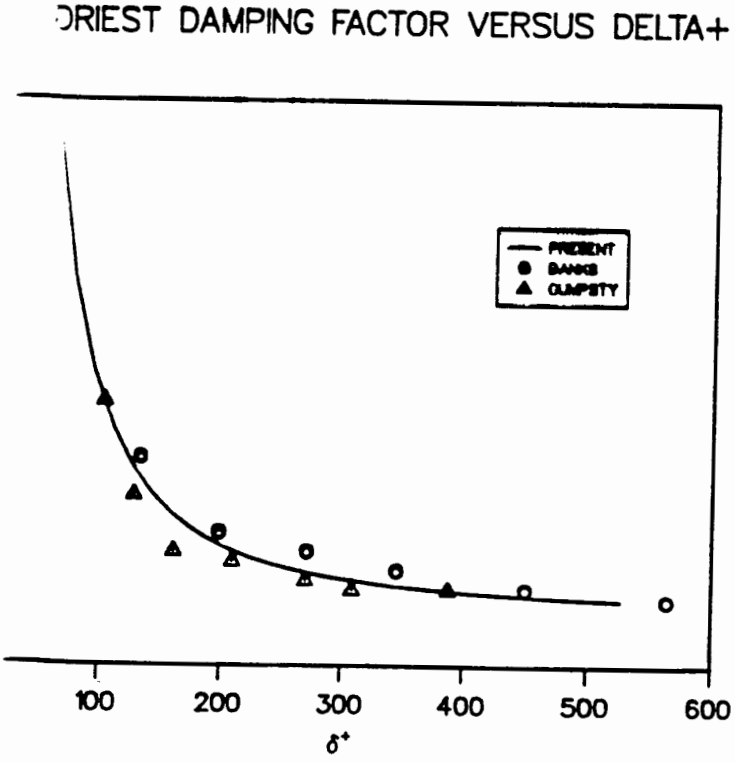

Figure 22

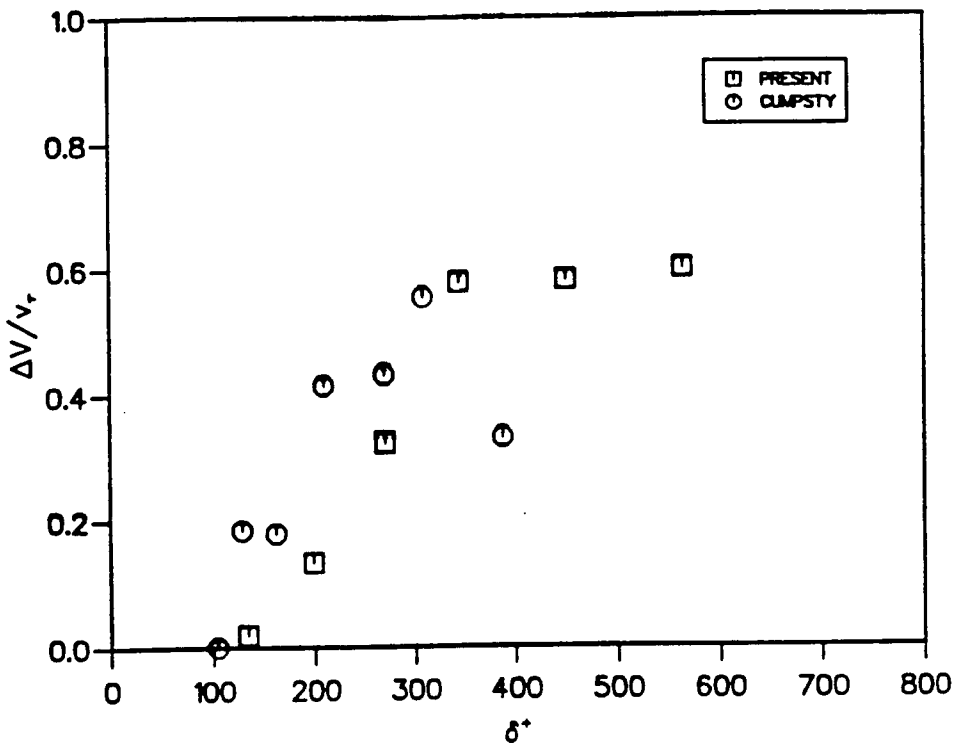
WAKE STRENGTH VERSUS DELTA+
PRESENT
CUMPSTY
1.0
0.8
0.6
0.4
0.2
0.0
ΔV/V
0
100
200
300
400
500
600
700
800
δ+

Figure 25

THE ROLE OF SEPARATION BUBBLES ON THE AERODYNAMIC CHARACTERISTICS OF AIRFOILS, INCLUDING STALL AND POST-STALL, AT LOW REYNOLDS NUMBERS

by

Hsun H. Chen* and Tuncer Cebeci**

Aerospace Engineering Department

California State University, Long Beach

Abstract

Airfoils at high Reynolds numbers, in general, have small separation bubbles that are usually confined to the leading edge. Since the Reynolds number is large, the turbulence model for the transition region between the laminar and turbulent flow is not important. Furthermore, the onset of transition occurs either at separation or prior to separation and can be predicted satisfactorily by empirical correlations when the incident angle is small and can be assumed to correspond to laminar separation when the correlations do not apply, i.e., at high incidence angles.

This is not the case at low Reynolds numbers. For chord Reynolds numbers between 100,000 and 500,000, rather large separation bubbles may occur on the airfoil even at low incidence angles: the onset of transition occurs inside the bubble and is separation induced. The turbulence model for the transition region becomes important[1,2] and plays a significant role in the prediction of the aerodynamic characteristics of an airfoil.

The present paper describes a turbulence model for the transition region at low Reynolds numbers. This model is incorporated into the Cebeci-Smith

* Associate Professor

** Professor and Chairman

algebraic eddy-viscosity formulation and is used in a calculation method that is based on the solutions of inviscid and boundary-layer equations with the onset of transition computed with the e^n-method based on linear stability theory.[3,4] Results will be presented for airfoils with large separation bubbles to demonstrate the ability of the turbulence model to predict the location of laminar separation and turbulent reattachment points. Results will also be presented to show the ability of the method to predict stall and post-stall flows on airfoils at low Reynolds numbers. These calculations will be performed with an improved Cebeci-Smith model that accounts for flows with strong pressure gradient and separation.

References

1. Walker, G.J., Subroto, P.H. and Platzer, M.F., "Transition Modeling Effects on Viscous/Inviscid Interaction Analysis of Low Reynolds Number Airfoil Flows Involving Laminar Separation Bubbles," ASME Paper 88-GT-32, Amsterdam, June 1988.
2. Walker, G.J., "The Role of Laminar-Turbulent Transition in Gas Turbine Engines: A discussion," Journal of Turbomachinery, Vol. 115, p. 207, April 1993.
3. Cebeci, T., "Essential Ingredients of a Method for low Reynolds Number Airfoils," AIAA Journal, Vol. 27, p. 1680, 1989.
4. Cebeci, T., Roknaldin, F., Carr, L.W., "Prediction of Stall and Post-Stall Behavior of Airfoils at Low and High Reynolds Numbers," AIAA Paper No. 93-3502, AIAA Applied Aerodynamic Meeting, Monterey, August 9-11, 1993

NASA/CP—2007-214667

THE ROLE OF SEPARATION BUBBLES ON THE AERODYNAMIC CHARACTERISTICS OF AIRFOILS, INCLUDING STALL AND POST-STALL, AT LOW REYNOLDS NUMBERS

by

Hsun H. Chen and Tuncer Cebeci
Aerospace Engineering Department
California State University, Long Beach

PURPOSE OF THE STUDY

- Study the calculation of separation bubbles on airfoils.
  - Examine the modelling of the transitional region.
  - Calculate transition as part of the solution procedure.
- Study the ability and the accuracy of the calculation method to predict the lift and drag characteristic of airfoils including low-drag airfoils.

CALCULATION METHOD, 1

- Based on stability/transition and interactive boundary-layer (IBL) approach in which the solutions of the panel and inverse boundary-layer methods are coupled to a transition prediction method based on linear stability theory using the e^n procedure.

- Turbulence model is based on the algebraic eddy-viscosity formulation of Cebeci-Smith (CS) with two improvements:

  1. Modelling of the transitional region

  2. Improving the accuracy of the model in strong adverse pressure gradient flows and flows with separation

CALCULATION METHOD, 2

To model the transitional region, consider

$$\gamma_{tr} = 1 - \exp\left[G(x - x_{tr}) \int_{x_{tr}}^{x} \frac{dx}{u_e}\right] \qquad (7b)$$

where

$$G = \frac{3}{c^2} \frac{u_e^3}{\nu^2} R_{x_{tr}}^{-1.34} \qquad (7c)$$

for separation-induced transition

$$c^2 = 213[\log R_{x_{tr}} - 4.7323] \qquad (19)$$

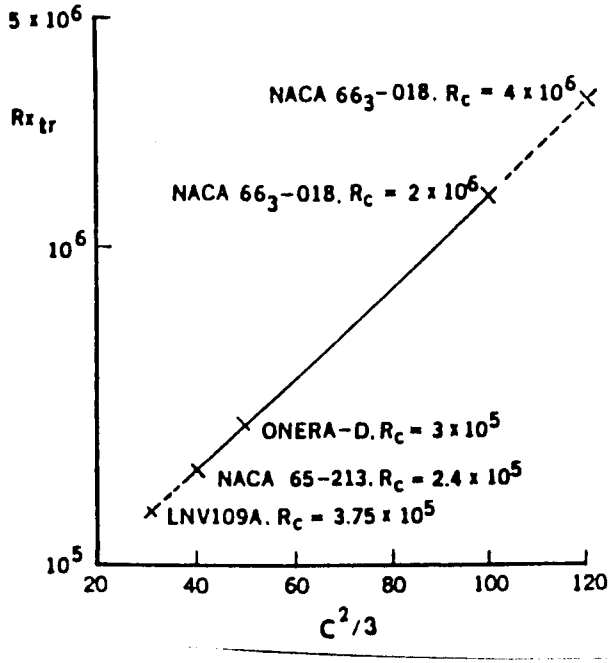

CALCULATION METHOD, 3

For strong adverse pressure gradient flows and flows with separation, consider

$$(\varepsilon_m)_o = \alpha \left| \int_0^\delta (u_e - u)dy \right| \gamma_{tr}\gamma$$

express α by

$$\alpha = \frac{0.0168}{F^{2.5}} \tag{14}$$

where

$$F = 1 - \beta \frac{\partial u/\partial x}{\partial u/\partial y} \tag{15b}$$

$$\beta = \begin{cases} \dfrac{6}{1 + 2R_t(2 - R_t)} & R_t < 1.0 \\ \dfrac{1 + R_t}{R_t} & R_t \geq 1.0 \end{cases} \tag{16b}$$

so that

$$\alpha = \frac{0.0168}{[1 - \beta(\partial u/\partial x)/(\partial u/\partial y)]^{2.5}} \tag{17}$$

In some ways, this improvement is similar to the Johnson-King model used for the CS model.

RESULTS FOR SEPARATION BUBBLES, 1

Take the Eppler airfoil as an example and conduct studies for R_c = 200,000 and 300,000 for the data of McGee et al.

R_c = 200,000

	Calculated			Experiment	
α	LS	$(x/c)_{tr}$	TR	LS	TR
-2	0.56	0.748	0.835	0.53	0.80
0	0.51	0.688	0.785	0.48	0.74
2	0.46	0.624	0.716	0.43	0.67
4	0.415	0.564	0.65	0.40	0.62
5	0.40	0.526	0.60	0.38	0.59
6	0.39	0.467	0.52	0.37	0.55

RESULTS FOR SEPARATION BUBBLES, 2

$R_c = 200{,}000$

$\alpha = 0°$

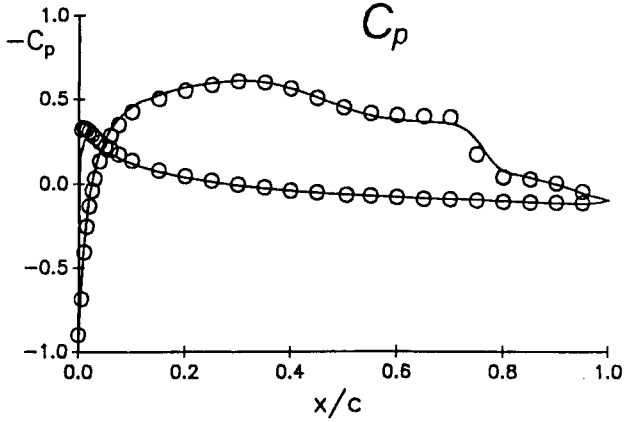

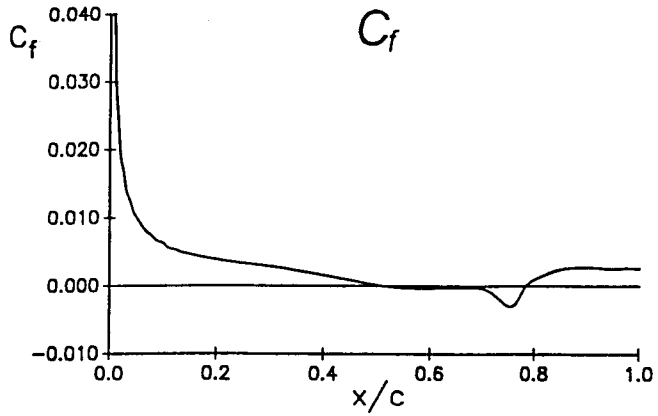

$\alpha = 4°$

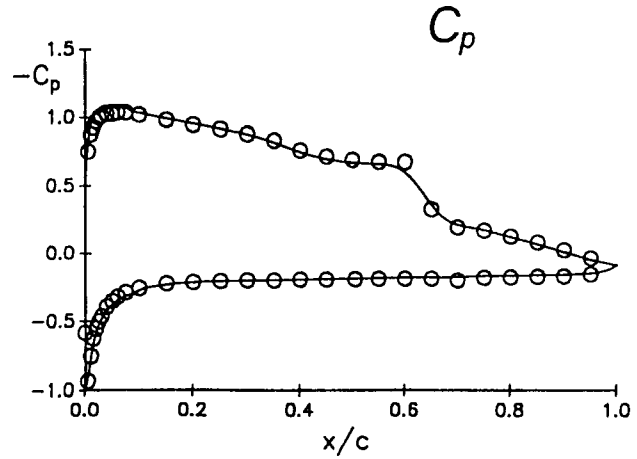

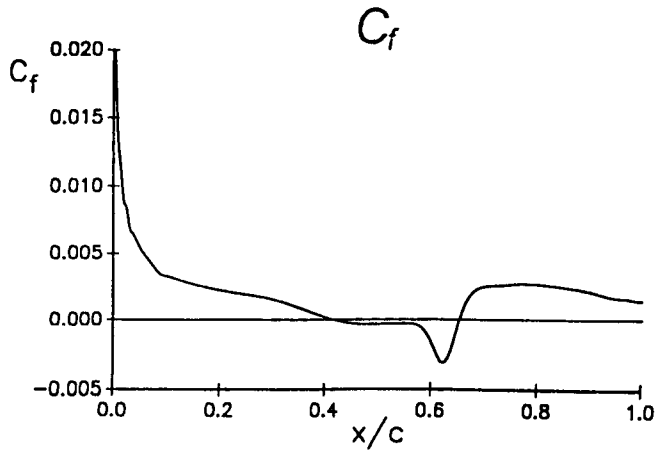

RESULTS FOR SEPARATION BUBBLES, 3

$R_c = 200{,}000$

$\alpha = 8°$

C_p

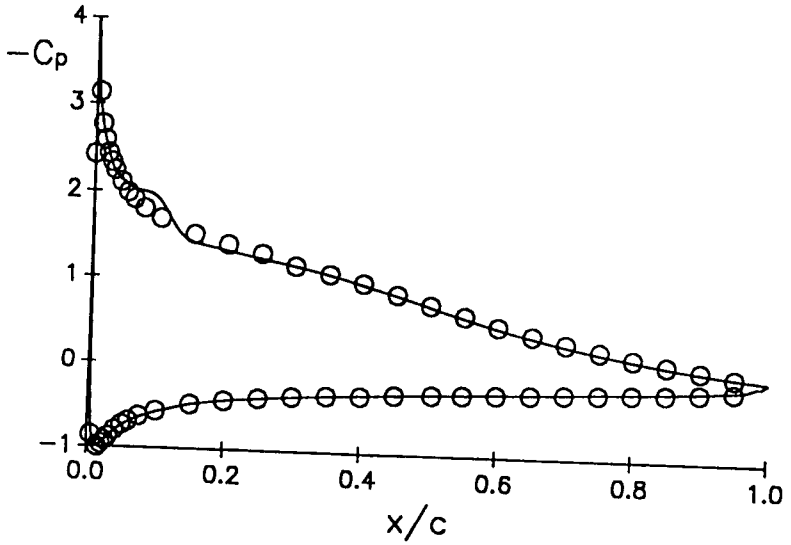

C_f

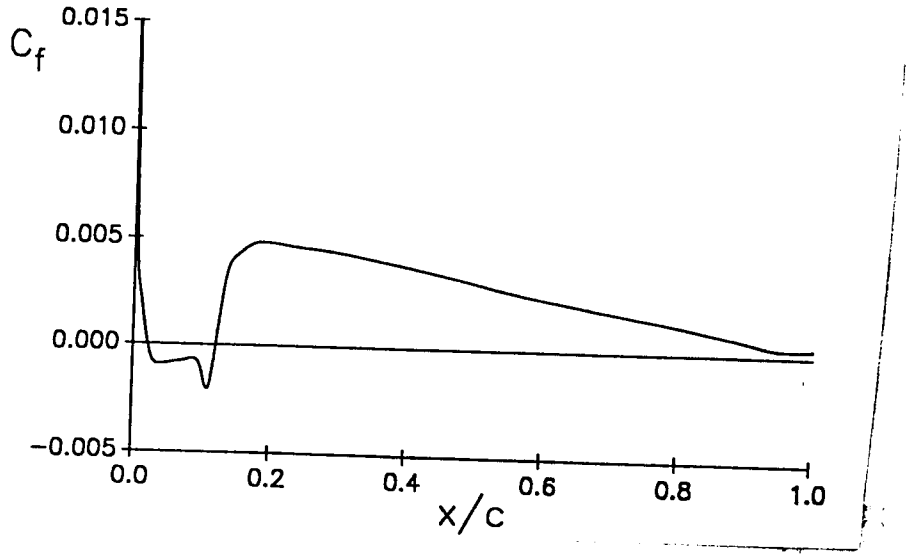

RESULTS FOR SEPARATION BUBBLES, 4

$R_c = 300{,}000$

	Calculated			Experiment	
α	LS	$(x/c)_{tr}$	TR	LS	TR
-2	0.56	0.714	0.785	0.53	0.74
0	0.515	0.653	0.72	0.48	0.69
2	0.465	0.604	0.676	0.45	0.62
4	0.42	0.541	0.60	0.40	0.58
5	0.415	0.495	0.544	0.39	0.55
6	0.41	0.427	0.45	0.38	0.50
8	0.008	0.061	0.085	-	-

RESULTS FOR SEPARATION BUBBLES, 5

$R_c = 300{,}000$

$\alpha = 0°$

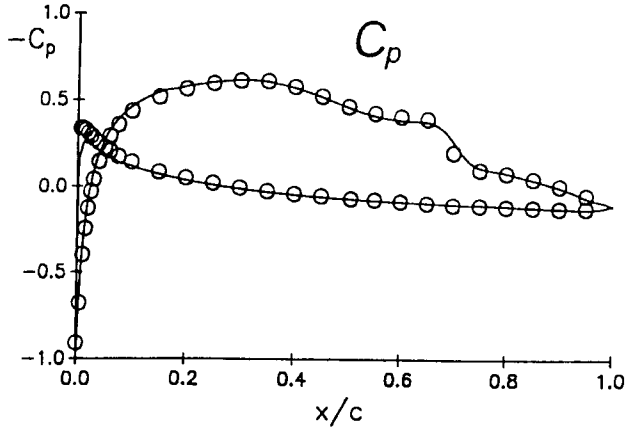

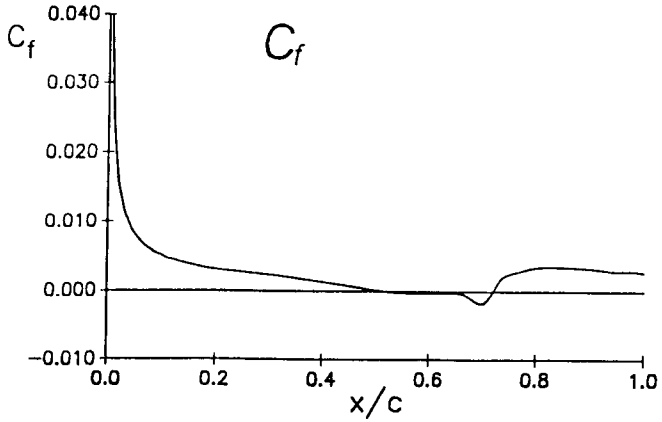

$\alpha = 4°$

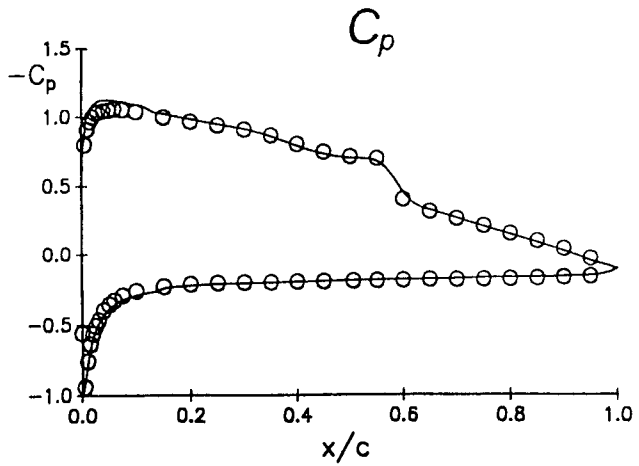

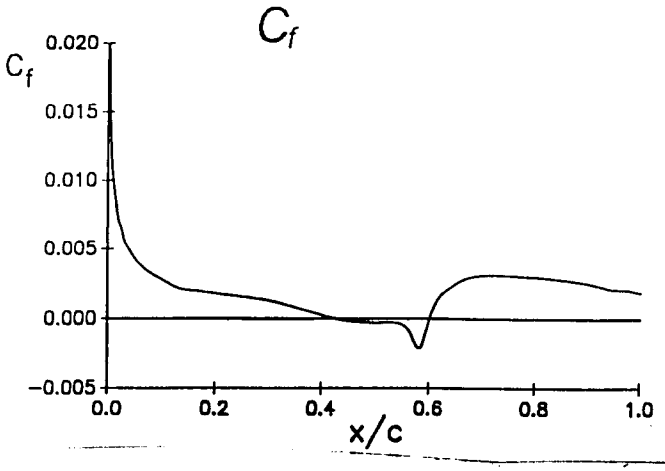

RESULTS FOR SEPARATION BUBBLES, 6

$R_c = 300{,}000$

$\alpha = 8°$

C_p

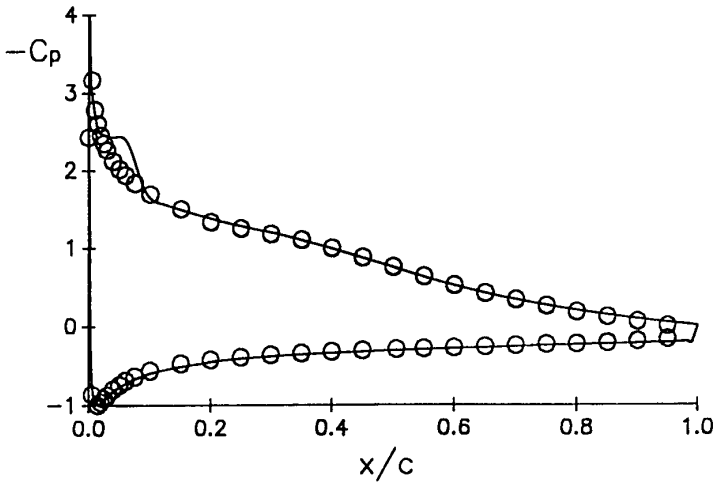

C_f

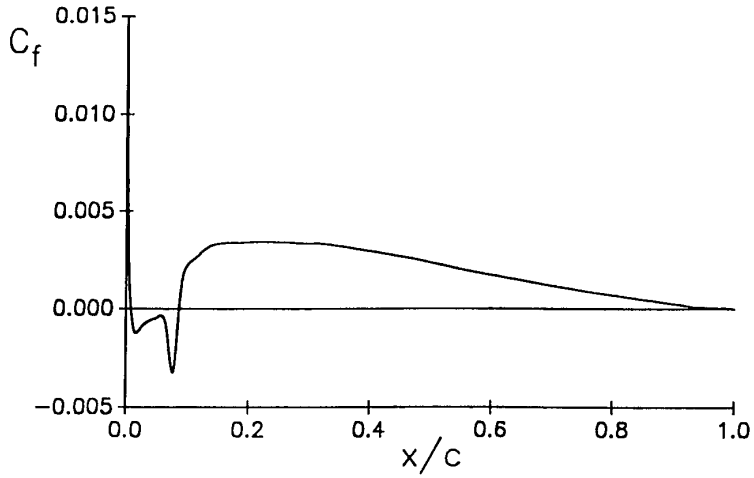

RESULTS FOR AERODYNAMIC CHARACTERISTICS, 1

Recent study

NACA 0012 Airfoil

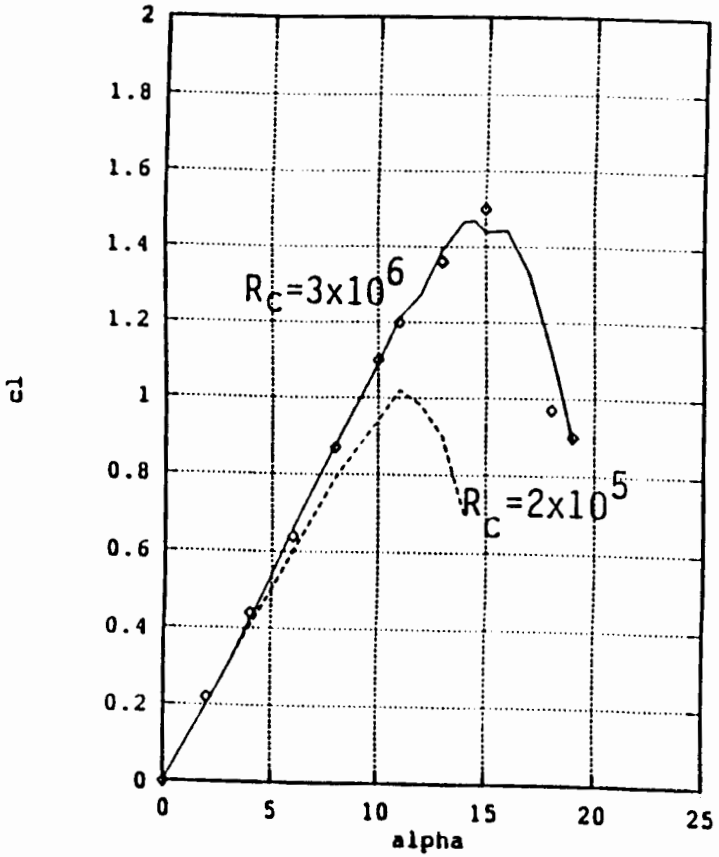

RESULTS FOR AERODYNAMIC CHARACTERISTICS, 2

Eppler Airfoil: Low Drag

$R_c = 200{,}000$

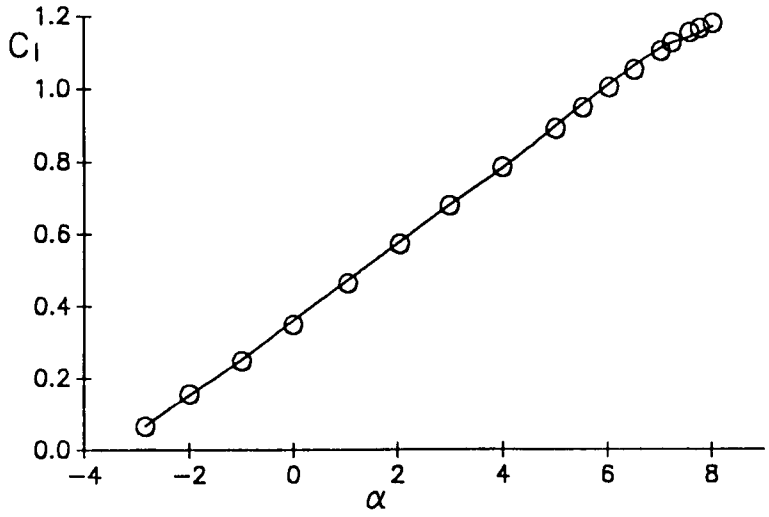

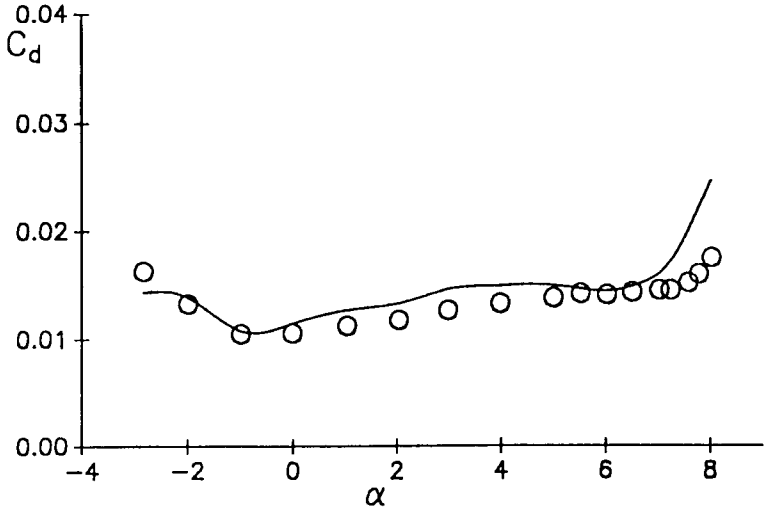

RESULTS FOR AERODYNAMIC CHARACTERISTICS, 3

Eppler Airfoil: Low Drag

$$R_c = 300{,}000$$

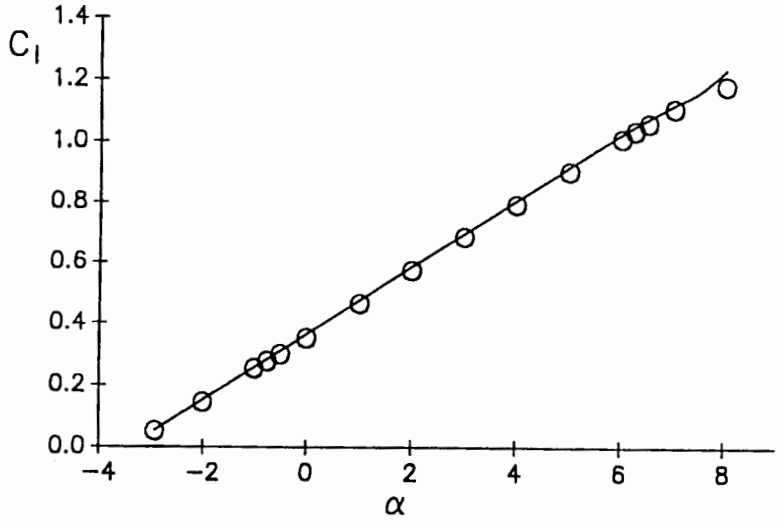

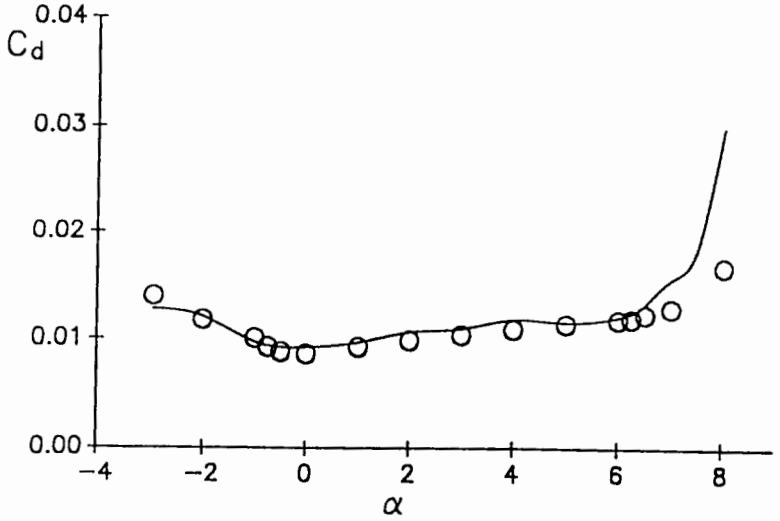

COMMENTS ON THE RESULTS

Features of this airfoil:

- **Separation bubbles away from the leading-edge of the airfoil at low and moderate α.**

- **Leading-edge separation bubbles at higher α, close to stall. Solutions are sensitive to transition location.**

CONCLUSIONS

At low Reynolds numbers

- The improved CS model, when incorporated into the calculation method based on a combination of e^n and IBL, is able to accurately predict separation bubbles on airfoils.

- For conventional airfoils, lift and drag can accurately be predicted for all angles of attack, including stall and post-stall.

- For low-drag airfoils, lift and drag can accurately be predicted for angles of attack up to stall.

Late Stage Hypersonic Boundary Layer Transition

Roger Kimmel
Wright Laboratory
Wright Patterson Air Force Base, OH 45433

Abstract

Our knowledge of late-stage hypersonic boundary layer transition is very limited, since most theoretical and experimental work has concentrated on the linear disturbance amplification regime. Although experiments show nonlinear higher harmonics beginning at approximately one-half the transition Reynolds number, there is no experimental evidence for subharmonics, in contrast to subsonic boundary layer transition. A practical definition of transition is the location where mean surface heat transfer first begins to rise above laminar values. Hot wire spectra show that prior to transition, spectral dispersion occurs, with second mode energy decreasing, and energy at neighboring frequencies increasing. Near the transition point, disturbance energy begins to spread from the critical layer toward the wall. Greater emphasis on the breakdown region is planned for future experiments.

DATA MATRIX

	ADIABATIC	COLD WALL
POWER SPECTRA	√	√
HEAT TRANSFER		√
SHADOWGRAPH		√
BL THICKNESS	√	
VELOCITY PROFILES	√	
BICOHERENCE	√	

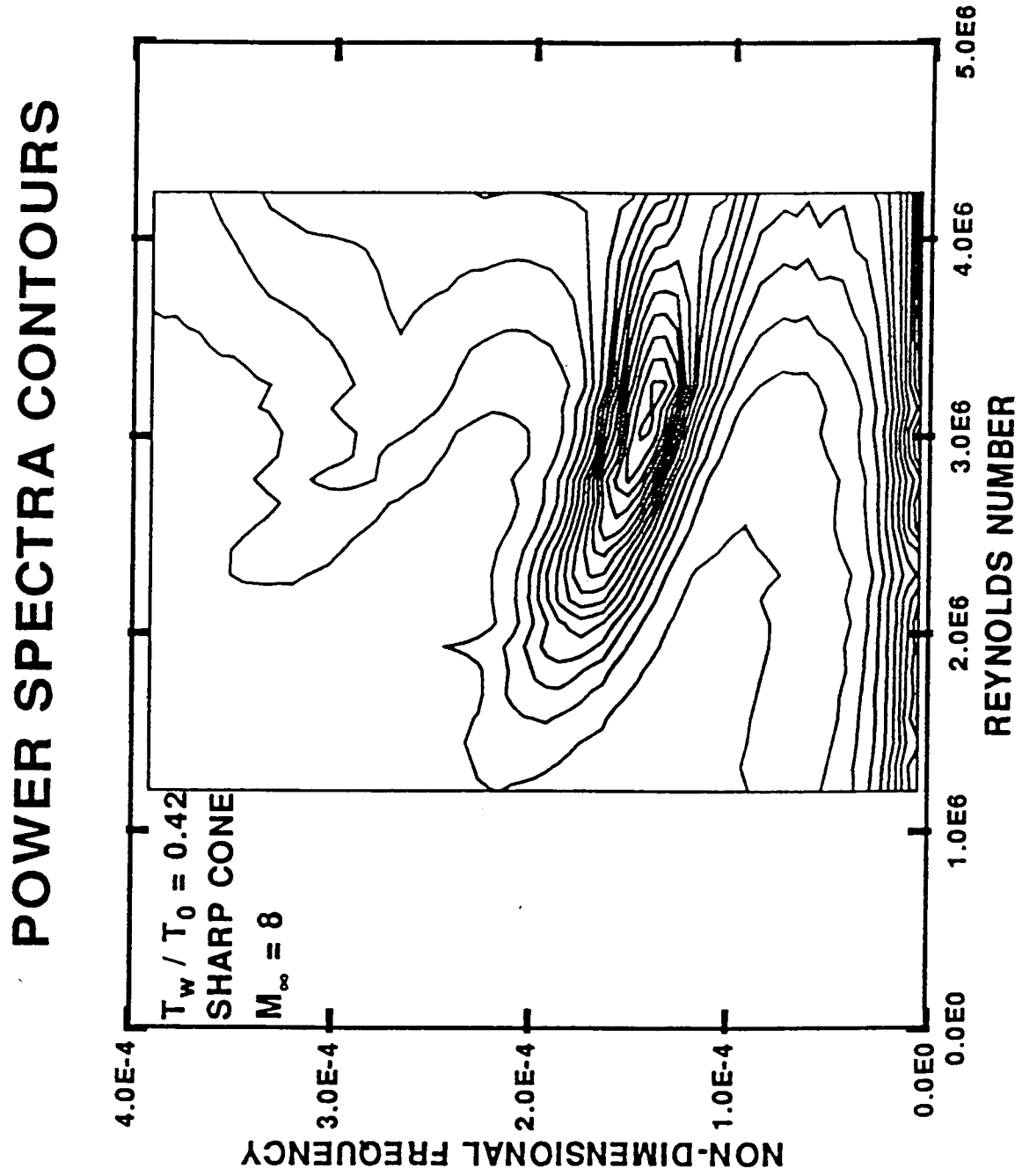
POWER SPECTRA CONTOURS
$T_w / T_0 = 0.42$
SHARP CONE
$M_\infty = 8$
NON-DIMENSIONAL FREQUENCY
4.0E-4
3.0E-4
2.0E-4
1.0E-4
0.0E0
0.0E0
1.0E6
2.0E6
3.0E6
4.0E6
5.0E6
REYNOLDS NUMBER

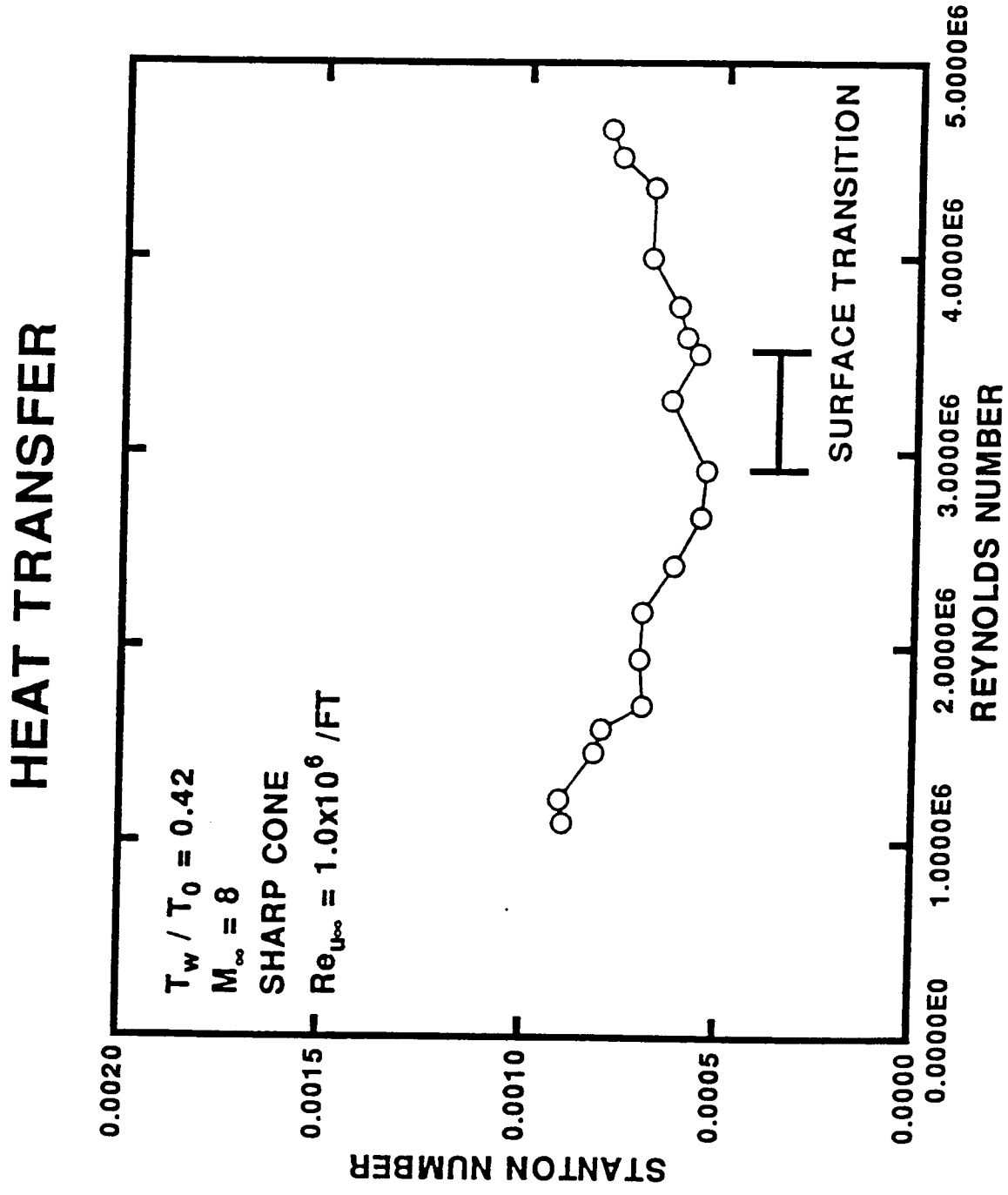
HEAT TRANSFER
$T_w / T_0 = 0.42$
$M_\infty = 8$
SHARP CONE
$Re_{U\infty} = 1.0x10^6$ /FT
SURFACE TRANSITION
STANTON NUMBER
0.0020
0.0015
0.0010
0.0005
0.0000
0.0000E0
1.0000E6
2.0000E6
3.0000E6
4.0000E6
5.0000E6
REYNOLDS NUMBER

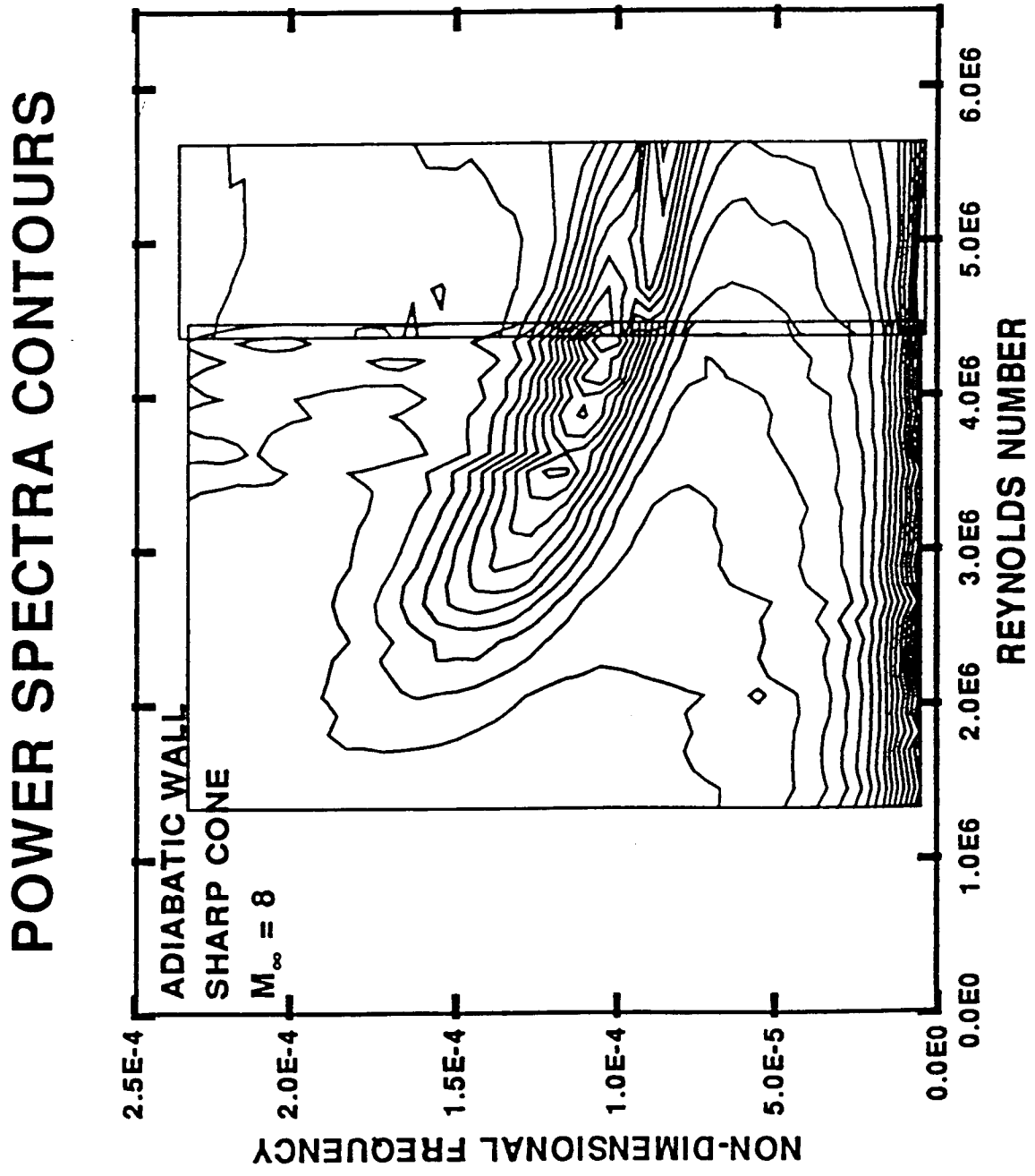
POWER SPECTRA CONTOURS
ADIABATIC WALL
SHARP CONE
M_∞ = 8
NON-DIMENSIONAL FREQUENCY
2.5E-4
2.0E-4
1.5E-4
1.0E-4
5.0E-5
0.0E0
REYNOLDS NUMBER
0.0E0
1.0E6
2.0E6
3.0E6
4.0E6
5.0E6
6.0E6

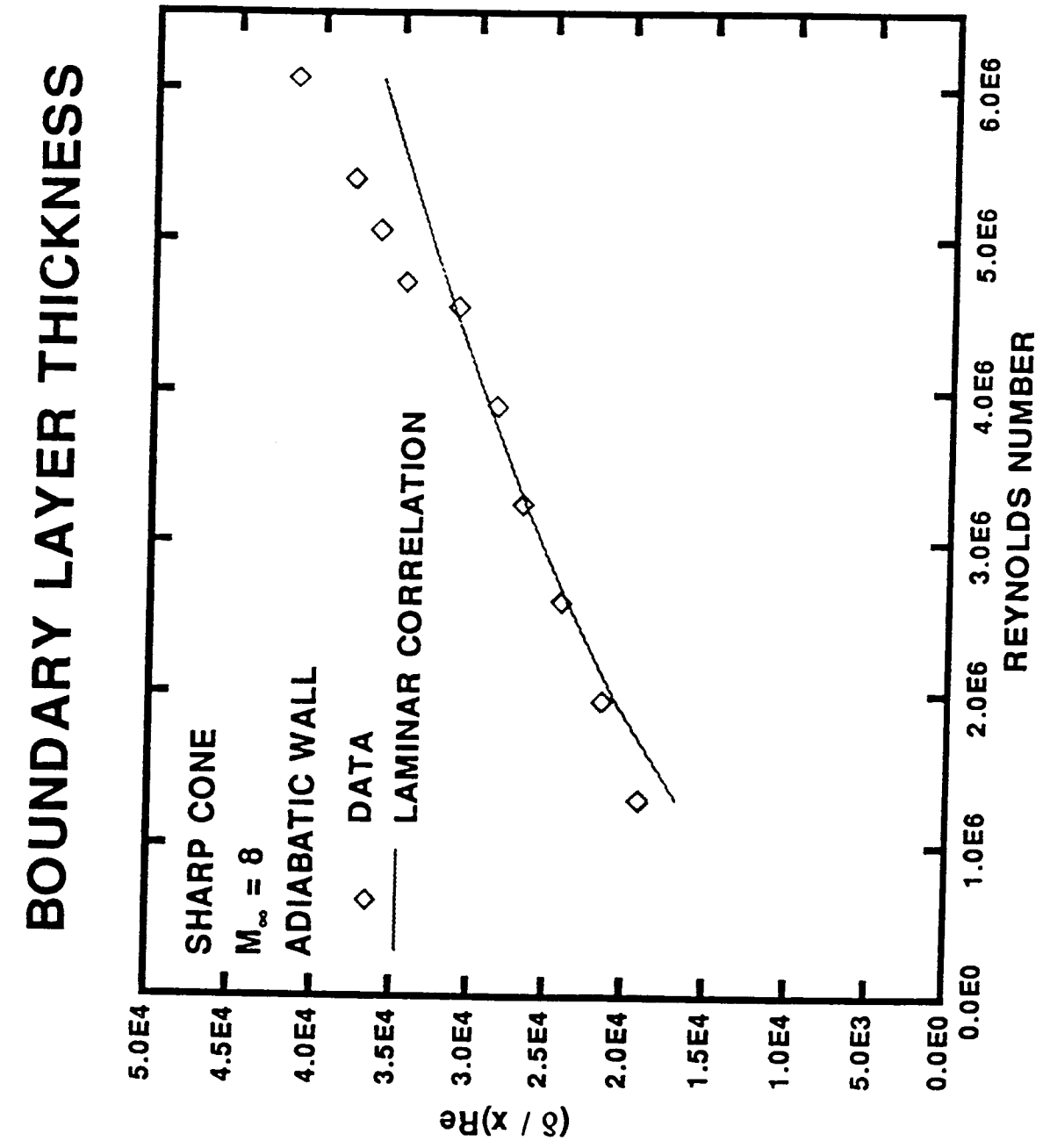
BOUNDARY LAYER THICKNESS
SHARP CONE
$M_\infty = 8$
ADIABATIC WALL
DATA
LAMINAR CORRELATION
$(\delta / x)Re$
REYNOLDS NUMBER
5.0E4
4.5E4
4.0E4
3.5E4
3.0E4
2.5E4
2.0E4
1.5E4
1.0E4
5.0E3
0.0E0
1.0E6
2.0E6
3.0E6
4.0E6
5.0E6
6.0E6

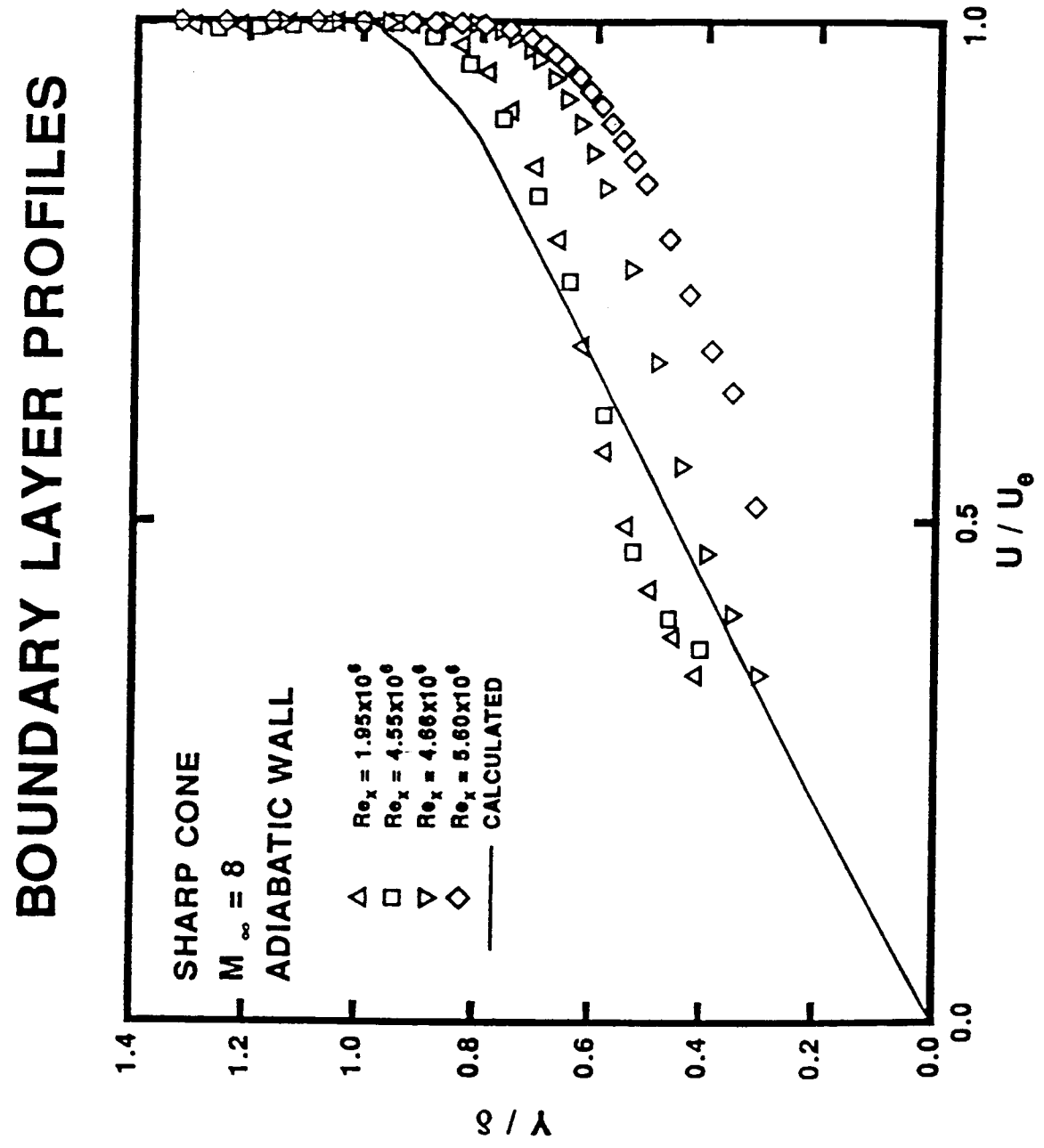
BOUNDARY LAYER PROFILES
SHARP CONE
M ∞ = 8
ADIABATIC WALL
Re x = 1.95x10^6
Re x = 4.55x10^6
Re x = 4.86x10^6
Re x = 5.60x10^6
CALCULATED
y / δ
U / U e
1.4
1.2
1.0
0.8
0.6
0.4
0.2
0.0
0.5
1.0

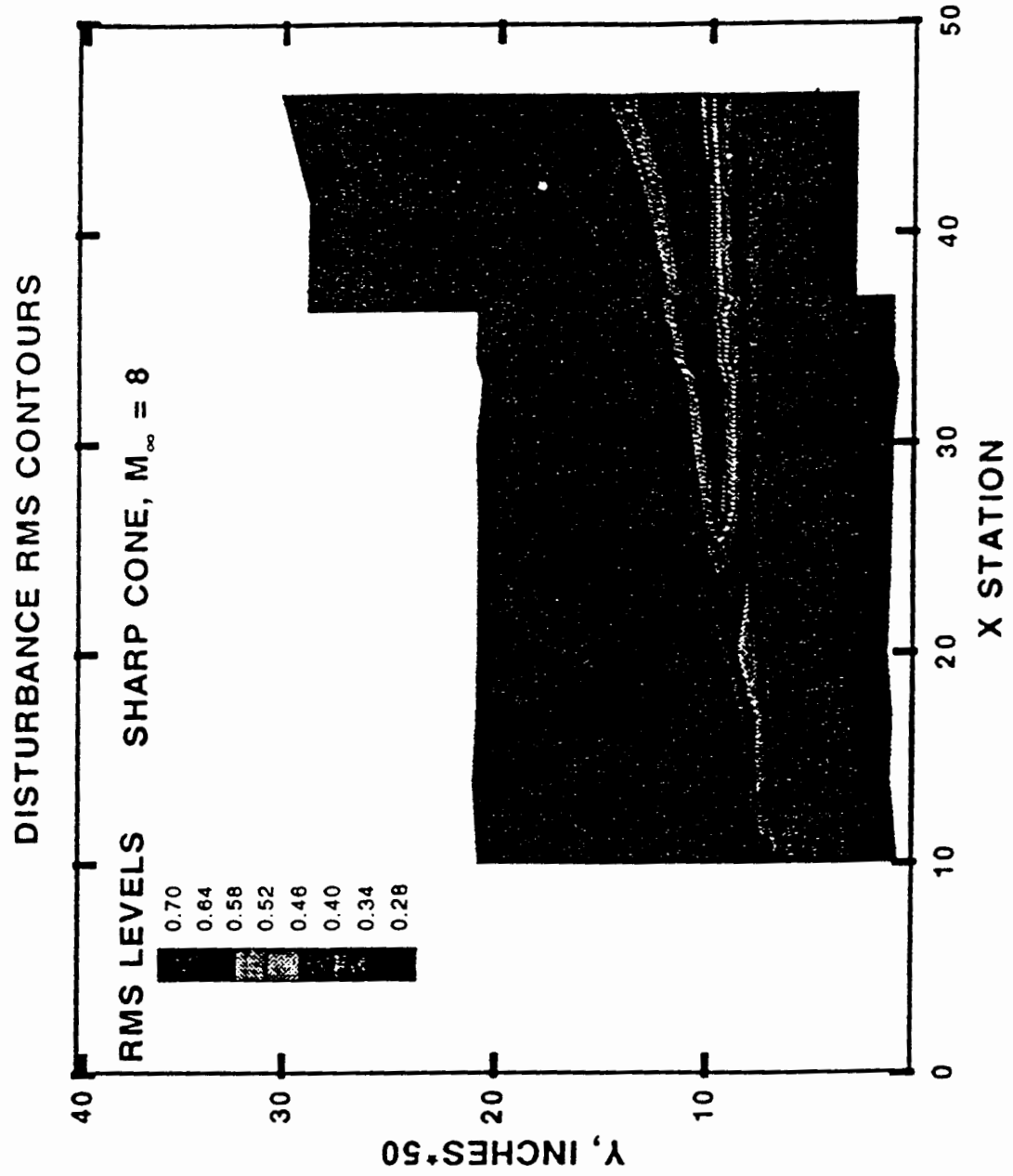
DISTURBANCE RMS CONTOURS
SHARP CONE, M_∞ = 8
RMS LEVELS
0.70
0.64
0.58
0.52
0.46
0.40
0.34
0.28
Y, INCHES*50
40
30
20
10
0
10
20
30
40
50
X STATION

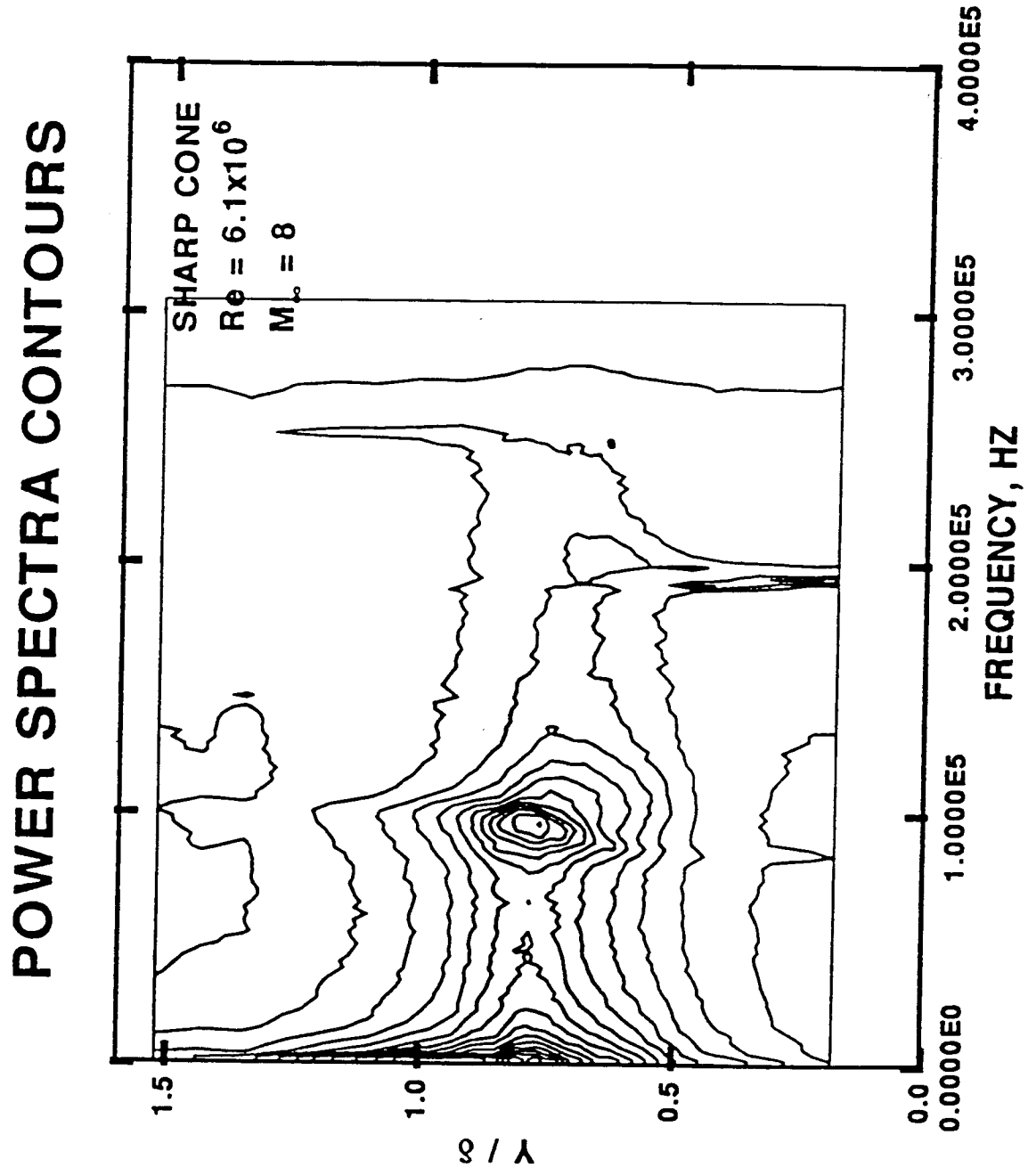
POWER SPECTRA CONTOURS
SHARP CONE
Re = 6.1x10^6
M∞ = 8
Y / δ
1.5
1.0
0.5
0.0
0.0000E0
1.0000E5
2.0000E5
3.0000E5
4.0000E5
FREQUENCY, HZ

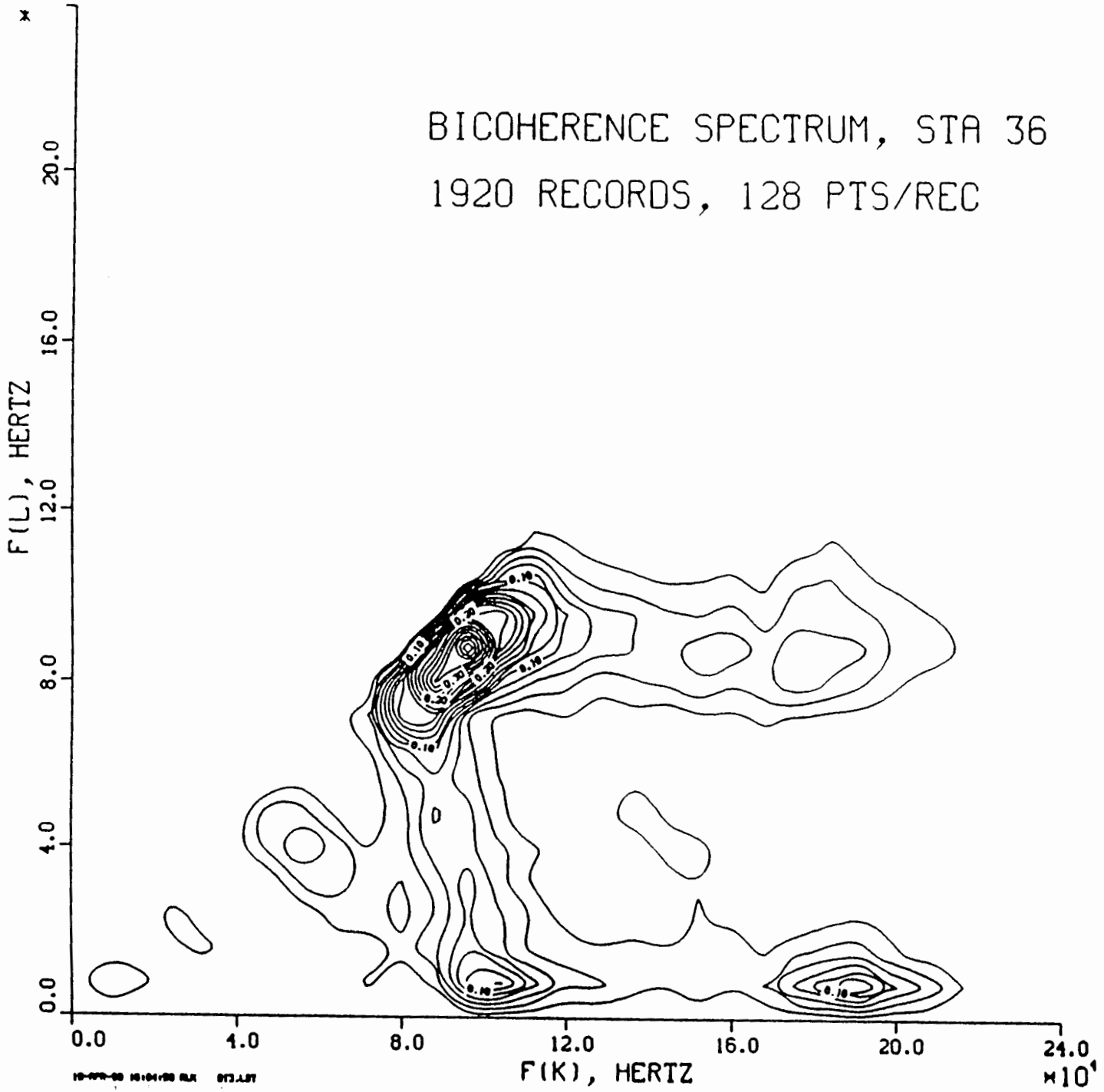
BICOHERENCE SPECTRUM, STA 36
1920 RECORDS, 128 PTS/REC
F(L), HERTZ
0.0
4.0
8.0
12.0
16.0
20.0
F(K), HERTZ
0.0
4.0
8.0
12.0
16.0
20.0
24.0
×10¹

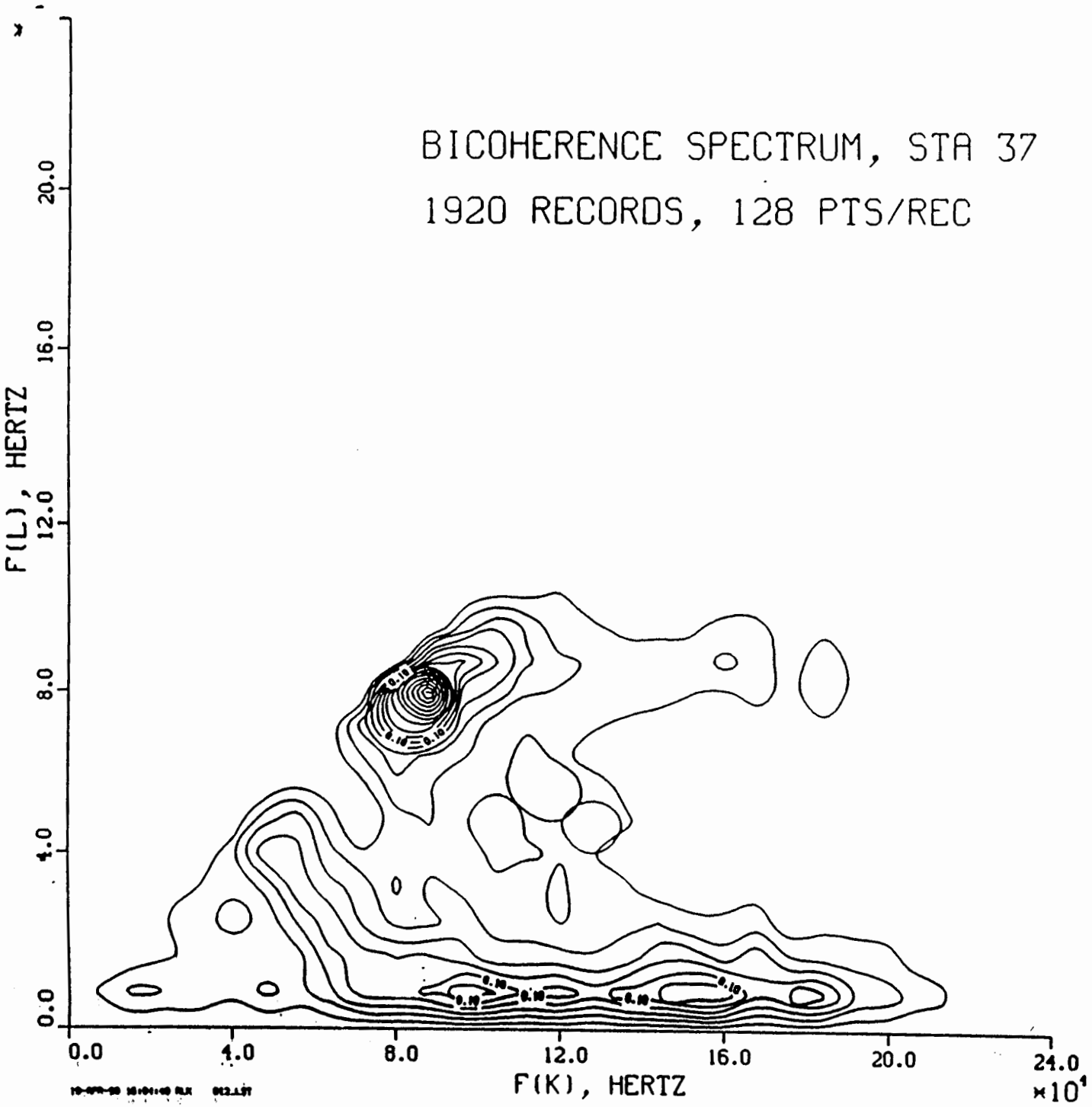
BICOHERENCE SPECTRUM, STA 37
1920 RECORDS, 128 PTS/REC
F(L), HERTZ
0.0
4.0
8.0
12.0
16.0
20.0
F(K), HERTZ
0.0
4.0
8.0
12.0
16.0
20.0
24.0
×10⁴

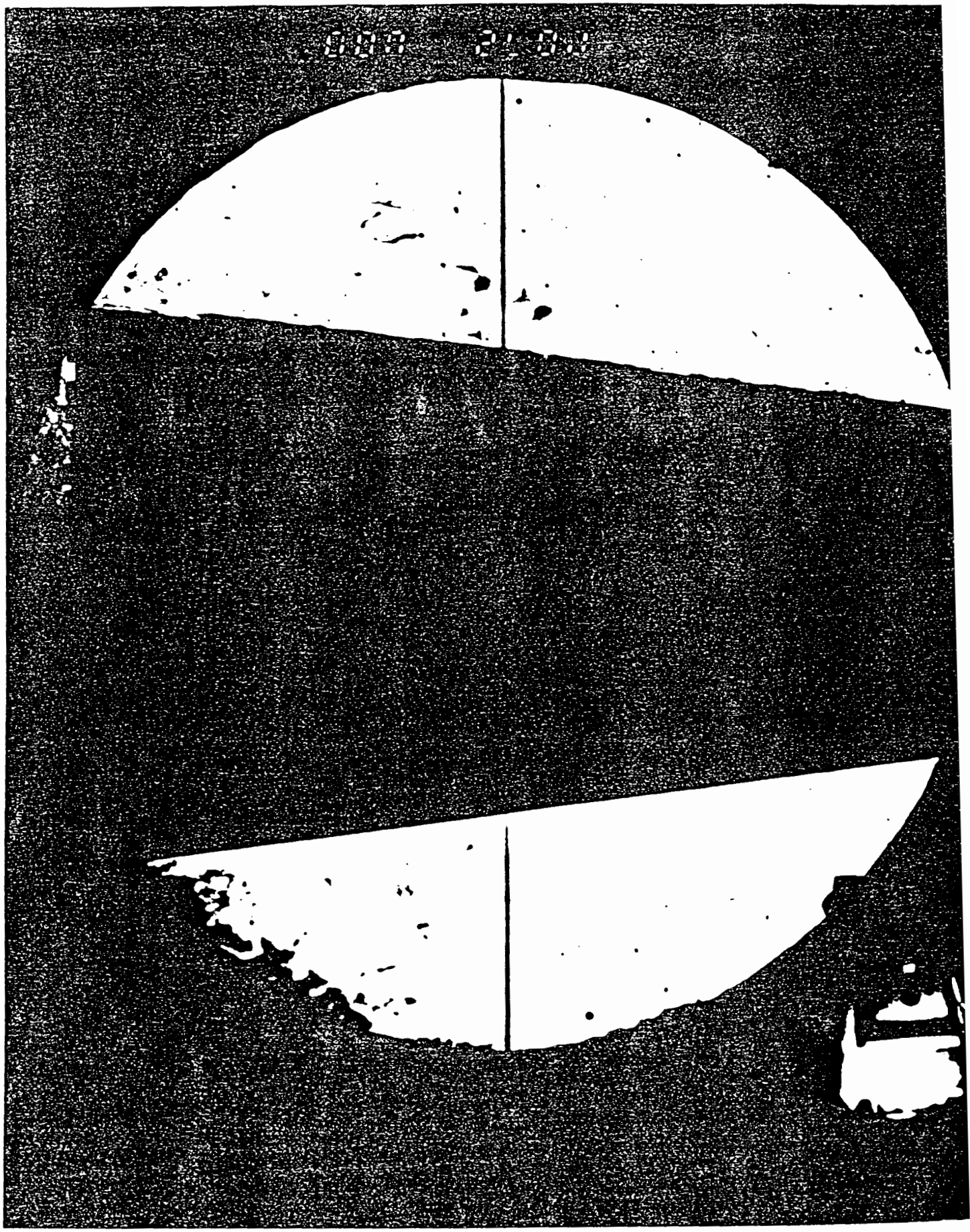

CONCLUSIONS

- HIGHER HARMONICS APPEAR EARLY
- NO EVIDENCE OF SUBHARMONICS
- SECOND MODE SATURATIONS MARKS:
  HEAT TRANSFER INCREASE
  BL THICKNESS INCREASE
  PROFILE FILLING
  DISTURBANCE SPREADING
  SPECTRAL DISPERSION
- ROLE OF BURSTS UNEXPLORED

TEXT TO ACCOMPANY "LATE STAGES OF HYPERSONIC BOUNDARY LAYER TRANSITION"

CHART 1. Title

CHART 2. The data presented in this talk consists of measurements taken at Arnold Engineering Development Center Tunnel B on sharp nosed cones at zero angle of attack at a freestream Mach number of eight. Two cases will be considered: adiabatic wall, and cold wall, with a wall-to-stagnation temperature ratio of 0.42. Heat transfer, shadowgraph, and contours of power spectral density will be presented for the cold wall case. Boundary layer thickness, velocity profiles, bicoherence, and power spectral density contours will be presented for the adiabatic wall case.

CHART 3. This graph shows contours of the power spectrum at the maximum energy point in the boundary layer (near the boundary layer edge) along the cooled cone. These data represent voltage fluctuations taken with an uncalibrated hot wire, and are thus qualitative only. Note the second mode growth which reaches maximum amplitude at a Reynolds number of about 3.2 million. There is no evidence of subharmonic growth.

CHART 4. This graph shows heat transfer from the cooled cone. The beginning of transition occurs between approximately 3.0 and 3.5 million Reynolds, in the same region where the second mode saturates.

CHART 5. This graph shows power spectrum contours for the adiabatic wall cone. Because the second mode is stabilized by the higher wall temperature, second mode saturation occurs at a higher Reynolds number, about 4.4 million, than the cold wall case. Although there is broad-band "filling-in" of valleys in the spectrum, there is no evidence of subharmonic growth.

CHART 6. Boundary layer thickness for the adiabatic wall begins to deviate above laminar correlations at approximately the same Reynolds numbers above which the second mode saturates.

CHART 7. Mean boundary layer profiles reflect the changes in other mean quantities near the second mode saturation point. Boundary layer velocity profiles collapse below a Reynolds number of 4.55 million, but become progressively fuller as the Reynolds number increases above this value.

CHART 8. Contours of constant broad-band rms show that disturbances are concentrated near the edge of the boundary layer, as expected for second mode mass flux and total temperature fluctuations. There is no significant "spreading" of these disturbances at Reynolds numbers lower than those where second mode saturation occurs (approximately station 36).

CHART 9. This graph shows contours of power spectrum with height at a fixed Reynolds number of 6.1 million on the adiabatic cone. Note that the inner portion of the boundary layer is relatively quiescent (in terms of the sensed variables), and that disturbances in this region are primarily lower frequency. Second mode disturbances are contained near the boundary layer edge.

CHART 10. This graph shows bicoherence for the sharp nose adiabatic cone at a Reynolds number of 4.68 million, which is where the peak second mode amplitude and the peak bicoherence occur. The bicoherence shows fairly strong self-interaction of the second mode fundamental (first harmonic) with itself to produce a second harmonic, weak evidence of first/second harmonic interaction to produce a third harmonic, and interaction of both the first and second harmonics with low frequency disturbances.

CHART 11. This graphs shows bicoherence at a Reynolds number of 4.8 million. The second mode amplitude in the spectrum has begun to decay, as well as the second mode/second mode bicoherence. The contours are now broader, indicating that a broad band of nonlinear interactions is occurring to fill in the spectrum.

CHART 12. The shadowgraph of the cold wall cone shows a well-ordered wave structure, with transition possibly beginning near the end of the cone on the top. This feature is transient, and does not appear in the one other shadowgraph taken at this condition.

CHART 13. Based on the data presented here, we can make several observations regarding transition in this wind tunnel environment.

1. There is no evidence of a strong subharmonic prior to boundary layer breakdown.

2. Higher harmonics of the fundamental arise prior to breakdown through non-linear wave interaction.

3. A saturation of the second mode (based on the average of 128 records) occurs near breakdown, and several changes in the boundary layer are correlated with this event:

   a. Surface heat transfer begins to increase.
   b. Mean boundary layer thickness begins to increase.
   c. The boundary layer profiles begin to fill out.
   d. Disturbances once contained near the edge of the boundary layer begin to "spread" to the surface.
   e. "Filling-in" of the spectral valleys begins to occur, apparently through non-linear wave interaction.

4. Second mode waves are present (at least on average) even after the boundary layer begins to show considerable mean distortion.

5. "Optical" transition tends to occur approximately half-way between the minimum and maximum heat transfer. The optical transition point is unsteady, but there is not enough data to measure this statistically. Also, the role of turbulent bursts is not fully explored.

Experiments in Transitional Boundary Layers with Emphasis on High Free-Stream Disturbance Level, Surface Concave Curvature and Strong Favorable Streamwise Pressure Gradient Effects

T. W. Simon and R. J. Volino
University of Minnesota
Mechanical Engineering Department
Minneapolis, MN 55455

Experiments on boundary layer transition with flat, concave and convex walls and various levels of free-stream disturbance and with zero and strong streamwise acceleration have been conducted. Measurements of both fluid mechanics and heat transfer processes were taken. Examples are profiles of mean velocity and temperature; Reynolds normal and shear stresses; turbulent streamwise and cross-stream heat fluxes; turbulent Prandtl number; and streamwise variations of wall skin friction and heat transfer coefficient values. Free-stream turbulence levels were varied over the range from about 0.3% to about 8%. The effects of curvature on the onset of transition under low disturbance conditions are clear; concave curvature leads to an earlier and more rapid transition and the opposite is true for convex curvature. This was previously known but little documentation of the transport processes in the flow was available. When at elevated free-stream disturbance levels, the curvature effect on the onset of transition is greatly diminished, though the effect of curvature on the later stages of transition and on turbulent transport downstream of transition is noticeable. Experiments were conducted with a zero streamwise pressure gradient, a constant-K ($K=\nu/U_\infty^2\ dU_\infty/dx$) of 0.75×10^{-6} and with a constant dU_∞/dx of 31 sec^{-1}. Various signal processing techniques were applied to both the hydrodynamic and heat transfer data. Probability density functions (PDF's) for temperature or velocity in the early transitional flow show a skewness, indicating the importance of a few, infrequent events for which the instantaneous velocity is low. In contrast, PDF's in fully-turbulent flow display a more Gaussian distribution, indicating a more uniform distribution with event size. Another processing technique is octant separation of turbulent shear stress and heat flux. In the transitional flow, an octant which represents a hot, wallward interaction, which is a rather unimportant octant in turbulent flow, emerges in importance. The importance of the hot wallward interaction remains when the flow is accelerated. Data on the combined effects of streamwise acceleration, concave curvature, and elevated free-stream disturbance levels were discussed. Profiles of the u'v' correlation show the separate effects of curvature and acceleration. A profile of u'v' processed from data taken from portions of the waveform for which u' is identified to be non-turbulent-like shows a small contribution of non-turbulent flow to the overall correlation value. Mean

temperature profiles show that if the acceleration effects on eddy diffusivity and the streamwise convection terms are included and if the turbulent Prandtl number measured by a triple-wire probe is employed, reasonable fits between the computed and measured profiles are attained. Power spectral distributions on u' are presented in fu'^2 v.s. log f coordinates (f is the frequency) and a peak in energy seems to roughly correspond to the frequency associated with convection of eddies of the integral scale size in the freestream. In an attempt to see the effect that the freestream may have on the boundary layer under such high bypass conditions, a ratio of the boundary layer spectrum to the freestream spectrum was taken. It appears to show considerable amplification at a frequency which roughly corresponds with that of the convected eddies. Further processing steps included computing the ratio of downstream to upstream spectra in the boundary layer divided by the same quantity but taken from the freestream data. The numerator shows the streamwise amplification in the boundary layer, the denominator shows the streamwise amplification in the freestream. It is interesting to note that the ratio remains at a value of 3 across the spectrum.

Upcoming activity includes measurements in stronger acceleration cases where a considerable transition length is expected in spite of the high disturbance level of the flow entering the test region.

Curvature Effect on Stanton Number
Tu=0.6%, Unaccelerated Flow

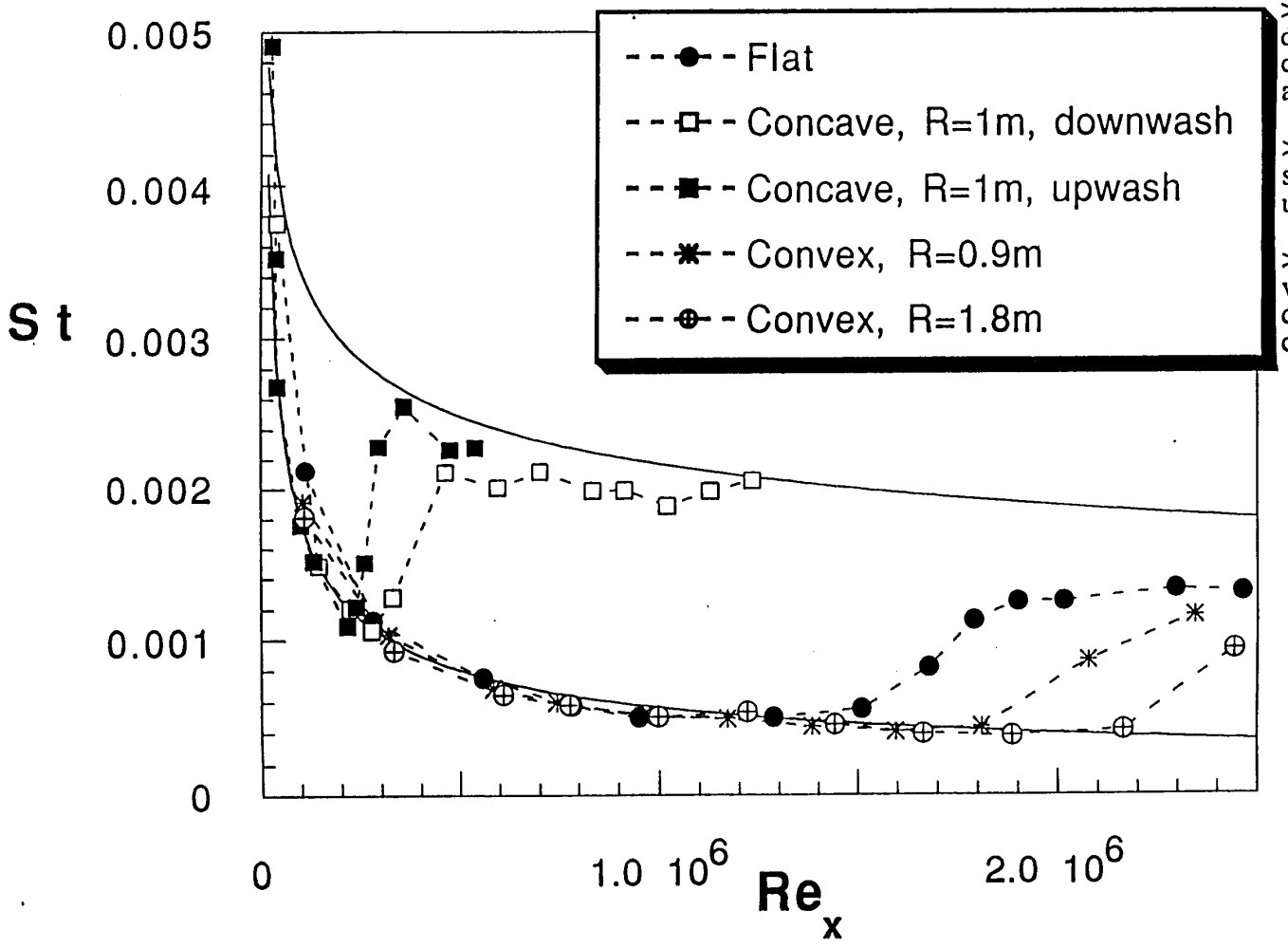

> Concave curvature is destabilizing, whereas convex curvature is stabilizing, relative to a flat wall.

> Concave case had an array of stationary Görtler vortices; hence, upwash and downwash regions.

> Convex effect should strengthen with magnitude of 1/R; hence, cases are out of order (R=0.9 m case is suspect).

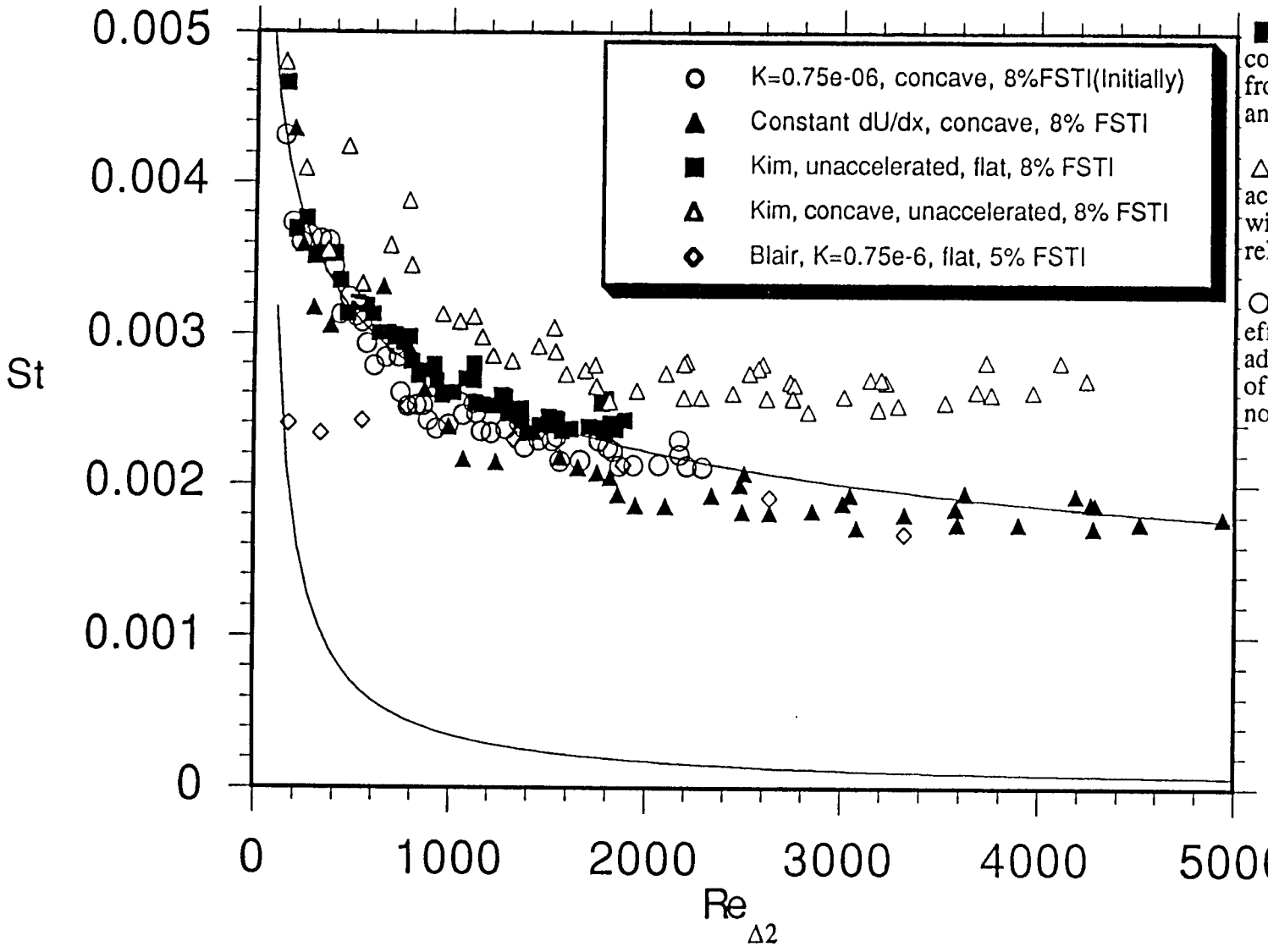

■ △ Comparison shows concave curvature effect (strong from very near the beginning -- and continually growing)

△ ▲○Comparison shows acceleration effect (decrease in St with increase of K, but no relaminarization tendencies)

○ ◇ Comparison shows an effect of slight FSTI rise and addition of curvature (note signs of transition in the ◇ case but no noticeable signs in the ○ case.

Stanton Numbers

OCTANT ANALYSIS

Instantaneous velocity and temperature signals divided into eight categories based on the signs of u', v' and t'.

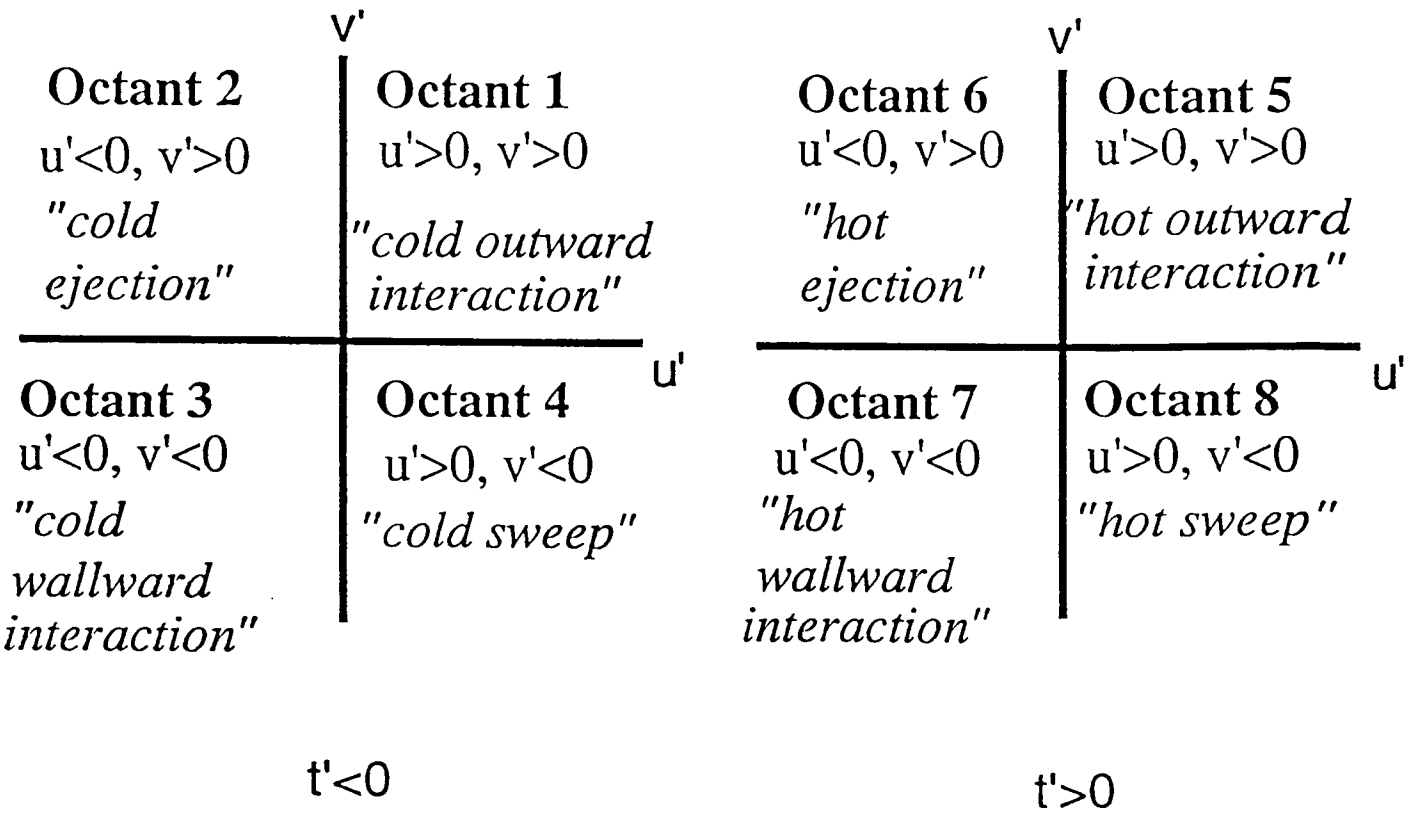

Names taken from Kawaguchi, Matsumori and Suzuki (1984).

Can correlate with particular eddy motions.

Examples of Ties to Flow Structure

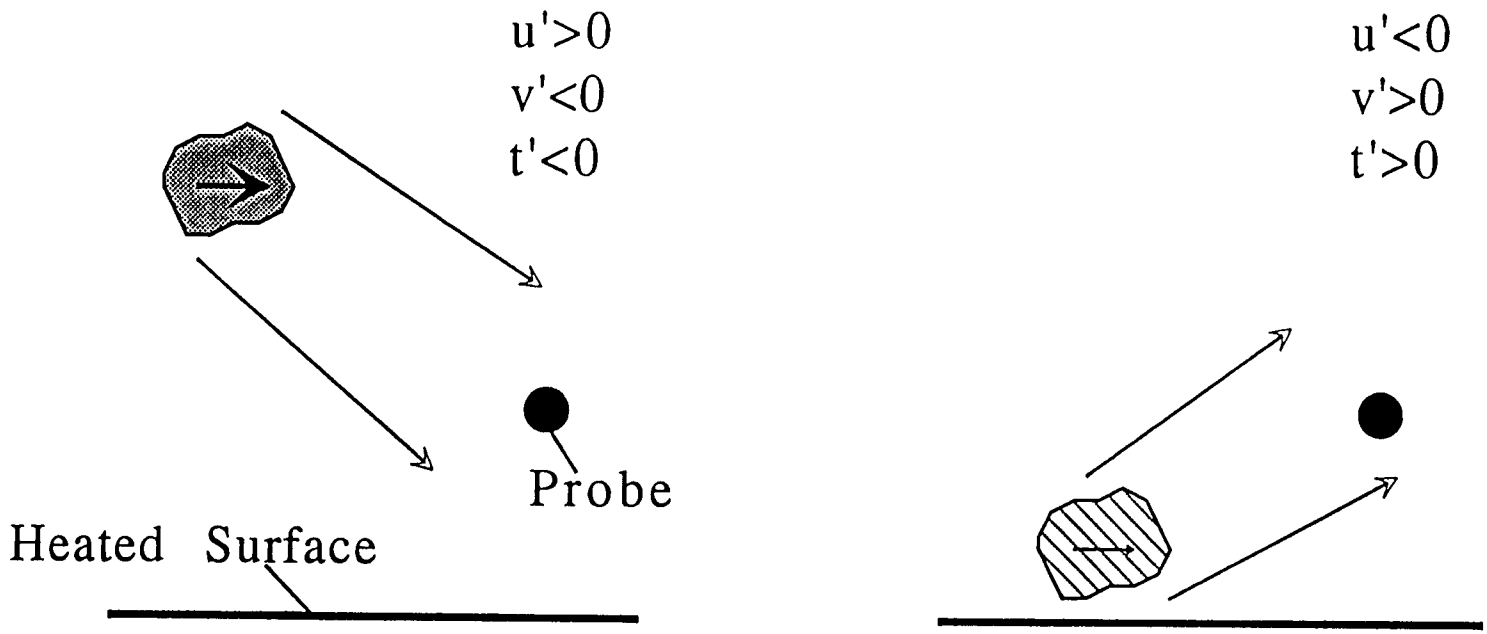

Octant 4
Cold Sweep

Octant 6
Hot Ejection

> These are the predominant terms in a turbulent boundary layer.

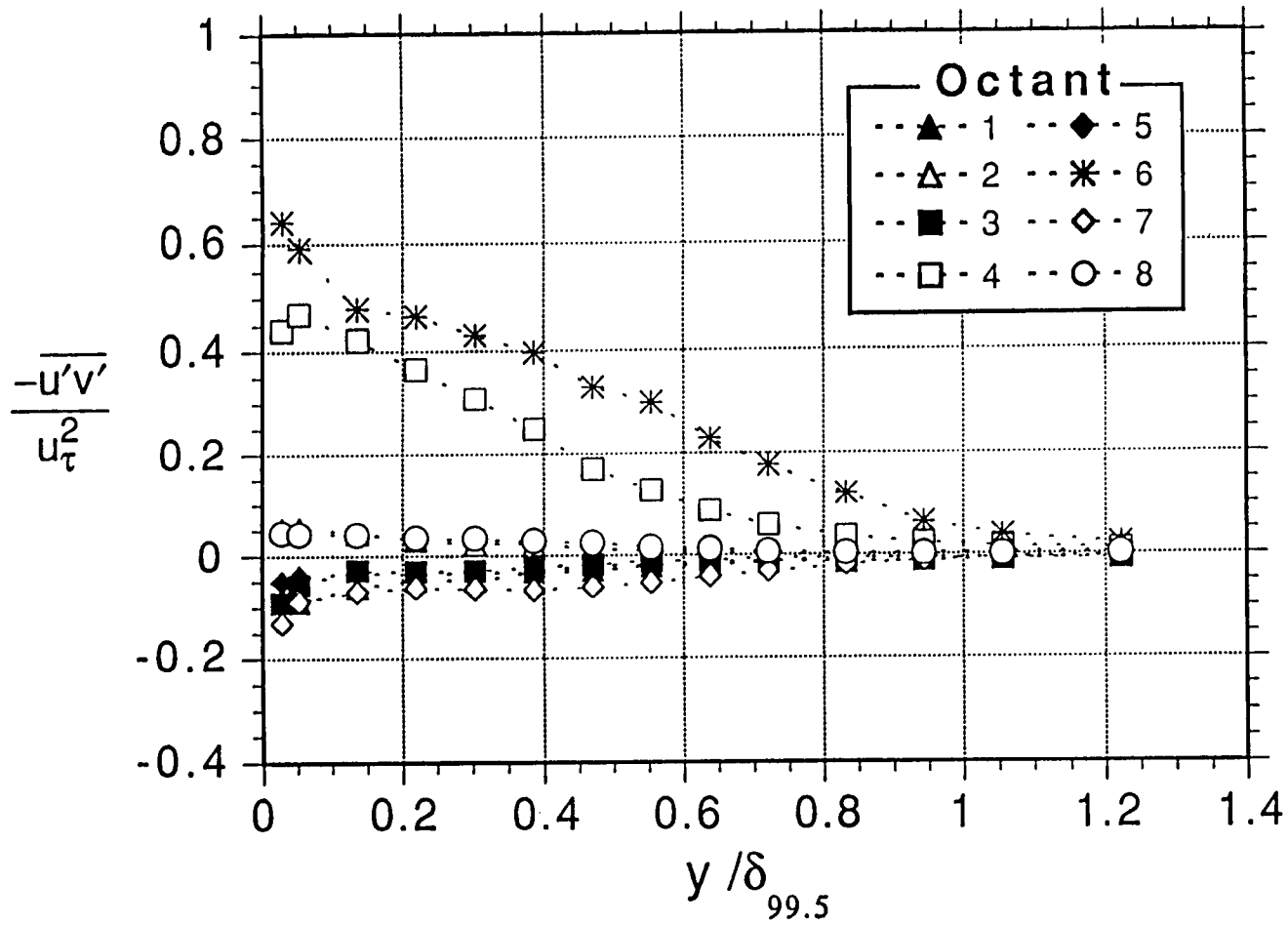

Turbulent shear stress profiles, 1.5% FSTI flat-wall case, fully-turbulent flow

Re_θ=1587, Re_x=1.062×10^6

> Note the importance of octants 4 and 6.

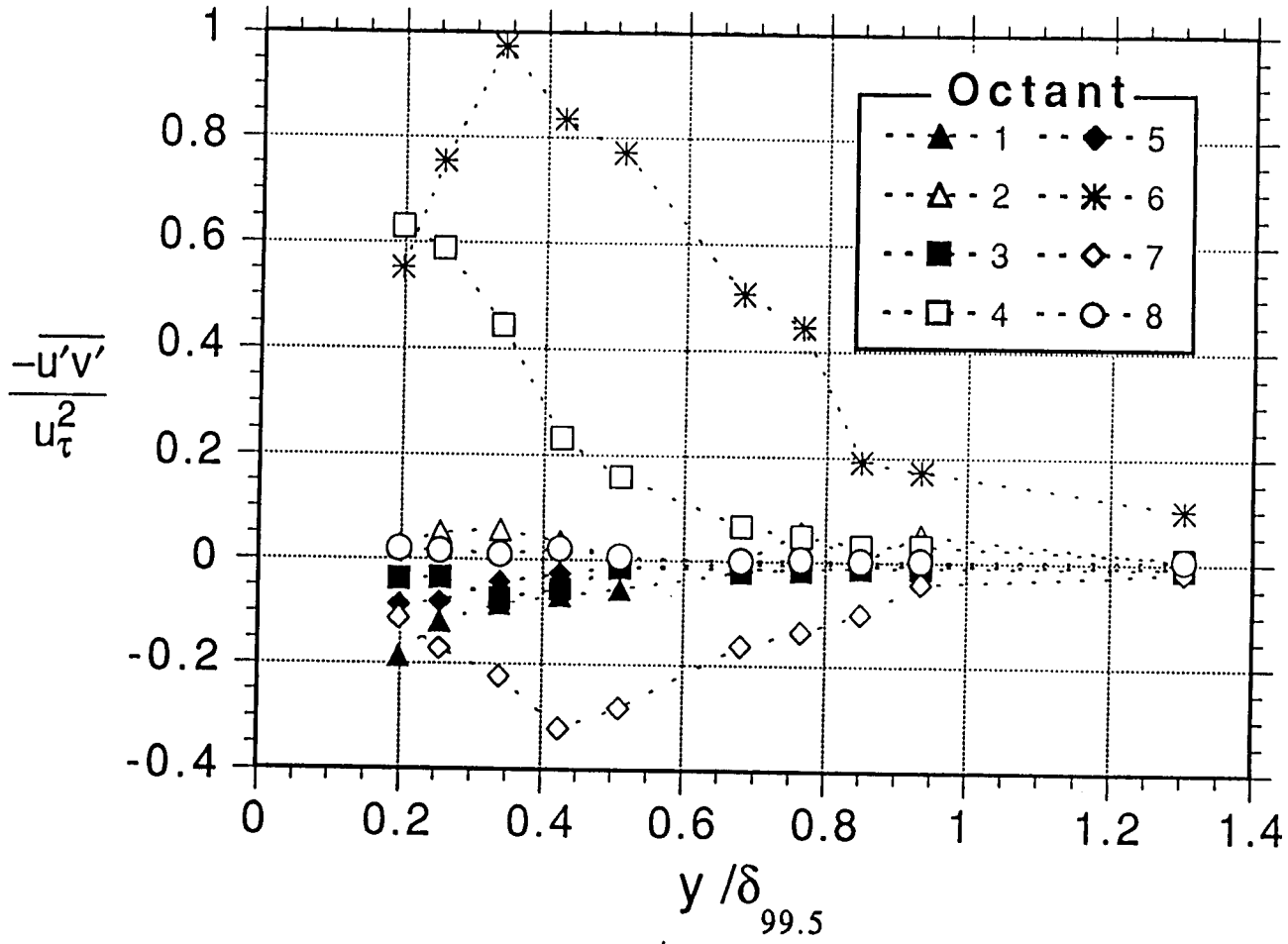

Turbulent shear stress profiles, 1.5% FSTI flat-wall case, transitional flow

Re_θ=379, Re_x=0.3442×10^6, γ=5% K=0.0

> Note the emergence of a positive $\overline{u'v'}$ contribution from octant 7 and the rise in importance of octant 6.

wo Wave Packet (TWP) Interaction; X=160cm Z=2cm Yma
Xp=30cm Zp=-4 and 8cm

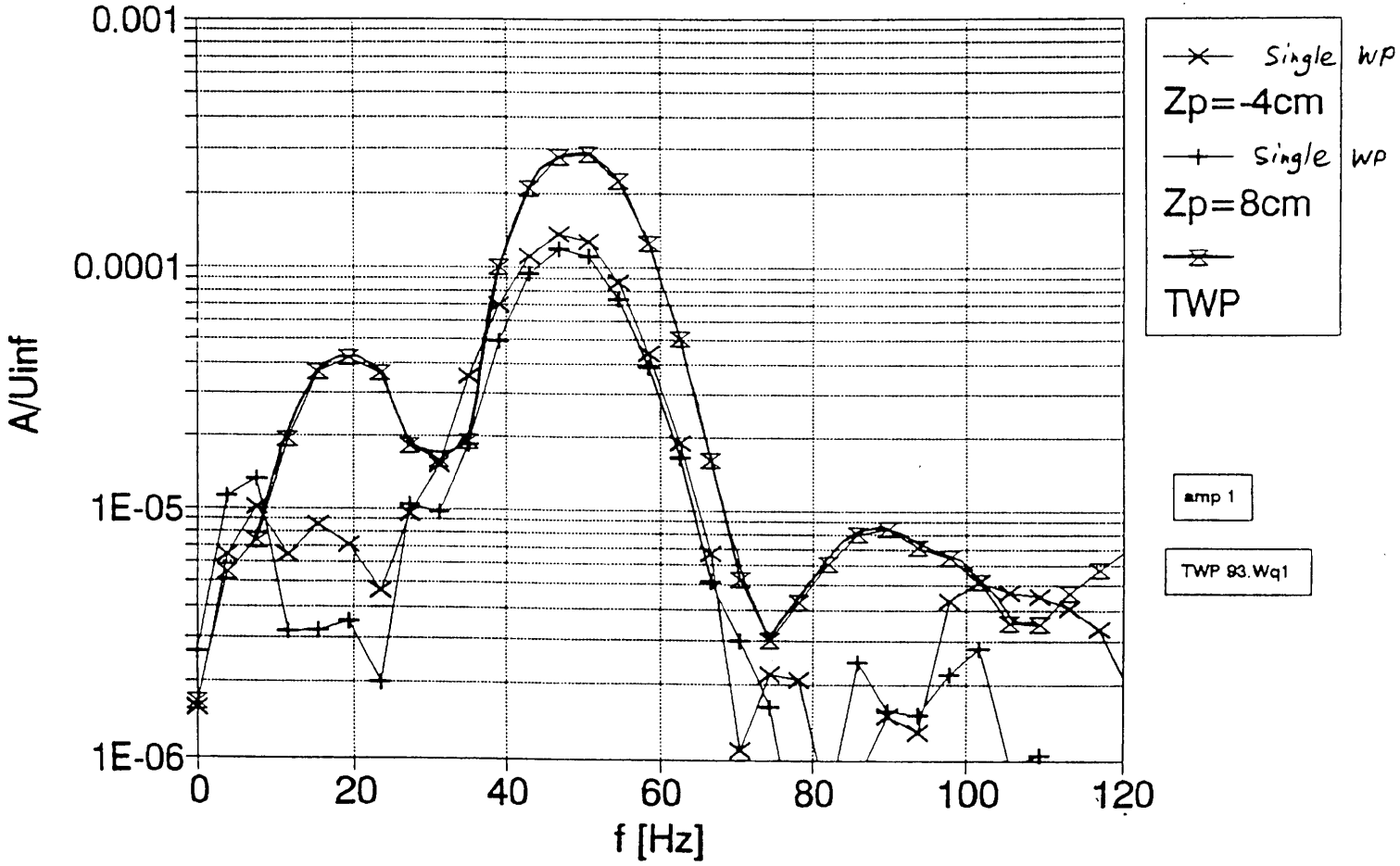

Appearance of a low band of f due to the Interaction

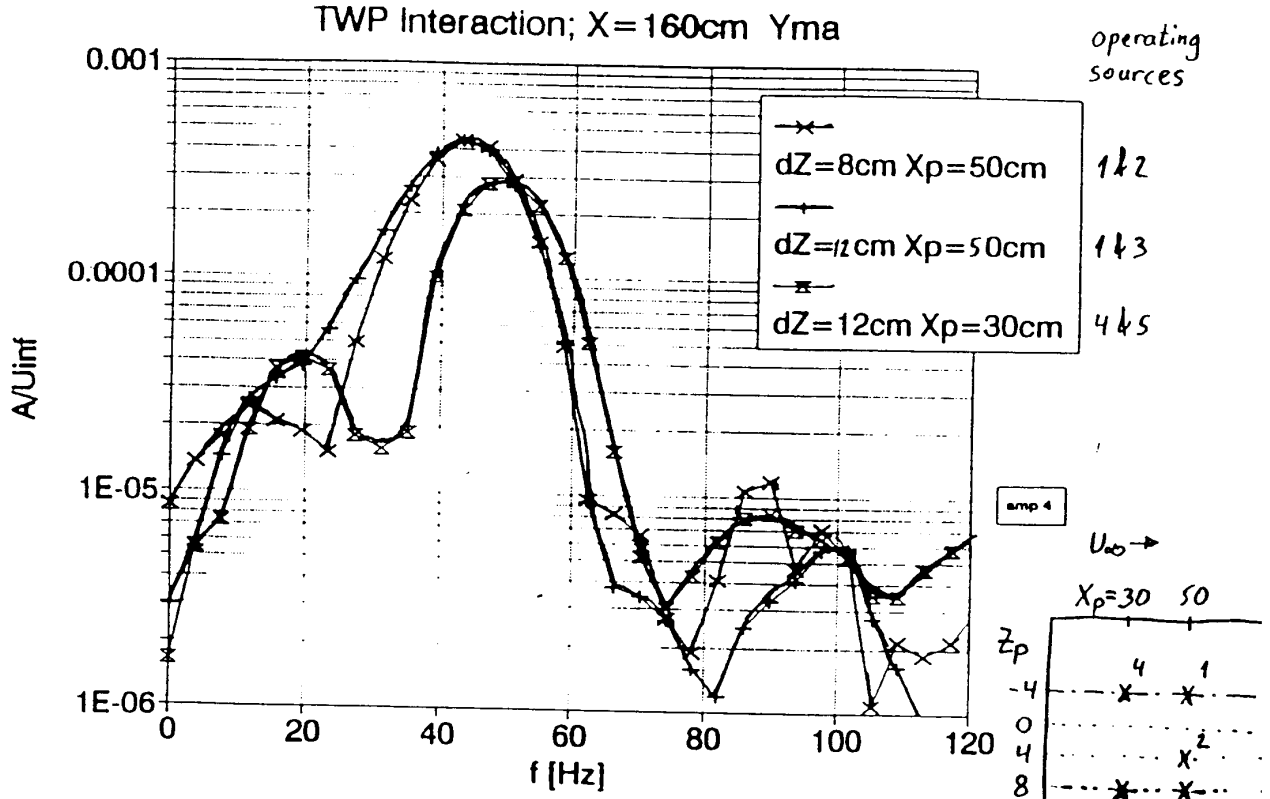

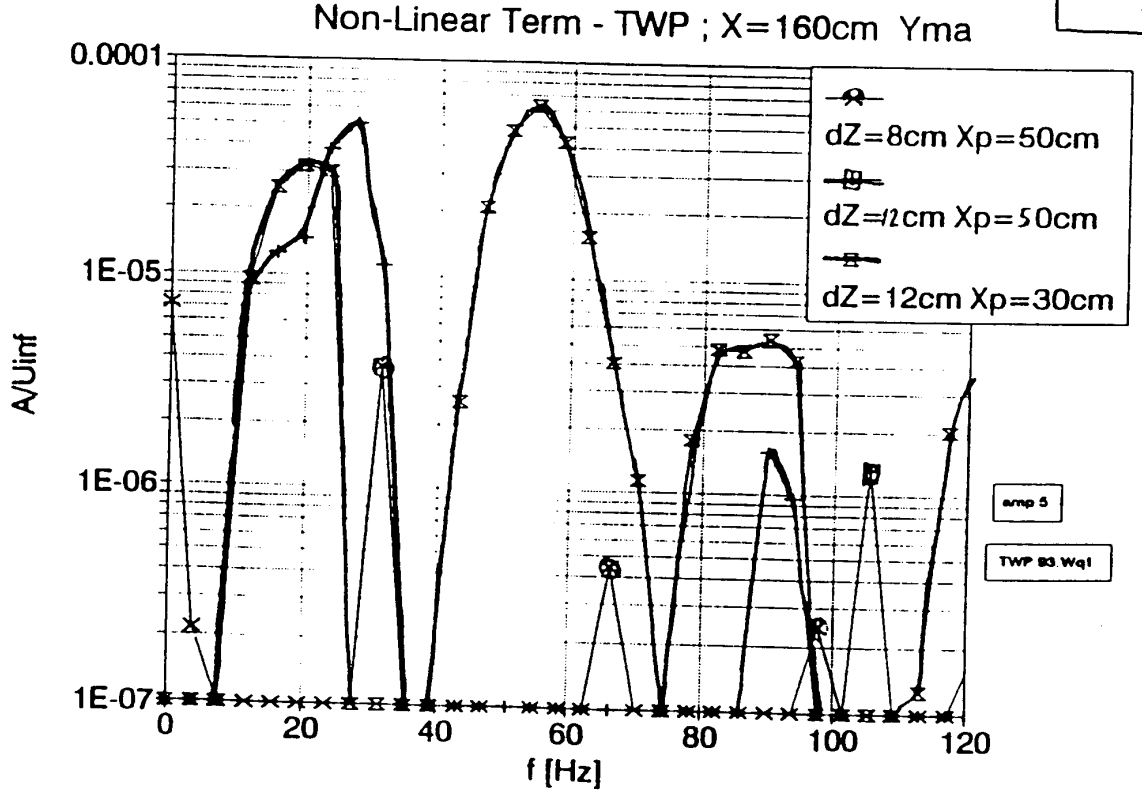

Effect of Spanwise Separation on Non-Linear term 12

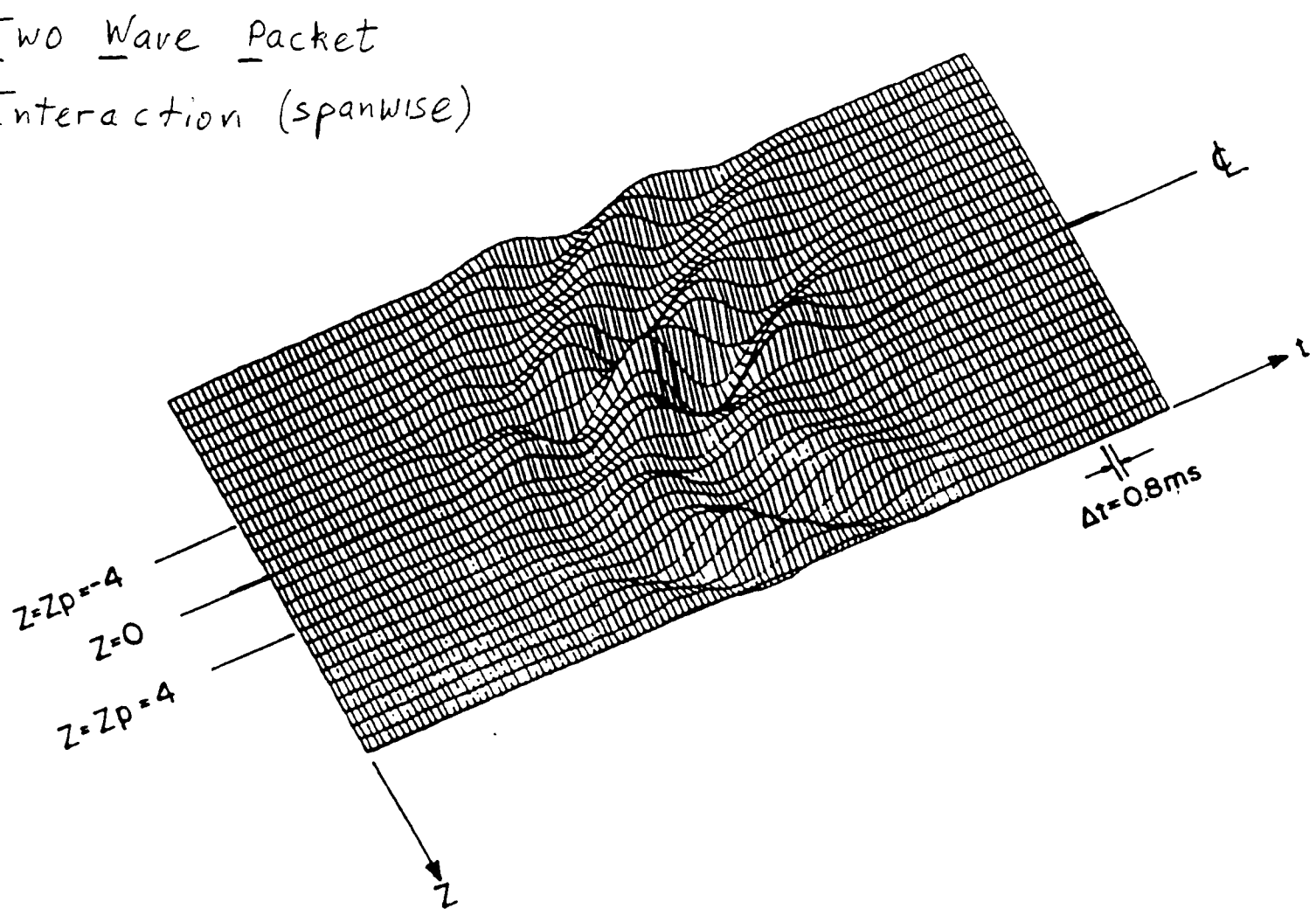

Fig. The velocity change due to the TWP passage at R_{δ^*}=1100 (X_s=55cm), Y≃Y_{max}, the whole TWP span. $U \sim 0.35 U_\infty$

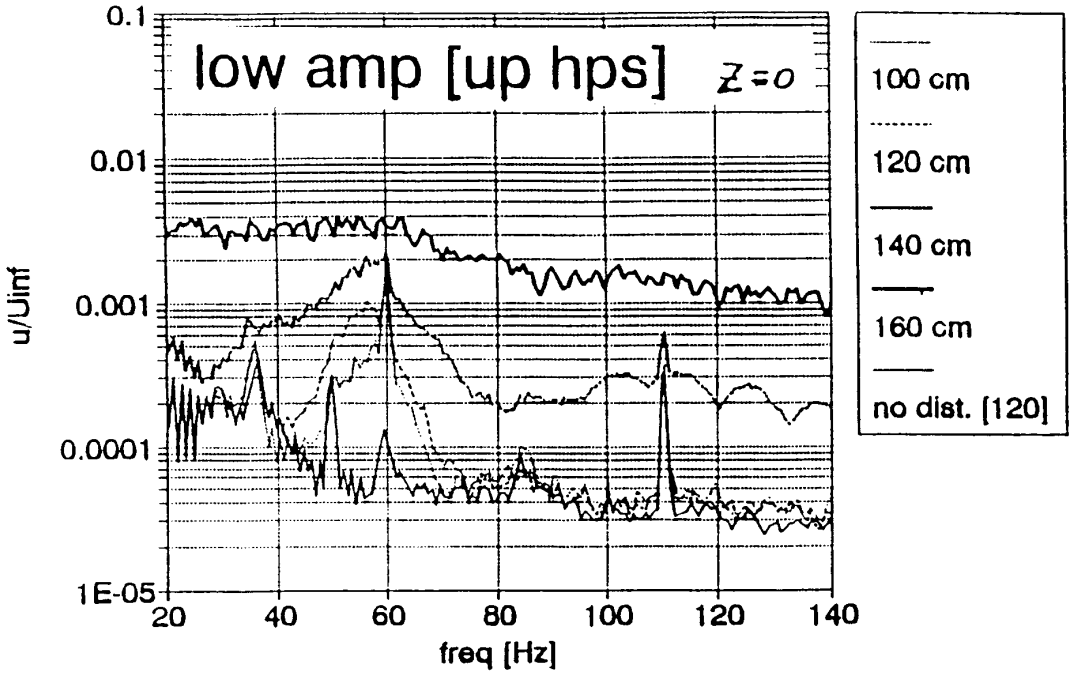

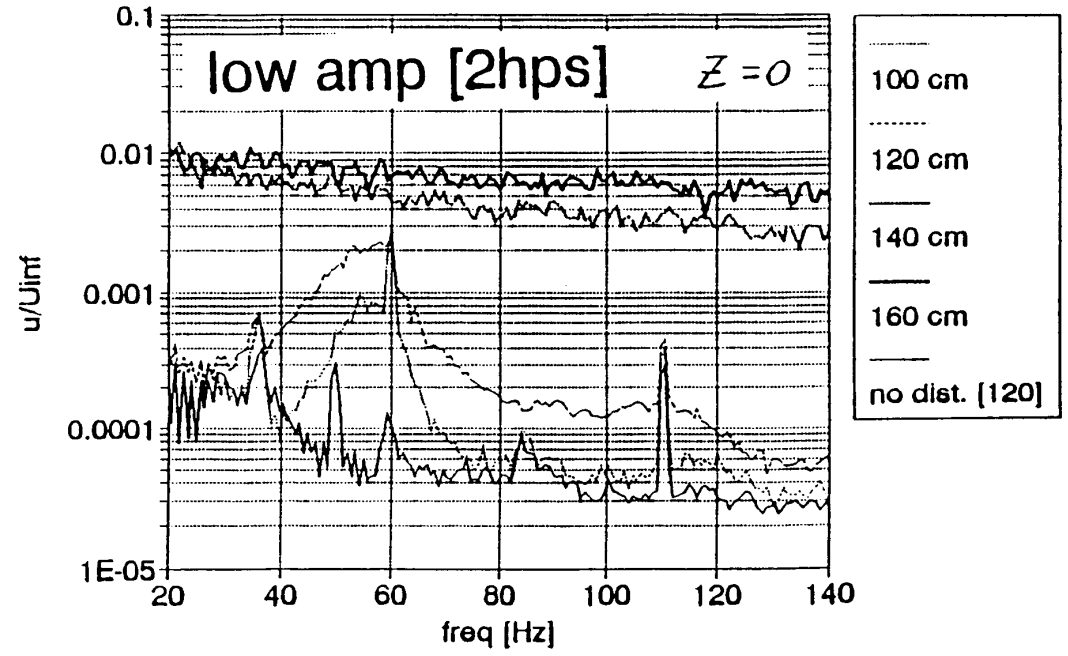

comparison between single HPS spectrum (up) and THPS (Interaction) spectrum.

9

PHASE LOCKED

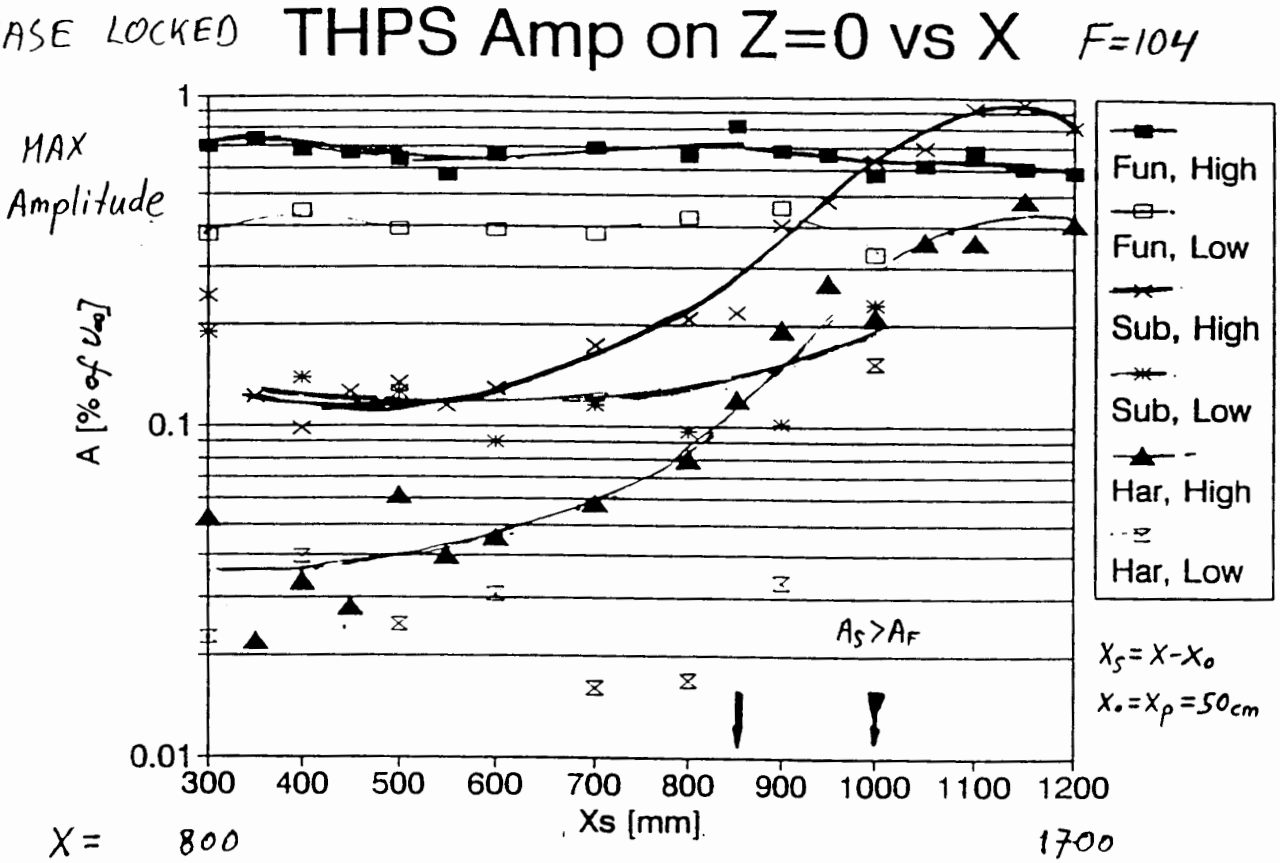

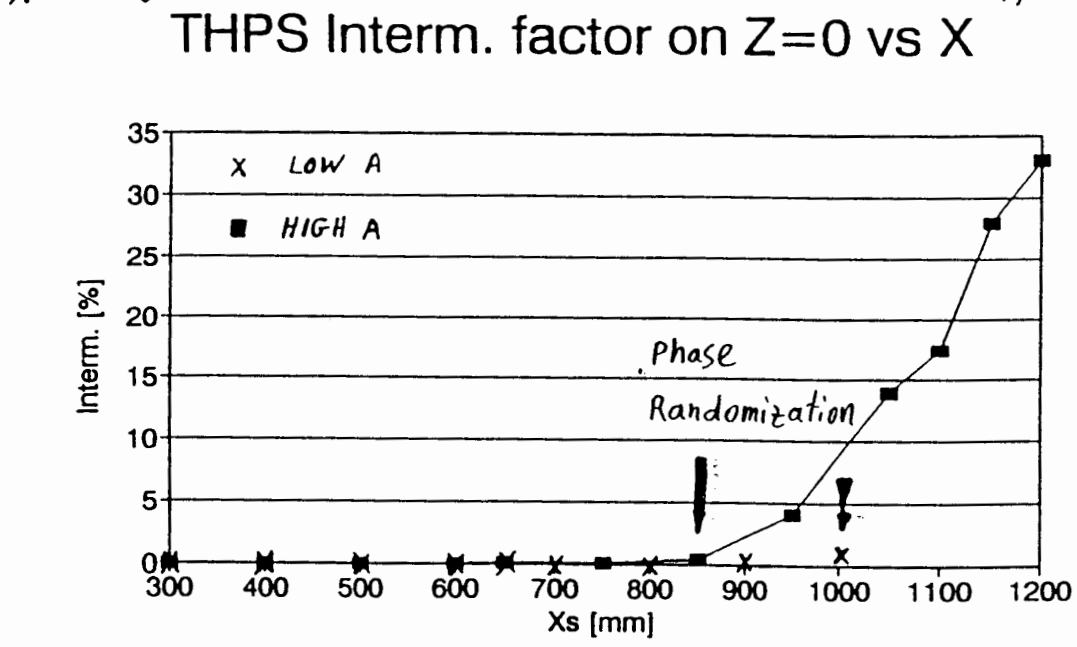

Two: Harmonic Point Source Interaction

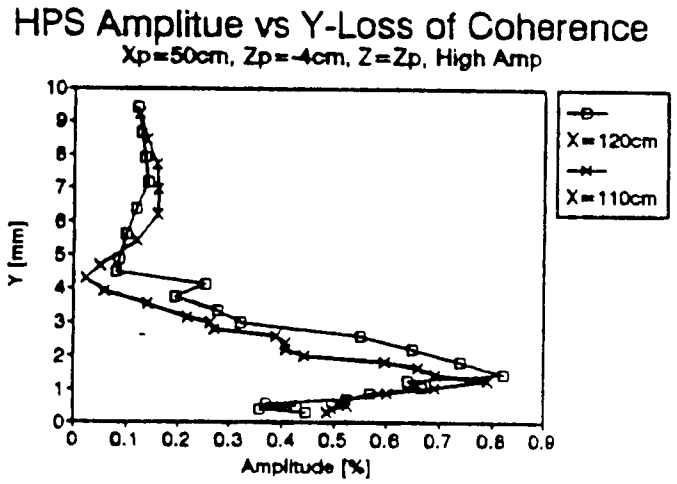

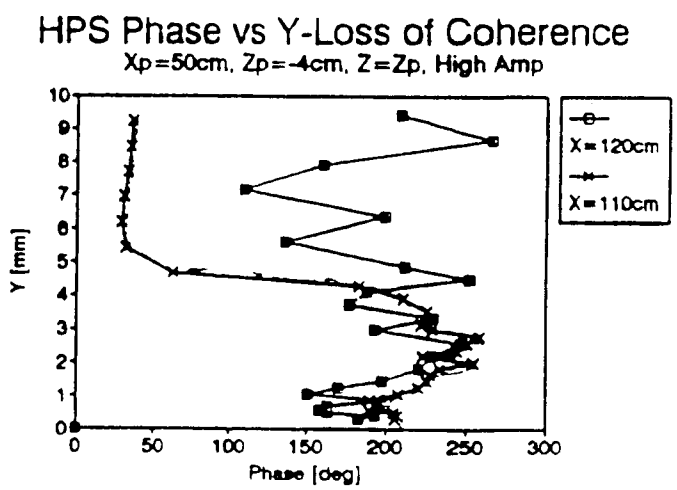

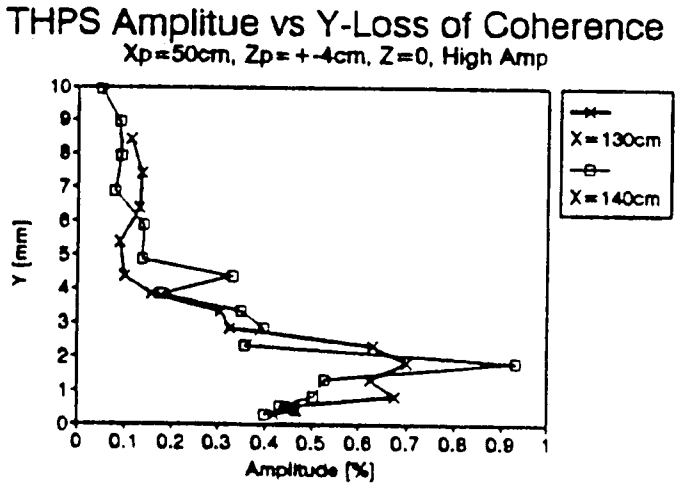

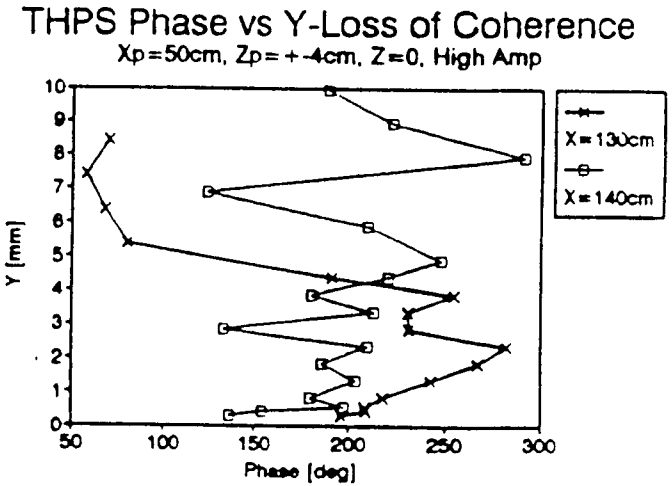

Phase Randomization prior to Breakdown

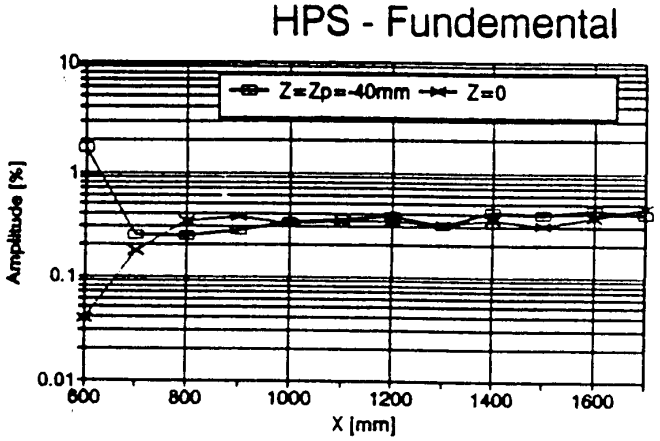

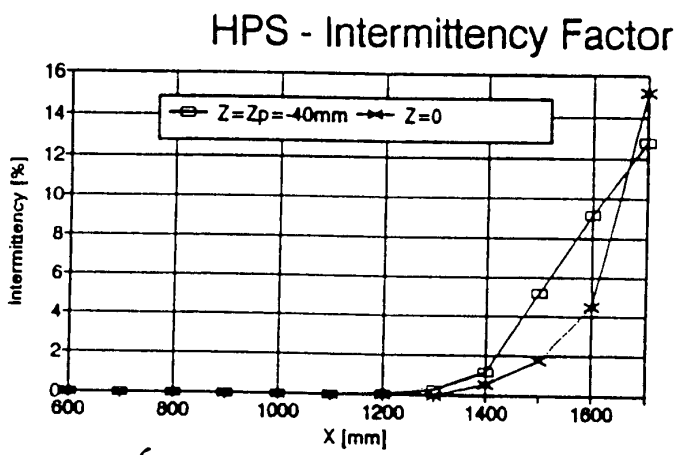

$F = 2\pi f \nu / U_\infty^2 = 104 \cdot 10^{-6}$

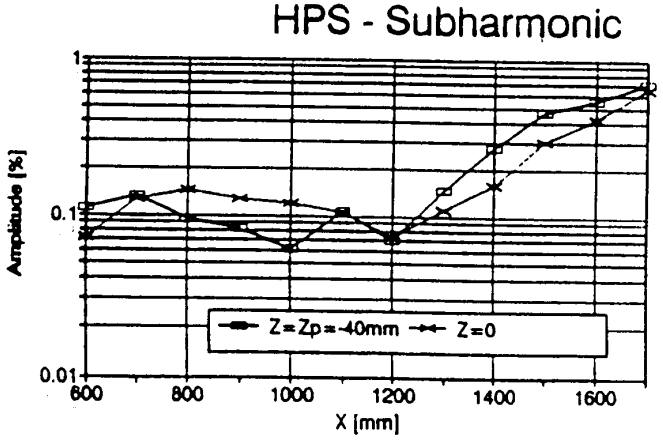

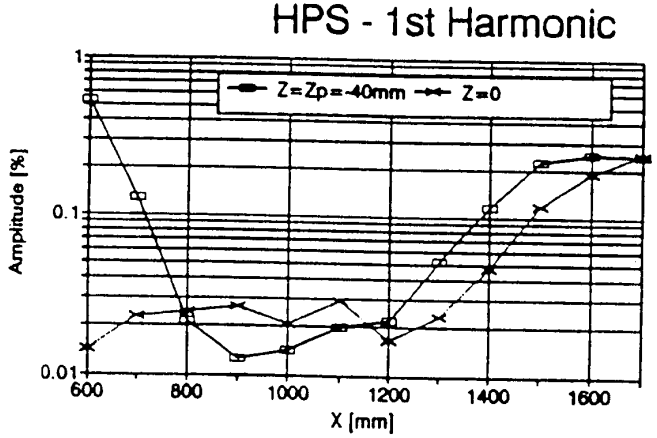

Max Amp (with respect to Y) Phase locked to the FUNDAMENTAL (F)

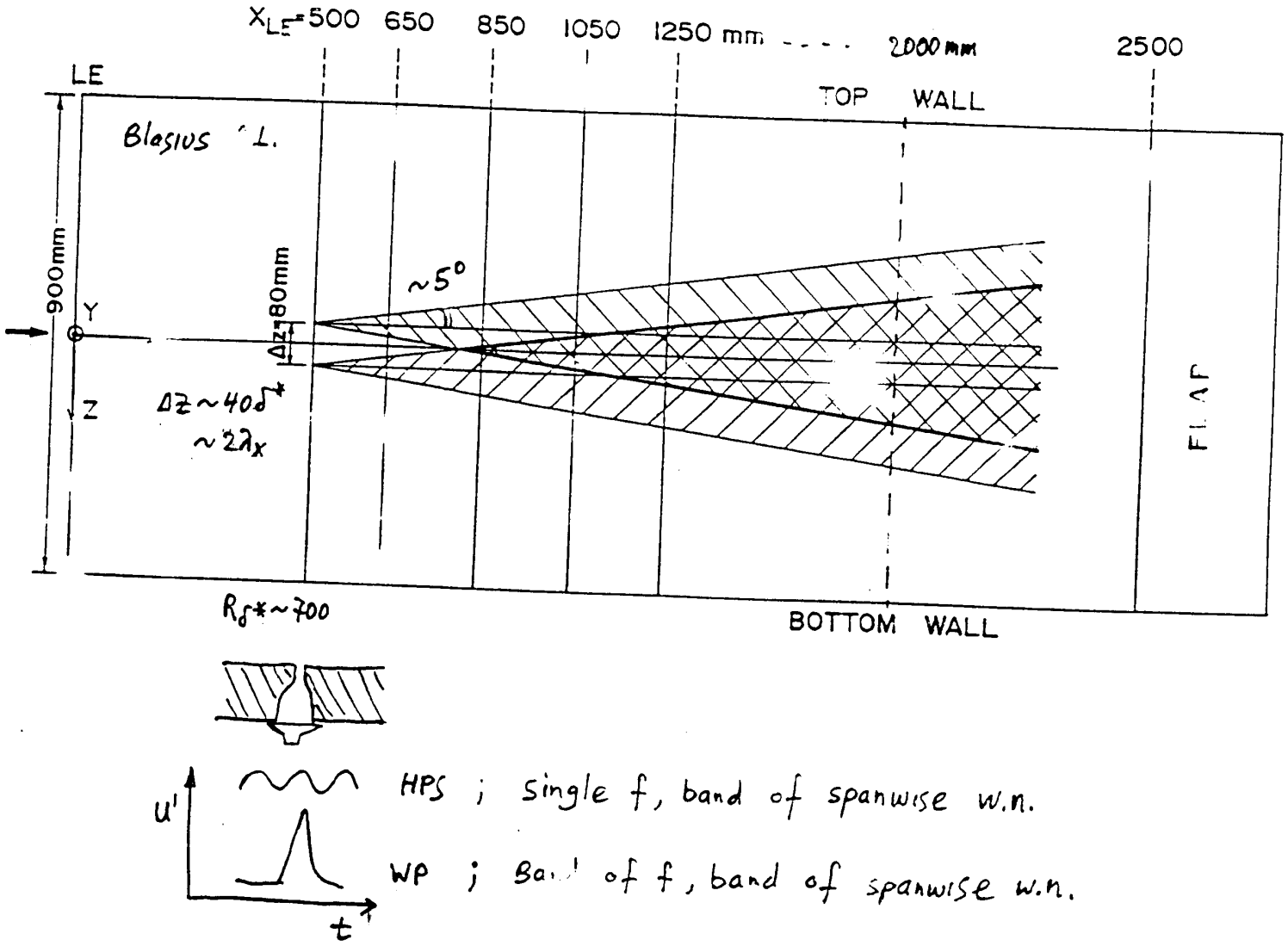
X_{LE}=500 650 850 1050 1250 mm ---- 2000 mm 2500
LE
TOP WALL
Blasius B.L.
900mm
Y
Z
J_∞
Δz 80mm
~5°
$\Delta z \sim 40\delta^*$
$\sim 2\lambda_x$
$R_{\delta^*} \sim 700$
BOTTOM WALL
FLAP
u'
t
HPS ; single f, band of spanwise w.n.
WP ; Band of f, band of spanwise w.n.

ON THE EVOLUTION OF LOCALIZED DISTURBANCES AND THEIR SPANWISE INTERACTIONS LEADING TO BREAKDOWN

A. Seifert
Department of Fluid Mechanics and Heat Transfer
Faculty of Engineering, Tel-Aviv University, ISRAEL

ABSTRACT

Localized Disturbances in a laminar boundary layers represent a more realistic model of transition than the extensively studied, two or quasy three-dimensional perturbations regardless of the fact if they evolve in a linear manner or not. Localized disturbances can originate by surface imperfections, insects or dust. The disturbances can be Harmonic (i.e. containing a single frequency and a complete set of spanwise wave numbers) or Pulsed (i.e containing a band of streamwise and spanwise wave numbers).

At sufficiently low amplitudes localized disturbances behave according to a linear stability model. It is highly probable that in a natural transition process such localized disturbances will overlap and interact. These interactions could either delay transition because of a partial wave cancellation resulting in an attenuation of the disturbance, or adversely enhance it by promoting non linear interactions. The non linearity could be simply amplitude dependent or cause a triad resonance. Non linear processes in a wave packet lead to breakdown and to the formation of turbulent spots. When the amplitude of the harmonic disturbance saturates, non linear prcesses widen the band of the lower amplified frequencies adjacent to the frequency of excitation.

Experimental results describing the spanwise interactions of harmonic and pulsed localized disturbances leading to breakdown will be presented and discussed. A comparison to the evolution and breakdown of a single localized disturbance will be provided.

1)

On the Evolution of Localized Disturbances and their Spanwise Interactions Leading to Breakdown

Dr. Avi Seifert
Tel-Aviv University

Acknowledgments: Y. Mitnik, B. Margaliot.

OBJECTIVES

DOES SPANWISE INTERACTION OF LOCALIZED DISTURBANCES PROMOTES TRANSITION ?

Comments about NATURE of TRANSITION
due to an ISOLATED:
Harmonic Point Source and Wave Packet

Relevance / Difference between TRANSITION
due to TWO HPS INTERACTION and TWO WP INTERACTION
(leading to breakdown)

SPECTRA RATIO

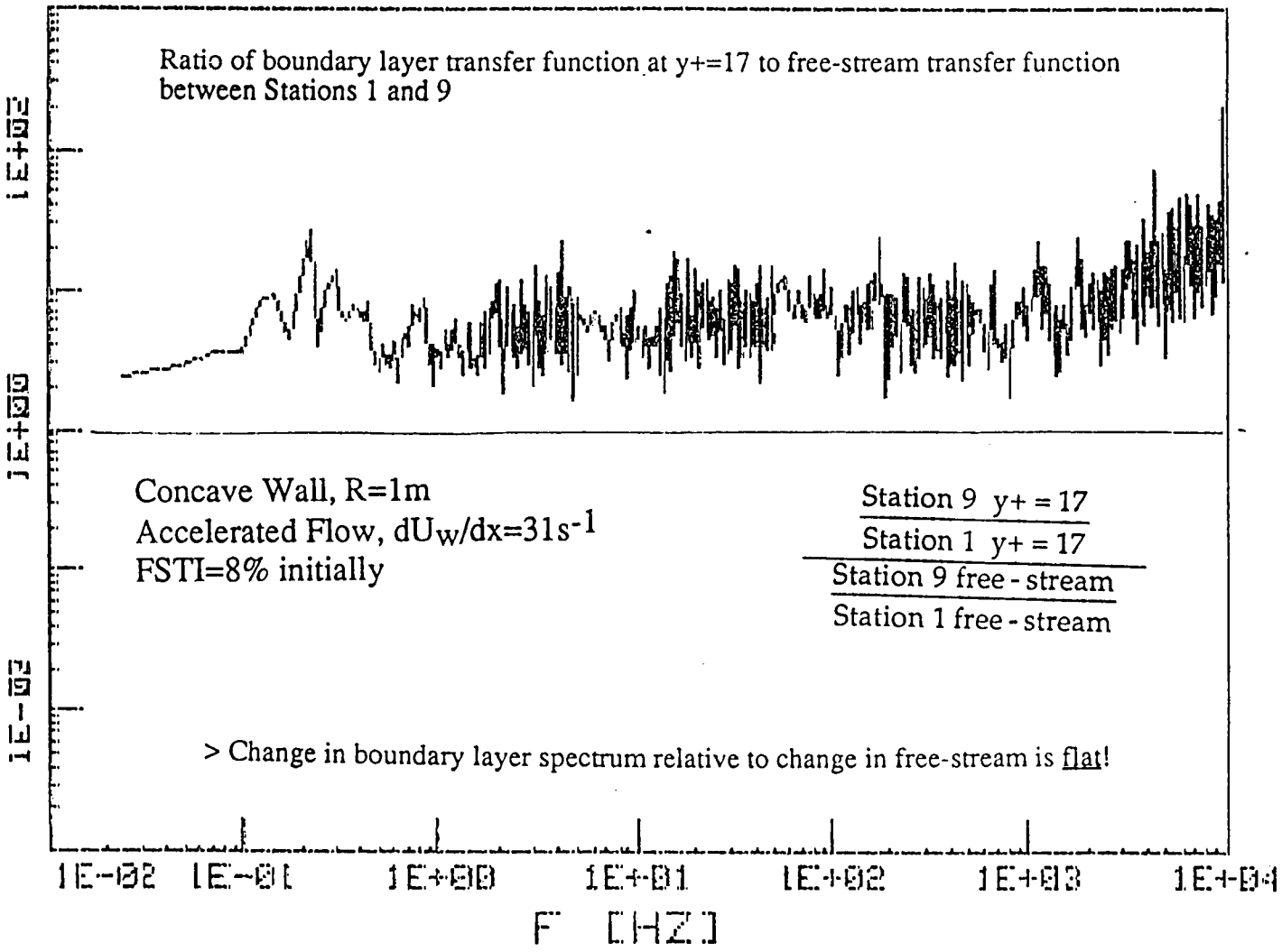

SPECTRA RATIO

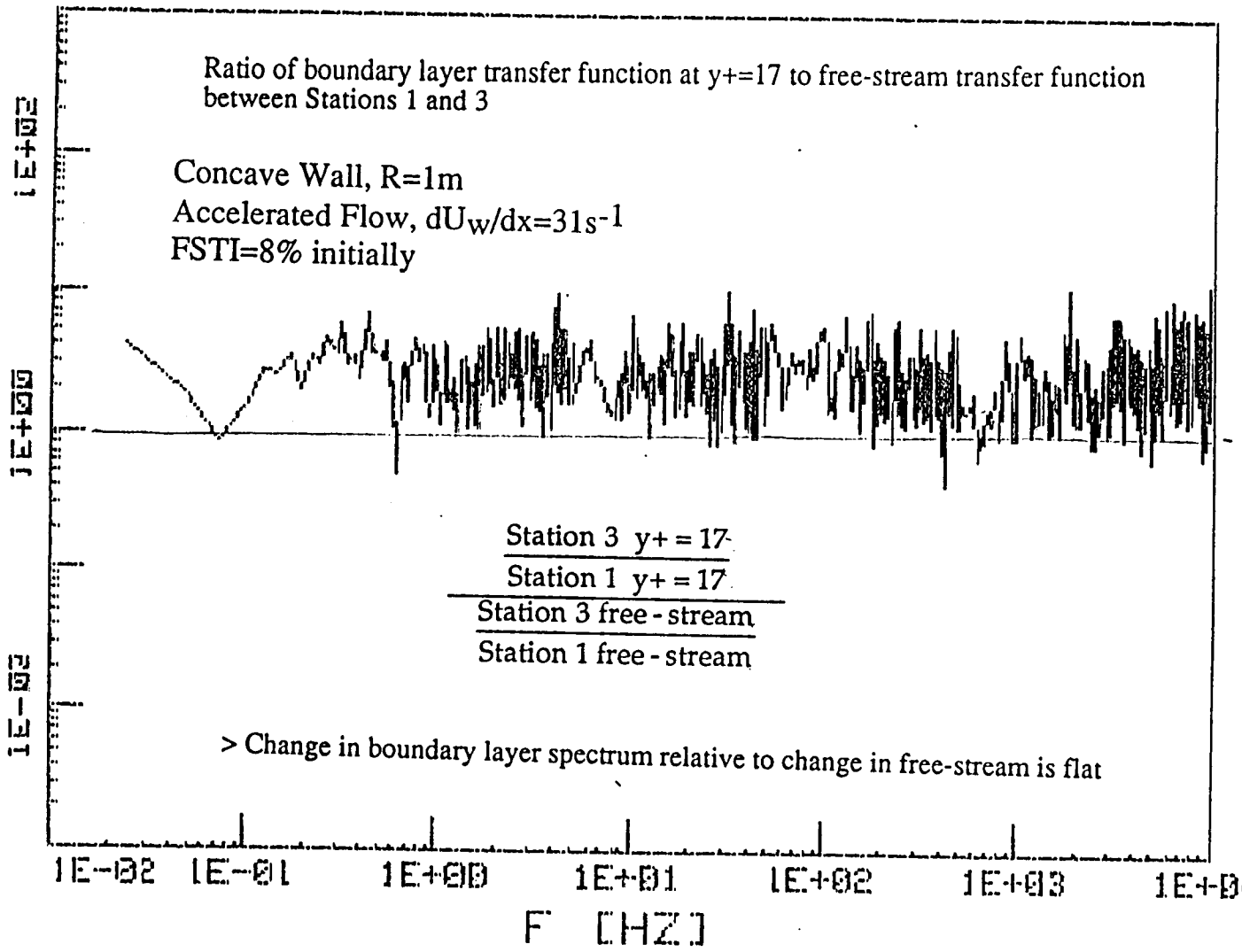

3L/14 3F/1F

3L/3F

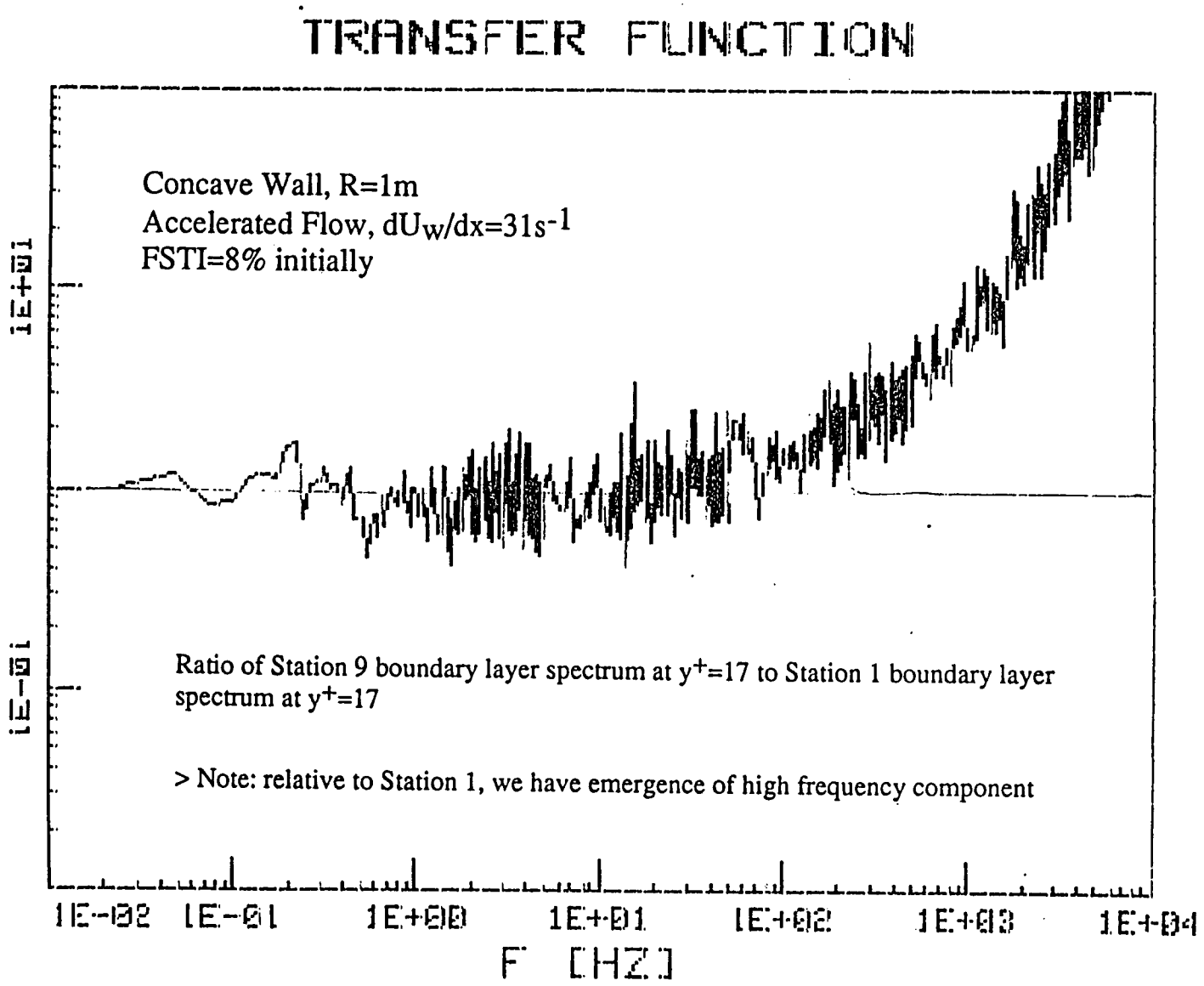
TRANSFER FUNCTION
Concave Wall, R=1m
Accelerated Flow, dUw/dx=31s-1
FSTI=8% initially
1E+01
1E-01
H
Ratio of Station 9 boundary layer spectrum at y+=17 to Station 1 boundary layer spectrum at y+=17
> Note: relative to Station 1, we have emergence of high frequency component
1E-02 1E-01 1E+00 1E+01 1E+02 1E+03 1E+04
F [HZ]

9L
1L

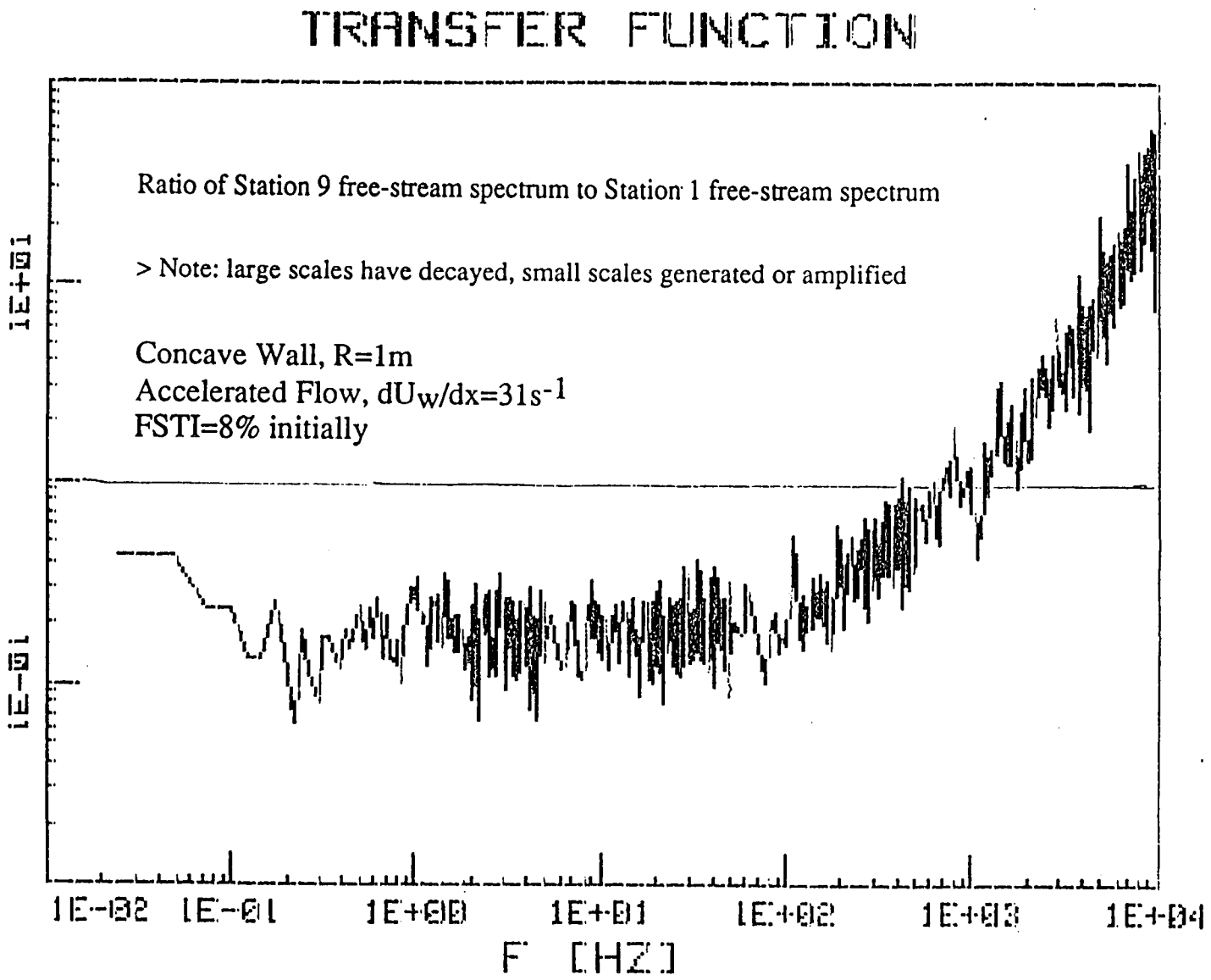
TRANSFER FUNCTION
Ratio of Station 9 free-stream spectrum to Station 1 free-stream spectrum
> Note: large scales have decayed, small scales generated or amplified
Concave Wall, R=1m
Accelerated Flow, dUw/dx=31s-1
FSTI=8% initially
1E+01
1E-01
H
1E-02
1E-01
1E+00
1E+01
1E+02
1E+03
1E+04
F [HZ]

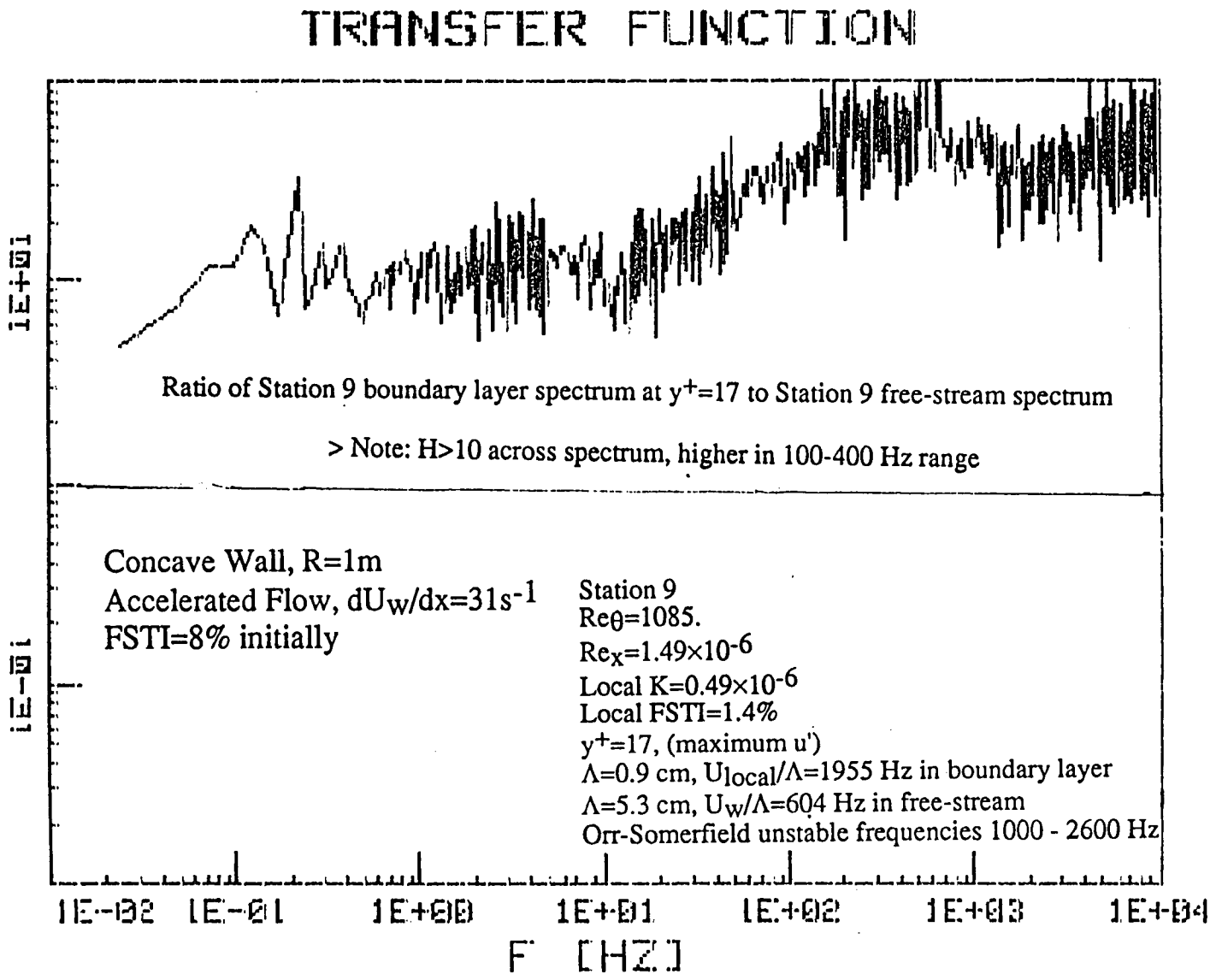
TRANSFER FUNCTION
1E+01
1E-01
Ratio of Station 9 boundary layer spectrum at y+=17 to Station 9 free-stream spectrum
> Note: H>10 across spectrum, higher in 100-400 Hz range
H
Concave Wall, R=1m
Accelerated Flow, dUw/dx=31s-1
FSTI=8% initially
Station 9
Reθ=1085.
Rex=1.49×10-6
Local K=0.49×10-6
Local FSTI=1.4%
y+=17, (maximum u')
Λ=0.9 cm, Ulocal/Λ=1955 Hz in boundary layer
Λ=5.3 cm, Uw/Λ=604 Hz in free-stream
Orr-Somerfield unstable frequencies 1000 - 2600 Hz
1E-02
1E-01
1E+00
1E+01
1E+02
1E+03
1E+04
F [HZ]

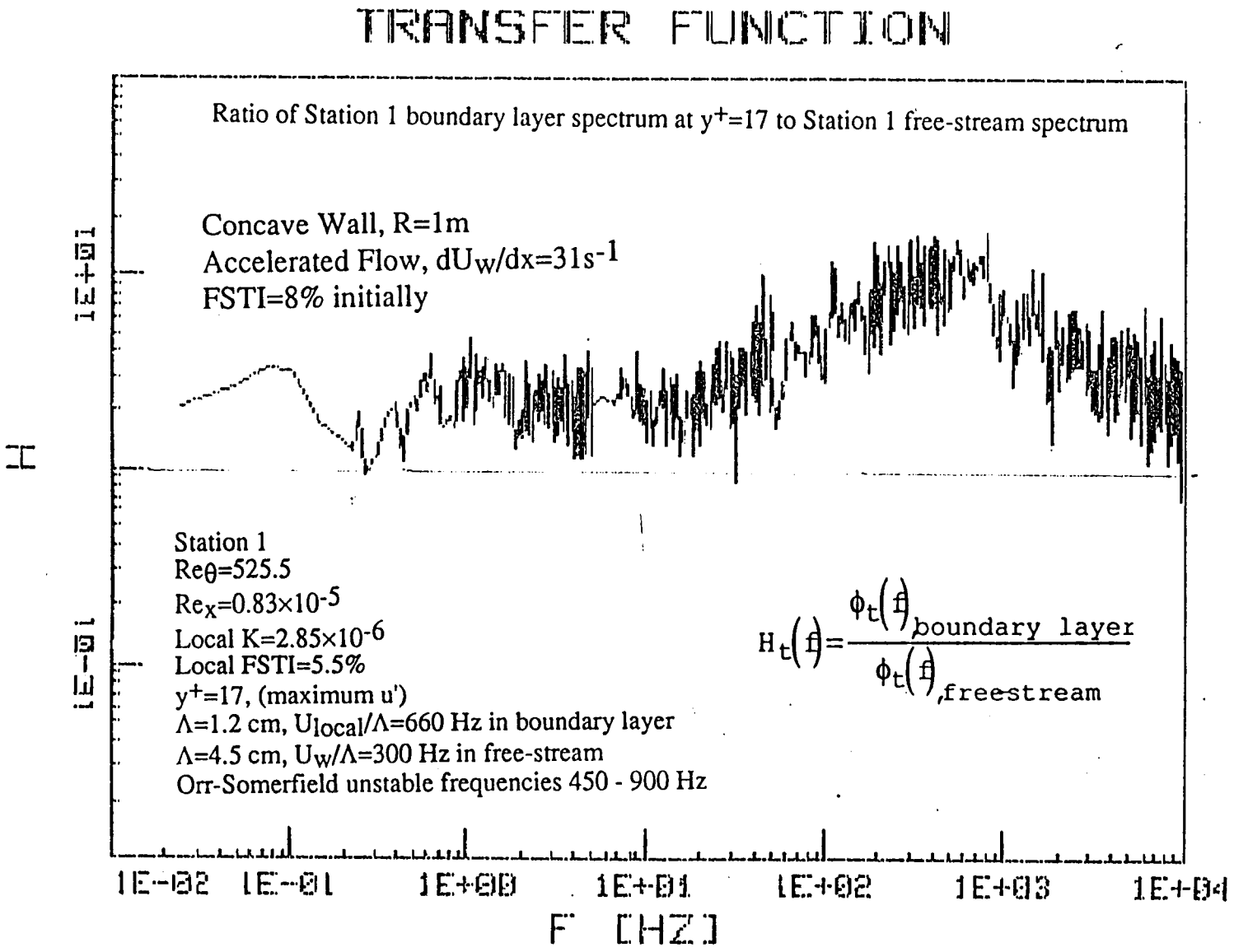
TRANSFER FUNCTION
Ratio of Station 1 boundary layer spectrum at y+=17 to Station 1 free-stream spectrum
Concave Wall, R=1m
Accelerated Flow, dUw/dx=31s-1
FSTI=8% initially
Station 1
Reθ=525.5
Rex=0.83×10-5
Local K=2.85×10-6
Local FSTI=5.5%
y+=17, (maximum u')
Λ=1.2 cm, Ulocal/Λ=660 Hz in boundary layer
Λ=4.5 cm, Uw/Λ=300 Hz in free-stream
Orr-Somerfield unstable frequencies 450 - 900 Hz
Ht(f)=φt(f),boundary layer / φt(f),freestream
1E+01
1E-01
H
1E-02 1E-01 1E+00 1E+01 1E+02 1E+03 1E+04
F [HZ]

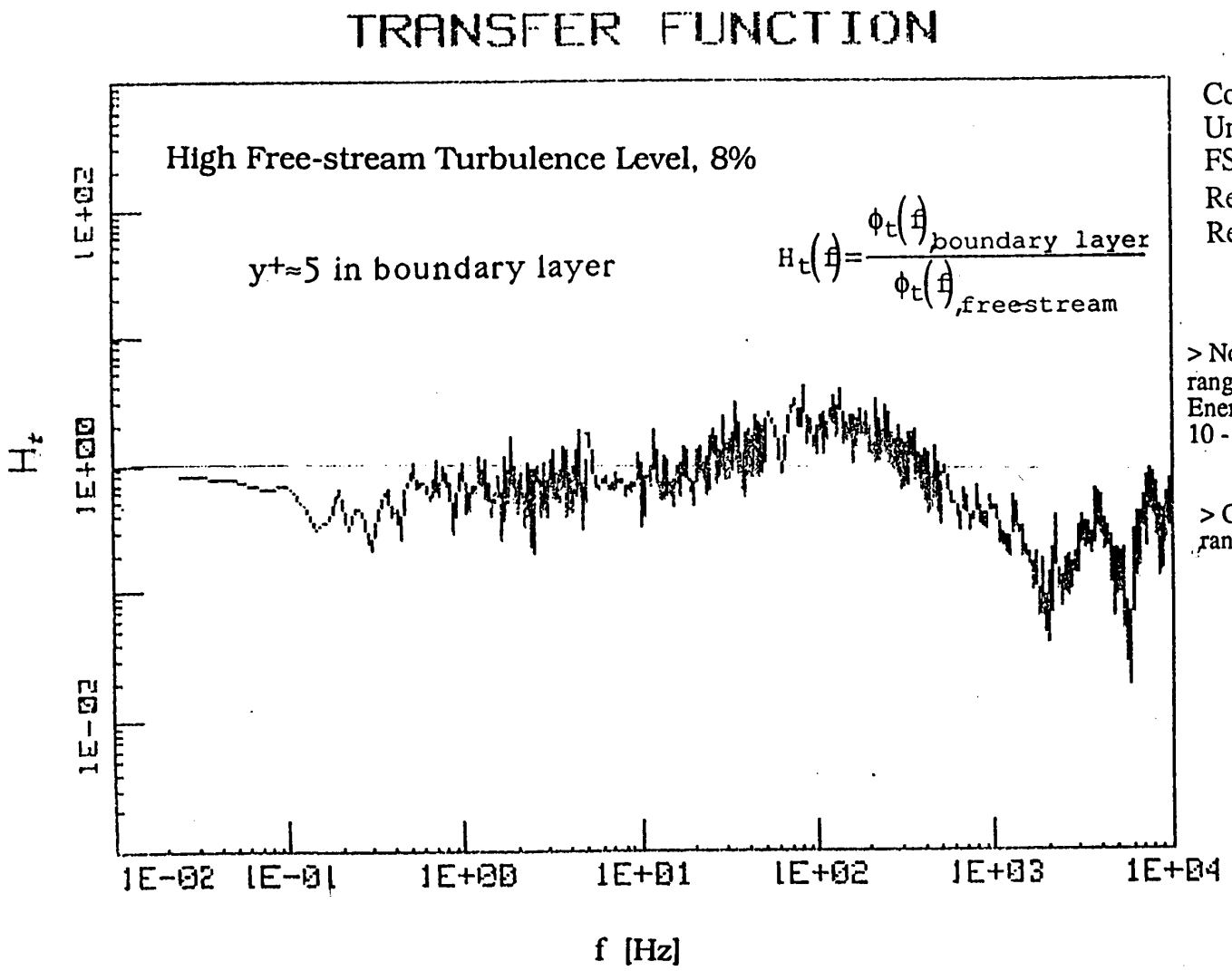

Concave Wall, R=1m
Unaccelerated Flow
FSTI=8%
$Re_x=1.12\times10^5$
$Re_\theta=366$

> Note, H≈2 in the 50 - 300 Hz range. Damped above 300 Hz. Energy in free-stream disributed over 10 - 2000 Hz.

> Orr-Somerfield unstable frequency range, 1200 - 1900 Hz.

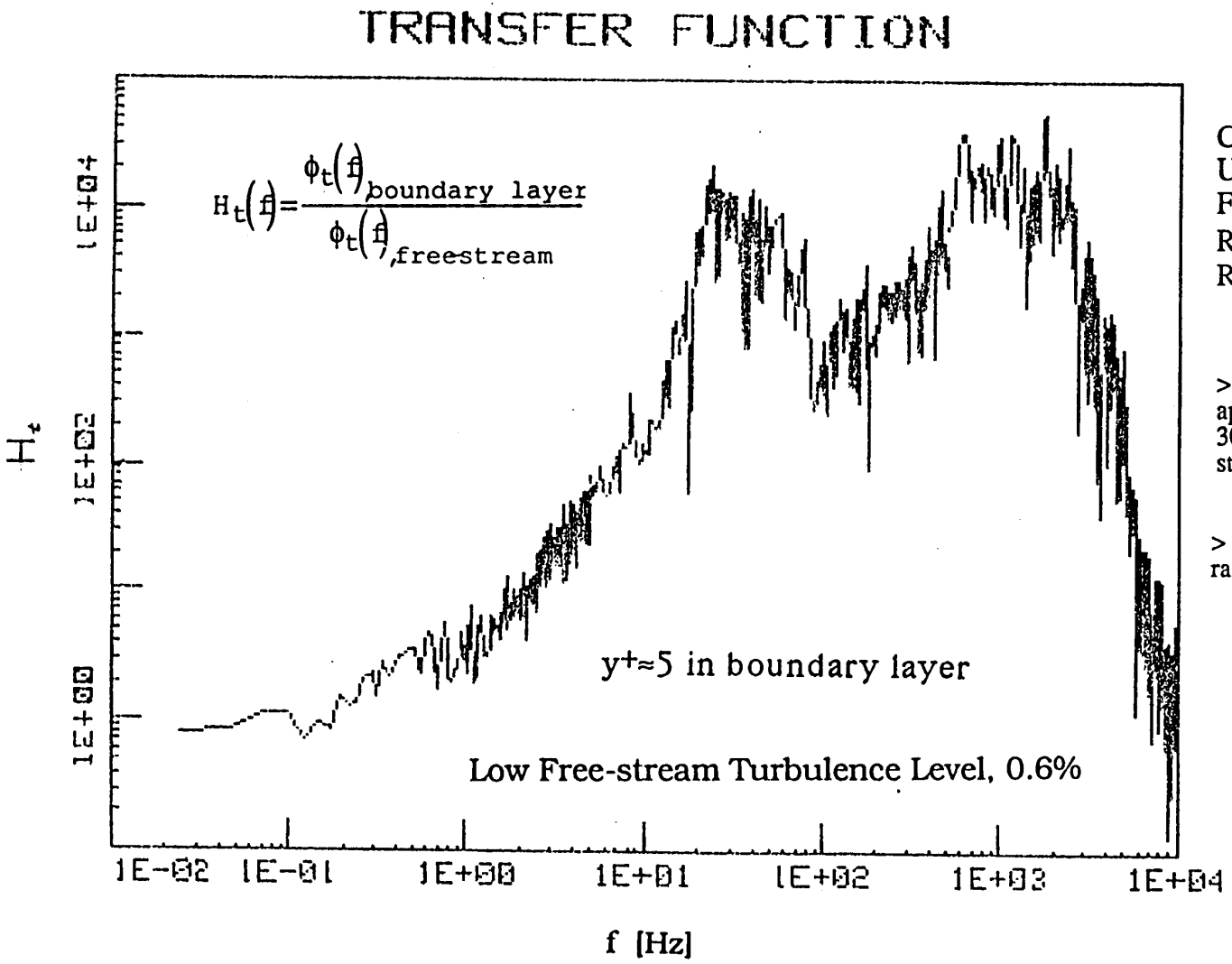

Concave Wall, R=1m
Unaccelerated Flow
FSTI=0.6%
$Re_x=3.6\times10^5$
$Re_\theta=560$

> Note, high ratios in the approximate ranges 20 - 60 Hz and 300 - 3000 Hz. Energy in the free-stream in range 0 - 20 Hz.

> Orr-Somerfield unstable frequency range, 310 - 840 Hz.

Normal Stress Profiles, Concave Wall, R=1m

Accelerated, $dU_w/dx = 31\ s^{-1}$, FSTI=8%

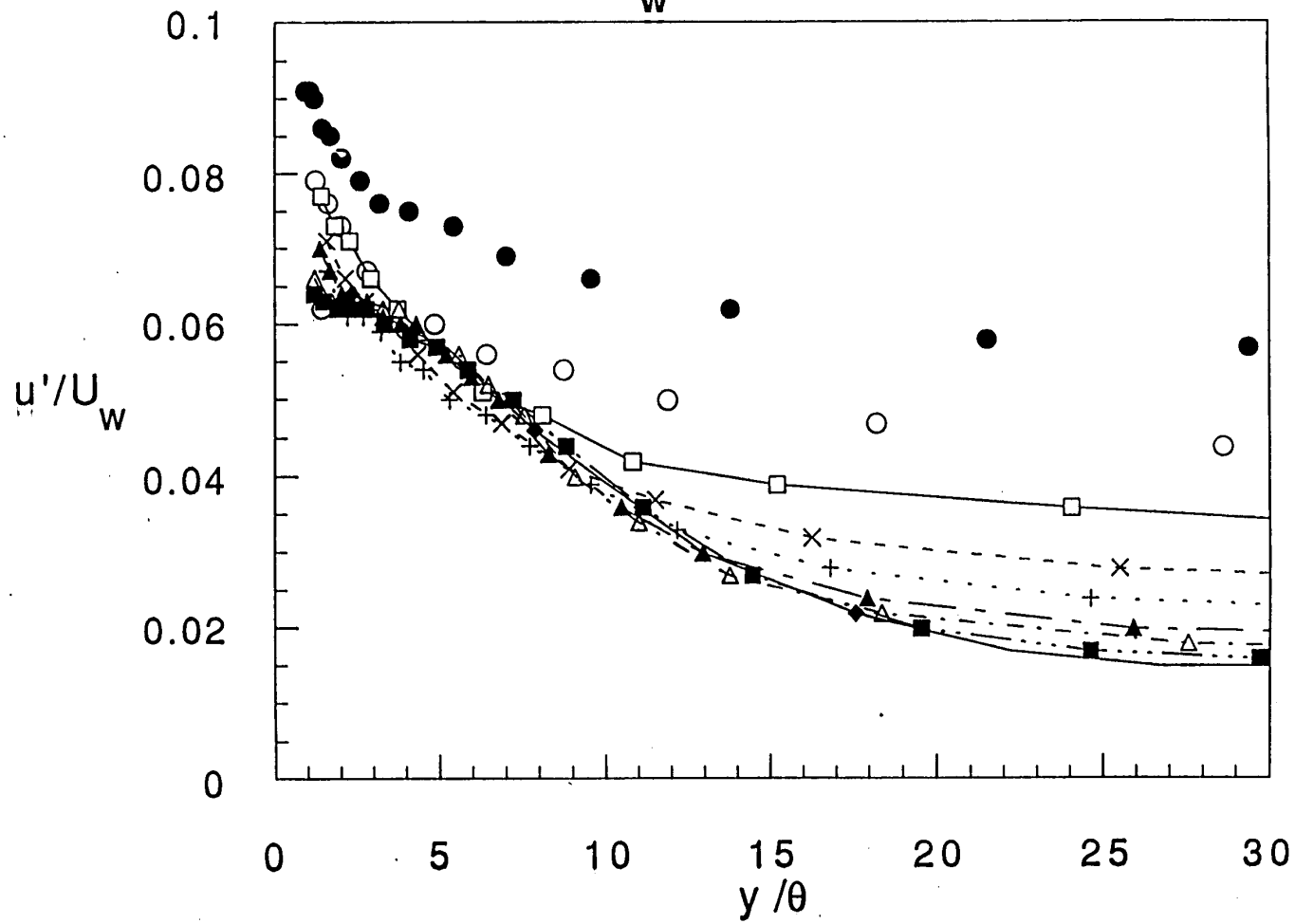

> For comparison to the next figure.

Reθ	$Re_x \times 10^{-5}$
525.5	0.83
462.4	1.85
467.9	2.93
488.6	4.49
549.2	6.23
689.1	7.96
839.4	9.86
920.9	12.4
1085.	14.9

Normal Stress Profiles, Non-Turbulent Zone
Concave Wall, R=1m, Accelerated
$dU_w/dx = 31\ s^{-1}$, FSTI=8%

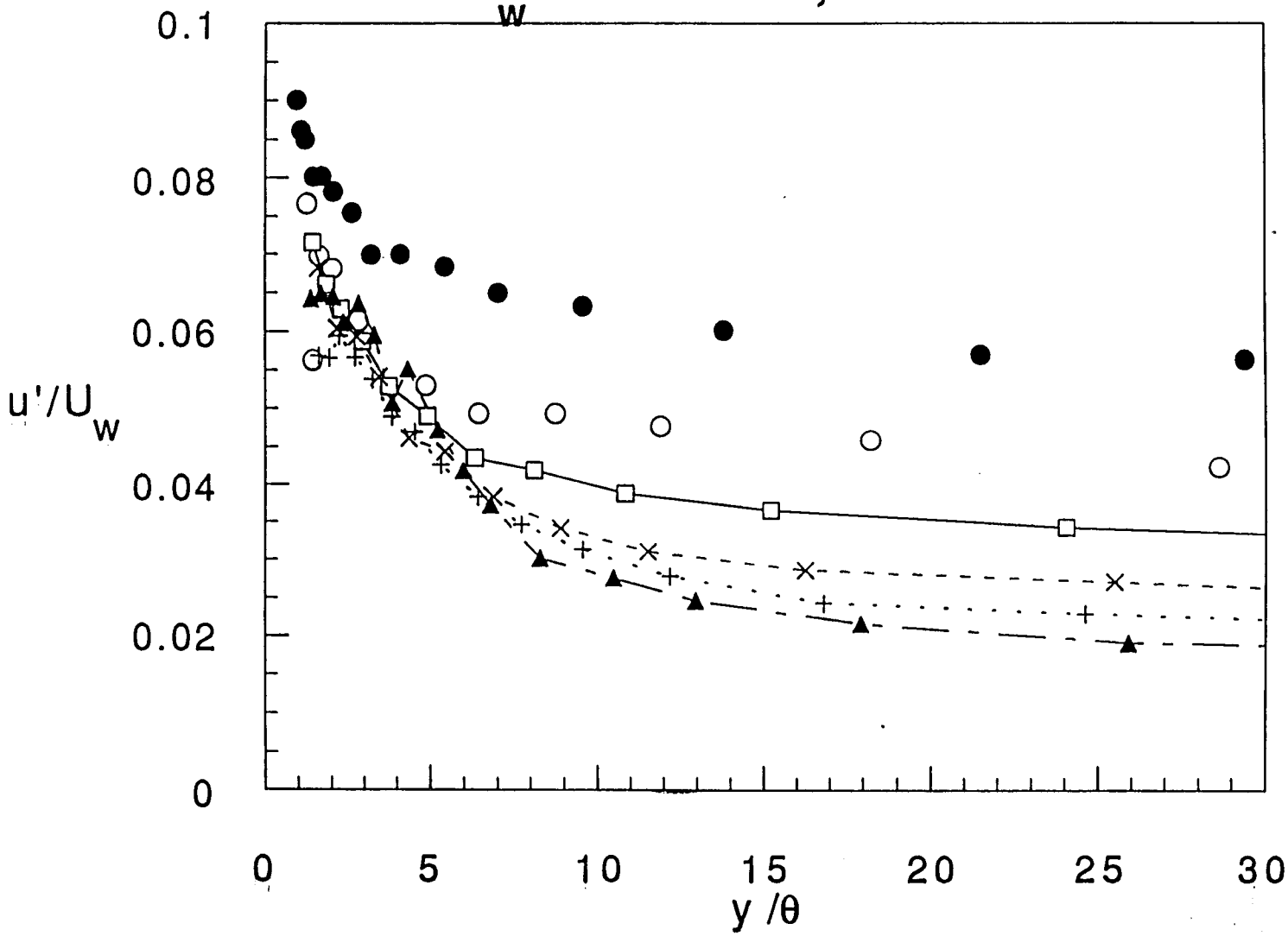

> Note the very large contribution from the non-turbulent zone.

Reθ	Re$_x$×10^5
525.5	0.83
462.4	1.85
467.9	2.93
488.6	4.49
549.2	6.23
689.1	7.96

> u' laminar -- values computed from measurements taken only when flow is identified to be non-turbulent -- based upon the u' signal.

Development of Velocity and Temperature Profile Correlations for Accelerated Flow

- Start with boundary layer equation

  Assume constant properties

$$\rho u\frac{\partial u}{\partial x}+\rho v\frac{\partial u}{\partial y}-\frac{\partial \tau}{\partial y}+\frac{dP}{dx}=0$$

- Do not make Couette flow assumptions
- Do not set dP/dx term to zero
- Eliminate v using continuity equation
- Intergrate from zero to y
- Convert to wall coordinates

  For convection terms,

$$\int(a)dy=\int(b)dy^{+}+\int(c)dx$$

  Assume history independent and set last integral to zero

- Resulting equation

$$\frac{\tau}{\tau_o}=1+p^{+}y^{+}+\left(\frac{K}{\sqrt{\frac{c_f}{2}}}+\frac{\nu}{U_\infty\frac{c_f}{2}}\frac{d\sqrt{\frac{c_f}{2}}}{dx}\right)\int_0^{y^{+}}u^{+2}dy^{+}$$

- Apply mixing length model with vanDriest damping

$$\frac{\tau}{\tau_o}=\left(1+\kappa^2y^{+2}\left(1-e^{-y^{+}/A^{+}}\right)^2\frac{du^{+}}{dy^{+}}\right)\frac{du^{+}}{dy^{+}}$$

  k=0.41

  Variable A^{+} as a function of p^{+}

- Solve for du^{+}/dy^{+} and integrate

$$u^{+}=\int_0^{y^{+}}\left[\frac{-1+\sqrt{1+4\left(1+p^{+}y^{+}+\left(\frac{K}{\sqrt{\frac{c_f}{2}}}+\frac{\nu}{U_\infty\frac{c_f}{2}}\frac{d\sqrt{\frac{c_f}{2}}}{dx}\right)\int_0^{y^{+}}u^{+2}dy^{+}\right)\left(\kappa^2y^{+2}\left(1-e^{-y^{+}/A^{+}}\right)^2\right)}}{2\left(\kappa^2y^{+2}\left(1-e^{-y^{+}/A^{+}}\right)^2\right)}\right]dy^{+}$$

- Similar derivation for temperature profile. For constant heat flux b.c.:

$$t^{+}=\int_0^{y^{+}}\left[\frac{1+\left(\frac{t_\infty^{+2}\nu}{U_\infty\frac{c_f}{2}}\frac{dSt}{dx}+\frac{Kt_\infty^{+}}{\sqrt{\frac{c_f}{2}}}\right)\int_0^{y^{+}}u^{+}dy^{+}-\left(\frac{K}{\sqrt{\frac{c_f}{2}}}+\frac{\nu}{U_\infty\frac{c_f}{2}}\frac{d\sqrt{\frac{c_f}{2}}}{dx}\right)\int_0^{y^{+}}u^{+}t^{+}dy^{+}}{\frac{1}{Pr}+\frac{\kappa^2y^{+2}\left(1-e^{-y^{+}/A^{+}}\right)^2}{Pr_t}\frac{du^{+}}{dy^{+}}}\right]dy^{+}$$

Velocity Profile, Accelerated Flow

$dU_w/dx = 31 s^{-1}$, Transitional Station

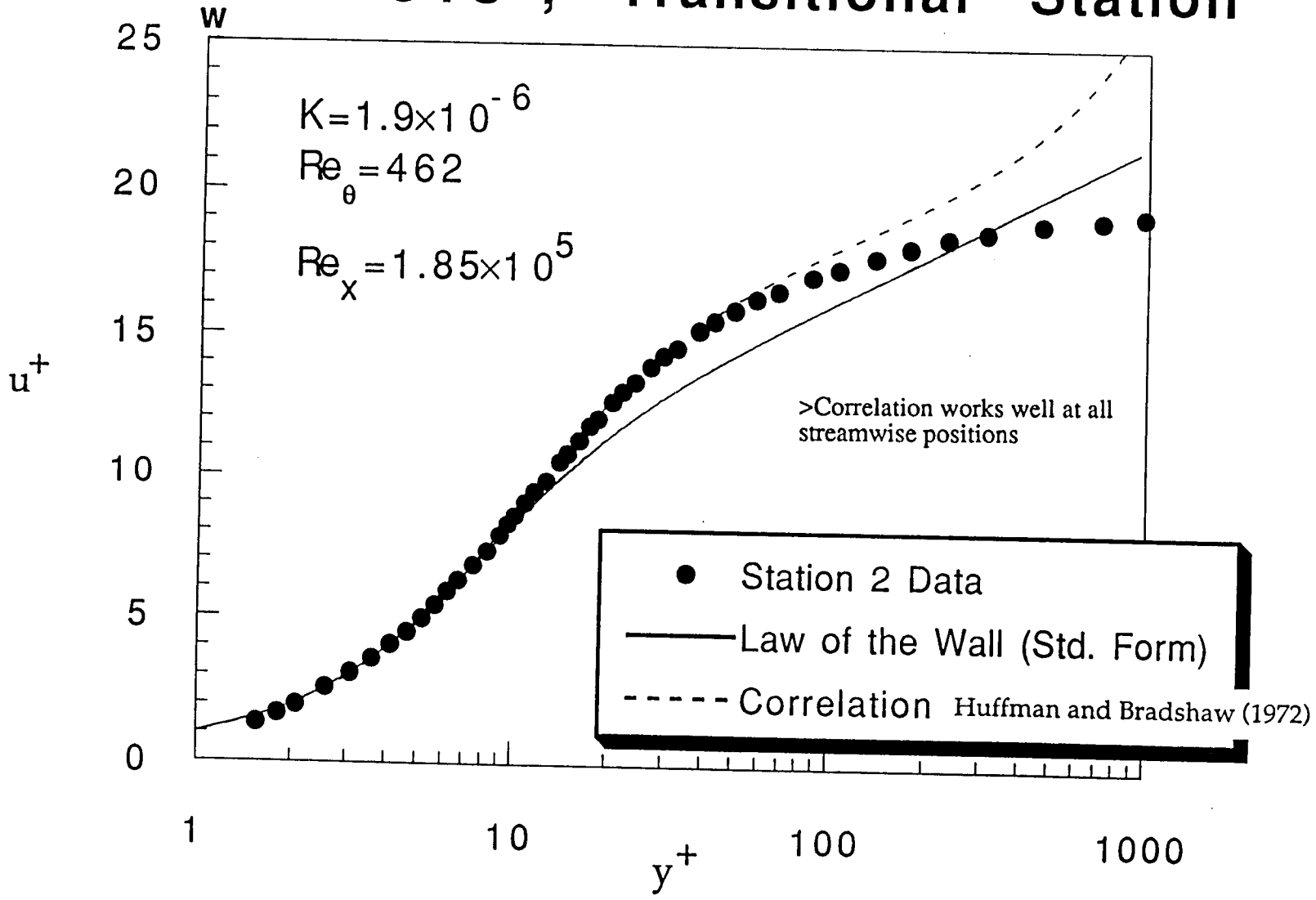

Temperature Profile, Accelerated Flow

$dU_w/dx = 31\,s^{-1}$, Transitional Station

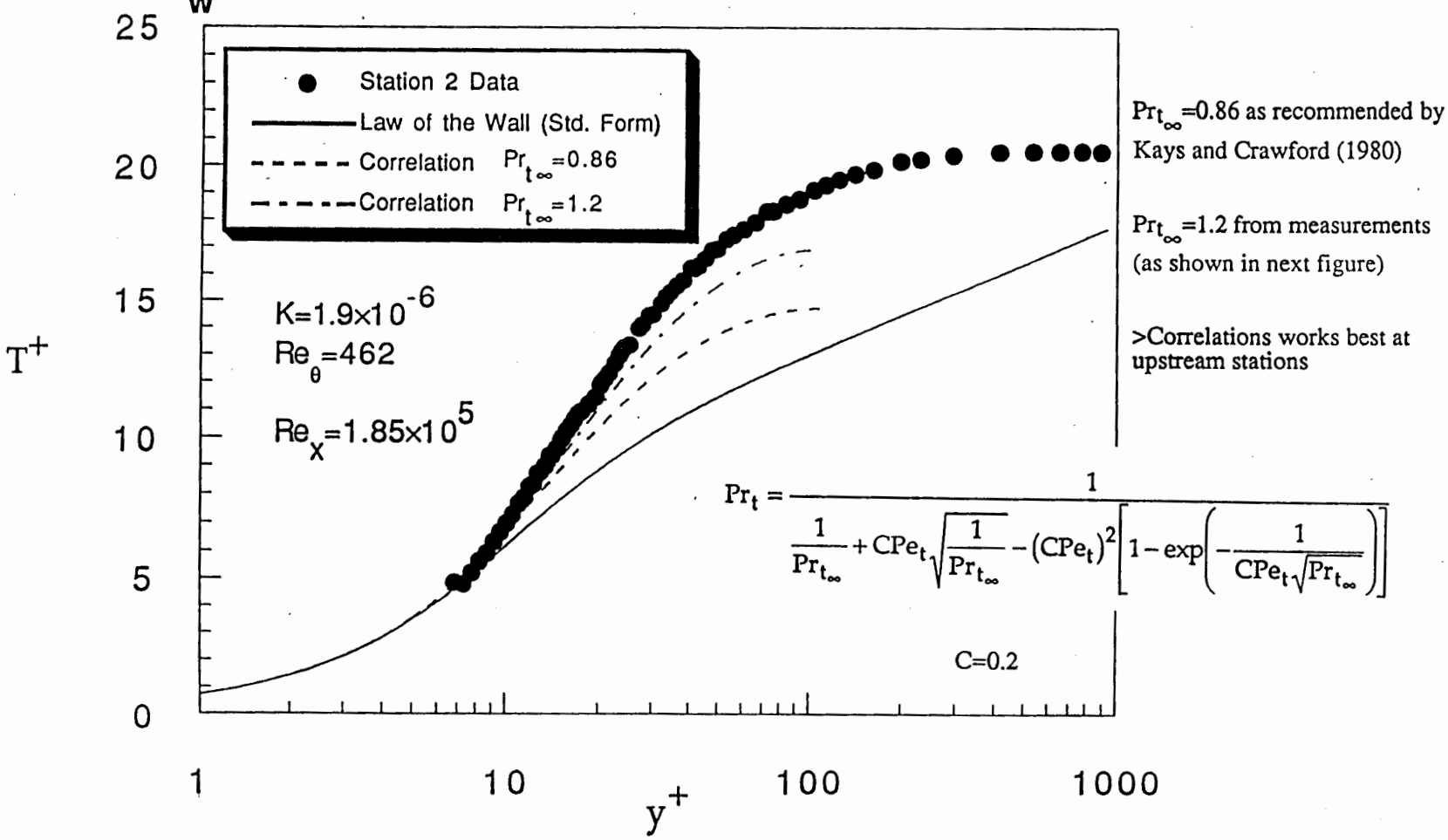

Turbulent Prandtl Number
Concave Wall, R=1m
Accelerated Flow, $dU_w/dx = 31 s^{-1}$

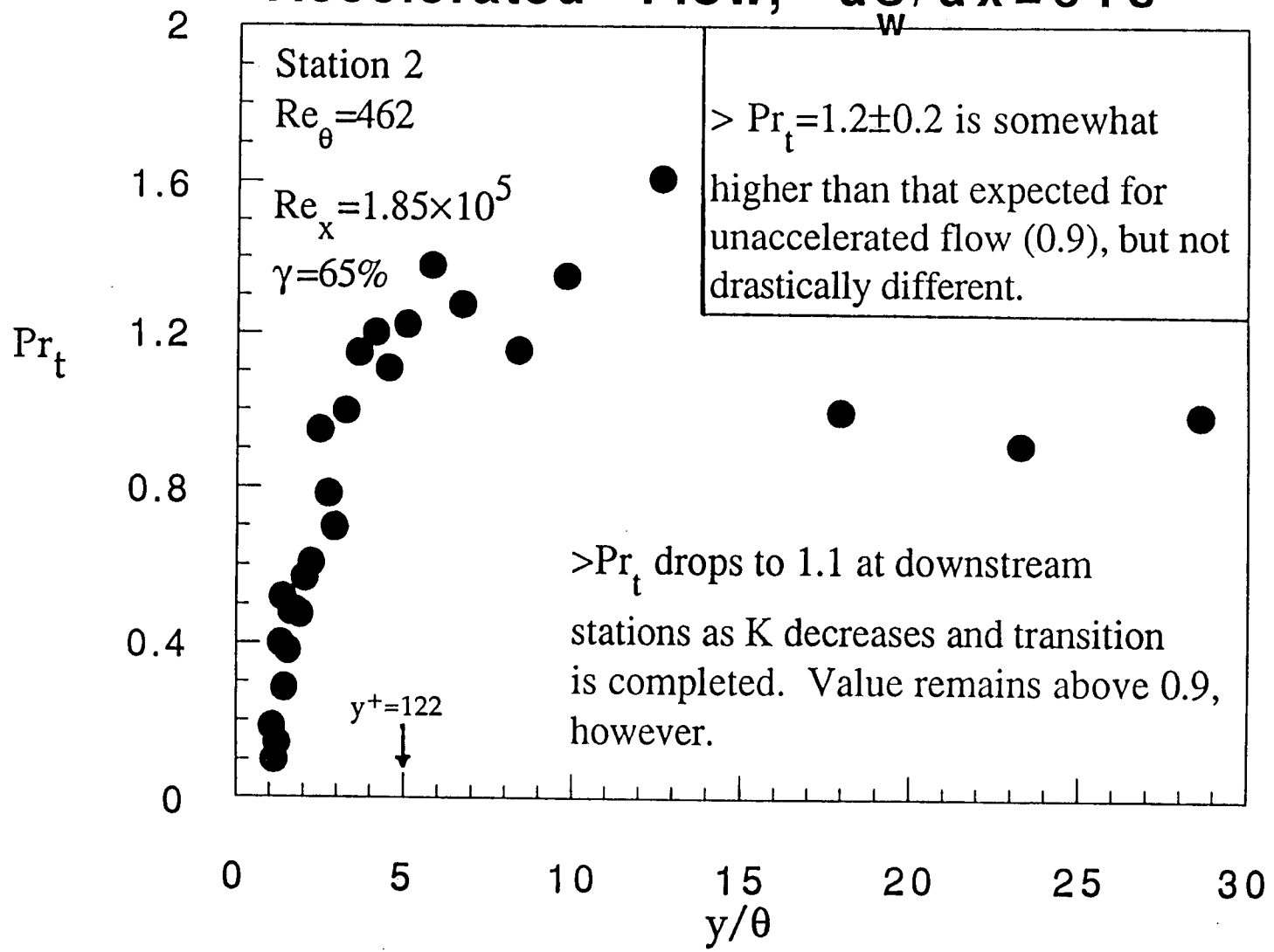

> Pr_t=1.2±0.2 is somewhat higher than that expected for unaccelerated flow (0.9), but not drastically different.

>Pr_t drops to 1.1 at downstream stations as K decreases and transition is completed. Value remains above 0.9, however.

BOUNDARY LAYER SPECTRA

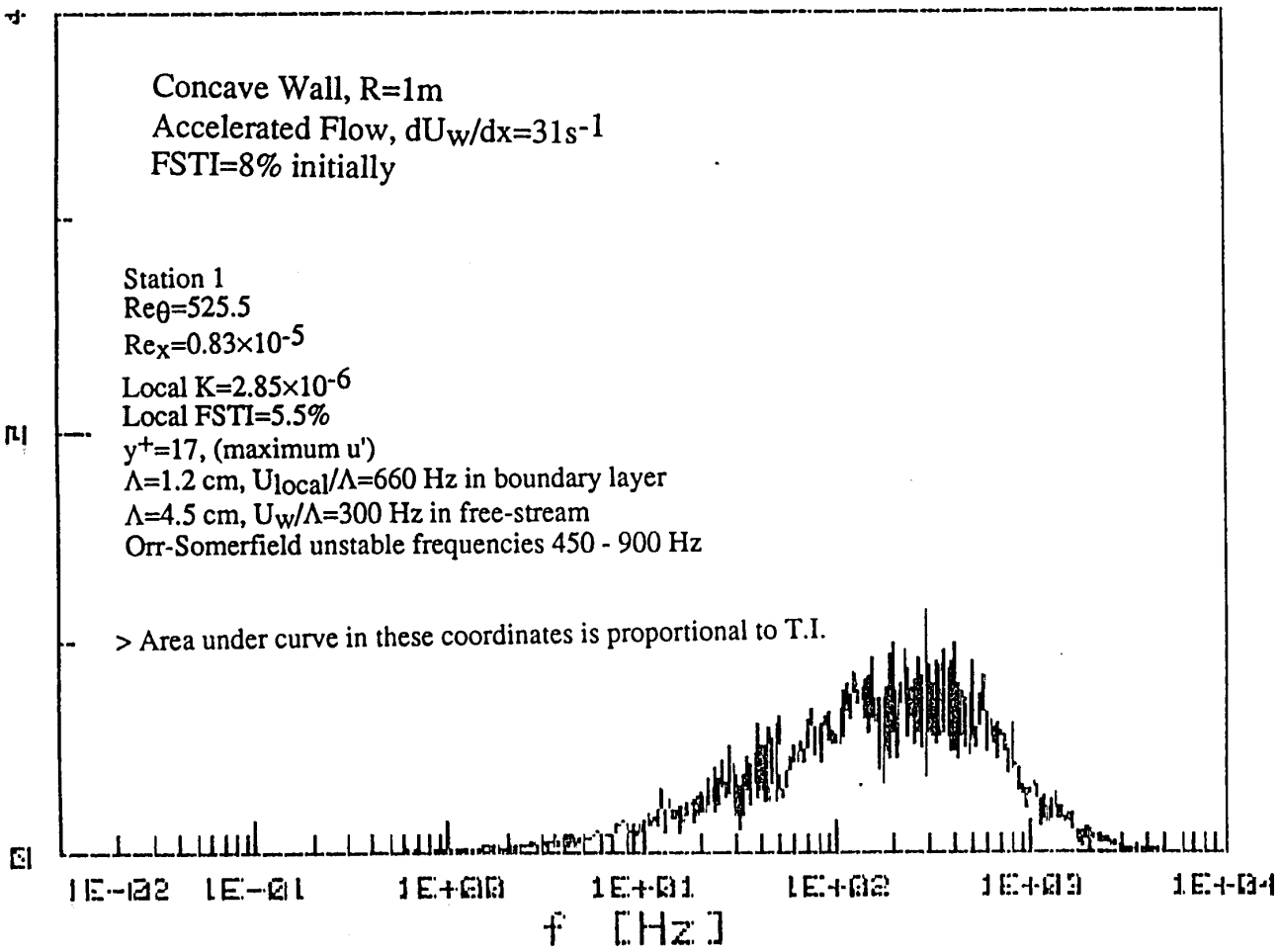

BOUNDARY LAYER SPECTRA
Concave Wall, R=1m
Accelerated Flow, dUw/dx=31s-1
FSTI=8% initially
Station 9
Reθ=1085.
Rex=1.49×10-6
Local K=0.49×10-6
Local FSTI=1.4%
y+=17, (maximum u')
Λ=0.9 cm, Ulocal/Λ=1955 Hz in boundary layer
Λ=5.3 cm, Uw/Λ=604 Hz in free-stream
Orr-Somerfield unstable frequencies 1000 - 2600 Hz
f × u'2(f,df) / df
m2/s2
f [Hz]
1E-02
1E-01
1E+00
1E+01
1E+02
1E+03
1E+04

4

BOUNDARY LAYER SHEAR STRESS SPECTRA

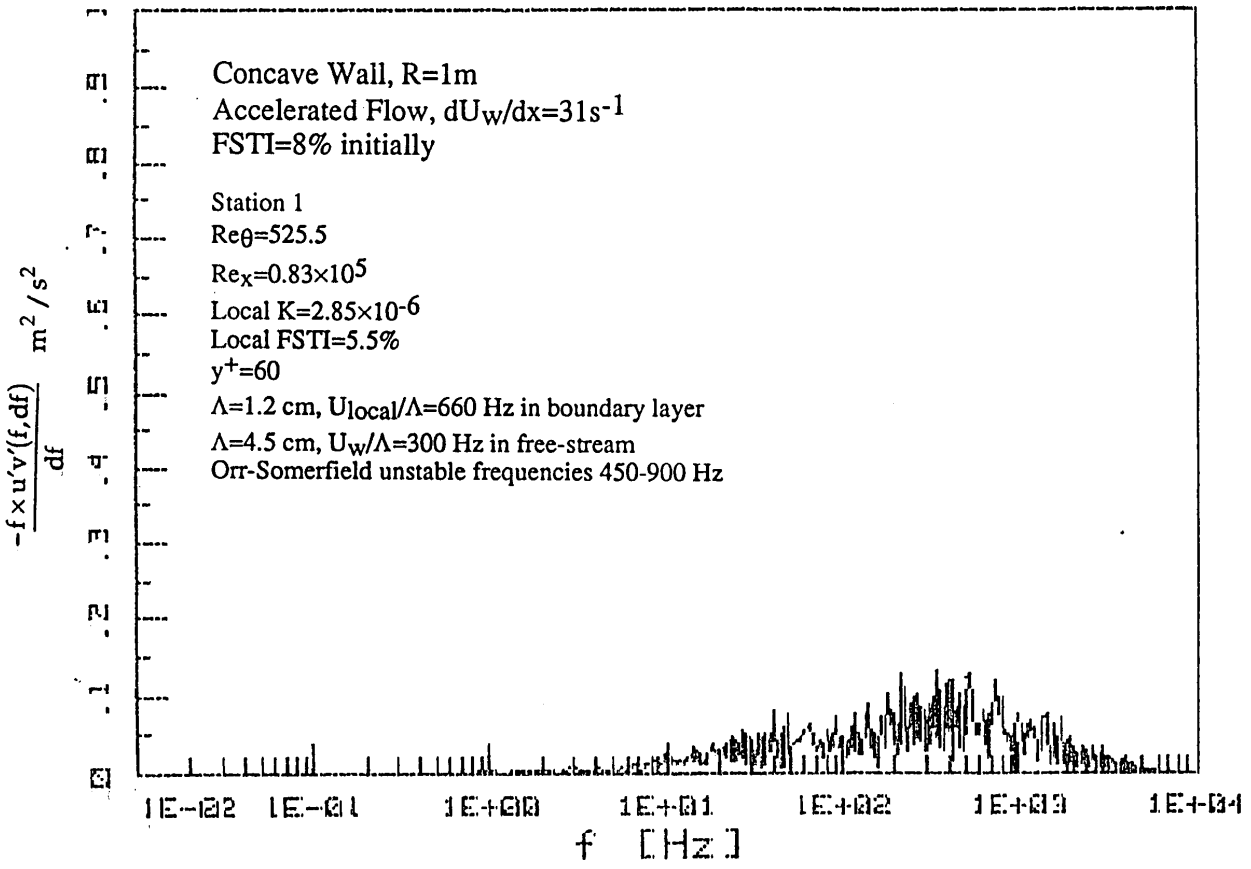

Station 1 $y^+=60$

BOUNDARY LAYER SHEAR STRESS SPECTRA

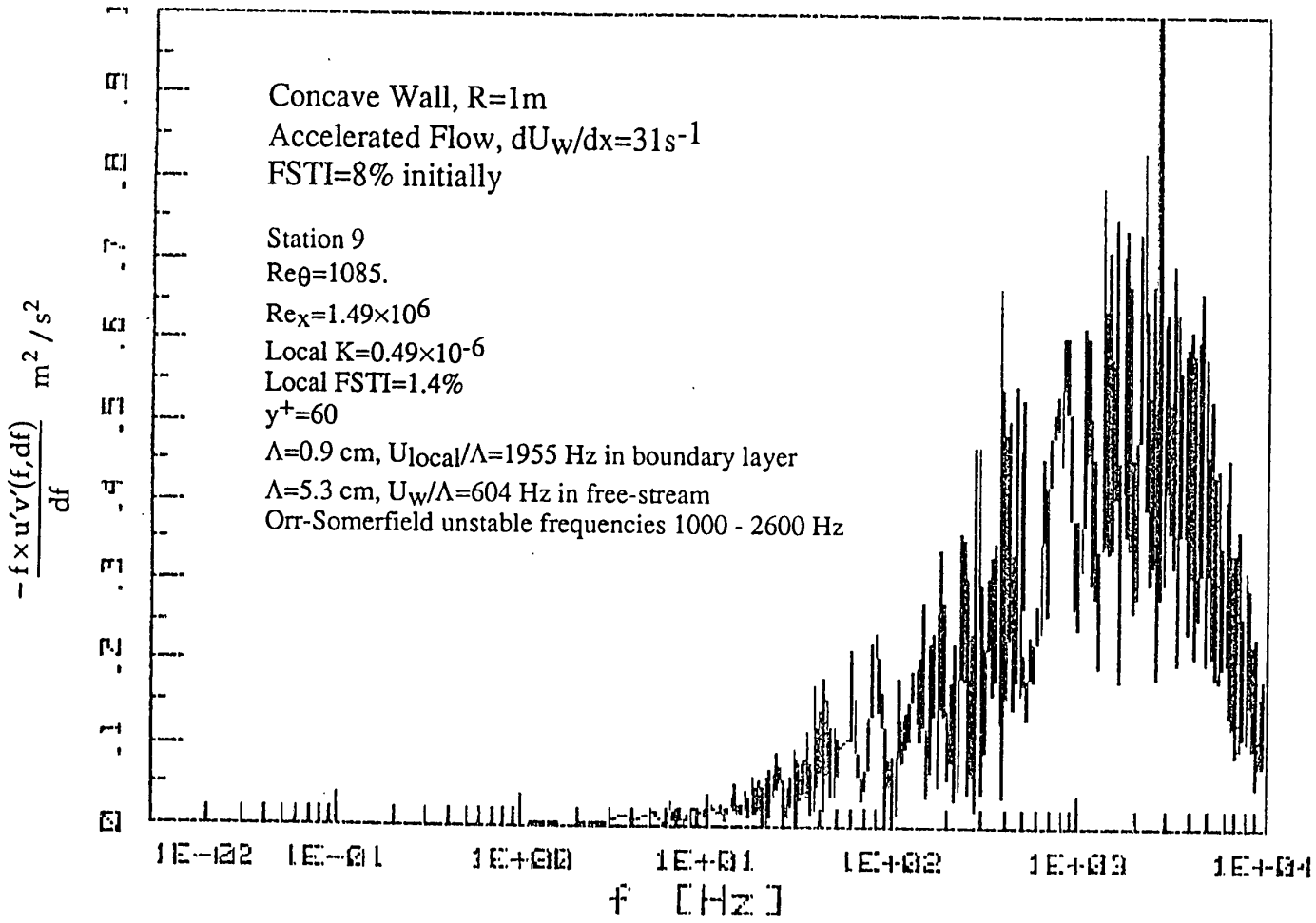

Shear Stress Profiles, Non-Turbulent Zone
Concave Wall, R=1m, Accelerated
$dU_w/dx = 31\ s^{-1}$, FSTI=8%

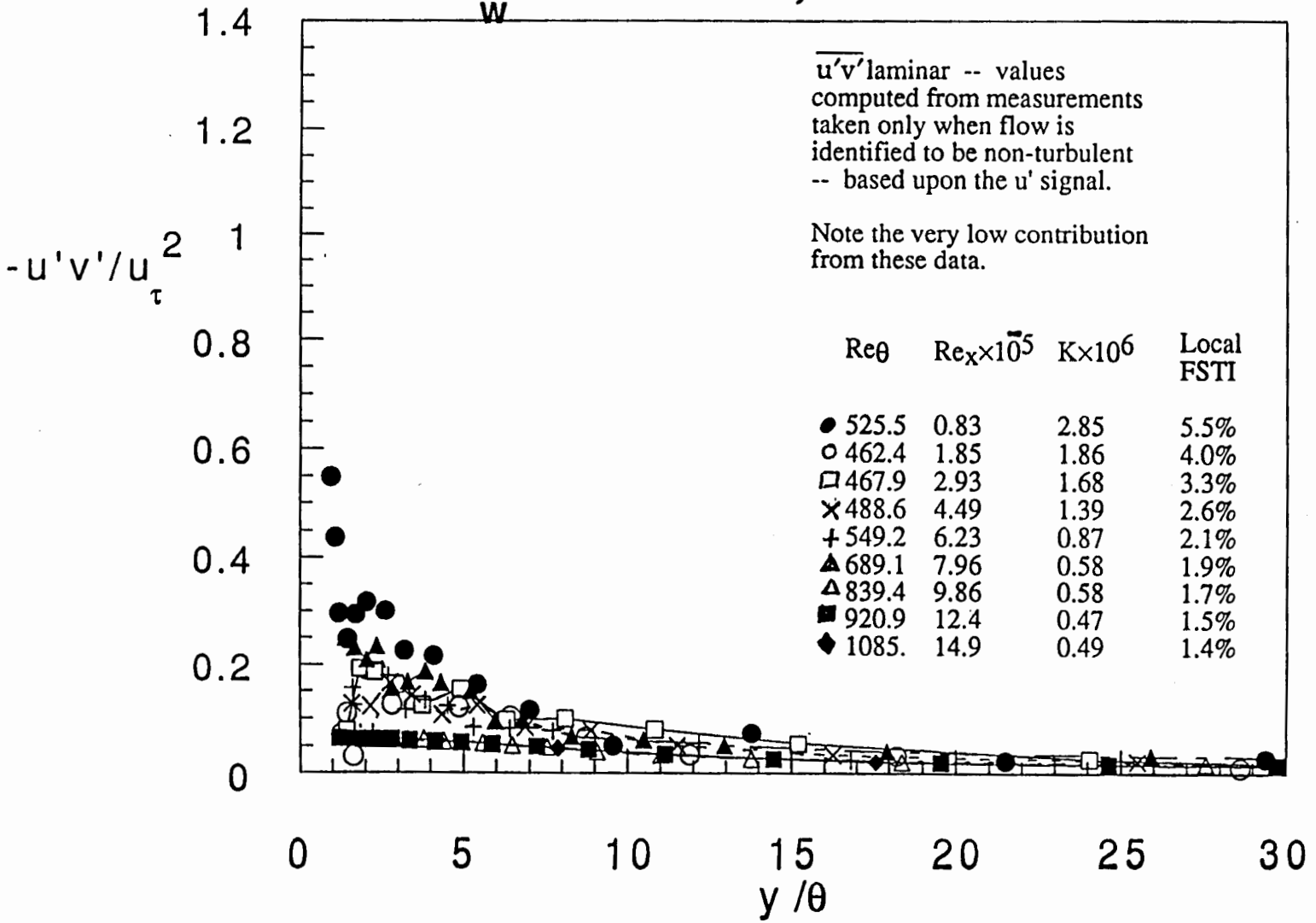

Shear Stress Profiles, Concave Wall, R=1m

Accelerated, $dU_w/dx = 31 s^{-1}$, FSTI=8%

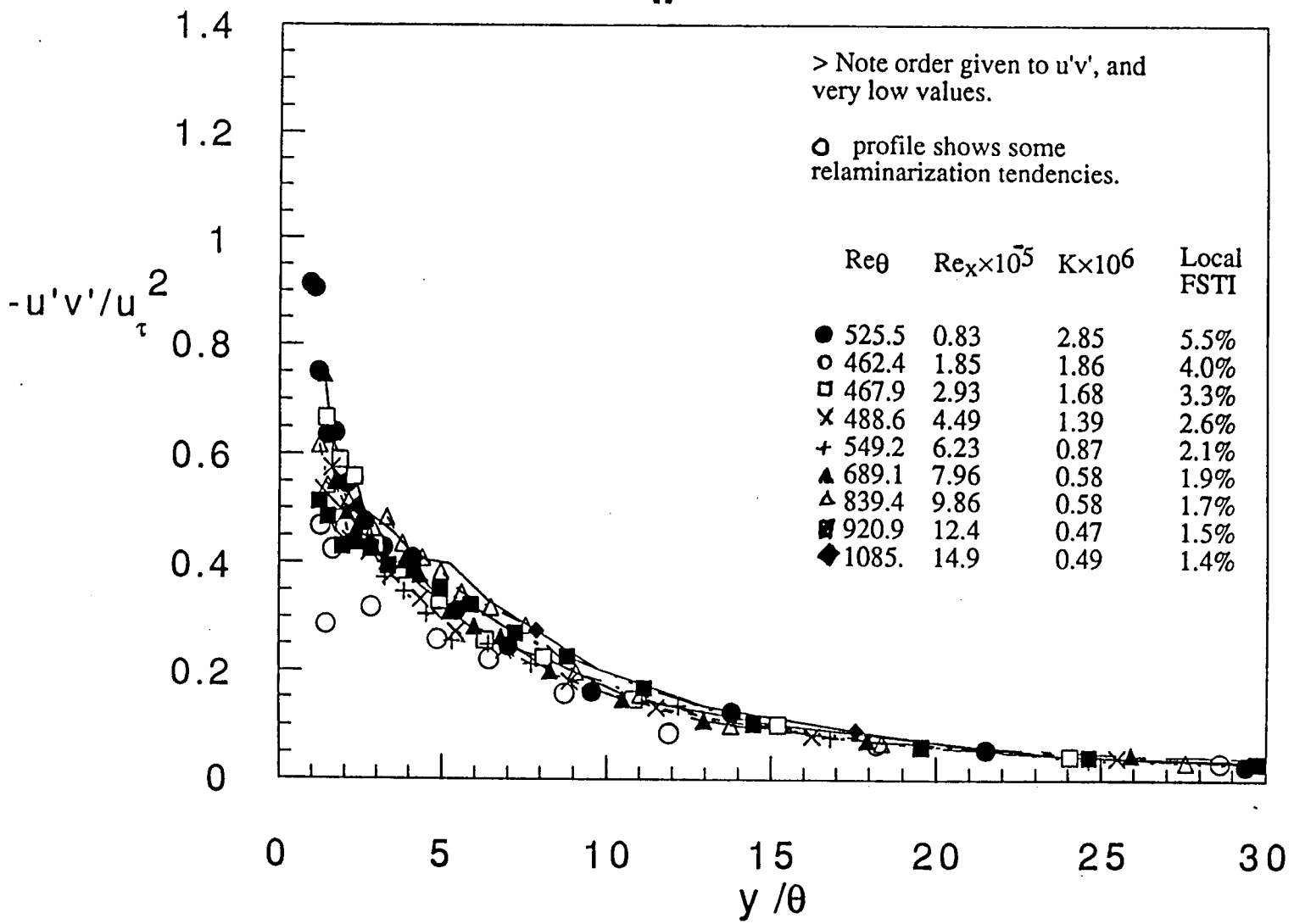

Shear Stress Profiles, Concave Wall R=1m, Unaccelerated, FSTI=8%

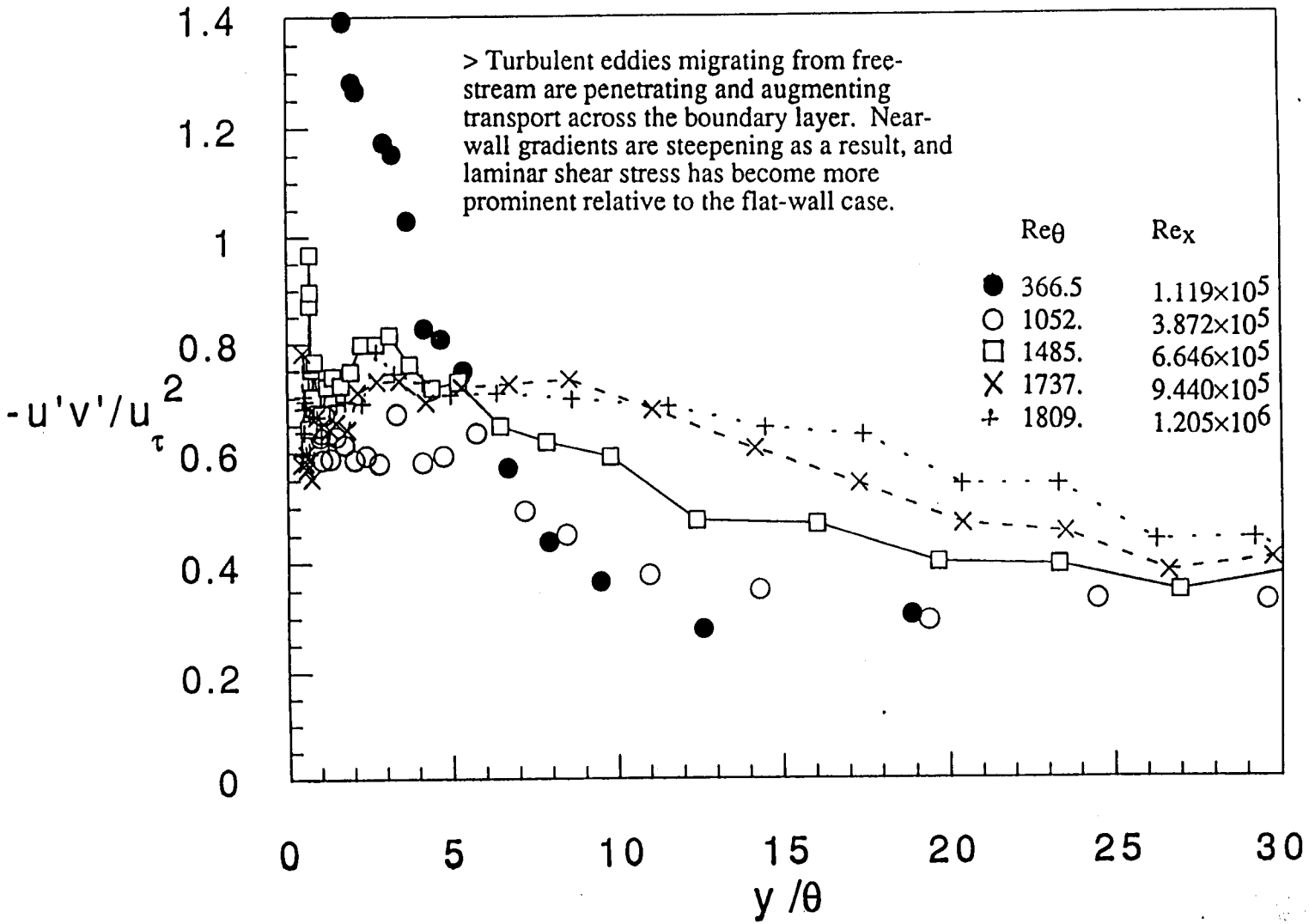

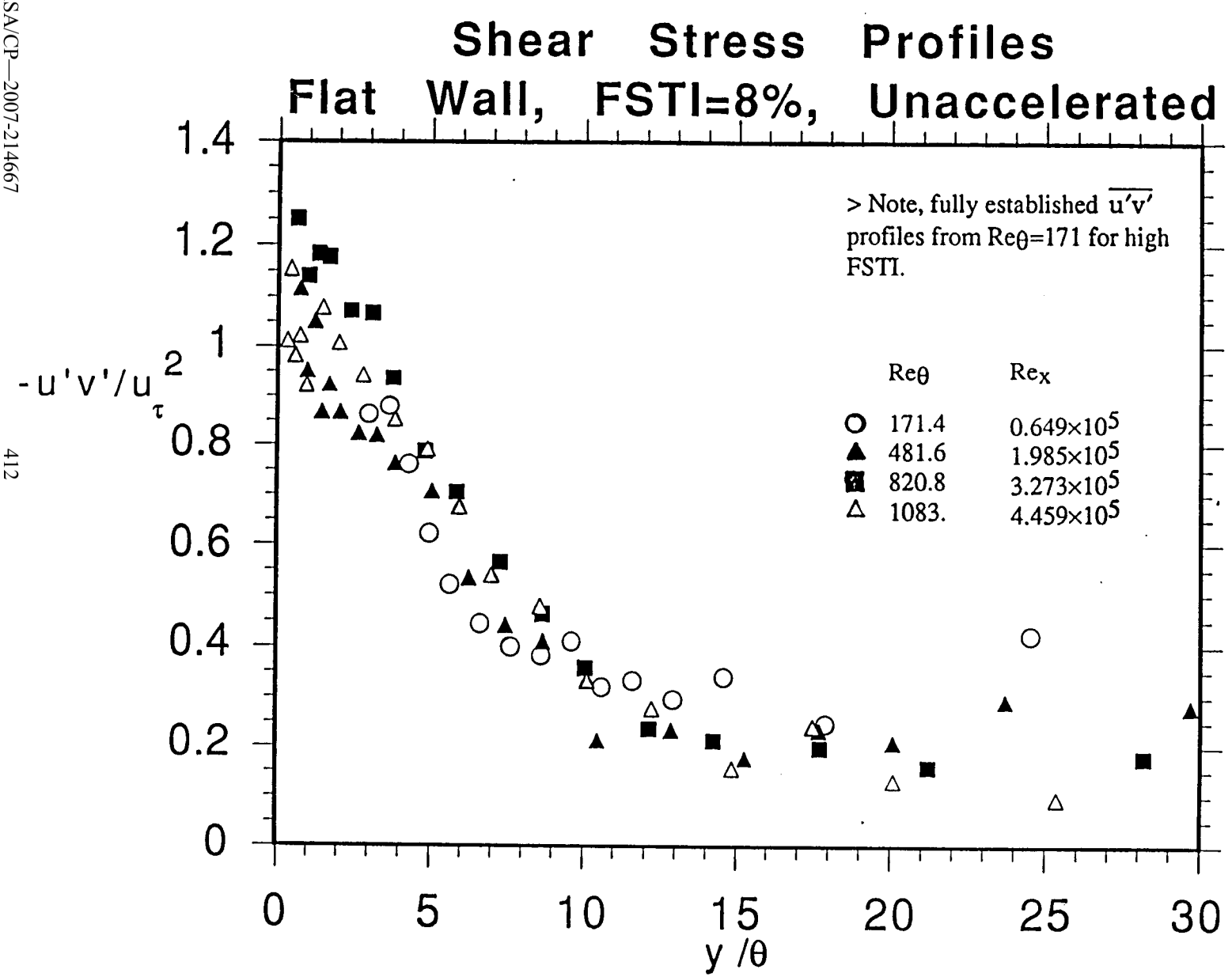
Shear Stress Profiles
Flat Wall, FSTI=8%, Unaccelerated
> Note, fully established u'v' profiles from Reθ=171 for high FSTI.
Reθ
Rex
171.4
0.649×10^5
481.6
1.985×10^5
820.8
3.273×10^5
1083.
4.459×10^5
-u'v'/u_τ^2
y /θ
0
0.2
0.4
0.6
0.8
1
1.2
1.4
0
5
10
15
20
25
30

Shear Stress Profiles
FSTI=8%

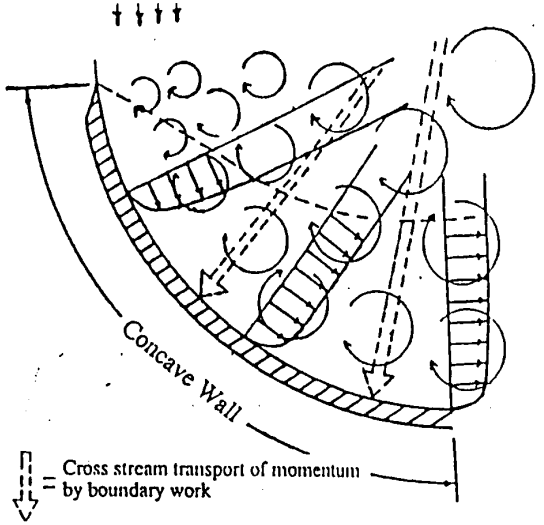

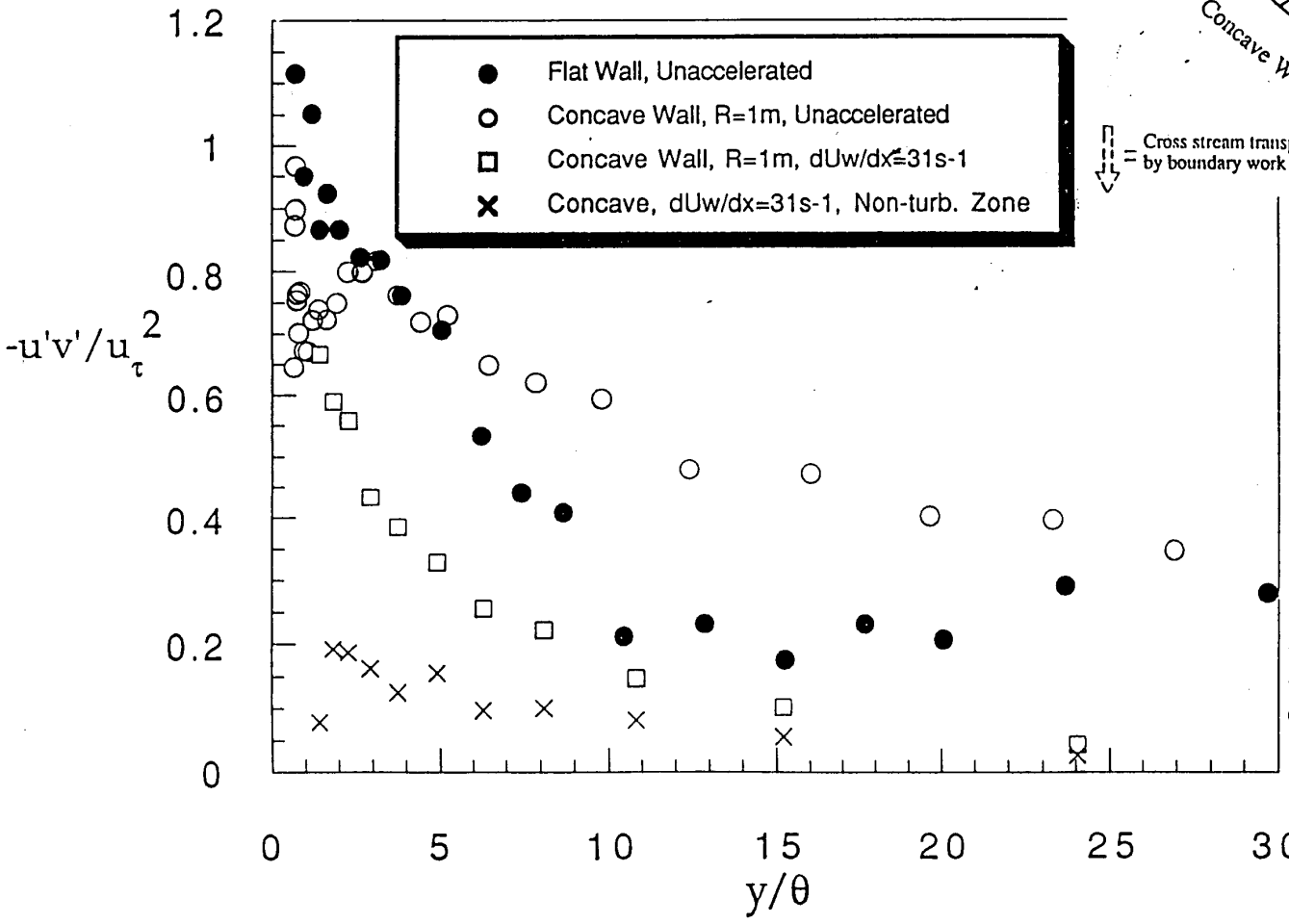

○ Turbulent eddies from the free-stream are penetrating and augmenting transport across the boundary layer relative to the flat-wall case.

□ Note very low values as acceleration is introduced.

× u'v' laminar -- values computed from measurements taken when flow is identified to be non-turbulent -- based upon the u' signal. Note the very low contribution from these data.

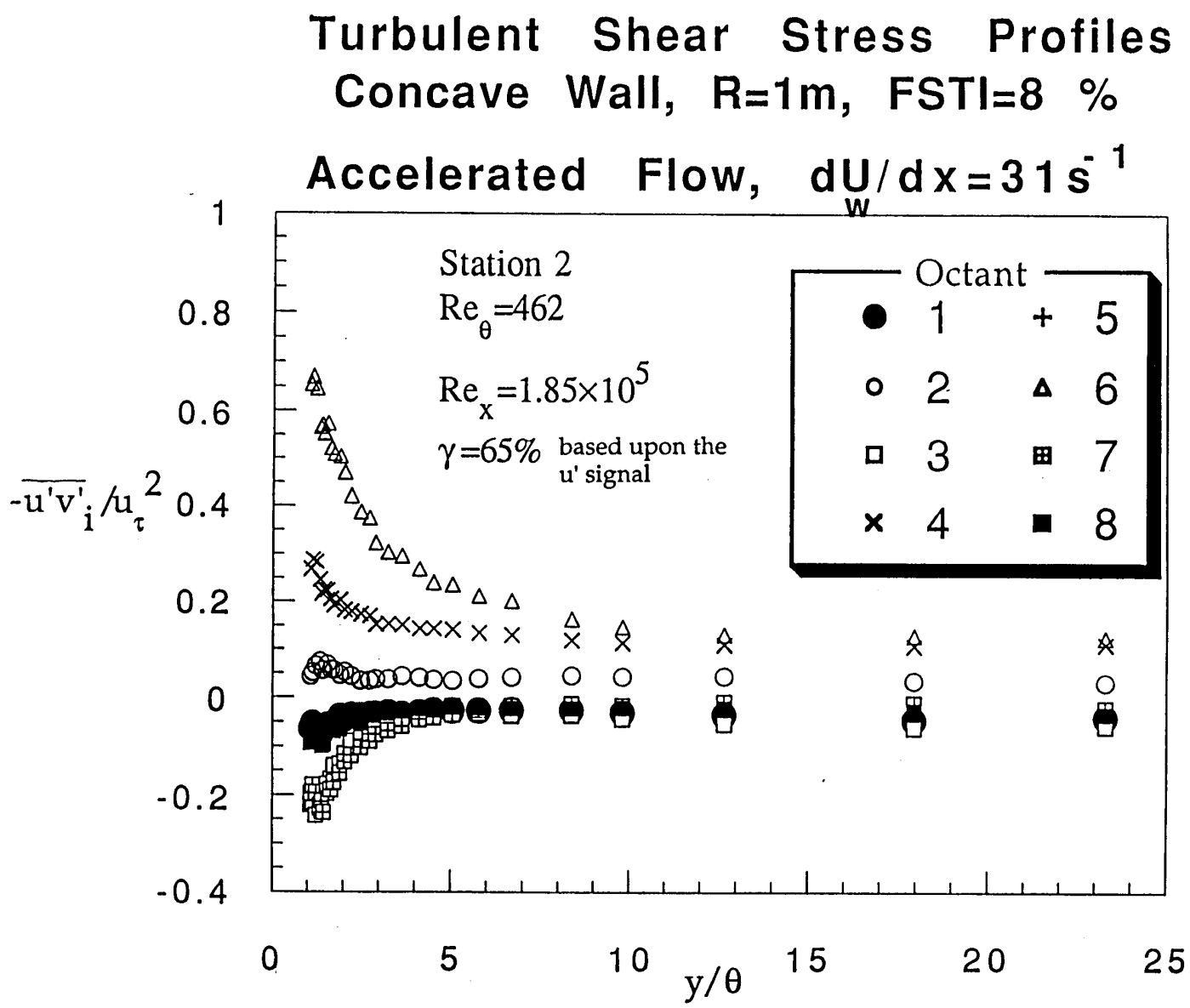
Turbulent Shear Stress Profiles
Concave Wall, R=1m, FSTI=8 %
Accelerated Flow, dU/dx=31s-1
w
Station 2
Reθ=462
Rex=1.85×10^5
γ=65% based upon the u' signal
Octant
1
2
3
4
5
6
7
8
-u'v'i/uτ2
1
0.8
0.6
0.4
0.2
0
-0.2
-0.4
0
5
10
15
20
25
y/θ

Maximum Intermittency in Profile
Concave Wall, R=1 m
Accelerated, $dU_w/dx=31s^{-1}$, FSTI=8%

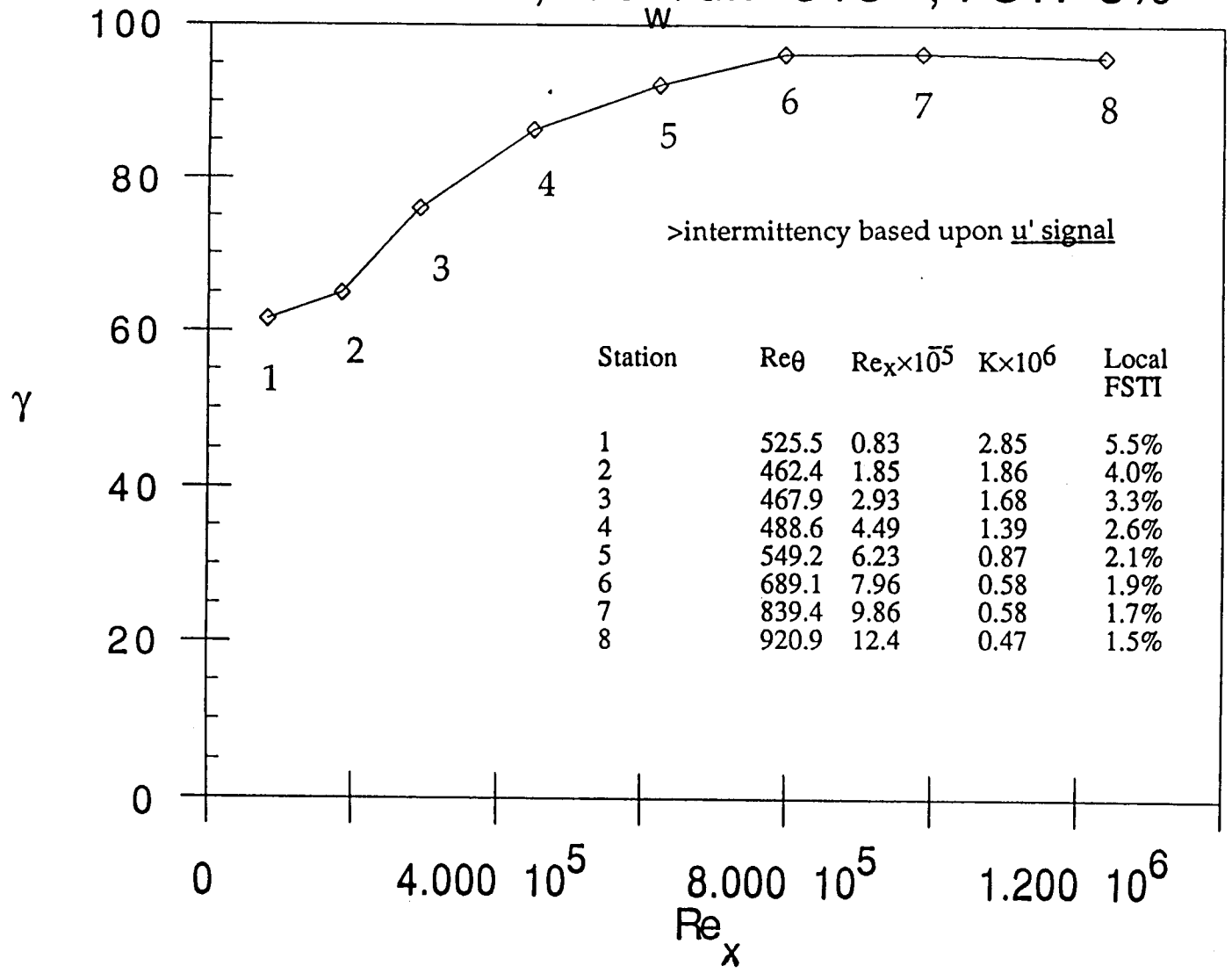

Station	Reθ	$Re_x \times 10^{-5}$	$K \times 10^6$	Local FSTI
1	525.5	0.83	2.85	5.5%
2	462.4	1.85	1.86	4.0%
3	467.9	2.93	1.68	3.3%
4	488.6	4.49	1.39	2.6%
5	549.2	6.23	0.87	2.1%
6	689.1	7.96	0.58	1.9%
7	839.4	9.86	0.58	1.7%
8	920.9	12.4	0.47	1.5%

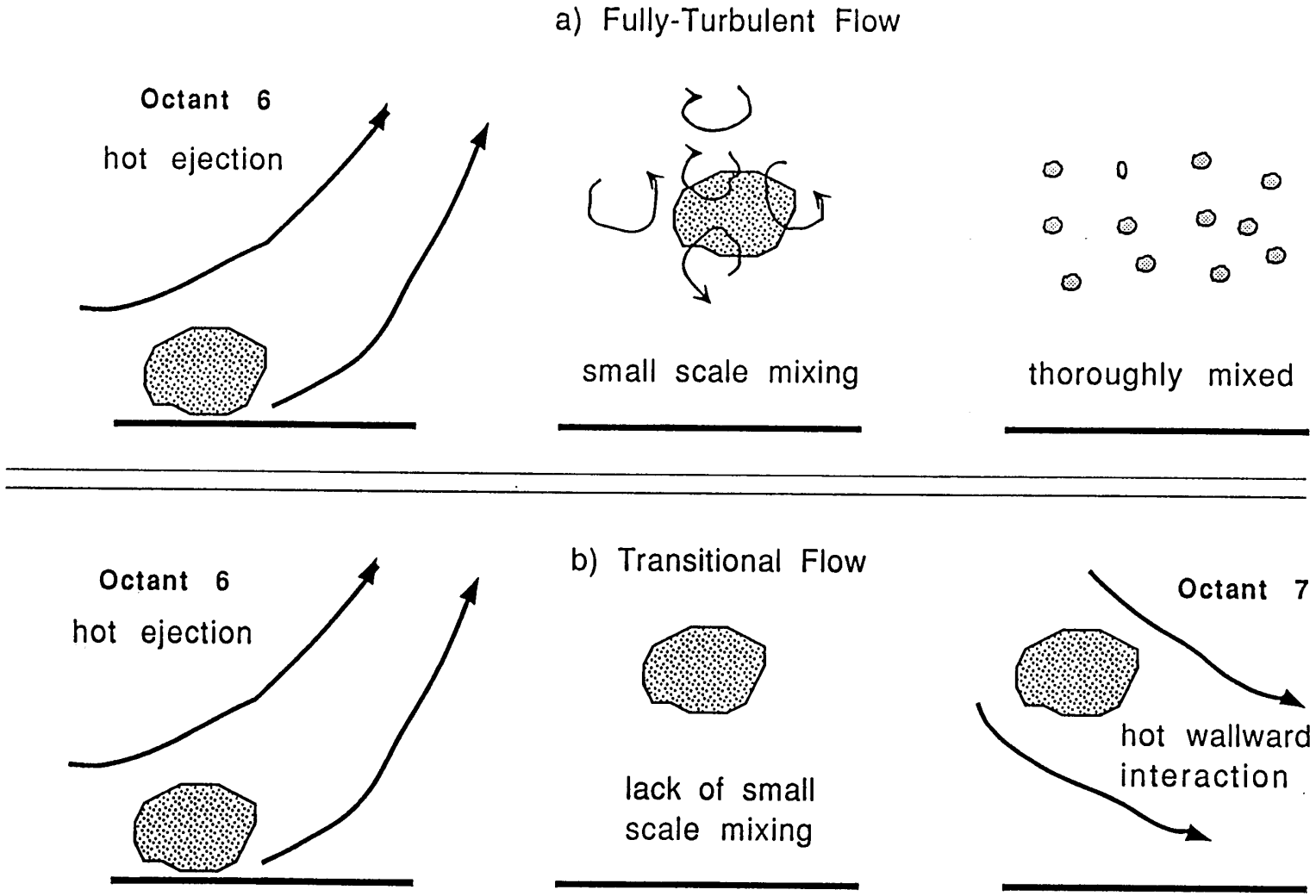

Proposed differences between fully-turbulent and transitional flow structures

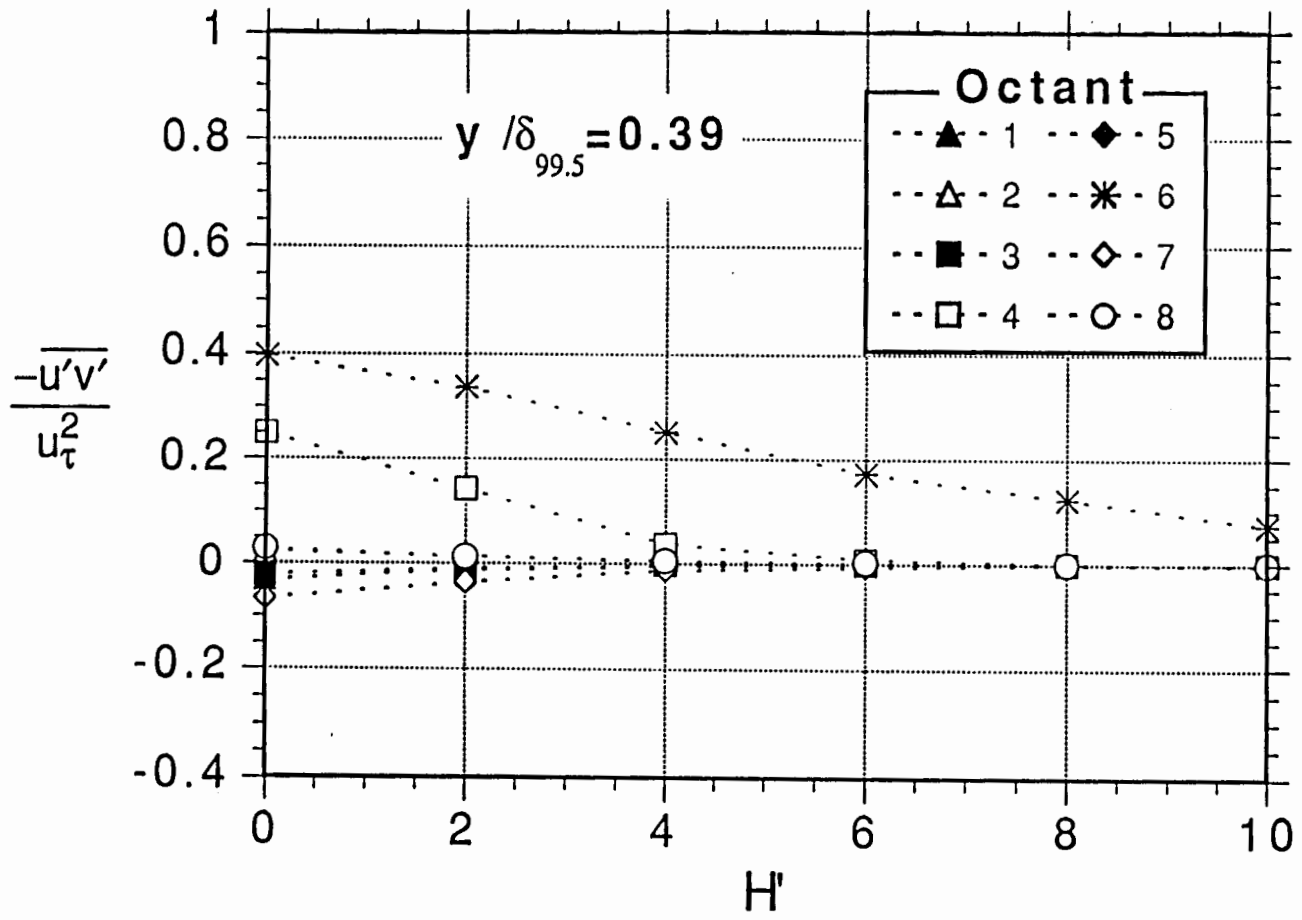

Turbulent shear stress vs hole size at $y/\delta_{99.5}=0.39$, 1.5% FSTI flat-wall case, fully-turbulent flow

$Re_\theta=1587$, $Re_x=1.062\times10^6$

> Note that in contrast to transitional flows, the contribution becomes small at large H' values.

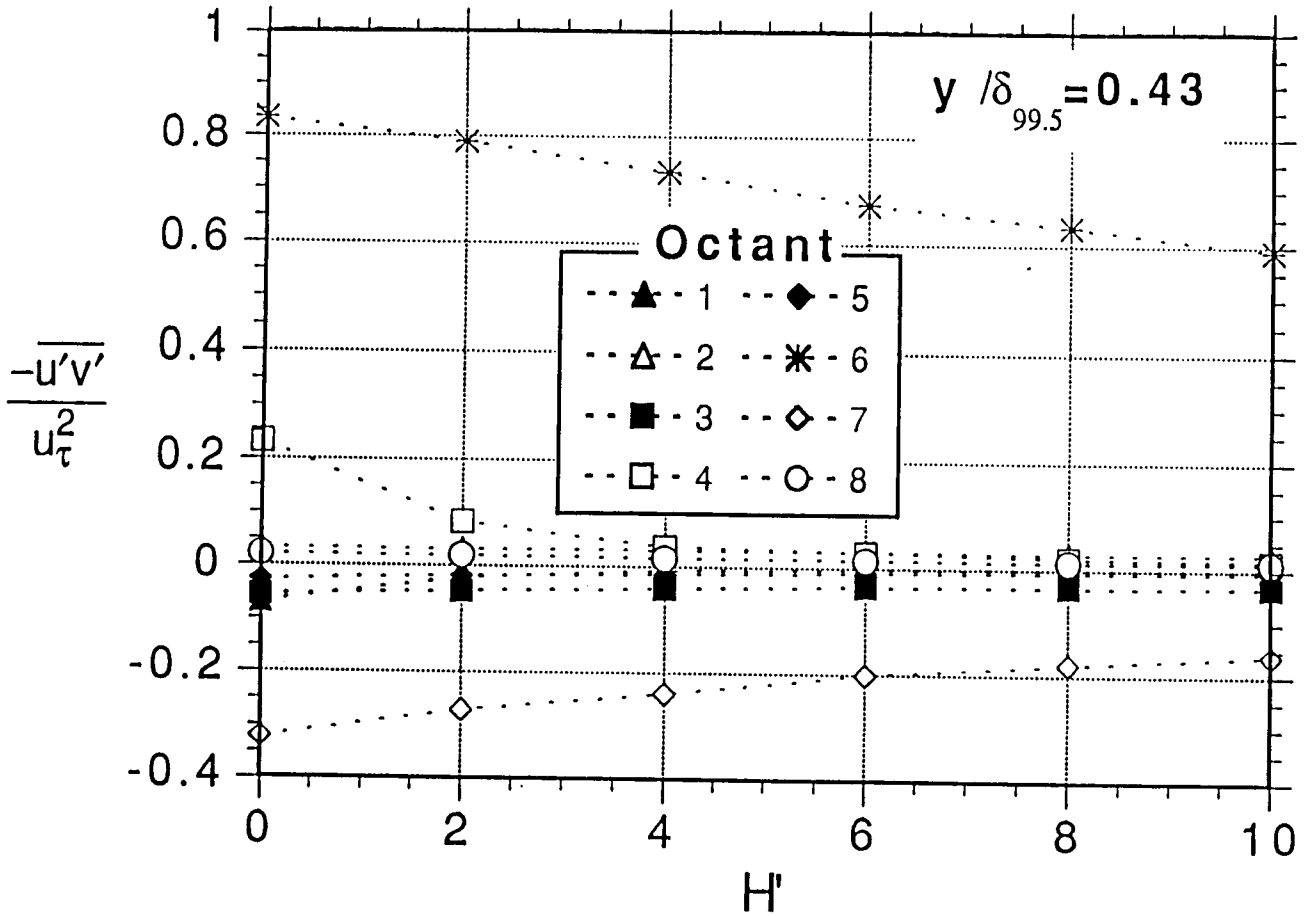

Turbulent shear stress vs hole size at $y/\delta_{99.5}=0.43$, 1.5% FSTI flat-wall case, transitional flow

$Re_\theta=379$, $Re_x=0.3442\times10^6$, $\gamma=5\%$

> When H'≠0, smaller values of u'v' are not used in processing $\overline{u'v'}$ octants. As H' increases, the filter threshold on u'v' grows. Thus, if values are large when H' is large, they come about due to strong events. Note that octants 6 and 7 remain large at large H' values.

CONCLUSIONS

SPANWISE INTERACTION OF LOCALIZED DISTURBANCES PROMOTES TRANSITION

- Increased Amplitude
- Different Spanwise Wavenumbers

THPS transition marked by Gradual Amplification of the Lower than Fundamental frequencies

TWP Transition marked by distinct lower band of Frequencies

Transition in Separating-Reattaching Boundary Layer Flows

Ed Malkiel
Mechanical Engineering Department
Resselear Polytechnic Institute
Troy, NY 12180

Abstract

Experimental work with leading edge separation bubbles is presented to clarify the issues regarding transition in separated regions. Hot-wire measurements, in the form of oscilloscope traces, turbulence intermittency and conditionally sampled velocity distributions are given. The resulting points of transition onset and spot production rates are compared to existing correlations.

OUTLINE

1) Problem

2) Experiment

3) Flow Results

4) Intermittency Results

5) Comparison to Correlations

6) Conclusions

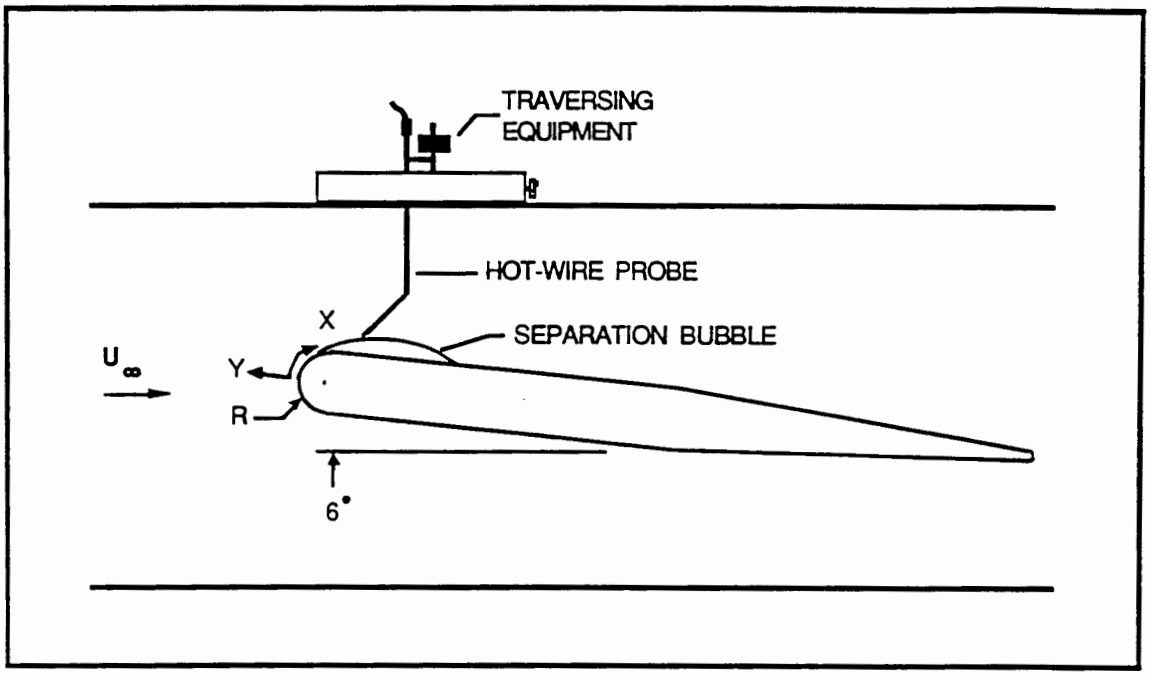

Fig. 1. Experimental Setup

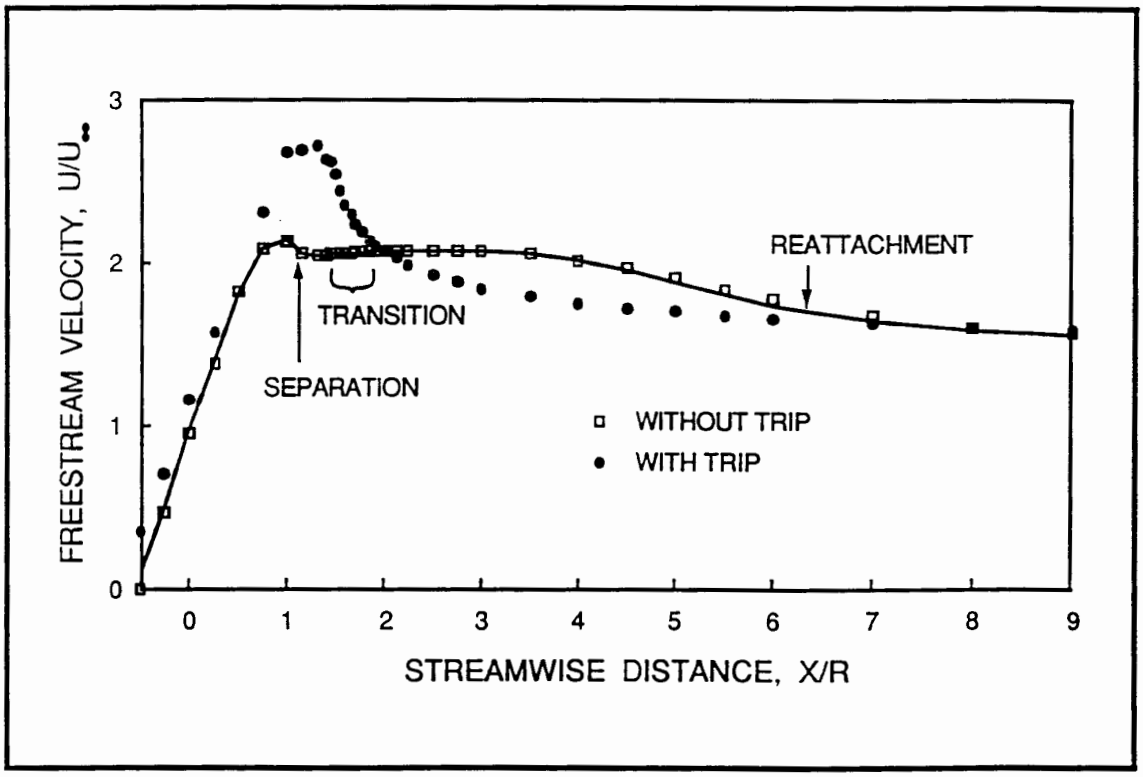

Fig. 2. Freestream Velocity

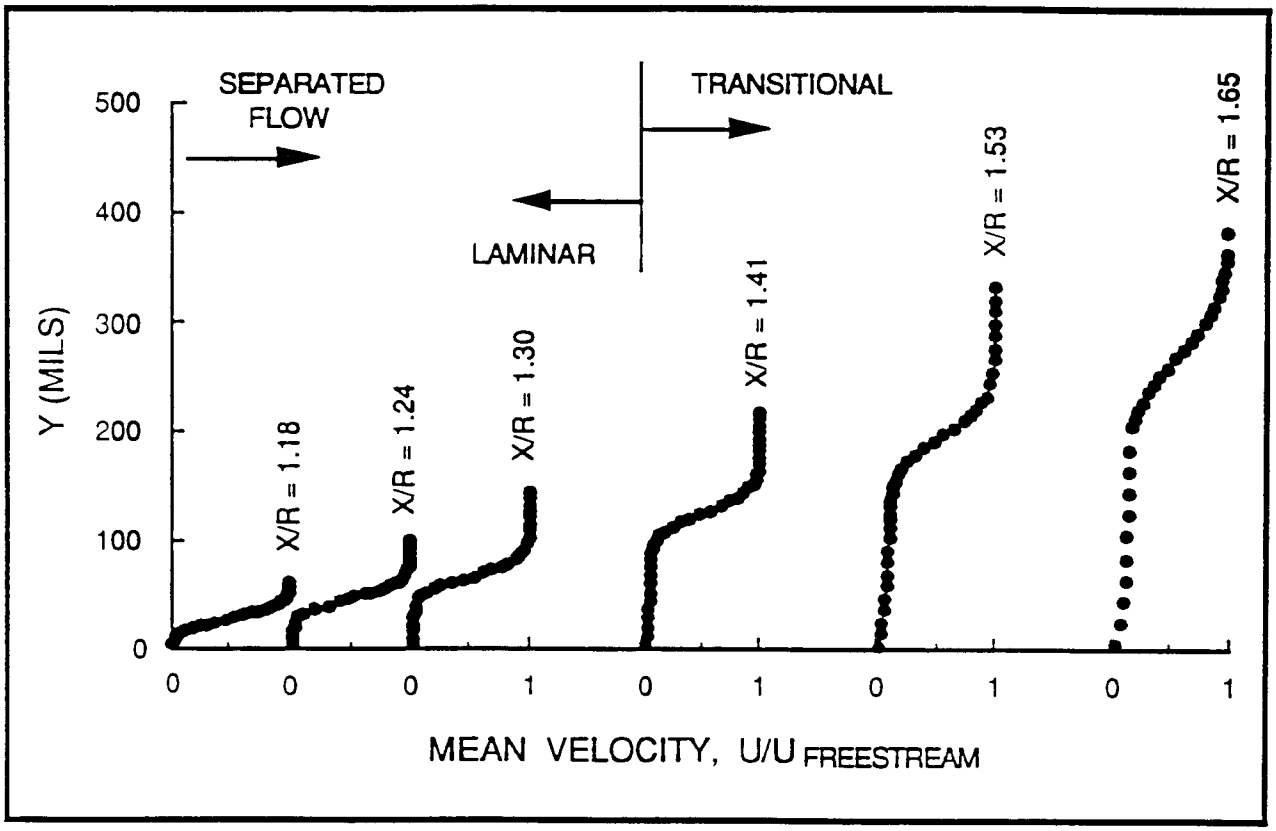

Fig. 3. Velocity Profiles

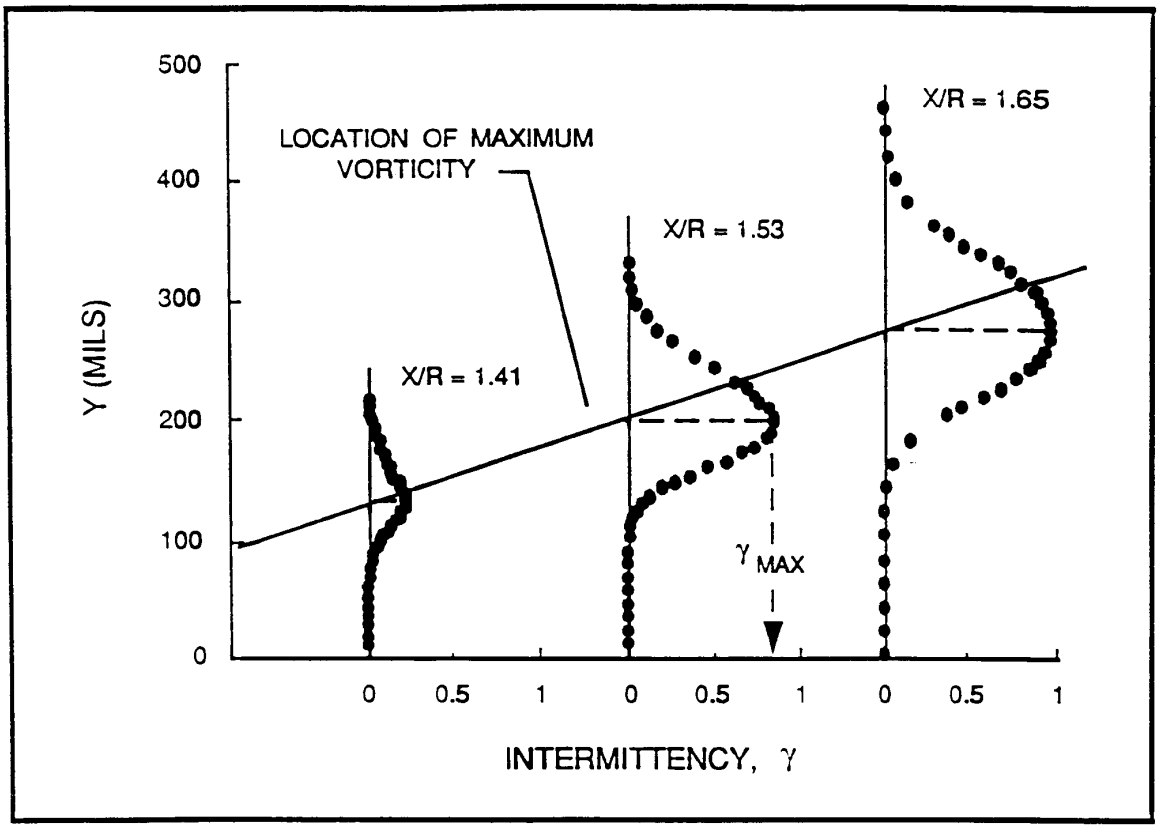

Fig 4. Intermittency Profiles

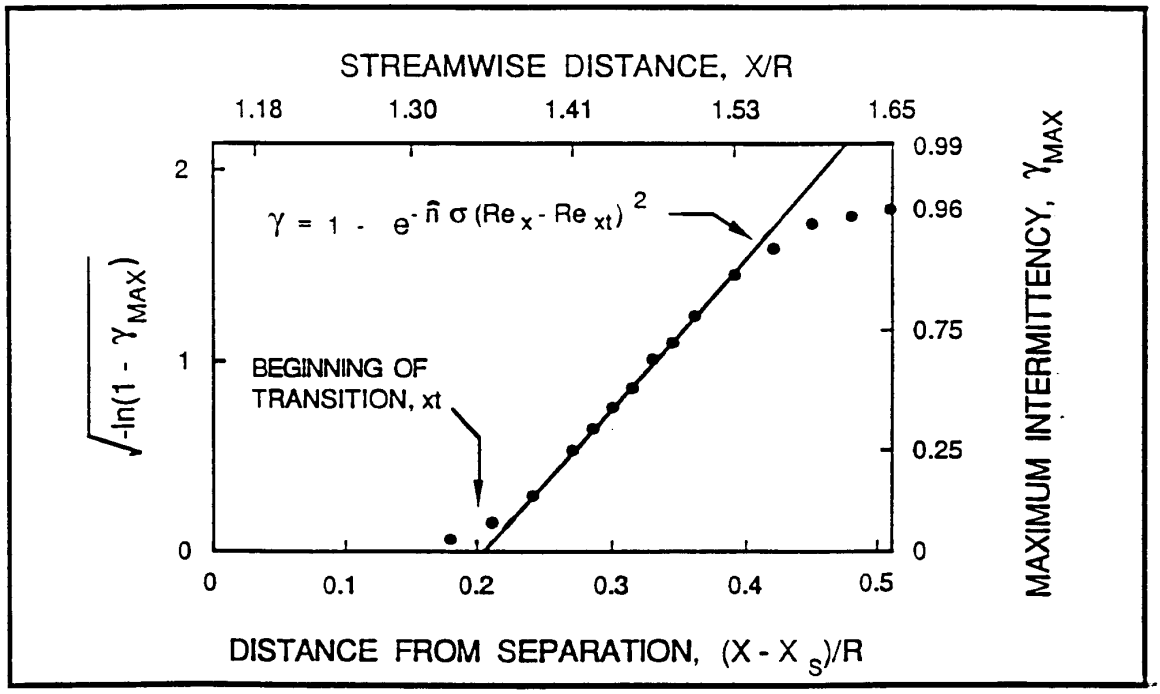

Fig. 5. Maximum Intermittency

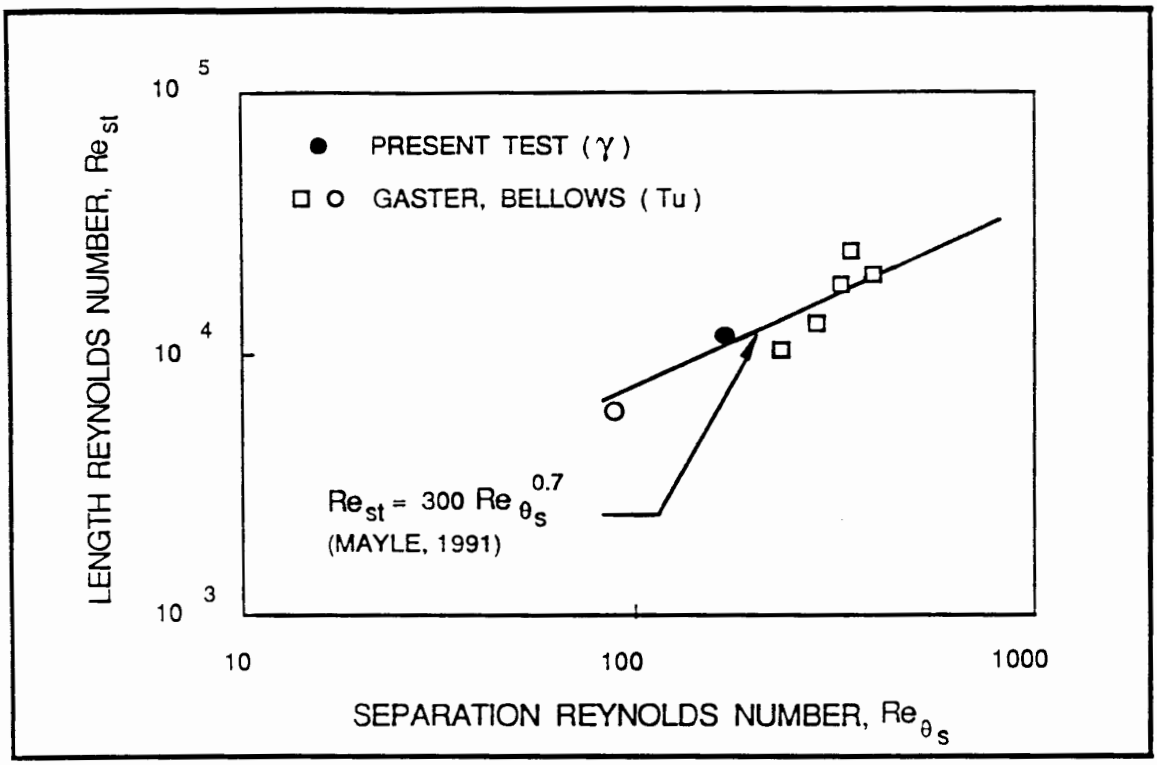

Fig 6. Beginning of Transition

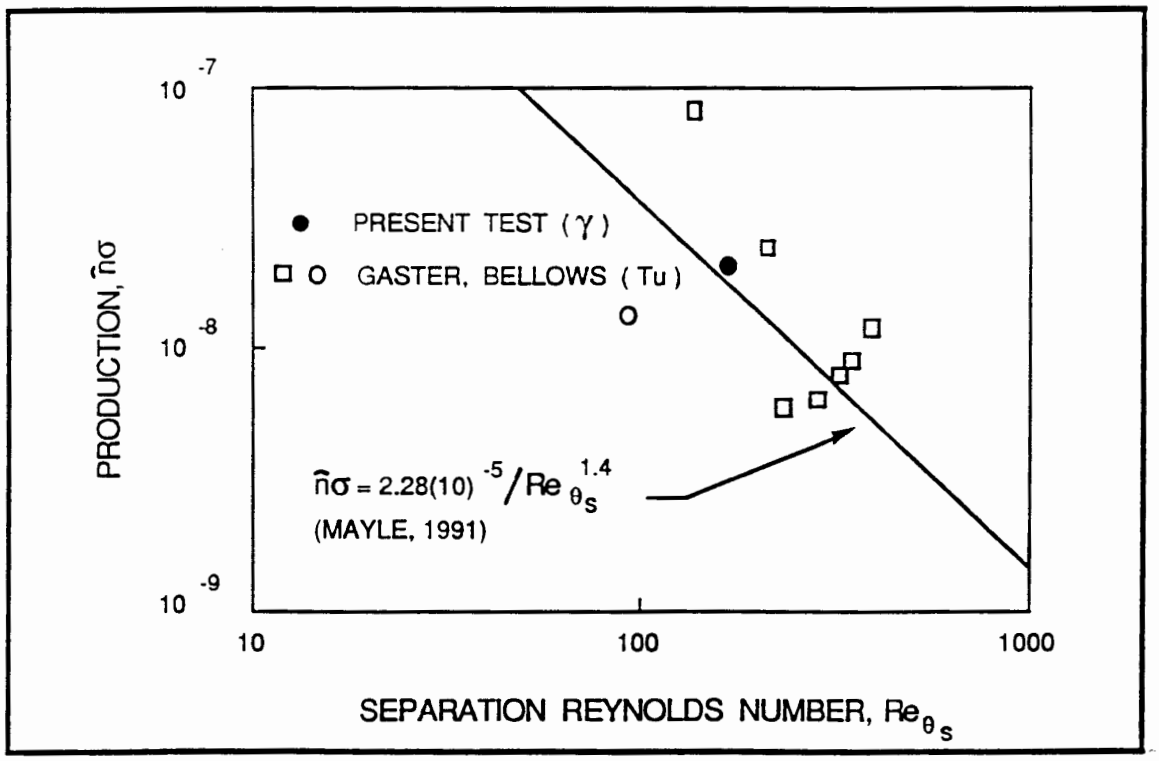

Fig. 7. Production Rate of Turbulent Spots

CONCLUSIONS

1) Transition occurs within the separated shear layer.

2) Intermittency profiles in the transition region are roughly Gaussian.

3) Maximum intermittency lies along the line of maximum vorticity in the shear layer.

4) Maximum intermittency grows as turbulent spot theory predicts.

5) More intermittency measurements in separated flow are needed.

6) Mayle's correlations seem to be reliable based on the experimental data acquired thus far.

Transition Zone Modeling

Eli Reshotko
Case Western Reserve University
Cleveland, OH 44106

This lecture reviews current practice as well as new modeling ideas for the calculation of at least skin friction and heat transfer between the onset and end of transition.

The principle means of transition zone modeling dating from the 1950's is through the intermittency models developed by Narasimha and colleagues. In these methods the length of the transition zone is closely correlated to mean boundary layer properties at the onset location and so the procedure is critically dependent on a correct determination of the onset location. The procedure is independent of the level or character of the free-stream disturbances implying independence of the spot generation mechanism or other detailed physics. Determination of onset location is principally by correlation methods of by e^N for quiescent streams. Recent development of PSE methods by Herbert and others provides a powerful method for calculating onset at all turbulence levels. Additional data for modeling of bypass transition over heated flat plates have been obtained by Sohu and Reshotko in the NASA-Lewis boundary layer channel. With a series or grids placed upstream of the contraction, free stream turbulence levels ranging from 0.4% to 6% can be produced. For Tu=0.4%, heating the plate advances transition as would be expected fro T-S considerations. For Tu>1%, there is negligible effect of heating on transition.

Rai and Moin (1990) have performed a direct Navier-Stokes (DNS) simulation of the grid 2 case of Sohu and Reshotko. This calculation which used about 8000 hrs. of CRAY-YMP time reproduced the onset of transition and most profile features through transition but missed the turbulent skin friction level. Such DNS simulation have to do better before they can be used as validation "experiment" for simpler modeling methods.

Sohu's intermittency conditioned mean profiles show that the nonturbulent part is Blasius near the beginning of transition but is fuller than Blasius as transition progresses. The turbulent part is initially less full than the standard turbulent boundary layer but approaches the Musker profile as transition is completed. Sohu's boundary layer spectra for Grids 2 and above are unambiguously turbulent. The spectra for Grid 0.5 and Grid 1 are somewhat ambiguous but our sense is that the bypass made is dominant. Sohu's spectra have some t-s features. Suder's spectra in the same facility for Grid 0 without plate heating fairly clearly document a T-S

path to transition. The turbulent spectra observed in bypass situations suggest that bypass transition might be modeled using turbulent flow methods. Additional experiments are under way for boundary layers with pressure gradients.

The balance of the presentation shows the experience to date of the Wu and Reshotko with a multiple-time-scale k-ε method. The skin friction results for the ERCOFTAC T3A case (Tu=2.8%) are reasonable but subject to improvement. The distributions of the k and ε components through transition are shown. More specifically, the low frequency component of k (kp) through transition is comparable to what is expected from such experiments including law-of-the wall similarity in the near-wall region. For turbulence levels above 12%, the law-of-the-wall similarity breaks down indicating that the outside turbulence is strong enough to change the near wall behavior thus altering the characters of the turbulent boundary layer at sub-elevated turbulence levels.

Work is continuing toward improving the MTS modeling and making the procedure more robust. Also it is important that the receptivity issue be examined toward identifying the physics of bypass initiation. Of particular interest in this regard are the forced algebraically growing subcritical "modes" identified recently by Henningson, Trefethen and colleagues.

INTERMITTENCY MODELS

$\gamma = \gamma(x)$ { Narasimha, Arnal, Chen and Thyson

Linear combination

$$( ) = (1-\gamma)( )_L + \gamma( )_T$$

Algebraic

$$\nu = \nu_m + \gamma(x)\,\nu_T$$

Narasimha

$$\gamma = 1 - \exp\left[-\frac{(x-x_t)^2 n\sigma}{U}\right]$$

x_t is onset location

n is spot formation rate

σ is a spot propagation parameter

$$\frac{n\sigma}{U} = \frac{0.41}{\lambda^2} = \frac{N}{\theta_t^2}\left(\frac{\nu}{U\theta_t}\right)$$

$$\lambda = \sqrt{\frac{0.41}{N}}\,\theta_t R_{\theta_t}^{\frac{1}{2}}$$

where λ is distance between $\gamma=0.25$ and $\gamma=0.$

N is dimensionless parameter thought to be nearly constant

θ_t is momentum thickness at x_t

DETERMINATION OF ONSET

Quiescent Streams $0 < Tu \lesssim 0.4\%$	Correlation, PSE, e^N, *
Weak Bypass ("Dangerous") $0.4\% \lesssim Tu \lesssim 2\%$	Correlation, PSE, *
Strong Bypass $Tu \gtrsim 2\%$	Correlation, PSE, * k-ϵ (DNS)

* Methods based on Henningson, Trefethen inspired techniques involving non-orthogonal forced modes, principally 3D!!

WHAT ARE THE ALTERNATIVES?

Quiescent Flows – Wilcox: e^4 followed by $g-\tau$

Bypass Flows – Many investigators:

Turbulent Flow methods

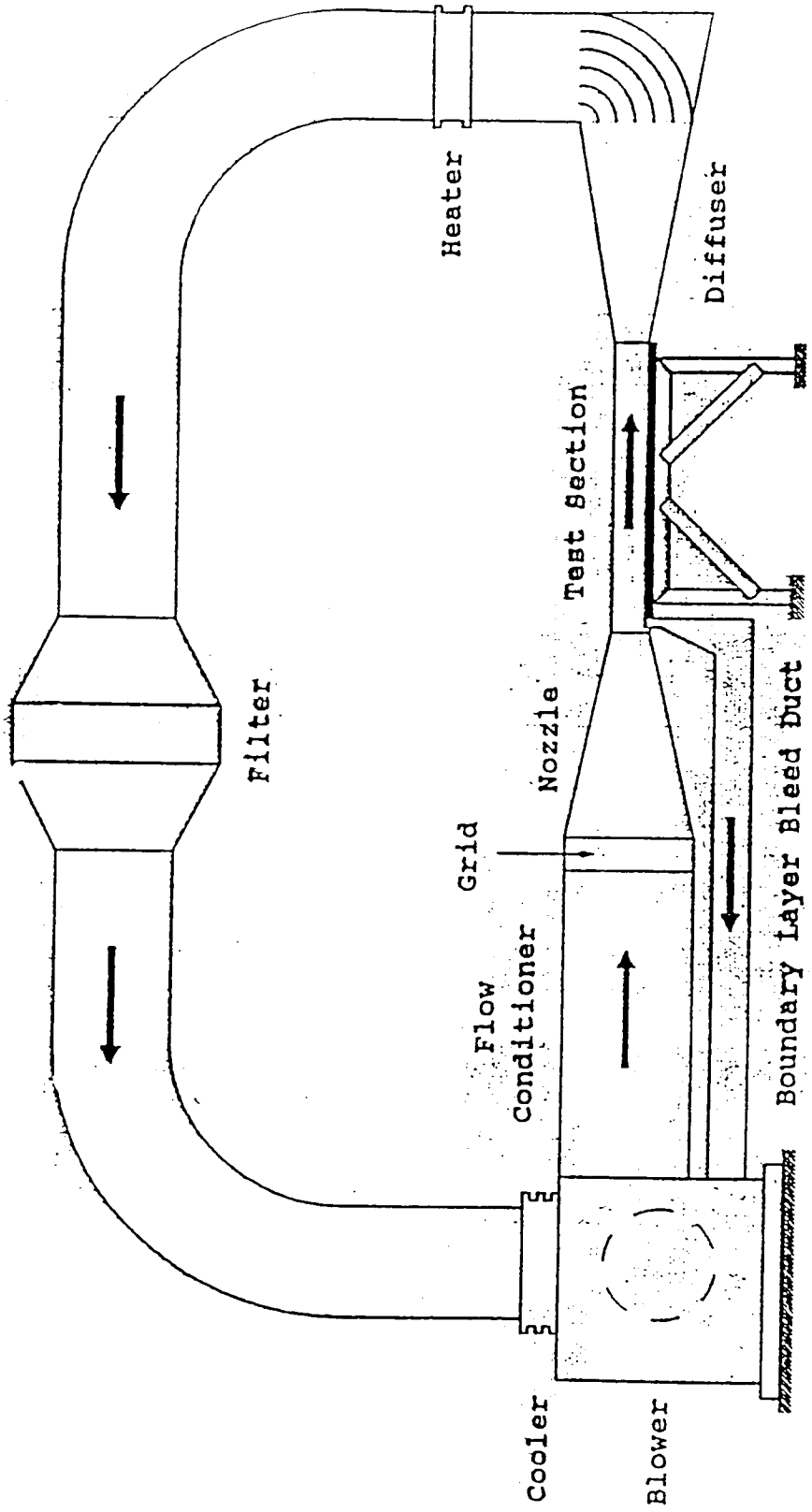

Fig. 1 Schematic diagram of the wind tunnel

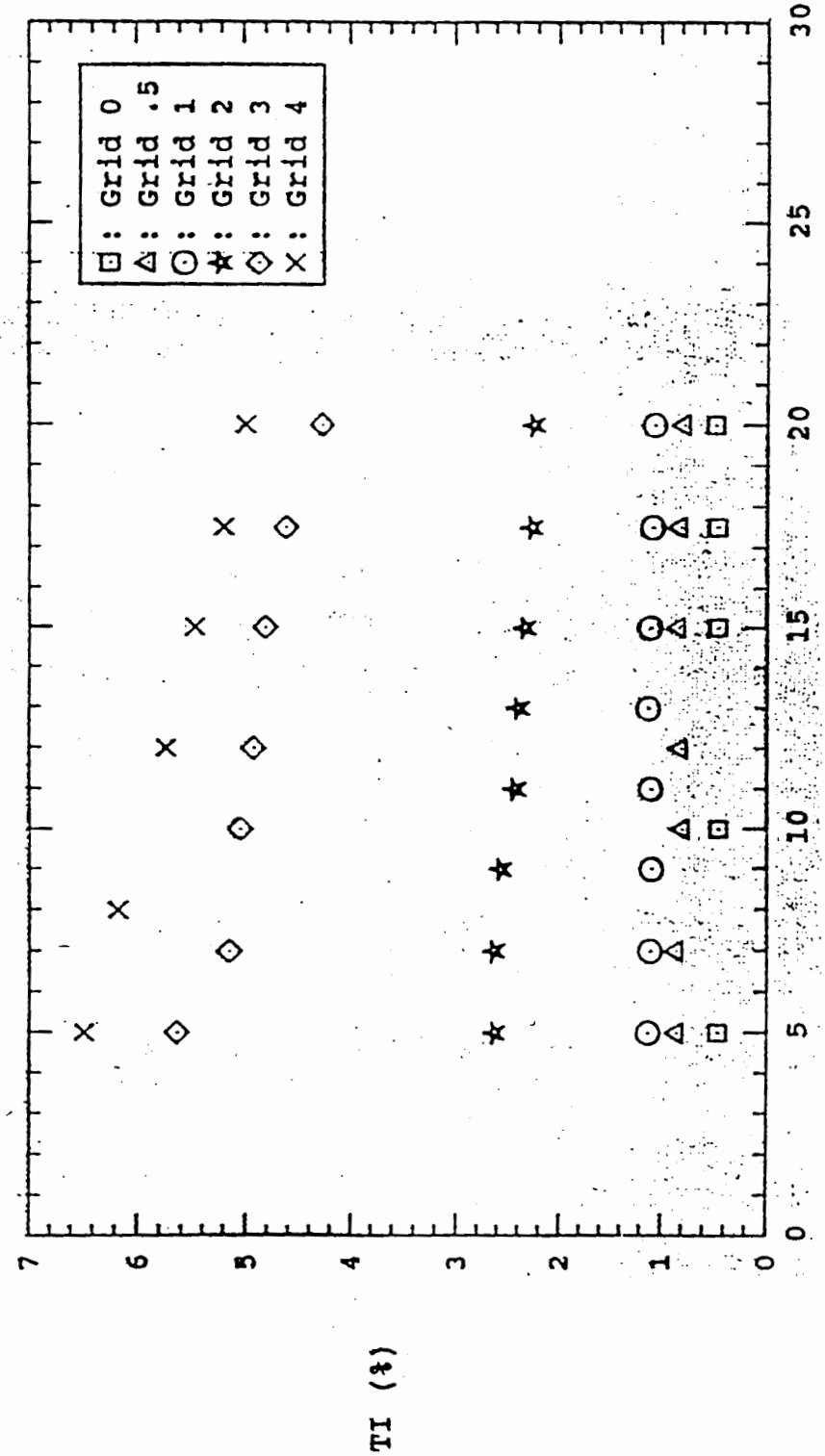

Fig. 19 Streamwise freestream turbulence intensity through the test section

SOHN

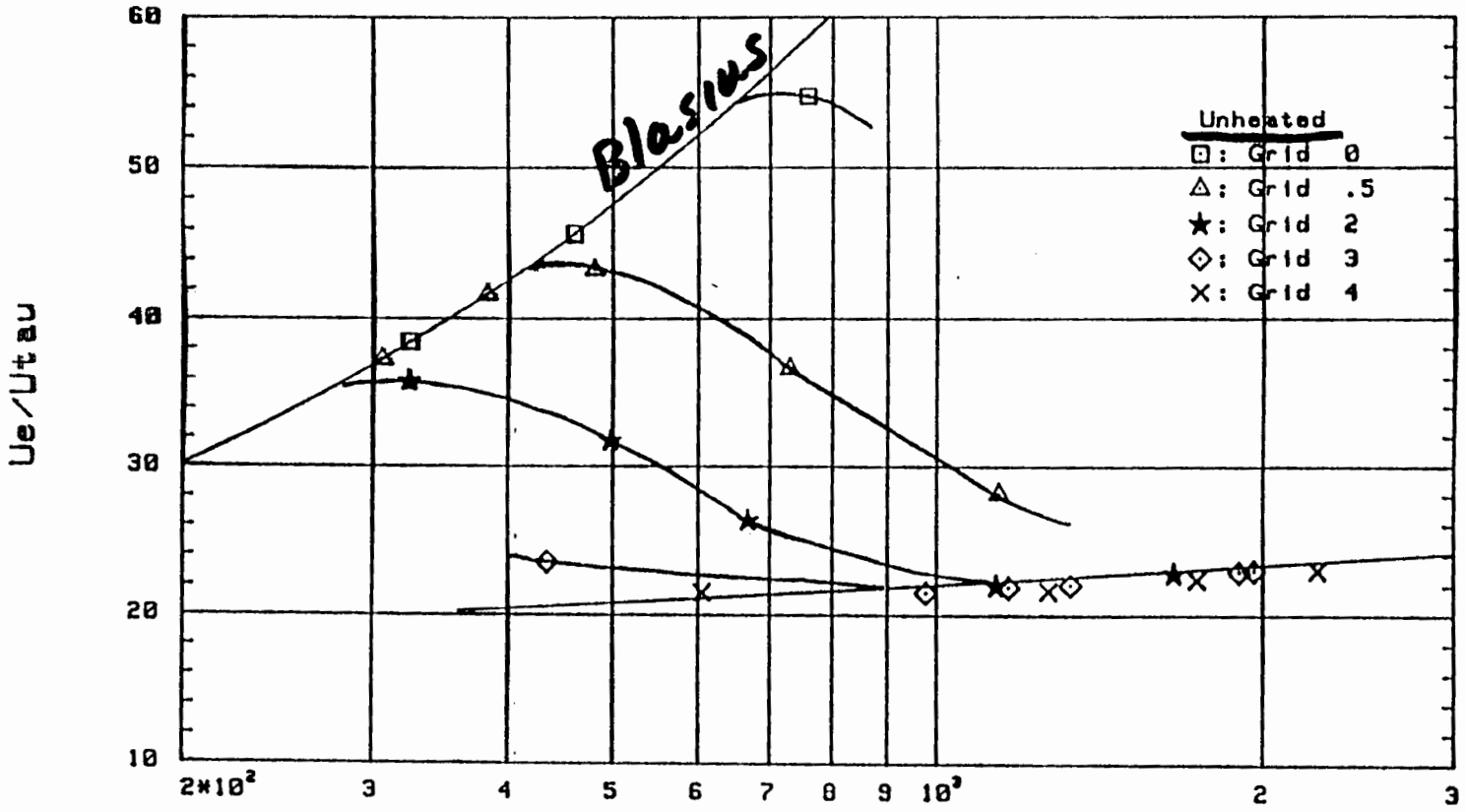

$$\frac{u_e}{u_\tau} = \sqrt{\frac{2}{c_f}}$$

Ue+ variation

SOHN

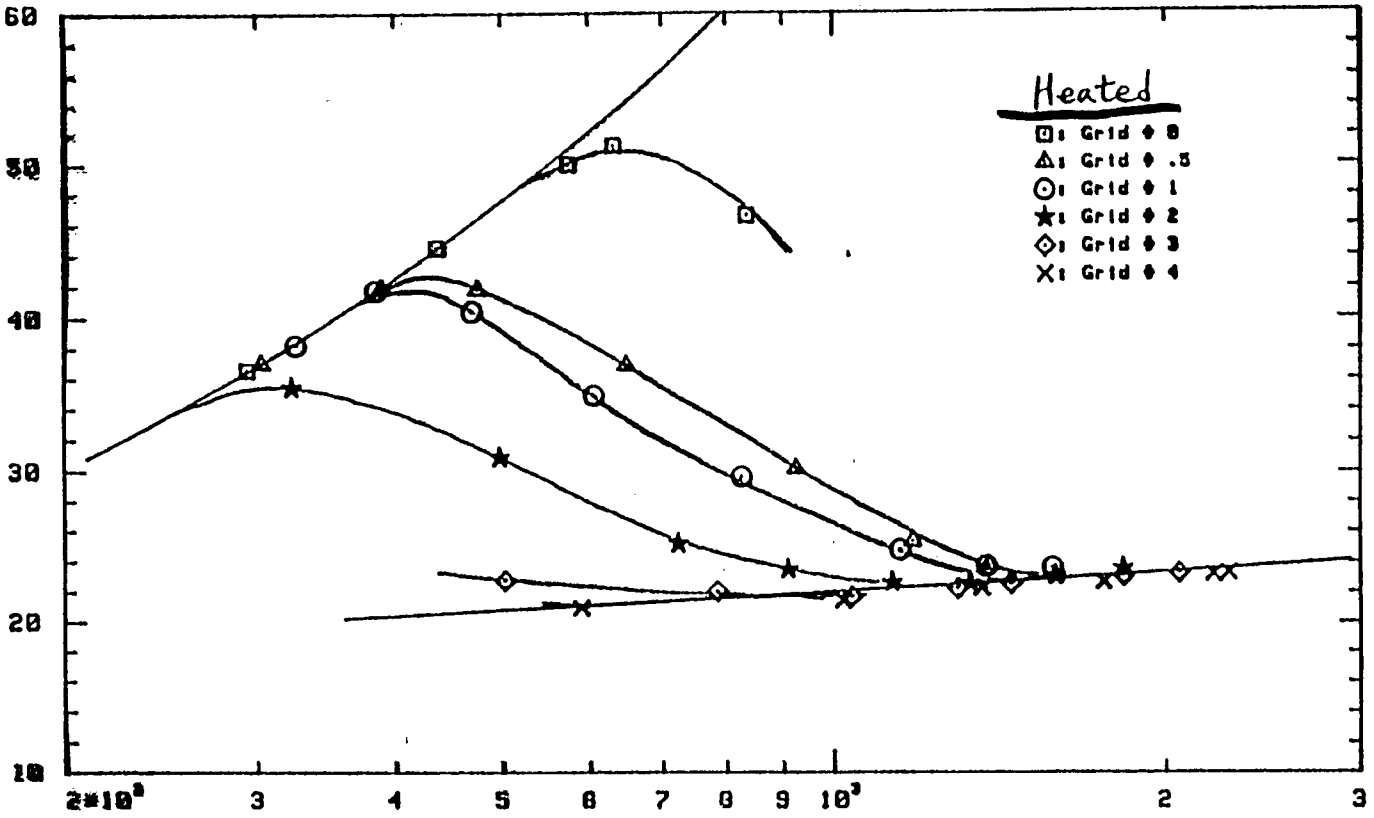

$$\frac{u_e}{u_\tau} = \sqrt{\frac{2}{c_f}}$$

Ue+ variation

($\Delta T \sim 15^{\circ}F$)

Heating reduces $Re_{x_{tr}}$ by about

20% for Grid 0 (T-S mode)

BUT HAS NEGLIGIBLE EFFECT ON

Re_{tr} FOR THE OTHER GRIDS

(Bypass mode dominant)

Note: For distibated roughness sufficiently large, stability modifiers are inoperative or may even have reverse effect. THIS IS ALSO A BYPASS.

FIG. 1. **Man Rai, NASA-Ames 1990**

SCHEMATIC OF COMPUTATIONAL REGION

(NOT IN SCALE)

GRID 2
of both Sieder and Blair

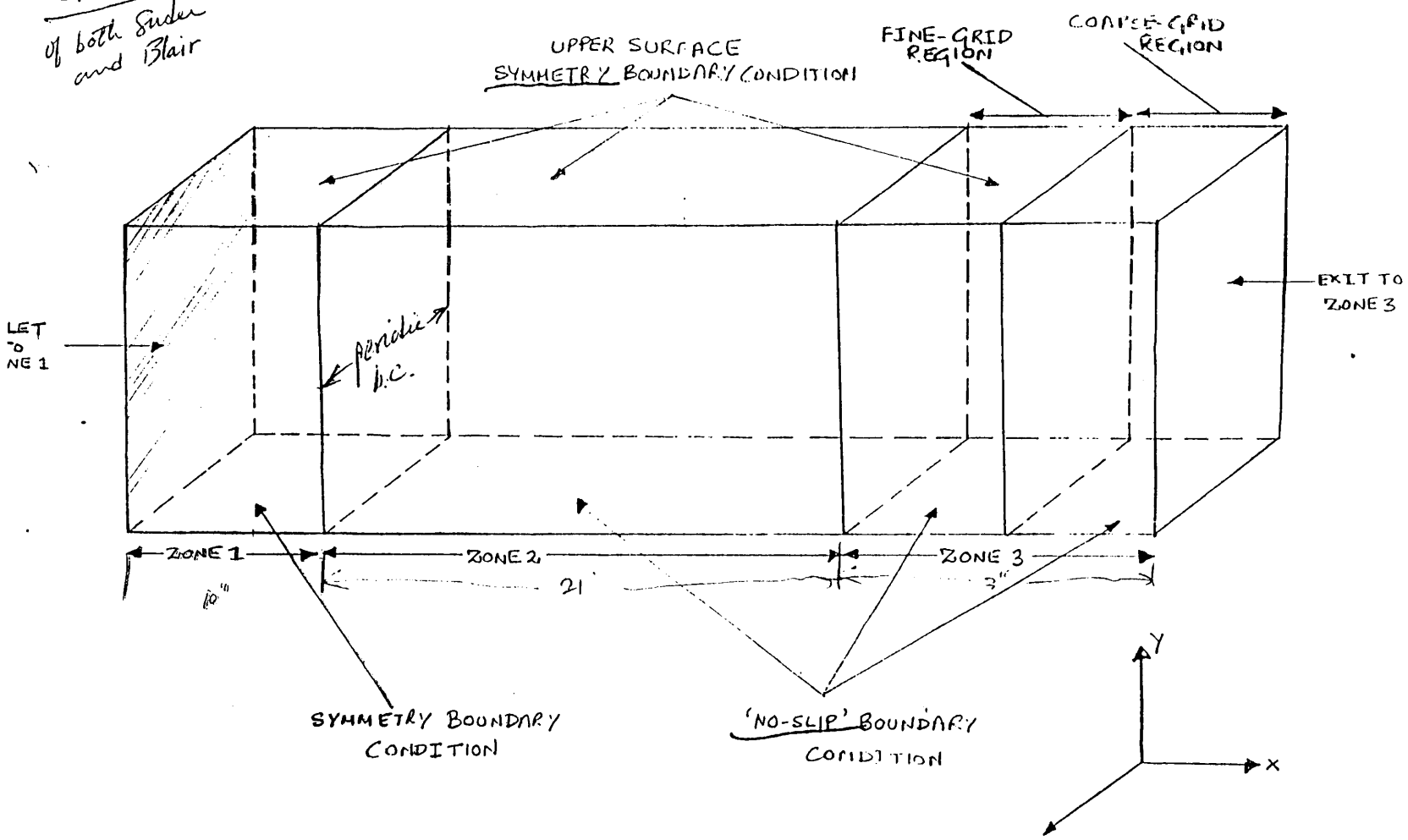

Rai, 1990

FIG. 2

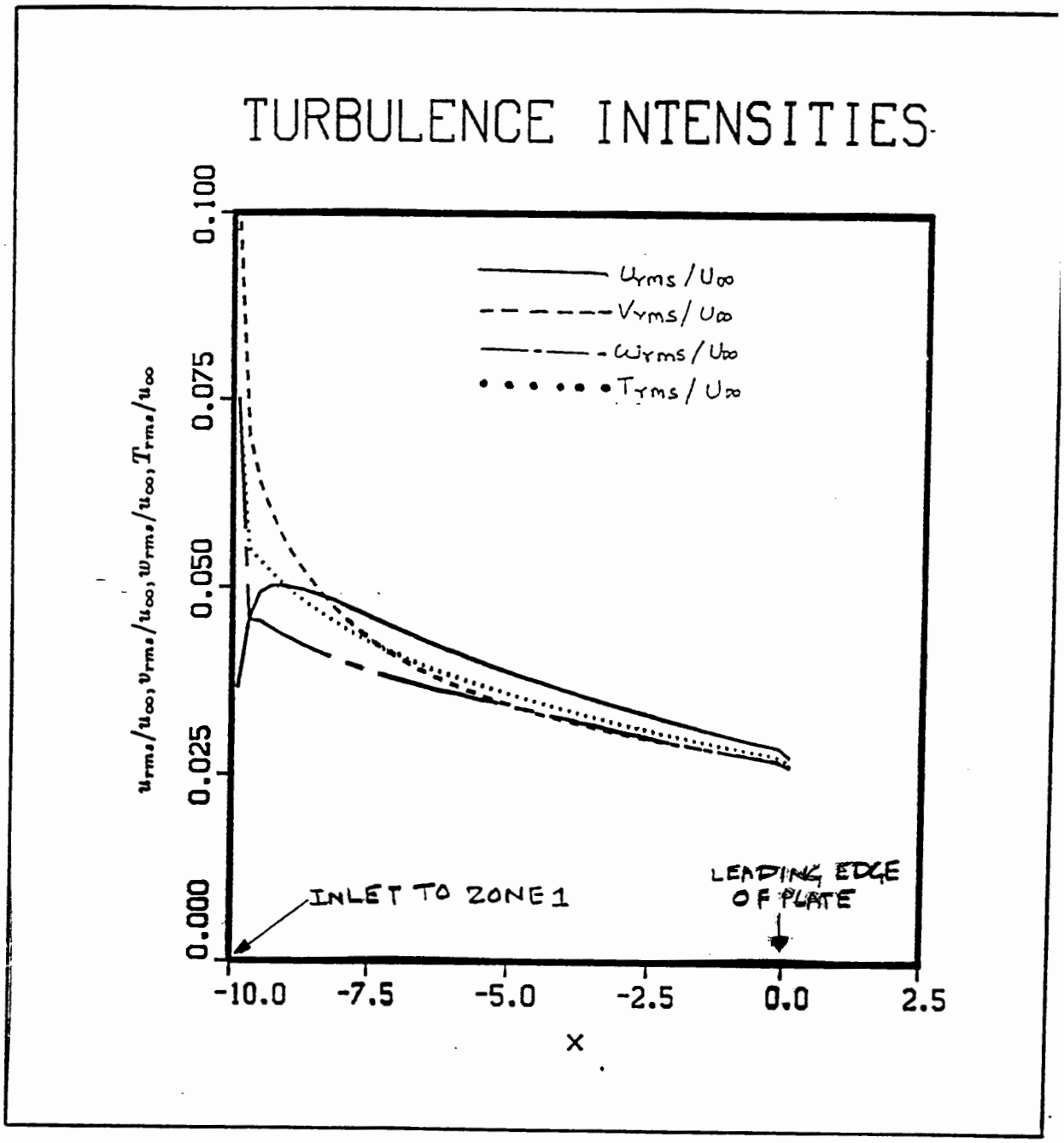

Rai, 1990

FIG. 3

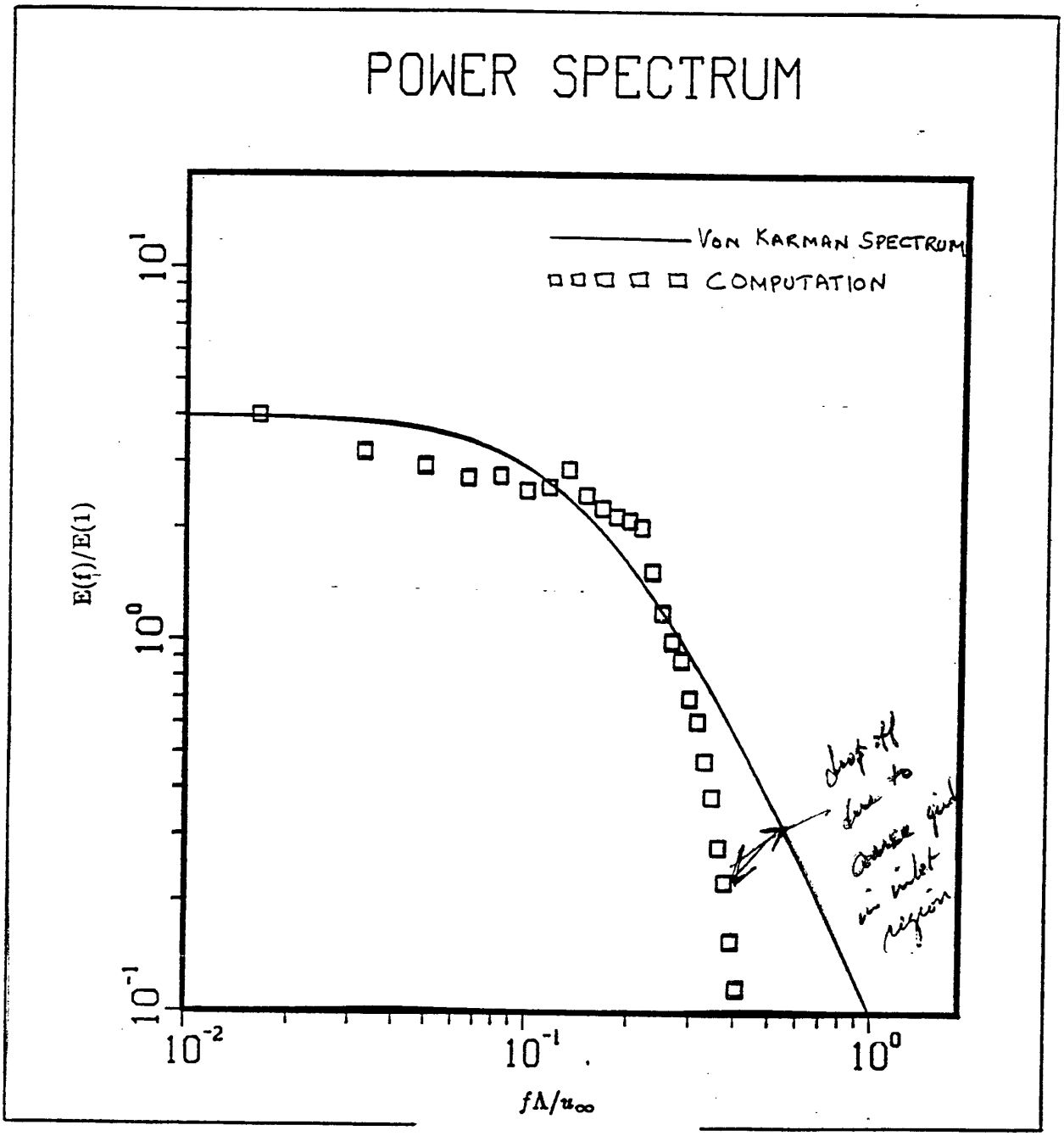

Rai, 1990

Would go a lot faster for M = 0.4 than M = 0.1

16.8×10^6 grid points 600-800 hrs on CRAY-YMP

FIG 5

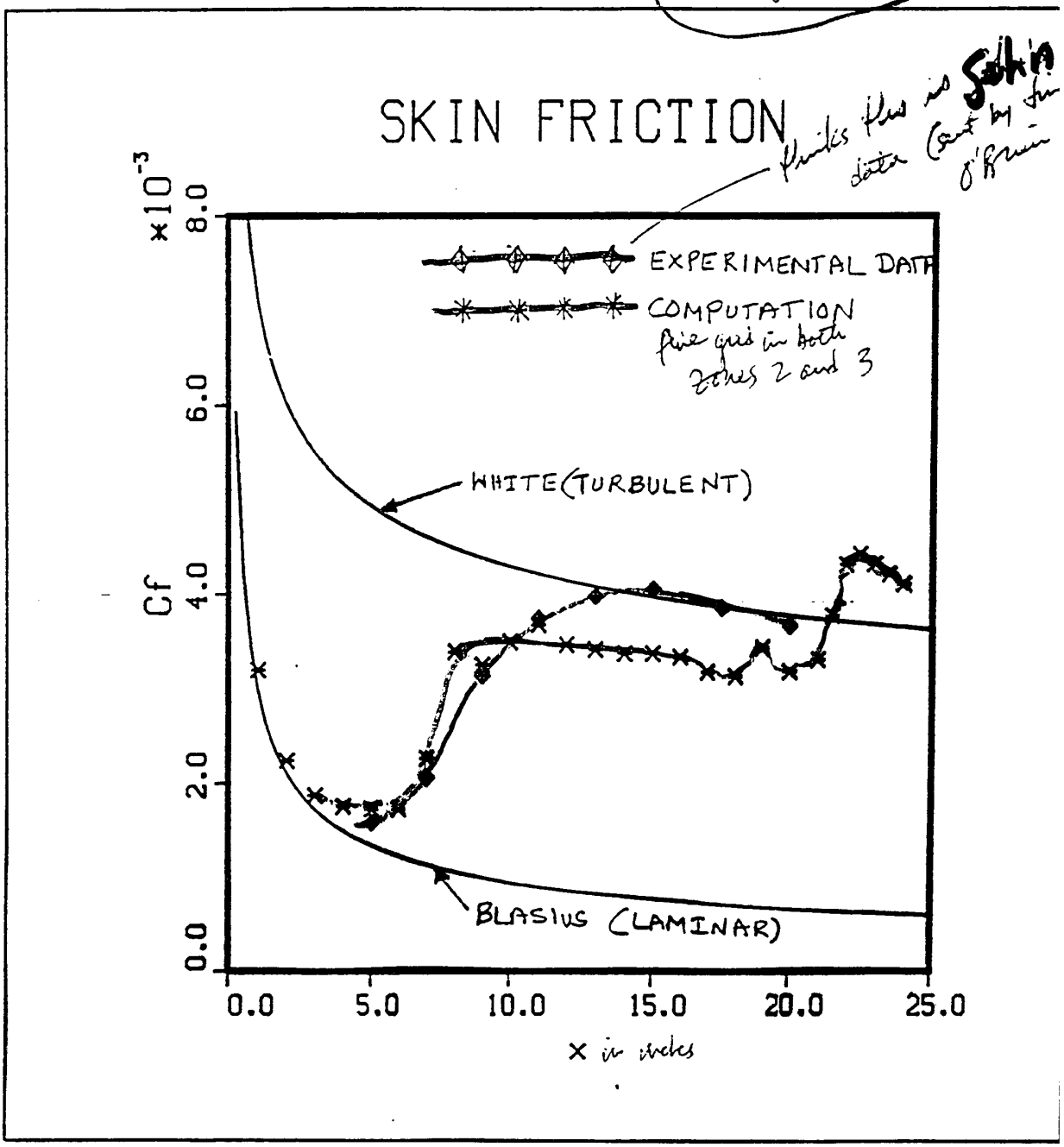

Rai, 1990

FIG. 6 $\Delta x^+ \approx 29$ $\Delta z^+ \approx 10$

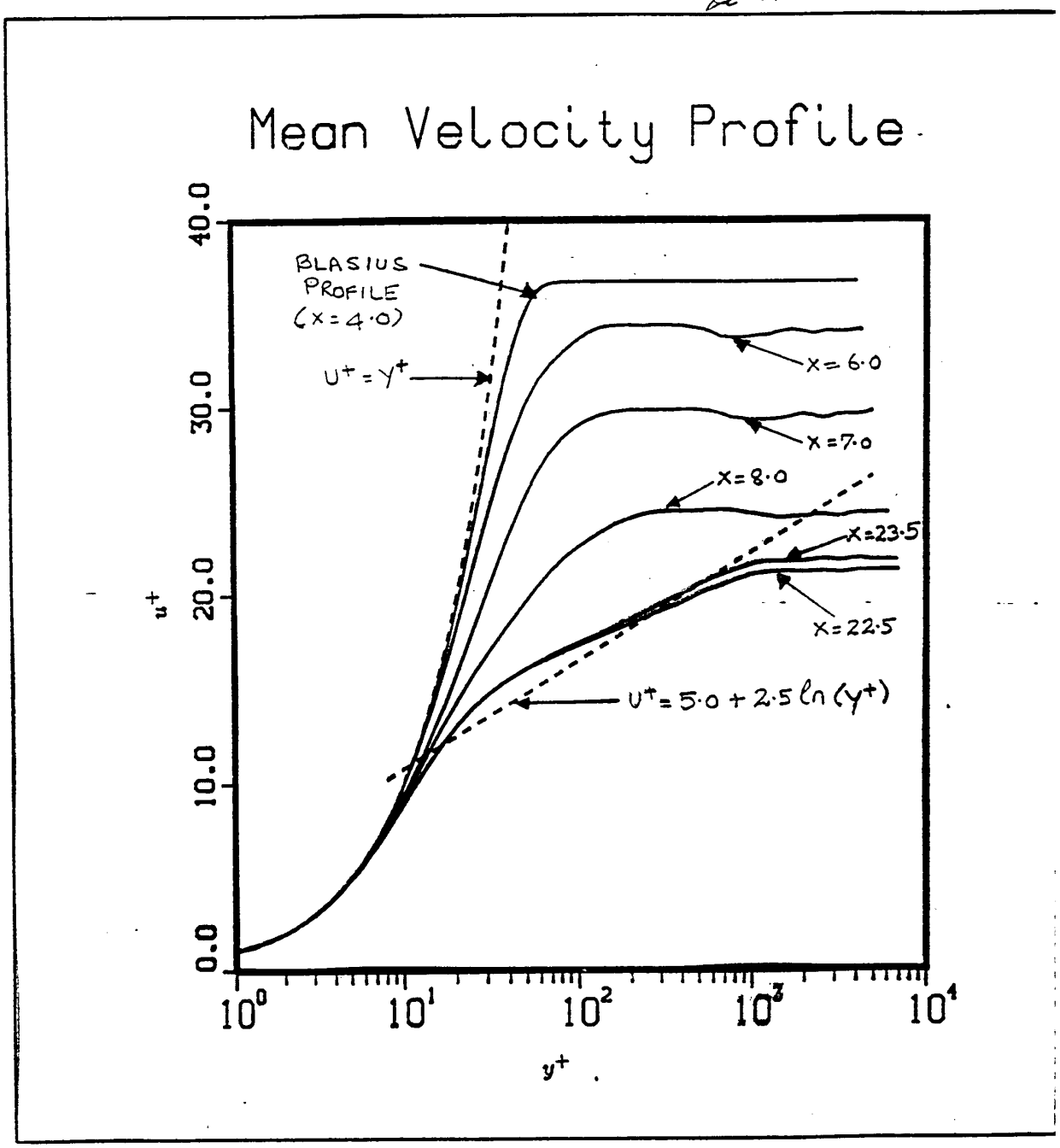

Rai, 1990

FIG. 7

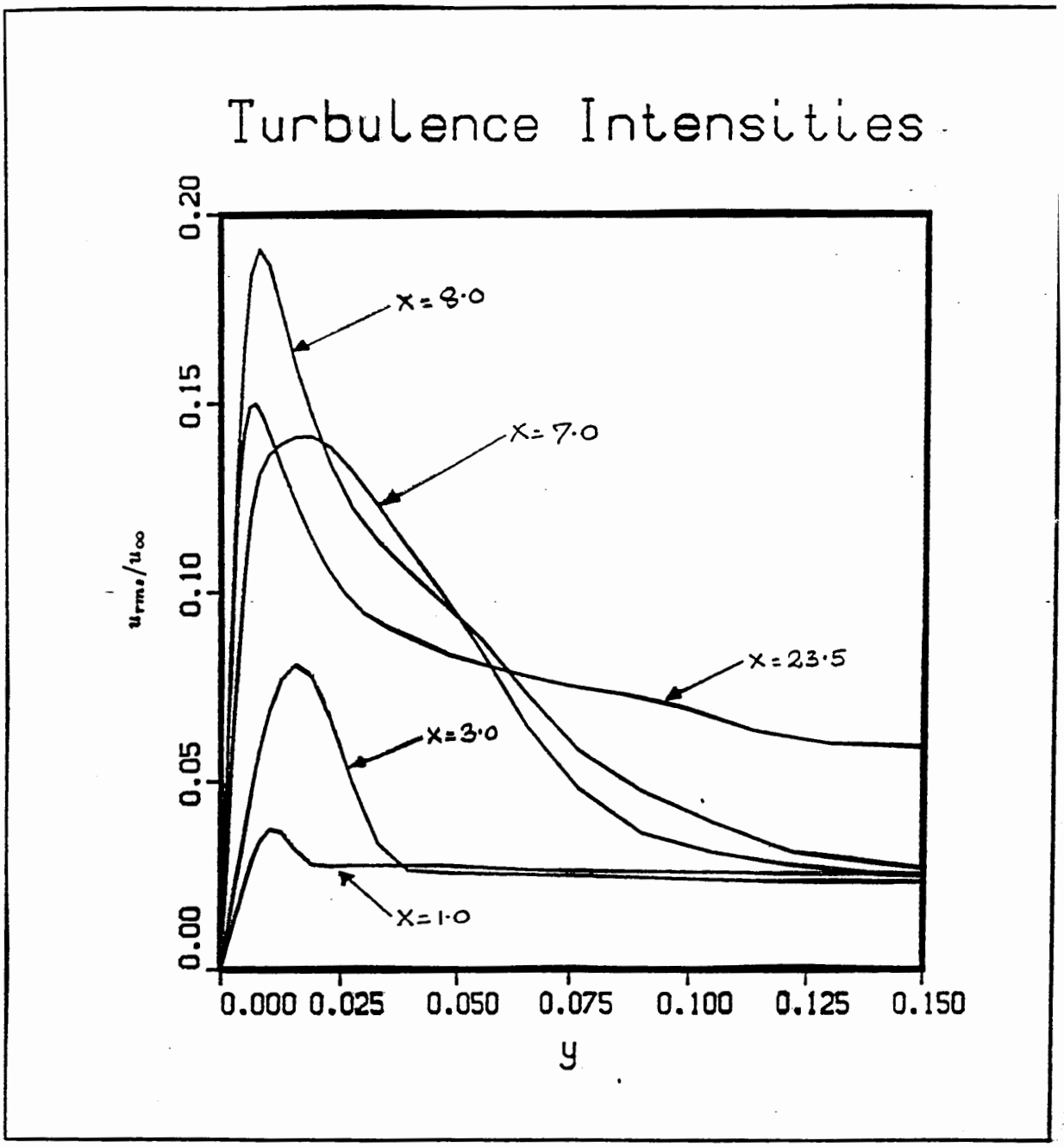

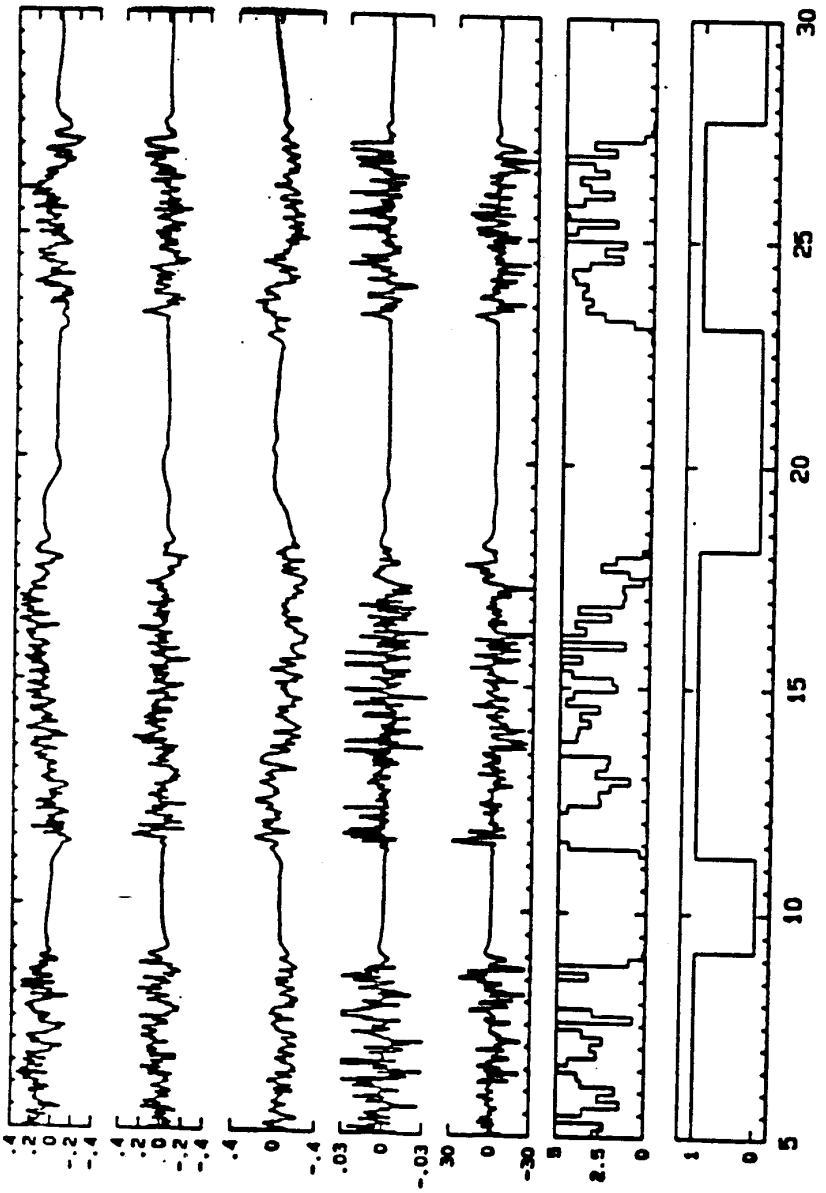

Fig. 18(b) Illustration of indicator function determination technique for 3-wire probe following Hedley and Keffer (1974)

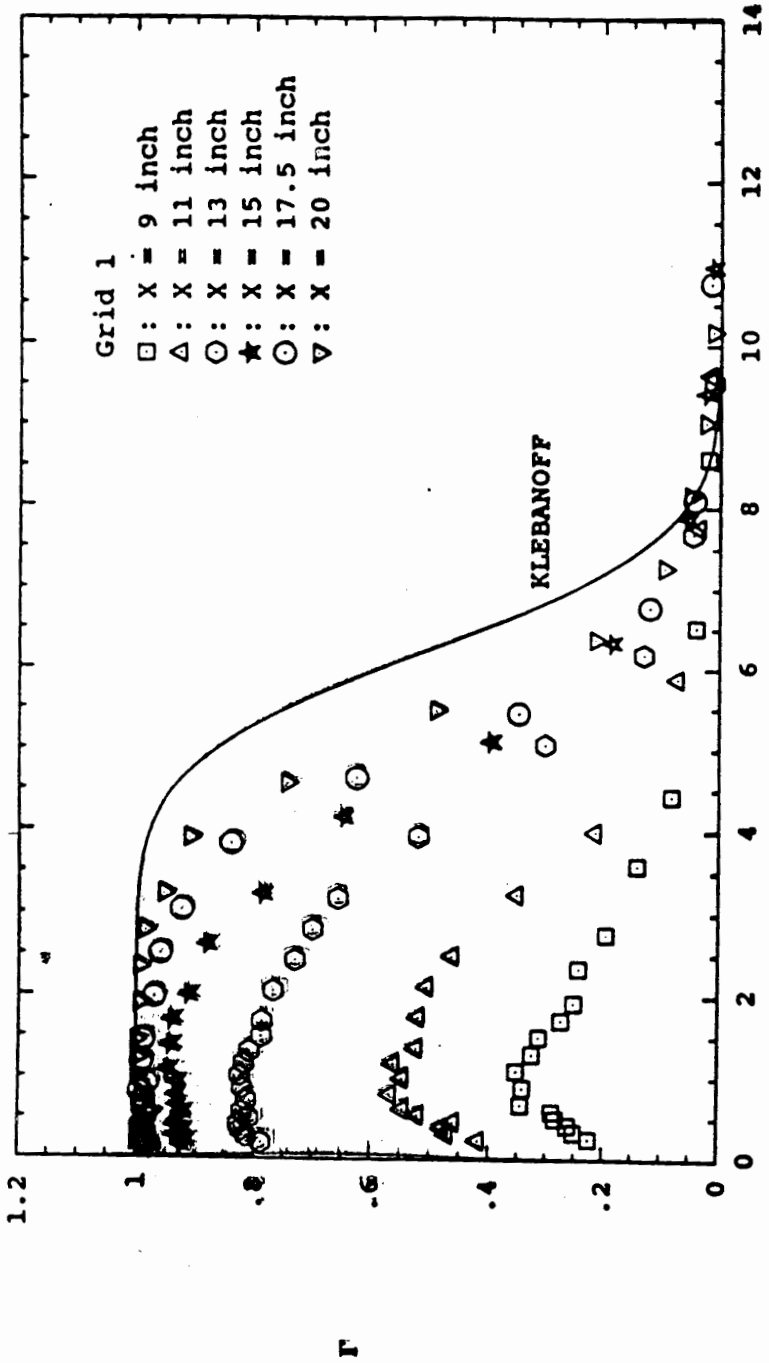

Fig. 28(a) Intermittency profiles across the boundary layer for grid 1

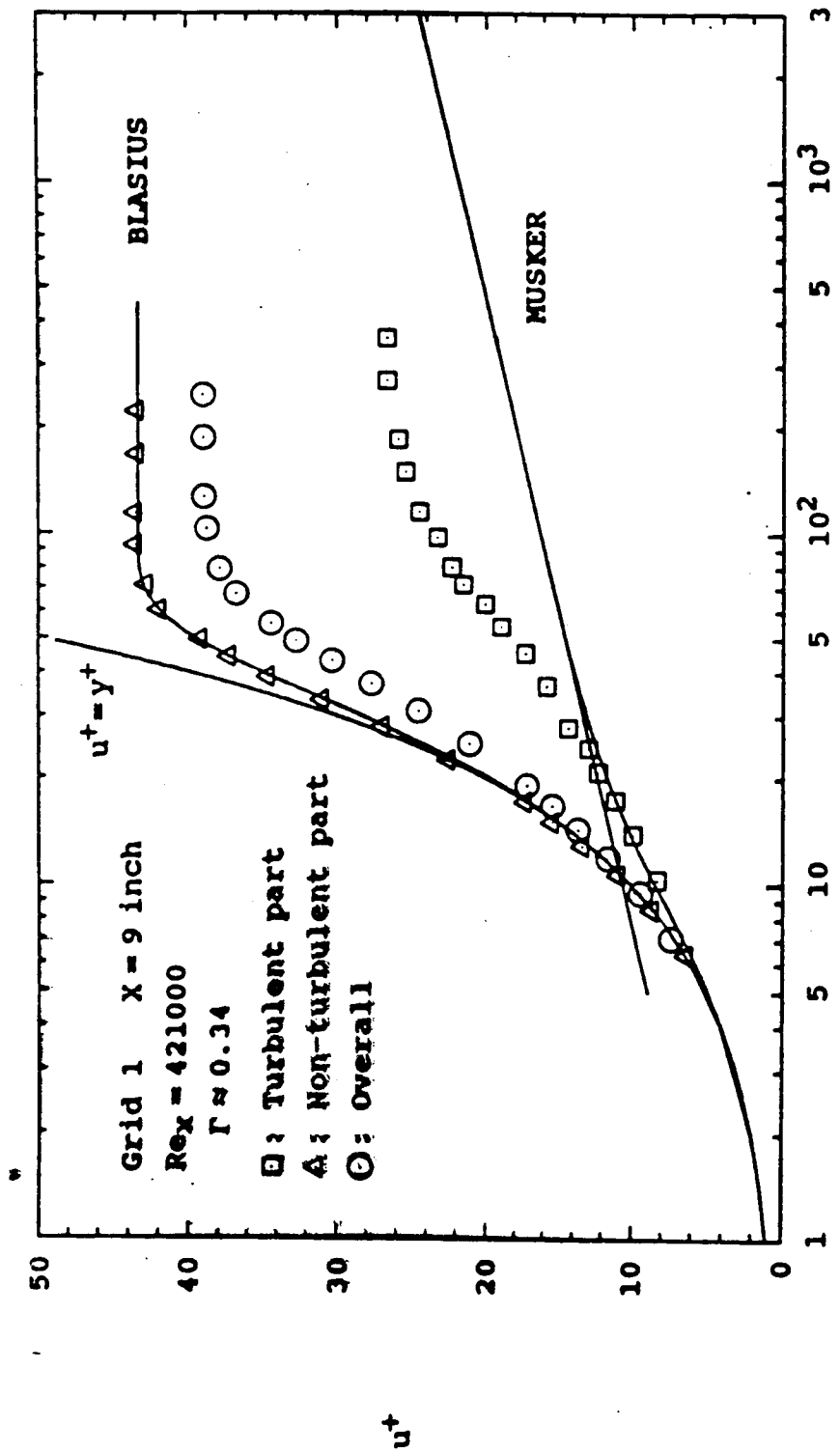

Fig. 29(a) Conditionally sampled mean velocity profiles in wall units at X=9 inches for grid 1

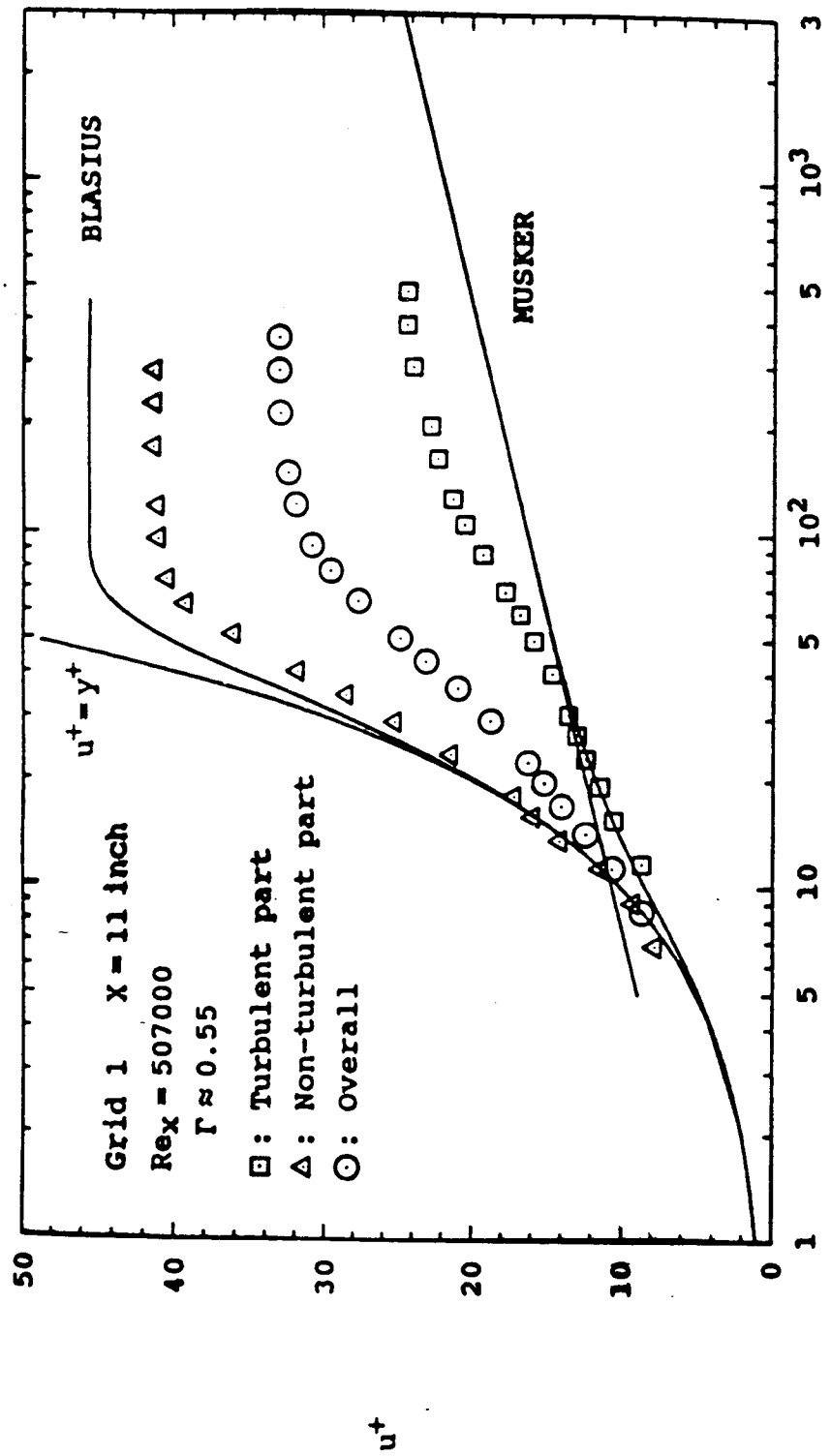

Fig. 29(b) Conditionally sampled mean velocity profiles in wall units at X=11 inches for grid 1

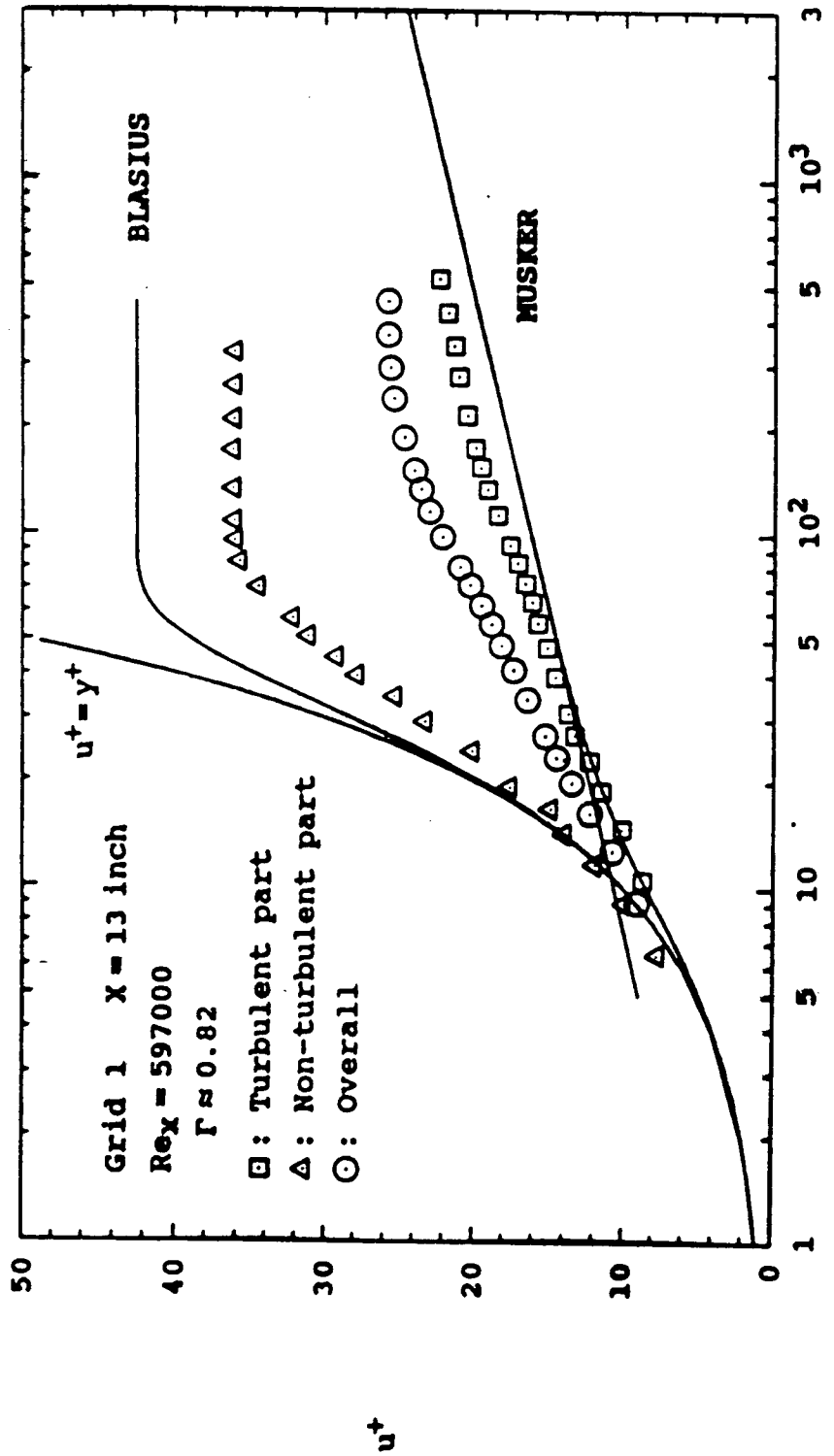

Fig. 29(c) Conditionally sampled mean velocity profiles in wall units at X=13 inches for grid 1

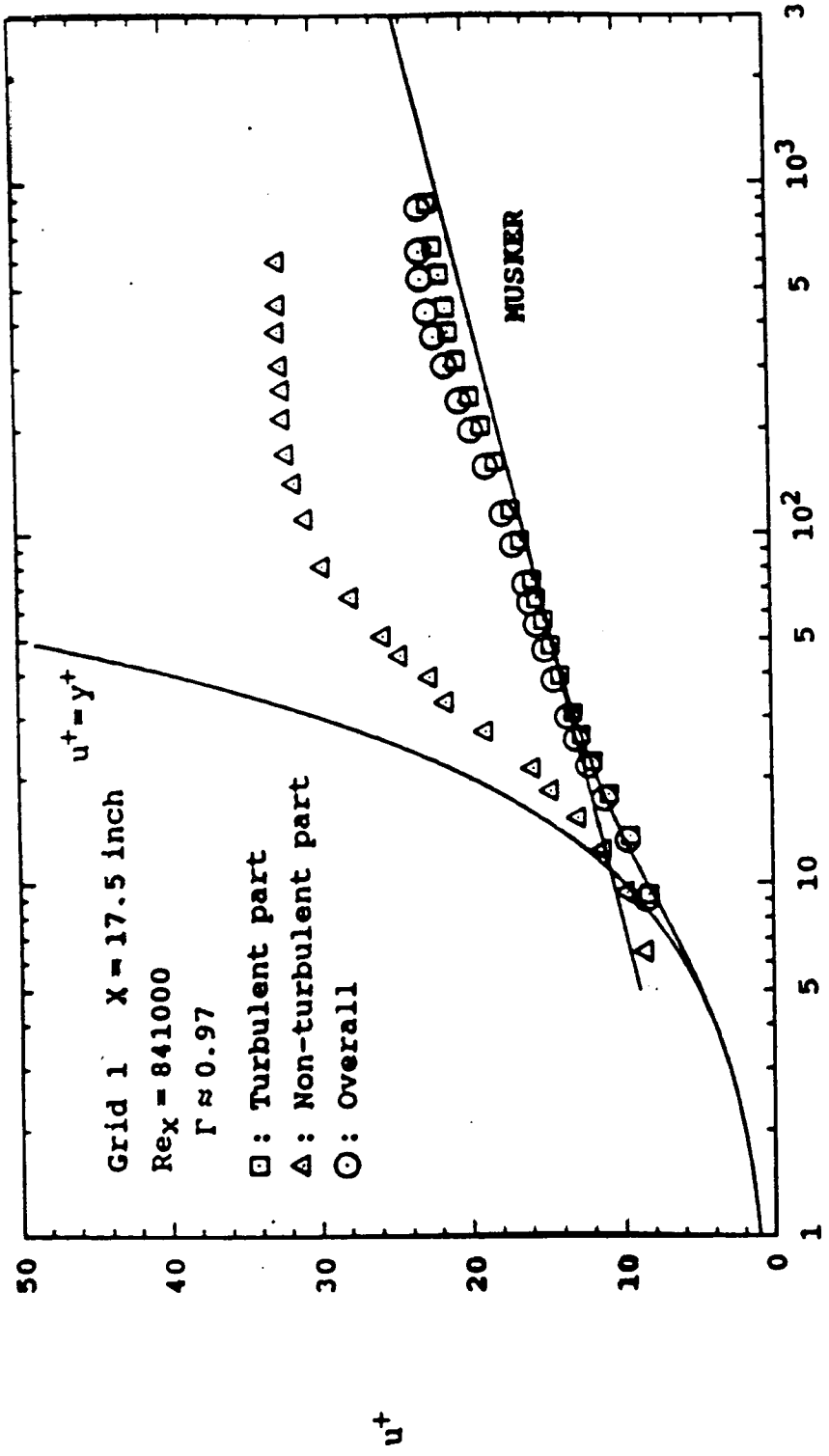

Fig. 29(e) Conditionally sampled mean velocity profiles in wall units at X=17.5 inches for grid 1

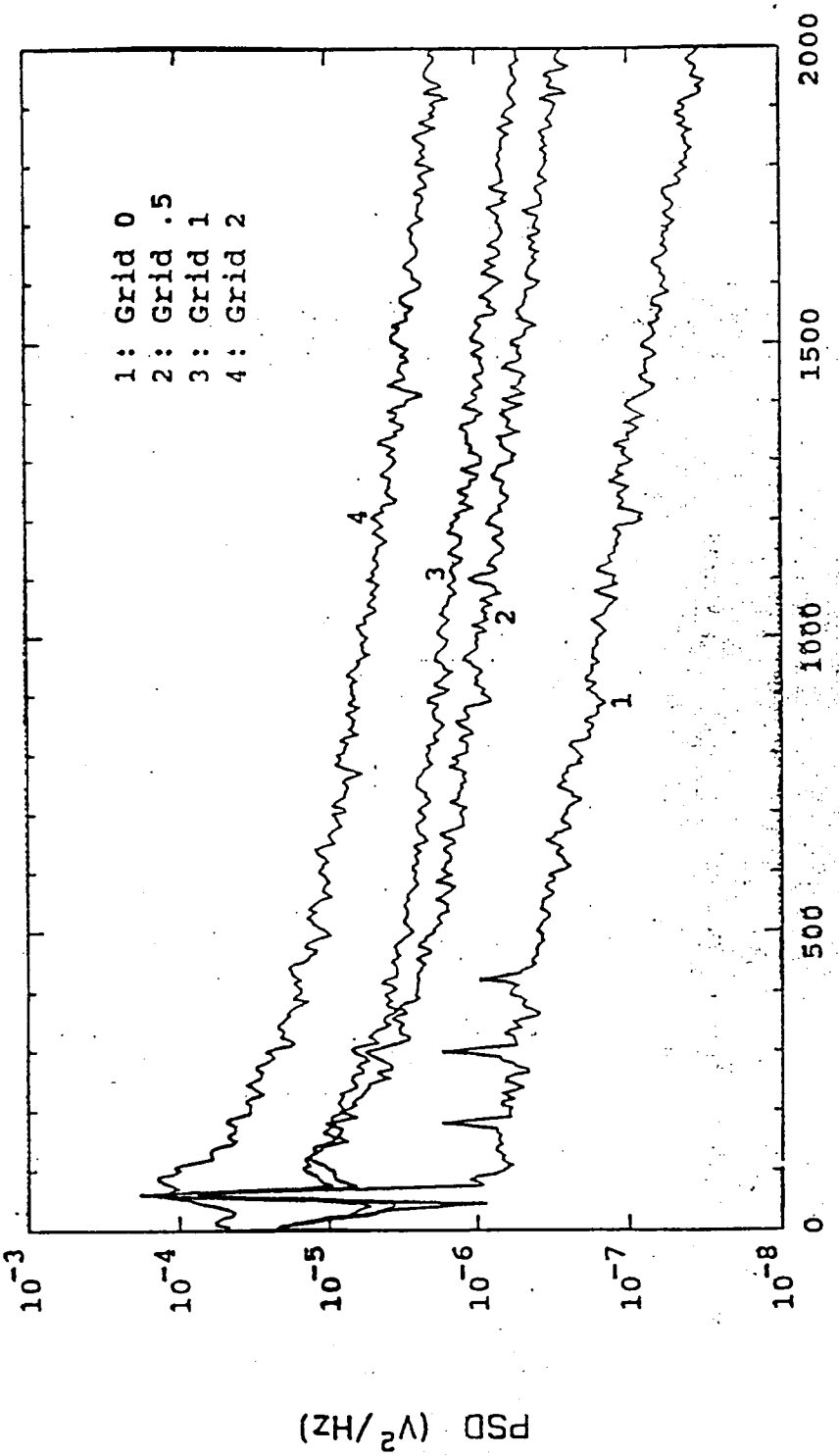

Fig. 54 Freestream spectra for 4 grids

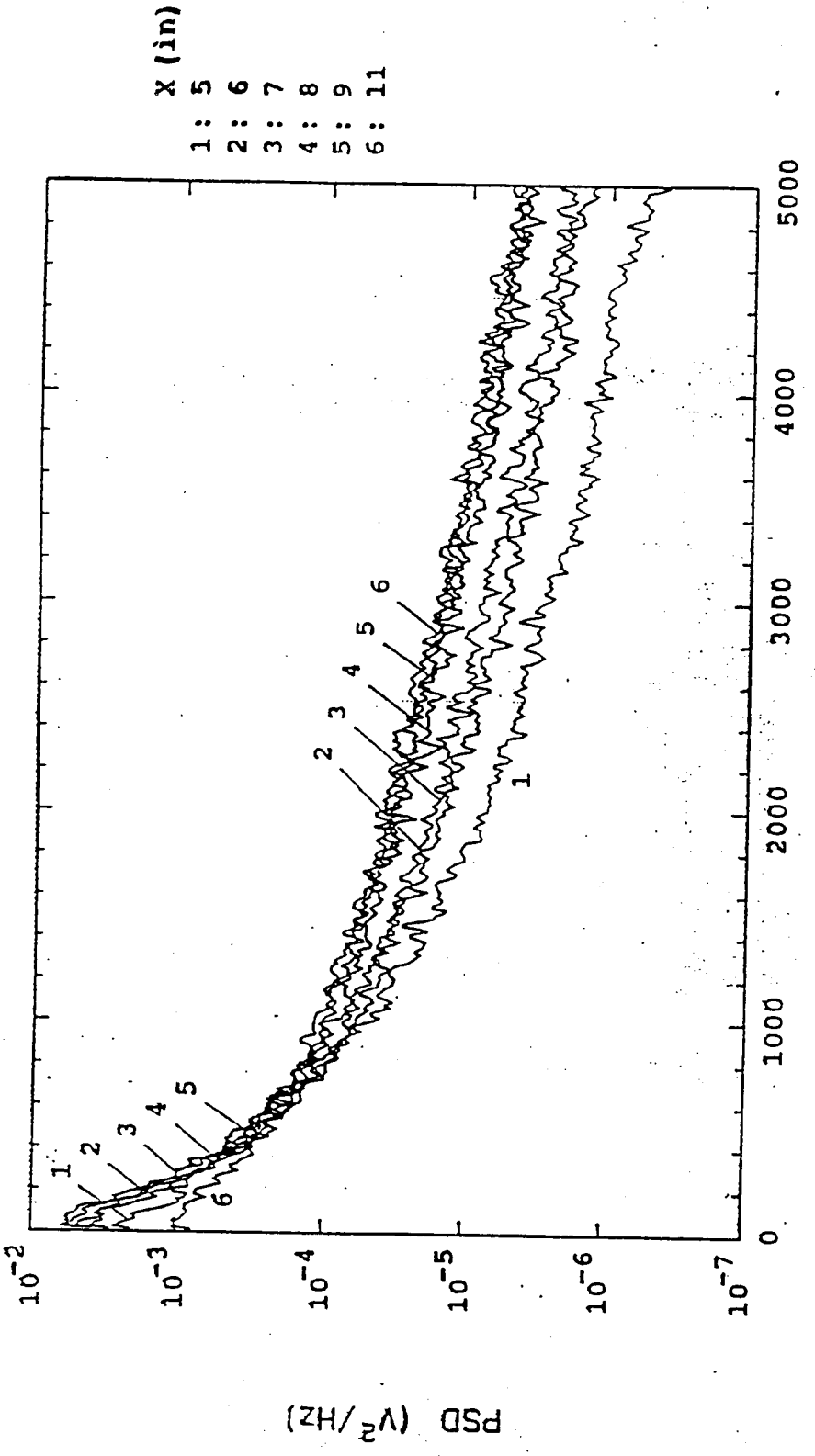

Fig. 53(d) Boundary layer spectra measured at locations where rms velocity reached maximum for grid 2

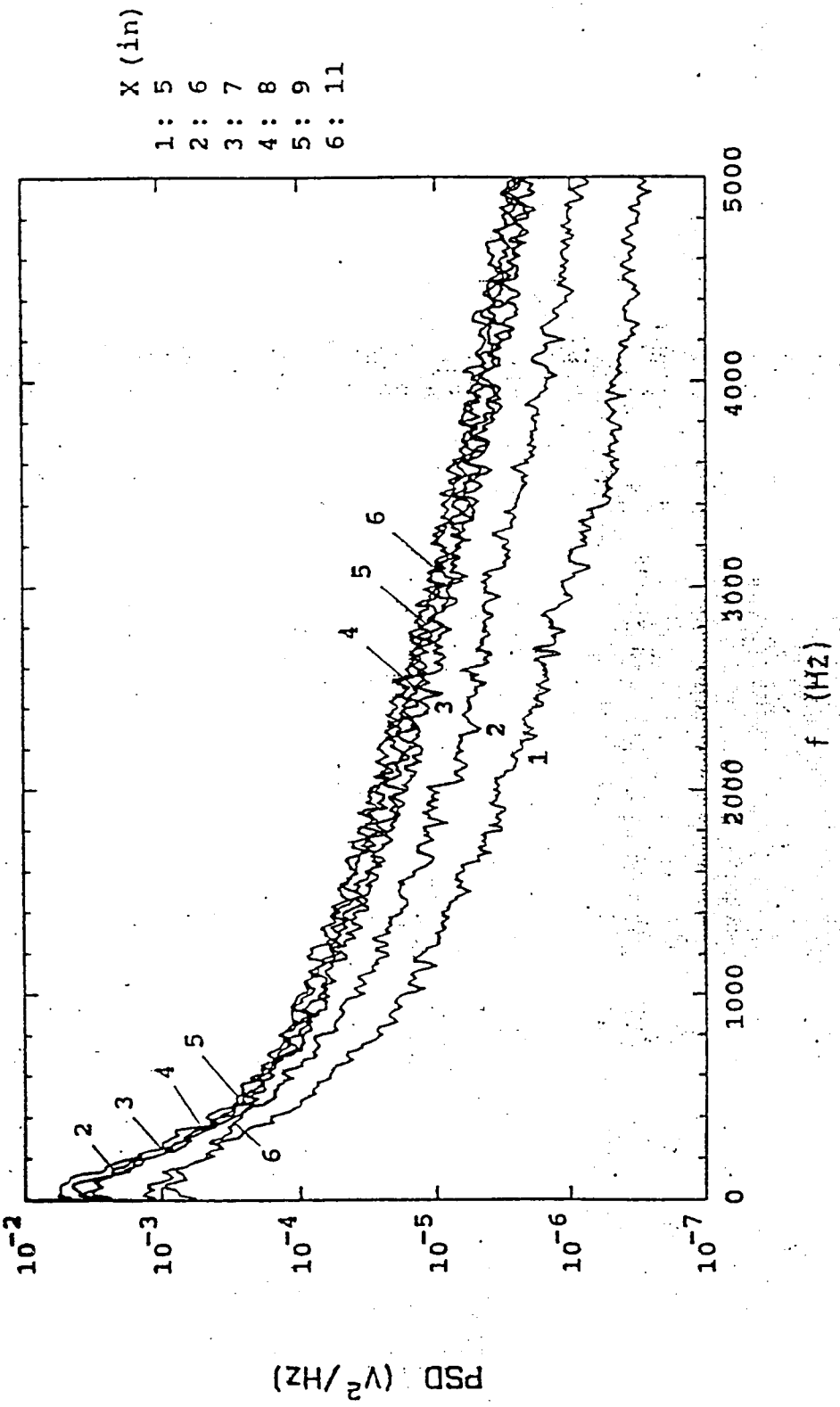

Fig. 52(d) Boundary layer spectra obtained at near-wall locations (Y_0) for grid 2

THIS SUGGESTS THAT BYPASS TRANSITION IN THE CONTEXT OF (Tu large) GAS TURBINE TECHNOLOGY, A MIGHT BE MODELED USING TURBULENT FLOW METHODS

THESE MUST ALL BE VALID IN THE LAMINAR LIMIT

- one-equation models (k)
- two-equation models (k-ϵ)
- Reynolds stress models
- DNS/LES

BUT - HOW DO YOU START THE CALCULATION?

ISSUE: RECEPTIVITY

K-ε APPROACHES

- Equations should have proper low-Reynolds-number form.
- Turbulence models should have correct near wall behavior for k, $-\overline{u'v'}$, ϵ
- Calculation algorithm should be compatible with equations and turbulence model

STARTING PROFILES FOR k, ϵ ?

FEATURES OF BYPASS TRANSITION TO BE MODELED

- Turbulent-like spectra throughout
- Intermittency $\gamma = \gamma(x,y)$
- With conditional sampling
  - Turbulent part approaches fully-turbulent characteristic as transition progresses
  - Non-turbulent part departs from laminar after transition onset

Intermittency: $\frac{\text{Non-turbulent part}}{\text{Low frequency}}$ $\frac{\text{Turbulent part}}{\text{High frequency}}$

MTS:

MODEL EACH PART SEPARATELY

DEVELOP INTERMITTENCY pde (following Kollmann)

COMBINE (We gave up on this.)

Multi-Time-Scale Low Reynolds Number k-ε Turbulence Model

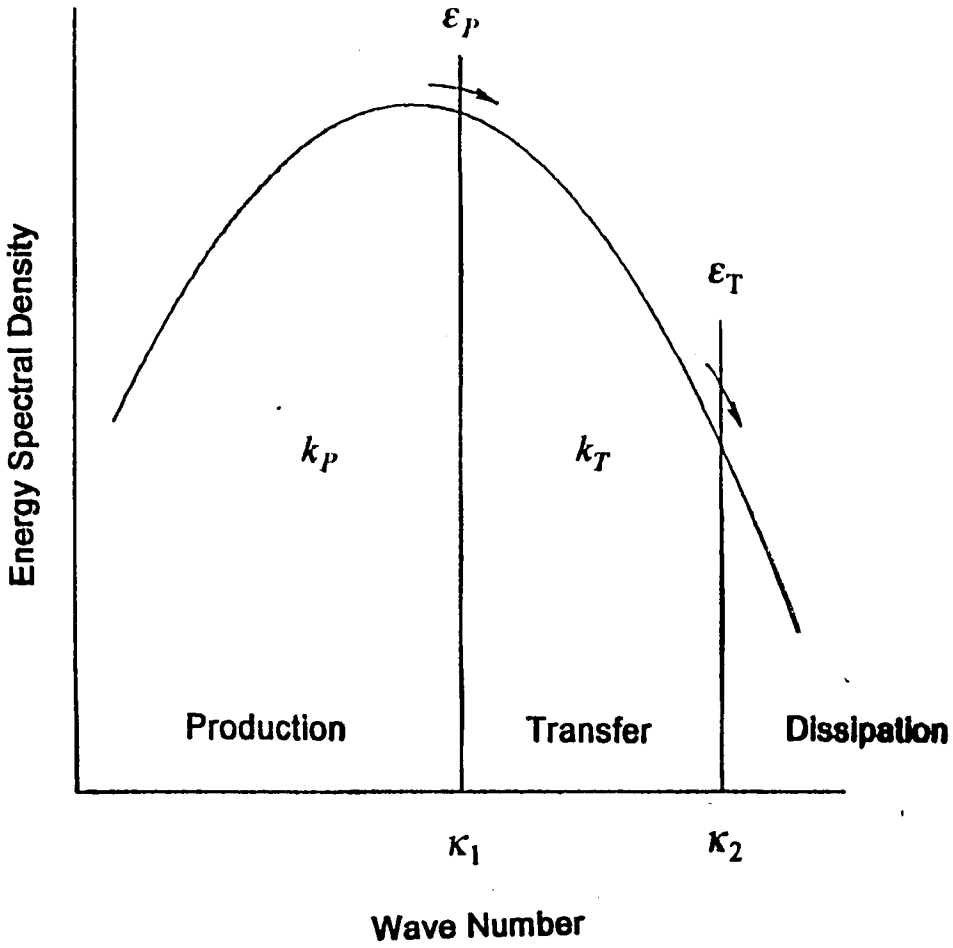

Hanjalić, Launder & Schiestel, 1980

Multi-Time-Scale Low Reynolds Number k-ε Turbulence Model

S-Y WU

$$U\frac{\partial k_P}{\partial x}+V\frac{\partial k_P}{\partial y}=\frac{\partial}{\partial y}\left[\left(\nu+\frac{\nu_t}{\sigma_k}\right)\frac{\partial k_P}{\partial y}\right]+P_k-\varepsilon_P$$

$$U\frac{\partial k_T}{\partial x}+V\frac{\partial k_T}{\partial y}=\frac{\partial}{\partial y}\left[\left(\nu+\frac{\nu_t}{\sigma_k}\right)\frac{\partial k_T}{\partial y}\right]+\varepsilon_P-\varepsilon_T$$

$$U\frac{\partial \varepsilon_P}{\partial x}+V\frac{\partial \varepsilon_P}{\partial y}=\frac{\partial}{\partial y}\left[\left(\nu+\frac{\nu_t}{\sigma_\varepsilon}\right)\frac{\partial \varepsilon_P}{\partial y}\right]+C_{P1}\left[\left(1+C'_{P1}\frac{P_k}{\varepsilon_P}\right)\right]P_k\frac{\varepsilon_P}{k_P}-C_{P2}f_{P2}\frac{\varepsilon_P^2}{k_P}$$

$$U\frac{\partial \varepsilon_T}{\partial x}+V\frac{\partial \varepsilon_T}{\partial y}=\frac{\partial}{\partial y}\left[\left(\nu+\frac{\nu_t}{\sigma_\varepsilon}\right)\frac{\partial \varepsilon_T}{\partial y}\right]+C_{T1}\left[\left(1+C'_{T1}\frac{\varepsilon_P}{\varepsilon_T}\right)\right]\varepsilon_P\frac{\varepsilon_T}{k_T}-C_{T2}f_{T2}\frac{\varepsilon_T^2}{k_T}$$

where $\quad P_k=\nu_t\left(\frac{\partial U}{\partial y}\right)^2 \qquad \nu_t=c_\mu f_\mu\frac{k^2}{\varepsilon_P} \qquad k=k_P+k_T$

at wall $\quad k_P=k_T=0 \qquad \varepsilon_P=2\nu\left(\frac{\partial\sqrt{k_P}}{\partial y}\right)^2 \qquad \varepsilon_T=2\nu\left(\frac{\partial\sqrt{k}}{\partial y}\right)^2$

Multi-Time-Scale Low Reynolds Number k-ε Turbulence Model

- **Patankar-Spalding method:**

  Grid point N=102

  Step size $\Delta x=0.1\delta_2$

  Non-uniform grid $\Delta\omega_n=1.02\Delta\omega_{n-1}$

- **Inlet condition:**

  Re_x=100

  U=Blasius solution

  k=Reshotko's profile $k=\frac{1}{2}U^2Tu^2\left(f'+\frac{\eta}{2}f''\right)^2$

  ε=Rodi's profile $\varepsilon_P=a_1k_P\frac{\partial U}{\partial y}$ $\varepsilon_T=a_1k_T\frac{\partial U}{\partial y}$

INFLUENCE OF THE STARTING LOCATION
Initial profiles: K and ε are Rodi's profiles
Freestream: $K_p=0.7K_e$

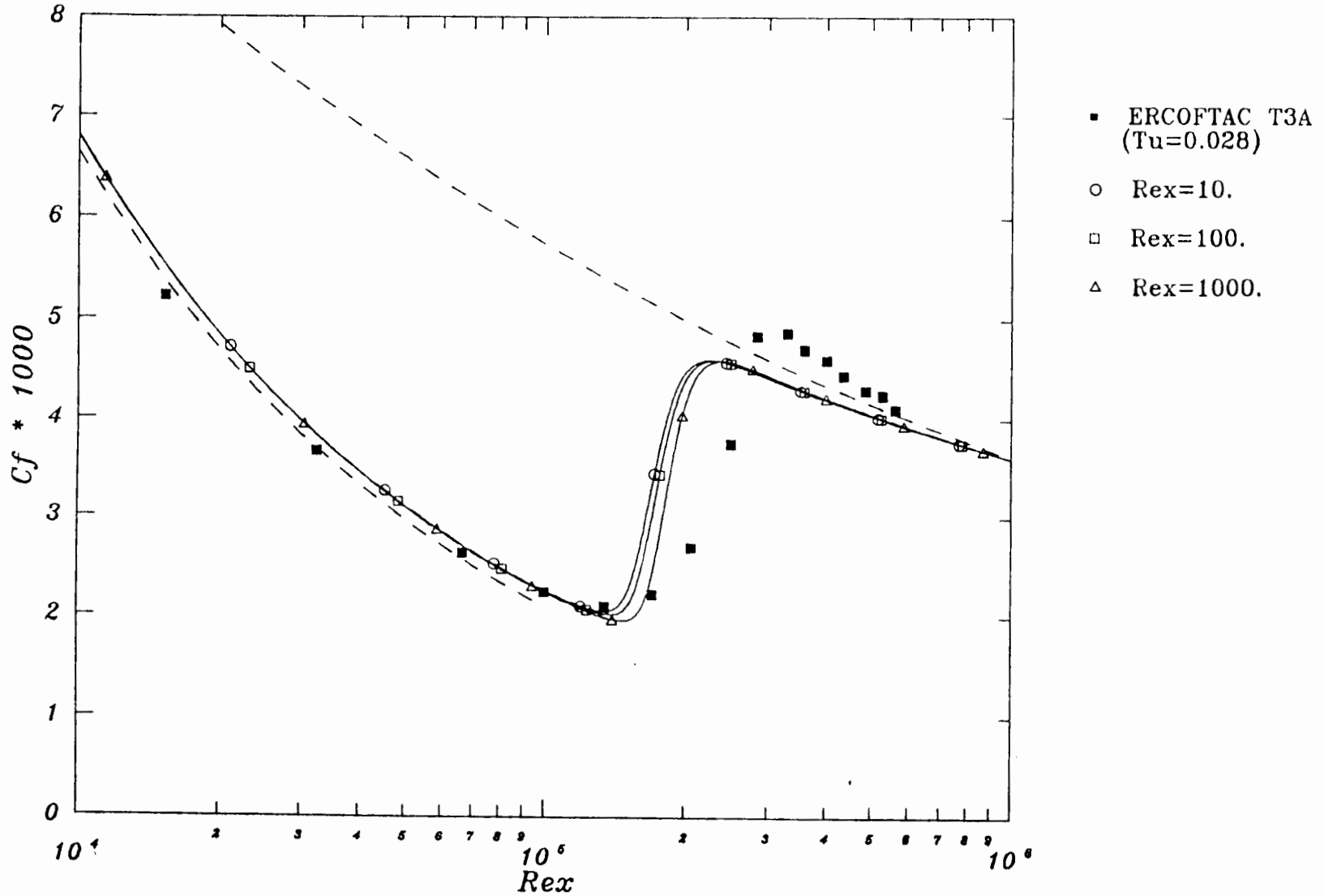

INFLUENCE OF THE PARTITION OF Kp AND Kt
Initial condition: K=Reshotko's profile, ε=Rodi's profile

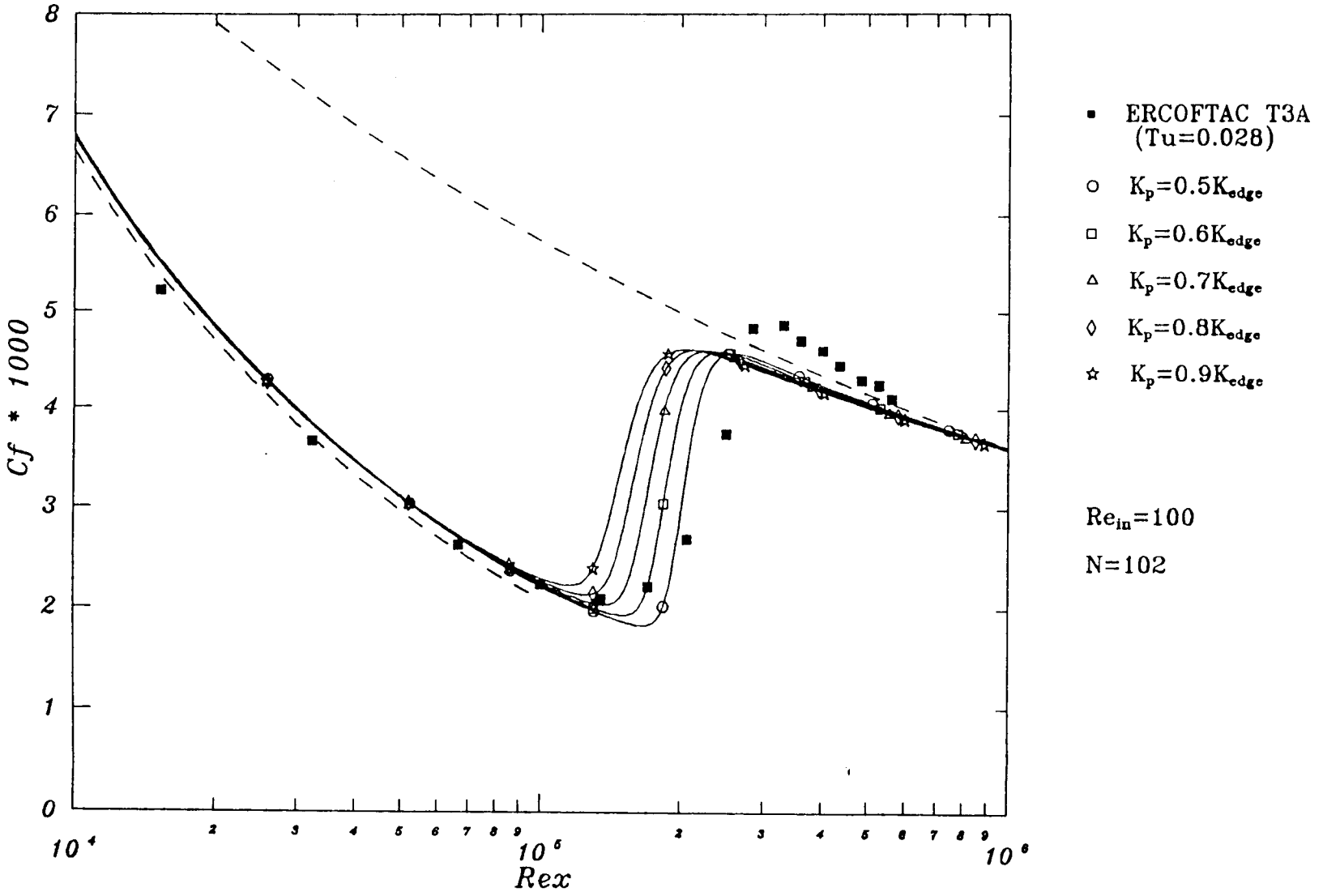

PRODUCTION ZONE TURBULENT KINETIC ENERGY, K_P^+,
Multi-time-scale k–ε Model
ERCOFTAC Test Case T3A

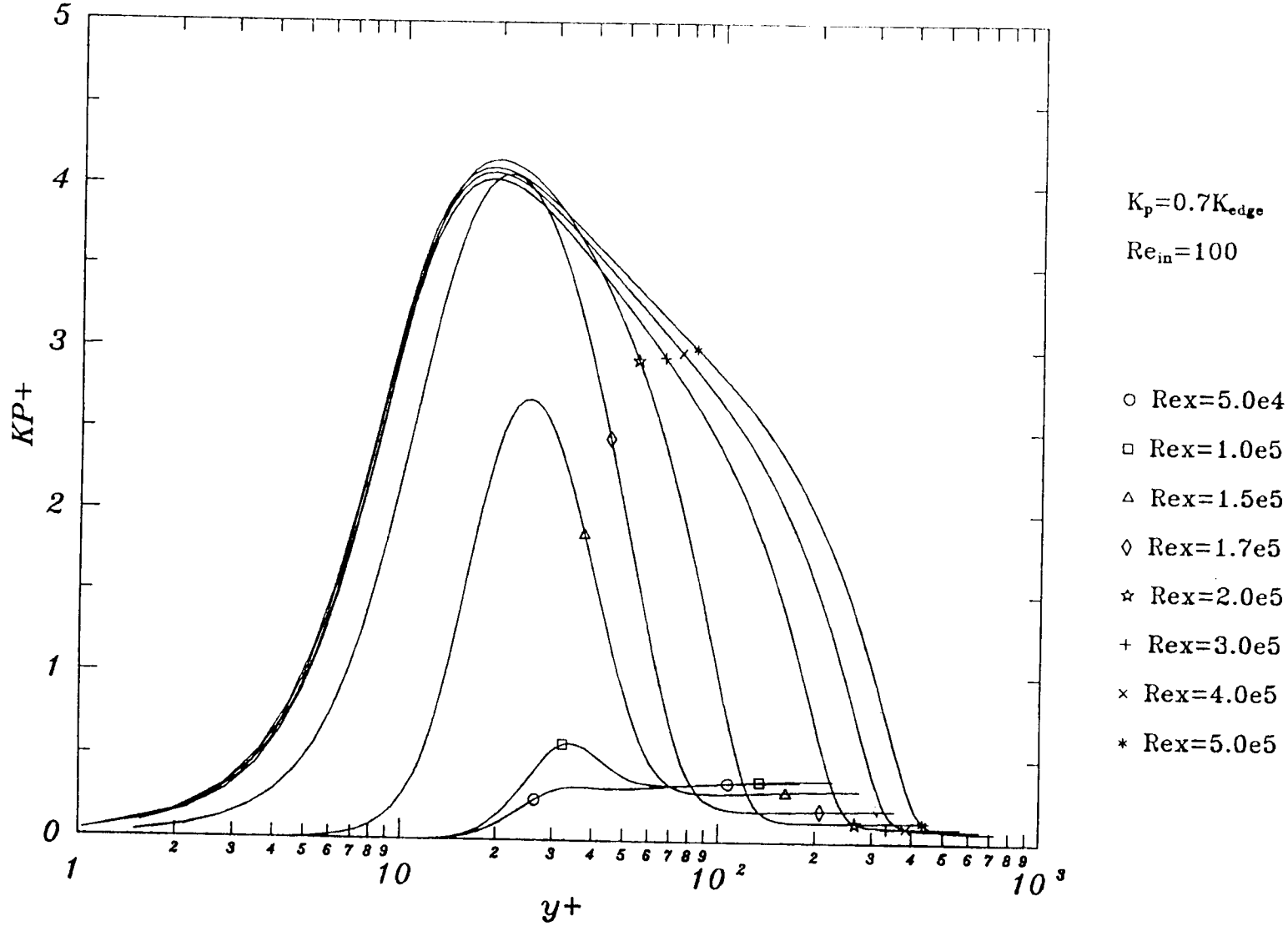

TRANSFER ZONE TURBULENT KINETIC ENERGY, K_T^+,
Multi-time-scale k-ε Model
ERCOFTAC Test Case T3A

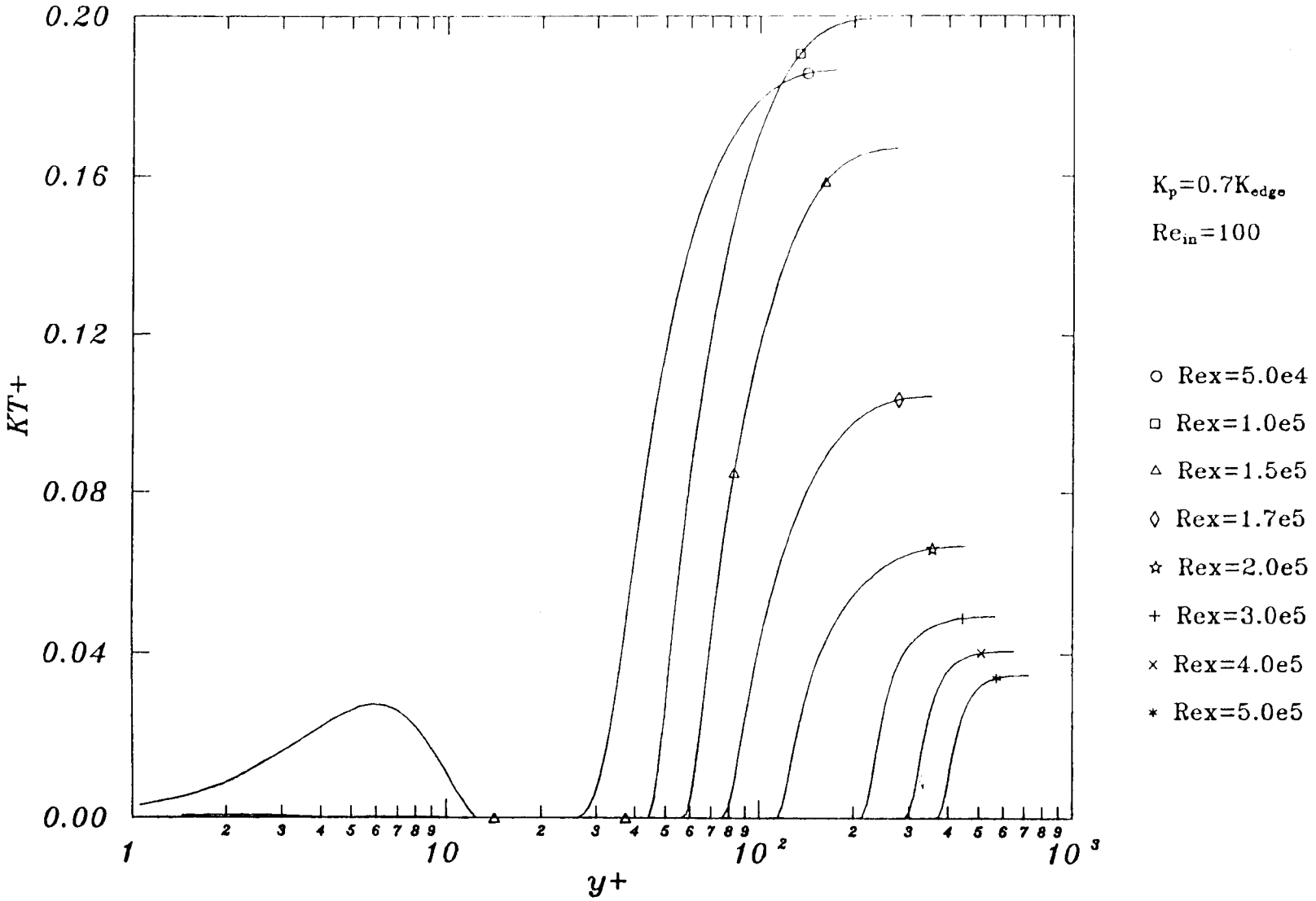

ENERGY TRANSFER FUNCTION, E_P^+,
Multi-time-scale k-ε Model
ERCOFTAC Test Case T3A

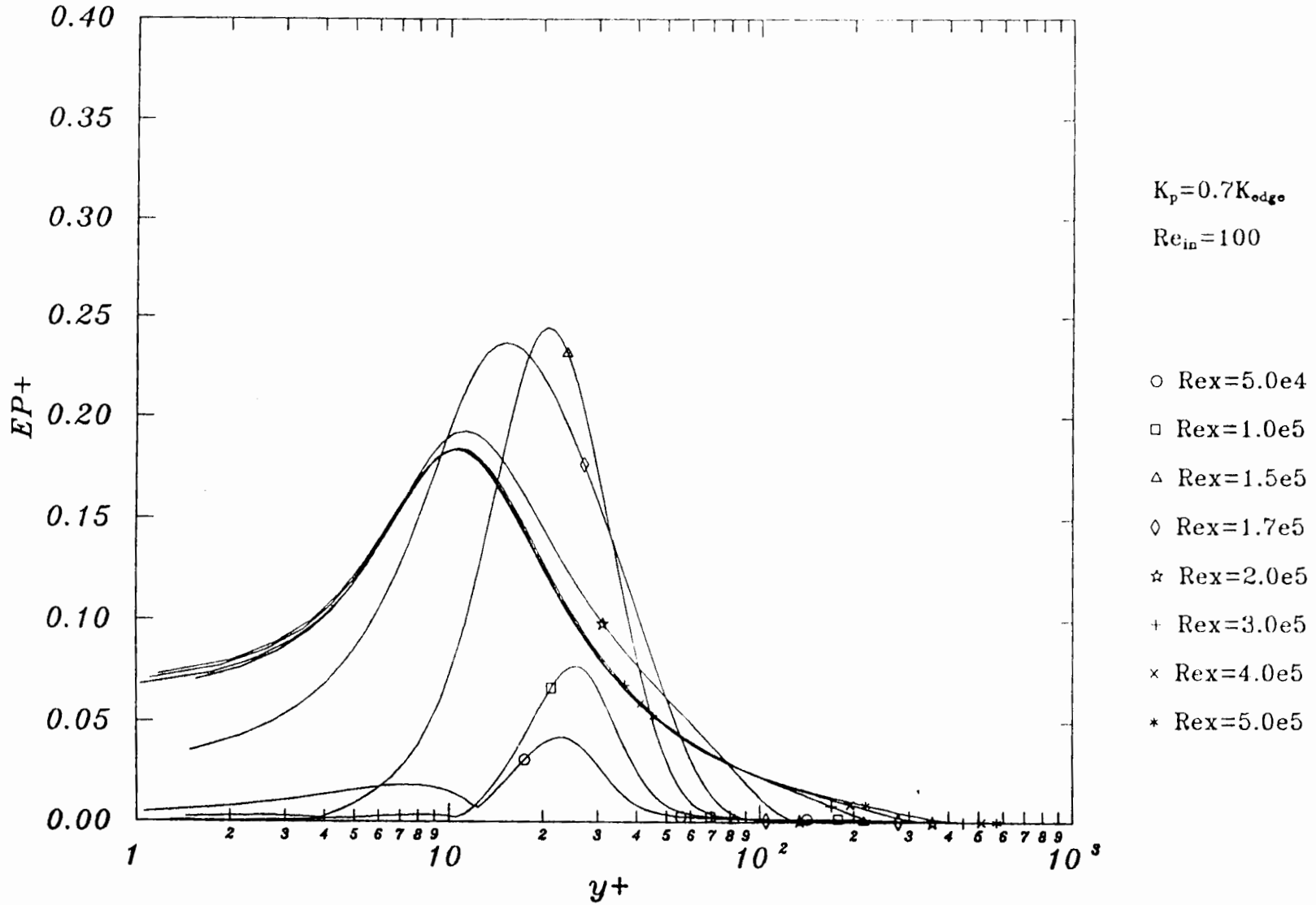

DISSIPATION, E_T^+,
Multi-time-scale k-ε Model
ERCOFTAC Test Case T3A

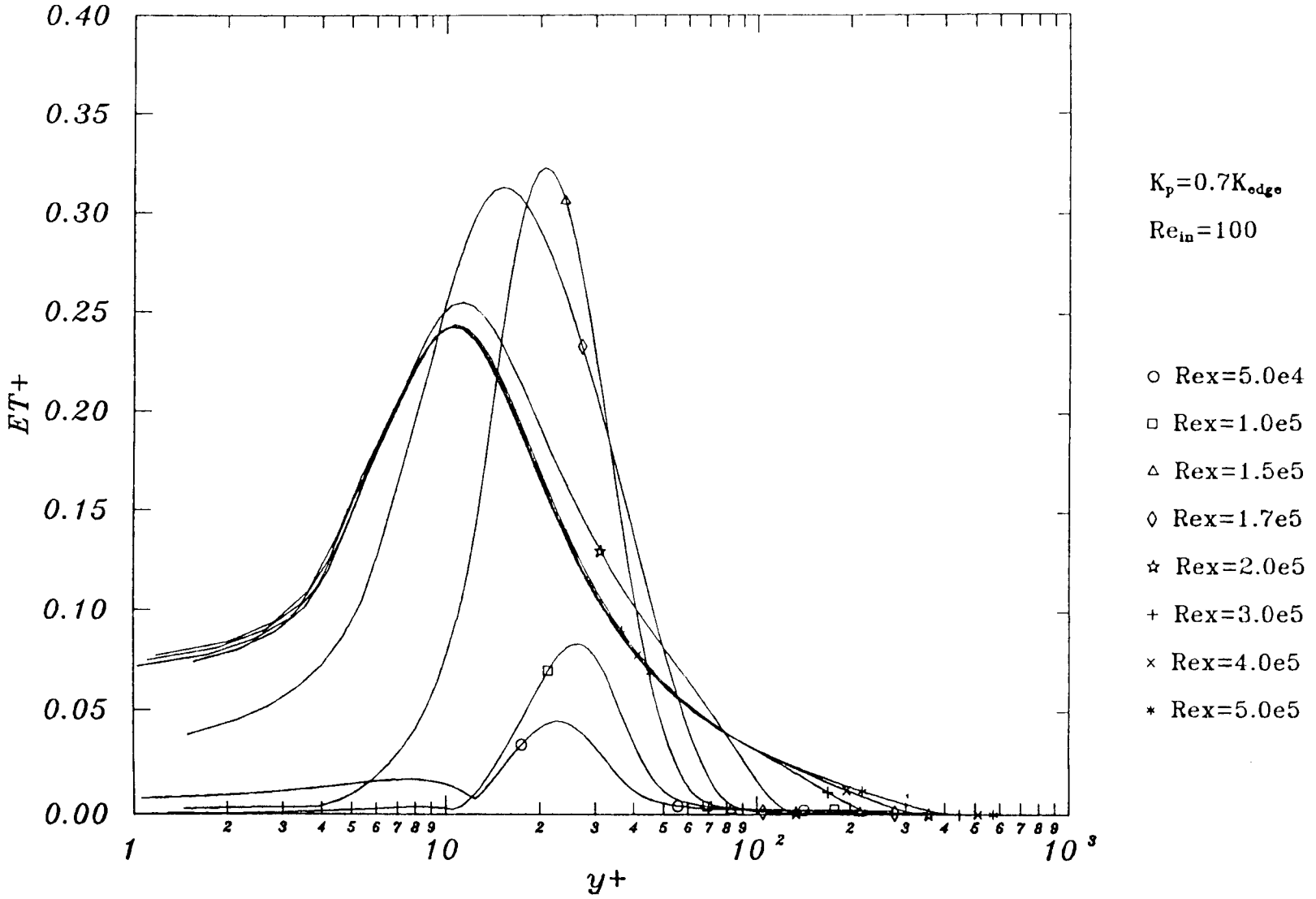

TURBULENT KINETIC ENERGY, K^+,
Multi-time-scale k-ε Model
High Free-Stream Turbulence, 12 percents

$\mathcal{E}_{e_{in}} = 798.$

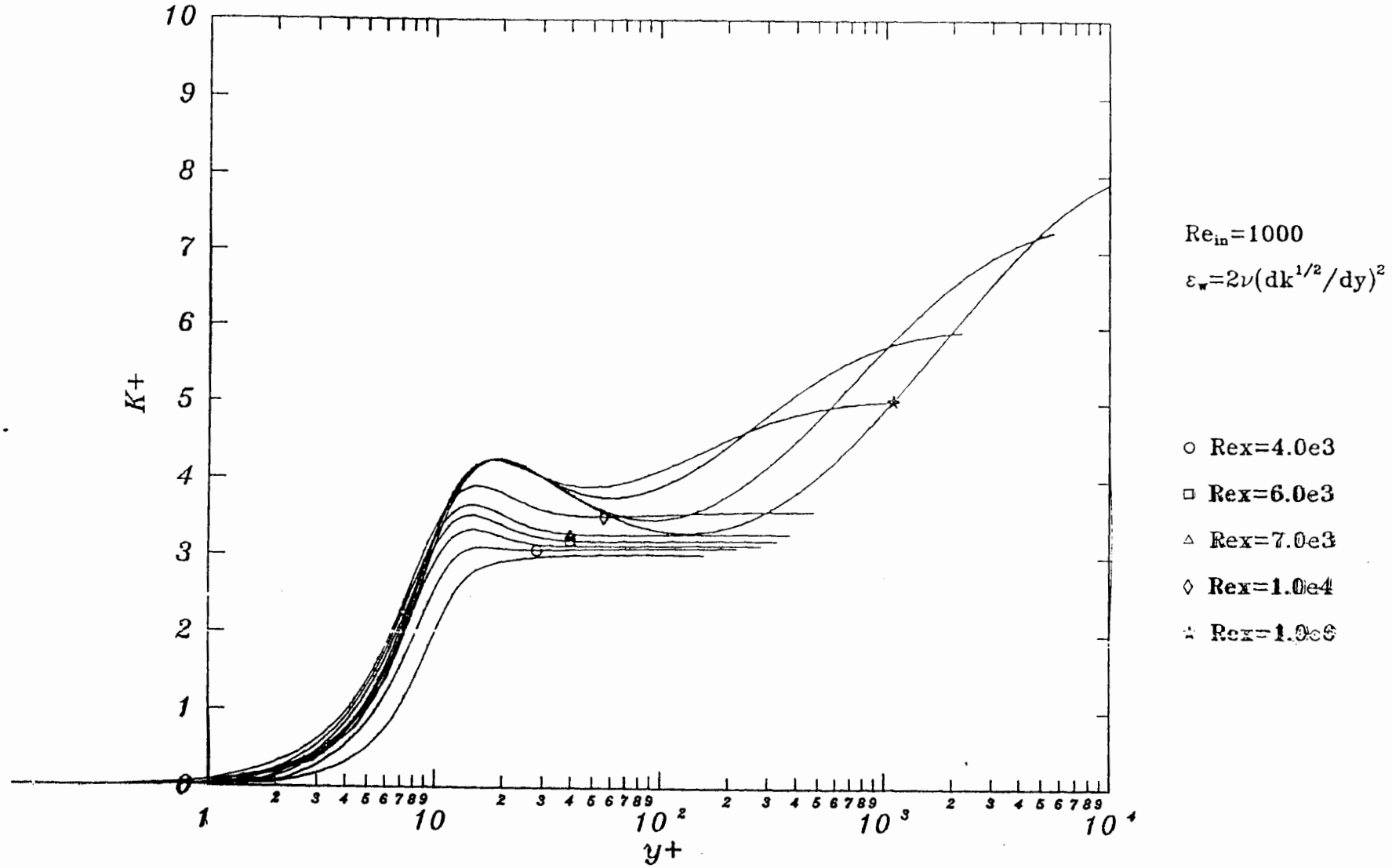

TURBULENT KINETIC ENERGY, K^+, Multi-time-scale k-ε Model High Free-Stream Turbulence, 15 percents

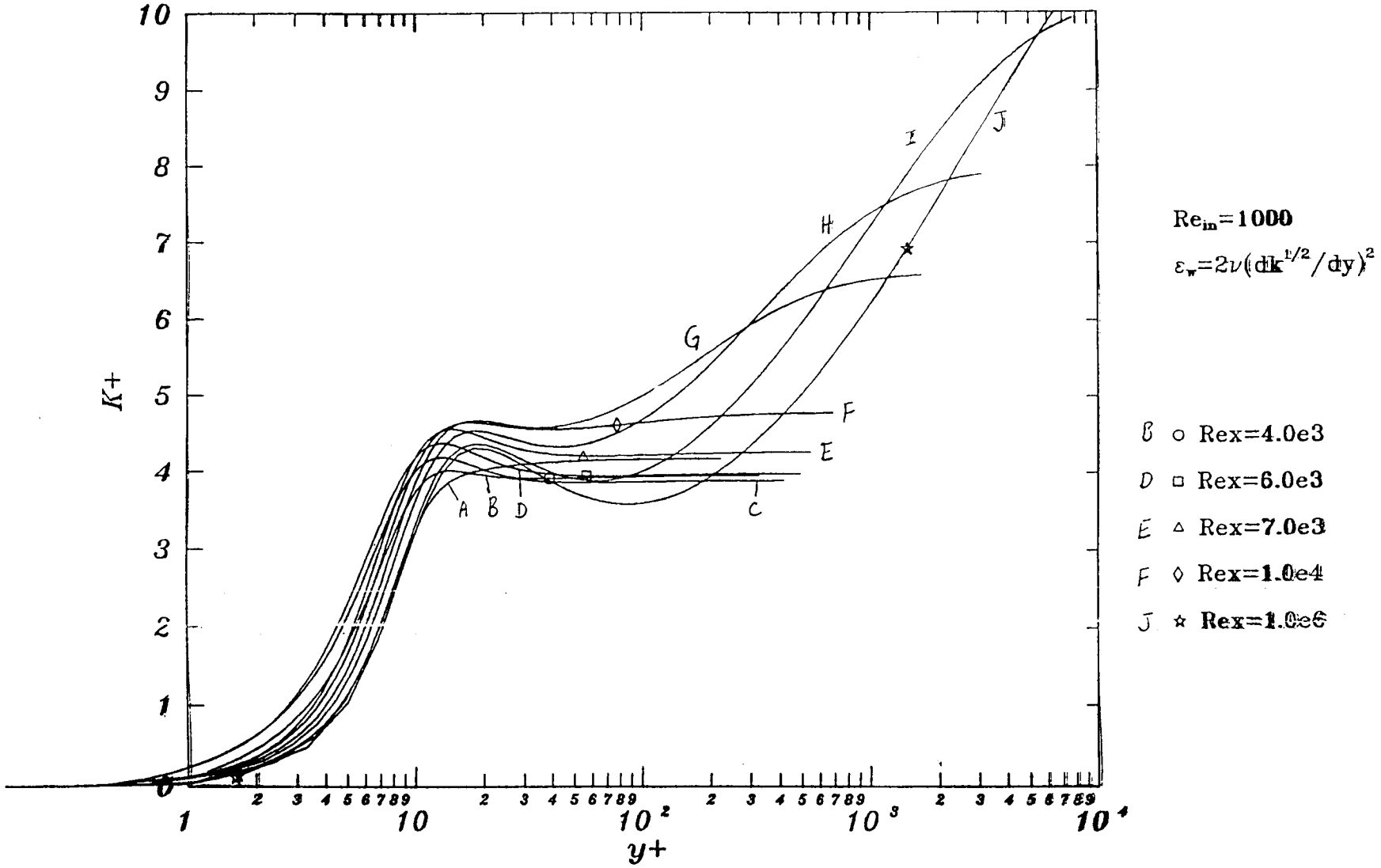

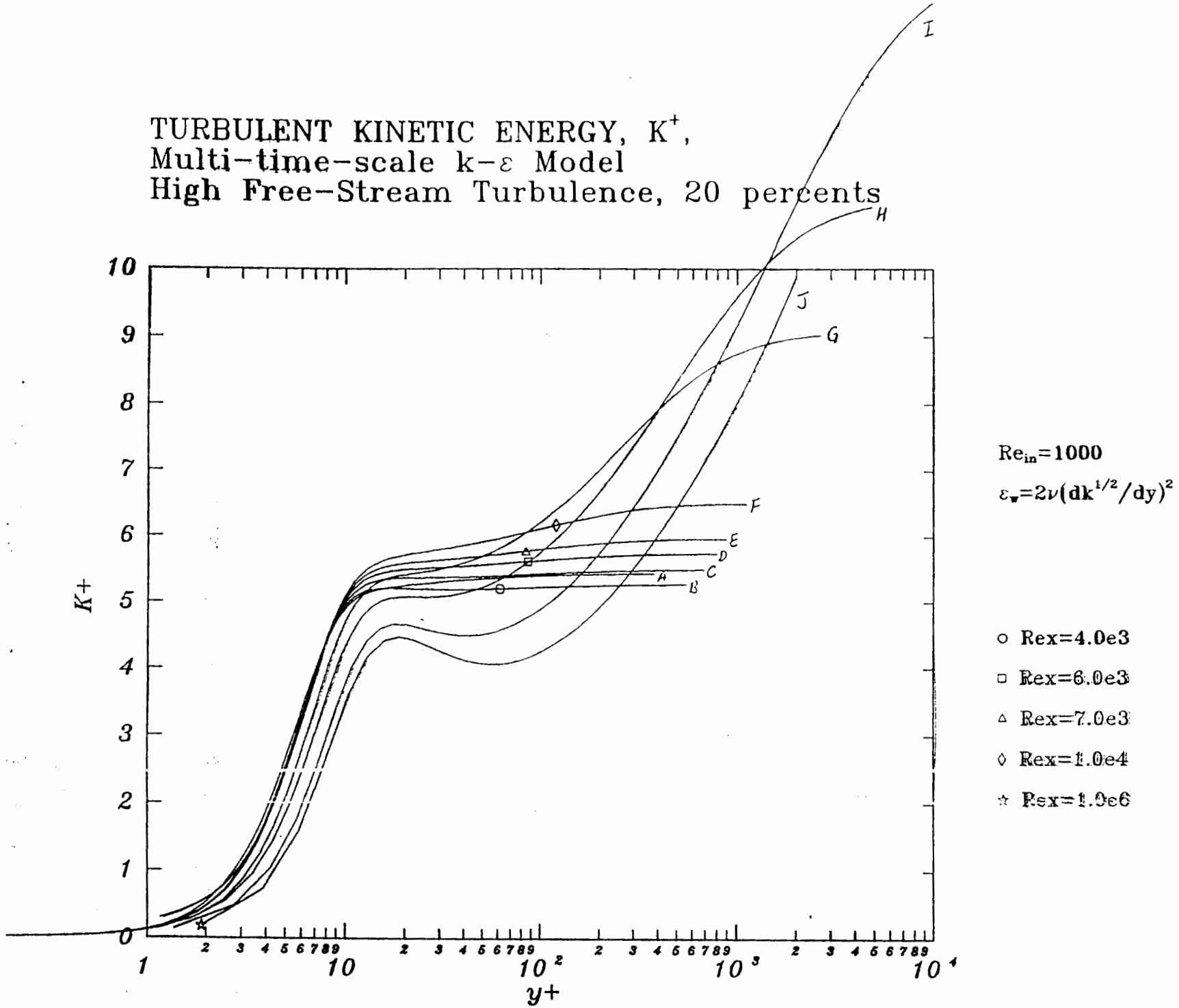
TURBULENT KINETIC ENERGY, K+,
Multi-time-scale k-ε Model
High Free-Stream Turbulence, 20 percents
K+
y+
I
H
J
G
F
E
D
C
B
A
Re_in=1000
ε_w=2ν(dk^1/2/dy)^2
Rex=4.0e3
Rex=6.0e3
Rex=7.0e3
Rex=1.0e4
Rex=1.0e6

DIRECTIONS

- CONTINUE EXPERIMENTAL STUDIES TO PROVIDE PHENOMENOLOGICAL DATA FOR MODELING VALIDATION
- REFINE MODELS (MTS, etc) TO BE USED FOR TURBINE BLADE DESIGN CALCULATIONS
- LOOK HARD AT "RECEPTIVITY" ISSUE TOWARD IDENTIFYING PHYSICS OF BYPASS INTIATION

EXPERIMENTS	–	BREUER, KENDALL
ANALYSIS COMPUTATION	–	LANDAHL, HENNINGSON SCHMID HERBERT (PSE)

Abstract submitted for the
Workshop on End Stage Transition
Blue Mountain Lake, New York, August 15 – 18, 1993

Simulations of Boundary-Layer Transition

Thorwald Herbert

Department of Mechanical Engineering
The Ohio State University, Columbus, OH 43210-1107 and
DynaFlow, Inc., Columbus, OH 43221-0319, USA

For incompressible benchmark flows, we have demonstrated the capability of the parabolized stability equations (PSE) to simulate the transition process in excellent agreement with microscopic experiments and direct Navier-Stokes simulations at modest computational cost. Encouraged by these results, we have developed the PSE methodology[1] for three-dimensional boundary-layers in general curvilinear coordinates for the range from low to hypersonic speeds, and for both linear and nonlinear problems. For given initial and boundary conditions, the approach permits simulations from receptivity through linear and secondary instabilities into the late stages of transition where significant changes in skin friction and heat transfer coefficients occur.

We have performed transition simulations for a variety of two- and three-dimensional similarity solutions and for realistic flows over swept wings at subsonic and supersonic speeds, the pressure and suction side of turbine blades at low and medium turbulence levels, and over a blunt cone at Mach number $Ma = 8$. We present selected results for different transition mechanisms with emphasis on the late stage of transition and the evolution of wall-shear stress and heat transfer.

NASA/CP—2007-214667

Simulations of Boundary-Layer Transition

Thorwald Herbert

The Ohio State University
&
DynaFlow, Inc.
Columbus, Ohio

Supported by AFOSR, ONR,
Wright Laboratories, and NASA

Outline

Parabolized Stability Equations

→ • PSE Development

• Stability Studies

? → • Receptivity, Forced Problems

• Transition Mechanisms

→ • Engineering Applications

Swept Wings

→ Gas Turbine Blades

High-Speed Flows

• Conclusions, Open Issues

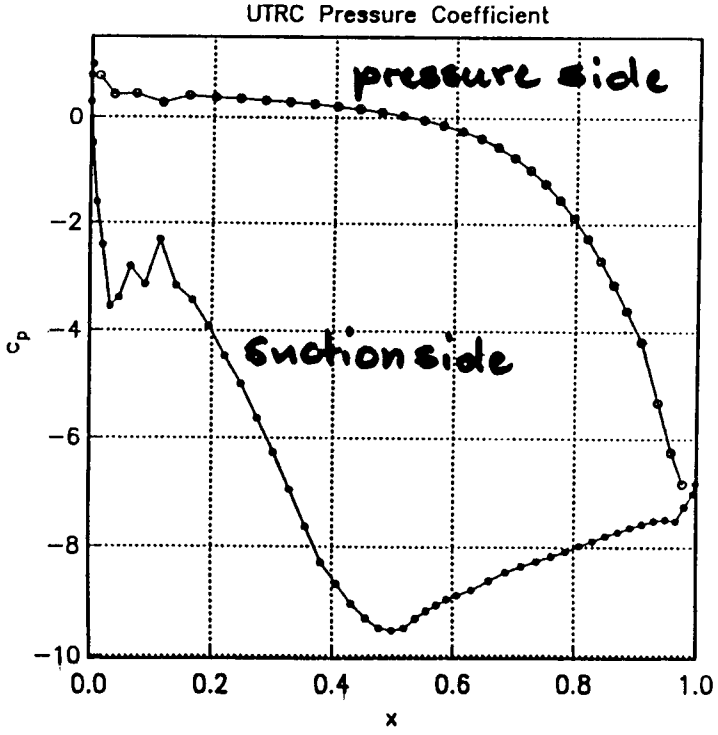
UTRC Pressure Coefficient
pressure side
suction side
c_p
x
0
−2
−4
−6
−8
−10
0.0
0.2
0.4
0.6
0.8
1.0

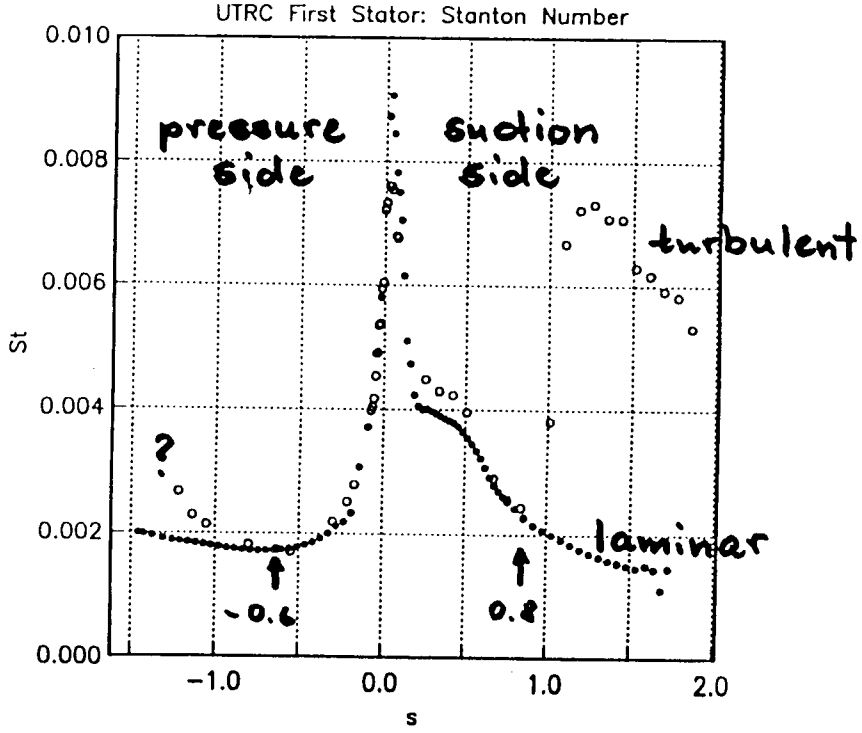
UTRC First Stator: Stanton Number
pressure side
suction side
turbulent
laminar
?
-0.6
0.8
St
s
0.010
0.008
0.006
0.004
0.002
0.000
−1.0
0.0
1.0
2.0

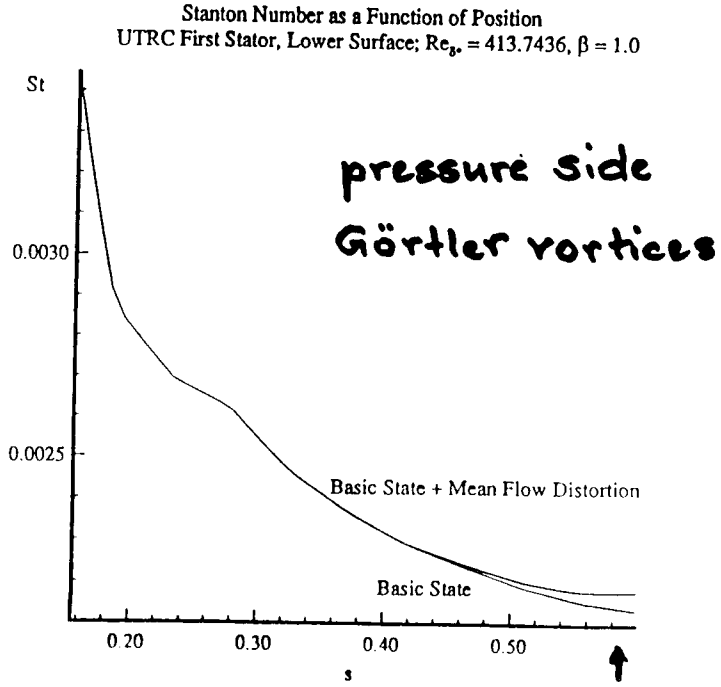
Stanton Number as a Function of Position
UTRC First Stator, Lower Surface; $Re_{\delta^*} = 413.7436$, $\beta = 1.0$
St
0.0030
0.0025
pressure side
Görtler vortices
Basic State + Mean Flow Distortion
Basic State
0.20
0.30
0.40
0.50
s

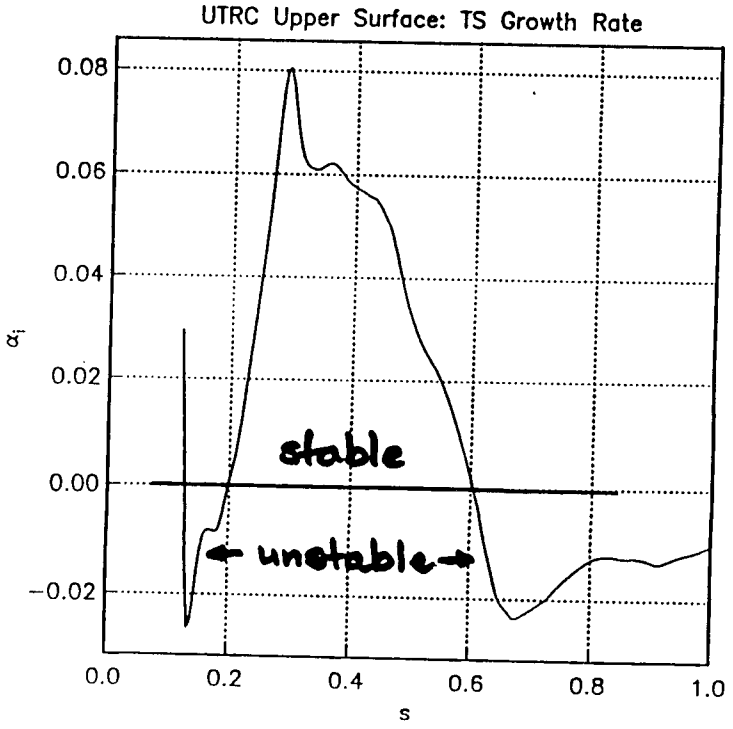
UTRC Upper Surface: TS Growth Rate
0.08
0.06
0.04
0.02
0.00
−0.02
α_i
stable
← unstable →
0.0
0.2
0.4
0.6
0.8
1.0
s

UTRC Turbine Experiments
First Stator Blade

Dring, et al, 1986, 1987

- Test run R53PD1 inlet conditions
  - 22.8 m/s
  - 15° C
  - 1 atm
- Uniform heat flux: 1.5775 kW/m^3
- Turbulence levels at inlet to first stator
  - 0.5% (grid out)
  - 9.8% (grid in)

HEAT TRANSFER ON GAS TURBINE BLADES

Dring et al. 1986

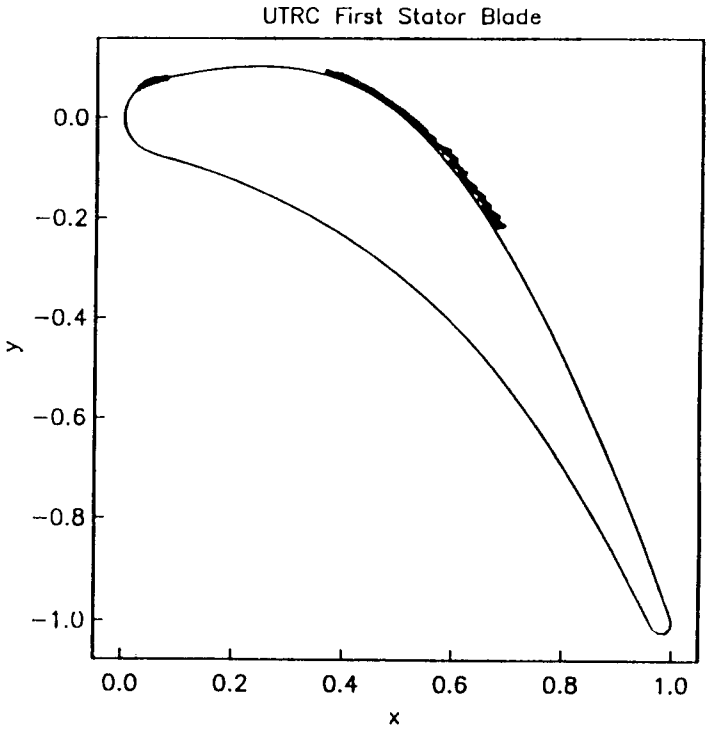

EFFECT OF STREAMWISE CURVATURE ON BYPASS TRANSITION

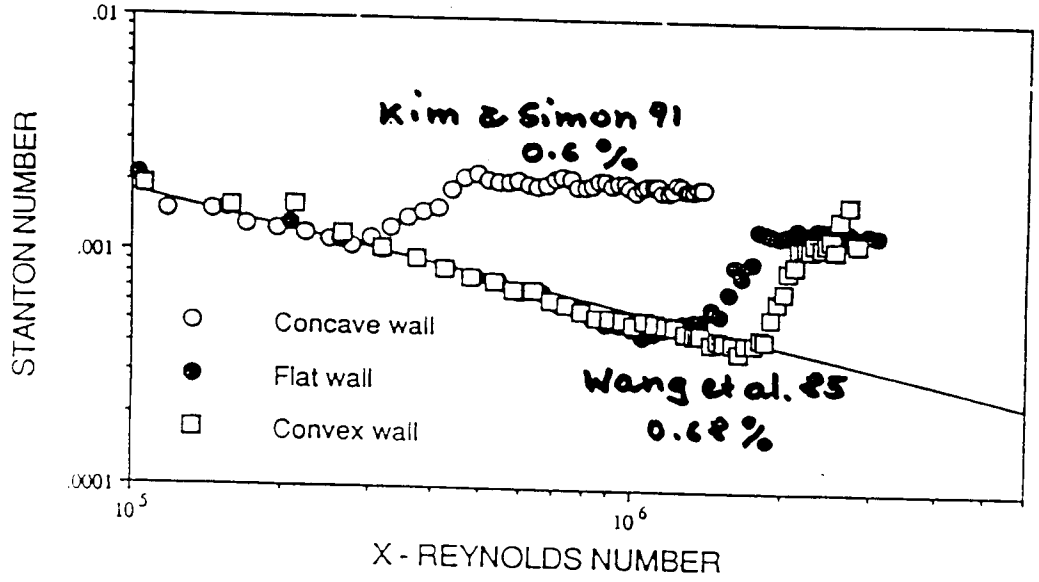

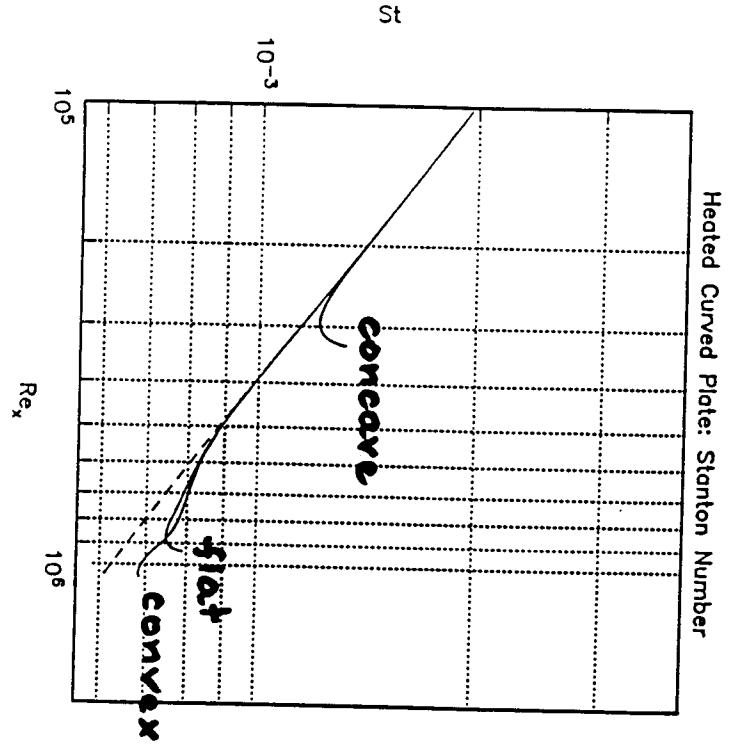

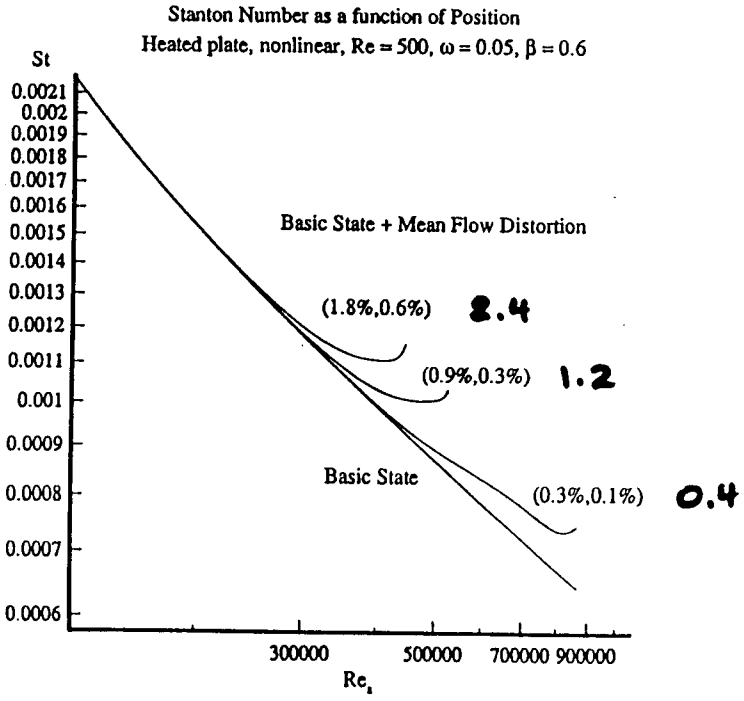

Experiments on Heated Curved Plates

Wang, Simon & Buddhavarapu 1985

- flat plate, $R=\infty$, $U_\infty=35\ m/s$, $Tu=0.68\%$
- flat plate, $R=\infty$, $U_\infty=15\ m/s$, $Tu=2\%$
- convex plate, $R=1.8\ m$, $0.9\ m$, $U_\infty=34\ m/s$, $Tu=0.68\%$
- convex plate, $R=1.8\ m$, $0.9\ m$, $U_\infty=15\ m/s$, $Tu=2\%$

Kim & Simon 1991

- flat plate, $R=\infty$, $U_\infty=28\ m/s$, $Tu=0.32\%$, (no heat)
- flat plate, $R=\infty$, $U_\infty=17\ m/s$, $Tu=1.5\%$
- concave plate, $R=0.97\ m$, $U_\infty=17\ m/s$, $Tu=0.6\%$

Experiments on Heated Flat Plates

Sohn & Reshotko 1991

- $U_\infty = 30.48\, m/s$
- Unheated starting length $35\, mm$
- Constant heat flux $0.42\, KW/m^2$
- Turbulence levels

  0.4% grid 0
  0.8% grid 0.5
  1.1% grid 1
  2.4% grid 2
  5.0% grid 3 (no transition point)
  6.0% grid 4 (no transition point)

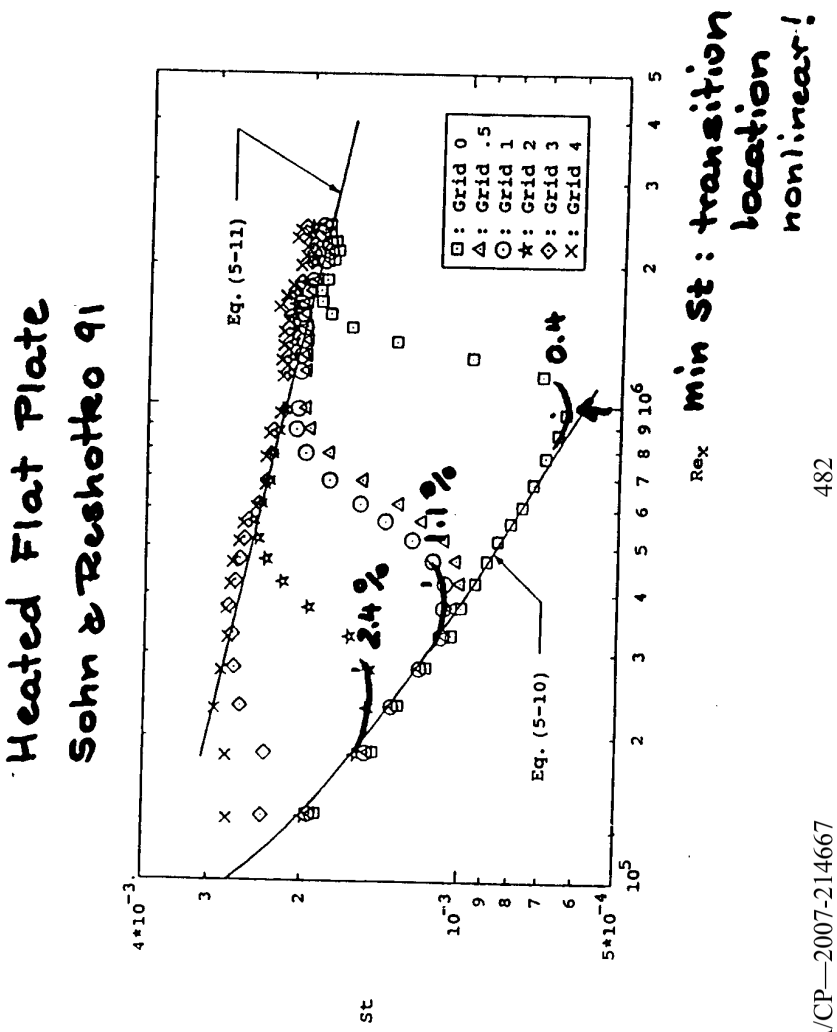

Input Model

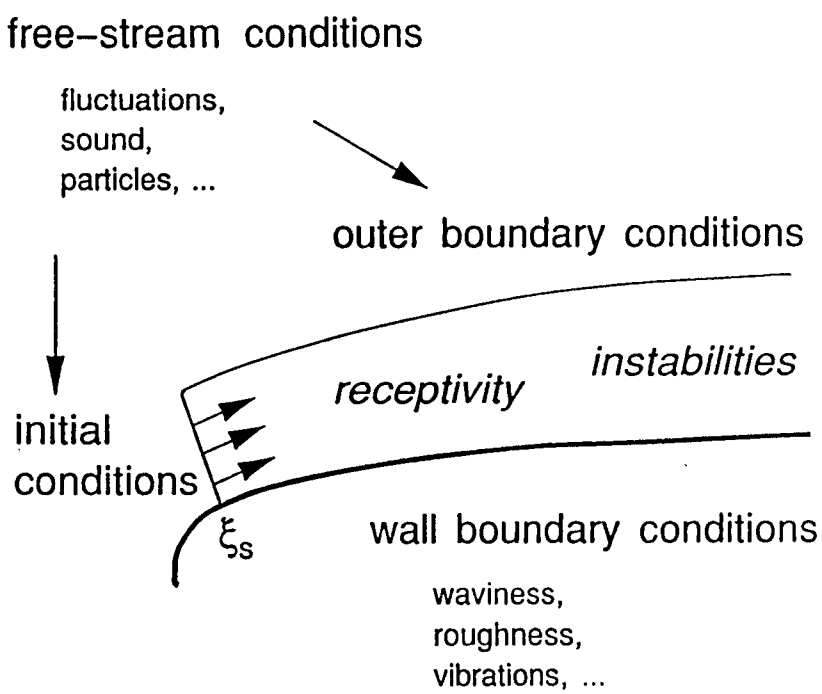

Need:

time scale, spanwise length scale, amplitudes

Model Environment

2D flow, wind tunnel, $Tu \geq 0.4\%$

- Initial conditions:
  receptivity
- Boundary conditions:
  area-distributed receptivity
- Spanwise scale:
  longitudinal vortex
  $\lambda_z \approx 2\delta$ (Kendall)
- Time scale:
  single frequency TS wave
  linear stability analysis
- Amplitudes:
  one "intelligent" guess
  linear receptivity

Code Development

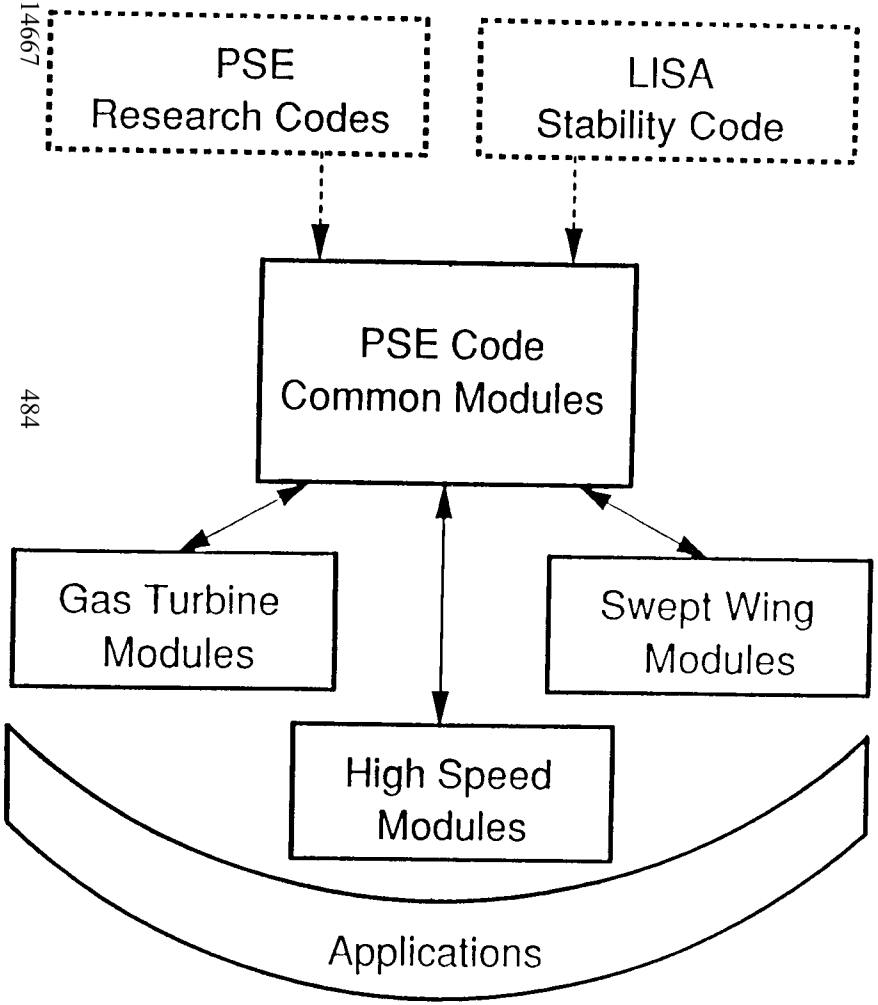

DF-93-H04

Support Codes

- Inviscid compressible flow in cascades:
  PCPANEL by E.R. McFarland (NASA Lewis)
  -- ported to Unix workstations
- Boundary-layer calculations:
  WING by Kaups & Cebeci,
  (undocumented version from NASA Langley)
  -- improvements/extensions implemented
- Local stability analysis:
  LISA by Th. Herbert,
  -- integrated with PSE code
- Codes for similarity solutions etc.

DF-93-H03

Engineering Method

- PSE Extension to
  compressible, hypersonic,
  3D boundary layers in
  general curvilinear coordinates
- \+ Modular Code Design
- \+ Numerical Methods
- \+ Basic Flow Interfaces, Interpolation
- \+ Support Codes
- \+ Real-Life Data, Smoothing
- \+ Efficiency, Robustness
- \+ Ease of Use

Major Problems

- Compressible Nonlinear Terms
- Numerical Integration
- Basic Flow Accuracy
- Basic Flow Interpolation
- Absence of Test Data
- Lack of Physical Understanding

Parabolized Stability Equations (PSE)

LOCAL STABILITY THEORY
Orr-Sommerfeld-type
ODE's
BVP, eigenvalue problem

↓

PSE APPROACH
Orr-Sommerfeld-type
parabolized PDE's
IBVP, marching solution in x

↑

SPATIAL DNS
Navier-Stokes
elliptic/hyperbolic PDE's
IBVP, marching solution in t

DF-92-D03

Validation of Concepts

(Blasius flow, Falkner-Skan flow)

Single Modes
- nonparallel linear stability
- direct calculation of N factors
- nonlinear evolution

Multiple Modes
- linear secondary instability
- mode interactions
- transition simulations
- studies at low frequencies

Conclusion: PSE

- are accurate and efficient, <30 min ~~Cray~~
- should replace existing e^N codes
- provide the potential for "transition prediction" in engineering practice

DF-93-D06

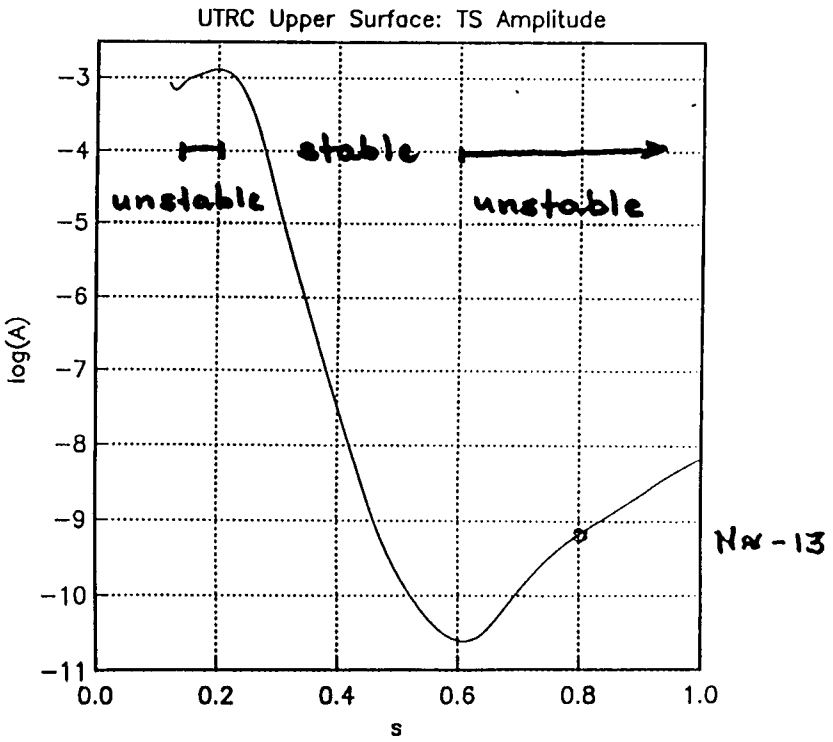

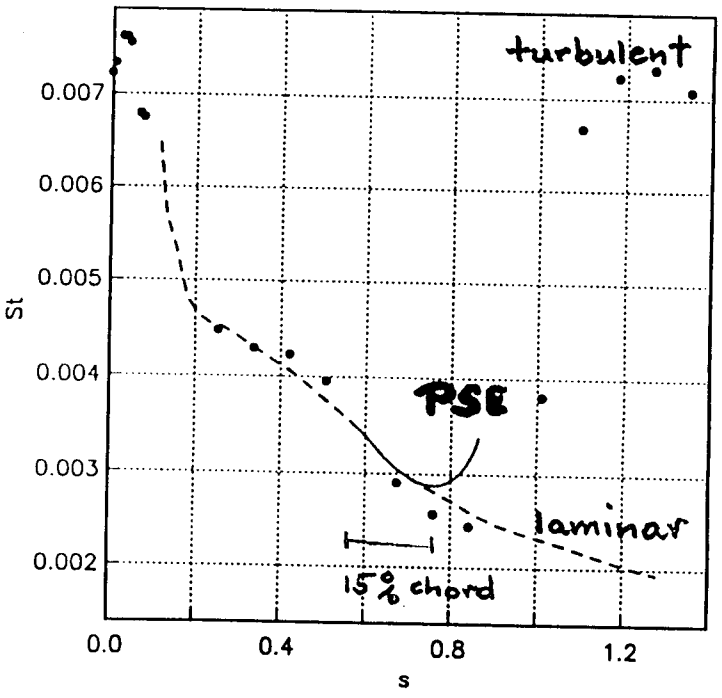

: also Rai & Moin AIAA 91-1607

Random noise 7.6% upstream →

Numerical Simulations of the Late Stages of Transition to Turbulence

N. D. Sandham

Department of Aeronautical Engineering
Queen Mary and Westfield College
Mile End Road
London E1 4NS, UK

References:

Sandham and Kleiser, JFM **245** (1992).
Sandham and Adams, ETC 4 (1992). [M=2.0]
Adams and Kleiser, (1993). [M=4.5]

(1)

CLASSICAL TRANSITION PROCESS
(vibrating ribbon experiments)

- linear instability - TS waves
- secondary instability - Lambda vortices
  K-type (Klebanoff) or H-type (Herbert)
- ? - spikes, hairpins, tertiary instabilities
- turbulence

Objective:

- clarify phenomena and mechanisms in the late stages of the transition process

(2)

NUMERICAL SIMULATION

Gilbert (1988), Gilbert & Kleiser (1990)

Overview

- plane channel flow geometry
- temporal development (periodic in x1, x2)
- 3d incompressible Navier-Stokes
  (no turbulence model)
- direct numerical simulation
  (spectral method)
- COMPLETE transition process simulated

Databases (constant Q, Re = 5000)

- K-type transition
- H-type transition
- Mixed-type transition

(3) Initial condition TS wave (3%)
oblique waves (0.1%)

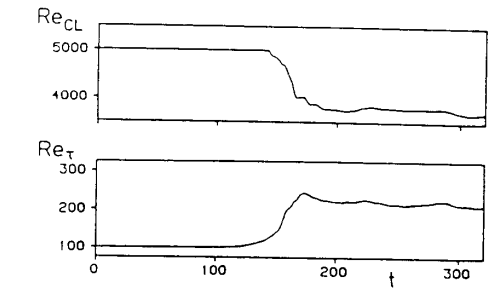

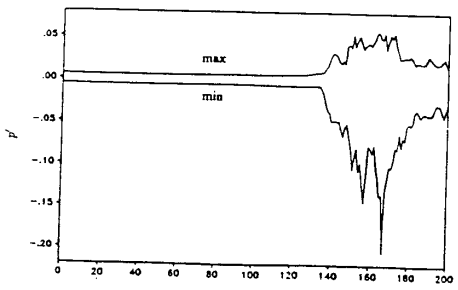

(4)

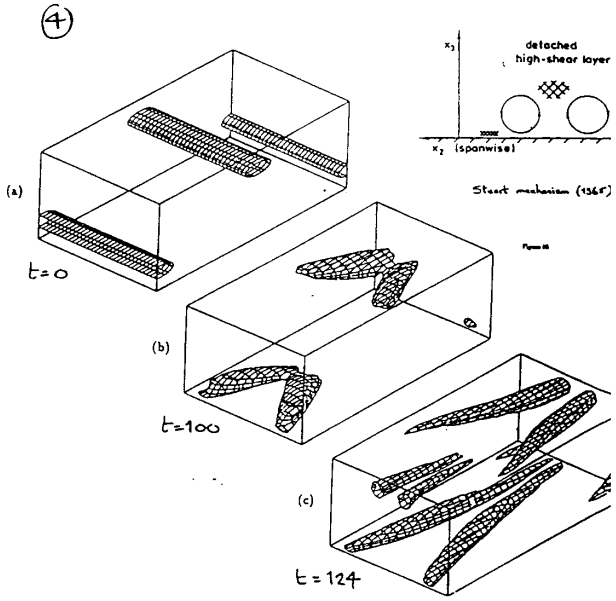

$$\Pi = \frac{\partial v_i}{\partial x_j}\frac{\partial v_j}{\partial x_i}$$

Figure 2

(13)

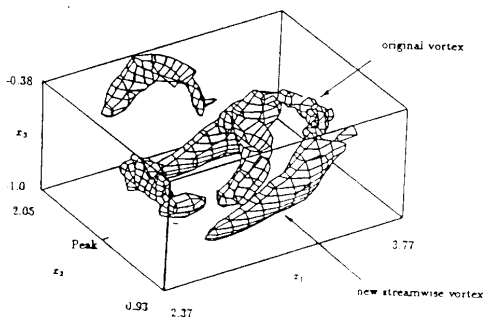

t = 156

Figure 14

(14)

Transition at M=2

1. Streamwise vortices
2. Decay and formation of new vortices
3. Vortex break-up

(see Sandham, Adams and Kleiser, 1994)

Transition at M=4.5

1. Mack mode of primary instability
2. Formation of Λ-vortices from random noise
3. Sonic layer important for Stuart mechanism
4. Lower shear layer develops first
5. Simulation results up to the beginnings of turbulence

Adams - dissertation (1993)
Adams and Kleiser (JFM, submitted)

(15)

M = 4.5

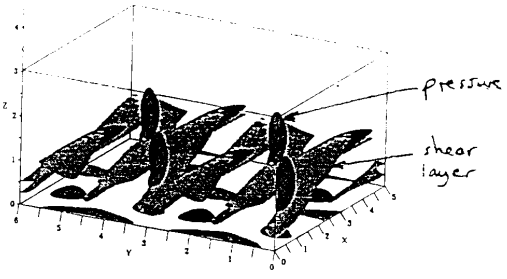

(a) Perspektive, in Spannweitenrichtung periodisch fortgesetzt.

(b) Draufsicht. (c) Seitenansicht.

Abbildung 7.20: p-Isoflächen ($p = 0.032237$, dunkel) und ω_y-Isoflächen ($\omega_y = 1.4$, hell) in $t = 492.70$.

not lower shear

(16)

Outlook

Advantages of DNS:
- controlled disturbances
- full flowfield data

Future developments:
- more databases (esp. compressible, 3D)
- higher Re, larger computational domains
- (more) complex geometries

(5)

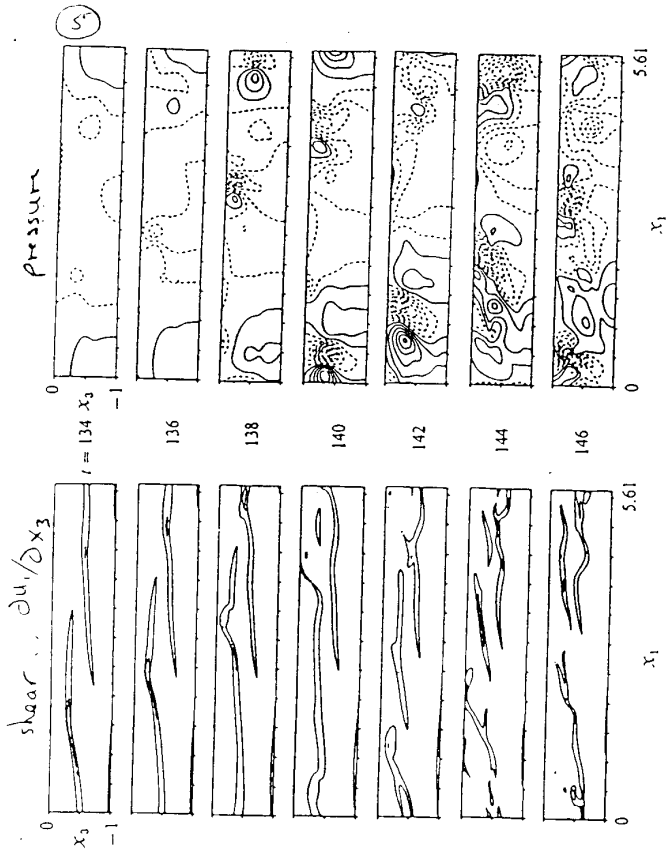

(6)

Late stages of transition to turbulence in channel flow

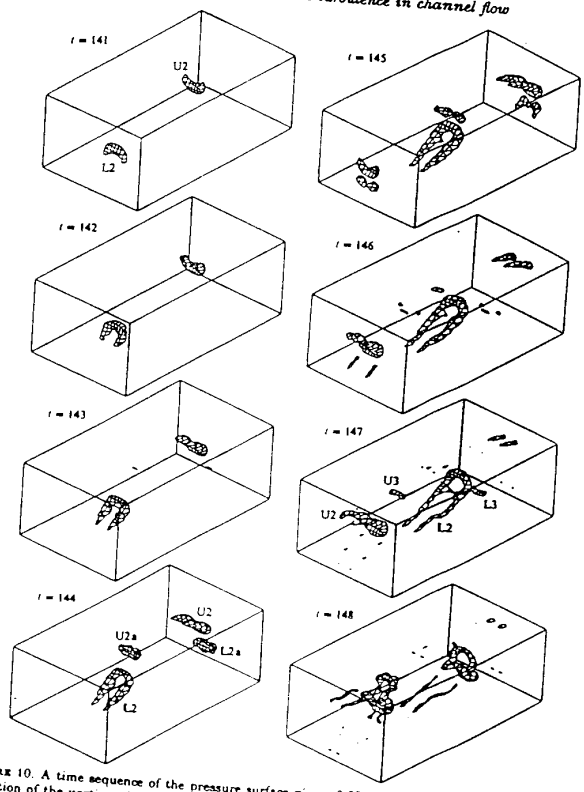

FIGURE 10. A time sequence of the pressure surface $p' = -0.025$ showing the three-dimensional evolution of the vortices that originate in the high-shear layer. Vortices L2 and U2 develop into pronounced hairpin vortices.

Sandham & Kleiser 1992

(7)

Streak development

$t = 155$

SHEAR ON WALL $\left.\frac{\partial u_1}{\partial x_3}\right|_w = 0, 10, 20$

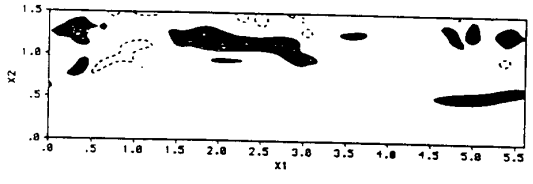

(8)

Wall Shear

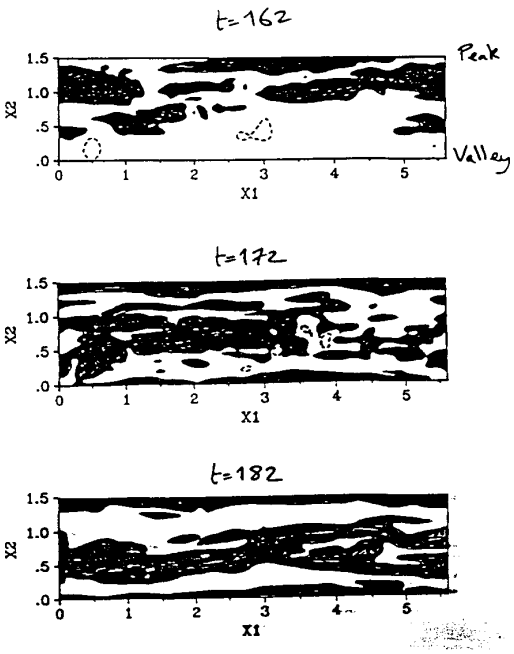

(9)

Development near-wall turbulence in the late stages of transition

TS wave

Λ - vortex, high-shear layer

shear-layer roll-up, vortex evolution

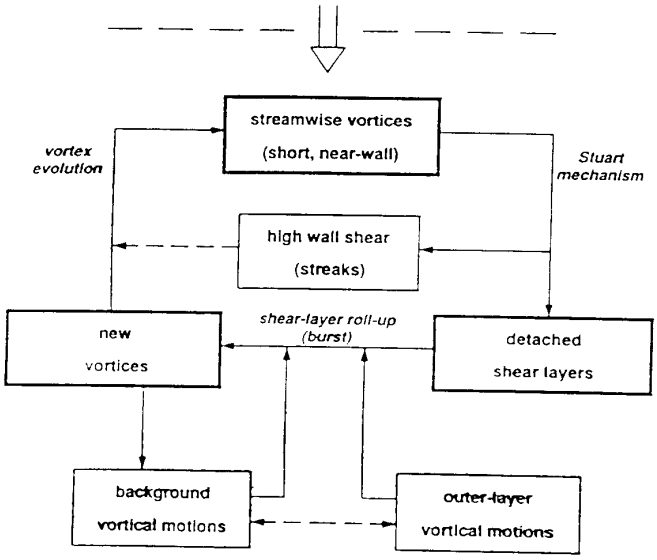

(10)

t = 150

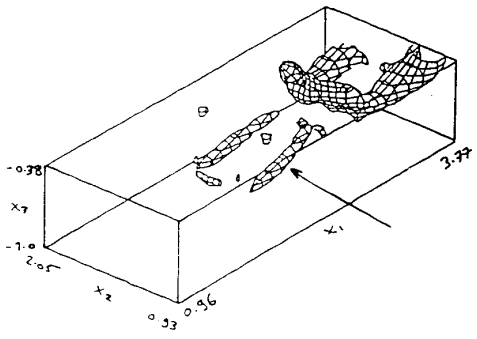

(11)

shear $\partial u_1/\partial x_3$

t = 151

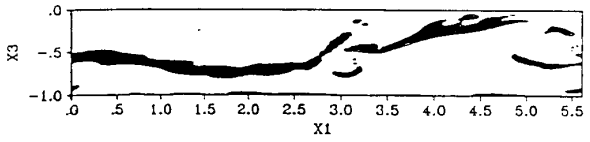

t = 153

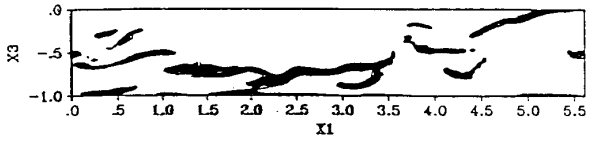

t = 155

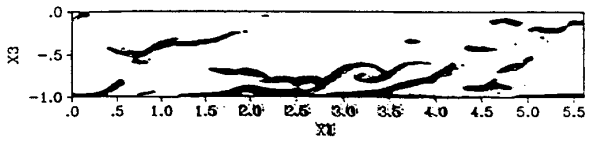

(12)

pressure

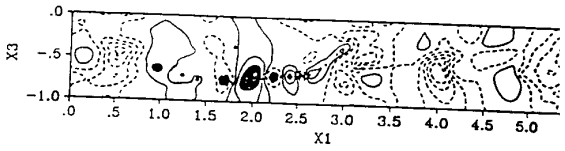

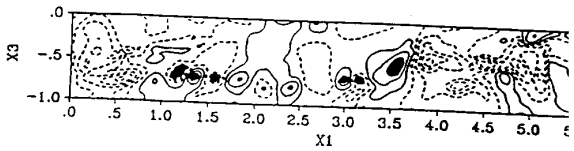

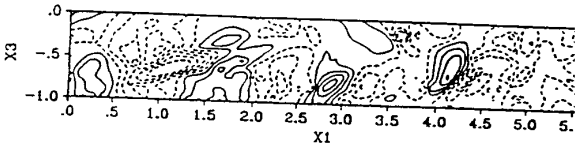

Turbulence Modeling for the Simulation of Transition in Wall Shear Flows

by
Michael E. Crawford
Mechanical Engineering Dept.
The University of Texas
Austin, TX 78712

Abstract

Our research involves study of the behavior of k-ε turbulence models for simulation of bypass-level transition over flat surfaces and turbine blades. One facet of the research has been to assess the performance of a multitude of k-ε models in what we call "natural transition", i.e. no modifications to the k-ε models. The study has been to ascertain what features in the dynamics of the model affect the start and end of the transition. Some of the findings are in keeping with those reported by others (e.g. ERCOFTAC). A second facet of the research has been to develop and benchmark a new multi-time scale k-ε model (MTS) for use in simulating bypass-level transition. This model has certain features of the published MTS models by Hanjalic, Launder, and Schiestel, and by Kim and his co-workers. The major new feature of our MTS model is that it can be used to compute wall shear flows as a low-turbulence Reynolds number type of model, i.e. there is no required partition with patching a one-equation k model in the near-wall region to a two-equation k-ε model in the outer part of the flow. Our MTS model has been studied extensively to understand its dynamics in predicting the onset of transition and the end-stage of the transition. Results to date indicate that it far superior to the standard un-modified k-ε models. The effects of protracted pressure gradients on the model behavior are currently being investigated.

Students involved in this research include Tzong-Huei Chen (Mechanical Engineering, The University of Texas at Austin) and Klaus Sieger (Institute for Thermal Turbomachinery, University of Karlsruhe, Germany). Sponsor for the majority of the research is the NASA-Lewis Research Center, with Mr. Fred Simon as technical monitor.

Turbulence Modeling for the Simulation of Transition in Wall Shear Flows

Professor Michael E. Crawford

Turbulence and Turbine Cooling Research Laboratory
Mechanical Engineering Department
The University of Texas at Austin

Bypass Transition Modeling Program

Objective: Develop turbulence model to account for effect of free stream disturbances on the laminar boundary layer and its transition region

Scope:

- Understand mechanisms of transition in existing 2-eqn models
- Develop improved modeling for bypass transition mechanism, friction and heat transfer

Governing Equations:

$$\frac{\partial}{\partial x}(\rho \bar{U}) + \frac{\partial}{\partial y}(\rho \bar{V}) = 0$$

$$\underbrace{\rho \bar{U}\frac{\partial \bar{U}}{\partial x} + \rho \bar{V}\frac{\partial \bar{U}}{\partial y}}_{Convection} = \underbrace{\frac{\partial}{\partial y}[\mu \frac{\partial \bar{U}}{\partial y} - \rho \overline{u'v'}]}_{Diffusion} \underbrace{-\frac{dp}{dx}}_{P_u}$$

$$\underbrace{\rho \bar{U}\frac{\partial \bar{i}^*}{\partial x} + \rho \bar{V}\frac{\partial \bar{i}^*}{\partial y}}_{Convection} = \underbrace{\frac{\partial}{\partial y}[\frac{\mathbf{Pr}}{\mu}\frac{\partial \bar{i}}{\partial y} - \rho c \overline{v't'}]}_{Diffusion} \underbrace{+\frac{\partial}{\partial y}(\mu \bar{U}\frac{\partial \bar{U}}{\partial y} - \overline{\rho u'v'}\bar{U})}_{P_i^*}$$

Turbulence Modeling:

Turbulent Reynolds Stress Model:

$$-\overline{u'v'} = \frac{\mu_t}{\rho}\frac{\partial \bar{U}}{\partial y}$$

Turbulent Heat Flux Model:

$$-\rho c\,\overline{v't'} = \kappa_t \frac{\partial \bar{t}}{\partial y} = \frac{\mu_t c}{\mathbf{Pr}_t}\frac{\partial \bar{t}}{\partial y}$$

Mixing Length Model:

$$\frac{\mu_t}{\rho} = \ell^2 \frac{\partial \bar{U}}{\partial y}$$

Two-Equation Model:

$$\frac{\mu_t}{\rho} = C_\mu f_\mu \frac{k^2}{\varepsilon}$$

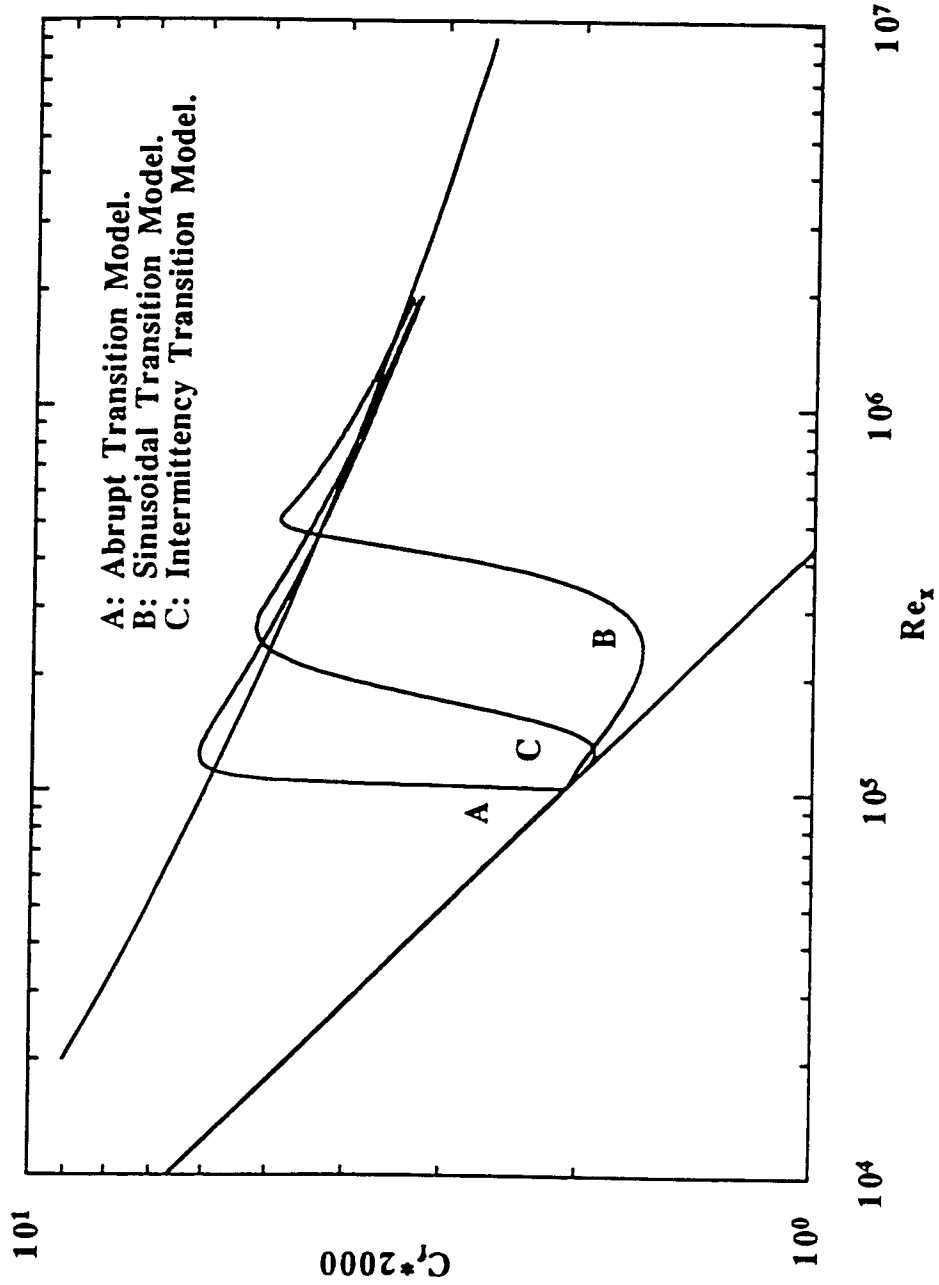

Figure 2: Examples of A^+ and γ calculations of transitional flow over a flat plate with a free stream turbulence level, Tu, of 3%.

Two-Equation Models:

$$\underbrace{\rho\bar{U}\frac{\partial k}{\partial x}+\rho\bar{V}\frac{\partial k}{\partial y}}_{\text{Convection}}=\underbrace{\frac{\partial}{\partial y}[(\mu+\frac{\mu_t}{\sigma_k})\frac{\partial k}{\partial y}]}_{\text{Diffusion}}+\underbrace{(-\rho\overline{u'v'})\frac{d\bar{U}}{dy}}_{P_k}-\underbrace{\rho\varepsilon}_{D_k}+D$$

$$\underbrace{\rho\bar{U}\frac{\partial \varepsilon}{\partial x}+\rho\bar{V}\frac{\partial \varepsilon}{\partial y}}_{\text{Convection}}=\underbrace{\frac{\partial}{\partial y}[(\mu+\frac{\mu_t}{\sigma_\varepsilon})\frac{\partial \varepsilon}{\partial y}]}_{\text{Diffusion}}+\underbrace{C_1 f_1\frac{\varepsilon}{k}P_k}_{P_\varepsilon}-\underbrace{\rho C_2 f_2\frac{\varepsilon^2}{k}}_{D_\varepsilon}+E$$

$$\text{where } -\overline{u'v'}=\upsilon_t\frac{d\bar{U}}{dy}=C_\mu f_\mu\frac{k^2}{\varepsilon}\frac{d\bar{U}}{dy}$$

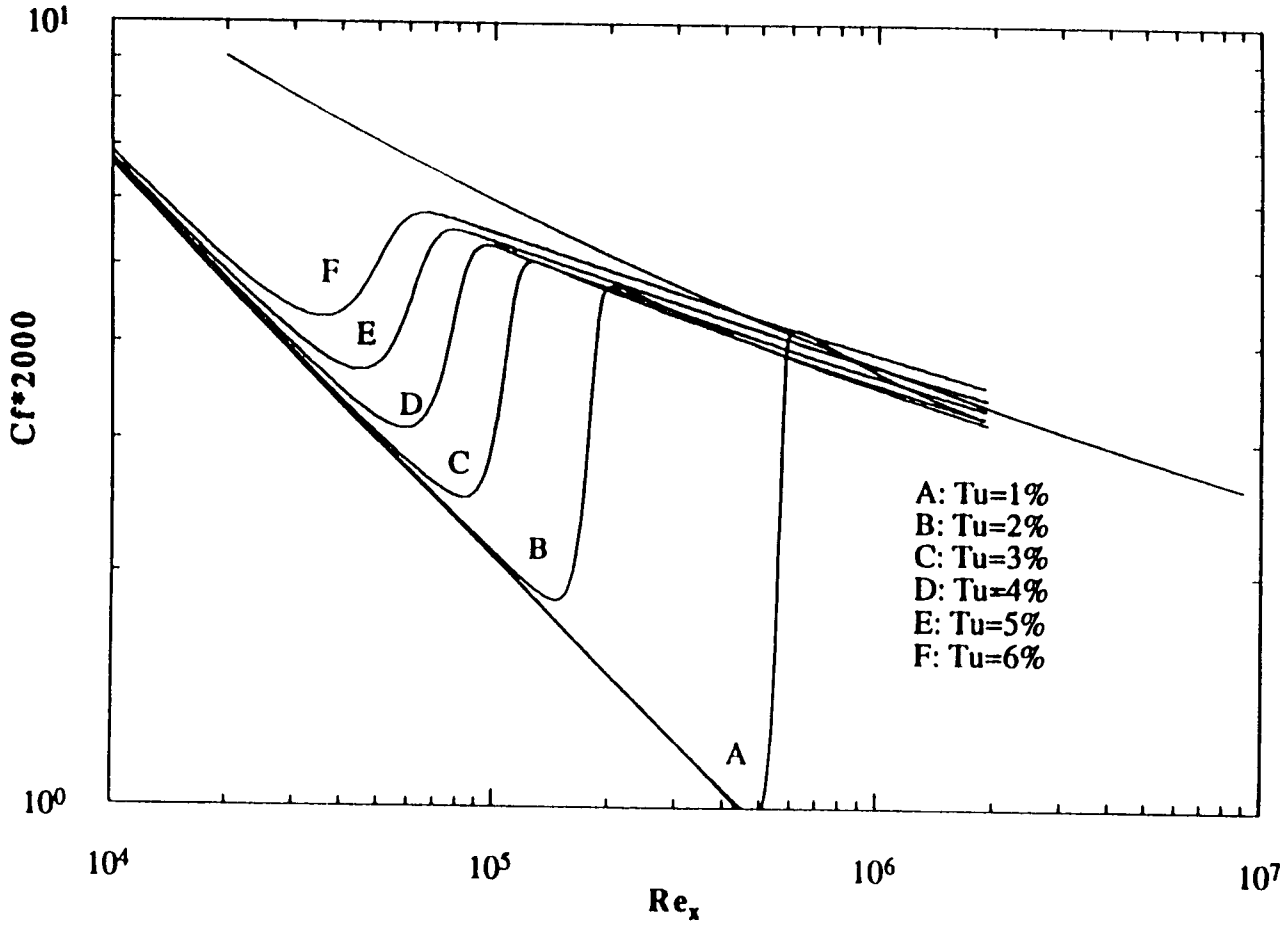

The prediction of transition for flow over flate plate using LS two-equation models

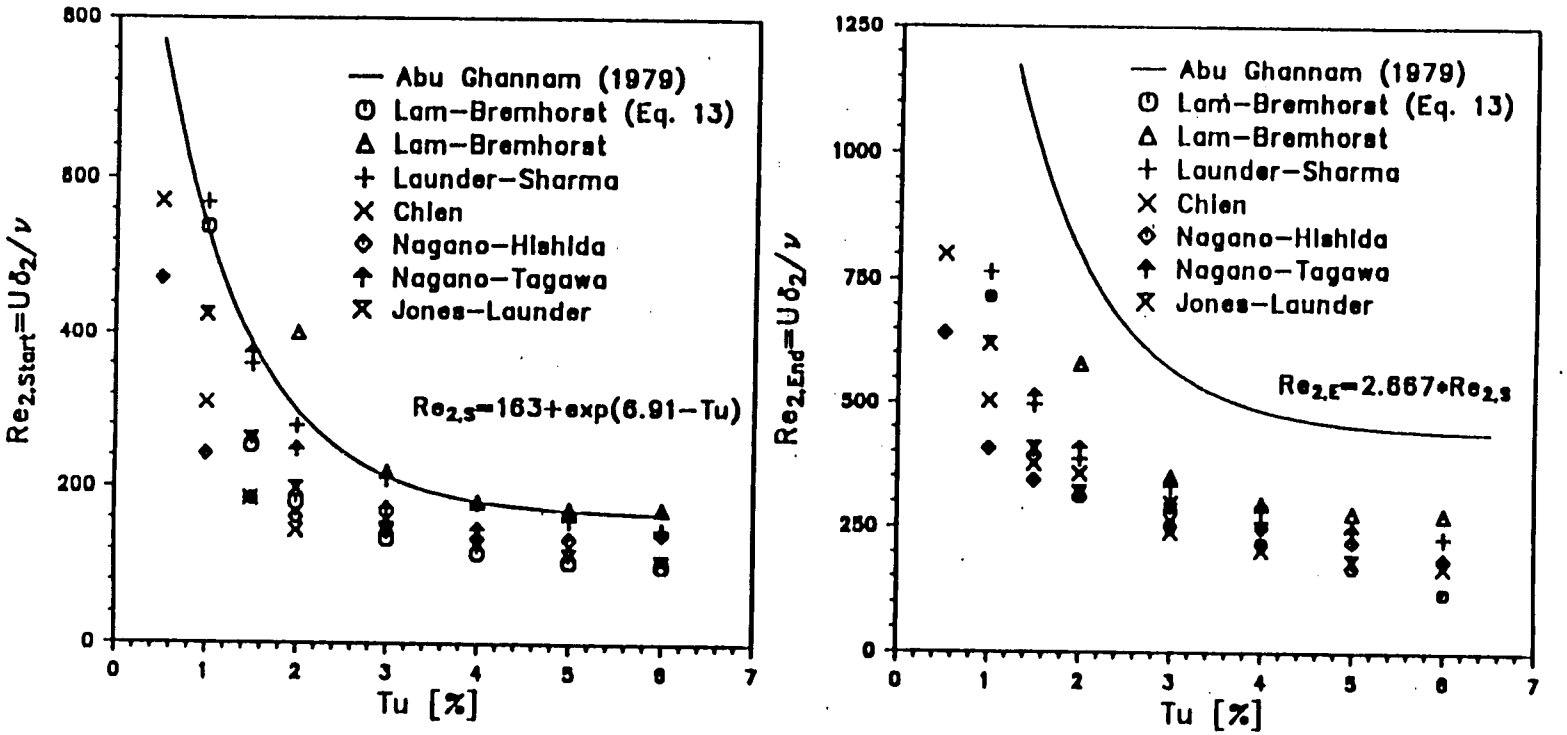

(a.) Start of Transition (b.) End of Transition

FIGURE 3: Computed momentum thickness Reynolds number at the start and end of transition in comparison to the correlation by Abu Ghannam (1979)

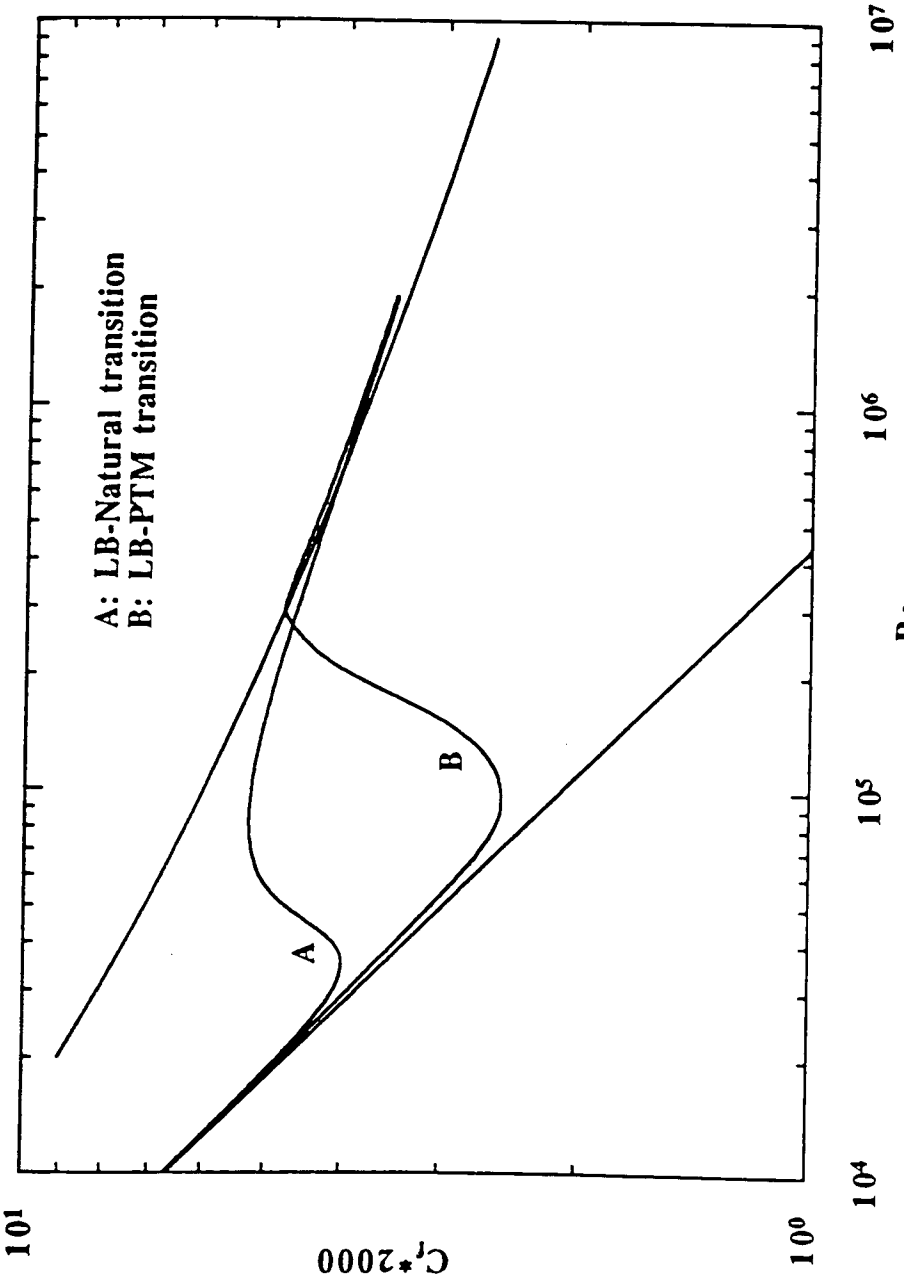

Figure 3: An example of natural transition and PTM transition for free stream turbulence level, Tu, of 3%.

Modified MTS Model:

$$\rho U\frac{\partial K_p}{\partial x}+\rho V\frac{\partial K_p}{\partial y}=\frac{\partial}{\partial y}[(\mu+\frac{\mu_t}{\sigma_{kp}})\frac{\partial K_p}{\partial y}]+P_k-\rho\varepsilon_p$$

$$\rho U\frac{\partial K_t}{\partial x}+\rho V\frac{\partial K_t}{\partial y}=\frac{\partial}{\partial y}[(\mu+\frac{\mu_t}{\sigma_{kt}})\frac{\partial K_t}{\partial y}]+\rho\varepsilon_p-\rho\varepsilon_t$$

$$\rho U\frac{\partial \varepsilon_p}{\partial x}+\rho V\frac{\partial \varepsilon_p}{\partial y}=\frac{\partial}{\partial y}[(\mu+\frac{\mu_t}{\sigma_{\varepsilon p}})\frac{\partial \varepsilon_p}{\partial y}]+C_{p1}P_k\frac{\varepsilon_p}{k_p}+\rho C'_{p1}k_p(\frac{\partial U}{\partial y})^2-\rho C_{p3}\frac{\varepsilon_p^2}{k_p}$$

$$\rho U\frac{\partial \varepsilon_t}{\partial x}+\rho V\frac{\partial \varepsilon_t}{\partial y}=\frac{\partial}{\partial y}[(\mu+\frac{\mu_t}{\sigma_{\varepsilon t}})\frac{\partial \varepsilon_t}{\partial y}]+\rho C_{t1}\frac{\varepsilon_t^2}{K_t}+\rho C_{t2}\frac{\varepsilon_p\varepsilon_t}{K_t}-\rho C_{t3}\frac{\varepsilon_t^2}{K_t}$$

$$\mu_t=\rho C_\mu f_\mu\frac{k^2}{\varepsilon_p}$$

$\sigma_{kp}=0.75$, $\sigma_{kt}=0.75$, $\sigma_{\varepsilon p}=1.15$, $\sigma_{\varepsilon t}=1.15$, $C_{p1}=0.21$, $C'_{p1}=0.11$, $C_{p3}=1.84$, $C_{t1}=0.29$, $C_{t2}=1.28$, and $C_{t3}=1.64$

Boundary Conditions:

$$\varepsilon_p\big|_w=\varepsilon_t\big|_w=\nu\,\partial^2k_p/\partial y^2\big|_w;\quad k_p\big|_w=k_p\big|_t=0$$

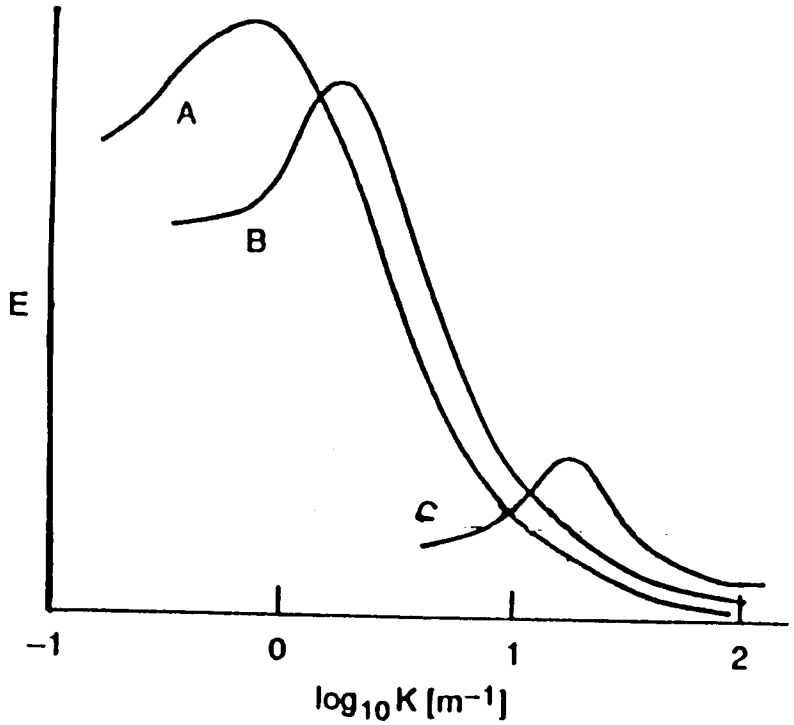

(a) Spectral density for inequilibrium turbulent flows, A: maximum shear location in a circular jet [20], B: center of a circular jet [20], C: free stream region of a boundary layer flow in zero pressure gradient [19].

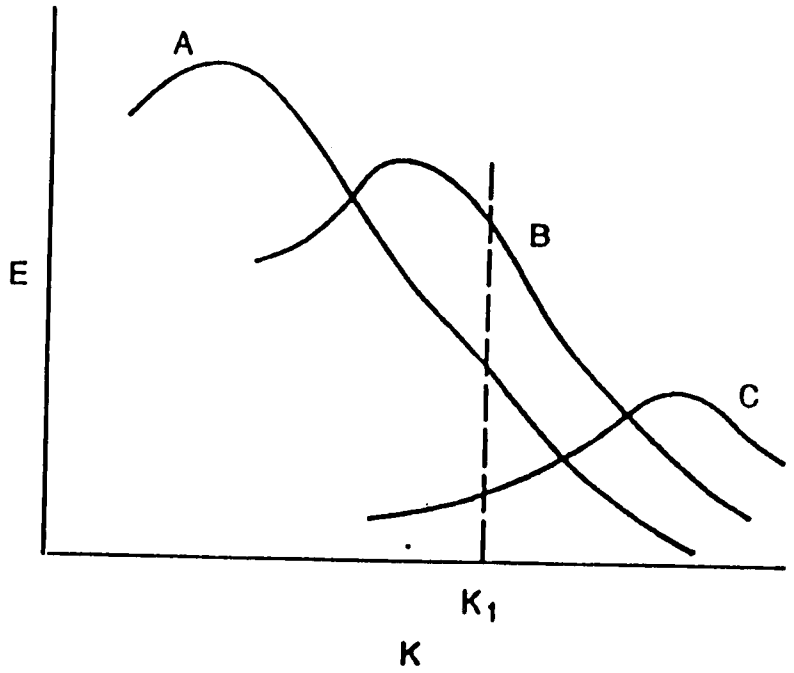

$$k_p = \int_{K=0}^{K_1} E dK, \quad k_t = \int_{K=K_1}^{\infty} E dK$$

(b) k_p/k_t for inequilibrium turbulent flow, A: $Pr/\epsilon_t > 1$, B: $Pr/\epsilon_t = 1$, C: $Pr \approx 0.0$.

Figure 2.—Spectral density.

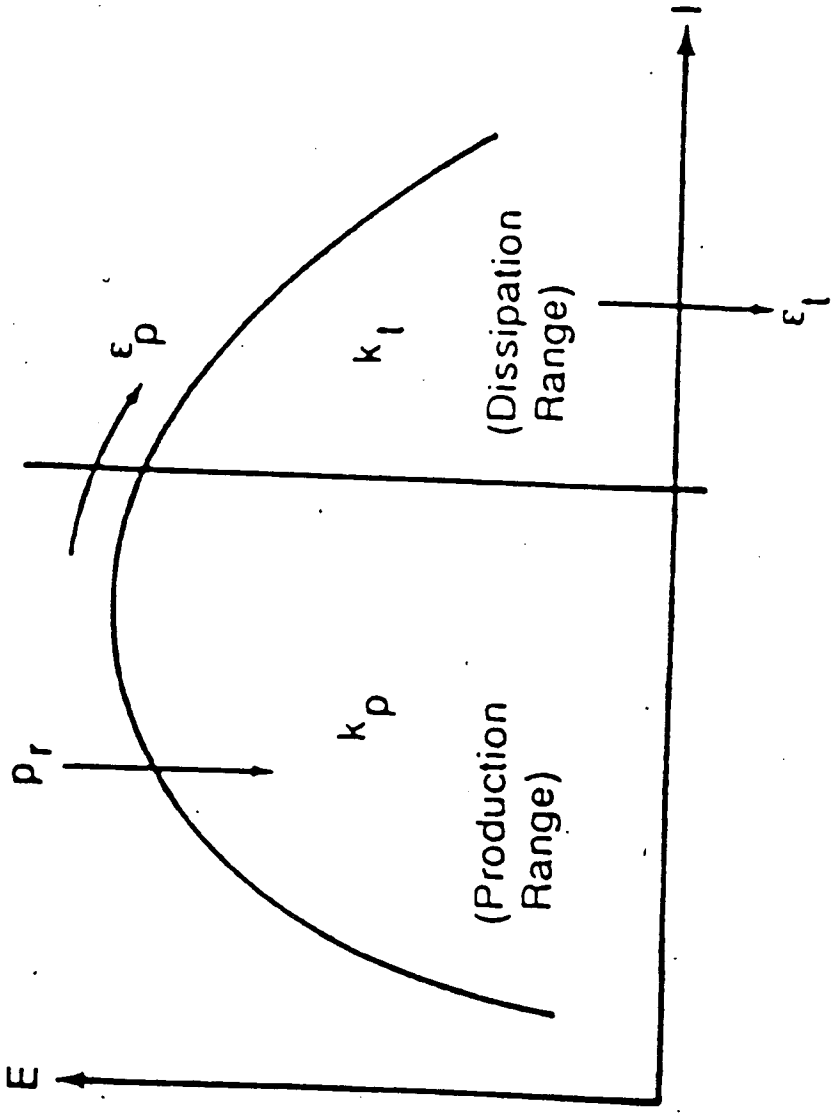
E
l
p_r
k_p
(Production Range)
ε_p
k_l
(Dissipation Range)
ε_l

Hanjalic, Launder , Shiestel (1980):

$$\frac{DK_p}{Dt} = -\varepsilon_p$$

$$\frac{DK_t}{Dt} = \varepsilon_p - \varepsilon_t$$

$$\frac{D\varepsilon_p}{Dt} = -C_{p2}\frac{\varepsilon_p^2}{K_p}$$

$$\frac{D\varepsilon_t}{Dt} = C_{t1}\frac{\varepsilon_p\varepsilon_t}{K_t} - C_{t2}\frac{\varepsilon_t^2}{K_t}$$

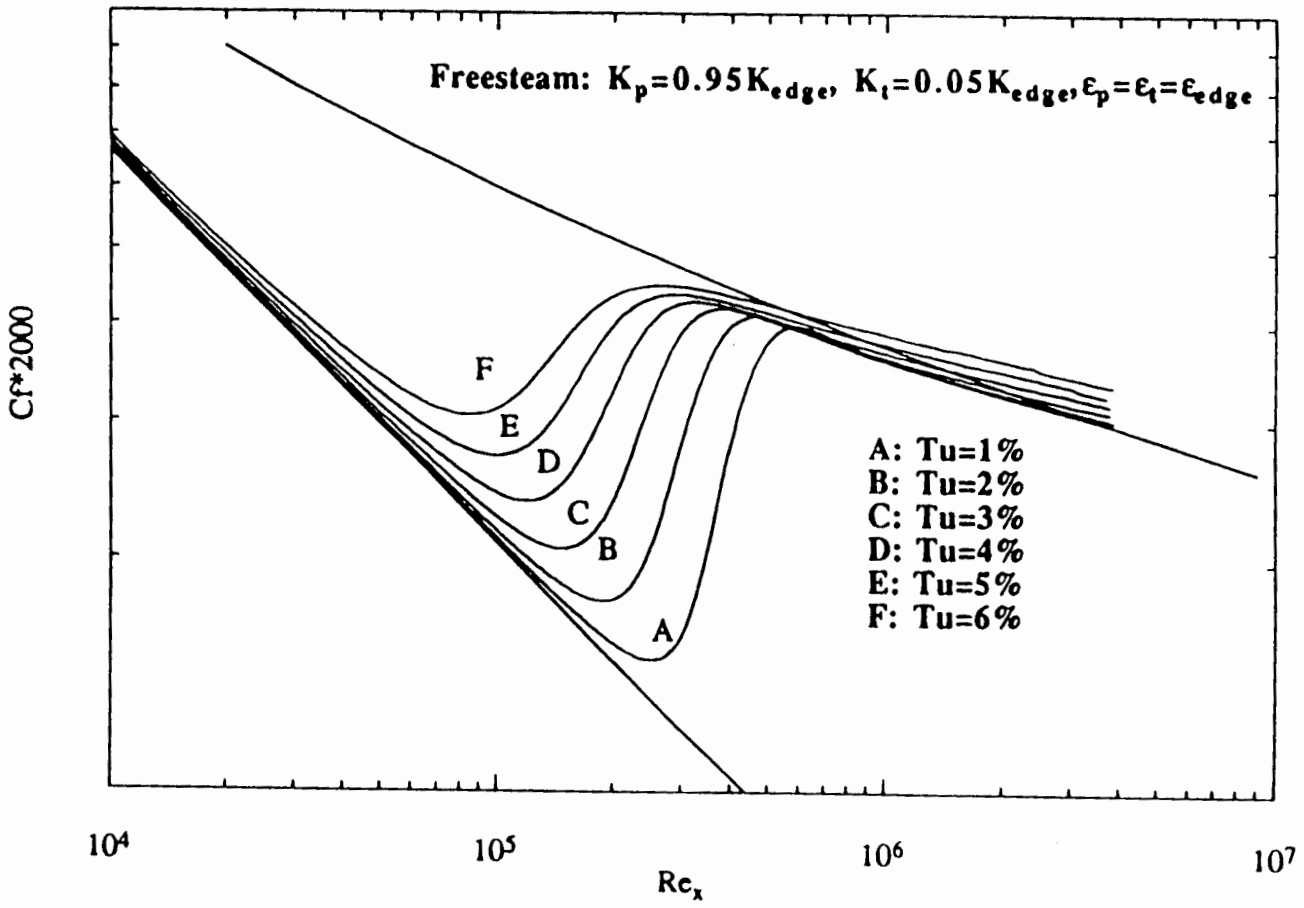
Freesteam: $K_p=0.95K_{edge}$, $K_t=0.05K_{edge}$, $\varepsilon_p=\varepsilon_t=\varepsilon_{edge}$
A: Tu=1%
B: Tu=2%
C: Tu=3%
D: Tu=4%
E: Tu=5%
F: Tu=6%
A
B
C
D
E
F
Cf*2000
10^4
10^5
10^6
10^7
Re_x

MTS Model

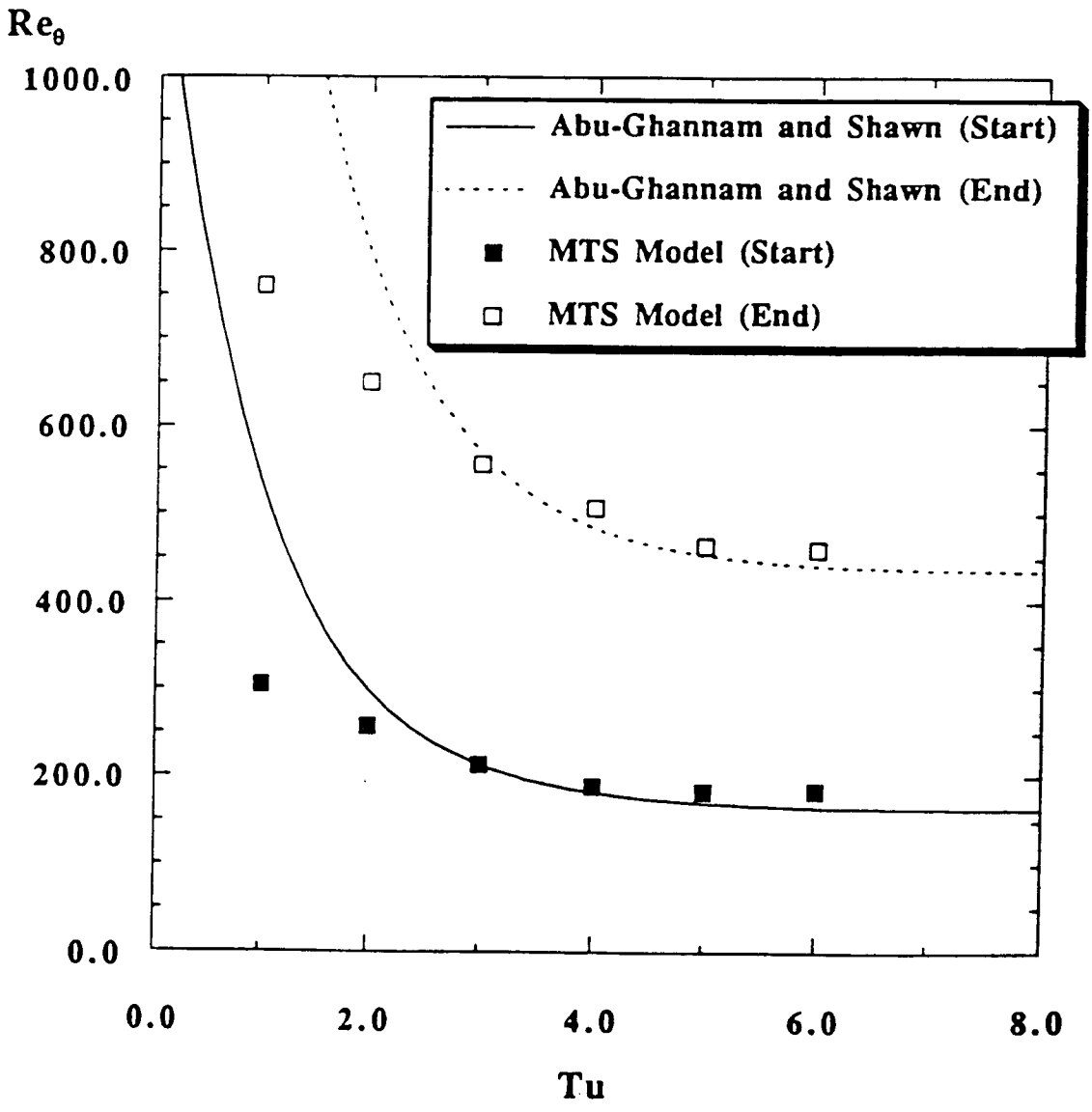
Re_θ
1000.0
800.0
600.0
400.0
200.0
0.0
0.0
2.0
4.0
6.0
8.0
Tu
Abu-Ghannam and Shawn (Start)
Abu-Ghannam and Shawn (End)
MTS Model (Start)
MTS Model (End)

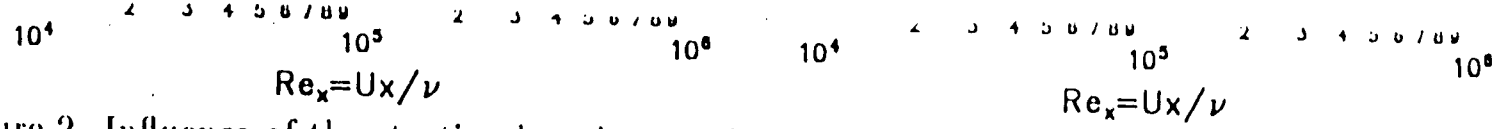

Figure 2. Influence of the starting location on the transition prediction

4.2. Effect of free-stream dissipation length scale

The laminar-turbulent transition depends strongly on the turbulence field in the free-stream, which is characterized by the turbulence level and the dissipation rate (or dissipation length scale) in the k, ϵ typ of model. The importance of a correct specification of the length scale is demonstrated in Fig. 3. Shown are calculations of the skin friction coefficient c_f for the test case T3B performed with the LS model. The corresponding turbulence decay is shown on the right hand side. The experimentally determined turbulence decay is given by the included correlation. The upper bound of the chosen length scales represents a frozen turbulence, i.e. k_∞ is constant. It becomes obvious that severe errors occure in the reproduction of the decay rate if the length scale specified at the starting location is incorrect. Due to this the predicted

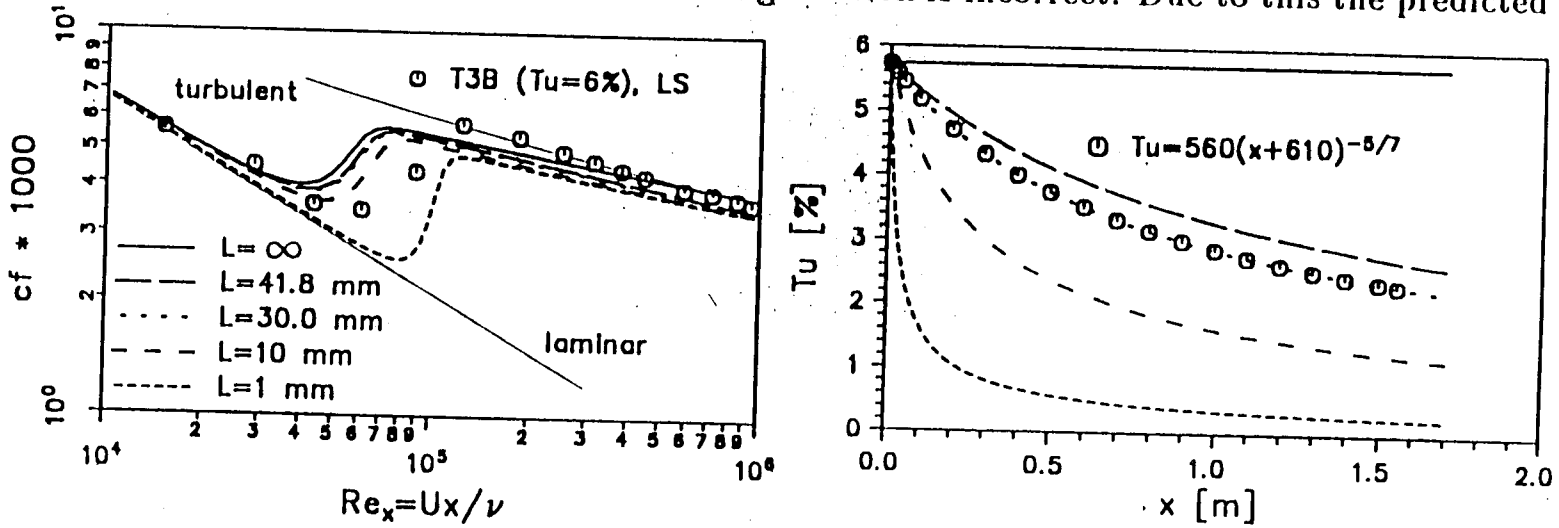

Figure 3. Influence of the free-stream dissipation length scale

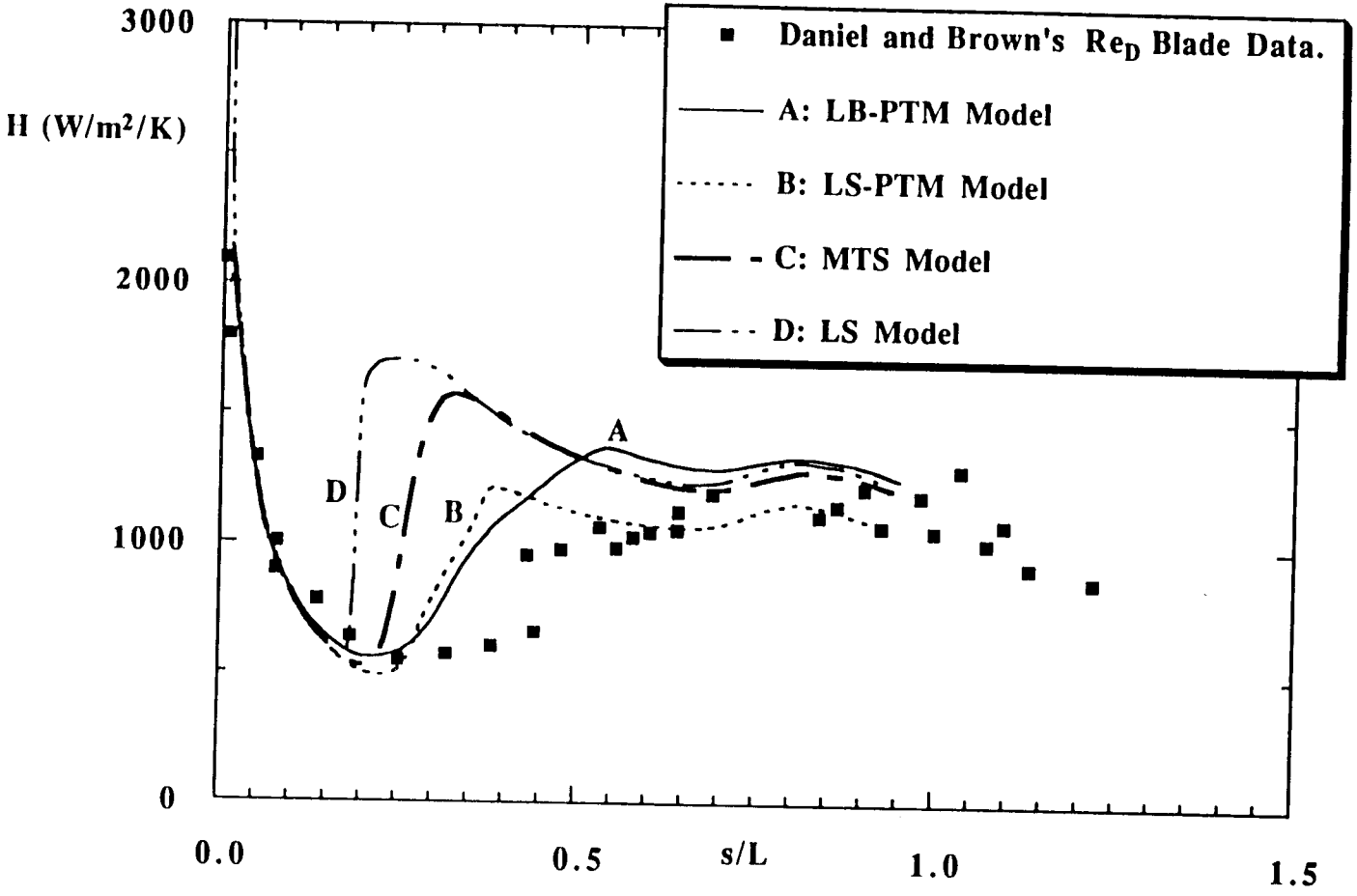

The comparison of the predicted heat transfer coefficient with the suction side of Daniel & Brown's blade data.

Conclusions & Recommendations

- Multi-time-scale model shows promise
- Free-Stream partition ?
- Fmu ? Time scales?
- Pressure gradient effect?

PERSONAL OBSERVATIONS
ON THE
WORKSHOP ON END-STAGE BOUNDARY LAYER TRANSITION

HELD AT
SYRACUSE UNIVERSITY/MINNOWBROOK CONFERENCE CENTER
BLUE MOUNTAIN LAKE, NEW YORK, USA
15-18 AUGUST 1993

by
Roddam Narasimha

Indian Institute of Science
and
Jawaharlal Nehru Centre for Advanced Scientific Research
Bangalore 560 012

WORKSHOP ON END-STAGE TRANSITION

SYRACUSE UNIVERSITY/MINNOWBROOK, 15-18 AUGUST 1993

Roddam Narasimha

Indian Institute of Science and Jawaharlal Nehru Centre for Advanced Scientific Research
Bangalore 560 012

Nearly 40 invited participants gathered on the evening of 15 August in the Minnowbrook Conference Centre on the shores of Blue Mountain Lake in the Adirondocks to discuss for the next two and a half days the late stages of transition in boundary layers. The Conference Centre, run by Syracuse University, provided the ideal ambience for an informal and stimulating workshop on a subject that is at once scientifically challenging and technologically important. The Workshop was unique in that it brought together, for the first time, those working on improving our understanding of transition phenomena with others concerned with handling and modelling transitional boundary layers in applications, especially in turbomachinery. Or, as Paul Gostelow (Sydney, who organized the meeting so effectively with John Lagraff of Syracuse and Terry Jones of Oxford) put it, the intention was to bring the JFM and ASME types together (he mentioned high and low church as well!).

The point was pursued by Roddam Narasimha (Bangalore) in his opening talk (his theme was The Many Worlds of Transition Research). Transition is a complex subject, and its investigation is being pursued in many sub-communities, respectively concerned with stability, receptivity, breakdown, turbulent spots, modelling, direct numerical simulation (DNS) etc. It is remarkable that there is not a single experimental investigation

of transition from laminar to turbulent flow in a boundary layer that goes the whole way - on any one of the many routes that everybody admits are possible.

The Workshop was dominated by discussions on turbulent spots - their genesis, properties and consequences - although Tom Corke (Illinois) described how transition could occur without spots. This spot-less or "scenic" route (as Narasimha called it - the road here is slow and long), discovered by the Novosibirsk group, was followed when a resonant interaction between a TS wave and a pair of oblique waves is arranged (- this is done, in Corke's experiment, by suitably programmed forcing through surface films excited thermally). There is in this case no evidence of rapid collapse into turbulent bursts, but only a gradual filling up of the spectrum. Although Corke finds that the route is followed even when there is some detuning, Narasimha felt that the spot-less route seemed contrived, and Mark Morkovin (Illinois Institute of Technology) questioned whether the disturbance field necessary was "environmentally realisable". Indeed, Morkovin emphasized that while the roads to turbulence are highly non-unique, the modes in which the final onset of bursting occurs are much less so.

Some very interesting discussion took place on the events leading to the birth of a spot. Jim Kendall (JPL) reported that the response of the boundary layer to weak free-stream turbulence (FST henceforth) - created in his tunnel by an array of 168 small jets directed upwind in the settling chamber - took three distinct forms. There is first of all a narrow Klebanoff mode peaking half

way across the boundary layer (- not to be confused with the peak-valley splitting also associated with his name); then there are wave packets, arising sporadically, narrower than Gaster's wave packet but with higher, randomly varying amplitude. Finally there are the TS waves. The dynamics of Kendall's wave packet is not clear. Mike Gaster (Cambridge), on the other hand, could track the birth of what appeared to be an Emmons spot within his type of wave packet, triggered by a surface-mounted microphone. Even when the input to the microphone is (deterministic) white noise, a modulated TS wave train appears, with a subsequent breakdown into a spot. Both experiments demonstrate incidentally how choosy the boundary layer is in picking out waves from whatever hash may be heaped on it.

While Gaster uses singular value decomposition and wavelet transforms to understand the time-frequency structure of the process of spot birth, a 3D view was presented by the flow visualization studies of Chuck Smith (Lehigh), who starts with a single hair-pin vortex generated by fluid injection at the surface. The key to the growth process, in his view, is strong vortex-surface interaction, which leads to more hair-pin vortices that amalgamate into a spot. Bart Singer (NASA Langley) could simulate similar primary and secondary vortices on the computer, but there is evidence of a counter-rotating wall vortex as well in his DNS results: the spot appears only after a rather long gestation period. Seifert (Tel Aviv) reported that two point disturbances separated spanwise, generated using Gaster's technique, interacted to promote transition.

Herbert's (Ohio State) parabolised stability equations (PSE) now take only 30 min. on a work-station and so have potential for engineering calculations. As they are in excellent agreement with both experiment and Navier-Stokes solutions, they can provide flow to the late stages of transition before onset at modest cost; DNS can take off from there on. Encouraged by this experience PSE methodology has now been extended to 3D boundary layers in curvilinear coordinates from low to hypersonic speeds, in both linear and nonlinear regimes. The message was that if the disturbance can be specified properly, and the mean flow is known sufficiently accurately, PSE can take one quite far.

There was much discussion, incidentally, of the possibility of "instability without eigenvalues", the title of a recent paper by Trefethen and coworkers (Science, 3 July 1993). Morkovin traced the history of related ideas; his assessment was that they were not particularly relevant to boundary layer transition, as the implied disturbances were again not "environmentally realizable".

How close to breakdown has basic theory been able to take us? Narasimha, in his opening remarks, was the only one to raise the question of the possible relevance of nonlinear dynamical-system theory to transition. He noted some broad similarities between a set of model equations he had studied with Bhat and Wiggins, and a set proposed by Herbert. These models do not of course reflect the full complexity of the 4-dimensional (3 space + time) forced nonlinear oscillator that the boundary layer is, so we cannot expect to encounter, in real-life transition, the relatively

simple routes to chaos so familiar in dynamical system theory. Although no insight of predictive value could be said to have come from these developments yet, he thought it would be surprising if dynamical chaos had nothing to do with transition. The data analysis methods being developed by Gaster's group could throw light on the problem in coming years.

In any case, according to Narasimha, all the work being done on the different routes to turbulence would eventually have to be codified into appropriate basins of attraction, especially in disturbance space. In general the number of dimensions involved would be too high, but he made proposals for simpler sets of experiments that could help define the concept. Morkovin felt that the number of dimensions would be 10 to 20, and doubted whether the resources - funds, man-power - would be available for undertaking such a task. He was generally pessimistic about the usefulness of the dynamical system approach. Frank Smith (London) described the nonlinear theories currently being pursued, falling into three classes: vortex-wave interactions (important at low input amplitudes), pressure-displacement interactions (medium input) and Euler-scale motions (high input). These theories are very suggestive, and direct comparisons with experimental data in channel flow is encouraging; nevertheless, predictions for flows of the type presented at the Workshop still do not appear to be an immediate possibility.

Wygnanski reviewed what is known about the structure and propagation of fully developed spots. Beyond a critical Reynolds number the TS waves that trail the wing tips of a spot can break

down, creating either apparently autonomous spots or "spotlets" that eventually merge with the parent and so make it grow: he found no support for the alternative view of spot growth, namely that it consists of lambda vortices whose numbers grow in proportion to the size of the spot. It is now well-known that favourable pressure gradients inhibit spot growth - possibly because the wing-tip TS waves are suppressed. Further evidence of this inhibition was presented by Terry Jones (Oxford). Gostelow finds that in adverse pressure gradients, on the other hand, the turbulent region of a spot can spread at a half-angle of 20 degrees, and the attendant wave packet at 29 degrees! Narasimha showed that flow distortion - i.e. a situation in which the streamlines are not parallel but there is no pressure gradient - results in a curved spot trajectory, with spread rates not significantly altered; however the spot is asymmetrical, being thicker on the outside of the bend and not spreading across streamlines necessarily. It is gratifying that spots are now beginning to be studied in more realistic environments, but clearly there may be many surprises in store as other situations are investigated. It is however important to remind ourselves that anomalous propagation is not read into a situation where the spot is not yet mature: the long gestation periods at low Reynolds numbers, known from the early Schubauer-Klebanoff work, can cause confusion in the interpretation of data if one is not careful.

In the real environment of applications, where are spots actually born? According to Morkovin locations are determined by sporadic extrema of the disturbances, but waves and wave packets act as mediators, at least under not highly disturbed conditions.

Narasimha hypothesises concentrated breakdown, i.e. most spots are born in a relatively narrow band around transition onset. The resulting universal intermittency distribution finds support from many measurements, including those presented at the Workshop by Fraser, Gostelow (in pressure gradients as well), Jones, Malkiel & Mayle (in a separation bubble, for the streamwise variation of the maximum value of the intermittency cross-stream, which occurs at the maximum vorticity point), among others. Ian Poll (Manchester) appeared to think that these distributions were being subjected to a rather heavy normalization process, but he also finds use for the same distributions in flow past swept wings, although his "intermittency" is not necessarily the fraction of time that flow is turbulent, as it is for all others, but what one may call a transition progression index, which may be different for different parameters such as skin friction, heat transfer, boundary layer thickness etc.

There is however no direct evidence for the hypothesis of concentrated breakdown, and Hodson (Cambridge) and Jones announced an Oxbridge "spot-hunting" project, which now appears feasible with the development of liquid crystal and multi-gauge surface heat film probes that Jones described at the Workshop. Such a project should in principle be able to track down each spot as it is born and as it propagates downstream. Spot-hunting should be a particularly enjoyable and rewarding exercise in pressure gradients so strong that intermittency distributions are not universal. The reason could be (as Narasimha has suggested) that growth rates vary with pressure gradient (as we know to be the case); but it could also be that breakdown is not sufficiently

concentrated. Spot-hunting could throw light on the question, and seemed to receive the warm support of all assembled.

Hodson's catalogue of the woes that beset turbomachinery fluid dynamicists - harsh environment, high curvature, three-dimensionality, awkward Reynolds numbers and so on - were partly illustrated by Wisler (GE Aircraft Engines), who showed hot film traces from a cascade facility depicting the whole range of phenomena from transition after tripping through attachment, relaminarisation and separation in a bubble, followed once again by transition and reattachment! The qualitative effects are so striking that it is not necessary to have the hot film properly calibrated to read shear stress. Ting Wang (Clemson) finds that acceleration may delay transition onset slightly, but can significantly affect transition zone lengths. Walker & Solomon (Tasmania) find that, on the stator blade of an axial compressor, with adverse pressure gradients that may cause laminar separation and intermittently turbulent reattachment, turbulent spots can appear periodically, following the growth of instability wave packets which lag behind wake passage. Lower FST does not alter the essential character of breakdown, confirming that FST is not the driving factor in adverse pressure gradients. Amidst all this talk of turbulence, Hodson reported some intriguing observations in a radial inflow turbine, where (in spite of relatively high Reynolds numbers and disturbance levels) the flow remains laminar or at best intermittent.

Hypersonics was on many people's minds but did not attract too much attention at the Workshop. Data obtained by Kimmel

(Wright-Patterson), including shadowgraphs and spectra, show that transition onset, as indicated by deviation of boundary layer parameters from laminar values, occurs where the second stability mode (clearly seen in the spectra) saturates. Whether this onset is accompanied by turbulent bursts of any kind is still not clear.

Modelling efforts appeared to fall into two classes: those that take explicit account of streamwise intermittency and those that do not. In the first class Fraser (Dundee) has a model that introduces new correlations for Narasimha's non-dimensional spot formation rate, and shows good agreement with Sharma's experiments on turbine blades, and the data of Abu-Ghannam & Shaw and Dhawan & Narasimha. Ashworth (Rolls Royce), after an assessment of surface film-gauge data under realistic conditions, concludes that transition in turbomachinery flows can be adequately modelled on the basis of Emmons's spots. Eli Reshotko (Case Western), reviewing models, said that the intermittency distributions of Narasimha, Arnal and Chen & Thyson all appeared viable, and that their use was now spreading surprisingly fast. PSE, in combination with e^n methods, was proving very useful in quiescent streams (FST < 0.4%), although Herbert found that if stability conditions were rapidly alternating, e^n could be a poor guide.

What about "by-pass"? There is a general tendency to use this word interchangeably with "high disturbance", but this was questioned at the Workshop. Are we on a by-pass if our hot-wire probes do not show TS waves? We cannot say yes, for Kendall can find TS waves in surface sensors when hot wires do not reveal them. Gaster thinks the TS mechanism may be operating even in the

absence of recognizable TS waves: the boundary layer may still be responding through a TS transfer function even if it has not picked out relatively pure TS waves. There is on the other hand the observation of Blackwelder (USC) that, when rigid particulates are introduced into a laminar boundary layer, turbulent spots arise from the disturbances due to the resulting wake that "scars" the boundary layer, rather than from the particulates themselves. Narasimha suggested that perhaps we should talk about a by-pass only if the mean flow were sufficiently modified to totally alter the transition mechanism. The issue was left hanging, and the participants found it convenient to ignore it for the moment, as they proceeded to talk of "weak" bypass (FST between 0.4% and 2%) and "strong" bypass (FST > 2%) as before (in spite of the fact that FST is not the dominating factor driving transition in adverse pressure gradient flows). By this definition all turbomachinery applications involve only by-pass routes: the disturbance environment is severe, with upstream blade rows often adding periodic wake-passage as another special dimension in disturbance space (as Hodson emphasized). Reshotko considered the weak bypasses the most dangerous, and advocated PSE and correlations to tackle them. For strong bypasses he added the $K\varepsilon$ equations. Max Platzer (Monterey) uses a modified Chen-Thyson model to compute flow past airfoils with separation bubbles, and finds that the incorporation of a transition model is crucial for predicting the bubble. Crawford (Texas at Austin) is developing two-equation models, especially for strong by-pass. Neither the Launder-Sharma models nor Crawford's mutliple time scale improvements seem able to predict the peak skin-friction and heat

transfer parameters that are now well known to occur towards the end of the transition zone. My own feeling is that differential models for transitional flow, without a built-in intermittency, cannot yet perform as well as properly constructed integral-type methods.

There is one silver lining in the cloud in turbomachinery fluid dynamics: blade Reynolds numbers are low enough to make direct numerical solution at full-scale feasible. Thus Manmohan Rai (now at NASA Langley) is able to simulate flow in a spatially developing boundary layer on a flat plate all the way to full turbulence. He finds rather narrow and elongated spot-like regions, more Kendall than Emmons, it seemed to me. Perhaps the rather narrow plate width (only about 130 momentum thicknesses) constrains turbulent regions. Neil Sandham (Queen Mary & Westfield), working with Kleiser at DLR, simulates the complete transition process in a channel: from the intermediate stages involving shear layers, their roll-up, lambda vortices, and, later on, sublayer streaks, ejections etc. The role of the Emmons spot in these simulations remains rather vague yet. But the question was raised, especially by Steve Robinson (NASA Langley), whether all the "captive" fluid mechanics produced on the computer is teaching us enough to be worthwhile? There was general agreement with Reshotko's proposal that DNS should now be done on a mission mode - planned like a flight experiment, say - and that the data must be easily available for interrogation by scientists through simple, well-understood procedures.

Transition control is in some sense an ultimate objective in

applications, but was not much discussed. Hodson thinks there may be optimum wake-passing frequencies from the point of view of the boundary layer. If wake impact triggers transition through wave packets, and a wake-induced turbulent slab conceals within itself a number of turbulent spots (as some experimental evidence suggests), alteration of wake impact frequency may change transition zone parameters in interesting ways. Nosenchuck & Brown (Princeton) are trying a more direct active method, using a wall-normal Lorentz force in the flow of an electrolyte past a flat plate. The Lorentz force is generated by a spanwise magnetic field acting on a streamwise current, and acts by inhibiting lift-up and bursting in the wall layer. Control is exercised through 'tiles' consisting of permanent magnet and stainless steel surface-mounted electrodes. Laser sheet views and velocity traces show dramatic changes when control is on; e.g. stresses are down by upto 90% at a Reynolds number of 1700 (based on momentum thickness), with an applied field of 1000 gauss and current density of 10 mA/cm^2.

On the last day of the Workshop, three working groups summarised their suggestions on what needs to be done. Apart from the question of where spots are born, there are many others that call for answers. Are celerities different from local free-stream velocities in pressure-gradient flows? Does spot growth occur by birth of offspring which amalgamate with the parent? How often do spots trigger the birth of other autonomous spots in the neighbourhood? How strong are spot-interaction effects? Do spot propagation parameters vary widely with pressure gradient? What

happens in strongly curved and 3D flows? And so on.

On the routes leading to spots, the respective roles of narrow Kendall-type wave packets and the wider Gaster-type needs to be clarified. The damped Klebanoff mode needs serious consideration as it may be important in both moderate and high free-stream turbulence. Is it enough to consider free-stream turbulence frozen, or does its evolution need to be accounted for? - this remained an open question.

Frank Smith made a strong plea for greater attention to the physics of the end game. This needs theory, computation and experiment to go hand in hand, but the manpower to do it is not visible. The rewards, on the other hand, are many, and include better transition models and greater understanding of the multiple roads to turbulence, and, eventually, more efficient transition management.

The meeting was one of the most rewarding and stimulating I have attended on transition, because it got two till-now distant communities together, put them in an isolated spot where interaction was easy, kept the group small enough for intimate discussions and organized a programme that had just the right pace - neither overcrowded nor leisurely. I wish there were more meetings like this one.

Final Plenary Session
Transcript

LaGraff In this plenary session discussions of the groups will be reported by spokesmen for the groups or by the moderators of sessions.

Spots

Okiishi At the application end in turbomachinery we see what look like spots/bursts, or some kind of turbulent activity, moving down the blade. There was a lot of interest because of this, and earlier comments on spots and what we mean by spots, to form a group to talk about spots their origin, generation, growth, interaction, structure and size under various conditions. Narasimha has volunteered to summarize the discussion on generation and origin, give us his perspective and lead a discussion. Our group produced a matrix which we consider to be a reasonable classification of spots. The matrix is also a framework for future work and discussion.

Narasimha There has been a lot of discussion about the spot generation process and about the kind of assumptions which could eventually lead to intermittency modeling. If we are going to get the intermittency right we need to know how, where and how many spots are generated and also how they propagate or grow. On spot generation there have been, at different times, hypotheses made on general arguments of a statistical nature and it seems to me that to start with the simplest hypothesis is the best approach. There is now the very exciting possibility that with the development of liquid crystal techniques backed up with large arrays of thin films we might be able to track down the spots as they are born. The proposal deserves our strong moral support. The experiments could also be done in water with a large facility, slow velocity and classical visualization techniques.

My personal feeling is that in the flow past a flat plate under zero pressure gradient it is doubtful if there will be surprises. On the other hand if you have pressure gradients and if you have all the other agencies that affect transition, let alone three-dimensional agencies, it would be very interesting to see how spots are generated and where they are generated. An example would be a body of revolution at an angle of attack. Non-symmetrical cases are also interesting. In our Bangalore experiments a favorable pressure gradient is followed by a zero pressure gradient; we were interested in seeing how spots themselves would behave on encountering a change in pressure gradient. The situation is subtransitional. These are not commonly-encountered pressure distributions. In aircraft wings and turbine blades we often tend to have favorable pressure gradients followed by adverse pressure gradients and with time, in engineering work, the pressure gradients are becoming more severe. It would therefore be very interesting to look at the spot generation and propagation aspects in different kinds of pressure gradient. Three-dimensional situations are largely untouched. There have been some studies on a swept wing, which is an obvious practical application. There may be great surprises in store with three-dimensional flows. There have already been surprises with the Bangalore experiment under a zero pressure gradient with diverging streamlines. Many other cases of great interest, both practical and fundamental, need to be studied here. Rotating cones and disks also give skewed boundary layers and need work. Gostelow has made some very interesting experiments on adverse pressure gradient flows. It is now time to work on pressure distributions which are representative of wings and turbine blades.

With regard to thin cylinders and transverse curvature, some studies on transition in axisymmetric boundary layers were made in Bangalore in the late 60's and early 70's. At that time the emphasis was on understanding the overall behavior of spots and relating them to intermittency distribution; we are now looking for more subtle details and a return to that problem would be worthwhile. Wygnanski has raised the question of very thick axisymmetric boundary layers. For a cone, either the spot eventually wraps around the body or it doesn't. This depends on the spread rate in relation to the cone angle. For a slender cone angle the spot quickly wraps around and the flow is like that on a cylinder. For a wider cone angle it is more like a plate; the boundaries of this behavior need to be established.

The transitions triggered by wakes hitting a blade are also interesting for both basic research and with regard to practical application. When you have a slab of turbulence caused by a wake hitting a blade the question arises of whether you have spots within or between the slabs. Is that slab a relatively homogeneous piece of turbulence? This is an interesting question and liquid crystal techniques might also might be useful here. Separation bubbles present another problem; understanding their role and dynamics needs work. Work by Van Atta on heat transfer in spots deserves re-visiting.

Singer How would you characterize the wake which impinges on a turbine blade? Do you have to run a gas turbine experiment to do this realistically?

Narasimha This can be done with a cylinder on a moving belt.

Ashworth We have looked at simulated wakes on a plane cascade under realistic engine conditions. We had a shock interaction as well as a wake interaction. One of the debates is what happens within that process. There appears to be a Reynolds number dependency. In our work the wake tripped the boundary layer immediately. Hodson believes he sees intermittent action within such a wake so that the turbulence is causing a breakdown process within the wake. You can get a range of mechanisms happening.

Singer If I were thinking of doing a calculation is there a good enough description of the flowfield impinging on the blade or do we have to wait for a better characterization?

Ashworth It is not such a big unknown - it is quite a convective process and lends itself to conventional modeling techniques.

Narasimha Are you thinking of DNS?

Singer Yes. We need a realistic simulation of the vortical flows coming in.

Wygnankski A Karlsruhe report by Rodi addresses this.

Walker You need to model the relative flow within the wake, not just the turbulence. Within the relative flow you either have a jet or a negative jet and this either removes the boundary layer or convects fluid onto the blade and these relative flows produce pertubations in pressure gradient which influence the stability characteristics..

Okiishi I have good collection of this literature which I can communicate to anyone. Calculations have been done at Ames and substantial measurements have been made in cascades and machines.

Morkovin How about spontaneous spot formation? Most of the work on spots is with triggered spots. Under what conditions do you have spontaneous formation?

Reshotko We have not really discussed the origin; Gaster had a proposed mechanism for origin and there was a discussion as to whether this was universal, and a feeling that it was not universal. Attention needs to be given to origin, not only where but how and why?

Narasimha I agree, but the Gaster spot was a forced spot.

Gaster I was putting white noise in to simulate the sorts of things you get in real life! The resulting boundary layer disturbances which evolve into the spike will depend on receptivity and what is in the free stream. There may be many mechanisms at different levels and we have not focussed attention on the theoretical aspects of these.

Morkovin I would not call the Gaster work forcing - it evolves. A sequence of pictures by Falco shows how rapidly the spot can occur. What does it take?

Narasimha It seems to me that what you are saying is that if you make point disturbances, using the kind of white noise that Gaster was using, then in the early stages, you are more likely to match the natural condition than by using ribbons.

Morkovin I haven't seen a spot after a ribbon.

Gaster We can follow it down to the birth of a spot.

Structure and Size

Okiishi Are there any questions for Wygnanski?

Frank Smith Are you sure you don't see T-S waves in a channel flow?

Wygnanksi I didn't do any channel work but the MIT work of Landahl and Widnall shows T-S waves upstream of the spot. They show the spot splitting into two spots. In a boundary layer the spot and Reynolds number increase as you move downstream. In a channel you have a pressure gradient and constant Reynolds number and so there is this significant blockage effect which causes T-S waves.

Gostelow Was the splitting of the spot associated with a forward extension of the calmed region?

Wygnanski I don't think so.

Morkovin There is no evidence of a calmed region in Poiseuille spots. The twinnning that occurs is at the low Reynolds number limit. It is a specialised situation and I don't think we are learning anything basic out of it.

Wygnanski The spot in the boundary layer has two things happening. The increase in Reynolds number is important and the divergence of the boundary layer. Our β=1 spot was an attempt to see what is significant when you have no divergence. We didn't see anything really different. For the Poiseuille flow spot the Reynolds number is constant and it is a different animal.

Singer Do you see any fundamental structural differences between a spot in a zero pressure gradient and one in an adverse pressure gradient?

Wygnanski I didn't do an adverse pressure gradient, ask Gostelow. I saw some interesting things in his work; it seems that some sort of T-S breakdown becomes dominant at the outer edges of the spot.

Singer There was some of that in your zero pressure gradient spot. To try to bring that out would an adverse pressure gradient spot be worth looking at?

Wygnanski We are set now for an adverse pressure gradient spot. We are hoping to get an adverse β=0.1 with no transition. What I saw yesterday was very fascinating. It seemed to me that behind the spot in the calmed region the skin friction was very much reduced. And this was after 128 ensemble averages so it wasn't just a single event.

Gostelow We set that experiment up for the maximum adverse pressure gradient that we could get without laminar separation. It has been traversed through from initiation to the turbulent layer and certainly the spot persists well through into a beginning turbulent layer. With ensemble averaging you can track these events through well and I think this is one legitimate use of ensemble averaging. The data are all new and has not yet been reviewed but there are many interesting things going on.

Wygnanski There used to be a concept that in designing an airfoil that transition occurs at the suction peak. Your data indicate that in the adverse pressure gradient region you might have many interesting things relating to transition occurring and these may take actual lengths which would be of interest.

Walker In the case of our compressor blades at negative incidence we can have an unstable laminar flow, from the suction peak to first breakdown, which may extend up to 50% chord.

Wygnanski The simple concept of transition at the suction peak is erroneous.

Walker Totally. The only place that might work is with a high incidence situation and peak suction pressure in the first 10% of chord.

Crawford Or a highly loaded blade.

Walker I wouldn't think so if the suction peak were at 30-40% chord.

Crawford Well the VKI data showed that on the suction surface of turbine blades.

Walker We need to distinguish between compressor and turbine blades here.

Crawford That's right.

Poll There is also the problem that on an airfoil the Reynolds number is high, compared to a blade so that, on an airfoil, transition takes place over a shorter distance.

Crawford It can be two million on a turbine blade. Isn't that high?

Poll It is for turbomachines. It is not just the pressure gradient, it's also the Reynolds number.

Wygnanski We are now interested in many low Reynolds flows where we were not a decade ago.

Reshotko In a confined flow, such as a cascade, the effects are different than for an airfoil.

Morkovin Wygnanski. Can you tell us about your experiences with pipe flows, which are different from the Poiseuille duct? Have you seen transition after a fully developed laminar flow? Didn't you say that transition in a pipe always occurs in the inlet flow? What do you need to do to get transition in a pipe?

Wygnanski If you keep the pipe flow very clean you can get a R_t of 100,000. Our pipe was only 500 diameters long. The flow stopped being parabolic and then produced slugs. On the other hand if you perturb the flow significantly, at a Reynolds number of 2,000 you can get a puff. You can generate a puff, which is analogous to a spot, either at the inlet or by a large perturbation.

We did an interesting experiment with a flow in a pipe of small diameter. It has a Reynolds number of 10,000 and is expanded in a slow diffuser. The Reynolds number drops but it starts with a turbulent flow. If a larger pipe is long enough you see puffs evolving in turbulent flow - similar to those in laminar flow. There is no interaction between development of a puff and turbulence. Is there a spot within turbulence? There should be a spot even if the flow is quite turbulent.

Poll I can add a physically different situation giving similar behavior. My investigations have concerned the turbulent attachment line. The turbulent cylinder had its largest diameter upstream. The Reynolds number decreases downstream. With a fully turbulent flow below a Reynolds number of 245 the flow reverts to intermittent and ultimately to laminar.

Morkovin The equilibrium puff is a wonderful creation to mimic mathematically. It is a very good target for cfd.

Wygnanski Another target for cfd is recomputing the spot, not using periodic boundary conditions, looking especially at the becalmed region.

Singer It takes too long right now. Does the adverse pressure gradient help by being faster?

Gostelow Yes - and it is more interesting.

Wygnanski Behind the spot you don't need the same density of grid points.

Singer You can shift the density of grid points but you have to be careful. It is a difficult calculation to do to go 400 δ^* downstream.

Low Disturbance Group

Kendall This group was concerned with low turbulence levels up to 0.5%. There was no discussion of pressure gradient effects. We discussed cases where turbulent spots were clearly the final breakdown mechanism. Our scheme was:-

Free-Stream Turbulence - wave packets (G; K) - higher instabilities (H; K) - spots.

Two different classes of packet, one type seen by Gaster and another type from my own work which does not spread laterally as rapidly as the Gaster packet. The distribution of its amplitude through the boundary layer is different from the Gaster case. Nevertheless the breakdown is similar.

The receptivity mechanism as to how packets come about is unknown at present. There is a seeding; there seems to be an injection of energy from the stream into the flow partly in the upstream regions, there is severe buffetting of the layer which may initiate a wave packet. The packet can sometimes be observed to become a burst. We suppose that the breakdown is H or K type, not C type. The Klebanoff mode of long streaky disturbances may depend almost linearly on free-stream turbulence. For high free-stream turbulence the K mode cannot be ignored. Whatever instabilities there are are taking place take place within that as an internal environment. Should free stream turbulence be thought of as frozen or evolving? There is no resolution on this. The structure of the free-stream turbulence will certainly be affected at the leading edge by pressure fields.

Morkovin If the turbulence is frozen as it passes the body the pressure field is the square of the fluctuation level. If it is rejuvenated you can have a fivefold increase in pressure fluctuation reaching the body. Especially if the turbulence is not moving with the free stream.

Walker We are measuring wave packets on compressor blades despite the fact the we have free stream turbulence levels much higher than 0.5%, under conditions of low Reynolds number and high positive pressure gradient.

Gostelow Just a quick comment on the high turbulence level environment - the question was raised of whether spots can occur under a high free-stream turbulence level of, say, 6%. I think we have demonstrated that this can happen. Mark - is this fair?

Morkovin Certainly. They can be quite distinct. The lesser the density of their seeding the more they are going to be evident, and a favorable pressure gradient gives you lesser density seeding.

Physics

Frank Smith A group of us got together to try to raise a flag for mechanisms. We came up with four questions for consideration:-

(i) Which aspects need more study?

We looked at the origins of the burst or spike. Vorticity dynamics, hairpin vortices. Regenerative cycle - one wants to understand λ_z and also the influence of viscosity. If that could be understood we might have some hope of understanding the small and large scale structure of spots and why they arise. Nonlinear receptivity.

(ii) How to do it ?

Computations, experiments and theory, and interactions between them. What new experiments can we perform with modern instrumentation?

(iii) What tools do we need but don't yet have?

Many. Manpower etc., there are not enough people looking at the fundamental physics.

(iv) Would such study help the community?

Yes. We need to understand current transition models and build better ones. Improve numerical simulation methods. Reduced systems for high Reynolds numbers. Understand the many transition paths and different properties of spots. Clarify the physics of the end-stage.

Fant What do you see as the value of the reduced systems at high Reynolds numbers - instead of DNS, solving LES etc?

Frank Smith Herbert is leading the way on this. He is solving an efficient reduced system which should take us up to high Reynolds numbers.

Herbert It works even better at high Reynolds number.

Ashworth Do you see a sequence or logical order for better understanding of the physics, in terms of spot initiation, structure, growth and spreading? Is there a path?

Frank Smith If we don't even understand the origin of the first spike from the viscous wall layer then we can't go on to address the vorticity dynamics or the regenerative process.

Gaster I agree with that. If we don't understand the lowest level of where the spike occurs and why it occurs the best model will not help for subsequent stages.

Morkovin This deals with disturbances after they have been internalised in a boundary layer. This is in the same ballpark as Trefethan and Henningsen. We agreed that it is a forced system. To that extent will we ever be able to put in the environment? This needs small groups for specialist environments. We cannot have response to all possible environments, this is wasteful. Klebanoff finally got good results when he cleaned his last screen. The Klebanoff mode had been hanging around and is now understood. In order to get closer to the approximation the designer needs, it is the designer's responsibility to specify the environment. It is up to individual groups of applications to provide the forcing documentation.

Narasimha The general explanation of the Russian group on spikes is that it occurs by phase locking. How far are we from predicting spikes?

Frank Smith I think of phase locking occurring prior to the spike. Most theories of phase locking are weakly nonlinear so that it occurs before the spike. The spike came out originally after K mode or after weak phase-locking. Is the spike of unique origin or are there many types?

Morkovin Klebanoff used the word spike for a very sudden change. People see spikes in hot wire signals that have nothing to do with turbulent breakdown. The word has been used across the board well beyond the specificity of the first tertiary signal in the K breakdown. It pollutes experimental literature.

Gostelow Did Nishioka use the word correctly?

Morkovin Yes he did. He was in touch with Klebanoff.

Gaster What word would you propose one uses? We see hot wire signals which have little spikes. These we call "spikes".

Morkovin I think it is fairly clear that it is the first hairpin in the Klebanoff tertiary breakdown.

Reshotko I don't think there is a real problem. When we talk of the K spike we refer to the first spike.

Sandham We are analysing data showing five spikes. I asked the question "What are they physically?" Specifically they were a shear layer followed by vortices. Only one was a hairpin vortex. The spikes that you see in experiments- you don't know what they are. The time scale for the formation of the shear layer is longer than the others and the time for the first stage, from the λ vortex stage, can be predicted by the Stuart mechanism.

Herbert In subharmonic breakdown you don't get a spike.

Sandham In the subharmonic case you do see a shear layer but it is not as strong.

Corke Subharmonic breakdown doesn't give inviscid instability. You don't need a 3% perturbation to give subharmonics. It starts at 0.05%.

Morkovin The word 'spikes' alone does not define the phenomenon.

Corke In some sense I agree. The word 'spike' alone does not describe it.

DNS

Crawford There is only a small group of workers, mostly in U.S.A., U.K. and Germany. The calculations are routine for workers with the codes but primarily temporal simulations. Workstations are replacing the Crays and this will enhance capabilities for at least the temporal DNS calculations, but they will be primarily low Reynolds number calculations.

Some issues that were brought up are as follows: The people working in the area need to work on as controlled (as opposed to stochastic) a set of initial conditions as possible. Stochastic conditions are still a problem. DNS fills in what we can't measure. DNS results are for given initial conditions and nothing else. If 20 variables are involved do we need 20 factorial calculations to cover them all? Realistic geometry will involve body fitted coordinates which will be memory- rather than speed-intensive. The question was raised as to whether we could use some of the low-disturbance PSE type computations for the first stage to get the computation started. In Rai's case he had four zones and zone 1 was tremendously intensive. Future DNS needs include stagnation region heat transfer, curved surfaces and pressure gradients. We need to clarify the diagnostics that can be used to evaluate the results of the computations. The final issue is the time commitment for DNS spatial calculations. Eight hundred Cray hours might be a typical time involvement. Do we proceed with man-year intensive calculations? Setting out is like travelling to a distant planet. Do we have the technology to do quality spatial DNS computations?

Sandham Spatial simulations are at the limit of the current capabilities. We can do a lot by temporal schemes, especially in the end-stage transition situation where the differences are probably not crucial.

Herbert In gas turbines the design of one blade costs half a million dollars, so why not proceed?

Robinson I have two rather different perspectives. Experimentalists can take more advantage of the data bases that are around. DNS computations create captive fluid mechanics and then the reasoning begins. From this experimentalists can learn a lot in deciding what experiments to do and what new types of experimental tools can be developed. It is wise for the people who own the DNS tools to make them widely available. The aeronautics side of NASA is questioning the value of DNS. Our steering committee has been challenged to justify why NASA should continue to do DNS. The first questions will be "How are the data bases being used? Are they being used fully?" Clearly the answer is absolutely not.

Crawford I agree. You need to be intimately involved with the Ames center. There has never been much of an attempt to bring it to the general community.

Robinson Generally you are right. NASA tries to make this available and there has been some attempt but it has not been a sufficient effort. Recent computations have raised eyebrows.

Herbert If someone sets out to do this it should be well planned.

Morkovin With respect to the Rai calculations he cannot extract the information that is needed, because it has all been averaged out. The parallel runs make it impossible to look at a specific region and focus on a spot.

Robinson It has a restart deck which makes it possible to investigate this. There is a lot of information in the Rai computations.

Gostelow What, then, is the constraint?

Robinson It is a combination of things. One is the realization that they are available. The taxpayers have paid and they are owned by the populace, just like the wind tunnels. Access is another thing. Many people do not have the facilities to take on board the data sets. The signal/noise ratio is low. That situation is improving. NASA has also been a little coy about keeping things to themselves. The attitude has been that this needs to be a formal collaborative project.

Herbert The NASA man wants to see his name on the paper.

Crawford It is difficult for academics to access the NASA stuff. There is a lot of frustration.

Morkovin The supervising committee for the CTR is addressing this. They will produce more specific guidance as to how it can be done. We have hit on this extremely hard and NASA Ames are providing an extra person to facilitate this. We can't do any more.

Robinson I don't agree. This community represents the need. By defining the need we shall decide whether work continues.

Morkovin That need has been addressed by the supervising committee for the CTR.

Reshotko Under what circumstances do you undertake a very computationally expensive program? They are singular events and need better planning. The Rai case should have been better planned and, perhaps, he should have been given more resources.

Crawford Rai should have been credited with the initiative. It went against the grain.

Reshotko It was against the grain but didn't have to be. It could have been organised as a group effort and carried through to an appropriate conclusion with the data set made available as a benchmark.

Robinson Had the planning happened there would have been no problem.

Morkovin He worked in isolation and that was unfortunate but there is more imprint of these specific computations. Steve and Neale have done an awesome job in interrogating the data base. You have put the inner (bursting) layer on a definite basis. This established a basis of certainty with which we can talk about turbulent boundary layers. That is an invaluable resource that some people will not appreciate but it is behind detail design. Unless you have these concepts quite certain you are not going to be able to be creative in your designs. More has been accomplished than you are giving credit for.

In this same vein there is a problem that is crying out for cfd. It is a by-pass problem. As you get to high Reynolds numbers what will kill you is roughness. Roughness conditions all high Reynolds number work. Single roughnesses are more or less in hand. The effect of distributed roughness is an unknown. With small distributed roughness if you put in an array of roughness elements too small to cause a Klebanoff mode then downstream transition occurs. We have not the slightest idea how that happens. In all probability they amalgamate giving larger scales necessary for initiation of spots. It is hard to see that we can do much more experimentally on this question. If you paint an airplane it makes a 3% difference in drag; that is smooth paint but these effects come in at high Reynolds number. cfd can tell us about the interaction of an array of vortices; small amounts of distributed suction can easily be simulated. No instrument could ever give you this resolution. This is a practically important problem and NASA should be aware of it.

Reshotko One of my PhD students is producing a DNS thesis on this. It needs a larger committment and it needs to be spatial rather than temporal. If we use suction there will be an argument as to whether it is the same mechanism. If we make the committment to an expensive calculation we should make sure that we get it right.

Morkovin The suction is an intermediate step and is much cheaper. This is extremely fundamental and we must have a go.

LaGraff I can think of no more appropriate an end than having Mark and Eli engaged in a spirited exchange of ideas. This symbolizes the more productive aspects of this workshop.

SPOTS, CLUMPS, BURSTS AND OTHER SIMILAR EVENTS

1. generation / origin
2. growth / interaction
3. structure / size

---

a. pressure gradient
b. wakes (as in turbomachines)
c. skew
d. flow separation
e. freestream content (high turbulence intensity)
f. heat transfer
g. high Mach and Reynolds numbers
h. surface curvature
i. other surface conditions (protrusions, film and impingement cooling etc.
j. rigid particulates
k. other (subharmonics etc.)

---

directions for the future

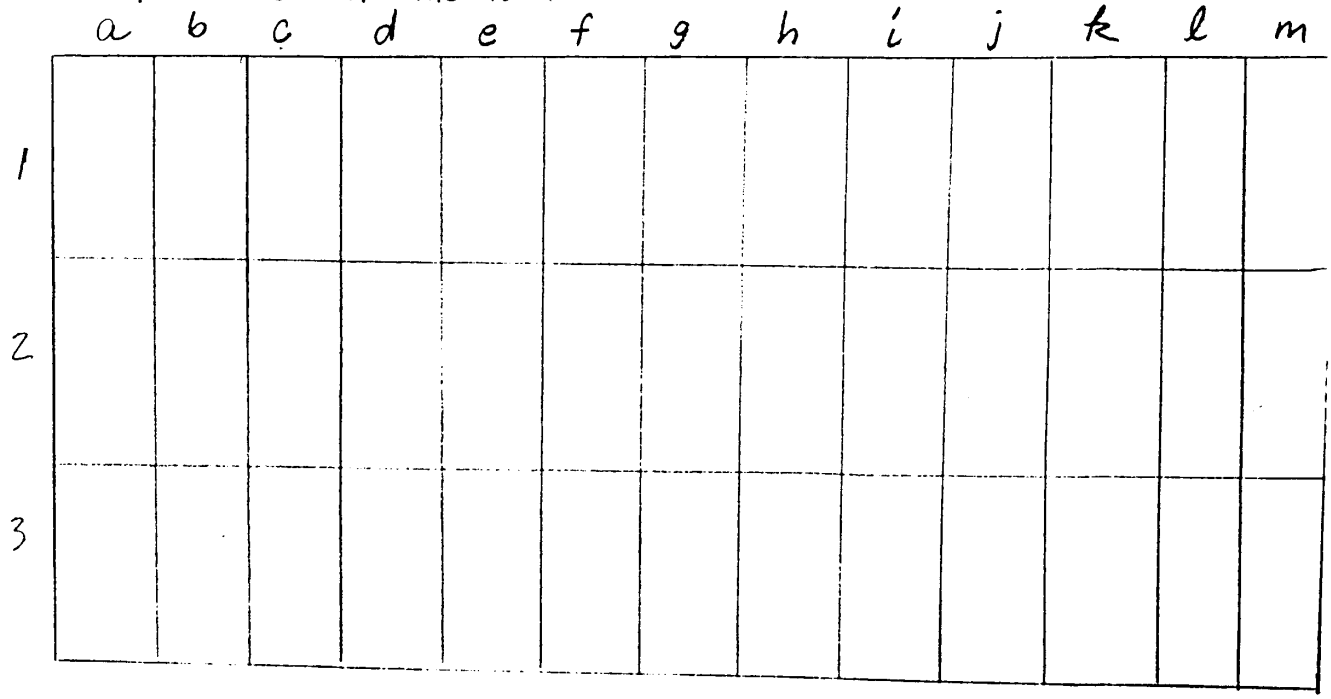

REPORT DOCUMENTATION PAGE	Form Approved OMB No. 0704-0188

1. REPORT DATE *(DD-MM-YYYY)*	2. REPORT TYPE	3. DATES COVERED *(From - To)*
06-04-2007	Conference Publication	

4. TITLE AND SUBTITLE
Minnowbrook I
1993 Workshop on End-Stage Boundary Layer Transition

5a. CONTRACT NUMBER

5b. GRANT NUMBER
NAG3-621

5c. PROGRAM ELEMENT NUMBER

6. AUTHOR(S)
LaGraff, John, E., editor(s)

5d. PROJECT NUMBER

5e. TASK NUMBER

5f. WORK UNIT NUMBER
WBS 561581.02.08.03.21.02

7. PERFORMING ORGANIZATION NAME(S) AND ADDRESS(ES)
National Aeronautics and Space Administration
John H. Glenn Research Center at Lewis Field
Cleveland, Ohio 44135-3191

8. PERFORMING ORGANIZATION REPORT NUMBER
E-15781

9. SPONSORING/MONITORING AGENCY NAME(S) AND ADDRESS(ES)
National Aeronautics and Space Administration
Washington, DC 20546-0001

10. SPONSORING/MONITORS ACRONYM(S)
NASA

11. SPONSORING/MONITORING REPORT NUMBER
NASA/CP-2007-214667

12. DISTRIBUTION/AVAILABILITY STATEMENT
Unclassified-Unlimited
Subject Categories: 02, 07, and 34
Available electronically at http://gltrs.grc.nasa.gov
This publication is available from the NASA Center for AeroSpace Information, 301-621-0390

13. SUPPLEMENTARY NOTES
Abstracts and viewgraphs prepared for the Minnowbrook I-1993 Workshop on End-Stage Boundary Layer Transition sponsored by Syracuse University, Blue Mountain Lake, New York, August 15-18, 1993. John E. LaGraff, Syracuse University, Syracuse, New York 13244.

14. ABSTRACT
This volume contains materials presented at the Minnowbrook I-1993 Workshop on End-Stage Boundary Layer Transition, held at the Syracuse University Minnowbrook Conference Center, New York, from August 15 to 18, 1993. This volume was previously published as a Syracuse University report edited by John E. LaGraff. The workshop organizers were John E. LaGraff (Syracuse University), Terry V. Jones (Oxford University), and J. Paul Gostelow (University of Technology, Sydney). The workshop focused on physical understanding of the late stages of transition from laminar to turbulent flows, with the specific goal of contributing to improving engineering design of turbomachinery and wing airfoils. The workshop participants included academic researchers from the United States and abroad, and representatives from the gas-turbine industry and U.S. government laboratories. To improve interaction and discussions among the participants, no formal papers were required. The physical mechanisms discussed were related to natural and bypass transition, wake-induced transition, effects of freestream turbulence, turbulent spots, hairpin vortices, nonlinear instabilities and breakdown, instability wave interactions, intermittency, turbulence, numerical simulation and modeling of transition, heat transfer in boundary-layer transition, transition in separated flows, laminarization, transition in turbomachinery compressors and turbines, hypersonic boundary-layer transition, and other related topics. This volume contains abstracts and copies of the viewgraphs presented, organized according to the workshop sessions. The workshop summary and the plenary discussion transcript clearly outline future research needs.

15. SUBJECT TERMS
Turbomachinery; Transition; Turbulence; Wakes; Boundary layers; Turbulent spots; Wavelets; Heat transfer; Unsteady flow; Compressors; Turbines

16. SECURITY CLASSIFICATION OF:			17. LIMITATION OF ABSTRACT	18. NUMBER OF PAGES	19a. NAME OF RESPONSIBLE PERSON
a. REPORT	b. ABSTRACT	c. THIS PAGE			David E. Ashpis
U	U	U		509	19b. TELEPHONE NUMBER *(include area code)* 216-433-8317